

Netherlands Geographical Studies 293

Sorting out sand and gravel

sediment transport and deposition

in sand-gravel bed rivers

Maarten G. Kleinhans

Utrecht 2002

The Royal Dutch Geographical Society/
Faculty of Geographical Sciences, Utrecht University

This publication is identical to a thesis submitted in partial fulfillment of the requirements for the degree of Doctor (Ph.D.) at Utrecht University, The Netherlands, 29 May 2002.

The investigations were supported by:

- The Netherlands Earth and Life sciences Foundation (“ALW”) with financial aid from the Netherlands Organisation for Scientific Research (“NWO”), grant number ALW-750.197.11
- The Directorate Eastern Netherlands of Rijkswaterstaat in the Netherlands and the National Institute for Inland Water Management and Waste Water Treatment (“RIZA”)
- St. Anthony Falls Laboratory, University of Minnesota, United States of America
- The Transport and Mobility of Researchers programme of the European Commission
- The consortium of Twente University, The Institute for Inland Water Management and Waste Water Treatment (“RIZA”) and WL | Delft Hydraulics
- Faculteit Ruimtelijke Wetenschappen van de Universiteit Utrecht
- Interuniversitair Centrum voor Geo-ecologisch onderzoek

Promotores:

Prof. dr. ir. L. C. van Rijn Faculty of Geographical Sciences, Utrecht University
/ WL | Delft Hydraulics

Prof. dr. E.A. Koster Faculty of Geographical Sciences, Utrecht University

Co-promotor:

Dr. J. H. van den Berg Faculty of Geographical Sciences, Utrecht University

Examination committee:

Prof. dr. J. Best School of Earth Sciences, University of Leeds

Prof. dr. ir. G. Parker St. Anthony Falls Laboratory, University of Minnesota

Prof. dr. ir. H. de Vriend Faculty of Civil Engineering and Geosciences, Delft University
of Technology / WL | Delft Hydraulics

Dr. W. ten Brinke Institute for Inland Water Management and Waste Water
Treatment (“RIZA”), Ministry of Transport, Public Works and
Water Management

Dr. ir. J. Ribberink Department of Civil Engineering, University of Twente

ISBN 90-6809-328-2

Copyright © Maarten G. Kleinhans, p/a Faculty of Geographical Sciences,
Utrecht University 2002.

Niets uit deze uitgave mag worden vermenigvuldigd en/of openbaar gemaakt door middel van druk, fotokopie of op welke andere wijze dan ook zonder voorafgaande schriftelijke toestemming van de uitgevers.

All rights reserved. No part of this publication may be reproduced in any form, by print or photo print, microfilm or any other means, without written permission by the publishers.

Printed in The Netherlands by Labor Grafimedia b.v. - Utrecht

Aan mijn vader,
die mij naar de natuur en de rest van het heelal leerde kijken (*“Observo, ergo sum”*),
en mij wel van de straat maar niet uit de goot wist te houden.

“The value of philosophy is, in fact, to be sought largely in its uncertainty. ... Philosophy, though unable to tell us with certainty what is the true answer to the doubts which it raises, is able to suggest many possibilities which enlarge our thoughts and free them from the tyranny of custom ... and it keeps alive our sense of wonder by showing familiar things in an unfamiliar aspect.” Bertrand Russell (1912, p. 91, *The problems of philosophy*, Oxford University Press, Oxford)

Contents

Figures 12

Tables 16

Acknowledgments - Voorwoord 17

1 Introduction 19

- 1.1 Rationale 19
 - 1.1.1 Between sand-bed rivers and gravel-bed rivers 19
 - 1.1.2 Emergent characteristics of sand-gravel bed rivers 19
 - 1.1.3 Relevance 20
- 1.2 General objective 21
- 1.3 Organisation of the thesis 23

2 Review, problem definition, objectives and hypotheses 25

- 2.1 Introduction 25
 - 2.1.1 Objective 25
 - 2.1.2 Sand-bed rivers and gravel-bed rivers 25
 - 2.1.3 Scope of this study 28
- 2.2 Sediment transport processes of uniform sediment 30
 - 2.2.1 Basic knowledge 30
 - 2.2.2 Interaction between bedforms and bedload transport 31
- 2.3 Sorting of sediment mixtures on the grain scale 31
 - 2.3.1 General observations 31
 - 2.3.2 Sorting in armour layers 32
 - 2.3.3 Incipient motion of sediment mixtures 33
 - 2.3.4 Hiding-exposure effects and deposition 35
 - 2.3.5 Incipient motion of unimodal and bimodal sediments 35
 - 2.3.6 Horizontal size-segregation and mobility in bimodal sand-gravel sediment 36
 - 2.3.7 The importance of turbulent shear stress variations near incipient motion 38
- 2.4 Sorting on the bedform scale 39
 - 2.4.1 General observations 39
 - 2.4.2 Bedform types in non-uniform sediment 40
 - 2.4.3 Vertical sediment sorting 43
 - 2.4.4 The combined role of turbulence and sediment sorting in bedforms 45
- 2.5 Sorting in meander bends 46
- 2.6 Shortcomings of the present approaches 48
- 2.7 Objectives 49
- 2.8 Hypotheses and conceptual modelling approaches 50
- 2.9 Integral conceptual model 51
- 2.10 The sky is not the limit 53
- 2.11 References 53

Part 1. Sediment transport in sand gravel bed rivers 57

3 Method and accuracy of sediment transport measurements in large sand-gravel bed rivers 59

- Abstract 59
- 3.1 Introduction 60
 - 3.1.1 Objective and definitions 60
 - 3.1.2 Review 60
- 3.2 Uncertainties in cross-channel integration of sediment transport 62
 - 3.2.1 Integration of measured data 62
 - 3.2.2 Sources of uncertainty in the integration 63
 - 3.2.3 Systematic interpolation error 63
 - 3.2.4 Stochastic uncertainty of transport sampling 65

	3.2.5	Combining all the uncertainties	65
3.3		Set-up of field measurements	66
	3.3.1	Field site and conditions	66
	3.3.2	Natural variability of sediment transport	68
	3.3.3	Sampling strategy for minimizing transport variance	70
3.4		Bedload transport measurement	70
	3.4.1	Instrumentation	70
	3.4.2	Calibration and sampling duration	72
3.5		Suspended load transport measurement	72
	3.5.1	Instrumentation	72
	3.5.2	Field check of the calibration of the acoustical sand transport meter	72
	3.5.3	Data processing	73
3.6		Results of the field measurements	74
	3.6.1	Hydrodynamics and sediment transport	74
	3.6.2	Effect of changing hydrodynamic conditions	75
3.7		Accuracy depending on sampling strategy	76
	3.7.1	Variation coefficients	76
	3.7.2	Uncertainty of integrated transport	77
3.8		Discussion	78
	3.8.1	Sources of uncertainty	78
	3.8.2	Bedforms	79
	3.8.3	Uncertainty of depth-integrated suspended transport	80
	3.8.4	Time and financial investment	80
3.9		Conclusions	81
		Acknowledgments	82
		Notation	82
		References	82
4		Bedforms and sediment transport over armour layers	85
		Abstract	85
4.1		Introduction	86
4.2		Review	86
4.3		Flume experiments	88
	4.3.1	Description of the experiments	88
	4.3.2	Results of the flume experiments	92
4.4		Field measurements	93
	4.4.1	Field measurements in the river Allier (France)	93
	4.4.2	Field measurements in the river Waal (The Netherlands)	95
4.5		Bedform stability diagrams	99
	4.5.1	Selection of diagrams	99
	4.5.2	Choice and effect of the grain size parameter	101
4.6		Effect of the supply limitation on bedform morphology	103
	4.6.1	Transitions between supply-limited bedform types	103
	4.6.2	Prediction of sediment supply-limited bedform morphology	104
4.7		Conclusions	109
		Acknowledgments	109
		References	109
5		Prediction of bedload sediment transport	113
		Abstract	113
5.1		Introduction	114
5.2		Types of bedload predictors	114
5.3		Prediction methods and parameters	115
	5.3.1	Modification of deterministic predictors for non-uniform sediment	115
	5.3.2	Modification to stochastic predictors (for non-uniform sediment)	117
5.4		Critical bed shear stress of particle size fractions in non-uniform sediment	118

5.4.1	Hiding-exposure correction	118
5.4.2	Critical Shields parameter (θ_{cr}) for D_i or $D50$	118
5.4.3	Critical bed shear stress of unimodal and bimodal sediment	120
5.5	Flume experiments	122
5.5.1	Setup of the flume experiments	122
5.5.2	Experimental evaluation of the Nikuradse grain roughness $k_{s,grains}$	125
5.6	Choosing the parameters	125
5.6.1	Effect of equation 3a/b (conversion from $\phi_{b,i}$ to $q_{b,i}$)	126
5.6.2	Hiding-exposure function	126
5.6.3	Effect of the stochastic parameter	129
5.6.4	Total bedload transport rates with the MPM bedload predictor	129
5.6.5	Effect of equations 7a/d (T_i in non-uniform VR predictor) and equations 8a/b (D_i in non-uniform VR predictor)	130
5.6.6	Fractionwise and total bedload transport rates with the VR bedload predictor	132
5.7	Hindrance at small transport rates	132
5.8	Validation	133
5.8.1	East Fork, Wyoming data	133
5.8.2	Sagehen Creek, California data	134
5.9	Discussion	136
5.9.1	Single- or multi-fraction approach	136
5.9.2	Deterministic or stochastic approach	137
5.9.3	Hiding-exposure	137
5.9.4	Hindrance and armouring	138
5.10	Conclusions	139
	Acknowledgments	139
	Notation	140
	References	141

Extreme hysteresis of bedload and suspended load transport during a discharge wave in the river Rhine
Abstract 143 143

6.1	Introduction	144
6.2	Measurement methods	144
6.2.1	Field site and general conditions	144
6.2.2	Determination of bedload and suspended load transport from direct measurements	145
6.2.3	Calibration of the applied bedload sampler	147
6.2.4	Determination of bedload transport from dunetracking	149
6.3	Results of the field measurements	150
6.3.1	Bedform development	150
6.3.2	Bedload transport from dunetracking	152
6.3.3	Bedload and suspended load sediment transport from sampling	153
6.3.4	Evaluation of the accuracy of the suspended and bedload transport rates	153
6.3.5	Sediment dynamics of the river bed	155
6.4	Bed shear stress determination	157
6.5	Hysteresis of suspended load transport	158
6.6	Hysteresis of bedload transport	159
6.6.1	Enumeration of potential explanations	159
6.6.2	Suspended sediment settling contributing to bedload transport and dune migration	160
6.6.3	Transport hysteresis due to degradation and fine sand scour	161
6.6.4	Transport hysteresis due to fine sand exchange with groyne fields	162
6.6.5	Transport hysteresis due to sand deposition in meander pools at low stages and entrainment at high stages	163
6.6.6	Transport hysteresis due to a downstream migrating fine sand wave	164
6.6.7	Transport hysteresis due to armouring	165
6.6.8	Transport hysteresis due to lag in dune height development	166
6.6.9	Transport hysteresis due to (antecedent) vertical sorting by dunes	167
6.7	Integration of the hypotheses	170

- 6.8 General value of the identified mechanisms causing transport hysteresis 171
- 6.9 Conclusions and recommendations 172
 - Acknowledgments 172
 - References 172

Part 2. Sediment sorting and deposition in sand gravel bed rivers 175

- 7 **Sorting in grain flows at the lee-side of dunes: review 177**
 - Abstract 177
 - 7.1 Introduction 178
 - 7.2 Basic sedimentological definitions, units and processes 178
 - 7.2.1 Bedforms and transport 178
 - 7.2.2 Deposits and sorting 180
 - 7.3 Sorting data in literature 183
 - 7.3.1 Vertical sorting in foresets in laboratory experiments 183
 - 7.3.2 Vertical sorting in foresets in rivers 187
 - 7.4 Grain fall process and deposition 188
 - 7.5 Sorting in foreset deposits from individual rolling grains 189
 - 7.5.1 The role of angles of repose 189
 - 7.5.2 Physical modelling of highly idealised conditions 191
 - 7.6 Sorting in foreset deposits from grain flows 193
 - 7.6.1 Initiation of the grain flow 193
 - 7.6.2 Sediment sorting within grain flows 195
 - 7.6.3 Sorting by grain flows rejuvenating underlying sediment 196
 - 7.7 Additional factors affecting sorting in dunes 197
 - 7.7.1 The effect of sediment bimodality 197
 - 7.7.2 Counterflow effects on the foreset and bottomset deposits 197
 - 7.7.3 The effect of sediment transport magnitude at the brinkpoint 199
 - 7.7.4 Armouring and bottomsets 202
 - 7.8 Synthesis: processes and variables 202
 - 7.8.1 Primary controls on grain fall, individual grains rolling and grain flows 202
 - 7.8.2 Hypothetical explanation for difference between segregation and stratification 204
 - 7.8.3 Conceptual model 205
 - 7.9 Concluding remarks 206
 - Acknowledgments 207
 - References 207
- 8 **Sorting in grain flows at the lee-side of dunes: experiments 211**
 - Abstract 211
 - 8.1 Introduction 212
 - 8.1.1 Scope and objective 212
 - 8.1.2 Review and definitions 212
 - 8.2 Setup of the flume experiments 213
 - 8.3 Results 216
 - 8.3.1 Basic data 216
 - 8.3.2 Vertical sorting 217
 - 8.3.3 Process description of sorting in the grain flow 221
 - 8.4 Discussion 223
 - 8.4.1 Dimensionless numbers affecting vertical sorting: theory 223
 - 8.4.2 Dimensionless numbers affecting vertical sorting: results 225
 - 8.4.3 Comparison between sorting in deltas, bars and dunes 226
 - 8.4.4 Applicability of the results to natural river dunes 228
 - 8.4.5 Comparison of the grain flow sorting process description with literature 230
 - 8.5 Conclusions 231
 - Acknowledgments 231
 - References 231

9	Linking the bedload transport process and sorted sand gravel deposits in fluvial channels with dunes	233
	Abstract	233
9.1	Introduction	234
9.1.1	Relevance of sediment sorting and scope	234
9.1.2	Cross-bedded and lag deposits	235
9.2	Flume experiments	236
9.3	Deposition and transport concept	237
9.4	Test of the concept with data from the river Rhine	239
9.4.1	Field site description	239
9.4.2	Dune height and sediment transport measurements	243
9.4.3	Gravel lag layers	244
9.5	Behavioural model of vertical sorting	247
9.5.1	Model rationale	247
9.5.2	Model description	248
9.5.3	Bedload transport prediction	250
9.5.4	Sorting modelling	251
9.6	Application of the model to the river Rhine	253
9.6.1	Boundary conditions	253
9.6.2	Modelled flow parameters, dune height and bedload transport	253
9.6.3	Modelled sediment sorting and lag deposits	255
9.6.4	Sensitivity analysis	256
9.7	Discussion	257
9.7.1	Effect of variability of dune height and scour depth on gravel lag layer depth	257
9.7.2	Effect of variability of trough scour depth on cross-set thickness	258
9.7.3	Effect of dune response time on stratigraphy	259
9.7.4	Effect of sorting function for cross-bedded (foreset) deposits	259
9.7.5	Future model development	260
9.8	Conclusions	260
	Acknowledgments	261
	List of symbols	261
	References	262
10	Sand-gravel sorting in channel beds by non-equilibrium, three-dimensional dunes	265
	Abstract	265
10.1	Introduction	266
10.1.1	Scope	266
10.1.2	Sorting in deposits of dunes in equilibrium and non-equilibrium conditions	266
10.1.3	Sorting in deposits of regular and irregular dunes	267
10.2	Setup of the flume experiments	267
10.3	Results	272
10.3.1	Flow, sediment transport and dunes	272
10.3.2	Sedimentary structures	274
10.3.3	Vertical sorting	277
10.4	Discussion	278
10.4.1	Controls on gravel lag formation	279
10.4.2	Controls on dune irregularity	281
10.4.3	Competition between deep scour and gravel lag layers	283
10.4.4	Deposits of dunes in lowering discharge	284
10.4.5	Towards modelling	286
10.5	Conclusions	287
	Acknowledgments	288
	Appendix: Effect of the difference between sediment feed and recirculation flumes	288
	Literature	289
11	Synthesis, conclusions and scientific recommendations	291
11.1	Introduction	291

- 11.2 Conclusions 291
- 11.3 A continuum from sand-bed rivers to gravel-bed rivers 293
- 11.4 Roles of sediment sorting on different scales 294
- 11.5 How to implement the results into (morphological) models? 295
 - 11.5.1 Modelling sediment sorting at the lee side of dunes 295
 - 11.5.2 Point model of sediment sorting and transport 296
 - 11.5.3 Continuous sorting in the Exner sediment continuity concept 297
- 11.6 Opening Pandoras Box: scientific challenges 298
 - 11.6.1 Shear stress acting on grains 298
 - 11.6.2 Hiding-exposure relations 299
 - 11.6.3 Interactions up- and downstream of river bifurcations 300
 - 11.6.4 Interactions with sediment sorting in meander bends 301
 - 11.6.5 Interactions with downstream fining 301
- References 302

Summary 304

Samenvatting voor de leek 308

Curriculum Vitae 315

Publications 316

Figures

- 1.1. Two 'grocery store examples' of phenomena that emerge only in rivers with both sand and gravel in the sediment. 20
- 1.2. A representation of a morphodynamic system for alluvial rivers. 21
- 1.3. Time-space diagram of alluvial processes and phenomena. 21
- 1.4. Oblique photograph of the bed in one of the flume experiments presented in chapter 4. A bedform is present which consists mainly of sand. In the trough zone and below the bedform, an armour layer is present. 22

- 2.1. Mobility of sediment in sand-bed rivers and gravel-bed rivers (after Parker in prep.). 27
- 2.2. Three ranges of flow and sediment conditions and their relations. The first (x-axis) is the relative proportion of sand (< 2 mm) and gravel (> 2 mm) in the bed. The second (y-axis) is the sediment mobility, which can also be expressed as flow discharge or shear stress. The third (z-axis) is the bimodality of the sediment. 29
- 2.3. Left: an armour layer with an imbricated pebble cluster on a bar in the river Waiho, New Zealand. Right: a pebble cluster on a sand ribbon in the laboratory experiments described in chapters 4 and 5. The largest grains are much more exposed to the flow than the small grains. 32
- 2.4. Critical bed shear stress according to the Shields curve and with equal mobility and Egiazaroff (1965) hiding-exposure corrections, and a hiding-exposure curve for strongly bimodal sediment (after Wilcock and McArdeell 1993, see text for explanation). 33
- 2.5. The mobility of sediment is determined by the flow shear stress and the critical shear stress, which both have a stochastic nature (after Grass 1970). 39
- 2.6. Illustrations of a number of bedform types, and the sorting within some bedforms. 42
- 2.7. Basic depositional units in dunes: a bottomset, a cross-foreset and a topset. 43
- 2.8. During rising and peak discharge the transported sediment is sorted in the grain flow at the lee side of a dune. In waning discharge, the dunes diminish and leave cross-bedding relicts. Due to selective deposition, an upward fining accumulation of lag deposits is created in addition (see chapters 6 and 9). 44
- 2.9. The structure of flow (to the right) over a dune. 45
- 2.10. Sediment sorting in the river Allier, France, in between Moulins and Chatel de Neuve. 47
- 2.11. Conjecture of extended morphodynamic system of a river bed with bedforms 52

- 3.1. Measurement positions in the cross-section (a) and in planform (b). 62
- 3.2. Hypothetical cross-channel distribution of transport and discrete approximations with seven subsections (figs. a-c), and the resulting interpolation error as a function of the number of subsections. 64
- 3.3. Field site location. 67
- 3.4. Discharge of the river Waal in the period March 1-14, 1997. 67
- 3.5. Sieve curves of bed material, bedload material and suspended material. 68
- 3.6. The nozzle of the adapted Helley Smith bedload sampler (HSZ) is suspended from the winch cable and thus

- lands on the bed after the frame and is lifted from the bed before the frame is. 71
- 3.7. Field check of ASTM concentrations (a) with pump concentrations (data from Ditzel & De Vos 1986) and a typical example (March 8, position -67 meter) of a vertical profile of suspended sediment transport (b). 73
 - 3.8. Stream velocity (a), bedload (b) and suspended load (c) sediment transport in the cross-section and a bed profile (d) of the cross-section. 74
 - 3.9. Bedload (a) and suspended load (b) sediment transport in the subsections as a function of discharge. The transports are corrected for changes in discharge during the period of the measurements for one complete cross-section. 75
 - 3.10. Sample size weighed variation coefficients of all subsections and the maximum variation coefficient of all bedload data. 76
 - 3.11. Relative uncertainty of suspended transport as a function of (a) the number of points in a vertical and (b) on the total suspended transport in the vertical. 76
 - 3.12. Relative uncertainty of cross-channel integrated bedload (a) and suspended load (b) transport as a function of the number of samples or verticals and the number (*k*) of subsections. 77
 - 3.13. Comparison of sample size weighed variation coefficients in a subsection as found in this study and in literature (Gaweesh & Van Rijn 1994; McLean & Tassone 1987 (in Hubbell 1987)). 79
 - 3.14. Accuracy of cross-channel integrated bedload (a) and suspended load (b) sediment transport estimates that can be achieved as a function of the duration of the measurement campaign for one cross-section. 81
- 4.1. Particle size distribution of the initial bed sediment in the flume experiments. 88
 - 4.2. Sequence of the experiments of Blom & Kleinhans 1999 (after Kleinhans 2000). 89
 - 4.3. Bedform types observed in the flume experiments. 91
 - 4.4. Bedform types and height as a function of depth-averaged flow velocity in the flume experiments. 92
 - 4.5. Location of the field measurements in the river Allier (arrow) and the river Waal (box). The area in the box in the Netherlands is enlarged in figure 7. 93
 - 4.6. Observations of migrating waves of sand on the immobile armour in the river Allier. 95
 - 4.7. The location of the measurement section in the river Waal in the Netherlands (arrow) is just downstream of the bifurcation point of the Rhine into the Pannerdensch Kanaal and the Waal. The flow direction is west. The location of this map is given in Figure 4.5. 95
 - 4.8. A) Flow discharge and dune height in the river Waal in October–November 1998, as well as a planform echosounding map of the river bed in the Waal just downstream of the bifurcation point with the Pannerdensch Kanaal. B) Two examples of dune profiles are given with large and with small dunes. 96
 - 4.9. Data of bedforms in non-uniform sediment plotted in the Southard & Boguchwal (1990) bedform stability diagram for 10°C-equivalent quantities and subcritical flow conditions 100
 - 4.10. Bedform data in non-uniform sediment in the diagram of Chiew (1991). 101
 - 4.11. Data of bedforms in non-uniform sediment plotted in the Van den Berg & Van Gelder (1993) bedform stability diagram. 102
 - 4.12. Transition of bedform types in response to changing flow velocity and bedload transport. 104
 - 4.13. Bedforms plotted against the modified Shields parameter (related to the grains of the transported sediment), and the ratio of predicted and measured bedload transport. 105
 - 4.14. The dimensionless transport layer thickness against the modified Shields parameter (based on shear stress on grains of the transported sediment) for flume (A) and field (B) conditions. 107
 - 4.15. Conceptual explanatory (but not predictive) model for the occurrence of bedforms in sediment supply-limited conditions. 108
- 5.1. Critical bed shear stress according to the Shields curve and with equal mobility and Egiazaroff (1965) hiding-exposure corrections. 119
 - 5.2. Effect on critical bed shear stress ($\tau_{cr,i,corrected}$) based on $\theta_{cr,Shields,D50}$ (straight dashed line) or $\theta_{cr,Shields,D_i}$ (curved line) in combination with a he-function (eq. 14). 120
 - 5.3. Critical bed shear stress of non-uniform sediment. 121
 - 5.4. The mobility of sand and gravel on different states of the bed surface with increasing bedload transport. 122
 - 5.5. Non-cumulative particle size distribution of the bed sediment used in the flume tests. 123
 - 5.6. Applied flow velocity and duration of the flow. 123
 - 5.7. Bedform types observed in the flume tests. 124
 - 5.8. Effect of conversion from $\Phi_{b,i}$ to $q_{b,i}$ with particle size parameters $D50$ and D_i (eq. 3). 126
 - 5.9. Comparison of predicted and measured relative fractional bedload rates for flume experiments T0, T5, T7, T9 and T10 with the Egiazaroff (1965) and the experimental he-function and the stochastic MPM. 127
 - 5.10. Average (of all tests included) experimental he-function compared to the Egiazaroff (1965) he-function. 128
 - 5.11. Comparison of predicted and measured total bedload transport rates with the stochastic MPM ($\alpha=5.7$) and

- VR for non-uniform sediment with the Egiazaroff (1965) and the experimental he-function. 130
- 5.12. A. The effect of (not) applying the he-function in the denominator of T_i on fractional bedload rates (eq. 7a/b). Calculations were done with D^*50 for experiment T7.
 - B. The effect of applying D^*50 or D^*i on fractional bedload rates (eq. 8a/b). Calculations were done without the he-function in the denominator of T_i for experiment T7. 131
 - 5.13. The hindrance factor function and observations from the Sand Flume experiments. 133
 - 5.14. Comparison of predicted and measured relative fractional bedload rates for the East Fork dataset for 4 flow velocity classes with the stochastic MPM with the Egiazaroff (1965) he-function. 134
 - 5.15. Comparison of predicted and measured total bedload transport rates with the stochastic MPM for non-uniform sediment with the Egiazaroff (1965) he-function of East Fork River and Sagehen Creek datasets, with and without the hindrance factor. 135
 - 5.16. Comparison of predicted and measured relative fractional bedload rates for the Sagehen Creek dataset for 5 bed shear stress classes with the stochastic MPM with $\theta_{cr,D50} = 0.0384$ (Andrews 1994) and with the Egiazaroff (1965) and the experimental he-function with $P = -0.887$ (Andrews 1994). 136
 - 5.17. Difference between the deterministic and stochastic MPM with the Egiazaroff (1965) he-function for the relative fractional bedload rates in Sand Flume experiments T7 and T10. 138
- 6.1. Map of the measurement positions of direct sampling of the sediment transport and flow in the river Waal, as well as the vibro-core positions. The whole (submerged) area given by the map was mapped with multibeam echosounders for dunetracking. 145
 - 6.2. a. Discharge of the Waal (lower curve) and Bovenrijn (upper curve) in the measurement period. b. Average grain size distribution of the bed sediment of the Bovenrijn and Waal, averaged over a depth of 0.8 m from the bed surface, determined from the vibro-cores (described in this paper). 146
 - 6.3. Dune height and length in the river Waal (a) resp. Bovenrijn (b), and migration rate in both rivers (c). 151
 - 6.4. Bedload transport computed from dune migration in the river Waal (a) resp. Bovenrijn (b). Numbers refer to dates in the period of 30 October to 19 November in 1998. In figure a, the bedload transport measured with the HSZ is given as well (see text for comparison and discussion). (c) The bedload transport computed from dune migration in the Bovenrijn in several discharge waves. 152
 - 6.5. a. Bedload transport in the river Waal by the HSZ, and the D90 of the bedload sediment. The percentages refer to the gravel abundance. b. Grain size distributions of the bedload sediment on October 31, November 3, 5, 9 and 12 (numbers 1-5). c. Suspended sand transport in the river Waal by the ASTM. d. Grain size distributions of the suspended load sediment. 154
 - 6.6. Observations of the deposits in the river Waal (a) and Bovenrijn (b). 156
 - 6.7. Grain size distributions of the sediment in the top and base of dunes in the Waal, and the fine sediment below the dune deposits. 157
 - 6.8. Total and grain-related bed shear stress measured in the Waal. 157
 - 6.9. Fraction of suspended load sediment that is potentially sampled with the HSZ (between 0 and 1, i.e. between 0% and 100%) (left vertical axis), and the suspended sediment transport between 0.2 and 0.3 m above the bed surface (right vertical axis). 161
 - 6.10. Conceptual model of sediment transport at two locations when fine sediment is eroded just upstream of the first location. 162
 - 6.11. Conceptual model explaining the observed hysteresis of sediment transport 170
- 7.1. Basic definitions of depositional units in river dunes in peak and waning discharge (after Kleinhans 2001). The dunes leave a lag deposit in the river bed below their troughs, which consists of coarse sediment that is no longer mobile. 179
 - 7.2. Flow conditions over dunes. 179
 - 7.3. Definitions of directions of sorting in four cases, in this case drawn in a cross-stratum, according to Allen (1984). Tangential and perpendicular refers to the direction of sorting relative to the direction of the moving sediment. Normal and reverse refers to the fining or coarsening trend in the deposit. 180
 - 7.4. a. Sorting and definitions in dune deposits after Hunter (1985b). b. Modified sorting in dune deposits for the case where only grain flow deposits are preserved. 181
 - 7.5. Vertical sorting measured in experiments. 185
 - 7.6. Vertical sorting measured in natural river dunes. 187
 - 7.7. Concepts of sorting mechanisms. 191
 - 7.8. Comparison of experimental (left) and modelling (right) results by Makse and coworkers (after Cizeau et al. 1999). 191
 - 7.9. Data of Hunter & Kocurek (1986). 201
 - 7.10. Conceptual model of sorting as a function of the most important variables. 205

- 8.1. A. Sorting and definitions in sand dune deposits (after Hunter 1985). B. Sorting in sand-gravel dune deposits, where only grain flow deposits are preserved on the lee slope. 213
- 8.2. Outline of the Delta Flume at St. Anthony Falls Laboratory (vertical scale exaggerated). 214
- 8.3. Grain size distributions of the sediment mixtures fed into the flume. See Table 8.1 for description. 215
- 8.4. The delta height and the delta celerity (downstream migration of the slip face). 216
- 8.5. a) Photograph showing the sediment sorting in delta M1. b) Examples of surface profiles of some experiments, which were used to determine the alluvial slope and the total volume of the delta. 218
- 8.6. The fining upward sorting in the deltas with the N sediment mixture. 219
- 8.7. Sorting in the deltas with the alternative sediment mixtures. 220
- 8.8. Plots of the sorting slope versus the variables celerity, delta height, geometric standard deviation and flow discharge above the delta top. 221
- 8.9. Conceptual model of the sediment deposition and sorting on the lee slope of the experimental deltas. The three stages of the process are given: 1,2: grain fall creating the sediment wedge and the toerset, 3: small grain flows with kinematic sorting, and 4,5: large grain flows that drag the top of the previous grain flow deposit downslope, leading to the fining upward. 222
- 8.10. Relation between dimensionless numbers and fining upward sorting. 224
- 8.11. Relation between dimensionless numbers and toerset deposition. 225
- 8.12. Comparison between field and experimental datasets from literature with the experiments presented here. 228
- 8.13. Examples of vertical sorting in experiments reported in literature, plotted in the same way as figures 6 and 7 for comparison. 229

- 9.1. Hypothesized channel bed deposits based on literature. During peak discharge the transported sediment is sorted in the grain flow at the lee side of a dune. In waning discharge, the dunes diminish and leave cross-bedding relicts. Due to selective deposition, an upward fining accumulation of lag deposits is created in addition. 235
- 9.2. Vertical sorting measured in the dunes in the flume experiments (Kleinhans 2000), expressed as the gravel fraction in the sediment ($D_{\text{gravel}} > 2\text{mm}$, rest is sand). 236
- 9.3. Conceptual model of sediment sorting with emphasis on the role of dunes in two subsequent discharge waves in order of decreasing magnitude (here only the gravel lag layers are shown, also see Figure 9.1). 238
- 9.4. Map of the measurement positions of direct sampling of the sediment transport and flow in the river Waal and of dunetracking in the Waal and Bovenrijn, as well as the vibro-core positions. The whole area was mapped with multibeam echosounders. 242
- 9.5. Measured sediment transport in the Waal during the discharge wave of 1998, given as total bedload divided by channel width. The measurements with the Helley Smith type bedload sampler (HSZ) have also been split in the gravel and sand bed load transport. 243
- 9.6. Observations of the deposits in the river Waal (a) en Bovenrijn (b). 246
- 9.7. The structure of the behavioural model for bedload transport and vertical sorting (a), a sketch of the principal parameters (b), and the different response of cross-bedded sorting in the model in rising and falling stage (c). 249
- 9.8. a) Discharge, water depth, flow velocity and grain shear stress, as well as the measured velocities, b) Dune height, as well as the measured dune heights, and c) Bedload transport of sand and gravel, as well as the measured transports (with Helley Smith). 254
- 9.9. Dune height (a) and sediment transport (b) as a function of discharge. 255
- 9.10. Model output: the final sorting of the river bed after the first two discharge waves (a, b). A gravel lag in the dune trough sinks into the bed as the dunes grow. In falling stage, a much thicker gravel lag is formed. In the second discharge wave the same happens, but at a smaller depth. 256
- 9.11. Statistics of dune scour depth of 417 dunes at positions varying from -100 m to +100 m from the river axis over a stretch of 0.5 km along the river Waal on 4 November (peak discharge). 257

- 10.1. Outline of the Tilting Bed Flume at St. Anthony Falls Laboratory (vertical scale exaggerated). 268
- 10.2. Time series of flow parameters (upper panel) and sediment transport (lower panel) of the Non experiments. (The average values of the same parameters of the Equ experiments are given in Table 10.1.) 270
- 10.3. Grain size distributions of the bed sediment (equal to the feed sediment) and the bedload sediment at the end of all experiments. 271
- 10.4. Photographs of the dunes in Equ2 and Equ3, which are comparable to those in Non4 and Non2 respectively. 273
- 10.5. Bed profiles at the end of all experiments. 274
- 10.6. Probability distributions of the bed surface, determined from time series of bed level taken at the end of the

- flume (11 m). 275
- 10.7. Sedimentary structures found in the experiments. 276
- 10.8. Correlation between the bed level variations in time (due to passing bedforms) and the deposition of gravel layers. 277
- 10.9. Vertical sorting in the bed, given as the gravel abundance ($D > 2\text{mm}$) of the samples against depth below the Non5 bed surface. 278
- 10.10. Grain size distributions of certain elements of the deposits. 279
- 10.11. Bedform stability diagram of Southard & Boguchwal (1990) from their Figures 10.3 and 10.8 for waterdepths of 0.1-0.4 m. 282
- 10.12. Probability distributions of the bed surface, determined from bed level profiles along the axis of the flume, from Blom & Kleinhans (1999) and from Blom et al. (2000). 283
- 10.13. Plot of the threshold for motion of uniform mixtures (critical shear stress as a function of grain size according to the Shields curve) and mixtures. 284
- 10.14. Conjecture of sediment sorting in the bed (key is the same as in Figure 10.7) in cases with equal mobility, and with lower mobility of the larger grains, and in cases with fast dune height adaptation to changing flow, and with slow or no adaptation. 285

Tables

- 3.1. Basic parameters of the field data set. 68
- 4.1. Experimental conditions (Blom & Kleinhans 1999, Kleinhans 2000). 90
- 4.2. Summary of the collected bedform, flow and sediment data in the river Allier. 94
- 4.3. Summary of the collected bedform, flow and sediment data in the river Waal. 97
- 4.4. Summary of flume and field data of flow, sediment and bedform types from literature. 98
- 5.1. Experimental conditions. 124
- 5.2. Summary of East Fork, Wyoming dataset with velocity group averages. 134
- 5.3. Summary of Sagehen Creek, California, dataset with bed shear stress group averages. 135
- 6.1. Calibration factors of the original (HS) and adapted (HSZ) Helley Smith. 148
- 6.2. Bedload transport hindcast parameters and results for the river Waal with and without the effect of fining of the active layer in falling stages (after Kleinhans 2001a). 169
- 7.1. Literature on vertical sorting data in grain falls and grain flows. 182
- 8.1. Description of the sediment mixtures fed into the flume. 214
- 8.2. Basic data of the experiments. 217
- 8.3. Description of the datasets used in the comparison between the experiments presented here, experiments in literature and three field datasets. 227
- 9.1 Basic data of the flume experiments presented by Kleinhans and Van Rijn (2002, see chapter 5) and Blom and Kleinhans (1999). 237
- 9.2. Basic data of the field measurements. 240
- 9.3. Predicted and observed depths (in $m \pm 0.1m$) below the low-stage bed level of gravel layers in the Rhine branches for two subsequent discharge waves. 245
- 9.4. Input and output parameters of the model for sediment transport and deposition. 248
- 10.1. Experimental conditions and results. The shear stress has been corrected for side-wall roughness with the method of Vanoni-Brooks. 269

Acknowledgments - Voorwoord

In the winters of 1994 and 1995, two extremely high discharge waves raged through the rivers Rhine and Meuse and threatened the artificial levees that protect urban and agricultural areas. The photograph on the cover of this book shows the flooding of the embanked floodplain of the river IJssel near Zwolle (The Netherlands). It was taken in the winter of 1995 by my father, a couple of hundreds of meters from where I grew up. The damage caused by the river was limited, but some of the feeling of safety had been flushed to the ocean; there was need for more knowledge and better safety measures. That was the soil in which this PhD-study rooted.

Blood, sweat, many sandwiches but only a few tears were the manure for this study. I hope that you will read the chapters with as much pleasure as I had in the past five years during the making. Please contact me if you want to obtain and use some of the datasets reported herein.

Als een promovendus (m/v) in één adem moet noemen aan wie hij allemaal wat te danken heeft voor zijn proefschrift, raakt hij onherroepelijk buiten adem, dus daar zal ik de nodige alinea's aan besteden. In the following duizeligmakend mixture of English en Nederlands, I would like to thank everyone who contributed and apologize beforehand lest I forgot someone.

First of all I thank my supervisors Leo van Rijn (“for those who like scatter”) and Ward Koster (“al is het je reinste onzin, als er maar niemand doorheen kan prikken is het goed”), who together guided me through the PhD process and stimulated me in their own way to form a suspension bridge between quantitative process research (sand grains and equations) and the qualitative synthesis of ‘armwaving’ geomorphology.

Second, my advisor Janrik van den Berg for his continuous support concerning sedimentology and the link between my clouds of datapoints and hypothetical relations (“dit is een tamelijk hopeloze zaak”). Je stond altijd voor mij klaar, zelfs als je het zelf erg druk had (“Je moet nou maar eens ophouden met schrijven want zo kom ik niet aan mijn eigen werk toe.”). Bedankt voor al je humor, hulp, steun en vertrouwen!

Third, Wilfried ten Brinke (Rijkswaterstaat-RIZA) (“neem de lezer bij de hand”), for all support and opportunities, like measuring morphological triangles on the river bed, working with the greatest field dataset in the world, and getting experience with the complex field measurement campaigns during high discharge waves in the river Rhine. In addition, you wear the first who taught me how to compose a scientific article.

Fourth, Gerrit Klaassen (IHE, WL|Delft Hydraulics) for many useful comments and discussions. Most importantly, you showed me two crucial ways to look at sediment sorting: in non-equilibrium conditions and in laboratory deltas.

Fifth, Gary Parker (St. Anthony Falls Laboratory, University of Minnesota, USA) (“In the Netherlands, the pore space in the sediment is already included in morphological computations. So the Dutch sell you both the donut and the air in the hole of the donut!”), for coming to the Netherlands to talk with me, for your invitation to SAFL while you knew I would maverick my way through the lab and camp overnight in your flumes, for your help with modelling and flume experiments and for the most inspiring classes I have ever had.

Those who worked (with me) during the 1997 and 1998 campaigns on the river Rhine: all the fieldworkers of the Meetdienst Oost Nederland, in specific Geert Otten, die mij hielp om de in de weg lopende tv-ploeg mores te leren tijdens hun opnamen aan boord van ons meetschip op de Waal (“één patat-friet!”) en zo het moreel tijdens de metingen in ijskoud en nat weer torenhoog

hielp houden, Jan Havekes, die ons en de meetapparatuur desondanks in toom wist te houden, en de scheepskapitein Koos de Boer (kapitein Smit Waalhaven) die ons net op tijd voor een aanstormend zes-baks duwvaartschip vandaan loodste, Leo van Hall en Dick Kos voor heel veel organisatie, en Anton van Oosten en Jan van 't Westende (samen Anja genoemd) die helemaal vanuit Middelburg kwamen om de AZTM-metingen te redden, wat overigens is gelukt.

For the flume experiments at WL|Delft Hydraulics I thank Astrid Blom, Klaus Basso, Nico Struiksmā, Erik Mosselman, Joop Ouderling, Freek de Groot and all European partners for the fantastic cooperation concerning 50 cubic meters of rather dirty Waal sediment (including car parts, boots, coal and underwear), experimental programs, the choking sediment recirculation system and the cooking competition with spaghetti-flambé for lunch and pancakes for dinner.

There is definitely a personal issue between me and sediment feeders, as I found out again in Minneapolis. They always fall apart when you need them the most. (Well, those machines really can't help it; imagine yourself chewing and spitting out gravel all the time...) I thank Scott, Mike and many others for repairing many, many sediment feeders and much more, Jeff Marr for helping me on the way and beyond, and Nikki (thanks for helping me with those scary things called differential equations), Jason, Michal, Rashmi, Jake, Horatio, Miguel, Alicia, Matt (good luck y'all with your theses!) and many more Minneapolitans for their help and friendship.

There is a host of colleagues and technicians I also want to thank. In order of appearance:

For the flume experiments and field measurements in the river Allier of my students and me: the magico-technicians of the Physical Geography department Bas van Dam, Hassan Arab, Henk Markies, Jaap van Barneveld, Kees Klāwer, Marcel van Maarseveen, and Theo Thiemissen, and the flume techno-wizard of the Earth Science department, Paul Anten.

For most of the graphs in chapter 4 and for processing all the photographs in this thesis I thank Magriet Ganzeveld, Rien Rabbers, Ton Markus and Margot Stoete of the Kartlab. For their help with a computer program which did not want to eat my dune profiles, I thank Kor de Jong and Cees Wesseling.

The room-mates, colleagues and friends for cooperation, help, conversations, discussions, comments on my work and happy tea-hours. Specifically: Johan Kabout, Marco Duiker, Kim Cohen ("At the end of every sentence I come to the point."), Annika Hesselink, die me af en toe tot de orde riep en met wie ik mee mocht denken over dat fantastische snelheidsmeetinstrument uit 1790, Esther Stouthamer, Irene Ruessink-van Enckevort, Antoine Wilbers, die een carrière als operazanger liet schieten om bij te dragen aan hoofdstuk 6 en mij regelmatig te verrassen met de waarheid omtrent duinverplaatsing, Bart Grasmeijer, die een webcam met weblink op Leo van Rijn's bureau richtte zodat ik hem de laatste maanden binnen 20 seconden na aankomst kon spreken in plaats van na de gebruikelijke 3 minuten, en natuurlijk Henk Berendsen ("Wacht maar tot Kleinhans afscheid neemt, dan gaat het niet over de structuur van de wereld maar over die van het heeal!") voor de liters thee en zijn stimulerende kijk op de mogelijke dwarsverbanden tussen het procesonderzoek en het kwartaargeologisch onderzoek ("Kansloos!").

Ik bedank de paranimfen Michal Kleinhans en Marcel Vonk voor hun steun bij de laatste loodjes, my father, Reinout, Jan, Marijke en Leonard for their lasting support, and Hester for discussing the first and last chapters of this thesis, and for much more which you already know.

Maarten Kleinhans

Utrecht, May 2002

1

General introduction

1.1 Rationale

1.1.1 Between sand-bed rivers and gravel-bed rivers

The behaviour of sand-bed rivers and of gravel-bed rivers is well understood compared to the behaviour of rivers with mixtures of sand and gravel (sand-gravel bed rivers). Sediment can be divided into sand (<2mm) and gravel (>2mm). Sand-bed rivers generally show the presence of subaqueous dunes as the dominant bedform type. The behaviour of the dunes is dependent on the bed sediment characteristics. In rivers with fine sand beds, the dunes emerge sooner and grow higher than in rivers with coarse sand beds. In gravel-bed rivers, dunes may never occur, but other bedform types (e.g. bars) may. More important, the river bed may be armoured by a coarse gravel layer, which prevents the entrainment of sediment during moderate discharges.

Between these two extremes, there are river reaches with both sand and gravel in the bed along a considerable length in between the upstream gravel-bed river and downstream sand-bed river. Large sections of the rivers Meuse (The Netherlands), Rhone, Allier (France), Fraser (Canada), Elbe (Germany), Mississippi (United States of America) and the Nile (Egypt) for example, have both sand and gravel in the bed. In the Dutch Rhine, significant amounts of gravel (circa 60-20%) are present in the bed over distances as far downstream as 60 kilometers in the Waal and 25 kilometers in the IJssel from the border between Germany and the Netherlands. These are all large river systems, in which dunes may occur simultaneously with sorting effects (e.g. armour layers). The interaction between these phenomena is not well understood. It is therefore important to gain more understanding of the fundamental processes in sand-gravel bed rivers.

1.1.2 Emergent characteristics of sand-gravel bed rivers

A mixture of sand and gravel may exhibit sorting phenomena that occur only in poorly sorted sediment. This is illustrated with two 'grocery store examples' (see fig. 1.1), which serve to illustrate that the knowledge of sand-bed and gravel-bed rivers cannot be straightforwardly applied to sand-gravel bed rivers.

Consider a (subaerial) pile of potatoes and lemons, over which a large bag of (dry) salt is poured out (see fig. 1.1). The salt will percolate downwards through the pores between the potatoes and lemons. This vertical sorting is only possible due to the large difference in 'grain size' between the two size classes but no grains of intermediate sizes. Sediments of this type are called bimodal, as opposed to unimodal sediment in which the intermediate grain sizes are abundantly present. Thus, in rivers with bimodal sediment, the percolation phenomenon may emerge and cause significant sorting.

Sorting may also occur with less large grain size differences. Consider a bowl of mixed nuts, which is being shaken (see fig. 1.1). The larger nuts will appear at the surface, while the smaller peanuts collect at the bottom of the bowl. Due to the shaking, the pore space between the nuts is

increased. The peanuts may move downwards through this pore space. As a result, the large nuts are pushed upwards, even though their mass is larger. Due to this kinematic sorting mechanism, rivers with coarse sand and fine gravel may exhibit significant sorting as well, both in a plane bed and in the bedforms.

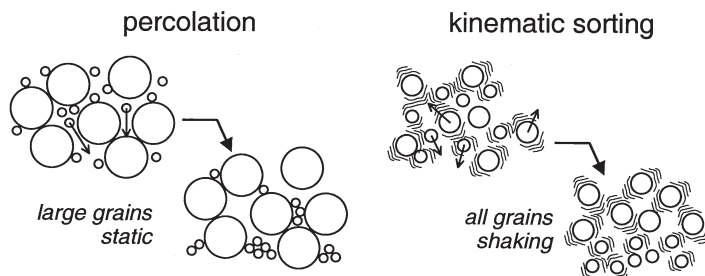


Figure 1.1. Two 'grocery store examples' of phenomena that emerge only in rivers with both sand and gravel in the sediment. In the first, the small grains (salt) percolates through the pore space of the large grains (potatoes and lemons). In the second, the size difference between the two grain species (large nuts and peanuts) is smaller, but the shaking enables the peanuts to move downwards, on average pushing upwards the large nuts.

1.1.3 Relevance

Understanding of the behaviour of dunes and of sediment transport is essential, because they are intimately related to local water levels of the rivers. The extremely high discharges in the rivers Rhine and Meuse (the Netherlands) during the winters of 1993-1994 and 1995 almost caused dike bursts and inundation of inhabited and economically important areas. Although rainfall and snowmelt in the river catchment area are the primary sources for the water discharge, the local water levels are also determined by the state of the river bed. At rising discharge, subaqueous dunes emerge on the bed of the river Rhine in the eastern Netherlands. These dunes have a height in the order of 0.5-1.5 m and length of 20-100 m, and have a much higher resistance to the flow than a plane river bed. Due to this additional resistance, the water level rises. How much it rises, is well known for lower river discharges that occur frequently. For extreme discharges on the other hand, the prediction of the exact water level rise is very uncertain, because the dune behaviour and development is, especially in sand-gravel sediment, not well understood.

On a decennium time scale, river bed degradation or aggradation is determined by changes in the sediment balance of the river, which depends on the gradients in sediment transport along the river and on human activities like sand mining in the river bed. Aggradation and degradation affect both the flood water levels and the water depth available for shipping. Shipping is intense on the river Rhine and of large economic importance for the Netherlands, Germany, France and Switzerland. Sediment transport of sand-gravel mixtures is, however, not well understood.

In the coming decennia, the flooding risks in the Rhine catchment may increase due to climate change. Climate-change based catchment models suggest that both very low and very high discharges will occur more frequently. In order to assess the impact on (1) water levels, the related flooding risks and (2) the navigation constraints, again the fundamental processes of sediment transport and dune behaviour must be understood for a large range of temporal and spatial scales, including the range beyond the most frequently occurring and observed conditions.

1.2 General objective

The process through which all natural morphological changes of the alluvial river bed take place, is (gradients in) sediment transport. The general approach to study river behaviour on short time scales, is to consider the river as a morphodynamic system (see figure 1.2). Morphological change is caused by gradients in the sediment transport (more sediment coming into a reach than going out results in aggradation, and vice versa for degradation). The morphological change will in turn affect the water flow.

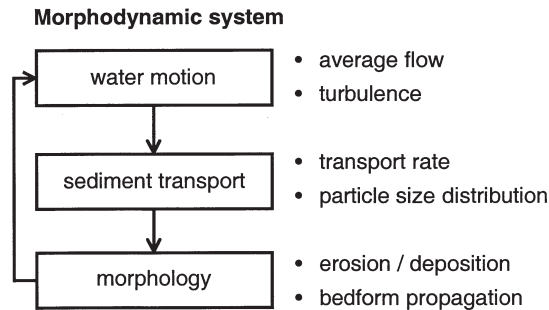


Figure 1.2. A representation of a morphodynamic system for alluvial rivers.

This study focusses on sediment transport processes. Sediment transport is the sliding, rolling, saltating and suspended motion of bed material due to the shear of the water flow over the river bed. The sliding, rolling and saltating motion is called bedload transport, and the other suspended load transport. The wash load, which consists of silt and clay, is not considered herein, because these play no role in the river bed dynamics of sand-gravel bed channels. They do play a role in floodplain building, which is not considered in this study.

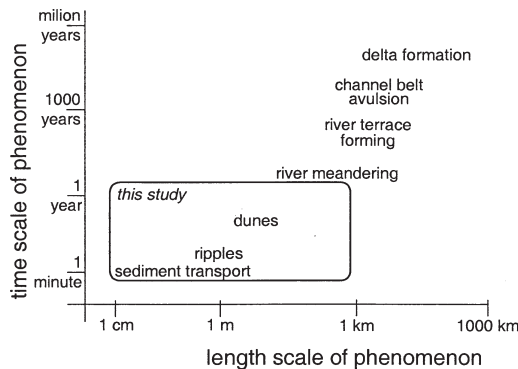


Figure 1.3. Time-space diagram of alluvial processes and phenomena. The extent of scales covered in this study is denoted with the box.

The sediment transport by the turbulent river flow takes place on a time scale of seconds and a length scale of meters at most (see figure 1.3), while the development of bend flow and river meanders is expressed on much longer scales. Phenomena occurring at different scales must obviously interact. On the 'river behaviour during one discharge wave' - scale, the smaller scale

turbulence might be considered a source of stochastic variation for that larger scale, while the river meandering and long term bed level change on the other hand, may be considered as an external forcing on the smaller scale.

However, it may be that a small-scale phenomenon also affects phenomena at larger scales, in which case the smaller-scale phenomenon can no longer be considered stochastic variation for the larger scale. This would lead to complex behaviour that cannot be understood at the scale of interest only. An example is sediment transport over dunes. Irregularities at the scale of grain movement grow out to larger scale phenomena like dunes, which then in turn affect the grain movement rate and spatial pattern of grain movement and grain size sorting. *The interaction of the process of sediment transport on the scale of grains and dunes is the central theme of this study.* The study is limited to the length scales of grains and bedforms, with those of turbulence and river meanders as boundary conditions, and the dune formation process is not addressed.

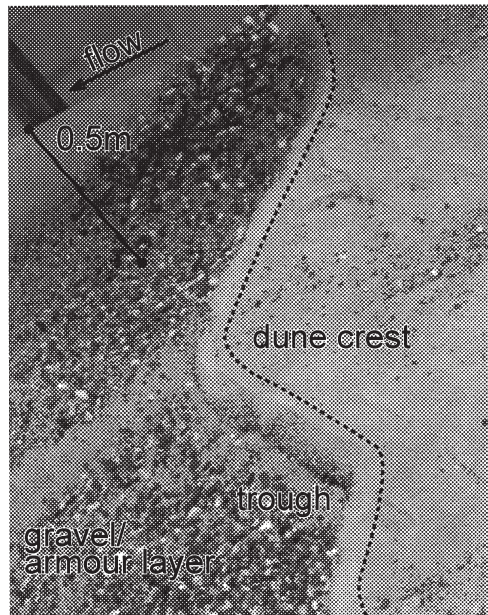


Figure 1.4. Oblique photograph of the bed in one of the flume experiments presented in chapter 4. A bedform is present which consists mainly of sand. In the trough zone and below the bedform, an armour layer is present.

In the past century, research by engineers and geophysicists on sediment transport primarily focussed on the scale of grains. Dunes were considered to have an effect on the flow only. At the same time, sedimentologists were attracted by deposits of dunes and other bedforms as the building units of alluvial sand (and gravel) bodies. However, it may be that the sediment mixture in these deposits is sorted. Sediment transport and dunes are then obviously related, because the deposits of dunes due to one discharge wave (waning phase) are re-entrained during the next discharge wave. Recently, physicists became interested in the complex behaviour of sediments with a range of grain sizes, and explored this behaviour from a physical point of view (mainly ignoring the work done by Allen and Bagnold and many others in the preceding decades). The three fields of knowledge are somewhat separated by a disciplinary gap: the sedimentologists concentrated on the, often qualitative, study of deposits and depositional processes, while

engineers and process-geomorphologists mainly studied the sediment transport process, and physicists studied sediment mixture behaviour in conditions that are hardly relevant for natural sedimentary systems. Driven by the practical necessity of managing rivers and flood mitigation, interaction between the fields has recently started. This Ph.D. thesis is a result of an attempt to bring the three further together.

Most rivers described in literature are either sand-bed or gravel-bed rivers, while rivers with a mixture of sand and gravel have received less attention. Yet, sand-gravel bed rivers deserve attention, as aspects of their behaviour cannot be understood from the knowledge of sand or gravel-bed rivers. In rivers with mixtures of sand and gravel, both the emergence of dunes as well as armouring is evident (see figure 1.4). Furthermore, a number of special effects occur, like vertical sorting of the sediment in the dunes, and the hiding of small grains in the lee of large grains, which in turn are more exposed to the flow. The impact of these effects on the river bed morphology and sediment transport depends in a rather subtle way on mixture characteristics such as the bimodality (bimodal sediment consists for instance of coarse gravel and fine sand, but not the fine gravel and coarse sand) and the gravel / sand ratio. Thus the response of a sand-gravel bed river to a discharge wave is not simply more sediment transport and larger dunes, but is the result of a complex interaction between the dune behaviour and the grain-size selective sediment transport. The morphological response may obviously be different from that in a river with only gravel or well sorted sand.

In the recent past, a number of morphodynamic models have been developed for the calculation of sediment mixture transport and the resulting morphological changes. However, it has not yet been possible to hindcast the relevant aspects of the behaviour of rivers with sand-gravel sediment during floods, because not all relevant processes are included in these model concepts and not all relevant processes are well understood.

Summarizing, the general aim of this thesis is to gain better understanding of the sediment transport and depositional processes of sand-gravel mixtures in the presence of dunes.

1.3 Organisation of the thesis

"Me and organised??" Paul Dekkers

The thesis is divided in two parts; **part 1** concentrates on the sediment transport process, and **part 2** concentrates on the sediment sorting in the depositional processes.

Chapter 2 summarises the literature which is relevant to the aim of this thesis, states the specific objectives and gives hypotheses with the insights distilled from the review. Most of the reviewed literature refers to the sediment transport process, and some to the sediment sorting processes in general.

The research reported in this thesis is essentially empirical, as it is based on flume experiments and field measurements. Field measurements of sediment transport, however, have notoriously large errors. The first step (in **chapter 3**) is therefore to determine an optimal strategy for *in situ* measurements of sediment transport in relation to the natural variability of sediment transport, and to find a decision tool for setting up a sampling program in a river based on a pre-defined level of accuracy (say, a stochastic error of 20%). This chapter is based on field measurements done in 1997 in the upstream stretch of Dutch Rhine branches, and investigates the spatial and temporal patterns of bedload transport in a large sand-gravel bed river with fixed banks and low sinuosity.

Chapter 4 is an inventory of observed bedform types in both literature and the experiments and measurements given herein. The occurrence and the stability of these bedform types are compared to those of bedforms in uniform sediment. The emphasis is on conditions with low or zero mobility of the coarse sediment in the river bed, which can be considered as one of the two limits of this Ph.D. study (the other limit is well-sorted sediment for which mobility differences between grains of different diameters are obviously irrelevant). The first (of three) set of experiments, which were done in the Sand Flume of WL|Delft Hydraulics, is introduced.

Chapter 5 attempts to adapt existing bedload sediment transport predictors for the case of sediment mixtures and flow conditions with incipient or full mobility of the coarsest sediment, including the effect of near-bed turbulence. The Sand Flume experiments and two existing datasets of sediment transport in natural rivers are used for the validation of the transport predictor.

Testing the relevance of the concepts developed so far, is done with field measurements in **chapter 6**. Using the measurement strategy developed in chapter 3, measurements during a large discharge wave in the Waal were done in 1998. In addition, the calibration of the instrument (i.e. systematic errors) is discussed and verified. The sediment transport in 1998 appeared to show a number of unexpected trends which could be related to sediment sorting and behaviour of dunes. A full hindcast of the sediment transport with the predictor constructed in chapter 5 is, therefore, found to give unrealistic results.

The study of dune behaviour, the effects on the flow (hydraulic resistance) and indirect effects on sediment transport is under way by Antoine Wilbers in his PhD project, while the sediment sorting and its effects on sediment transport is addressed in **part 2** of this thesis.

In **chapter 7**, data and concepts related to the sediment sorting process in grain flows at the lee-side of dunes are reviewed. This reveals that those sorting processes are not well understood at all and have not yet systematically been studied in experiments or in the field. The available data is synthesised to excerpt the most important phenomena and variables for the benefit of experiment design.

The second set of experiments (**chapter 8**) provides a systematic dataset and observations of the sediment sorting processes at the lee side of dunes. This set of experiments was done in a small flume at St. Anthony Falls Hydraulics Laboratory with several sediment mixtures and systematic variation in the flow conditions, the design of which was based on the findings in chapter 7. The applicability of this dataset to natural dunes is evaluated by comparison of the variables that are the most important for sorting in the experiments, and in three field datasets.

The next step (in **chapter 9**) is to determine how sediment is sorted by bedforms in the channel bed in the course of several discharge events, and how this sorting affects the sediment transport process. The result is a behavioural model of vertical sorting by dunes, of which the results compare favourably with the data of the river Rhine (chapter 6).

A controlled set of experiments was done in the Tilting Bed Flume at St. Anthony Falls Hydraulics Laboratory (**chapter 10**) to study the sediment sorting by irregular dunes in non-equilibrium conditions. A sand-gravel mixture was subjected to two discharge peaks in order of decreasing magnitude, with periods of low flow before, in between and after the events. The observations of sorting in the bed sediment corroborate that the sorting in the deposits is largely determined by dune behaviour.

The results of the whole project are synthesized (**chapter 11**). The role and importance of the interaction between the transport on the grain scale and the bedforms is discussed for a range of conditions. Furthermore, it is discussed which processes and interactions should be included in future models for realistic modelling of the river. Finally, a number of serious hiatuses in the present understanding of the sediment transport and deposition processes are outlined.

2

Review, problem definition, objectives and hypotheses

“... the success of current scientific theories is no miracle. It is not even surprising to the scientific (Darwinistic) mind. For any scientific theory is born into a life of fierce competition, a jungle red in tooth and claw. Only the successful theories survive - the ones which in fact latched on to actual regularities in nature.” Bas van Fraassen (1980: p. 40, *The scientific Image*, Clarendon Paperbacks, Oxford)

2.1 Introduction

2.1.1 Objective

The objective of this review is to discuss the controls on sediment transport in a large range of river flow and sediment characteristics with special emphasis on sorting processes in sand-gravel mixtures. First some general characteristics of sand-bed and gravel-bed rivers are given. Points of discussion are what the characteristics of sand-gravel bed rivers may be, and to what extent the characteristics of both sand and gravel-bed rivers may occur in sand-gravel bed rivers. In addition, typical phenomena for sand-gravel bed rivers are indicated. Next a short review is given of the present engineering approaches to the prediction of sediment transport of uniform sediment. Then, the controls of sediment sorting on sediment transport are discussed for three length scales: the grain scale, the bedform scale, and the meander scale. On the grain scale, the effect of sorting is mainly on the incipient motion. This is discussed for unimodal and bimodal mixtures. Furthermore the role of near-bed flow turbulence is elaborated. On the bedform scale, sorting mainly determines the availability of different grain sizes for bedload transport. Both horizontal and vertical sorting are discussed, as well as the interaction between flow turbulence, bedforms and the sorting in bedforms. Sorting on the meander scale is discussed to determine whether this acts as a large-scale boundary condition on the sediment transport, or must be considered in the same detail as bedforms. Finally, the shortcomings of present approaches to non-uniform sediment transport prediction are identified in the light of sorting on different length scales.

2.1.2 Sand-bed rivers and gravel-bed rivers

When a river is followed in its course from the mountains to the sea, the bed sediment of rivers generally appears to fine downstream. Although many small rivers are either sand-bed or gravel-bed rivers depending on the characteristics of the sediment delivered from their catchments, many large rivers show a downstream fining trend in their sediment and therefore have stretches with bed sediment composed of a mixture of sand and gravel in varying proportions. In addition, sediment input from tributaries may lead to wide mixtures.

In the past, the processes in sand-bed rivers and gravel-bed rivers have been studied extensively. Bedform stability and height predictors are available, as well as sediment transport predictors (cf.

Van Rijn 1993). Typical characteristics of many sand-bed rivers are summarized below, with emphasis on the lower river Rhine (lower Waal and Merwede) in the Netherlands:

- low energy gradient, significant low discharges and high magnitude floods for periods in the order of weeks,
- meandering planform, with pools in the outer bend and pointbars in the inner bend, and riffles in between the bends, and rather stable banks (although there exist some sand-bed rivers that are braided),
- rather well sorted bed sediment, and silt and clay in the bank and overbank deposits,
- ripples at low discharges, and dunes at higher discharges, and in some conditions secondary dunes superimposed on primary dunes,
- significant sediment transport, even at low discharges, as the critical threshold for initial motion of sand is very low compared to the occurring flow conditions.

Gravel bed rivers have been studied as well (cf. Mosley 2001), although the emphasis has been on small rivers rather than on large ones. This is because large gravel-bed rivers are rare, and because the technical difficulties of field measurements in large gravel-bed rivers are large. Consequently, not many predictors are available for the armour layer composition, sediment transport, bedform and bar stability and planform (cf. Mosley 2001). Yet a number of predictors are available, and much is qualitatively known of gravel-bed rivers. Typical characteristics of gravel-bed rivers are:

- high energy gradient, very low discharges and flashfloods for periods in the order of hours or days,
- step-pool or braided planform, with braid bars and unstable banks (although there exist meandering gravel bed rivers as well),
- poorly sorted sediment and a range of grain sizes represented in the bed,
- when the gravel is mobile, the finer sediment is already fully in suspension,
- coarse gravel surface layer ('armour layer') during low discharge, which breaks up at a high discharge above the critical entrainment threshold of the armour layer,
- almost no sediment transport below the critical entrainment threshold of the armour layer, and large transports only in high-magnitude floods,
- sediment transport is partly a function of the armour layer development in previous floods.

The mobility of the sediment is thus one of the most important parameters to explain differences between sand-bed and gravel-bed streams. The dimensionless Shields parameter (dimensionless shear stress) gives the balance between sediment entrainment and settling forces and thus indicates the sediment mobility. Figure 2.1 gives the mobilities of a dataset of sand-bed and gravel-bed rivers, and of the experiments and data provided in this thesis. The point of this figure is not that it is exhaustive with data representing all types of rivers in the world, but that there seems to be a natural divide between sand-bed streams and gravel-bed streams. A similar divide between a population of sand-bed rivers and gravel-bed rivers is apparent in a dataset of rivers used for a river pattern analysis by Van den Berg (1995).

There are many possible reasons for this (see Parker in prep. for discussion). One reason is that some catchments have such rock characteristics that they mainly deliver cobbles and gravel, while other rock types yield mainly sand. Another reason is that the river sorts and abrades its sediment along its course, mostly with a downstream fining trend as a result. The gravel grains suddenly fall apart into sand grains leading to a sudden transition from gravel-bed to sand-bed rivers. Yet, many rivers and river reaches can be found (for example in Japan (Parker in prep.)) which have sand and gravel in comparable amounts in the bed. As examples, the sand-gravel reaches of the

rivers Allier (France) (Van den Berg et al. 2000), Meuse (The Netherlands) (Duizendstra 1999) and Rhine near Pannerdensche Kop (The Netherlands) (Ten Brinke 1997) are plotted in figure 2.1, and indeed they plot in between the two populations.

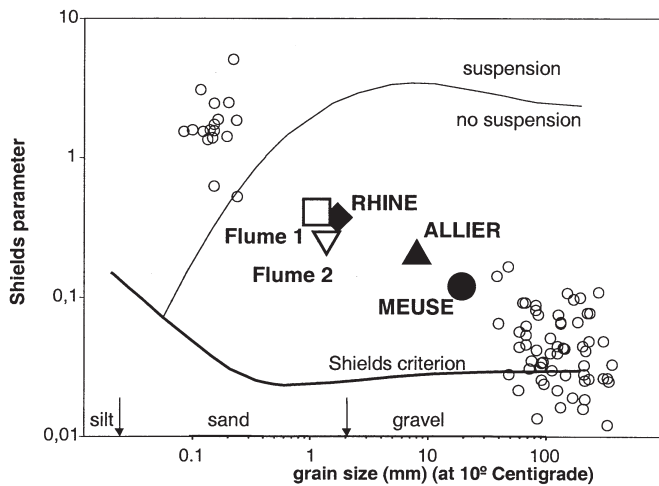


Figure 2.1. Mobility of sediment in sand-bed rivers and gravel-bed rivers (after Parker in prep.). The Shields parameter is a dimensionless shear stress, in this case for bankful discharge. The grain size is the median size. The data are from small gravel-bed rivers in Wales (UK), Alberta (Canada) and Idaho (USA), and sand-bed streams extracted by Wright & Parker (in prep.) from Church & Rood (1983). The criteria of Shields and Bagnold indicate the transitions from immobile bed to bedload transport and from bedload to suspended load, respectively. In addition, points representing the rivers Allier (near Moulins, France, see chapter 4), Rhine (near Pannerdensche Kop, The Netherlands, see chapter 6) and Meuse (Grensmaas near Maaseik, The Netherlands) are given, as these rivers play a role in this thesis. Also the laboratory flume conditions (peak discharge) of two of the experimental programmes reported in this thesis are given (Flume 1 is Sandflume in the Netherlands, see chapter 4 and 5, Flume 2 is Tilting bed flume in Minneapolis, USA, see chapter 10).

Rivers with both sand and gravel in the bed may be expected to exhibit characteristics that are related to both sand and gravel-bed rivers. These characteristics could for example be:

- intermediate positions between long discharge peaks (of many meandering sand-bed rivers) and flash floods (of many braided gravel-bed rivers), if the sand-gravel bed river is the transition stretch between its upstream gravel-bed and downstream sand-bed river,
- low but significant transport during low flow, even though an armour layer may exist,
- sandy, isolated bedforms migrating over an armour layer in low discharge, and sand-gravel or gravel dunes in higher discharges.

The question is to what extent a sand-gravel bed river is comparable to either a sand or gravel-bed river. This will depend on the fractions of sand and gravel in the bed. For instance, a certain minimum amount of gravel may be necessary for the formation of an armour layer, and a certain minimum amount of sand may be necessary for the formation of dunes. In addition, the flow regime of the river determines the mobility of the gravel. In a gravel-bed river with some sand and low flow energy, the bed may be heavily armoured, while in a gravel-bed river with the same sediment but much higher flow energy, the armour layer may only be marginally developed (e.g. Reid & Laronne 1995). Thus the behaviour of a sand-gravel bed river depends on the sediment mixture and on the flow regime.

In addition, there may be emergent characteristics of sand-gravel bed rivers that do not occur dominantly in sand-bed or gravel-bed rivers. One example is kinematic sorting (e.g. Sallenger 1979, see **chapter 7**). When a sediment mixture is in motion due to stirring, flow shear, or gravity-driven sediment flow, the sediment expands and the pore space increases because of the extra space taken by the individual and colliding grains. The fine sediment is able to move into the pores between the large grains under the influence of gravity, meanwhile working up the coarse sediment because that cannot move into the pores. This promotes a coarsening upward sorting. A related phenomenon is percolation, which occurs when gravel grains rest on each other and have empty pore spaces (clast-supported sediment), so the fine sediment may fall through the pores even if the gravel is immobile. When there is more sand and pea-gravel in the mixture and the gravel grains do not rest on each other (matrix-supported sediment), then dilation is necessary for sorting. Ikeda & Iseya (1988) found that the transition between clast-supported to matrix-supported sediment is sudden for bimodal sediment and causes a sudden change in water surface slope, mobility of the sediment and sediment transport.

It is emphasised that sand-bed, gravel-bed and sand-gravel bed rivers are not separate classes but gradual transitions. For the given examples of sand-gravel bed rivers Rhine, Allier and Meuse, this behaviour differs widely. The armour layer in the Meuse is well developed and bedforms occur only during extreme discharges. In the river Rhine on the other hand, an armour layer is probably present but not very important, while significant dunes occur at moderate discharges. The Allier is somewhere in between the Rhine and Meuse.

2.1.3 Scope of this study

For simplicity, the range of possible flow conditions and sediment characteristics is split into three factors:

1. the sand and gravel abundance in the bed sediment, that is, whether the river is a sand-bed, a gravel-bed or a sand-gravel bed river,
2. the mobility of the sediment, that is, the discharge regime of the river, and
3. the bimodality of the sediment.

In figure 2.2, a range of sediment conditions is considered from pure sand-bed rivers to pure gravel-bed rivers, with sand-gravel bed rivers in between (x-axis in fig. 2.2). The latter class of rivers is the object of study herein. The understanding of sediment transport of uniform sediment cannot simply be extrapolated to sediment mixtures. The sediment grains of different sizes interact in a number of ways that cannot be represented by using uniform sediment methods, because the relative sizes of the grains determine the interaction. Furthermore, while bedforms may already have significant effects on sediment transport in uniform sediment, the effects for sediment mixtures are even larger, because the sediment is sorted in various ways. These effects will be discussed below.

In addition, the flow conditions in the river also determine which part of the sediment is in transport (y-axis in fig. 2.2). In small rivers with a 50/50% sand-gravel mixture, the largest grains may not be in motion, while the sand is in motion as migrating sandy bedforms over an immobile gravel lag. In large rivers with a similar bed, the whole mixture may be in motion as sand-gravel dunes, but then the sorting of sediment within those bedforms may be a complicating factor.

A third feature of sediment mixtures must be considered. A 50/50% sand-gravel mixture may either be unimodal or bimodal or anything in between, and in very special (laboratory) conditions even trimodal. Rivers with unimodal and bimodal sand-gravel sediments both occur in nature. Usually, the sand is the first mode and the gravel is the second mode, with a relatively low

abundance of grains with a diameter of about 2 mm. It seems from literature that the bimodality has severe effects on the sediment transport and the occurrence of bedforms (see chapter 5). This is then the third range of conditions which must be studied for the understanding of sediment transport (z-axis in fig. 2.2) This study is mainly concerned with slightly bimodal sediment. This is rather arbitrarily defined as mixtures of which the grain size distribution shows two modes that are just discernable.

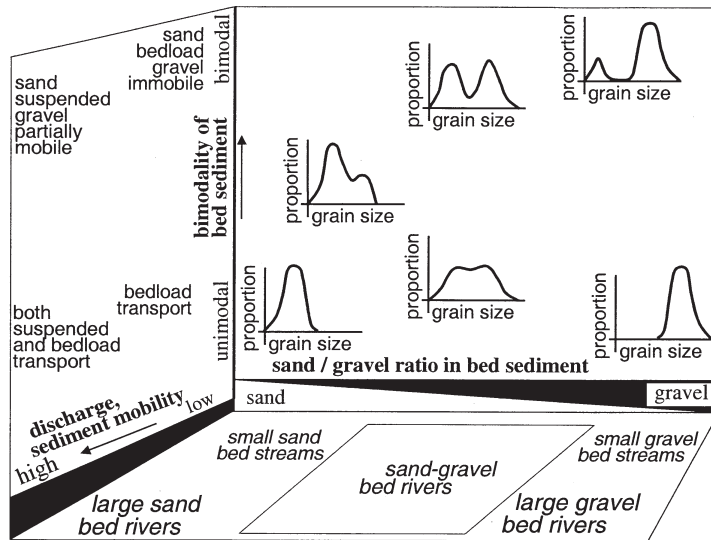


Figure 2.2. Three ranges of flow and sediment conditions and their relations. The first (x-axis) is the relative proportion of sand (< 2 mm) and gravel (> 2 mm) in the bed. The second (y-axis) is the sediment mobility, which can also be expressed as flow discharge or shear stress. The third (z-axis) is the bimodality of the sediment. The first and third are necessary to describe the sediment. The relation between the first and second determines the difference between large and small rivers and sand, sand-gravel and gravel-bed rivers. The relation between the second and the third determines the mobility of the sand and gravel, and the relative importance of partial (bedload) mobility, bedload and suspended load transport.

The definition of bimodality of sediment is difficult. Three aspects are important in a description: the relative proportions of the two modes (usually sand and gravel), the standard deviation of each mode, and the diameter difference between the two modes. To circumvent the necessity of clearly defined describing parameters, the full grain size distributions are given where possible.

Thus, the objective of this review is to discuss the controls on sediment transport in the ranges of low mobility to high mobility, of sandy gravel to gravelly sand, and of unimodal to bimodal sediment. First the basic knowledge of sediment transport processes of uniform sediment is summarized. Next the processes in non-uniform sediment are reviewed and discussed. The sorting of sediment transport involves three length scales which are referred to in this discussion: the grain scale, the bedform scale and the meander bend scale. Obviously these scales are not strictly separated, but the grain scale entails interactions between grains only, while the bedform scale

entails sorting phenomena, e.g. grain flows, that occur only in bedforms but not on smaller scales, and the meander scale refers to large scale flow patterns that do not occur on smaller scales. For clarity, these scales are discussed separately.

2.2 Sediment transport processes of uniform sediment

2.2.1 Basic knowledge

Sediment transport is driven by the bed shear stress, defined as $\tau = \rho g h \sin(i)$, approximated as $\tau = \rho g h i$ for energy slopes below 0.01 (m/m), in which g is the gravitational acceleration (9.81 m/s²), h is the water depth and i is the energy slope. Furthermore, sediment transport depends on grain size, since large grains are less easily transported.

The opposing force is the resistance of the sediment against movement, which depends mostly on grain size, form, density and the local bed slope. A grain can only be moved if the bed shear stress exceeds a certain threshold. This Shields threshold is incorporated in many sediment transport predictors and is usually defined by the Shields curve (1936, in Van Rijn 1993). From the Shields curve it follows that the critical bed shear stress depends strongly on the median diameter of the sediment. In reality, this threshold does not define the absolute beginning of sediment motion. Unfrequent motion occurs far below the Shields criterion, and is related to the near-bed flow turbulence and the stochastic nature of the grain positions on the bed and their exposure to the flow (Paintal 1971).

Thus, most sediment transport predictors for uniform sediment are based on the excess shear stress above critical value. Furthermore they need a measure for bed shear stress and grain size as principal independent input parameters (e.g. Einstein 1950, Engelund & Hansen 1967, Kalinske 1947 (adapted by Van den Berg 1987), Meyer-Peter & Müller 1948, Parker et al. 1982, Van Rijn 1984a, Zanke 1990).

Bedforms are the result of sediment transport, and their propagation can be seen as a measure for the bedload transport. The bedforms dissipate energy by creating flow separation just downstream of the top, and modify the near-bed flow conditions. Thus, there is a feedback between flow shear stress, sediment transport and bedforms.

Most predictors use only the part of the bed shear stress that is exerted on the grains, while excluding the part that is lost due to the friction caused by bedforms. These effects can be accounted for by separating the total shear stress in a bedform-related component and a grain-related component. The latter is called the grain shear stress. The grain shear stress is usually determined as the shear stress due to the friction of a representative roughness length, e.g. 1-3 D_{90} , depending on the sediment size (Van Rijn 1993, $D_{90} = 90^{\text{th}}$ percentile of the grain size distribution of the bed sediment, see [chapter 5](#)).

Unfortunately, the behaviour of bedforms is not well predictable yet, and neither are the effects on shear stress and sediment transport, especially in changing flow conditions like a discharge wave (see [chapter 6](#)). Often the bedform development lags behind the changing flow during a discharge wave (Allen & Collinson 1974). At rising stages the bedforms are still small and their flow resistance is likewise small. At waning flow stages the bedforms are larger and dissipate more flow energy. The flow is then less able to transport bed sediment, therefore the bedload transport is often lower at falling stages than at rising stages.

Concluding, the sediment transport of uniform sediment is relatively well understood. The interaction between the flow, bedforms and sediment transport is less well understood, while it

may have large effects. More specific, the relation between turbulence and bedform generation, and between turbulence generation and flow over bedforms, is unclear (Bennett & Best 1995). Nevertheless, when the grain shear stress can be computed, the sediment transport of uniform sediment can usually be predicted with an accuracy of a factor 2-3 (e.g. Van den Berg 1987, Van Rijn 1993).

2.2.2 Interaction between bedforms and bedload transport

The role of bedforms in the sediment transport process is large. Bedforms affect sediment transport in two ways (see Livesay et al. 1996 for a review):

1. they create variations in bed roughness which may significantly affect the near-boundary flow structure and thus the bedload and suspended load transport, and
2. they produce marked spatial and temporal variations in both total and fractional bedload transport rates.

Bedforms in sediment mixtures affect sediment transport in two additional ways (Livesay et al. 1996):

3. they generate distinct patterns of sediment sorting, and
4. they control the spatial availability of individual size-fractions for sediment transport.

In theory these sorting phenomena must be incorporated in prediction methods based on uniform sediment, because they affect the incipient motion as well as the abundance and availability for transport of sand and gravel at the bed surface (see **chapter 9**). In practice, not all may be necessary.

The importance of bedforms for sediment transport over a mixed sediment bed is at present recognized (e.g. Whiting et al. 1988), but this has not yet lead to integrated models with quantitative relationships for mixed sediment transport. There are a great many observations on bedforms in laboratory conditions, and also many in field conditions (see **chapter 6**). No model exists yet that describes the relations between those bedforms, sediment characteristics and flow (see **chapter 9**).

2.3 Sorting of sediment mixtures on the grain scale

2.3.1 General observations

As discussed earlier, sediment sorting is discussed for three length scales: the grain scale, the bedform scale and the meander scale. In this section the grain scale is considered. In general, the following phenomena have been observed to be important on the grain scale (see fig. 2.3), and are discussed in the following sections:

- the flow is turbulent and varies strongly, and may entrain grains that are stable in the average flow,
- small grains hide in the lee of large grains, while the large grains are more exposed to the flow. This is called the hiding-exposure effect,
- in low flow in (sand-) gravel-bed rivers, a coarse surface layer may develop that inhibits the entrainment of finer, underlying sediment. This coarse surface layer is called 'armour'

layer’.

- in the armour layer, the largest grains are often surrounded by a cluster of smaller grains. In addition, the asymmetric, flattened stones dip in the upstream direction, which is called ‘imbrication’,
- sediment is often horizontally sorted: the sand is concentrated in patches (often bedforms like flow-parallel sand ribbons, or patches in niches in the gravel bed, further discussed in section on sorting on the bedform scale); in addition the sediment may be sorted in cross-sectional or downstream direction (e.g. sorting in meander bends or on tops of bars).

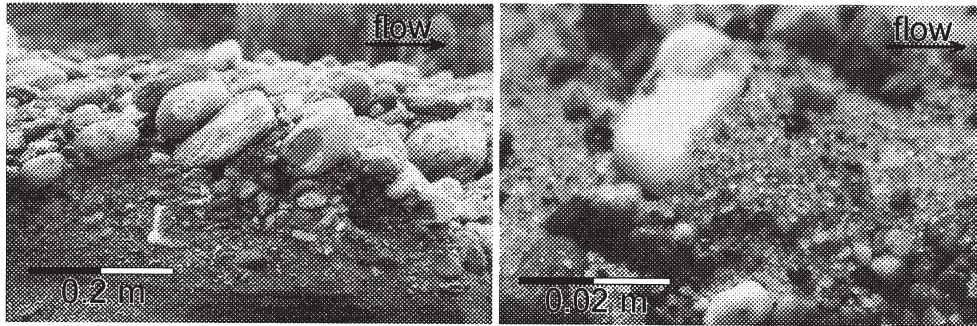


Figure 2.3. Left: an armour layer with an imbricated pebble cluster on a bar in the river Waiho, New Zealand. Right: a pebble cluster on a sand ribbon in the laboratory experiments described in chapters 4 and 5. The largest grains are much more exposed to the flow than the small grains.

2.3.2 Sorting in armour layers

At this point it is necessary to distinguish between mobile and stable armouring. A stable armour layer (Gessler 1971) forms if the upstream sediment input is cut off for some reason, e.g. a dam or upstream armouring. Large discharge waves remove all grains that can be moved from the armour layer and just below. The armour layer then reflects the largest discharge wave in the recent past. The bed surface sediment is only entrained when the discharge exceeds that of the largest historical flood. If this type of armour is broken, the bed sediment is suddenly entrained in large quantities. At the lowering of the flow a new, coarser armour layer is formed.

A mobile armour layer (Parker & Klingeman 1982) on the other hand is present at a large range of discharges except extremely high discharge, and is a direct consequence of the hiding-exposure phenomenon. At the lowest flows only the finest sediment is entrained and transported over the armour layer. At higher flows coarser sediment is entrained, and is exchanged with the bedload sediment because the pockets in the bed that are left open by entrained grains, are preferentially filled with grains of the same size. The bedload obtains the same grain size distribution as the bed sediment at extremely high discharges. At that point there is no longer an armour layer, but with lowering flow the armour layer is reformed.

Parker et al. (1982) did flume experiments with a sediment mixture in a narrow, sediment feeding flume. They showed that an armour layer can coexist with motion of all grain sizes, because the motion is sporadic in their conditions. The largest grains are less mobile as they are heavier, and consequently become overrepresented at the bed surface. Thus an armour layer emerges, which in turn decreases the mobility of the small grains. The result appears to be equal mobility of all fractions. In this condition, the grain size distribution of the bedload material is the same as the substrate, or sub-armour layer material, which both are finer than the armour layer material. The

equal mobility concept was corroborated in their experiments and in some field measurements. The stability of natural armour layers is often increased by pebble clusters or imbricate clusters, which are formed by colliding flat gravel grains (e.g. De Jong 1995). An obstacle (e.g. large pebble) prevents a pebble from being transported. Subsequent collisions of other pebbles in transport form a pebble cluster parallel to the flow, with an imbricated structure (middle axis dipping in upstream direction). A pebble cluster has less resistance to the flow than a cluster structure of the same pebbles in an area (De Jong 1995), or in other words, it is more difficult to break up a pebble cluster than to transport the pebbles separately. Evidence for this is also found in other rivers. Reid et al. (1985) found for a natural gravel-bed river that incipient motion during rising flow was at a much larger shear stress than the end of motion in waning flow. They attributed this to the destruction of an armour layer with pebble clusters, while the pebble clusters were absent in the waning flow.

2.3.3 Incipient motion of sediment mixtures

The initiation of general sediment motion is described well by the Shields curve for uniform sediment. Unfortunately, the Shields curve is no longer valid when the bed sediment consists of a large range of diameters. Larger grains are more exposed to the flow and therefore have lower critical shear stresses. Smaller grains are hiding in the wake of larger grains and therefore have higher critical shear stresses. This is called the hiding-exposure phenomenon (see figs. 2.3 and 2.4 and chapter 5).

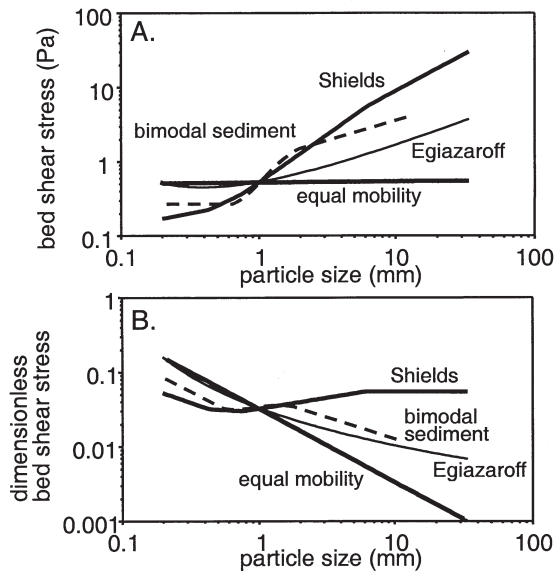


Figure 2.4. Critical bed shear stress according to the Shields curve and with equal mobility and Egiazaroff (1965) hiding-exposure corrections, and a hiding-exposure curve for strongly bimodal sediment (after Wilcock and McArdell 1993, see text for explanation). The hiding-exposure corrections are computer here for sediment with a median grain size of 1 mm.

A. Dimensional representation.

B. Dimensionless representation comparable to original Shields curve.

The effect on sediment transport was first quantified by Egiazaroff (1965), who theoretically derived a hiding-exposure correction for all grain sizes D_i (see fig. 2.4):

$$\theta_{cr,i, corrected} = \theta_{cr,D50} \cdot \frac{1.66667}{\left[\log \left(19 \frac{D_i}{D_{50}} \right) \right]^2} \quad (1)$$

in which $\theta_{cr,D50}$ = the critical Shields shear stress and $\theta_{cr,i,corrected}$ = Shields critical shear stress corrected for the hiding-exposure effect. The dimensionless Shields shear stress is related to critical shear stress (τ_{cr}) as $\theta_{cr} = \tau_{cr} / ((\rho_s - \rho)gD_{50})$, in which $(\rho_s - \rho)$ is the density of sediment minus that of water.

In practice, the critical shear stress of each fraction is often corrected with an empirical relation of the form:

$$\theta_{cr,i, corrected} = \theta_{cr,D50} \cdot \left(\frac{D_i}{D_{50}} \right)^p \quad (2)$$

The power p is determined from datasets in several ways. One way is to measure the grain size distribution of transported material during low transports and extrapolate the shear stresses for each fraction to the extremely low transport that represents incipient motion (e.g. Wilcock 1993). Another method is to estimate visually the boundary between transport and no transport for each fraction (Shields 1936, in Van Rijn 1993). Buffington & Montgomery (1997,1998) gave an overview of most existing empirical relations, which are as numerous and diverse as the studies themselves. They conclude that no universal relation can be found, but defensible values should be used for each set of application, measurement instruments and definition of incipient motion. The power p is not accurately known and differs for each dataset. The theoretical curve of Egiazaroff can be approached by a range of powers p , depending on grain size. If the power p is -1, then all fractions are equally mobile. Parker et al. (1982) hypothesized that this is the case if the largest fraction is in motion, because a mobile armour layer is not broken up but stays intact. In the mobile armour layer the differences in hiding and exposure of the fractions have the effect that the critical Shields value is the same for every grain size. If, however, the bed shear stresses are lower than critical (or twice critical in some studies) for the largest fraction, the power p decreases.

If a completely mixed bed is taken as a starting point, and the power p is in between 0 and -1, then first the finest material is eroded away. The fine material behind larger grains are winnowed out down to a certain depth, on which the hiding / exposure is in equilibrium. If this point has been reached, the bed surface is relatively coarse, equivalent to desert pavements. A moving bed of this type is often called pavement or mobile armour layer, a fixed, stable bed with mainly large grains at the surface is called stable armour layer.

Concluding, sorting mechanisms on the grain scale are related to relative grain sizes, which cause the hiding-exposure phenomenon, and consequently the armouring process and pebble clusters. The hiding-exposure phenomenon and armouring obviously will have a large effect on sediment transport by reducing the mobility of fine sediment, and increasing that of coarse sediment.

The hiding-exposure phenomenon obviously must be incorporated in sediment transport predictions. A transport predictor for uniform sediment can be used to calculate the transport of

sediment mixtures as follows (see **chapter 5**). The mixture is divided into size fractions, and for each size fraction the transport is calculated while correcting the critical shear stress of each size fraction with an appropriate hiding-exposure correction. In this way the composition of the transported material is calculated.

2.3.4 Hiding-exposure effects and deposition

Depositional mechanisms have received much less attention than entrainment mechanisms. Everts (1973, in Carling 1990 and Powell 1998) argued that sediment sorting during deposition is controlled by processes very similar to those that determine the relative mobility of different size fractions at entrainment. The mobility of a grain is in part determined by the pocket geometry in which it rests (hiding / exposure). During deposition, larger grains are less likely to deposit on a finer bed except where coincidental accumulations of other larger grains provide a suitable pocket, or where the wake of these other grains reduce the drag force (Carling 1990, see Powell 1998 for a review).

The efficiency of this process may in part be determined by local turbulence characteristics of the bed surface in two ways. First, flow turbulence results in a more thorough removal of fine sediment from an initially poorly sorted bed surface. Second, local turbulence inhibits the deposition of finer material, therefore only coarser material can settle. The role of near-bed turbulence will be discussed later.

Depending on the abundance of certain fractions in the bedload material, the bed surface may preferentially consist of clasts larger than can be entrained by local turbulence, but even coarser fractions are not deposited on the bed because these do not fit in the pockets of the clasts in the bed. In this way a relatively well sorted bed surface is created on a bar (Powell 1998). This is called the 'like-seeks-like' effect.

Concluding, a like-seeks-like effect may occur in which grains of equal size can be deposited while larger grains remain fully exposed and smaller grains are winnowed. The like-seeks-like effect is not described by the hiding-exposure equations. Yet it causes the sediment to be horizontally size-segregated, which may lead to different sediment transports in each area (Paola and Seal 1995). The latter phenomenon will be discussed in the section on sorting on the bedform scale.

2.3.5 Incipient motion of unimodal and bimodal sediments

The incipient motion of unimodal sediment is well described with the hiding-exposure correctors described in the previous section. Bimodal sediment on the other hand, shows combined behaviour of uniform and mixed sediment. With increasing bimodality of the bed sediment, the sand and gravel part show different behaviour. The gravel fractions show slightly size selective transport, while the sand part shows equal mobility (Wathen & al. 1995). The size selectivity of transport of the gravel part is caused by the coarsest fractions that rarely are in motion (Wilcock & McArdeall 1993 and **chapter 5**). The result is a relation between the critical Shields parameter and grain size that lies in between the Shields curve (representing uniform sediment) and the horizontal equal mobility curve (representing extreme hiding-exposure for non-uniform sediment) (fig. 2.4).

The effect is that the sand may already be in motion while the gravel is still immobile. Due to the like-seeks-like mechanism described in the previous section, this may lead to a horizontal segregation of sand and gravel, resulting in patches with relatively uniform sediment (Paola and

Seal 1995) and other bedforms. The gravel patches are usually immobile while the sand patches can be mobile in low flow. This grain size segregation obviously causes the segregated gravel and sand to behave even more like uniform or unimodal sediment. Strictly, the segregation of sediment is probably not in the horizontal direction but in the vertical, because the sandy patches are in fact lying on top of gravel. For practical purposes of sediment transport prediction during one discharge wave, however, it can be considered as a horizontal segregation.

Consequently Wilcock & McArdell (1993) define a condition of partial transport between fully mobilized transport and immobile bed, that is between one and two times the critical shear stress for a fraction. During conditions of partial transport the finer fractions are in motion, while the coarser are not. In former studies this finer fraction was called 'wash load' or 'throughput load' (e.g. Parker et al. 1982). The term 'wash load' is generally used for sediment that is transported by the river without being deposited on the river bed. In this case, there is no interaction because of an armour layer, but the sand is present in the bed below the armour layer. Therefore the term 'throughput load' is preferred here.

It can be assumed that the throughput load is mostly limited by the availability of material. This limitation is caused by the immobility of the armour layer, which protects the fines in the bed against entrainment. Thus the throughput load is - for this condition - independent on the underlying sediment but only dependent on upstream supply, and therefore is probably unpredictable. The throughput load may be expected to occur more often in strongly bimodal sediments, in which the mobility of the coarse sediment is unrelated (by the hiding-exposure phenomenon) to that of the fine throughput sediment.

During conditions of partial mobility (Wilcock & McArdell 1993), the bed coarsens with increasing flow strength because only the fine material is mobilised. Above two or three times the critical shear stress for the largest grains, the bed surface becomes finer again, because fine material is released from below the armour layer for transport as more and more large grains move from their places. Obviously this behaviour is comparable to that described by Parker et al. (1982) in their equal mobility hypothesis. Wilcock & McArdell (1993) compared data of their flume experiments to field data of Goodwin Creek (Kuhnle 1992) and Oak Creek (Milhous 1973, in Parker et al. 1982), and found that partial transport conditions occur frequently in both rivers, and probably also in many other rivers. The difference between Wilcock & McArdell's (1993) results and the equal mobility hypothesis is twofold: the shear stresses in the experiments of Wilcock & McArdell are available between immobile bed and the critical shear stress needed to move the largest grains, while equal mobility occurs mostly above that critical shear stress. Second, the mixtures used in the experiments are highly bimodal, while equal mobility seems to occur mostly in unimodal mixtures.

Concluding, the influence of the rate of bimodality on the correction of bed shear stress of individual fractions is large (Wilcock 1993). The effect of bimodality can be interpreted as a reduced mixture effect: critical shear stresses for strongly bimodal sediments are intermediate between uniform sediment values (Shields curve) and unimodal mixture values (approaching equal mobility, same shear stress for all fractions). The effect on the finer fractions is larger than on the coarser fractions (Wilcock 1993). Another consequence of sediment bimodality is that armour layers are expected to occur more often in bimodal sediment than in unimodal sediment, because the gravel is less mobile.

2.3.6 Horizontal size-segregation and mobility in bimodal sand-gravel sediment

The trends mentioned above cannot be explained by the hiding-exposure concept as proposed by

Egiazaroff (1965), because the horizontal segregation of sand and gravel is not incorporated. This segregation has been observed in numerous experiments in the form of longitudinal sand ribbons and other bedform types on gravel beds (see chapter 4), and in the form of patches initiated by the like-seeks-like mechanism.

If finer sediment is concentrated in more homogeneous zones, then the critical shear stress will approach those of uniform sediment. The coarse part of the surface will then show increased flow shielding and increased rolling resistance, resulting in a higher critical shear stress than would be in the case of a unimodal sediment with one critical value for all fractions. This is confirmed by Wilcock (1993), who found that in almost unimodal sediments all sizes began to move at nearly the same shear stress, forming low dunes, while more bimodal sediments had increasingly longer trajectories of incipient transport of only the finer fractions, forming flow-parallel ribbons or isolated bedforms.

Horizontal sediment sorting was investigated by Seal et al. (1996) with laboratory experiments in sediment-feed flumes. First they experimented with a 70% gravel and 30% sand mixture in a narrow flume (width 0.3 m), to make lateral sorting impossible. The experiments produced deposits with downstream fining with a sharp gravel-sand transition, independent of the rate of deposition. The second set of experiments was done in a much wider flume (width 2.4 m) with several mixtures. The mixture of 70% gravel and 30% sand showed only weak lateral segregation and produced a fining pattern comparable to the narrow flume experiments, although with a less sharp transition. When the sand content in the feed-mixture was increased to 50%, clear patches of fine and coarse material developed and a continuous downstream fining pattern with no clear transition. These experiments confirm that the bimodality rate of a mixture determines whether patches form or not.

Comparable experiments (Ikeda and Iseya 1988) indicate that the sediment behaviour changes rather suddenly when the sand content is above 50%, because at that point the sediment changes from clast-supported to matrix-supported. In the latter case, the sand starts to move as bedforms over the bed surface, while the gravelly areas in between are immobile.

The effect of horizontal segregation on sediment mobility is further illustrated by the results of Kuhnle (1993), who did experiments in a recirculating flume with a bimodal sand-gravel mixture with several ratios between sand and gravel content. In experiments with only the sand or the gravel mixture, all grain sizes began to move at nearly the same critical shear stress, which is equivalent to near equal mobility. However, in the bimodal sand-gravel mixtures the formation of a coarse surface layer (armour layer as described by Parker et al. 1982) was inhibited when there was more than 50% sand in the mixture. This sand mode prevented a portion of the smaller sizes of gravel from being removed from the surface layer, because the sand filled all interstices of the gravel. As a result, the initiation of motion of the gravel fraction was still dependent on size. Interestingly, all sand fractions consistently began to move at nearly the same critical shear stress in all experiments, also in the bimodal experiments, and therefore seem to behave independent from the gravel fractions.

Concluding, the behaviour of sand and gravel in a bimodal sediment mixture may be understood in terms of trends, but a unique description of incipient motion based solely on size distributions is not available. The application of critical shear stresses of bimodal sediment in transport predictors is therefore still ambiguous and the role of the sediment bimodality unclear. There is some evidence for asymmetric roles for sand and gravel, as the sand content of the bed determines the sediment mobility of the mixture, and as the sand grains remain equally mobile while the gravel shows size-selective entrainment.

2.3.7 The importance of turbulent shear stress variations near incipient motion

In many rivers with sand-gravel bed material the sand fraction is in motion while the gravel fraction is mostly immobile. Using a deterministic bedload predictor with a critical bed shear stress for incipient motion, the predicted transport of the gravel fraction in the bed might then be zero, while the true transport is non-zero. When the larger sediment grains are below the threshold for motion, the stochastic nature of bedload transport due to flow turbulence should also be represented, because the grain sizes that are on average immobile, may be responsible for some transport due to the turbulence. The effect of turbulence on sediment transport near the threshold of motion was first modelled in detail by Einstein (1937), Kalinske (1947) and Paintal (1971). There are now several new stochastic predictors available, e.g. Bridge and Bennett (1992), Zanke (1990) and Van Rijn (1993).

In the calculation of excess shear stress both the exerted shear stress and the critical shear stress may be considered as a stochastic variable (Grass 1970). In the determination of critical shear stress, a subjective boundary between motion and no motion is taken. The Shields curve for example represents motion of about 10% of the grains on the surface (Zanke 1990). Einstein (1937), Zanke (1990) and others have constructed probability distributions for the beginning of movement of sediment.

It is a matter of discussion whether flow turbulence or sediment characteristics or both are the principal sources of variation (see Mosselman and Akkerman (1998) and **chapter 5**). Fact is that flow turbulence is the only possible source of variation in the driving forces. On the other hand the grains of a mixture show many (static) variations: shape, density, imbrication and other surface formations. Since critical shear stresses are measured in flows that are turbulent, the variation due to flow turbulence and sediment characteristics is difficult to distinguish.

Grass (1970), Paintal (1971) and Zanke (1990) argued that the Shields threshold of incipient sediment motion is not a strict threshold but a gradual increase from no motion to full motion, due to the stochastic properties of the grain stacking and the near-bed flow. Buffington and Montgomery (1997, 1998) compared most available literature on incipient motion, and found that the Shields parameter value depended on the method or criterion for incipient motion. They argued that no value is more correct than others, but that defensible values should be used for each specific problem. Zanke (1990) empirically found a probability function for the incipient motion, which is dependent on shear stress. He was able to incorporate this function as a correction factor to his bedload transport predictor to yield more reliable predictions just above and below the Shields criterion. The distribution gives probabilities between zero and unity for a range in which motion is beginning. However, this approach does only work with predictors that do not have the critical threshold itself incorporated. If they had, these predictors would predict zero transport below the threshold, while in reality there is some transport just below the Shields criterion. Therefore Zankes function cannot be used with most predictors.

Many others consider turbulence as the prime source of variation. Van Rijn (1987, in 1993) assumed that bed shear stresses are normally distributed, and proceeded to implement the assumed distributions into a bedload predictor based on relative excess shear stress (see 'incipient motion') (see fig. 2.5). This approach was also followed by Bridge and Bennett (1992), who varied the bed shear stress only, according to a normal or lognormal probability distribution. The transport is calculated for each probability and integrated to yield the total transport for the considered probability distribution. Since this method only affects the shear stress and not the critical shear stress, it can be applied to most predictors. Bridge and Bennett applied this method to a fractionwise predictor of bedload transport.

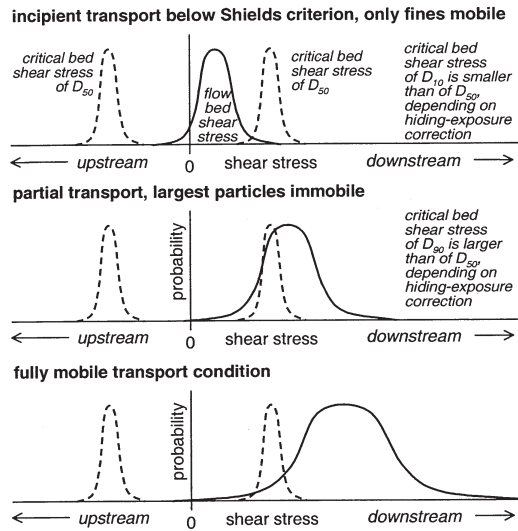


Figure 2.5. The mobility of sediment is determined by the flow shear stress and the critical shear stress, which both have a stochastic nature (after Grass 1970). Note that in turbulent flow the momentaneous shear stress may be in the upstream (to the left) and downstream direction (to the right).

Concluding, partly due to flow turbulence, the beginning of motion is a stochastic phenomenon. There are at least two general methods for incorporating turbulent flow variations into a predictor to account for very low transport just above and below the Shields critical threshold of motion. It is however not clear how to apply these methods to existing bedload predictors, while it is obvious that this phenomenon is important for sediment mixtures at incipient motion for a part of the mixture (see chapter 5).

2.4 Sorting on the bedform scale

2.4.1 General observations

There are many different types of bedforms in uniform sediment and in mixtures (see fig. 2.6 and chapter 4). In sand-gravel mixtures, the following bedform types have been recognised:

- ripples: only in sand, crests flow-perpendicular, assymetric and triangular, height related to grain size, length circa 10 times height,
- dunes: crests flow-perpendicular, assymetric and triangular, height about 15% of water depth, length circa 20 times height,
- sand ribbons: flow-parallel features, height related to grain size, width related to flow structure,
- barchans: parabolic dunes with the points pointing downstream,
- bedload sheets: low relief bedforms, height circa 2 times grain size, crests flow-perpendicular, sediment sorting is the most outstanding feature: large grains in leading

- edge and fine upstream,
- other low relief features: low relief bedforms, symmetric forms, height related to grain size,
- patches: areas of fine immobile sediment, no specific form but present in lee of boulders or other niches

In addition, there are many sorting phenomena associated with these bedforms (cf. Allen 1984, see fig. 2.6), among which:

- horizontal sorting in bedload sheets: coarsest sediment in leading edge and finer sediment upstream,
- Fining Upward (FU) in ripples, barchans, bars and dunes: coarsest sediment lower in the bedform and finer sediment near tops,
- gravel lag or armour layer in troughs of barchans and dunes (also see fig. 1.4).

2.4.2 Bedform types in non-uniform sediment

Between the scale of bars and pebble configurations there is a large range of bedform types. Bedforms in uniform sediment have been classified in genetic terms of sediment diameter and shear stress (or velocity), e.g. by Simons-Richardson (1966), Van den Berg & Van Gelder (1993), Van Rijn (1989) and Southard and Boguchwal (1990). It is not clear whether these classifications can be extrapolated to sand-gravel mixtures.

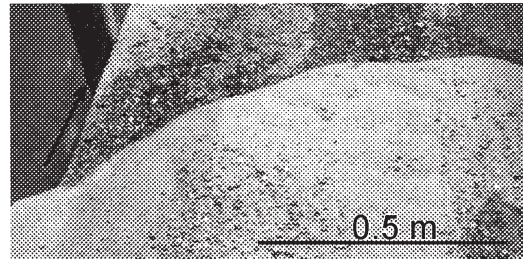
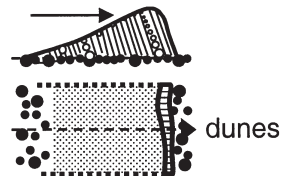
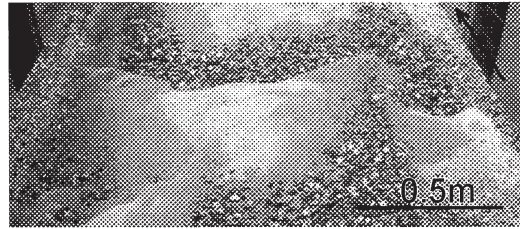
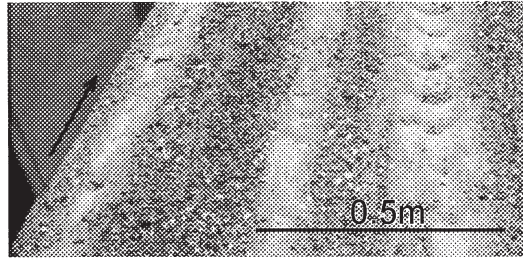
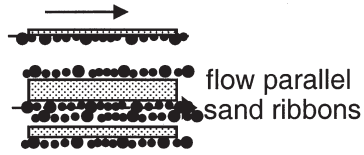
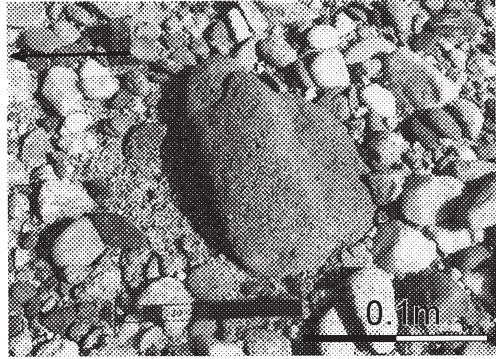
Carling (1999) presented an overview of the available data on bedforms in coarse sediments. These data were confronted with the bedform stability diagrams of Allen (1984) and Southard and Boguchwal (1990). It appeared that the stability fields of bedforms in sand could be extended in the gravel grades (Carling 1999). Thus, dunes made up of gravel and sand dunes are found in the same range of values of the Shields parameter. However, Carling's data refer mostly to rather unimodal sand or gravel sediments, bimodal sand gravel mixtures were not considered.

It was demonstrated (Klaassen 1986, Chiew 1991) that the stability of bedforms may be significantly influenced by sediment sorting. In poorly sorted sediments the relatively finer-grained fractions may become mobilized so that bedforms, such as dunes, form in finer sediment and override the coarser underlying armour layer. The following phases in transport were distinguished for a unimodal sand-gravel mixture (Klaassen 1986):

- during low flow over an armour layer no movement occurs,
- during higher flow fine sand is winnowed out of the armour layer through small instabilities,
- during increasingly higher flow small dunes are formed of the winnowed sand. In the troughs of the dunes the bed shear stress on the armour layer is higher due to the turbulence of the flow separation. More and more sand and coarser material is extracted from the bed below the armour layer, and the armour layer itself sinks away and becomes partly buried,
- during decreasing flow the dunes still travel on top of the armour layer.

These phases were observed in a straight flume, obviously without the three-dimensional effects that may occur in natural meandering rivers. In a meandering river, the inner bend and deepest pools may provide temporary storages of fine sediment, which is entrained to form dunes overriding the armour layer. Also, the bedforms migrating through a bend with a lower waterdepth at the inside than at the outside, may behave different than indicated here, because

sandpatch
in the lee
of a cobble



ripples over a dune

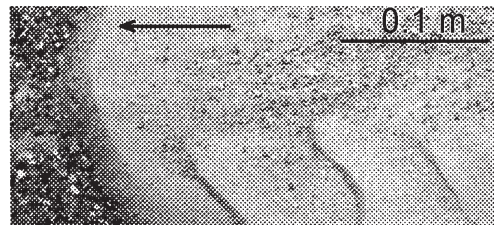


Figure 2.6. Illustrations of a number of bedform types, and the sorting within some bedforms. The sand tail in the lee of a cobble was found in the river Allier, France, while the other bedform types were observed in the Sandflume experiments described in chapters 4 and 5.

the flow pattern in the dune troughs is modified (Dietrich and Smith 1984, Kisling-Møller 1993). This is, however, not important in rivers with a small sinuosity. This is further discussed in the section on sorting on the meandering scale.

Wilcock (1993) found that dunes superceded a lower-stage plane bed at higher bed shear stresses in sediments with a log-normal grain size distribution, while bedforms called bedload sheets formed after a lower-stage plane bed in bimodal mixtures. A bedload sheet is the result of a longitudinal sediment sorting process in which bed material moves in very low amplitude waves with distinct coarse fronts followed by transitional and smooth zones. These features migrate downstream as large grains eroded from upstream are able to move easily over the smooth section (overpassing) before coming to rest in the next congested zone. This zone is then filled and covered with sand, but later re-emerges towards the tail. Grains are able to move more rapidly over the sand zone because the flow cannot adjust to the rapidly changing roughness states, so a similar shear stress is applied to all zones, but since the critical shear stress is lower over the sand zone, grains can be entrained and transported more readily (Sambrook Smith 1996). Bedload sheets have both been found in the field (e.g. Whiting et al. 1988) and afterwards described in laboratory conditions (e.g. Iseya & Ikeda 1987).

It has been hypothesized by many authors that bedload sheets in poorly sorted sand-gravel mixtures and gravels are the counterpart of dunes in sandy material (e.g. Livesay et al. 1996, Bennett & Bridge 1995, Best 1996). Ikeda & Iseya (1987) studied the influence of the sand content in sand-gravel mixtures on bedforms. They found that with increasing sand content the bedforms more and more resembled sand dunes, while with low sand contents the bedforms were in fact bedload sheets or very low dunes in gravel. The transition to dunes most likely results from a rise in the importance of flow separation as a control on bedform geometry and an increase in the mobility of coarser fractions with increasing shear stress. Also the presence of sand on the bed increased the mobility of the gravel because of the overpassing mechanism.

Bennett & Bridge (1995) described three forms of low-relief bed forms: pebble clusters, bedload sheets and low-relief bars. They propose a sequence of bed features on a mixed-size and mixed-density bed under increasing bed shear stress, bed mobility and sediment transport: (1) selective entrainment and transport of the relatively fine fractions and their incorporation into bedload sheets that migrate over a partially armored, coarser bed containing pebble clusters; (2) increase in the height and number of bedload sheets present (incipient dunes); and (3) amalgamation of bedload sheets and development of dunes. Bars are expected to coexist with bedload sheets and dunes.

Concluding, a plethora of bedform types exists in sand-gravel sediment, but there is no systematic study of their occurrence that covers most observed types. The results suggest that bedload sheets occur in bimodal sediment, while dunes occur in unimodal sediment and very sandy bimodal sediment. Sand ribbons and pebble clusters were observed in both sediments (see chapter 4). The bedforms themselves can be seen as patches of different sediment than the surrounding bed. These patches may have a considerable effect on the sediment transport because of that grain size difference. In addition, it was found that dunes with significant flow separation and turbulence generation may contribute to the formation of an armour layer.

2.4.3 Vertical sediment sorting

Sediment in bedforms may be sorted in the vertical direction, especially in larger bedforms like dunes. In sedimentological literature this sorting is often described. A well known feature of dunes in rivers is the cross-stratified deposit, caused by the propagation of the bedforms by discontinuous avalanching of bedload sediment at the lee side of a dune (e.g. Allen 1970, see chapters 7 and 8). Within a cross-stratified set the sediment appears often sorted vertically (see fig. 2.7). The gravel is mainly deposited on the lower part of the lee slope, while the finer grades are predominantly deposited in the upper part. The result is an upward fining deposit with cross-stratification. Although this sorting principle related to avalanching is well known, a mathematical description of the process is not available. The processes at the lee side of bedforms and their deposits are described in more detail below.

Within the dunes, three basic units can be distinguished, being a toeset, a cross-stratified set consisting of many foresets, and a topset (Allen 1984, see fig. 2.7). Bedload sediment is transported on top of the dune, and may be preserved as a topset. A toeset may be preserved when the dune overruns it; it is then called a bottomset.

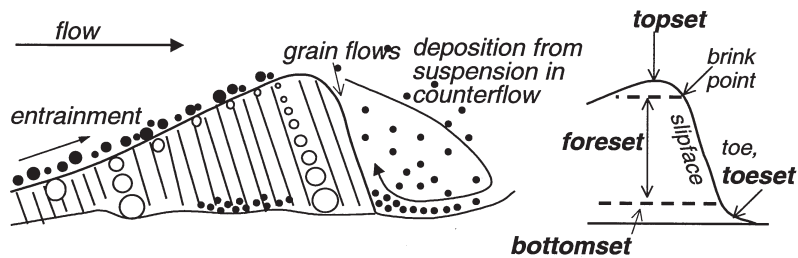


Figure 2.7. Basic depositional units in dunes: a bottomset, a cross-foreset and a topset. Note that the combination of coarse gravel in transport and a fine toeset is unlikely, but given here for the purpose of definition.

Sediment that arrives at the brinkpoint of the dune, is partly deposited on the lee slope. A finer part of the sediment is suspended, to be deposited on the lee slope, in the trough zone or on the stoss side of the downstream dune when the turbulent energy in the trough zone is small (Jopling 1969). Obviously, there is a gradual transition between the bedload mode and suspension. The sediment on the lee slope will accumulate until the angle of repose of the sediment is exceeded. The angle of repose is sometimes called angle of internal friction, to denote the critical angle of a mass of sediment (internal friction) as opposed to that of the individual grains (repose). Then the accumulated sediment will roll or flow down the lee slope of the dune. This gravity-driven movement stops at the toe of the lee slope, where the local bed slope decreases. The moving layer of sediment on the lee slope is deposited as a cross-stratum. A number of cross-strata are called the cross-stratified set. Cross-stratified sets may range in thickness from a few millimeters in ripples to more than one hundred meter in Gilbert-type deltas.

Suspended sediment must be included in this discussion, since it may affect the vertical sorting. The suspended sediment is partly captured in the counterflow and settles on the lee slope and in the trough to form a bottomset (Jopling 1969). The part of the bottomset at the toe of the lee slope is sometimes called the toeset. The sediment in the trough is transported both upstream and downstream, depending on the position relative to the reattachment zone. Both the counterflow and the coflow may form ripples. With relatively small flow energy, the bottomset may be preserved when the dune migrates over it by deposition of cross-strata at its lee side on top of the

bottomset (Boersma et al. 1968). With higher flow energy, an armour layer may form when the largest grains of the sediment are partially mobile or immobile, while the smaller grains are winnowed from the bed and suspended. In high-energy conditions the formation of a toe deposit is obviously very unlikely.

Consider a river with dunes in the order of 0.5-1 m and a sand gravel mixture with 50% sand. During rising flow the bedform trough level is lowered while sediment is entrained into the migrating and growing bedforms. During waning flow the trough level rises again while the bedforms become smaller (e.g. Allen and Collinson 1974). Meanwhile, the sediment is vertically sorted in the grain flow along the lee side of bedforms. Thus, a sedimentological record is left in the river bed. More important, this vertically sorted sediment is the bed sediment that will be entrained again in the next discharge wave. Thus the historic record of discharge and sediment sorting in the river bed is bound to play a role in the sediment transport (see fig. 2.8 and chapter 9).

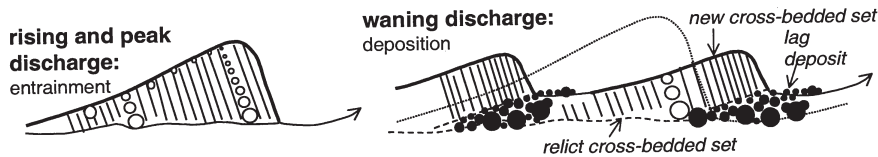


Figure 2.8. During rising and peak discharge the transported sediment is sorted in the grain flow at the lee side of a dune. In waning discharge, the dunes diminish and leave cross-bedding relicts. Due to selective deposition, an upward fining accumulation of lag deposits is created in addition (see chapters 6 and 9).

During the different stages of discharge waves, grain size selective entrainment and deposition of the sediment mixture may also lead to a vertical sorting. The largest grains that are in motion during the peak discharge, will be deposited in lowering discharge while the smaller grains remain in transport. In the avalanching process the larger grains are preferentially transferred to the trough zone (Klaassen 1991). Thus the larger grains will preferentially be deposited in the troughs of the dunes, resulting in an upward fining accumulation of lag deposits (see fig. 2.8). Obviously the process of sorting in grain flows at the lee side of dunes cooperates with the selective transport process to create an upward fining sorting of sediment that is preserved in the river bed.

In a number of publications it was pointed out that sediment transport and deposition in sand-gravel bed rivers cannot be understood without considering vertical sorting (e.g. Klaassen 1987, 1991, Klaassen et al. 1987, 1999, Wilcock 1993, Wathen et al. 1995). Also the importance of the dune height has been shown, in the sense that the sediment from below the transporting layer of dunes is entrained in the (deepest) troughs (Ribberink 1987). The sorting in the bed was modelled in two layers by Ribberink (1987), but neither the historic sorting of previous discharge waves, nor the sorting within dunes were incorporated. Recently Parker et al. (2000) developed a mathematical model concept with a continuous description of sediment sorting in the dunes and the bed, comparable to the concept proposed by Klaassen et al. (1987). Klaassen et al. and Parker et al. could not implement their concepts because a general predictor for the sediment sorting in depth was not available.

Concluding, vertical sorting in bedforms potentially is very significant for the sediment transport process, because the sorting is recorded in the river bed, and is the boundary condition (as bed sediment varying with depth) for sediment transport in following discharge waves (see chapters 6, 9 and 10). So far, this effect has largely been neglected. Quantitative descriptors or models of vertical sorting in bedforms are unavailable.

2.4.4 The combined role of turbulence and sediment sorting in bedforms

If transport has to be calculated in the presence of bedforms, then the use of a single, constant value of bed shear stress is no longer sufficient. In summarizing parameters (from literature) the probability distributions of bed shear stress due to turbulence has to be used, following Van Rijn (1987, in 1993), with or without the variation of turbulence intensities over the bedform. This is further complicated with grain size variations over bedforms, which significantly influence the roughness and shear stress variations over bedforms. All variations might be included in a stochastic approach combined with information on spatial distributions on grain sorting and diameter, and turbulence intensities.

In the case of large dunes, the problem of sediment transport prediction based on an average shear stress and an average hiding-exposure function is even more problematic. The hiding-exposure phenomenon assumes that the sediment at the bed surface is fully mixed, while this is almost never the case due to the presence of bedforms. Both the shear stress and the grain size distribution of the bed surface vary systematically over the length of the dune (see fig. 2.9). These two patterns (of shear stress and of sediment sorting) interact to yield the average bedload transport (expressed by the propagation of the dune). In the bedform trough the average bed shear stress is on average zero but has large fluctuations. At the same location the sediment may be rather coarse, because it is in effect the eroding base of the upstream dune. At the top of the dune, the turbulent fluctuations relative to the average shear stress have diminished, and the sediment at the surface has changed to fine and better sorted. This structure on average yields the bedload transport. It is obvious that the assumptions underlying the bedload predictors are not very realistic in the presence of dunes. This also suggests that a universal hiding-exposure function will be difficult to find, because it intimately depends on the bedform type and sorting within the bedform (see chapter 11).

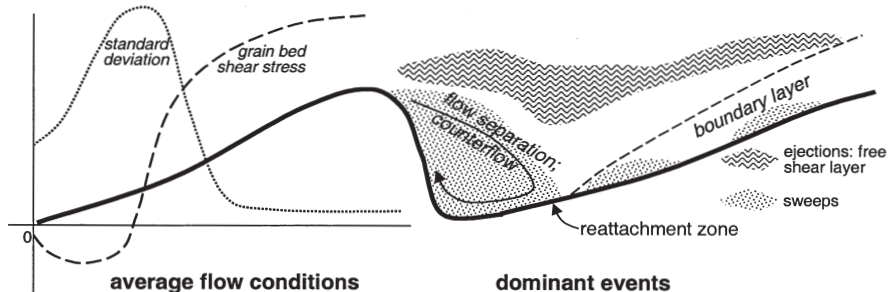


Figure 2.9. The structure of flow (to the right) over a dune. In the left half of the figure, the average characteristics of the flow are given as the average grain-related bed shear stress and its standard deviation. The standard deviation is the largest in the trough region of the dune, since the flow is separated downstream of the dune top and reattaches on the bed in the trough zone. In the right half of the figure the dominance of two turbulent event types is given (after Bennett and Best 1995). An ejection is a relatively fast upward motion, and a sweep is a relatively slow downward motion. The ejections at the dune top lead to a free shear layer, and suspend sediment. The sweeps entrain sediment near the bed.

In the flow separation zone (downstream of the brinkpoint), the flow has almost no net velocity but consists mainly of turbulence (see fig. 2.9). This is important in the entrainment of sediment. The length scale of turbulence may or may not play a role in the development and length scales of bedforms (cf. Best 1996 for an overview). More important, turbulent fluctuations above the bed (ejections and sweeps) have a skewed distribution that cause temporal high shear stresses. Since

bedload transport is dependent on shear stress to a power $p > 1$, a major part of the transport is caused by the high tail of the shear stress distribution. Also, the same temporal high shear stresses may exceed the critical shear stress of a grain that is too large to be moved by the average shear stress.

In the presence of bedforms, this is even more complicated because of the spatial variation of the different contributions to turbulence. Nelson et al. (1993) measured these structures in flumes, and comparable results from the Fraser river are found by Kostaschuk & Church (1993). The measured parameters are described, and in general it was found that ejections are the most important on the crest and top of dunes. An ejection is a relatively fast and upward directed flow. Ejections provide a mechanism for the entrainment and suspension of sediment. Sweeps are most important in the trough and at the reattachment point. A sweep is a relatively slow and downward directed flow, and thus provides the mechanism for erosion of the lower stoss side of dunes and deposition on the top.

There have been two recent attempts to predict the sediment transport along a bedform to account for the structural variation of shear stress, turbulence and sediment sorting. Livesey et al. (1995) used the bedload transport model of Bridge & Bennett (1992) to predict the spatial pattern of total and fractional bedload transport rates over low-relief bedforms. Turbulent fluctuations were also incorporated to account for transport of fractions near the threshold of motion. They were rather successful in the case of bedload sheets. The applicability for dunes however is very limited, since dunes have a much more pronounced vertical sorting while the turbulent structure over the bedform is much more complicated.

McLean et al. (1999) measured the turbulent flow structure above dunes with the objective to couple it to the bedload transport averaged over the length of the dune. They found that it was not possible yet to predict the bedload transport over the length of a dune, especially because the bed shear stress characteristics in the separated flow zone were not well predicted by the model. Instead they proposed that the turbulent flow model be used to predict the turbulent shear stress at the top of the dune. With the assumption that dunes are triangular and move at a constant celerity, the sediment transport at the top of the dune is twice the average sediment transport (Hamamori 1962). Thus the sediment transport prediction at the dune top was used to predict the average sediment transport. This is however only possible for dunes of uniform sediment or dunes without vertical sorting. For dunes with fining upward sorting and almost immobile gravel in the troughs, it is the question how the sediment must be represented in the prediction method, therefore this method cannot yet be used in most non-uniform sediments.

Concluding, there is no method yet for combining the phenomena related to bedforms with sediment transport prediction, while these phenomena cannot be neglected. Both flow turbulence and sediment characteristics have been incorporated as stochastic variables in sediment transport predictors, but always for plane beds or low relief bedforms. No predictors are known that explicitly include spatially variable turbulence and grain characteristics.

2.5 Sorting in meander bends

In this section, the role of sediment sorting on the length scale of meander bends is discussed, to determine whether this sorting scale must be addressed in as much detail as the bedform scale. In a hypothetical meandering river with graded sediment and no interaction or influence between different sediment sizes, the flow in the meander bends would induce a lateral sorting of bed material with coarse sediment in the outer bend and fine sediment in the inner bend.

The sorting is caused by a helicoidal motion of the flow, which develops in the bend (secondary

circulation) and causes a slight inclination of bed shear stress vectors towards the inner bank of the river. A meander bend in equilibrium therefore shows a sloping bed profile which is deepest at the outer bend (pool) and shallowest in the inner bend (pointbar).

The effect of helicoidal motion in the hypothetical river on sediment transport is as follows. The gravitational force on grains down the slope is proportional to the grain mass, while the drag force of the flow (with a component towards the inner bank) is proportional to the surface. For the same near-bed velocity a larger grain will be directed to the outer bank (topographic sorting), while a smaller grain will be directed inwards. In an infinitely long bend in the hypothetical river (without interaction between the different sizes), the streamlines of the different grain sizes will eventually become parallel, which means that the bed material is sorted completely (Olesen 1987).

Dietrich & Whiting (1989) combined theoretical research on flow and sediment entrainment in river meanders with field measurements of sediment transport and bed surface sorting. They found that in beds of moderately to well sorted sand in flows generating boundary shear stresses well above critical (such as in large sandy rivers), downstream varying boundary stress is matched by topographically induced cross-stream transport of sediment. In meanders with high excess shear stress but poorly sorted coarse sand and fine gravel, boundary shear stress variation downstream is partially matched by surface grain size adjustments (e.g. armouring) and by net cross-stream sediment flux. This is in effect a sedimentological change instead of a morphological change. The effect is a much less clear bend sorting with coarse sediment in both inner and outer bend (see fig. 2.10) than would have occurred without the surface grain size adjustments.

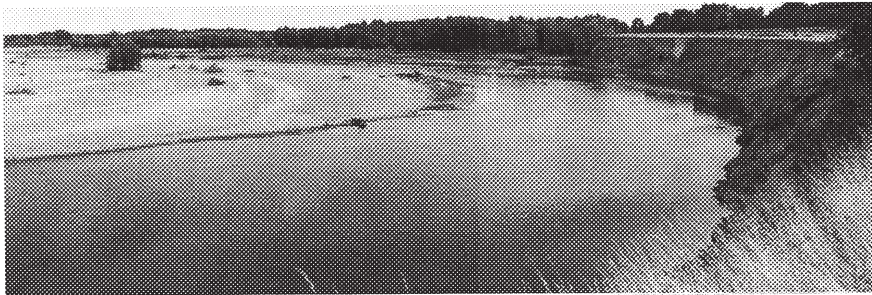


Figure 2.10. Sediment sorting in the river Allier, France, in between Moulins and Chatel de Neuve. The bed of the river Allier consists of sand and gravel. Some bend sorting was observed, but gravel was found abundantly in both inner and outer bend. The river bed is armoured in both the inner and outer bend. Flow is from back to front. Sand ribbons and patches (light) can be seen on the armour layer (darker) as well.

Maxima of bedload transport rate and boundary shear stress do not correspond in some areas. In gravel-bedded meanders with low excess boundary shear stress and low sediment supply, bedload may be much finer than the bed surface, and significant areas of bar surface are covered with grain sizes that constitute a very small portion of the bedload. Substantial bedload transport may only occur over a narrow portion of the bed width where boundary shear stress relative to critical stress of the surface is highest and where the sediment flux from upstream is locally concentrated. In this case grain size adjustments dominate over topographically induced cross-stream sediment transport in controlling the relationship between boundary shear stress and bedload transport fields (Dietrich & Whiting 1989).

Dietrich & Whiting (1989) show that incorporation of the interactions between different grain sizes have the effect that poorly sorted material in a bend can not be completely sorted out, because the bed surface adjusts sedimentologically to the flow. This effect is further enhanced by the presence of minerals with different densities in the sediment mixture (Bridge 1992).

In addition to topographically induced near-bed flow, Dietrich & Smith (1984) and Kisling-Møller (1993) highlight the importance of cross-stream transport caused by strong troughwise currents along the crests of bedforms that have skewed forms. These currents attribute to the lateral sorting of sediment. The skewness of the bedforms is caused by shoaling induced outward flow, causing a net outward directed bed shear stress in the innermost part of the bend. On the location where this outward flow meets the inwards directed flow due to secondary motion, a scroll bar may be formed.

Klaassen (1991) compared flume experimental results (Sand Flume, width 1.5m length 50m) with a sediment mixture with results of a physical meandering scale model with the same mixture. He found hardly any significant behavioural differences between the two. The most important difference was in the armour layer. In the straight flume an armour layer developed on the whole bed, but in the meandering model the armour layer only developed in the middle of the river, while the inner bends formed sand-beds and the outer bends formed gravel beds (bend-sorting). Therefore there was some difference during conditions below incipient motion of the coarser fractions between hydraulic roughness and sediment transport in the two flumes.

In rivers in which the gravel is even less mobile, the gravel is often found on the upstream ends of the point bars. It may be deposited there because, coming from the cross-over in the riffle, the flow experiences a widening of the river when entering the next meander bend, and therefore decelerates. This gravel deposit has been observed in the river Allier and in a scale model of the river Meuse by the writer. Fine sand, on the other hand may collect on the point bars or in the pools, to become available for transport in rising discharge (Lisle and Hilton 1999, Duizendstra 1999).

Concluding, sediment sorting processes on the grain scale counteract those on the meander scale to some extent. It is expected that a meandering river with low sinuosity will therefore not have an extremely pronounced bend sorting. Thus the effects on sediment transport of sorting on the grain and bedform scale may be dominant, and the sorting on the scale of a meander bend may be considered as a weak forcing parameter on the scale of bedforms and grains.

2.6 Shortcomings of the present approaches

Above, the present approaches to sediment transport calculation of sand-gravel mixtures were reviewed, and the relevance of natural phenomena like sediment bimodality was discussed. There are hiatuses in the fundamental knowledge of processes, a number of relations between processes and between processes and deposits is not well known, and there are questions about the application of the knowledge in practical predictors and models. The fundamental questions are:

- i. The mobility of different grain sizes varies with flow conditions and mixture characteristics, but whether, and how it varies systematically, is not known. Bimodal sediment seems to behave in a distinctly different way than unimodal sediment, but it is not understood how and why (see [chapter 5](#)).
- ii. A plethora of bedform types have been observed in sediment mixtures, but it is not known systematically in what conditions these bedform types occur (see [chapter 4](#)).
- iii. It is not known whether and how the turbulent flow structure associated with dunes interacts with the vertical sediment sorting in dunes. In the troughs, the sediment is coarse

and near the threshold of motion except for strong bursts. Yet in this region, the entrainment and winnowing of sediment from the bed takes place when the dunes grow, and in this region an armour layer may form (see **chapter 10**).

- iv. The processes at the lee side of bedforms that lead to vertical sediment sorting are not well understood, and only little quantitative information is available how the sediment is sorted (see **chapters 7 and 8**).
- v. The discharge hydrograph, bedforms and armour layers may leave a historic record in the river bed in the form of vertically sorted sediment. The sediment transport and the grain size distribution of the transport material is at least partly determined by this vertically sorted sediment in the bed. It is not known how antecedent sorting affects the sediment transport process, e.g. how much hysteresis in transport rates it may cause (see **chapters 6 and 8**).

The more practical questions are:

- vi. The entrainment of different size fractions from a mixture is often calculated with the hiding-exposure approach. However, the empirical equations developed for the hiding-exposure correction of critical shear stress differ between rivers and between laboratory experiments, and it is only partly known why (see **chapter 5**).
- vii. Flow turbulence is important for the entrainment of sediment. It is not clear whether one should use a stochastic approach to turbulence or to the threshold of incipient sediment motion (see **chapter 5**).
- viii. It is not clear how sediment transport predictions can be done for conditions with vertical sediment sorting in dunes and armour layers below dunes and how the effects of a historic record of sediment sorting in the bed can be incorporated in sediment transport predictors (see **chapters 6, 9, 10 and 11**).

2.7 Objectives

The general objective in this thesis is to describe and quantify the processes of sediment transport in rivers in case of non-uniform sediment, with emphasis on mixtures of sand and gravel and the interaction between processes on the grain scale and the bedform scale. Specific objectives in this thesis are to:

- i. develop a predictor for selective sediment transport of mixtures, including the probability of movement for different size-fractions near incipient motion and fully mobile conditions (for permanent flow), and including sediment sorting on the grain scale (hiding-exposure phenomenon) (see **chapter 5**),
- ii. identify the bedform types that occur in sediment mixtures, and their significance for the sediment transport, both for permanent and non-permanent (floods) hydraulic conditions,

and develop a predictor for the bedform types (see **chapter 4**),

- iii. identify vertical sediment sorting processes and determine their role in sediment transport, in specific for the combination of dunes and armour layers (see **chapters 6 and 10**),
- iv. identify and quantify the effect of dune development, armouring and other sorting processes in the bed on sediment transport in non-steady conditions (discharge wave) (see **chapters 6, 9 and 10**),
- v. develop a model for bedform-related sorting processes of bed sediment and determine the effects of the vertical sorting on selective sediment transport of mixtures (see **chapters 9 and 11**).

2.8 Hypotheses and conceptual modelling approaches

Below, hypotheses are given that correspond to the objectives and shortcomings discussed above. Part of the hypotheses is based on the literature review, while other parts are conjectures. In addition, modelling approaches are suggested at the end of each hypothesis.

- i. The transport of a sediment mixture can be considered as the sum of the sediment transport of each uniform grain size fraction for all grain sizes present in the mixture. In that case, the hiding-exposure phenomenon is taken into account. In addition, the near-bed turbulence must be taken into account, as this affects the transport of the largest grain sizes which are near or below their threshold of motion.
Thus the transport might be computed with predictors for uniform sediment as follows. The sediment mixture is divided into grain size fractions. For each fraction, the transport can be computed with the predictor for uniform sediment. The hiding-exposure phenomenon can be incorporated by correcting the critical Shields parameter for each grain size fraction. The shear stress acting on the grains can be varied stochastically to account for near-bed flow turbulence. Even when the average shear stress is below the assumed threshold of motion, this stochastic approach should yield small transports. Thus the partial transport condition, averaged over the length of several dunes, can be adequately modelled (see **chapter 5**).
- ii. Bedform types in sediment mixtures are, just like their counterparts in uniform sediment, dependent on the flow conditions and sediment size. However, whether a bedform type is able to develop, is also dependent on the amount of sediment available for the formation of the bedforms, and the grain size of that available sediment. In the case of partial transport or an immobile armour layer, the bedforms may not be able to develop from the local bed sediment, because the entrainment or transport of finer sediment is inhibited by the overlying immobile coarse sediment. In those conditions, the bedform type is dependent on the upstream sediment input (see **chapter 4**).
- iii. Two processes may cause vertical sorting in the river bed, acting simultaneously. The first is grain size-selective entrainment and deposition of sediment, due to which a gravel lag may develop on the bed below the moving sediment (see **chapters 9 and 10**). The second

process is the vertical sorting in the grain flow at the lee-side of bedforms, which may also be preserved in the river bed (see **chapters 7 to 9**).

It is not clear how these two sorting processes and their interaction could be modelled. The grain-size selective deposition of a gravel lag in the troughs of dunes might be predicted with a fractionwise bedload transport predictor (given in hypothesis i.), but this is not likely to work since the predictor does not account for the flow structure in bedform troughs (see the previous section). The grain flow process is only qualitatively understood; a predictive model is not available.

- iv. Due to the vertical sorting processes mentioned in the previous hypothesis, the sediment in a river bed is sorted during a discharge wave. The depth from which this sorted sediment is entrained during a subsequent discharge wave, is determined by the depth of the bedform troughs during that discharge wave. Since bedload sediment transport partly depends on the grain size and mixture characteristics of the sediment available in the bed, the sorting affects the transport rate in rising discharge when the sediment is entrained from increasing depths below the bed surface. Thus both the sediment transport and the vertical sorting in the river bed are then expected to depend partly on the discharge history of the river as preserved in the river bed (see **chapters 9 and 11**).

The history effects of sediment sorting on sediment transport depend partly on the bedform height, which might be measured, or modelled with an appropriate predictor. Whether bedforms occur at all, could be predicted with the method given under hypothesis ii. The bedform height then determines the thickness of a transport layer, in which the sediment is entrained and sorted. The bedload transport of the transport layer could be computed with a fractionwise bedload transport predictor (given in hypothesis i.). The vertical sorting due to the two mechanisms described under hypothesis iii. can, however, not yet be predicted except with empirical formulae derived from flume or field measurements for reasons mentioned before.

2.9 Integral conceptual model

The hypotheses and modelling approaches given in the previous section can be combined into an integral conceptual model, which could be implemented in numerical models. This conceptual model is based on the morphodynamic system as described in the introduction (**chapter 1**, see fig. 1.2), in which all phenomena, conditions and sediment types are in principle incorporated. In figure 2.11 the structure of a morphodynamic system is given, including bedforms explicitly and thus emphasising the relations between the scales of grains and bedforms.

Every relation has a number and is described below. As given in the specific objectives, only relations 1, 2, 4, 7, 8 and 9 are addressed in this thesis. The net bed level change at the meander length scale, sorting at the meander scale, and the undulations due to dune migration are not referred to here because the morphodynamic model as sketched here refers to one single position on the river bed. It could in principle be applied to all positions in the framework of a two-dimensional morphological model.

1. The relation between water motion and sediment transport is given by a sediment transport predictor as described in hypothesis i. This relation only accounts for processes on the grain scale (see **chapter 5**).

Morphodynamic system

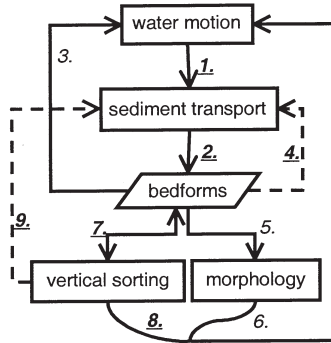


Figure 2.11. Conjecture of extended morphodynamic system of a river bed with bedforms (compare to figure 1.2). The relations are numbered, see text for explanation. The fat underlined numbers denote relations that are addressed in this thesis. Dashed lines indicate that there is no direct feedback but a history effect.

2. The transported bedload sediment is accumulated in the bedforms. The bedform type is dependent on the flow conditions, the sediment available for transport and the characteristics of the transported sediment as described in hypothesis ii (see **chapters 4 and 9**).
3. Bedforms change the flow characteristics. The flow separation at the brinkpoint of the bedforms causes turbulent vortices. This turbulence is the cause of hydraulic form roughness. The dimensions of the flow separation zone are dependent on the bedform brinkpoint height. In addition, the turbulence in the bedform trough partly determines the winnowing and entrainment of sediment. As argued in shortcoming vi. and hypothesis iii. it is not clear how to model this effect (see **chapter 6**).
4. The bedform height determines from what depth the bed sediment is entrained as described in hypothesis vi. If the bed sediment is vertically sorted as described under relation 7, then the dune height and sorting both determine what sediment is available for entrainment and transport. The dashed line in figure 2.11 denotes that this is not an immediate feedback but a history effect. Relations 4, 7 and 9 together form a strong interaction between the grain and bedform scale (see **chapter 9**).
5. If there is a net gradient in transport then the bed aggradates or degradates.
6. There is a feedback between bed level and water motion: local erosion of the bed will result in a larger water depth, which means a decrease in flow velocity, and vice versa.
7. The existence of bedforms in non-uniform sediment leads to a vertical sorting of sediment as described in hypothesis iii. This sorting has its own feedback mechanisms (arrows both ways). The base level of the bedforms is enriched with untransportable sediment, which will lead to a decrease and eventually complete arrest of the winnowing process (entrainment of sediment from the bedform troughs). This may be seen as a variant of the armouring process (see **chapters 4 and 9**).
8. The bed surface grain size (resulting from the sorting processes) has a small influence on the water motion, as it determines the hydraulic grain roughness (as described in the literature review) (see **chapter 5**).

9. The sedimentological history in the bed due to vertical sorting by bedforms determines partly what sediment is available for sediment transport as described in hypothesis iv. The dashed line in figure 2.11 denotes that this is not an immediate feedback but a history effect (see chapters 6 and 9 to 11).

2.10 The sky is not the limit

This study has been constrained within a certain range of phenomena, conditions and sediments, given here in order of decreasing length scale:

- Braided rivers are not considered, because of their widely differing planform (wandering bars) compared to meandering rivers,
- The spatial scale not larger than one meander bend and not smaller than the scale of hiding/exposure (see fig. 1.2),
- Sediment sorting is only studied in the vertical direction (e.g. caused by bedforms), not in the horizontal direction like sorting in meander bends, patchiness,
- No flow calculations are done: flow is a (measured) boundary condition, and turbulence is described with straightforward statistical techniques, thus excluding relations 4 and 9,
- No extensive bedform generation mechanisms are considered, the presence of bedforms is a boundary condition, which excludes relation 9,
- No morphological modelling of bed level change is done, this study is limited to the sediment entrainment, transport and deposition processes at a point, thus excluding relations 3 and 4,
- No extensive armour layer generation mechanisms are considered,
- Only bedload sediment transport is included presently, suspended bed sediment transport is only addressed when necessary to understand the vertical sorting in bedforms, thus excluding part of relation 1.

2.11 References

- ALLEN, J. R. L. (1970), The avalanching of granular solids on dune and similar slopes. *Journal of Geology* 78. pp. 326-351.
- ALLEN, J. R. L., (1984), *Sedimentary structures, their character and physical basis*, 1. *Developments in Sedimentology* 30; Elsevier, Amsterdam, The Netherlands, 593 pp.
- ALLEN, J. R. L., & COLLINSON, J. D. (1974), The superimposition and classification of dunes formed by unidirectional aqueous flows, *Sedimentary Geology* v. 12, p. 169-178.
- BENNETT, S. J. & BEST, J. L. (1995), Mean flow and turbulence structure over fixed, two-dimensional dunes: implications for sediment transport and bedform stability. *Sedimentology* 42 pp. 491-513.
- BRIDGE, J. S. & BENNETT, S. J. (1992), A Model for the Entrainment and Transport of Sediment Grains of Mixed Sizes, Shapes and Densities. *Water Resources Research* 28 (2) pp. 337-363.
- BOERSMA, J. R., VAN DE MEENE, E. A. & TJALSMA, R. C. (1968), Intricated cross-stratification due to interaction of a mega ripple with its lee-side system of backflow ripples (upper-pointbar deposits, Lower Rhine), *Sedimentology* 11 pp. 147-162.
- BUFFINGTON, J. M. & MONTGOMERY, D. R. (1997), A systematic analysis of eight decades of incipient motion studies, with special reference to gravel-bedded rivers. *Water Resources Research* 33 (8) pp. 1993-2029.

- BUFFINGTON, J. M. & MONTGOMERY, D. R. (1998), Correction to "A systematic analysis of eight decades of incipient motion studies, with special reference to gravel-bedded rivers". *Water Resources Research* 34 (1) pp. 157-157.
- CARLING, P. A. (1990), Particle over-passing on depth-limited gravel bars. *Sedimentology* 37, pp. 345-355.
- CARLING, P. A. (1999), Subaqueous gravel dunes. *Journal of Sedimentary Research*, 69(3), pp. 534-545.
- DE JONG, C. (1995), Temporal and spatial interactions between river bed roughness, geometry, bedload transport and flow hydraulics in mountain streams - examples from Squaw Creek (Montana, USA) and Lainbach/Schmiedlaine (Upper Bavaria, Germany). Institut für Geographische Wissenschaften der Freien Universität Berlin. 1-229, 1995. Ph.D thesis.
- DIETRICH, W. E. & SMITH, J. D. (1984), Bed load transport in a river meander. *Water Resources Research* 20 no. 10., pp. 1355-1380.
- DUIZENDSTRA, H. D. (1999), Sedimenttransport in de Grensmaas. Rijkswaterstaat, Rijksinstituut voor Zoetwaterbeheer en Afvalwaterbehandeling (RIZA), werkdocument 99.158x.
- EGIAZAROFF, I. V. (1965), Calculation of nonuniform sediment concentrations. *Journal of the Hydraulics Division, ASCE* 91 (HY4) pp. 225-248.
- EINSTEIN, H. A. (1937), Bed load transport as a probability problem. In: H. W. Shen (ed.) *Sedimentation*. Zurich:Verlag Rascher & Co. 1-105.
- EINSTEIN, H. A. (1950), The bed-load function for sediment transportation in open channel flows. Washington, D.C.:U.S. Dep. of Agriculture, Soil Conservation Service. Technical Bulletin, 1026..
- ENGELUND, F. & HANSEN, E. (1967), A monograph on Sediment transport. Technisk Forlag, Copenhagen, Denmark.
- GESSLER, J. (1971), Critical shear stress for sediment mixtures. *Hydraulic research and its impact on the environment*. Conference Proc. IAHR 3 Paris, pp. c1-1 - c1-8.
- GRASS, A. J. (1970), Initial instability of fine sand bed. *J. of the Hydr. Div., ASCE*, 96 no. HY3, pp. 619-632.
- HAMAMORI A. (1962), A theoretical investigation on the fluctuation of bed-load transport, Delft Hydraulics, report R4, Delft, The Netherlands.
- IKEDA, H. & ISEYA, F. (1988), Experimental study of heterogeneous sediment transport, University of Tsukuba, Environmental Research Center, Paper no. 12.
- ISEYA, F. & IKEDA, H. (1987), Pulsations in bedload transport rates induced by a longitudinal sediment sorting: a flume study using sand and gravel mixtures. *Geografiska Annaler* 69A, no. 1 pp. 15-27.
- JOPLING, A. V. (1965), Laboratory study of the distribution of grain sizes in cross-bedded deposits, in: MIDDLETON, G. V. (ed.) *Primary sedimentary structures and their hydrodynamic interpretation*, spec. publ. no. 12, Soc. of Econ. Paleontologists and Mineralogists, Oklahoma, U.S.A.
- KALINSKE, A. A. (1947), Movement of sediment as bed load in rivers. *Transactions, American Geophysical Union* 28 (4) pp. 615-620.
- KISLING-MØLLER, J. (1993), Bedform migration and related sediment transport in a meander bend. *Special Publications of the International Association of Sedimentology* 17, pp. 51-61.
- KLAASSEN, G. J. (1986), Morphology of armoured river beds, experiments with high discharge waves (in Dutch), Delft Hydraulics report M2061.
- KLAASSEN, G. J. (1987), Armoured river beds during floods. *Euromech 215*, Genova, Italy, September 15-19, also Delft Hydraulics publication 394, Delft, The Netherlands.
- KLAASSEN, G. J. (1991), Experiments on the effect of gradation and vertical sorting on sediment transport phenomena in the dune phase. *Grain Sorting Seminar*, 21-25 October, 1991, Ascona (Switzerland).
- KLAASSEN, G. J., RIBBERINK, J. S. & DE RUITER, J. C. C. (1987) On the transport of mixtures in the dune phase. *Euromech 215 Colloquium*, Genova, Italy, September 15-19, also Delft Hydraulics publication 394, Delft, The Netherlands.
- KLAASSEN, G. J., LAMBEEK, J., MOSSELMAN, E., DUIZENDSTRA, H. D. & NIEUWENHUIJZEN, M. E. (1999), Re-naturalization of the Meuse river in the Netherlands. In: KLINGEMAN, P.C. (1998), *Gravel-bed rivers in the environment : workshop held at Gold Bar, Washington, 20-26 August 1995*. Highlands Ranch [CO-USA] Water Resources Publications, pp. 655-674.
- KUHNLE, R. A. & WILLIS, J. C. (1992), Mean size distribution of bed load on Goodwin Creek. *Journal of Hydraulic Engineering* 118 (10) pp. 1443-1446.

- KUHNLE, R. A. (1993), Incipient motion of sand-gravel sediment mixtures. *Journal of Hydraulic Engineering* 119 (12) pp. 1400-1415.
- LISLE, T. E., & HILTON, S. (1999), Fine bed material in pools of natural gravel bed channels; *Water Resources Research*, 35(4), pp. 1291-1304.
- LIVESEY, J., BENNETT, S. J., ASHWORTH, P. J. & BEST J. L. (1996), Flow, sediment transport and bedform dynamics in bimodal sediments. *International Workshop on Gravel-bed Rivers IV 1996*, Goldbar, Washington, USA.
- MEYER-PETER, E., & MUELLER, R. (1948), Formulas for bed-load transport; 3rd Conf. Int. Assoc. of Hydraul. Res. Stockholm, Sweden, pp. 39-64, 1948.
- MOSSELMAN, E. & AKKERMAN, G. J. (1998), Low-mobility transport of coarse-grained material. *Delft Hydraulics report Q2395.40*, Delft, The Netherlands.
- MOSLEY, M. P. (ed.) (2001), *Gravel-bed rivers V*, pp. 212-214, New Zealand Hydrological Society Inc, Wellington, New Zealand.
- OLESEN, K. W. (1987), Bed topography in shallow river bends. *Communications on Hydraulic and Geotechnical Engineering No. 87-1*, PhD thesis Delft University of Technology, Delft, The Netherlands.
- PAINTAL (1971), Concept of critical shear stress in loose boundary open channels, *J. Hydr. Res., IAHR*, Vol 9 No. 1.
- PAOLA, C. & SEAL R. (1995), Grain size patchiness as a cause of selective deposition and downstream fining. *Water Resources Research* 31 (5) pp. 1395-1407.
- PARKER, G. P., DHAMOTHARAN, S., & STEFAN, H. (1982), Model experiments on mobile paved gravel bed streams. *Water Resources Research* 18 (5) pp. 1395-1408, 1982.
- PARKER, G. P., KLINGEMAN, P. C., & MCLEAN, D. G. (1982), Bedload and size distribution in paved gravel-bed streams. *Journal of Hydraulic Engineering* 108 (HY4) pp. 544-571.
- PARKER, G. P., & KLINGEMAN, P. C. (1982), On why gravel bed streams are paved. *Water Resources Research* 18 (5) pp. 1409-1423.
- PARKER, G. (in prep.), Transport of gravel and sediment mixtures. In: *Manual 54, Chapter 3*, American Society for Civil Engineering.
- PARKER, G., PAOLA, C. & LECLAIR, S. (2000), Probabilistic Exner sediment continuity equation for mixtures with no active layer, *Journal of Hydraulic Engineering* 126 (11) pp. 818-826.
- POWELL, D. M. (1998), Patterns and processes of sediment sorting in gravel-bed rivers. *Progress in Phys. Geogr.* 22 (1) pp. 1-32.
- REID, I., FROSTICK, L. E. & LAYMAN, J. T. (1985), The incidence and nature of bedload transport during flood flows in coarse-grained alluvial channels. *Earth Surf. Proc. Land.* 10 pp. 33-44.
- REID, I., & LARONNE, J. B. (1995), Bed load sediment transport in an ephemeral stream and a comparison with seasonal and perennial counterparts. *Water Resources Research* 31 (3) pp. 773-781.
- RIBBERINK, J. S. (1987), Mathematical modelling of one-dimensional morphological changes in rivers with non-uniform sediment. Ph.D. thesis, Delft University, The Netherlands.
- SALLENGER, A. H. (1979), Inverse grading and hydraulic equivalence in grain-flow deposits. *J. of Sed. Petr.* 49 (2) pp. 553-562.
- SEAL, R., TORO-ESCOBAR, C., CUI, Y., PAOLA, C., PARKER, G. P., SOUTHARD, J. B. & WILCOCK, P. R. (1996), Downstream fining by selective deposition: theory, laboratory and field observations. *International Workshop on Gravel-bed Rivers IV 1996*, Goldbar, Washington, USA.
- SIMONS, D. B., & RICHARDSON, E. V., 1965. A study of variables affecting flow characteristics and sediment transport in alluvial channels; In: *Federal Inter-agency Sediment Conf. 1963 Proc.*, Misc. Pub. US Agric. 970, Washington, USA, pp. 193-207.
- SOUTHARD, J. B., & BOGUCHWAL, A., 1990. Bed configurations in steady unidirectional water flows. Part 2. Synthesis of flume data; *Journal of Sedimentary Petrology*, 60 no. 5, pp. 658-679.
- TEN BRINKE, W. B. M. (1997), *De bodemsamenstelling van Waal en IJssel in de jaren 1966, 1976, 1984 en 1995*. Rijkswaterstaat, Rijksinstituut voor Zoetwaterbeheer en Afvalwaterbehandeling (RIZA), rapport 97.009.
- VAN DEN BERG, J. H. (1987), Bedform migration and bed-load transport in some rivers and tidal environments. *Sedimentology* 34 pp. 681-698.
- VAN DEN BERG, J.H. (1987), Bedform migration and bed-load transport in some rivers and tidal

- environments. *Sedimentology* 34 pp. 681-689.
- VAN DEN BERG, J. H., & VAN GELDER, A., 1993. A new bedform stability diagram, with emphasis on the transition of ripples to plane bed in flows over fine sand and silt; *Spec. Publs. Int. Ass. Sediment.* 17, pp. 11-21.
- VAN DEN BERG, J. H. (1995), Prediction of alluvial channel pattern of perennial rivers. *Geomorphology* 12, pp. 259-279.
- VAN DEN BERG, J. H., DE KRAMER, J., KLEINHANS, M. & WILBERS, A. (2000), De Allier als morfologisch voorbeeld voor de Grensmaas. I: vergelijkbaarheid en rivierpatroon. *Natuurhistorisch Maandblad*, juli 2000, pp. 118-122.
- VAN RIJN, L. C. (1984), Sediment transport, part I: bed load transport. *Journal of Hydraulic Engineering* 110 (10) pp. 1431-1456.
- VAN RIJN, L. C. (1993), Principles of sediment transport in rivers, estuaries and coastal seas, Oldemarkt: Aqua Publications.
- WATHEN, S. J., FERGUSON, R. I., HOEY, T. B. & WERRITTY A. (1995), Unequal mobility of gravel and sand in weakly bimodal river sediments. *Water Resources Research* 31 (8) pp. 2087-2096.
- WHITING, P. J., DIETRICH, W. E., LEOPOLD, L. B., DRAKE, T. G., & SHREVE, R. L., 1988. Bedload sheets in heterogeneous sediment; *Geology*, 16, pp. 105-108.
- WILCOCK, P. R. (1993), Critical shear stress of natural sediments. *Journal of Hydraulic Engineering* 119 (4) pp. 491-505.
- WILCOCK, P. R. & MCARDELL B. W. (1993), Surface-based fractional transport rates: mobilization thresholds and partial transport of a sand-gravel sediment. *Water Resources Research* 29 (4) pp. 1297-1312.
- ZANKE, U. (1990), The beginning of sediment motion as a probability problem (in German). *Wasser + Boden* 42 (1).

3

Method and accuracy of sediment transport measurements in large sand-gravel bed rivers

"First get your facts; then you can distort them at your leisure." Mark Twain

Abstract

The accuracy of cross-channel integrated sediment transport of bed-material is determined with an elaborate set of field measurements in the river Waal, the Netherlands. The measurements were done during a discharge wave in the upstream part of the river, which has a bimodal sand-gravel-bed.

The sampling strategy should take both spatial and temporal aspects into account to obtain maximum accuracy. Presence of moving bedforms, differences in bed sediment grain size in the cross-section and presence of preferential transport lanes dictate that at least 5 subsections for sampling in the cross-section are necessary.

The accuracy of cross-channel integrated bedload transport depends mainly on the measurement strategy. An uncertainty of less than 20% (bedload) and 7% (suspended load) of cross-channel integrated sediment transport is shown to be feasible if 30 samples of bedload and 2 vertical profiles of suspended bed-material load are taken in one subsection, provided that the cross-section of the river is divided into at least 5 subsections. The samples in one subsection should be distributed over the length of the bedform.

Changes of discharge during the measurements cause systematic differences between the subsections. To minimize this uncertainty a compromise between the spatial and temporal accuracy is necessary. Therefore, when only one vessel with instruments is available for doing the measurements, the number of sampling positions and subsections must be reduced if the rate of change of discharge is large.

Based on the results a prediction method is given to estimate the feasible accuracy in the planning phase of future campaigns, and the necessary time and financial investment for that accuracy.

This chapter is reproduced from:

Kleinhans, M. G. & Ten Brinke, W. B. M. (2001). Accuracy of cross-channel sampled sediment transport in large sand-gravel-bed rivers. *Journal of Hydraulic Engineering* 127(4), ASCE, pp. 258-269, reproduced with permission of the ASCE.

3.1 Introduction

3.1.1 Objective and definitions

Accurate assessment of cross-section integrated sediment transport in a river is important for many research and engineering questions. Sediment transport in rivers is often estimated by inter- and extrapolation of measurements in a cross-section. Samples taken with a trap-type instrument (e.g. Helley Smith and Nile Sampler) are small and the duration of sampling is short relative to the spatial and temporal variations in transport. This is also true for locally determined vertical profiles of suspended transport. In large rivers these variations may lead to unacceptable large errors in mean transport, even after averaging of repetitive measurements.

This paper deals with the question of accuracy of sediment transport estimates based on *in situ* measurements in the Dutch river Waal. This is done by an empirical assessment of the contributions of systematic errors, stochastic errors and natural variability. Although some stochastic errors could not be separated from natural variability with the present dataset, they are discussed separately to be able to minimize them effectively in the measurement strategy and data processing procedures. By choosing a sampling strategy that covers the important time and spatial scales of transport variation the contribution of natural variability to the overall uncertainty can be minimized. The strategy of sampling in relation to the natural variability of sediment transport is the main object of this paper. Measurements of sand-gravel transport were done with a trap-type (Helley Smith like) bedload sampler and a 1-D (acoustical) suspended load instrument. As a second goal, the study aims at finding a decision tool for setting up a sampling program in a river based on a pre-defined level of accuracy.

For practical reasons, bedload transport is defined as the transport of bed material between the bed and the height of the bedload sampler. Suspended transport is then defined as the transport of bed material above the bedload sampler. Wash load (clay and silt $< 64 \mu\text{m}$) is not included in this study.

Uncertainty is defined herein as a relative standard error (given in percentages of the average values), which can be calculated as the difference between the average value and the value of the 67% error margin.

3.1.2 Review

Spatial variations of sediment transport in meandering sand-gravel-bed rivers are mainly caused by bedforms and systematic grain size sorting of bed sediment in meander bends due to cross-sectional flow distribution. Temporal variations of sediment transport in a single point are mainly caused by turbulence, changes in bed shear stress due to variations in discharge and water surface gradient and the movement of bedforms at that point. Both spatial and temporal variations of transport have been studied extensively (e.g. Gaweesh & Van Rijn 1994; Kuhnle 1996; Powell 1998). Implications of these variations for the strategy of field measurements to obtain an accuracy as high as possible, however, have received relatively little attention. The available studies were done in very small channels mostly.

Emmett (1980) mentions that cross-channel and temporal variations of bedload are significant but does not quantify the effects. From experience Emmett estimates that 20 equally spaced samples across the river are necessary for a 15 m wide sand-gravel-bed river. This number is a

subjective compromise between the necessary spatial coverage and the time needed for sampling across the river. It is not clear how accurate this method is.

Hubbell (1987) studied the effect of temporal and cross-channel variation of bedload transport on the uncertainty of the cross-channel averaged bedload transport. Hubbell found that both temporal and spatial variations affect the final uncertainty. With high temporal variations in transport Hubbell recommended fast repetitive sampling of the cross-section at only a few points. With high spatial variation, sampling is recommended at those positions only that are required to identify the lateral distribution of mean transport. In this way the measurement effort is minimized. Hubbell found that an uncertainty of less than 20% is feasible with between 100 and 200 samples when variation of transport in the cross-section is moderate, but no method could be given to choose the appropriate strategy beforehand.

Recently, Gomez & Troutman (1997) modelled bedform behaviour at moderate transport conditions to obtain the best sampling scheme. They found that an optimal compromise between spatial and temporal variation was to sample four or five times across the river and collect 20-40 samples over a period of 3-8 hours. However, these results are obtained for small rivers and neglect performance of samplers and large scale spatial variability of flow and bed material.

Powell et al. (1995) measured bedload transport in small ephemeral channels with only three to five recording bedload traps. They found that the cross-stream variability is larger and more complex for wider channels and with higher stages. Powell et al. (1995) hypothesized that secondary flow can develop better in wider channels and during higher stages, which explains the higher variability of the sediment transport. This indicates that the total uncertainty of cross-channel sampled bedload transport may be larger in wider rivers, depending on the measurement strategy.

Gaweesh & Van Rijn (1994) estimated the uncertainty of cross-channel integrated bedload transport with field measurements on the rivers Nile (Egypt) and Rhine (The Netherlands). These rivers are much larger than previous examples, but the discharge (and therefore the temporal variation in transport) was low and constant. The measurements were done with a ship-board operated trap-type (like a Helley Smith, e.g. Emmett 1980) bedload sampler ('Nile-sampler'). Both meandering rivers had depths of a few meters and widths of a few hundred meters. The river beds consisted of medium and coarse sands and were covered with dunes with heights of a few decimeters and lengths of several tens of meters. The cross-section was divided in 7 subsections, in all of which samples were taken on five fixed locations along a bedform from trough to top, thus accounting for a part of the spatial and temporal variation. At each position on the dune ten samples were taken with the bedload sampler, in contrast with Emmett (1980) and Hubbell (1987), who only took one sample at every measurement position. All samples in each subsection were used to determine the relative error of the mean transport as a function of the number of samples. This function was combined with the uncertainty of width of subsections in an error analysis to calculate the uncertainty of the cross-channel integrated transport. Gaweesh & Van Rijn (1994) found that the uncertainty was about 20 percent if the cross-section was divided in seven subsections, in which 25 samples were taken on 5 positions distributed along the bedform length.

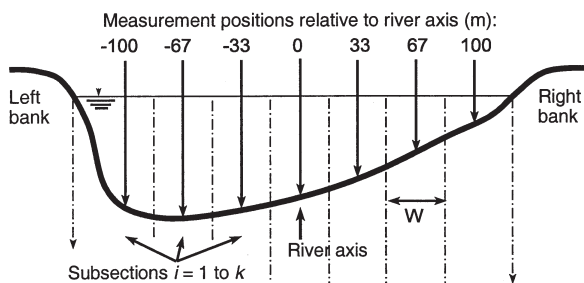
Van Rijn (1993) estimated the uncertainty of cross-channel integrated suspended load transport. The same approach as in Gaweesh & Van Rijn (1994) was followed: the relative error of the integrated transport was calculated as a function of the variance of velocity, concentration, height above the bed and an interpolation error. Van Rijn found that the final uncertainty was about 20% if the cross-section was divided in six subsections, and if the vertical profiles of suspended transport ('verticals') had at least 6 levels above the bed. No data were available of suspended transport measurements in the presence of dunes.

If a pavement or armour is present, then initial sediment transport and bedform development only occur above certain threshold shear stresses. These threshold shear stresses are only exceeded during high discharge waves. In large sand-gravel-bed and gravel-bed rivers, it is therefore most interesting to do measurements of sediment transport during high discharge waves. However, the accuracy in these cases was unknown until now, since most findings are restricted to bedload in small streams or during low discharges.

3.2 Uncertainties in cross-channel integration of sediment transport

3.2.1 Integration of measured data

A. Measurement positions in the cross-section



B. Measurement positions in planform

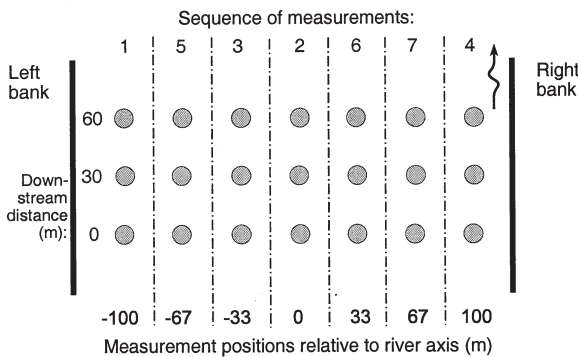


Figure 3.1. Measurement positions in the cross-section (a) and in planform (b).

The uncertainty of cross-channel integrated transport, and the strategy to minimize it, can partly be derived from the integration method, which is as follows. The cross-section is divided in a number of subsections in which samples of bedload transport and vertical profiles of suspended load ('verticals') are taken distributed over the length of bedforms (see Fig. 3.1). First the average transport of each subsection is calculated for unit width. Then the average

transport is multiplied with the width of the subsection. The sum of transports in all subsections finally gives the cross-channel integrated sediment transport:

$$Q_s = c \sum_{i=1}^k (\bar{q}_{s,i} \Delta W_i) \quad (1)$$

in which Q_s = cross-channel integrated bedload or suspended load transport; c = correction for all systematic errors; k = number of subsections in the cross-section, $\bar{q}_{s,i}$ = mean measured bedload or suspended load transport for unit width in subsection i ; and ΔW_i = width of subsection i . Both terms between brackets have uncertainties, that will be quantified separately.

3.2.2 Sources of uncertainty in the integration

The accuracy of cross-channel integrated transport depends on two factors: first, the measurement techniques including the method for integrating the data across the river, and second, the strategy of sampling with respect to the natural variability of transport. It is important to distinguish between systematic errors, stochastic errors and natural variability. Systematic errors have an effect on the amount of transport, but not on its accuracy in terms of relative 'error' margins. Stochastic errors and natural variability have an effect on the final relative accuracy of the transport, but not on its absolute amount.

The measurement techniques may have systematic errors and stochastic errors. Systematic errors are accounted for with calibration factors of the measurement instruments (correction c in equation 1), and are not discussed extensively in this paper. Stochastic errors originate from the measurement techniques and their shortcomings, e.g. the positioning of the instruments. Natural variability will be discussed later.

The width of most subsections is defined in the strategy (see Fig. 3.1), except for the subsections at both river banks. The width of the outer two subsections depends mostly on bank morphology and presence of constructions (e.g. groynes) in relation to the water level. It is assumed that the exchange of sediment between the bed and the area between the groynes is negligible compared to the transport in the channel. The sediment transporting width of the outer subsections and its error may be estimated from cross-channel bathymetry. Thus the error in width (ΔW_i) only has to be included for subsections $i = 1$ and $i = k$.

3.2.3 Systematic interpolation error

To determine the total sediment transport rate, the transport distribution must be integrated over the cross-section. The smooth cross-channel distribution of transport is represented with k line segments. Therefore, a systematic interpolation error is made, which has to be included in the constant (c) in equation 1. This error can be estimated by comparison of hypothetical 'true' distributions and a discrete approximation with k subsections (see Fig. 3.2). By taking a hypothetical 'true' distribution the effect of a systematic interpolation error is effectively separated from measurement errors and calibration errors. It is expected that more subsections will give a better approximation of the true cross-channel distribution of transport, because an infinite number of subsections results in a zero interpolation error.

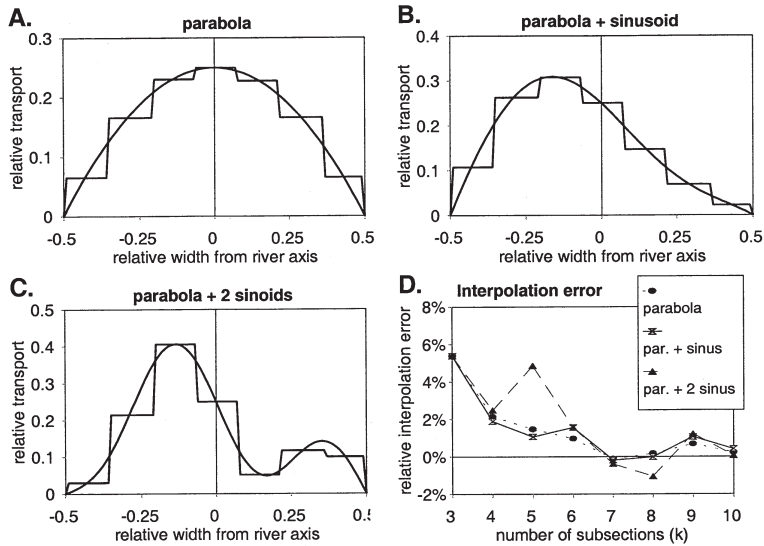


Figure 3.2. Hypothetical cross-channel distribution of transport and discrete approximations with seven subsections (figs. a-c), and the resulting interpolation error as a function of the number of subsections.

The measured distribution of sediment transport over the (regular) cross-section of a river often can be described with a parabola or skewed parabola (Hubbell 1987; Kleinhans 1997b). This parabola is approximated with segments of the width of the subsections in which the sampling was done. In the middle of a subsection the transport is by definition the same as the hypothetical one at that point (see Fig. 3.2). The true area of a parabola is calculated and compared to the area of the histogram with k columns, the same number as the number of subsections. The difference between the area of the discrete approximation and the true area of the hypothetical distribution is the interpolation error. The effect of the number of subsections can be assessed by varying k .

To show that this analysis is not very sensitive to the assumption of a simple parabolic distribution, three hypothetical distributions are tested (see Figs. 2a-c): a parabola, a skewed parabola and a double parabola. These distributions are considered as idealized examples of a straight river section, a meander bend section and a section in a braided river with one mid-channel bar respectively.

As expected, the interpolation error is inversely proportional to the number of subsections and the irregularity of the distributions (see Fig. 3.2d). It is also shown that the interpolation error is on average positive which means an overestimation of true surface. The systematic interpolation error is smaller than 2% with five to seven subsections, and the form of the histogram resembles the true form of the distribution with 5 or more subsections. The rise in interpolation error at 9 subsections (see Fig. 3.2d) is part of the damped oscillation of the error with an increasing number of subsections due to the specific form of the distributions and the small number of subsections in the discrete approximation.

3.2.4 Stochastic uncertainty of transport sampling

The uncertainty of the average of samples in a subsection is given in relative form as the variation coefficient (VC), here defined as:

$$VC_s = \frac{s_{\bar{q}_s}}{\bar{q}_s \sqrt{n}} \quad (2)$$

in which VC_s = variation coefficient of q_s in a subsection; s_{q_s} = standard deviation of all bedload samples or suspended load verticals in a subsection; and n = number of bedload samples or verticals of suspended transport. With the assumption that sampled sediment transport is normally distributed, the use of the square-root of n in the denominator is allowed. In this way the uncertainty of q_s depends on the number of samples.

3.2.5 Combining all the uncertainties

The uncertainties of the two terms q_s and ΔW_i have to be combined to get the uncertainty of the integrated transport Q_s . For simplicity it is assumed that both uncertainty parameters are normally distributed and are stochastically independent. Furthermore it is assumed that the hydrodynamic conditions are constant during sampling of the cross-section. The effect of changing hydrodynamic conditions will be addressed in the discussion section.

The combination of the uncertainties is done with straightforward error analysis rules. The error of width is included for $2j$ subsections, with j = the number of channels. If a river has only one channel, then $j = 1$ (two banks), and if a river has islands or more than one channel, this should be adapted by including the error of width as many times as there are banks in the cross-section. Therefore, the variance of transport of the outer subsections is a sum of the squared relative error of width and the squared (relative) uncertainty of transport in a subsection:

$$Rel_{s,i}^2 = VC_s^2 + \left(\frac{s_{\Delta W}}{\Delta W} \right)^2 \quad (3)$$

in which $s_{\Delta W}$ = uncertainty of width and $Rel_{s,i}^2$ = relative variance of sediment transport in subsection i . For the other $k-2j$ subsections only the VC_s^2 has to be added:

$$Rel_{s,i}^2 = VC_s^2 \quad (4)$$

To be able to sum the uncertainties of all subsections according to the rules of error analysis, the variances of the transport in each subsection i must not be written in relative but in absolute form:

$$(s_{Q_s})^2 = \sum_{i=1}^k (\bar{q}_{s,i} \cdot Rel_{s,i})^2 \quad (5)$$

in which $(s_{Q_s})^2$ is the absolute variance of the cross-channel integrated transport. This final uncertainty is made relative with the cross-channel integrated transport:

$$\left(\frac{s_{Q_s}}{Q_s}\right)^2 = \frac{\sum_{i=1}^k (\bar{q}_{s,i} \cdot Rel_{s,i})^2}{Q_s^2} = \sum_{i=1}^k \left(\frac{\bar{q}_{s,i}}{Q_s} \cdot Rel_{s,i}\right)^2 \quad (6)$$

By adding the relative variances of equation 3 and 4 for $k-2j$ resp. k subsections in equation 6, the following equation for the relative variance of cross-channel integrated transport is found:

$$\left(\frac{s_{Q_s}}{Q_s}\right)^2 = \sum_{i=1}^{2j} \left[\frac{\bar{q}_{s,i}}{Q_s} \sqrt{VC_{s,\max}^2 + \left(\frac{s_{\Delta W}}{\Delta W}\right)^2}\right]^2 + \sum_{i=1}^{k-2j} \left[\frac{\bar{q}_{s,i}}{Q_s} VC_{s,\max}\right]^2 \quad (7)$$

The first part of the right hand side is the relative variance of the $2j$ subsections next to the river banks, and the second part is the relative variance of the other $k-2j$ subsections. The VC_s is a.o. calculated with the standard deviation of the transport measurements (see equation (2)). Since especially bedload samples tend to be grouped in small and large catches due to systematic variation on bedform crests migrating into the sampler, these standard deviations generally underestimate the true, longer-term variability of bedload based on relatively small numbers of bedload samples. To compensate for this potential error the maximum $VC_{s,\max}$ of all subsections instead of the measured $VC_{s,i}$ is taken. The variation coefficients can be determined with measurements of the transport.

The ratio $q_{s,i}/Q_s$ for each i implies *a priori* knowledge of the cross-channel distribution of transport, which is unavailable in the planning phase. Since the average transport $q_{s,i}$ in a subsection is equal to Q_s/k , the average ratio $q_{s,i}/Q_s$ is $1/k$. The equation can now be simplified by substituting $1/k$ for $q_{s,i}/Q_s$:

$$\left(\frac{s_{Q_s}}{Q_s}\right)^2 = 2j \left[\frac{1}{k} \sqrt{VC_{s,\max}^2 + \left(\frac{s_{\Delta W}}{\Delta W}\right)^2}\right]^2 + (k - 2j) \left[\frac{1}{k} VC_{s,\max}\right]^2 \quad (8)$$

This simplification is useful since the uncertainty related to different strategies can now be assessed *a priori*. The effect of the simplification is studied below by comparing the outcome of (7) and (8).

3.3 Set-up of field measurements

3.3.1 Field site and conditions

The measurement location was the upstream section of the river Waal, the Netherlands (see Fig. 3.3.). The river Waal is heavily shipped, and its banks are protected with groynes. The

average width of the river between the groynes is 240 m and the local water depth varies between 3 and 12 m. The average discharge of the Waal is 1350 m³/s, with peaks up to 8000 m³/s. With high discharges bedforms develop with lengths of 10 to 20 m and heights of 0.5 m over the full width of the river at the measurement location (Wilbers 1998).

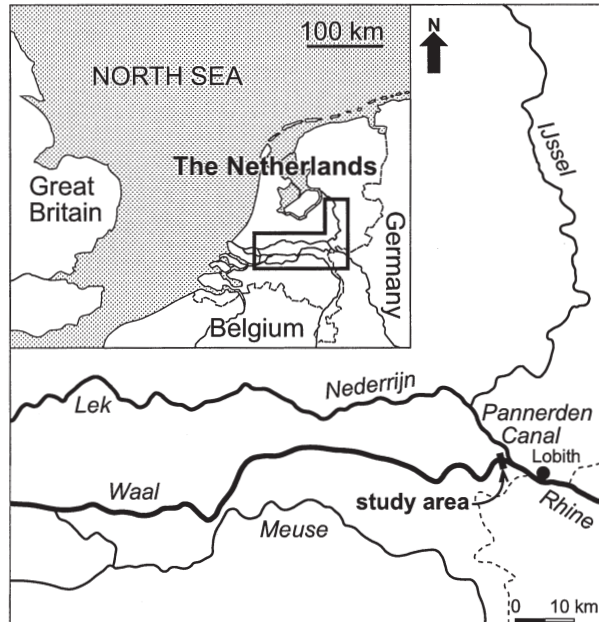


Figure 3.3. Field site location.

The measurements were done on March 1 to 14, 1997. In Table 1 the basic parameters of the field data are given. In Figure 3.4 the discharge curve is given and the measurement moments in time. The river was crossed two times (labels 1 and 2), giving two subsets of data for which the accuracy can be determined. After the discharge peak four extra detailed measurements were done at the same location (labels 3).

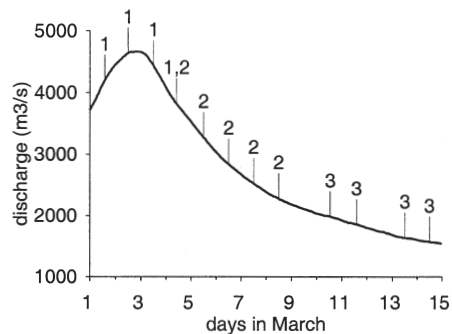


Figure 3.4. Discharge of the river Waal in the period March 1-14, 1997. Tags denote times of measurements, labels denote cross-section numbers.

At the measurement location the bed consists of a bimodal sand-gravel mixture with a median diameter of 2.8 mm, with the two modes at 0.5 mm and >8 mm. The bedload material is finer than the bed material, especially at the coarse end of the sieve curve (see Fig. 3.5). The

D90 of suspended sediment is about $300\ \mu\text{m}$, while the mesh bag of the bedload sampler has a mesh size of $250\ \mu\text{m}$. This means that the bedload sieve curve was hardly influenced by suspended load that was accidentally sampled with the bedload sampler.

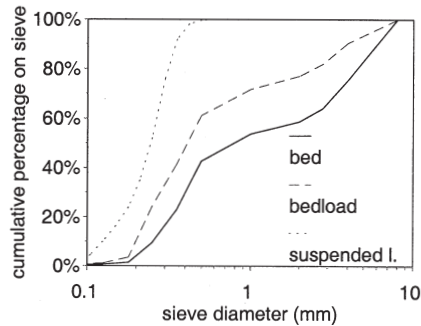


Figure 3.5. Sieve curves of bed material, bedload material and suspended material.

3.3.2 Natural variability of sediment transport

Natural variability of transport in a cross-section has many components on different scales of time and space. Here only the components are included that are of importance on the scale of a measurement campaign in one cross-section during a discharge wave. Contributions to the spatial variation are:

1. presence of preferential transport lanes,
2. cross-channel variation in grain size / sorting of bed sediments,
3. presence of bedforms, also cross-sectional differences in bedforms.

Contributions to the temporal variation are:

4. propagation of bedforms, resulting in a quasi-cyclic transport pattern,
5. macro-scale turbulence and
6. change of flow conditions during one set of measurements in a cross-section, especially during a discharge wave.

Table 3.1. Basic parameters of the field data set.

*	in m from river axis, positive coordinates are at the right half of the river when looking downstream
¶:	average water discharge during measurements in first river crossing: $4205\ \text{m}^3/\text{s}$ and in second $2645\ \text{m}^3/\text{s}$ (excluding 10-14 March)
†:	due to technical problems no data available
‡:	relative standard deviation, in table averaged per subsection (see text for explanations of symbols)
§:	corrected transport for changes in discharge (not done for subsections 84, 16, -16 and -84 m), see text
ASTM:	Acoustic Sand Transport Meter
HSZ:	Helley Smith Sand, adapted Helley Smith bedload sampler for sand-gravel sediment

Table 3.1 (continued). Basic parameters of the field data set.

Days in March 1997	Subsection	Discharge of Waal	Temperature	Suspended Transport	s_p/q_p †	number of verticals	Corrected suspended transport	Water Depth at ASTM	Flow Velocity ASTM	Bedload Transport	s_p/q_p †	number of catches	Corrected bedload transport
m*	m ³ /s †	g/sm	°C	g/sm	-	g/sm §	m	m/s	g/sm	-	g/sm §	g/sm §	
1	-100	4219	8.2	501	0.010	2	494	10.0	1.18	220	1.1	31	255
2	-33	4622	8.3	528	0.010	3	369	11.0	1.22	104	1.4	30	106
2	67	4655	8.3	306	0.020	3	203	8.7	1.22	212	1.2	30	207
3	0	4477	8.4	151	0.020	3	125	9.3	0.91	161	0.5	30	169
3	100	4347	8.4	114	0.080	3	100	7.8	1.07	68	1.6	29	75
4	-67	3813	8.5	306	0.020	3	467	8.7	1.22	91	1	30	123
5	33	3301	8.7	†	†	†	†	†	†	157	0.6	30	246
5	-100	3231	8.7	†	†	†	†	†	†	8	1	30	7
6	-33	2861	8.7	†	†	†	†	†	†	67	0.9	31	70
6	67	2807	8.7	†	†	†	†	†	†	100	0.9	30	106
7	100	2549	9.0	15	0.09	3	17	5.7	0.90	29	1.7	30	36
7	0	2511	9.0	41	0.132	3	48	8.2	0.72	78	0.8	30	98
8	-67	2299	9.2	23	0.360	3	43	8.4	0.97	61	1	30	86
8	33	2261	9.2	16	0.104	3	26	6.6	0.97	84	1.3	30	125
10	-84	1986	9.5	25	0.030	5	§	8.5	0.79	18	1.4	75	§
11	84	1859	9.7	6	0.162	4	§	4.7	0.71	55	1.3	59	§
13	16	1638	10.0	11	0.090	5	§	5.9	0.81	28	1.2	75	§
14	-16	1574	10.0	16	0.100	5	§	6.6	0.84	59	1.3	75	§

The contributions of cross-channel variations in grainsize / sorting and of transport (1 and 2) can be minimized with an adequate number of subsections (Hubbell 1987; Gaweesh & Van Rijn 1994). The contributions due to bedforms (3 and 4) include turbulence over bedforms. These contributions can be assessed with repetitive streamwise echosoundings of the bedforms and subsequently choosing a number of measurement locations distributed over the bedform length. Contributions 3, 4 and 5 (macro-scale turbulence) to uncertainty of suspended transport are incorporated in the variance of integrated suspended transport verticals. The only way to minimize contribution 6 is to keep the time needed for one cross-section as short as possible, or to use more than one ship. On the other hand, a minimum number of subsections in one cross-section is needed to represent the cross-sectional distribution of transport, and a large number of samples must be done over the length of bedforms. This leads to a conflict between minimizing uncertainty due to spatial variation on the one hand and minimizing the effect of uncertainty due to temporal variation on the other hand. For each situation another compromise must be found that must be based on some *a priori* knowledge of presence of bedforms and rate of change of discharge. For the river Waal this leads to the sampling strategy given below.

3.3.3 Sampling strategy for minimizing transport variance

The cross-section of the river was divided in 7 subsections (see Fig. 3.1) centered at the river axis and 33, 67 and 100 m from the axis at both sides. The width of a subsection, therefore, is about 33 m, except for the outer sections at the banks, which are approximately 40 m wide. Four extra detailed subsections were added at 16 and 84 m on both sides of the river axis in the last phase of the campaign (waning flow), resulting in more samples and smaller spacing.

Three measurement positions were chosen in each subsection (five in the extra subsections) (see Fig. 3.1). It was not possible to distribute the measurement positions over the length of bedforms in a strict sense, since the bedforms (length 10-15 m, height 0.2-0.4 m) were too small and the bedform celerities (24-30 m/day) too high for positioning the instruments on specific positions on the bedforms. Therefore, a distance of 30 m between the positions (15 m in the extra subsections) was chosen. By doing so it was assumed that samples were taken at different positions on the bedforms.

At each position in every subsection the bedload was measured 10 times and in the four extra subsections 15 times. At each position in every subsection one suspended transport vertical was measured. This resulted in a dataset with 30 samples per subsection (75 in the extra subsections during waning flow) and 3 suspension verticals per subsection (5 in the extra subsections). 3.5 days were needed for seven subsections in one cross-section. The subsections were visited in the order shown in Fig. 3.1.

3.4 Bedload transport measurement

3.4.1 Instrumentation

Bedload transport was measured with an adapted version of the classical Helley-Smith bedload sampler: the Helley Smith for sand-gravel sediment ('HSZ') (see fig. 3.6). The dimensions of the sampler orifice are the same as in the original: 7.62 cm wide and high. The mesh bag had a

mesh diameter of 250 μm , which is smaller than the 10% diameter percentile of the bed material in the upstream part of the river Waal.

Contributions to the stochastic errors of a trap-type bedload sampler in field conditions are insufficient contact between the sampler nozzle and the bed in the presence of ripples or stones. These effects can be assessed with a video-camera mounted on the sampler. However, with high wash loads the orifice of the sampler is invisible, and a video-camera near the orifice of the sampler may disturb the flow near the nozzle of the sampler and thus have large effects on the sampling efficiency.

If a trap-type sampler is lowered in deep rivers, extra problems arise: uncontrolled sideward movements during lowering; initial effect of landing during which bed material is stirred up and caught in the sampler; dredging bed material when the sampler slides over the bed due to ship movements; and finally dredging bed material when the sampler is lifted up from its downstream position relative to the boat or bridge.

To diminish uncontrolled sideward movements the present sampler was adapted with extra weight of 100 kg and larger vanes. The result was that it could be lowered to the bed in a calm and smooth way even during the highest discharges and the added weight made sure that the sampler remained on its landing place on the bed. Ship movement was prevented by anchoring the boat with a vertical pole in the bed. Also passing ships were asked to slow down to decrease wave heights.

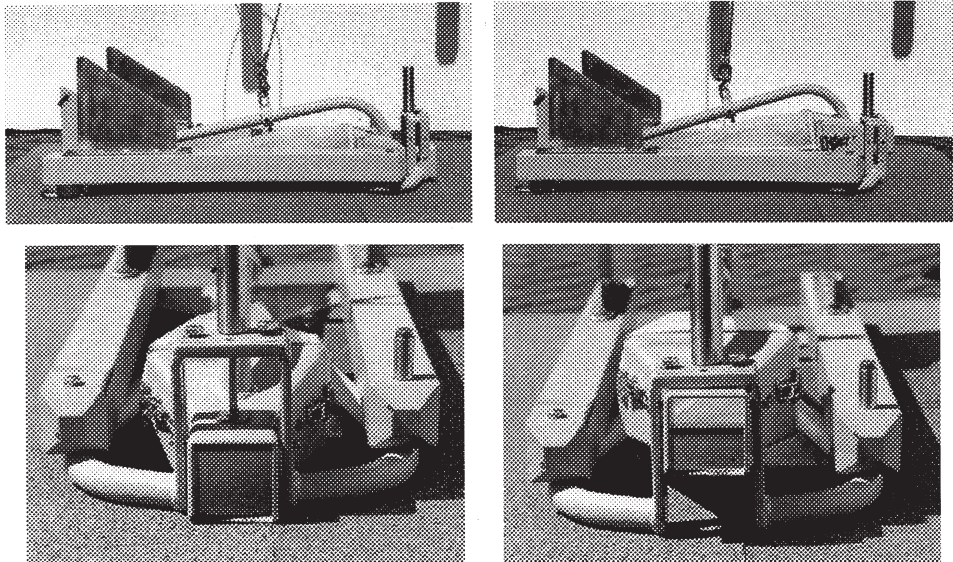


Figure 3.6. The nozzle of the adapted Helley Smith bedload sampler (HSZ) is suspended from the winch cable and thus lands on the bed after the frame and is lifted from the bed before the frame is. The 'flow' is from right to left. The cylinder on top of the nozzle frame is the damped spring.

The orifice of the sampler settles to the bed in a few seconds after the frame of the Helley Smith was positioned onto the bed (see Fig. 3.6). This prevents bed material to be scooped from the bed during landing and lifting. The sampler is suspended from a winch cable connected to the orifice, which hangs in its upward position in the frame of the Helley-Smith. When the frame lands on the bed, the orifice takes about five seconds to lower itself slowly to the bed by means of a damped spring construction. When the sampler is lifted again, first the

orifice is lifted because it is attached to the winch directly and a few moments later the frame comes up too, making dredging very unlikely. This was visually confirmed in flume tests (Delft Hydraulics 1996; 1997).

3.4.2 Calibration and sampling duration

Delft Hydraulics (1996, 1997) calibrated the HSZ in flume tests and found a calibration coefficient for the adapted Helley Smith of 1.15. This is a systematic error for the cross-channel integrated transport and is, therefore, not important for the present analyses of stochastic errors and natural variability.

The sampling time was chosen in such a way that the samples did not fill up the mesh bag for more than 50% to prevent reduction of the efficiency of the sampler. The sample duration was between 0.5 and 2 minutes.

3.5 Suspended load transport measurement

3.5.1 Instrumentation

Suspended sediment transport is equal to the product of velocity and concentration integrated over the water depth. Both velocity and concentration were measured at several levels above the bed with an Acoustical Sand Transport Meter ('ASTM'). Contributions to the stochastic error of an ASTM in field conditions are the varying height above the bed due to downstream and sideward movements of the frame, and the variability of velocity and concentration because of the small sampling time with respect to large scale turbulence.

It was found that the variation of suspended sand transport was mainly caused by macro-scale turbulence near the bed on a time scale of one minute (Mulder et al. 1985; Van den Berg 1984; Rijkswaterstaat 1985). Mulder et al. measured suspended transport in a tidal channel with a sand-bed covered with large bedforms. Their data indicate that two minutes sampling time per point with 2 Hz sampling frequency is enough to get an average with about 10% uncertainty.

All other factors that influence the measured concentration, e.g. water temperature, salinity and wash load, are corrected for in the calibration curves determined in the laboratory.

The ASTM concentration signal slightly depends on the diameter of the sediment. The suspended sediment in the river Waal is comparable to the material for which the ASTM was originally designed. Therefore, a correction of concentration for grain diameter is not necessary. The grain diameters of the suspended material were determined with pump sampling close to the measurement volume of the ASTM.

3.5.2 Field check of the calibration of the acoustical sand transport meter

Two field checks of the calibration of the ASTM are available (Ditzel & De Vos 1986; De Vos unpublished results 1995). The measured velocities of the ASTM were compared to Ott current meters, and the measured concentrations of the ASTM were compared to pump

samples. The pump concentrations were corrected for non-isokinetic pumping with the method of Nelson & Benedict (1950). The pairs of ASTM/pump concentrations were corrected for the time lag between ASTM sampling and pumping up by allowing the pump to fill the hoses with the water from the measurement position before ASTM sampling was started.

The pairs of ASTM and Pump concentrations at all levels above the bed are given in Figure 3.7a. The Figure shows a very good result. The regression line (see Fig. 3.7a) has an intercept of almost zero, being of the same order as the lowest measured concentrations near the water surface, and has a slope of approximately unity. The scatter and the non-zero intercept may very likely be due to uncertainty of the pump sampling instead of uncertainty of the ASTM measurements. The results for the velocity are comparable. In this paper the calibration of the transports measured with the ASTM is therefore assumed to be reliable.

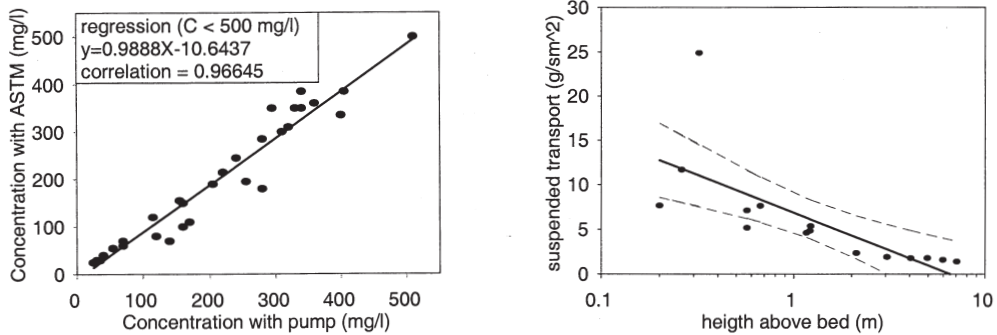


Figure 3.7. Field check of ASTM concentrations (a) with pump concentrations (data from Ditzel & De Vos 1986) and a typical example (March 8, position -67 meter) of a vertical profile of suspended sediment transport (b). The thick line (b) is the function fitted to the vertical profile, and the dashed lines are the 95% margins of the regression. The function is integrated from the top of the bedload sampler to the water surface to obtain the depth-integrated suspended sediment transport at this position in the river.

3.5.3 Data processing

At 0.20, 0.50 and 1.0 m above the bed the suspended transport was measured three times for 2 minutes at each level. From 1.0 m up to the water surface the suspended transport was measured for 2 minutes with increments of 1 m. The ASTM frame was lowered to the bed and then progressively lifted to the next heights.

The mean suspended load transport in a subsection was determined by averaging the depth-integrated transports of all verticals in that subsection. Nearly all the transport verticals of the present dataset appeared to be straight lines on a semi-logarithmic plot. Measuring near bed concentrations below 20 cm above the bed was impossible. Therefore, the form of the transport vertical between the bedload layer and 20 cm above the bed is not known. The vertical of suspended transport is therefore extrapolated to the top of the bedload sampler as described below.

The procedure of integration of the transport verticals is as follows. A semi-logarithmic regression is done on the transport vertical (see Fig. 3.7b), which subsequently is integrated between the top of the bedload sampler and the water surface. This method was verified by comparing the depth integrated suspended transport from the regression equation to a discrete

integration for all depth intervals for a subset of measured verticals. Both methods yielded equal transport values. A second verification was done by extrapolating the fitted function down to the bed for comparison with the measured bedload transports. The measured bedload was of the same order of magnitude as the extrapolated suspended transport. Finally, the difference in outcome after repeating these two verifications with a power function was only 10%, from which it can be concluded that the calculations are insensitive to the form of the fitted function.

The standard deviation s_{q_s} of the suspended transport in equation (2) is herein related to the scatter of the transport measurements around the log-linear regression function of transport against height above the bed. Thus it is assumed that all natural fluctuations of transport in the vertical are manifested in this scatter. The s_{q_s} of suspended transport is calculated depending on the residues between the predicted and measured transport at a certain height above the bed as:

$$s_{q_s} = \frac{1}{n - p} \sum_{i=1}^n (q_{s,i} - \hat{q}_{s,i})^2 \quad (9)$$

in which $\hat{q}_{s,i}$ is the transport predicted with the regression function and p is the number of parameters fitted in the regression ($p=2$ in this case). Thus $n-p$ is the number of degrees of freedom in the regression.

3.6 Results of the field measurements

3.6.1 Hydrodynamics and sediment transport

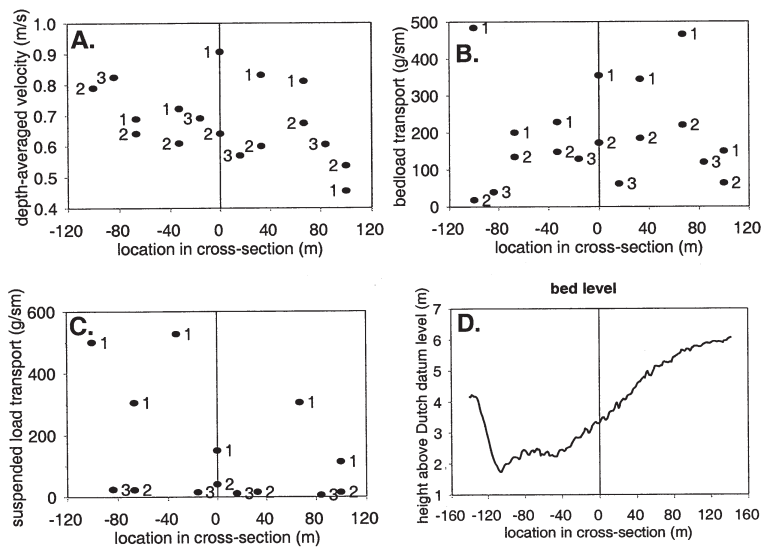


Figure 3.8. Stream velocity (a), bedload (b) and suspended load (c) sediment transport in the cross-section and a bed profile (d) of the cross-section. Labels denote cross-section numbers.

In Figure 3.8 the distribution of current velocity (Fig. 3.8a) and sediment transport (Fig. 3.8b,c) in the cross-section is given, as well as the bathymetry (Fig. 3.8d). The maximum measured depth averaged velocity was about 1 m/s. During cross-section 1 measurements the velocities were highest in the middle of the channel, but during cross-section 2 measurements and the extra measurements 3, when the discharge was lower, the position with the highest current velocities shifted to the deepest part of the river cross-section. Suspended load transport exhibits two effects. First, suspended load transport is almost zero during the second cross-section measurements. Second, the suspended load is highest in the deepest part of the channel.

3.6.2 Effect of changing hydrodynamic conditions

The ideal situation in which measurements in all subsections are done simultaneously is impractical and dangerous on a heavily shipped river. Thus the water discharge changes when measuring in a cross-section and inevitably some information on temporal and spatial variation is lost. A tentative method to solve this problem is suggested here. Note that this method does not affect the relative accuracy of the measurements according to equation (6, 7) because it is applied after determining the accuracy.

The effect of changing hydrodynamic conditions is corrected for by translation of measurements (s, Q pairs) in one cross-section parallel to an empirical power function ($s = aQ^b$) between transport and discharge (see Fig. 3.9). This function is fitted with the least-squares method to the datapoints of all subsections. The datapoints, having a measured discharge, are translated to the average discharge of the period in which all points in the whole cross-section were measured. Numerically, this procedure amounts to predicting the sediment transport for one point with the power function for both the measured (S_p, Q_m ; with $p =$ predicted and $m =$ measured) and average discharge (S_p, Q_a ; with $a =$ average), and then correcting the measured transport (S_m with the ratio between the two predicted values to yield the corrected measured transport (S_c ; $c =$ corrected) as follows: $S_c = [(S_p \text{ for } Q_a)/(S_p \text{ for } Q_m)]S_m$. The sediment transport varies systematically in the width of the river, but it must tentatively be assumed that the same empirical function can be used for all subsections because the dataset is too small to allow the derivation of empirical functions for all subsections. The corrected transports of the subsections (S_c, Q_a pairs) can now be integrated to a cross-channel transport for a certain discharge.

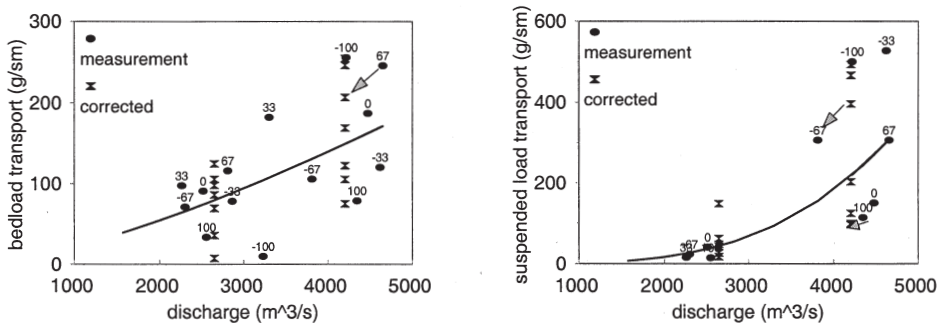


Figure 3.9. Bedload (a) and suspended load (b) sediment transport in the subsections as a function of discharge. The transports are corrected for changes in discharge during the period of the measurements for one complete cross-section.

3.7 Accuracy depending on sampling strategy

3.7.1 Variation coefficients

All bedload samples in a subsection were used to calculate the sample size weighed variation coefficients of the bedload in the subsections with equation (2) for n samples, but also for $n-1$, $n-2$ etc. In this way a variation coefficient curve can be constructed of all of the subsections (see Fig. 3.10). As expected, the variation coefficient generally decreases with an increasing number of samples in a subsection. The envelope curve is constructed out of the maximum variation coefficients (see Fig. 3.10). This $VC_{bedload} = VC_{s,max}$ is the input for equation (7).

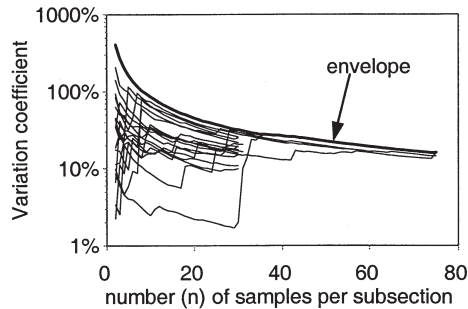


Figure 3.10. Sample size weighed variation coefficients of all subsections and the maximum variation coefficient of all bedload data.

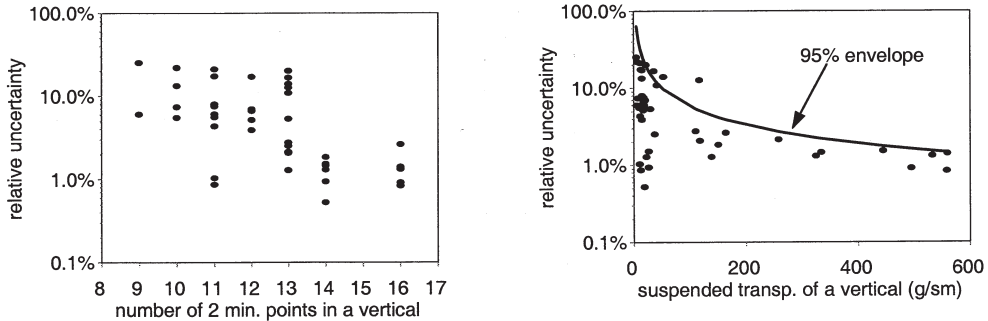


Figure 3.11. Relative uncertainty of suspended transport as a function of (a) the number of points in a vertical and (b) on the total suspended transport in the vertical. The points in the vertical are measurements over time periods of 2 minutes each.

The variation of suspended transport in a vertical is derived from the scatter of the measurements around the regression functions of the transport verticals above the bed. It was found that the uncertainty of suspended transport depends weakly on the number of points in a vertical (see Fig. 3.11a), which is expected. However, it seems to depend strongly on the total transport in the vertical (see Fig. 3.11b). Although it could be argued that the variability in the uncertainty is large while the uncertainty itself is independent on the transport magnitude, the empirically found dependence is taken into account to obtain realistic uncertainty estimates for this dataset. This means that all accuracy calculations have to be done for several magnitudes of transport. For this purpose an envelope curve of maximum

variation $s_{q_s, max}$ as a function of transport was constructed (see Fig. 3.11b). The envelope curve is described as: $s_{q_s, max}/q_s = 2.3q_s^{-0.8}$. This empirical curve is used to calculate the uncertainty of suspended transport in a subsection, taking $s_{q_s, max} = s_{q_s}$ and n is the number of verticals in a subsection in equation (2).

Strictly, the uncertainty of suspended load transport in a vertical depends on the velocity, concentration and level above the bed. With the approach taken above, the uncertainties of velocity and concentration are incorporated in the uncertainty of transport, and the uncertainty of level above the bed is incorporated in the regression. Thus the covariance between velocity and concentration does not need to be included explicitly.

3.7.2 Uncertainty of integrated transport

The uncertainty in width of the two outermost subsections near the banks of the present field location was estimated to be 2 m, which means that with 95% certainty the error in width was 4 m. This was estimated from the echosounding accuracy of the position of the groyne toes on the alluvial bed. This position barely changes with discharge, and the only variation is a small excursion of the sediment in transport onto the steep slope in between the groynes. With outer subsections of at most 40 m wide, this resulted in a relatively small uncertainty of 5% ($s_{\Delta W}/\Delta W$).

The uncertainty of cross-channel integrated bedload transport was calculated with equation (7). The empirical envelope curves of maximum VC_s were used to emphasize the fact that standard measurements in nature were the basis of this analysis. With 7 subsections and 30 samples per subsection the uncertainty of integrated bedload transport was 12%, which is small compared with all variations of transport at one position.

The outcome with equations (7) and (8) were compared to assess the effect of the simplification in the latter. The final uncertainty of cross-channel integrated bedload transport with (7) for 7 subsections was 12.9% against 11.8% with (8) and for 3 subsections 19.0% against 18.1%. It is concluded that the simplification from equation (7) to (8) is allowed and can be used in the assessment of different strategies and in the planning phase of a new campaign. The calculation of final uncertainty thus was repeated with equation (8) for smaller numbers of samples and different numbers of subsections (see Fig. 3.12a).

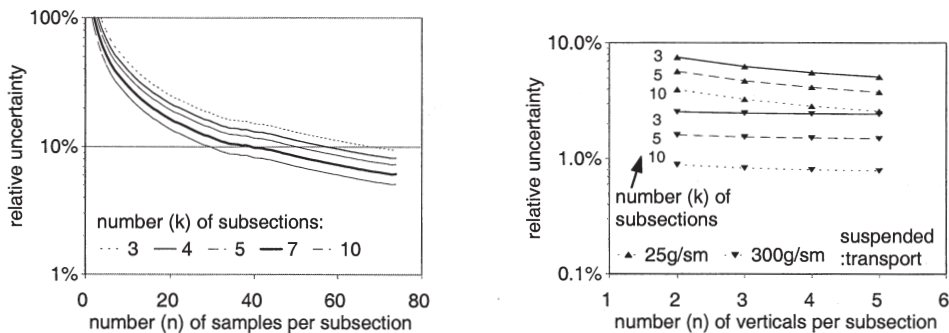


Figure 3.12. Relative uncertainty of cross-channel integrated bedload (a) and suspended load (b) transport as a function of the number of samples or verticals and the number (k) of subsections. For suspended load transport curves are given for upper and lower transport magnitudes.

For suspended load transport the s_{qs} in equation (2) was estimated for several magnitudes of transport with the 95% envelope of the uncertainty of a suspended transport vertical as a function of the transport itself (see Fig. 3.12b). With equation (7) the final uncertainty of cross-channel integrated suspended transport was calculated for varying numbers of verticals and subsections and two extreme transport magnitudes. As can be seen in Fig. 3.12b, the uncertainty of suspended transport thus may vary between 0.7% and 8%, depending on the conditions and strategy. With 5 subsections and 3 verticals distributed over the length of the bedform the uncertainty is between 1% and 6%, which is much smaller than the uncertainty of bedload transport.

3.8 Discussion

3.8.1 Sources of uncertainty

Two main sources of uncertainty were discussed: stochastic errors and natural variability. The natural variability was examined in terms of spatial and temporal variability. The natural small scale spatial and temporal variability during the measurement at a single position due to turbulence and small moving bedforms cannot be separated from the stochastic measurement errors in the present approach.

The large scale spatial variability is related to the meandering of flow and related bed level and bed sediment composition variation. From the present dataset the effect of these factors on the cross-channel accuracy of sediment transport cannot be separated. Furthermore, the spatial variability may very well vary in time, which can not be analysed with the present dataset. The effect of all large scale spatial variability can be assessed from Figure 3.12 only for constant spatial structures. In reality, these spatial structures vary in time and along the river and the impact of this variation on sediment transport cannot be quantified here accurately for logistic reasons. Preliminary analysis of three-dimensional dune tracking indicates that the cross-sectional distribution of bedload transport quantified with migrating dunes resembles the theoretical one in Figure 3.2b quite closely (Wilbers, pers. comm.). Thus, the more rapid and less expensive method of dune tracking seems promising for determining large scale spatial variability.

The large scale temporal variability is related to the changes in discharge. The application of an empirical transport-discharge relation is usually associated with a lot of scatter, of which a large part is due to the systematic variation of transport across the river, as can be concluded from the labels in Figure 3.9a. Therefore, it is the opinion of the authors that using an empirical power function for the translation of transport in subsections to one water discharge is acceptable if changes in discharge during a set of cross-section measurements are not larger than about 25% and if only data of a single campaign is used for the empirical relation. A larger change indicates that another compromise between accuracy and change over time should have been chosen with less measurements per cross-section or subsection.

In collecting the present dataset the river was crossed only twice, which is not enough to determine a more generally valid power function. More measurements at higher discharges would have improved the function and might even have been used to derive power functions for each subsection instead of all subsections lumped together. The correction for changes in discharge might thus be improved. For the present dataset no better method is available. In retrospect, the variation of discharge during one crossing of the river in the present campaign is rather large while the number of subsections in the cross-section could have been reduced to

5 instead of 7 with only a small loss of accuracy. This reduction would have led to less large scale temporal variability and less large corrections for changes in discharge. Furthermore the reduction in subsections might have made an extra river crossing possible. The discharge cannot be predicted more than two or three days ahead, however, which makes *a priori* choices of the strategy difficult.

3.8.2 Bedforms

Gaweesh & Van Rijn (1994) did their measurements during low discharges with relatively large and stagnant bedforms. In their case it was possible to have five sampling positions on different parts of the bedforms. On the location studied here, bedforms had relatively short lengths and large celerities. It was therefore not possible to sample on specific parts of the bedforms. This introduced large quasi-cyclic variations of transport in the subsections. This means that the accuracy of cross-channel integrated transport may be higher in other situations with larger dunes or very small bedforms or plane bed. The authors therefore argue that relatively small dunes as in this paper present a worst case scenario for the accuracy. This is confirmed by comparison of the variation coefficient envelope (for a single subsection, not for the cross-channel integrated transport) with results from literature (Gaweesh & Van Rijn 1994; McLean & Tassone 1987 (in Hubbell 1987)). The variation coefficients from the present measurements are the largest (see Fig. 3.13).

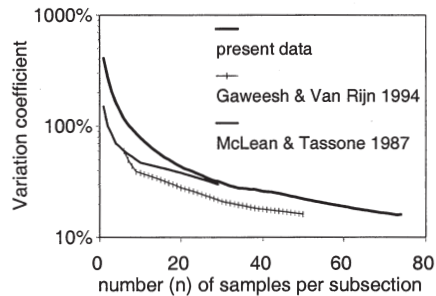


Figure 3.13. Comparison of sample size weighed variation coefficients in a subsection as found in this study and in literature (Gaweesh & Van Rijn 1994; McLean & Tassone 1987 (in Hubbell 1987)).

Gaweesh & Van Rijn (1994) derived the interpolation error from predicted cross-channel distributions of transport with 40 subsections in comparison with cross-channel distributions with smaller numbers of subsections. They found that the interpolation error was about 15% for seven subsections. Gaweesh & Van Rijn calculated their cross-channel distribution of transport from interpolated measurements of water depth and flow velocity in the calculations of transport with the predictor of Engelund-Hansen. Thus their interpolation error includes the uncertainties of the flow measurements and transport predictor and, therefore, is not a true interpolation error. In this paper the true error due to the integration method is not calculated from measurements, but from hypothetical distributions without measurement and prediction errors. The cross-channel distribution of transport is assumed to be of a smooth form without irregularities resulting from small-scale temporal variations in the transport process and measurement errors. Thus the error calculated in this paper is an estimate of the systematic

interpolation error due to the discrete integration method only and has no stochastic components of measured parameters that are not related to the integration method. The interpolation error appeared to be negligible.

In the derivation of equation (7) it is explicitly assumed that sediment transport samples are normally distributed. The probability distribution function (PDF) of bedload, however, is not altogether normal. Hamamori (1962) derived a strongly skewed probability distribution function (PDF) for instantaneous bedload transport rates from the combined movement of small ripples over larger bedforms. Kuhnle (1996) on the other hand reported bedload measurements of gravel that were approximately normally distributed. It is likely that the normal PDF and Hamamori PDF represent two extremes of possible measured probability distribution functions. The effect of a skewed distribution is that the uncertainty as presented in this paper would be asymmetrically divided above and below the average transport, probably with a larger uncertainty margin above the average cross-channel integrated transport. By using the envelope of the sample size weighed variation coefficient (see Fig. 3.10) the possible effect of a skewed distribution is thought to be incorporated in our uncertainty calculations.

3.8.3 Uncertainty of depth-integrated suspended transport

Suspended transport is in effect the downstream movement of small clouds of suspended sediment. At low transports the number of clouds is very small. The lowest measured transports of say 25 g/sm can, therefore, not be measured accurately with pumps or the ASTM in the given time period, giving more scatter than during high transport. The correlation between depth and transport is, therefore, lower during lower transport. This indicates that 2 minutes sampling is not long enough at low transport. This result is not influenced by the choice for a semi-logarithmic regression instead of a power function, because the latter gave about the same correlations.

Van Rijn (1993) derived the uncertainty of depth-integrated suspended load transport with estimates of the uncertainty of flow velocity, concentration, level above the bed and of an interpolation error. The interpolation error strongly depended on the number of points and on the distribution of points over the depth. This is to be expected because the integrated transport strongly depends on the high near-bed transport. Combining all contributions to uncertainty the total uncertainty became 21%. In this paper the uncertainty of a single vertical was between 0.7% and 8%, depending on the amount of transport. The two methods are difficult to compare, but the data in this paper represent a more direct field estimate of the uncertainty during low and high transport in the presence of bedforms and heavy shipping, while Van Rijn (1993) presented only higher transport data with guesses for the relative errors of concentration and velocity.

3.8.4 Time and financial investment

The total time needed for a measurement campaign was calculated from the time needed to finish a subsection and the demanded maximum uncertainty of the final cross-channel integrated transport (see Fig. 3.14). It was assumed that variation in the cross-section was adequately sampled with 5 to 7 subsections. The time to complete a position with 10 samples was about 60 minutes (including navigation) with one boat and one bedload sampler. The time to complete a position with 3 verticals with 13 points in height above the bed was about

40 minutes (including navigation) with one boat and one suspended transport instrument. From Figure 3.14a,b the necessary time and cost investment at predefined demanded levels of maximum uncertainty in the results can be calculated for future campaigns. For suspended transport two curves are given, one for very low transports and one for high transports.

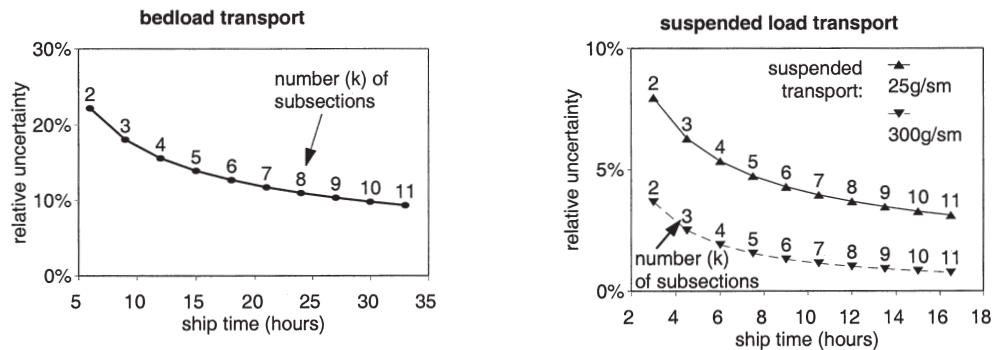


Figure 3.14. Accuracy of cross-channel integrated bedload (a) and suspended load (b) sediment transport estimates that can be achieved as a function of the duration of the measurement campaign for one cross-section.

3.9 Conclusions

Cross-channel integrated suspended and bedload transport can be measured with an uncertainty of 10 to 20% in a large sand-gravel-bed river during high discharge. The uncertainty depends mainly on the balance between the number of subsections and measurement positions, and the rate of change of hydrodynamic conditions. Sampling of 30 bedload samples and 2 suspended transport verticals per subsection in 5 subsections, however, is considered to be the minimum effort in a single channel.

The error in width of the two subsections next to the river banks only has a minor effect on the final uncertainty of cross-channel integrated sediment transport. In the presence of banks or islands and low-sloping river banks this error may be much larger.

Presence of bedforms is an important contribution to the final uncertainty. The temporal and spatial variations due to moving bedforms are sufficiently included when at least 30 samples of bedload and 2 verticals of suspended load are taken distributed over the length of the bedform.

Variation in hydrodynamic conditions during a discharge wave cause systematic differences in transport between the subsections belonging to one cross-section, thus fouling the pure spatial variation. This can be corrected for by calculating a discharge-transport relationship and using this relationship to recalculate all transports such that they all refer to the same discharge. The maximum acceptable correction of transport with this method is estimated to be 25%. Therefore, the time to complete a cross-section must be kept as low as possible to minimize the change in hydrodynamic conditions. Since a minimum of samples is necessary for covering the spatial variation in transport, a compromise has to be found between the number of subsections and the rate of change of the discharge.

Acknowledgments

The National Institute for Inland Water Management and Waste Water Treatment (RIZA) and the Directorate Eastern Netherlands, both institutes of Rijkswaterstaat in the Netherlands, financed and carried out the measurements.

The authors would like to thank A.W. Hesselink (who also drew figure 3), E. Stouthamer, J.H. Van den Berg, L.C. Van Rijn, E. Pebesma and two anonymous reviewers for their comments. The pleasant cooperation with the Rijkswaterstaat - ANIM crew during the measurement campaign is thankfully remembered.

Notation

c	=	correction for all systematic errors (-)
i	=	indicator of subsection number or number of point measurement above the bed
j	=	number of channels (with $2j$ = number of banks)
k	=	number of subsections in the cross-section (-)
n	=	number of samples (-)
$q_{s,i}$	=	mean measured bedload transport (kg/s)
$\hat{q}_{s,i}$	=	suspended transport estimated with regression function at level i above the bed
Q_s	=	cross-channel integrated bedload transport (kg/s)
R	=	correlation coefficient of regression analysis (-)
$Rel_{s,i}$	=	relative variation of sediment transport in subsection i (-)
s_{qs}	=	standard deviation of q_s of all samples in a subsection (kg/s)
s_{Q_s}	=	standard deviation of Q_s (kg/s)
$s_{\Delta W}$	=	uncertainty of width (m)
VC_s	=	variation coefficient of bedload transport (-)
ΔW_i	=	width of subsection i (m)
α	=	calibration coefficient of measurement instrument (-)

References

- DELFT HYDRAULICS (1996), Test and calibration measurements with an adapted Helley Smith for bedload transport measurements in sand-bed rivers. (in Dutch) Delft Hydraulics report Q2141, Delft, The Netherlands.
- DELFT HYDRAULICS (1997), Calibration and comparison Helley-Smith Sand. Delft Hydraulics report Q2345, Delft, The Netherlands.
- DITZEL, H. & DE VOS, W. (1986), Afnametests gemodificeerde AZTM. (in Dutch) Rijkswaterstaat Directie Zeeland notitie DDWTZ 86.382.
- EMMETT, W.W. (1980), A Field Calibration of the Sediment-Trapping Characteristics of the Helley-Smith Bedload Sampler. Geol. Surv. Prof. Pap. 1139, U.S. Dep. of the Interior, U.S. Gov. Print. Office, Washington.
- GAWEESH, M.T.K. & VAN RIJN, L.C. (1994), Bed-Load Sampling in Sand-Bed Rivers. J. Hydr. Eng., ASCE, 120 12, pp. 1364-1384.

- GOMEZ, B. & TROUTMAN, B.M. (1997), Evaluation of process errors in bed load sampling using a dune model. *Water Res. Res.* 33 10, pp. 2387-2398.
- HAMAMORI, A (1962), A Theoretical Investigation on the Fluctuation of Bed-Load Transport. Delft Hydraulics report R4, Delft, The Netherlands.
- HUBBELL, D.W. (1987), Bed Load Sampling and Analysis. In: *Sediment Transport in Gravel-Bed Rivers*. Eds. Thorne, C.R., Bathurst, J.C. and Hey, R.D., John Wiley & Sons.
- KLEINHANS, M.G. (1997b), Sediment Transport in the Waal: Discharge peak of March 1997. (In Dutch) Netherlands Centre for Geo-ecological Research, report 97/7, Utrecht University, The Netherlands.
- KUHNLE, R.A. (1996), Unsteady Transport of Sand and Gravel Mixtures. In: *Advances in Fluvial Dynamics and Stratigraphy*. Eds. CARLING, P.A. & DAWSON, M.R., John Wiley & Sons.
- MCLEAN, D.G. & TASSONE, B. (1987), Discussion of HUBBELL (1987), In: *Advances in Fluvial Dynamics and Stratigraphy*. Eds. CARLING, P.A. & DAWSON, M.R., John Wiley & Sons.
- MULDER, H.P.J., KOHSIEK, L.H.M. & VANDERKOLK, A.C. (1985), Turbulence in terms of coherent structures and their relation to sand concentration in tidal channels. *Euromech 192 symposium*.
- NELSON, M.E. & BENEDICT, P.C. (1950), Measurement and analysis of suspended sediment loads in streams. *Proc. ASCE*, 76 pp. 1-28.
- POWELL, D.M., REID, I., LARONNE, J.B. & FROSTICK, L.E. (1995), Cross-stream Variability of Bedload Flux in Narrow and Wider Ephemeral Channels During Desert Flash Floods. 4th Int. Workshop on Gravel-Bed Rivers, Gold Bar, Washington, U.S.A..
- POWELL, D.M. (1998), Patterns and Processes of Sediment Sorting in Gravel-Bed Rivers. *Progress in Phys. Geography* 22,1 pp.1-32.
- RIJKSWATERSTAAT (1985), 1-D Acoustic Sand Transport Meter (in Dutch). Internal report DDWT 85.22.
- VAN DEN BERG, J.H. (1984), Determination of the Suspended Sand Concentration. In: *The Closure of Tidal Basins*. Eds. HUIS IN 'T VELD, J.C., STUIP, J., WALTHER, A.W. & VAN WESTEN, J.M. Delft University Press 1984.
- VAN RIJN, L.C. (1993), *Principles of Sediment Transport in Rivers, Estuaries and Coastal Seas*, Aqua Publications, Amsterdam, The Netherlands.
- WILBERS, A.W.E. (1998), Spatial Variability of Dune Characteristics in the Waal during a Discharge Wave in 1997. (in Dutch) Netherlands Centre for Geo-ecological Research report 98/19, Utrecht University, The Netherlands.

4

Bedforms and sediment transport over armour layers

Abstract

The stability of bedforms generated in gravel and mixtures of gravel and sand is not well understood. Two bedform types are characteristic for mixed sand and gravel sediment, flow parallel sand ribbons and flow transverse barchans. Flume experiments and field data presented here show that gradual transitions exist from sand ribbons to barchans, and from barchans to fully developed dunes. Barchans and sand ribbons occur when not enough transportable sediment is available for the formation of fully developed ripples or dunes. The reason is that a part of the bed sediment is immobile, e.g. with an armour layer, which limits the sediment supply and thus the volume of sediment available for the formation of bedforms.

Bedform stability diagrams are shown to be extendable to sediment supply-limited bedforms in sand-gravel sediment, if the particle parameters of the diagrams are derived from the transported sediment instead of the bed sediment. Barchans and transitional forms to fully developed dunes plot in the dune stability fields. Sand ribbons on the other hand plot in the ripple, lower plane bed and dune fields.

In the case of sediment supply limitation, bedforms apparently are partly or completely related to the characteristics of the sediment supply from upstream. The sediment underlying the bedforms may be a stable armour and the exchange of sediment particles between this armour and the bedforms may be small or non-existent. As a consequence, bedform characteristics in sand-gravel mixtures in supply-limited conditions are not predictable from the local hydraulic and sediment characteristics. A descriptive stability diagram with dimensionless parameters is given for the occurrence of the bedform types. Thus, barchans are the supply-limited counterpart of dunes, with barchanoids as a transitional form. Sand ribbons are even more supply-limited bedforms.

This chapter is reproduced from:

Kleinhans, M. G., Wilbers, A. W. E., De Swaaf, A. & Van den Berg, J. H. (2002). Sediment supply-limited bedforms in sand-gravel bed rivers. In press by Journal of Sedimentary Research, September 2002 issue, reproduced with permission of JSR.

4.1 Introduction

The stability of bedforms in sandy material in steady and uniform flow is well understood. Many bedform stability diagrams for uniform sand have been proposed in the past decennia, e.g. Simons & Richardson (1965), Allen (1984), Southard & Boguchwal (1990) and Van den Berg & Van Gelder (1993; 1998). Bedforms in sediments with both gravel and sand have only recently received attention. An outstanding property of (bimodal) sediment mixtures is that the larger particles become practically immobile during some critical lower flow stage, while the smaller particles are propagating downstream as bedforms (Wilcock, 1998; Carling et al., 2000a;b). The effect of the partial mobility of sediment on bedform characteristics and morphology is not well known.

The objectives of this paper are 1) to describe the bedform types that occur in sediments with sand and gravel, 2) to test the applicability of bedform stability diagrams for uniform (sand) sediment to sediment mixtures, and 3) to determine the effect of sediment supply on bedform morphology. For this purpose, data from series of flume experiments are used that provide information on bedforms at conditions ranging from extremely transportable sediment-supply-limited to supply-unlimited. Furthermore new data are presented for bedform types in natural rivers with (bimodal) sand-gravel sediment. These data together with a selection of data from the literature are used to infer the main factors determining bedform stability and morphology in sediment supply-limited conditions. The data are applied to existing bedform stability diagrams to determine whether stability fields for unimodal sand can be extended to sand-gravel sediments.

4.2 Review

Dinehart (1989; 1992) observed active gravel dunes in the North Fork Toutle river, proving that dunes do exist in very coarse sediment. Superimposed on and migrating over these dunes, features were found that seemed to be transitional forms between bedload sheets and small dunes.

Carling (1999) presented an overview of published data on bedforms in coarse sediments. These data were applied to the bedform stability diagrams of Allen (1984) and Southard & Boguchwal (1990). It appeared that the stability fields of bedforms in sand could be extended in the gravel grades (Carling, 1999). Thus, gravel dunes and sand dunes are found in the same range of Shields-parameter values. However, the data used by Carling refer mostly to rather unimodal sand or gravel sediments, bimodal sand-gravel mixtures were not considered.

The effect of sediment sorting on bedform stability was experimentally determined by Chiew (1991). Lognormal distributed sediments with a D_{50} of 0.6 mm and a Trask sorting coefficients varying from 1.2 to 5.5 were subjected to steady flows of 0.3 to 2 m/s in a small recirculating flume. Chiew found that differences with uniform sand were: the armouring tendency, the absence of antidunes and the fact that bedform sizes at intermediate flows were dependent on the availability of fine sediment at the bed surface. Chiew did not provide information on detailed bedform morphology and sediment transport.

Three bedform types seem to be characteristic of sand-gravel sediment:

1. bedload sheets: thin accumulations of bedload sediment of about two grain diameters thick and in the order of one half to two meters long in sand and gravel respectively. They are mainly recognisable by their flow-transverse sorting with the coarse grains at the leading edge.
2. flow parallel sand ribbons: created by near-bed helical flow cells in combination with

selective transport of bed sediment (e.g. Allen, 1970; McLelland et al., 1999). The sand is concentrated in flow parallel ribbons, a few grains thick and in the order of 0.1 m wide, and are transported over the immobile gravel. The spatial segregation of fine and coarse sediment enhances this flow structure, providing a positive feedback for sand ribbon formation (Colombini, 1993; McLean, 1981; McLelland et al., 1999).

3. flow transverse barchans: crescent shape with the horns pointing downstream, and height and lengths in the same order as dunes, and they migrate over an immobile base. They are well known features in subaerial settings and have a stable form; here, barchans were observed to preserve their form while migrating over long distances (Hesp & Hastings, 1998). The transportable sediment supply is limited because the base either is wet and thus cohesive due to a high groundwater table, or the base is more or less immobile in case of a desert pavement or sabkha. As a very special case, on a frozen solid, migrating snow barchans may occur (McKee, 1979; Pye & Tsoar, 1990; Hesp & Hastings, 1998).

The first occurrence of barchans in fluvial literature known to the authors is McCulloch & Janda (1964). They gave visual observations of barchan dunes migrating over an immobile gravel lag in an Alaskan river. They conclude that subaqueous barchans are formed in response to a limited sand supply due to the immobility of the coarser particles. Recently, Carling et al. (2000a;b) described large sandy barchans migrating over an armour layer in an eroding stretch of the river Rhine (Germany) downstream of a hydropower dam which limits the upstream sediment supply. In addition, researchers mention barchans migrating over armour layers in flume experiments (Klaassen, 1986; Rosza & Jozsa, 1999).

As compared to their subaqueous counterparts subaerial dunes are not limited in height due to an infinite air 'depth' while dunes in flumes or shallow rivers react strongly on changes in water depth (e.g. Southard & Boguchwal, 1990). An important similarity is that the height of subaerial barchans is often sediment supply-limited. Sometimes the limitation of sediment supply does not mean that barchans become smaller as the sediment supply diminishes. Instead, the number of barchans simply declines due to the declining availability of mobile sediment for bedform formation. This agrees with the observation of Rubin & Topping (2001) that in case of extreme winnowing, coarsening of the bed may be accompanied by reduction in surface area of transportable sediment patches on the riverbed. Subaerial dunes can only be limited in height by sediment supply, while subaqueous dunes may be limited in addition by water depth.

The phrase supply-limited is here intended to refer to a limitation of available, transportable sediment from which the bedforms are moulded. With a fully mixed bed as initial condition, this could also be seen as a flow limitation. The critical shear stress of the larger grains in the bed is not exceeded by the flow, which leads to coarsening of the bed, and less sediment in transport than would have been the case in fully mobile bed conditions. Thus the limit on entrainment is strongly related to the critical shear stress of all grain size fractions. This effect is different for different sediment mixtures. In bimodal sediment the finer grades are much more mobile than in unimodal sediment, while in both cases the mobility of the finer grades is less than in uniform sand (Wilcock, 1998; Kleinhans & Van Rijn, 2002, see chapter 5). However, in case of an armour layer formed during a previous discharge wave or period of low flow, sediment supply-limitation is not seen as a flow limitation, because that condition does not relate to the present flow. Such an armour layer (history effect) inhibits the entrainment of finer sediment from the underlying bed, that would otherwise have been entrained in the present flow.

An important question is how the supply limit relates to the stability and morphology of subaqueous bedforms. Belderson et al. (1982) observed migrating sand ribbons and sand barchans over a clay substrate on the oceanic shelf. They presented a semi-quantitative model of bedform morphology ranging from sand ribbons to dunes overlying a clay substrate. The main factor in

this model is the availability of sediment for bedload transport. McKee (1979) presents a qualitative model to illustrate the continuous sequence of subareal transverse dunes to transitional forms (herein called barchanoids) to barchans with unidirectional wind and diminishing sand supply. No model is available to illustrate a similar sequence for bedforms in rivers.

Barchanoids are herein defined as transitional forms between barchans and dunes. While barchans are individual unconnected bedforms migrating over an immobile base visible between the bedforms, barchanoids have partly grown together (coalesced barchans), both in flow-transverse and flow-parallel direction, because more transportable sediment is available leading to more bedforms. Dunes, finally, occur when the active riverbed (down to the deepest dune troughs) is fully mobile. Thus, in between barchanoid bedforms (in all directions), large patches of immobile sediment can be observed, while this is not the case with dunes which, in contrast to barchans, have their crests connected. Obviously the transition is gradual.

Existing diagrams of bedform stability refer to supply-unlimited, non-aggrading conditions, where the bedforms are moulded from the underlying bed and therefore can directly be related to overall characteristics of bed material and flow conditions. In the case of supply limitation, bedforms apparently are partly or completely related to the characteristics of the sediment supply from upstream. Therefore, in contrast to the unimodal case, bedform characteristics in (bimodal) mixtures at supply-limited conditions may therefore be unpredictable from the local hydraulic and sediment characteristics. This hypothesis is tested herein.

4.3 Flume experiments

4.3.1 Description of the experiments

The objective of the flume tests was to study the bedload transport process of a sand-gravel mixture in equilibrium conditions. Herein, only the results with respect to bedform morphology are given. Kleinhans (2000) presents an overview of all results.

The experiments were done with slightly bimodal sediment (Fig. 4.1) from the uppermost reach of the river Waal, a distributary of the Rhine in the Netherlands. To prevent choking of the flume recirculation system, all particles larger than 16 mm (D_{95} of the original mixture) were excluded from the mixture.

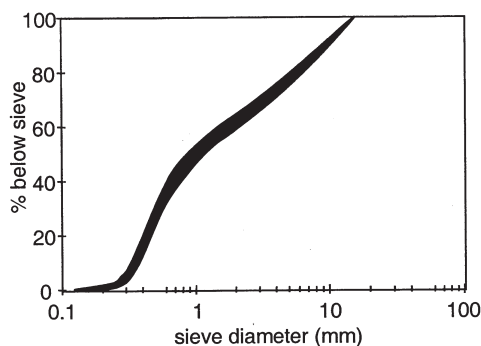


Figure 4.1. Particle size distribution of the initial bed sediment in the flume experiments. The distribution is given as the envelope of the distributions of five large samples.

The flume experiments were started with a mixed bed, installed at a bed slope equal to the water

surface slope. The bed was carefully saturated with water, the flow was started slowly (over 15 minutes) to prevent bed damage. The flow was maintained until the system was in equilibrium (Fig. 4.2). The equilibrium phase was pragmatically defined as the time at which changes in flow roughness, bedform dimensions and sediment transport became smaller than the measurement accuracy and variability. The flume was then drained of water, and the bed was photographed and sampled. The next step was to apply a different bed shear stress on the old bed until equilibrium was again reached (Fig. 4.2) (Blom & Kleinhans, 1999; Kleinhans 2000). The experiments during which the bed was allowed to attain equilibrium are hereafter referred to as equilibrium experiments. The rising and waning flow stages between the equilibrium experiments are referred to as transitional experiments. Conditions of most experiments were near incipient motion for most diameters, but some experiments had shear stresses well above critical for most diameters. Sediment transport in suspension was negligible. A summary of experimental data is given in Table 4.1.

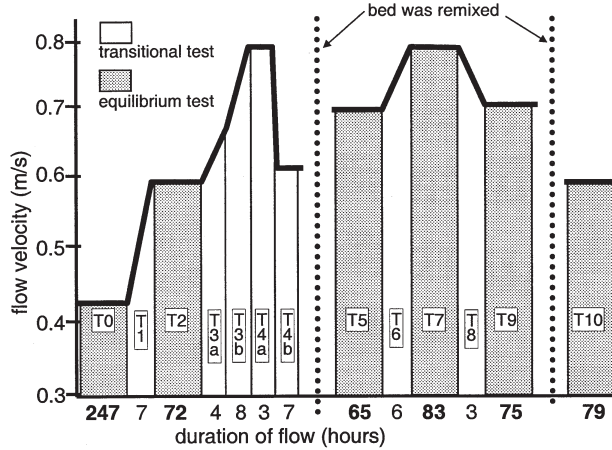


Figure 4.2. Sequence of the experiments of Blom & Kleinhans 1999 (after Kleinhans 2000).

It is assumed that the bedload transport depends on the grain-related bed shear stress (grain shear stress) (Van Rijn 1984; Van den Berg & Van Gelder, 1993). The grain fraction of the shear stress therefore must be constant in the equilibrium experiments. The grain bed shear stress is herein defined as $\tau' = \rho g (u/C)^2$, in which ρ = density of water (1000 kg/m^3), g = gravitational acceleration (9.81 m/s^2), u = depth-averaged flow velocity (m/s), and C = Chezy ($\text{m}^{0.5}/\text{s}$) roughness parameter related to grain friction (explained later). It was assumed that the roughness coefficient related to grains C' (skin friction) remained constant in the experiments. Based on this assumption, Kleinhans & Van Rijn (2002) successfully hindcasted the sediment transport with a bedload predictor for these flume experiments, which suggests that the assumption is reasonable. C' was calculated using the White-Colebrook equation and assuming a Nikuradse grain-related roughness $k' = D_{90}$ (m) in which D_{90} = 90th percentile of the original sediment mixture: $C' = 18 \log(12h/k')$ in which h = water depth (m). Alternative methods, which subtract bedform-related roughness from total roughness to obtain grain roughness, are subject to large uncertainties related to the measurement of the total roughness and the determination of the bedform roughness. An advantage of the present method is that the depth-averaged flow velocity can be determined with high accuracy, and the grain-related Chezy parameter is rather insensitive to the chosen grain size.

In order to keep the grain-related shear stress for each experiment at a constant value, the cross-section- and depth-averaged flow velocity ($= Q/A$, with Q = flow discharge (m^3/s) and $A = hW$ is

Table 4.1. Experimental conditions (Blom & Kleinhans 1999, Kleinhans 2000). To obtain constant flow velocities during a test, both the water depth and discharge were adapted. Therefore these parameters are given as a range. The given water surface slope approximates the average bed slope.

experiment condition	water depth * (m)	discharge * (m ³ /s)	flow velocity ** (m/s)(Q/A)	water surface θ' slope (10 ⁻⁴)	transport	thickness of D50 transp. layer (mm)	final bed state
bed was mixed and bed slope installed							
T0	0.20 - 0.20	0.13 - 0.13	0.40 - 0.44	-4.48	0.073	0.001	flat bed, flow parallel sand ribbons
T1	0.20 - 0.37	0.13 - 0.33	0.42 - 0.59	-4.48	0.102	0.001	flat bed, flow parallel sand ribbons
T2	0.37 - 0.37	0.33 - 0.33	0.59 - 0.60	-5.22	0.056	0.000	flat armoured bed
T3a	0.37 - 0.46	0.33 - 0.50	0.59 - 0.73	-4.53		0.001	flat armoured bed
T3b	0.49 - 0.61	0.60 - 0.78	0.78 - 0.87	-7.06		0.002	small barchans over armour layer
T4a	0.49 - 0.52	0.60 - 0.60	0.77 - 0.82	-6.38	0.193	0.008	small barchans over armour layer
T4b	0.38 - 0.35	0.33 - 0.33	0.59 - 0.64	-4.88	0.134	0.008	small dunes over armour layer
bed was remixed and new bed slope installed							
T5	0.21 - 0.25	0.22 - 0.26	0.68 - 0.73	-14.72	0.170	0.008	small barchans over armour layer
T6	0.24 - 0.33	0.26 - 0.38	0.70 - 0.79	-14.62	0.217	0.017	dunes over armour layer
T7	0.34 - 0.36	0.41 - 0.43	0.77 - 0.81	-15.20	0.241	0.028	large dunes over armour layer
T8	0.35 - 0.27	0.42 - 0.30	0.79 - 0.70	-15.71		0.029	large dunes over armour layer
T9	0.25 - 0.27	0.26 - 0.28	0.68 - 0.72	-16.94	0.204	0.027	large dunes over buried armour layer
bed was remixed and new bed slope installed							
T10	0.14 - 0.19	0.14 - 0.19	0.49 - 0.60	-11.06	0.126	0.002	small barchans over armour layer

Notes

Water temperature in all experiments: 14 degrees Centigrade

* To obtain constant flow velocities during an equilibrium test, both the water depth and discharge were adapted. Therefore these parameters are given as a range.

** The flow velocity in the equilibrium experiments was constant, the given range is twice the standard error. The average velocity was used in the graphs.

*** The water surface slope approximates the average bed slope.

cross-sectional area (m^2), W =width of the flume (m)) had to be kept constant while bedforms developed. This cannot be established with a constant flow discharge, because the growing bedforms will lead to increasing form roughness and hence to decreasing grain bed shear stress. The consequence was that both the water depth (controlled by a downstream weir) and discharge had to be adjusted iteratively several times a day. At the same time the flow was kept uniform. It is acknowledged that the assumption of constant C' may not hold in changing surface compositions of sediment mixtures in different conditions, but the alternative of keeping the flow discharge constant would have led to a much less constant τ .

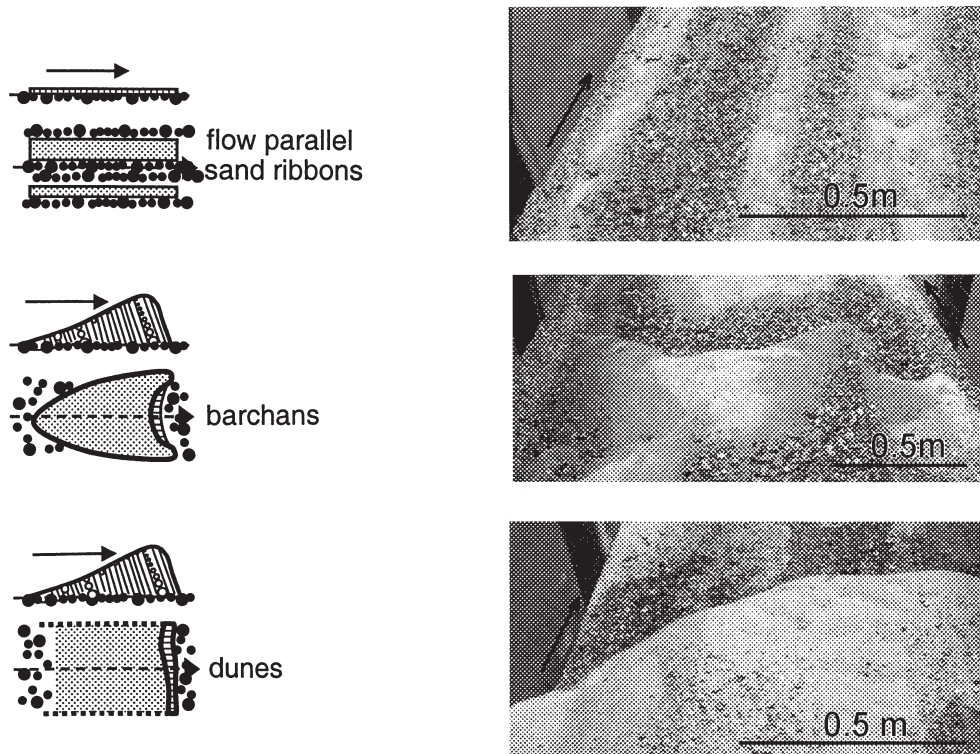


Figure 4.3. Bedform types observed in the flume experiments. Arrows denote flow direction and scale bars are 0.5 m. Stippled areas are sand and dots are gravel.

The experiments were conducted in the straight Sand Flume of Delft Hydraulics Laboratory, which is 50 m long and 1.5 m wide (Bakker, 1984). The water discharge, Q , may be varied between 0.03 and $0.8 \text{ m}^3 \text{ s}^{-1}$. The sediment is recirculated. Bed- and water surface levels are automatically recorded at every centimetre along the axis of the flume with electromagnetic water and bed surface profilers on a cart that runs on rails.

The total bed shear stress was calculated from the bed- and water surface profiles and corrected for flume sidewall roughness with the method of Vanoni-Brooks. The water temperature was kept constant at 14°C . The average flow velocity and the average water depth of each test are used to calculate the grain bed shear stress.

During the experiments the sediment transport was measured in the recirculation system. The sediment transport per size fraction has been determined from the bulk transport (kg/s). Samples were taken from the transported sediment, and were analysed by sieving and settling tube to

determine the particle size distributions of the transported sediment. In experiment T2, the sediment was not recirculated to have an armour layer developed.

The bed profiles were detrended and analysed with the computer program Dunetrack 2D (Wesseling & Wilbers, 1999). The output of this program is a number of bedform parameters: height, length, volume, and number of bedforms. This was done for all profiles.

4.3.2 Results of the flume experiments

In Figures 3 and 4, the observed bedform types are given as a function of depth-averaged flow velocity and bedform height. The flow parallel ribbons occurred in the lowest flow velocities (T0 and T2). The sand in the ribbons migrated downstream in the form of superimposed small ripples, which sometimes had barchanoid forms. Between the ribbons the bed surface consisted mainly of gravel. Barchans occurred in experiments T3b, T4a, T5 and T10. Dunes occurred in experiments T4b, and T6-T9. The armour layer under the barchans was broken up and entrained in the troughs of the barchans.

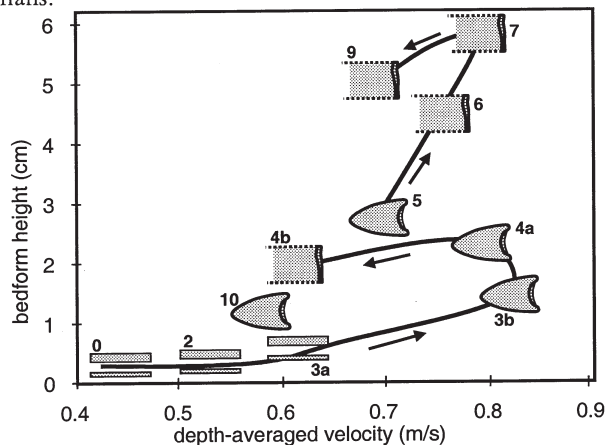


Figure 4.4. Bedform types and height as a function of depth-averaged flow velocity in the flume experiments. Labels refer to the flume experiments. The key to bedform type is shown in figure 3. The arrows indicate the order of the experiments. Note that the two series of experiments cannot be connected, because their flow histories and therefore armour layers are different.

Furthermore, sheets were observed to migrate over the dunes. The sheets had the height of ripples but were somewhat longer and sometimes showed a longitudinal sorting with the coarser grains at the leading edge. The sheets resembled both sand ripples and bedload sheets. However, these features have not been described in detail and were not detectable in the bed profiles.

The findings are interpreted as follows. During low flow, armouring almost inhibits bedload transport and only a very small portion of the bed is covered by bedload sediment in sand ribbons, bedload sheets or barchans. At rising stages the armour layer remains unbroken up to a certain point. This point may be determined by the threshold of motion of the imbricated particles and pebble clusters in the armour layer. In this case, the armour layer was broken up by the turbulence in the bedform troughs, as was also found by Klaassen (1986). As soon as such an armour layer is broken or mobile, more sand becomes available and the bedforms may eventually grow together into sand dunes. Also, at high flow velocities, part of the armour layer may be mixed into the

bedforms, resulting in sand-gravel dunes.

The history of sorting in the bed partly determines the outcome of the experiments. In the absence of an initial armour layer, a higher shear stress mobilises more sediment and larger grains, leading to the observed transition from sand ribbons to barchans to dunes (cf. T0, T10, T5 and T7). The outcome of T7 would have been the same for a fully mixed bed as initial condition, because the turbulence in the troughs of barchans and dunes becomes strong enough to override the armouring tendency, as was also observed by Klaassen (1986). However, when an armour layer is allowed to develop (as in T2) by cutting off the upstream sediment supply, then the critical shear stress for mobilising the armour layer is much larger. Once the armour layer is mobilised, the same transitions from sand ribbons to barchans and dunes occur (in T3 and T4), though at much higher shear stresses, and probably within a much narrower range of shear stresses. Consequently, although the experiments represent only a subset of all possible realisations, they range from the end-members of a strong armour layer to a fully mixed bed as initial conditions. Concluding, during low flow most of the sediment is immobile, leading to strong sediment supply-limited conditions with sand ribbons. With increasing flow strength more and more sediment was transported, which yielded a gradual change from sand ribbons to barchans, barchanoids and finally dunes and complete burial of the bed armour.

4.4 Field measurements

4.4.1 Field measurements in the river Allier (France)

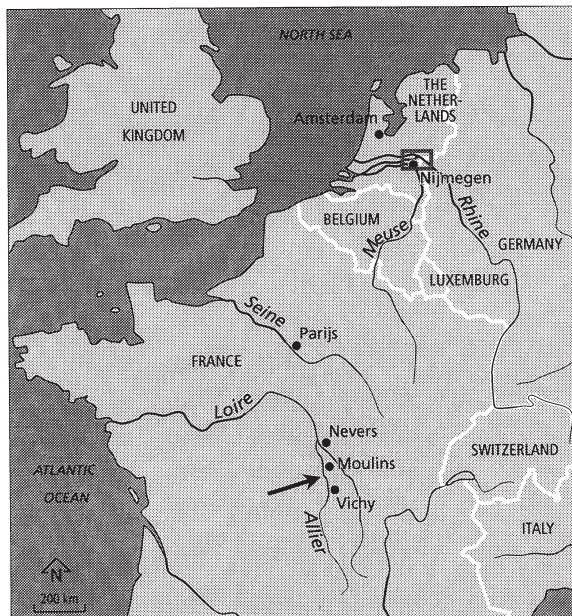


Figure 4.5. Location of the field measurements in the river Allier (arrow) and the river Waal (box). The area in the box in the Netherlands is enlarged in figure 7.

The river Allier, south of Moulins, in the centre of France, is one of the few meandering sand-

gravel bed rivers without artificial bank protection over distances of a number of meanders that still exist in Europe. The measurements were done 4 km to the south of Moulins (Fig. 4.5). At a bankfull discharge, which is about 900 m³/s, the width of the river varies between 60 and 100 m. During a period of high discharge the banks in outer bends may erode several tens of meters. Point bar morphology is well developed, with riffle spacings of about 600 m. The river bed is mostly armoured during low flow, with D_{50} =18 mm, D_{90} =40 mm and 85% gravel in the armour layer. The underlying bed sediment is distinctly bimodal with modes at 0.7 and 24mm, D_{50} =7 mm, D_{90} =32 mm and has 68% gravel.

Observations and measurements were made in summer during low flow with discharges of 20 - 40 m³/s. Bedforms consisting of sand with a D_{50} of 0.5 mm migrated over the armoured bed. Data collected at locations with bedforms comprised estimations of bedform dimensions (height, width, length) and the surface area covered by the bedforms. Vertical velocity profiles and water depths were obtained at several locations above and near the bedforms with an Electro Magnetic Flow device (EMF) mounted on a portable frame. The flow velocity was measured at the following levels above the bed: 0.05, 0.10, 0.15, 0.20, 0.25, 0.30, 0.40, 0.50 and 0.70 m. From these values, depth-averaged flow velocities, bed shear stress and roughness length data were obtained at the location of the bedforms. The bed and bedforms at the measuring location were sampled after the measurements and sieved for grain size analysis.

Several types of bedforms were observed (Table 4.2): sand ribbons, barchans and dunes, often concurrent in the same stretch of the river. Barchan varied in height between 0.01 and 0.05 m, dune heights were between 0.05 and 0.25 m. The sand coverage of the bed varied from 0 to 100 %. Relict gravel dunes were found on the surface of bars above the low flow water surface, indicating that these form during periods of higher discharge.

Table 4.2. Summary of the collected bedform, flow and sediment data in the river Allier.

bedform type	water depth*	flow velocity*	θ' transport*	thickness of transport layer*	D50 transport*
	(m)	(m/s)		(m)	(mm)
dune	0.85 - 1.10	0.55 - 0.80	0.052 - 0.118	0.030 - 0.100	0.42 - 0.91
barchan	0.53 - 1.04	0.52 - 0.74	0.066 - 0.112	0.004 - 0.009	0.53 - 1.04
sand ribbon	0.32 - 0.70	0.27 - 0.62	0.018 - 0.131	0.001 - 0.002	0.46 - 0.58
lower plane bed	0.32 - 1.25	0.41 - 0.71	0.032 - 0.088	0.001 - 0.004	0.33 - 1.54

Notes

Water temperature during the whole period: 20 degrees Centigrade

* Range of data within the bedform class. In total, 32 datapoints were collected.

Meander pools often contained deposits of fine sand between 0.1 and 1 m thick. These are probably waning or low flow deposits as described by Lisle & Hilton (1999). During the fieldwork period, a small peak in the discharge occurred, which allowed a wave of sand to detach from the sand deposit in the pool (Fig. 4.6). The sand reservoir in the pool was not emptied. The wave of sand provided a spatially varying sediment supply for bedforms in equal flow conditions. Near the pool, dunes with sinuous crests occurred, that gradually changed into barchanoid features downstream. Further downstream barchans occurred concurrently with sand ribbons, while even further only sand ribbons occurred. At the extreme front end of the wave of sand the armour was fully exposed. In time the volume of sand in the wave decreased, as the downstream propagating sand infiltrated into the armour layer.

At other locations, downstream migrating waves of sand of a few to a few hundred square meters were found. These waves of sand may have originated from the sand deposits in pools or from

bank failures. The same pattern of bedform types and order was observed as in the wave of sand derived from the meander pool deposit, but in this case it was mirrored in both the upstream and downstream direction (Fig. 4.6). This set of bedforms migrated downstream during low flow. For all locations and bedform types the flow conditions were more or less equal and the armour layer was stable.

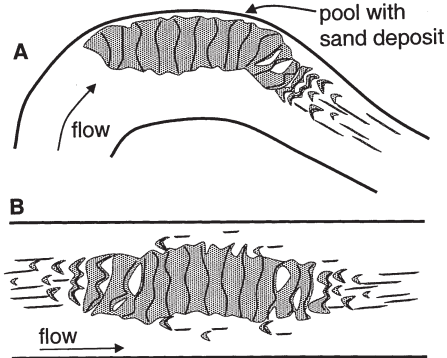


Figure 4.6. Observations of migrating waves of sand on the immobile armour in the river Allier. A) bedforms originating from a sand deposit in a meander pool. Bedform crests are denoted by solid lines, and sand by stippled patches. B) bedforms in a migrating wave of sand.

Concluding, a large range of bedform types was found in the river Allier at flow conditions in which the gravel was immobile. These bedform types were the same as found in the flume experiments. Contrary to the experiments, the flow conditions were about the same for all bedform types, and the armour layer was not broken up. The main factor causing the differences in bedform type was the availability of mobile sand for the formation of the bedforms.

4.4.2 Field measurements in the river Waal (The Netherlands)

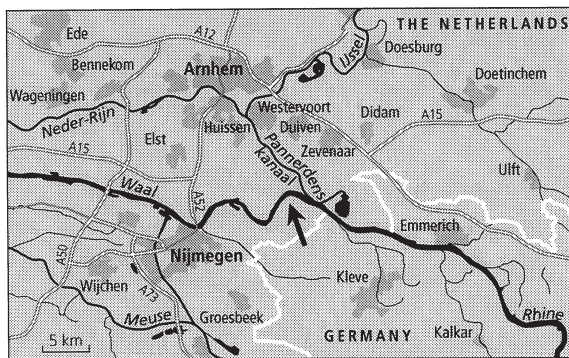


Figure 4.7. The location of the measurement section in the river Waal in the Netherlands (arrow) is just downstream of the bifurcation point of the Rhine into the Pannerdens Kanaal and the Waal. The flow direction is west. The location of this map is given in Figure 4.5.

The measurement location was the upstream section of the river Waal (Fig. 4.7). For navigation purposes and bank protection, both sides of the river have a system of groynes. The average width

of the river (between the groynes) is 240 m. Here, the water depth varies between 3 and 12 m. The median discharge of the Waal is 1350 m³/s with peaks up to 8000 m³/s. At high discharges bedforms develop with lengths of 10 to 20 m and heights of 0.5 m over the full width of the river (Wilbers, 1999).

The measurements were made in October and November 1998 (Kleinans, 1999; 2000) during a flood wave with a peak discharge of 6400 m³/s. At the measurement location the bed consists of a bimodal sand-gravel mixture with a median diameter of 2.8 mm, with the two modes at 0.5 mm and 10 mm. The D_{90} of suspended sediment is about 300 μm , while the mesh bag of the Helley-Smith type bedload sampler had a mesh size of 250 μm .

Three-dimensional echo sounding of the bed was done with a multibeam echo sounder, yielding on average a coverage of 15 points per m² over a width of at most 100 m at both sides of the middle of the channel. The riverbed was measured twice a day over 1 km along the river. Dunetrack 2D (Wesseling & Wilbers, 1999) software was used to calculate bedform dimensions and statistics (Wilbers, 1999).

The observed bedform type was straight-crested transverse dunes c.q. two-dimensional dunes. The bedforms attained their maximum height one day after the discharge peak (Fig. 4.8 and Table 4.3). After the peak discharge, smaller dunes emerged that propagated over the immobile and gradually disappearing large dunes. Allen & Collinson (1974) attribute this superposition of small active bedforms on inactive large dunes to the fast change in discharge.

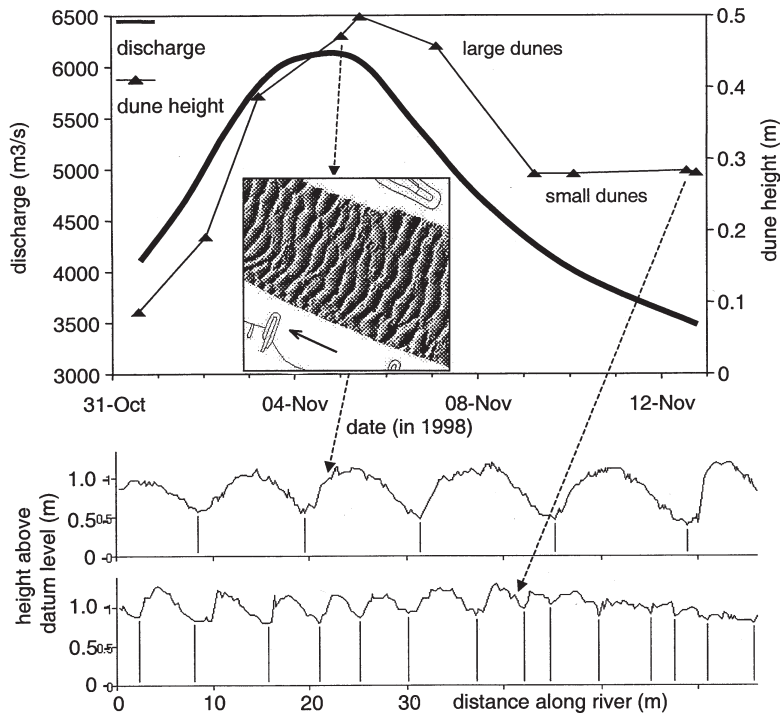


Figure 4.8. A) Flow discharge and dune height in the river Waal in October-November 1998, as well as a planform echosounding map of the river bed in the Waal just downstream of the bifurcation point with the Pannerdensch Kanaal. B) Two examples of dune profiles are given with large and with small dunes.

Table 4.3. Summary of the collected bedform, flow and sediment data in the river Waal.

date	bedform type	discharge (m ³ /s)	water temp. (C)	water depth (m)	θ' transport	dune height (m)	dune length (m)	dune volume (m ²)	thickness of D50 transp. layer transport* (mm)
31-Oct-98	small dunes	3993	12	9.2	0.313	0.09	3.22	0.20	0.063
02-Nov-98	small dunes	5032	12	9.7	0.361	0.19	7.02	0.83	0.118
03-Nov-98	dunes	5741	11	10.2	0.489	0.39	8.69	1.87	0.215
05-Nov-98	dunes	6097	11	10.7	0.521	0.47	10.93	2.86	0.261
05-Nov-98	dunes	5891	11	10.5	0.577	0.50	12.37	3.41	0.276
07-Nov-98	dunes	5114	10	10.1	0.316	0.46	18.86	4.68	0.248
09-Nov-98	small dunes	4198	10	9.4	0.287	0.28	6.53	0.98	0.150
10-Nov-98	small dunes	3899	10	9.2	0.344	0.28	6.53	0.98	0.150
12-Nov-98	small dunes	3407	9	8.7	0.392	0.28	6.19	0.95	0.154
12-Nov-98	small dunes	3372	9	8.6	0.390	0.28	6.08	0.92	0.152

Notes

* D50 of transported sediment determined from Helley-Smith bedload trap samples, averaged over the width of the river.

Concluding, during discharge peaks in the river Waal the bedform type is two-dimensional dunes with no significant armour layers in the troughs. Supply-limited bedforms were not observed, which does not mean that they did not occur. They might have been too small to be seen with the echo-sounder. In waning flow the large dunes become inactive and small active dunes are superimposed on the large.

Table 4.4. Summary of flume and field data of flow, sediment and bedform types from literature.

author	condition	bedform type	approx. water temperature (Centigrade)	water depth (m)	θ' transport	thickness of transport layer (m)	D50 transport (mm)
Bennett & Bridge (1995)	flume	bedload sheets	25	0.074 - 0.076	0.103 - 0.116	0.004 - 0.005	2.18 - 2.32
		low relief bars (small dunes)*	25	0.074 - 0.076	0.103 - 0.116	0.006 - 0.008	2.18 - 2.32
Blom et al. (2000)	flume	barchans	18	0.155	0.093 - 0.094	0.008 - 0.009	1.34 - 1.36
		dunes	18	0.320	0.126	0.034	1.34
Carling et al. (2000)***	field	barchans	unknown	2.7 - 6.65	0.078 - 0.211	0.051 - 0.099	0.9 - 0.9
Chiew (1991)	flume	dunes	unknown	0.17	Chiew does not give these parameters, only bed sediment and stream power.		
		ripples	unknown	0.17			
		lower plane bed	unknown	0.17			
Dinehart (1992)	field****	dunes	8 - 10	1.40 - 2.24	0.105 - 0.245	0.079 - 0.226	22 - 36
Horton et al. (2000)	flume	ripples	25	0.172 - 0.181	0.168 - 0.264	0.002 - 0.002	0.55 - 0.88
		bedload sheets	25	0.173 - 0.181	0.217 - 0.264	0.004 - 0.006	0.55 - 0.88
		low relief bedforms (small dunes)*	25	0.176 - 0.178	0.247 - 0.264	0.007 - 0.008	0.73 - 0.88
		ripples	25	0.138 - 0.15	0.119 - 0.221	0.002 - 0.003	0.54 - 2.78
		bedload sheets	25	0.139 - 0.15	0.119 - 0.221	0.004 - 0.007	0.57 - 2.78
Hirano & Ohmoto (1988)**	flume	low relief bedforms (small dunes)*	25	0.139 - 0.142	0.119 - 0.221	0.004 - 0.006	0.78 - 2.78
		sand ribbons	unknown	0.050	0.077	0.002	0.70
McLelland et al. (1999)	flume	sand ribbons	unknown	0.100	0.044	0.0005	0.87

Notes

* Low relief bedforms and bars are here interpreted as small dunes.

** For additional data, Carling & Goelz (1993) was used.

*** In McLelland et al. (1999).

**** North Fork Toutle river.

4.5 Bedform stability diagrams

4.5.1 Selection of diagrams

A number of bedform stability diagrams are available in literature. None of these diagrams however extend into the zone of medium to coarse gravels. This is due to lack of data, both from the field as from flume experiments. This means that part of the data used in this analysis will plot beyond the range considered in these diagrams. Hereinafter it will be assumed that the bedforms outside the range can be predicted by extrapolation of boundaries between bedform states as provided by the stability diagrams.

The Simons & Richardson (1965) diagram has two parameters, being the total stream power and the grain size:

$$\text{Bedform type}_{\text{Simons \& Richardson (1965)}} = F(\omega, D),$$

with $\omega = \tau u$ is stream power and D is sediment diameter. Chiew (1991) plotted the same streampower against sorting of the bed sediment to determine the effect of sorting of sediment on the transition between bedform types:

$$\text{Bedform type}_{\text{Chiew (1991)}} = F(\omega, \sigma_g),$$

with σ_g = geometric standard deviation of the (bed) sediment.

The Southard & Boguchwal (1990) diagram is the result of a very detailed and thorough compilation and analysis, in which the parameters are corrected for temperature effects. The diagram contains the flow velocity and grain size, and were constructed for several classes of water depth:

$$\text{Bedform type}_{\text{Southard \& Boguchwal (1990)}} = F(u, h, D).$$

A disadvantage of these three diagrams is that they require information on the energy gradient of the flow, or, alternatively, the total hydraulic roughness (comprising bedform and skin friction) in order to calculate the bed shear stress. In rivers these parameters generally are not measured with the required accuracy.

The bedform stability diagram of Van den Berg & Van Gelder (1993) does not have the above mentioned disadvantage. In addition to this, the transition to high Froude number related bedforms is provided for a number of waterdepths by a series of lines that cross-cut the diagram (Van den Berg & Van Gelder, 1998). Bedforms are plotted as a function of a dimensionless mobility versus a dimensionless grain number. The mobility, or skin friction related Shields parameter is given as $\theta' = \tau' / ((\rho_s - \rho)g D_{50})$, in which D_{50} is the median diameter of the bed sediment, g is the gravitational acceleration, $\rho_s - \rho$ is the submerged density of sediment, and τ' is the grain-related bed shear stress. It is assumed that the total shear stress is the sum of the grain-related shear stress and the bedform related shear stress. Thus, it is assumed that the grain shear stress determines the bed-load transport and therefore also the bedform type and dimensions. The grain, or Bonnefille parameter is given as $D^* = D_{50} = [(\rho_s - \rho)g / (\rho v^2)]^{1/3}$, in which v is the dynamic viscosity (m^2/s). Thus:

$$\text{Bedform type}_{\text{Van den Berg \& Van Gelder (1993)}} = F(\theta', D^*).$$

To investigate the nature of the bedforms in the datasets, the data are applied to three bedform stability diagrams, as they apply to conditions well below supercritical: Southard & Boguchwal (1990), Chiew (1991) and Van den Berg & Van Gelder (1993). In addition, a number of datasets with different types of bedforms in sand-gravel mixtures were collected from literature (Table 4.4),

which are also used in the diagrams.

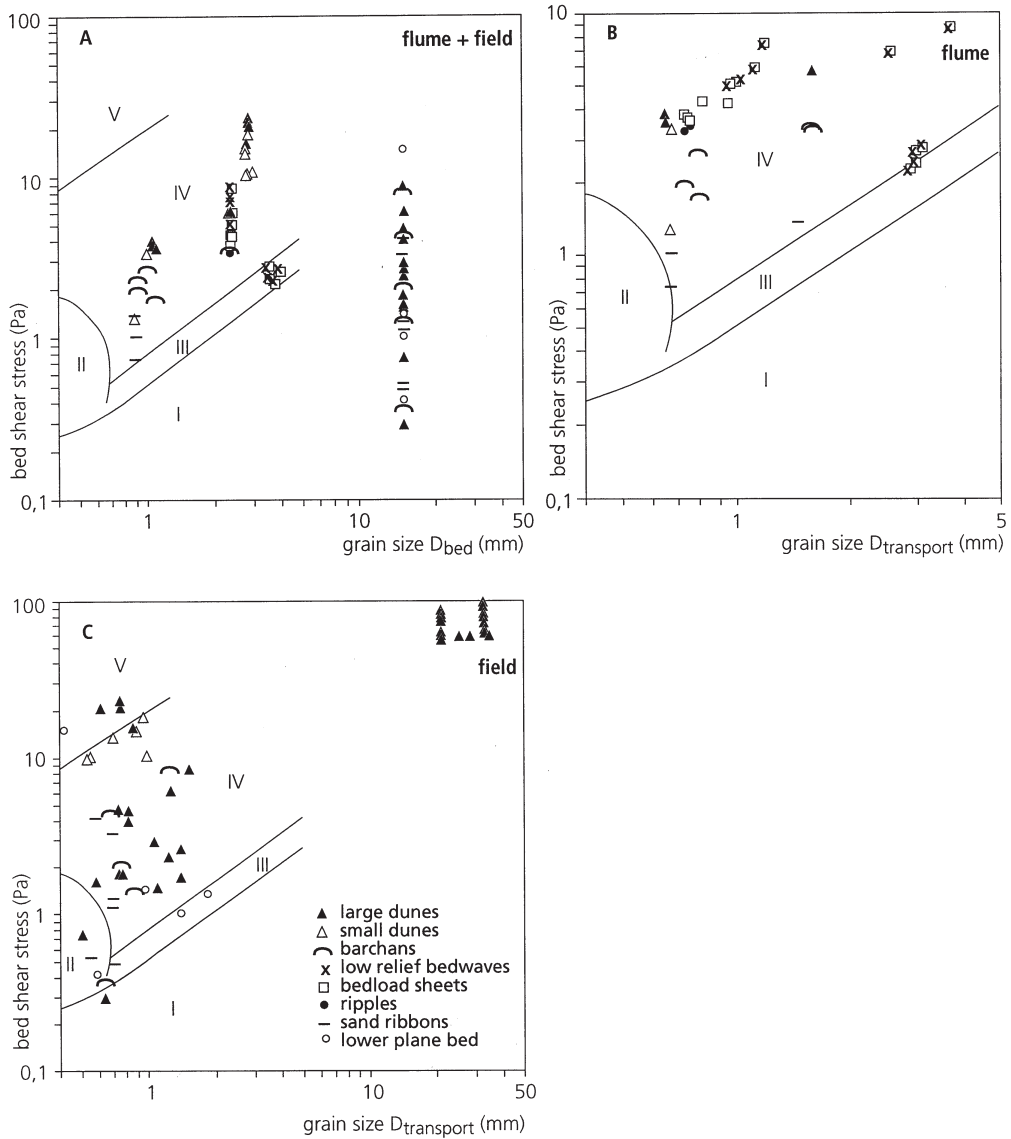


Figure 4.9. Data of bedforms in non-uniform sediment plotted in the Southard & Boguchwal (1990) bedform stability diagram for 10°C-equivalent quantities and subcritical flow conditions. A) Flume and field data, D_{50} determined from bed sediment. B) Flume data, D_{50} determined from transported sediment. C) Field data, D_{50} determined from transported sediment. Labels for regions: I, no movement on plane bed; II, ripples; III, lower plane bed; IV, dunes; V, upper plane bed.

4.5.2 Choice and effect of the grain size parameter

Figure 4.9 shows the flume and field data (described in Tables 1 to 4) in the diagrams of Southard & Boguchwal (1990). In Figure 4.9A, the D_{50} was determined from the bed sediment (points not shown if unavailable for a dataset). In uniform sediment, the bed and bedload consist of the same sediment, therefore the bed and bedload sediment are about the same. It might be argued that, also in the case of non-uniform sediment, the bed is where the bedforms derive their sediment from. In non-uniform sediment, however, the larger grain size fractions may be immobile. Bedforms then depend not only on the grain size of the mobile sediment, but also on the availability of this mobile sediment, which may deviate considerably from the grain characteristics of the immobile bed surface. Therefore it is hypothesised that the relevant grain size for bedform stability is the transported sediment (measured bedload sediment), because the bedforms comprise this sediment (Figs. 4.9B and C).

For the diagram based on bed sediment (Fig. 4.9A), a considerable number of barchans and dunes plot in the lower plane bed stability field. These are the bedforms in the Allier (this study) and in the Niederrhein (Carling et al., 2000a,b) (Table 4.4). For the diagrams based on the transported sediment the result is much better as was expected. Barchans all plot in the dune field. Sand ribbons plot both in the dune, ripple and lower plane bed range.

Chiew (1991) plotted streampower against sorting of the bed sediment to determine the effect of sorting of sediment on the transition between bedform types. Here (Fig. 4.10), streampower is plotted against the D_{90} / D_{50} of the bed sediment. For the Chiew data it is assumed that the sediment was lognormally distributed and the $D_{90} = D_{50}\sigma^{1.3}$, in which σ is the Trask sorting as given by Chiew. The data mostly plot in the fields as indicated by Chiew. The conclusion of Chiew (1991) that the sorting of the sediment has no effect on the bedform stability, as implicitly suggested also by all other existing bedform stability diagrams is confirmed.

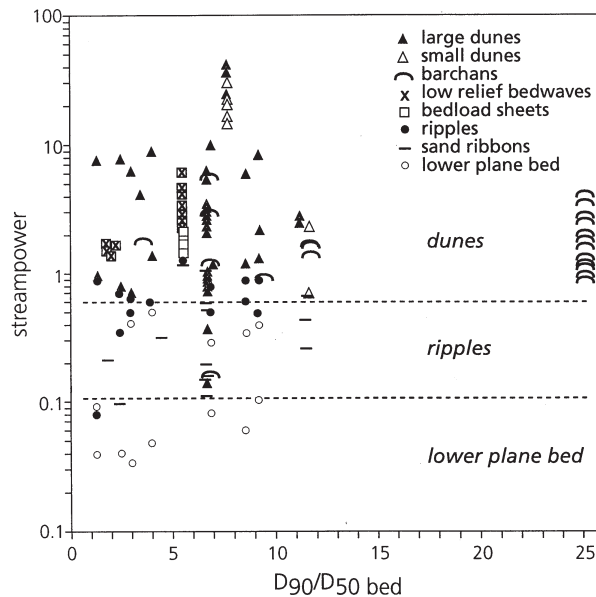


Figure 4.10. Bedform data in non-uniform sediment in the diagram of Chiew (1991). The D_{50} and D_{90} are determined from the bed sediment.

The Van den Berg & Van Gelder stability diagram is given in Figure 4.11. Note that the D_{50} and D_{90} of the bed or transported sediment are incorporated directly in the Shields parameter related to grain roughness. In Figure 4.11A the bedform types plot in the correct stability fields, but the field data in Figure 4.11B plot extremely low in the lower plane bed field. In Figure 4.11C and D, in which the D_{50} and D_{90} of the transported sediment are used, the bedform types plot reasonably well within the correct bedform stability fields. The only exception is the Dinehart data, which apparently plots partly in the lower plane bed field. Again the bedload sheets and low relief bedforms in the Bennett and Horton datasets plot in the dune fields. The sand ribbons plot in the lower plane bed as well as in the ripple and dune fields. Again, the classification is not successful when particle parameters of the bed sediment are taken, but is successful when size parameters of the transported sediment are taken.

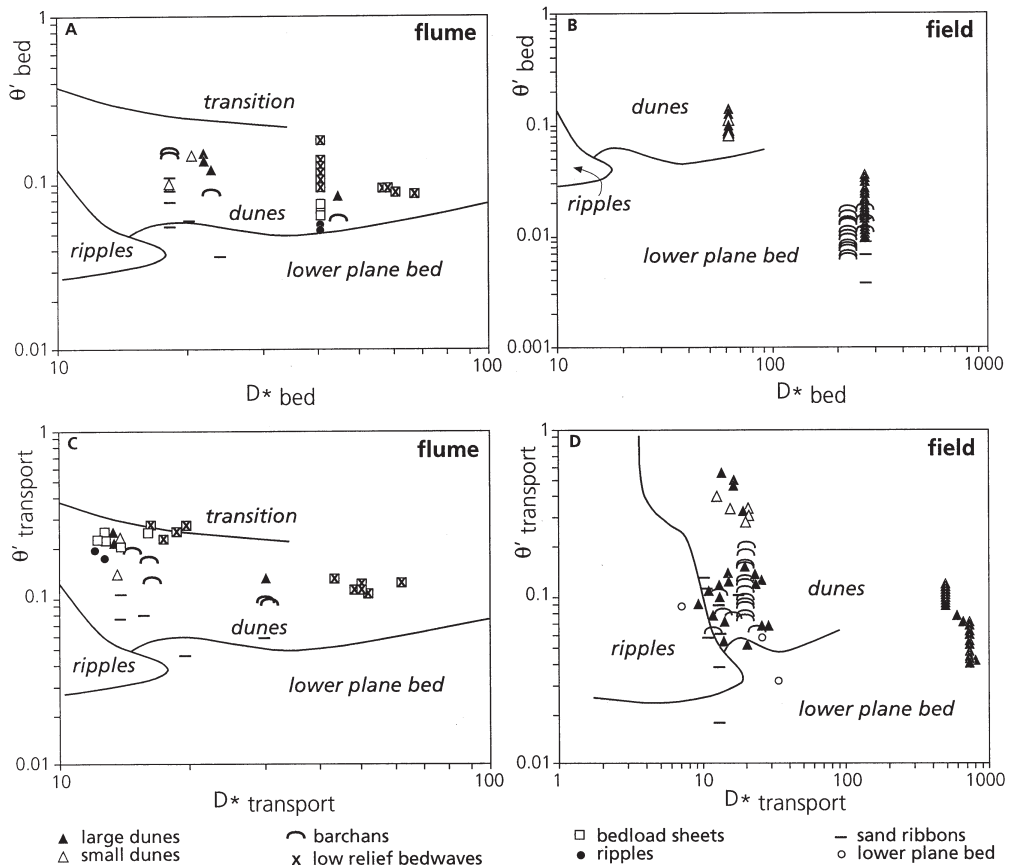


Figure 4.11. Data of bedforms in non-uniform sediment plotted in the Van den Berg & Van Gelder (1993) bedform stability diagram. A and B are flume and field data, respectively, D_{50} and D_{90} determined from bed sediment. C and D are flume and field data respectively, D_{50} and D_{90} determined from transported sediment.

Note that ripples from the Horton dataset (Table 4.4) would have plotted in the dune range at grain sizes larger than 0.7 mm, while Costello & Southard (1981) noted that ripples do not exist for grain sizes larger than 0.7 mm. Horton (pers. comm.) indicates that the ripples consisted of sand with grain sizes smaller than 0.7 mm, which migrated over the other bedforms, as has often been observed in the flume experiments and in the Allier. Data of superimposed ripples in the dune regime have been excluded from the diagrams.

There has been some discussion in literature about the nature of bedload sheets (e.g. Whiting et al., 1988; Iseya & Ikeda, 1987; Bennett & Bridge, 1995), particularly their relation with ripples or dunes. Dinehart (1989; 1992) and Whiting et al. (1988) observed bedload sheets that were superimposed on dunes. Just like the ripples of Horton these sheets may plot in the dune stability field because the bed is in the dune phase, but this does not mean that they are in the dune phase as well. Bedload sheets seem not to be supply-limited since they do not occur when the coarser particles are immobile. If the coarse particles were immobile, then another bedform type would probably emerge, like barchan ripples or dunes. Thus bedload sheets are probably not very relevant in the present discussion of supply-limited bedforms.

Concluding, the extended bedform stability diagrams describe the observed bedforms in non-uniform sediment reasonably well, provided that the grain size parameters are derived from the transported sediment instead of the bed sediment, bed surface or substrate. This proviso is the consequence of the sediment supply limitation. However, bedload sheets and barchans plot almost without exception within the dune stability fields, while sand ribbons plot within the lower plane bed, as well as in the ripple and dune stability fields. Thus the bedform stability diagrams have a limited predictive capacity to discriminate between the different bedform types in supply-limited conditions.

4.6 Effect of the supply limitation on bedform morphology

4.6.1 Transitions between supply-limited bedform types

Until now the focus was on the classification of bedform types. In reality however, gradual transitions exist, as was shown by the flume experiments and field data presented here. Barchans and transitional forms (here called barchanoids) to fully developed dunes plot in the dune stability fields of bedform stability diagrams, indicating that the sediment supply limitation determines whether a bedform will have a barchan form. It is interesting to note that barchan forms may occur in the ripple and in the dune stability fields. It suggests that bedform morphology is not limited to a certain bed state. Thus a supply limit of sand may cause both a ripple and a dune to obtain a barchan form.

The same accounts for sand ribbons. Obviously they are stable in both the ripple regime and the dune regime. (Actually, migrating ripples were sometimes observed in sand ribbons in flume and nature.) It seems that the dominant factor determining the occurrence of sand ribbons is a strong limit of the sediment supply, even stronger than in the case of barchans.

The effect of sediment supply on transitions between barchans and dunes is illustrated with a subset of data containing the experimental results. In experiment T4b the flow velocity and the bedform height are lower than in T4a. The bedforms in T4b became lower as a response to the lower flow velocity and water depth (flow depth-limitation). Thus sand became available for extension of the width of the bedforms, which lead to a transition from barchans to dunes (Fig. 4.12).

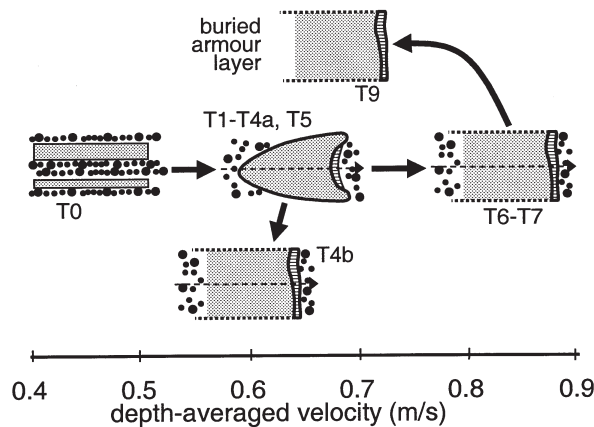


Figure 4.12. Transition of bedform types in response to changing flow velocity and bedload transport. The arrows indicate the order of the experiments; see Figure 4.3 for key to bedform types.

The same principle lies behind the difference in bedform type between T5 and T9, which have almost equal flow velocities. In T5 there was not enough sand available in the beginning for the formation of dunes, so the type was barchanoid. However, in T7 much more sand was in transport because it was winnowed from the bed below the armour layer. In T9 the sand of the large dunes of T7 was redistributed into the lower dunes of T9. The deposition of bedload sediment in T9 was so large that the armour layer of T7 was buried.

In Fig. 4.12 the bedform type transition observed in the flume experiments is sketched. Note, that the boundaries between bedforms stages are gradual, from barchans to barchanoids, to barchanoids with increasing slipface lengths, to dunes with barchanoid characteristics like crescentic slipfaces and tails, to dunes with irregular slipfaces, to more or less two-dimensional (transverse) dunes. These gradual transitions were also observed in the Allier.

4.6.2 Prediction of sediment supply-limited bedform morphology

The question now is how the bedform morphology in this continuum can be predicted. Obviously the sediment supply should somehow be incorporated in a predictive method for bedform morphology. Several approaches are discussed below.

Belderson et al. (1982) presented their semi-quantitative model for the oceanic shelf with flow velocity as the only parameter. In decelerating flow the sand settled from suspension and the supply for bedload increased, leading to a development from ribbons to dunes. Thus the main factor is the sediment supply. However, in many riverine conditions the reason for the sediment supply limit is not that all the sediment is suspended, but because the sediment on the bed surface cannot be entrained. Therefore their qualitative model is not generally appropriate for rivers. The qualitative model of McKee (1979) illustrates the continuous sequence of subareal transverse dunes to barchanoids to barchans with unidirectional wind and diminishing sand supply, but offers no quantification.

The problem might be approached by comparison with the uniform sediment case. The armouring tendency in non-uniform sediment causes the sediment supply limitation in the flume experiments. Keeping in mind that the available bedload transport predictors (e.g. Meyer-Peter & Müller, 1948) for uniform sediment neglect this armouring, a comparison between predicted transport and measured transport will reveal whether the sediment is supply-limited. A

computation of this supply-limitedness for a large range of conditions or an estimate of the sediment supply in the same range of conditions would allow an estimation of the occurrence of the supply-limited bedform types and their relative importance for that specific system. In Figure 4.13 the bedforms of the flume dataset (Kleinhans, 2000) are plotted against a modified Shields parameter (related to the grains of the transported sediment) and the ratio of predicted and measured (dimensionless) transport. For perfect supply unlimited bedload predictions, the latter ratio is unity. The bedload transport was predicted with the Meyer-Peter & Müller (1948) predictor, based on the (measured) transport sediment parameters and the modified Shields parameter instead of the original combined with the original ripple factor. This choice of parameters is discussed in detail in Kleinhans & Van Rijn (2002). Obviously the different bedform types are reasonably separated, with dunes the nearest to the fully mobile conditions and sand ribbons at the other end with barchans in between. So, if the sediment transport rate is predictable and the true transport has been measured, then the bedform type is predictable.

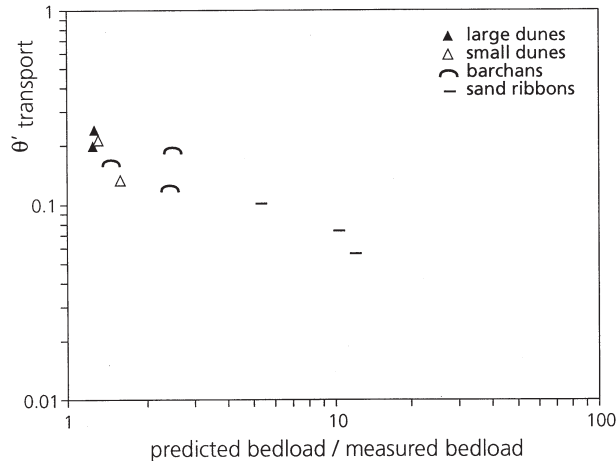


Figure 4.13. Bedforms plotted against the modified Shields parameter (related to the grains of the transported sediment), and the ratio of predicted and measured bedload transport. The prediction was done with the equation of Meyer-Peter & Müller (1948) based on the (measured) transported sediment parameters.

This is confirmed by Van der Zwaard (1974), who followed a comparable approach for determining the bedform-related flow roughness in the case of unimodal sand moving over an immobile coarse gravel layer (artificial bed protection). Increasing the sand feed-rate in a flume, the range of bedform types of barchans to fully developed dunes (without any gravel at the surface) was observed. The sediment transport and flow roughness in the latter case were the same as in experiments without the gravel. From the measured sediment feed-rate, Van der Zwaard was able to hindcast the flow roughness.

Unfortunately, this approach is impractical for the present purpose because the true transport rate must be measured. In the field, these measurements are difficult and expensive to do (Kleinhans & Ten Brinke 2001, see chapter 3). A cheap mapping of the bedforms with echosounders would directly answer the question about bedform morphology.

Moreover, the prediction of the sediment transport rate provides a problem in rivers with an armour layer. In a recirculating flume the sediment supply is determined by the conditions in that flume, but in natural rivers it is not. Waves of sediment may propagate through the system, which are derived from sudden collapse of upstream river banks during floods and other non-steady and

history effects. Thus the sediment supply is not (directly) related to the local flow and the local composition of the river bed (the latter excludes the overlying bedload sediment) just upstream of the bedforms. This almost erratic sediment supply can in no way be predicted. In practice the method of discrimination given in Figure 4.13 will therefore not be very feasible. The knowledge of the initial conditions is limiting the prediction in this respect.

As an alternative to the transport rate, the availability of sediment for the formation of bedforms can be expressed in a thickness of the transport layer. Roughly, this is the thickness of the layer of transported sediment that is obtained after distributing the sediment of the bedforms evenly over the bed. The thickness is computed by estimating the volume of sediment in each bedform, multiplying this by the fraction of the bed that is actually covered by the bedforms, and dividing the result by the total area in which the bedform dimensions were collected. For fully developed dunes that cover the armour layer, the thickness can also be obtained from bedform height (H) alone. The volume per meter width (here equivalent to thickness of the transport layer) for regular triangular dunes is $0.5H$ by definition, and up to $0.7H$ for more convex dunes (e.g. Havinga 1983). Here, $0.55H$ is taken, assuming near-triangular forms (Shinohara & Tsubaki (1959); Jinchi (1992)). For plane bed conditions the D_{90} of the bedload sediment is taken as the thickness.

The thickness of the transport layer does not alone determine the bedform morphology, since the waterdepth also was shown to have a large effect. A tentative approach is to rely on the relation between bedform height and flow depth, since most dune height predictors depend on the flow depth in some way (Van Rijn, 1993). As a first approximation the transport layer thickness is simply divided by the water depth to obtain a dimensionless parameter for sediment availability. This means that the flume and field datasets must be considered separately, as dunes in flumes are relatively higher (30% of flow depth as a rule of thumb) than in rivers (15% of flow depth).

Also here a prediction might be attempted with a bedform height predictor to estimate the bedform height for the same conditions but for uniform sediment. However, predictions of bedform height are even more uncertain than the prediction of bedload transport. Furthermore, it was concluded that bedforms in non-uniform sediment only plot correctly in bedform stability diagrams if the parameters of the transported sediment are used instead of the bed sediment. We expect that parameters of the transported sediment are also necessary for a correct prediction of bedform height. The composition of the bedload sediment should be predicted as well, which is also very uncertain. Therefore the prediction of bedform height is not attempted.

A plot (Fig. 4.14) of the dimensionless transport layer thickness against the modified Shields parameter shows a reasonable division between the bedform types in flumes and in rivers. The barchans plot to the left of the dunes, while the sand ribbons are even further to the left. Both ripple, sand ribbon and bedload sheet height are unrelated to the water depth, which explains their scatter in the plot (Fig. 4.14A). The dunes of the Waal dataset plot in the barchan range (Fig. 4.14B), which is not correct. At the large modified Shields values of these observations, all grain size fractions in the bed are already in motion. This deviation may have to do with the delayed response of large dunes to changes in the flow, as the dune height in the Waal dataset is much larger than in the other datasets.

With two alternative dimensionless parameters it was not possible to obtain a separation between the different bedform types. The first alternative that was tried, was the transport layer thickness divided by the D_{90} of the transported sediment, with the idea that the ripple and sand ribbon height might be related to the D_{90} of the sediment. The second alternative was the square of the D_{90} of the transported sediment divided by the product of transport layer thickness and water depth, with the idea that the ripples and sand ribbons are related to the surface area of the grains (and the drag force that acts on that surface), and to low water depth combined with small transport layer thickness. Neither of the parameters gave any consistent outcome when plotted on the horizontal axis of Figure 4.14.

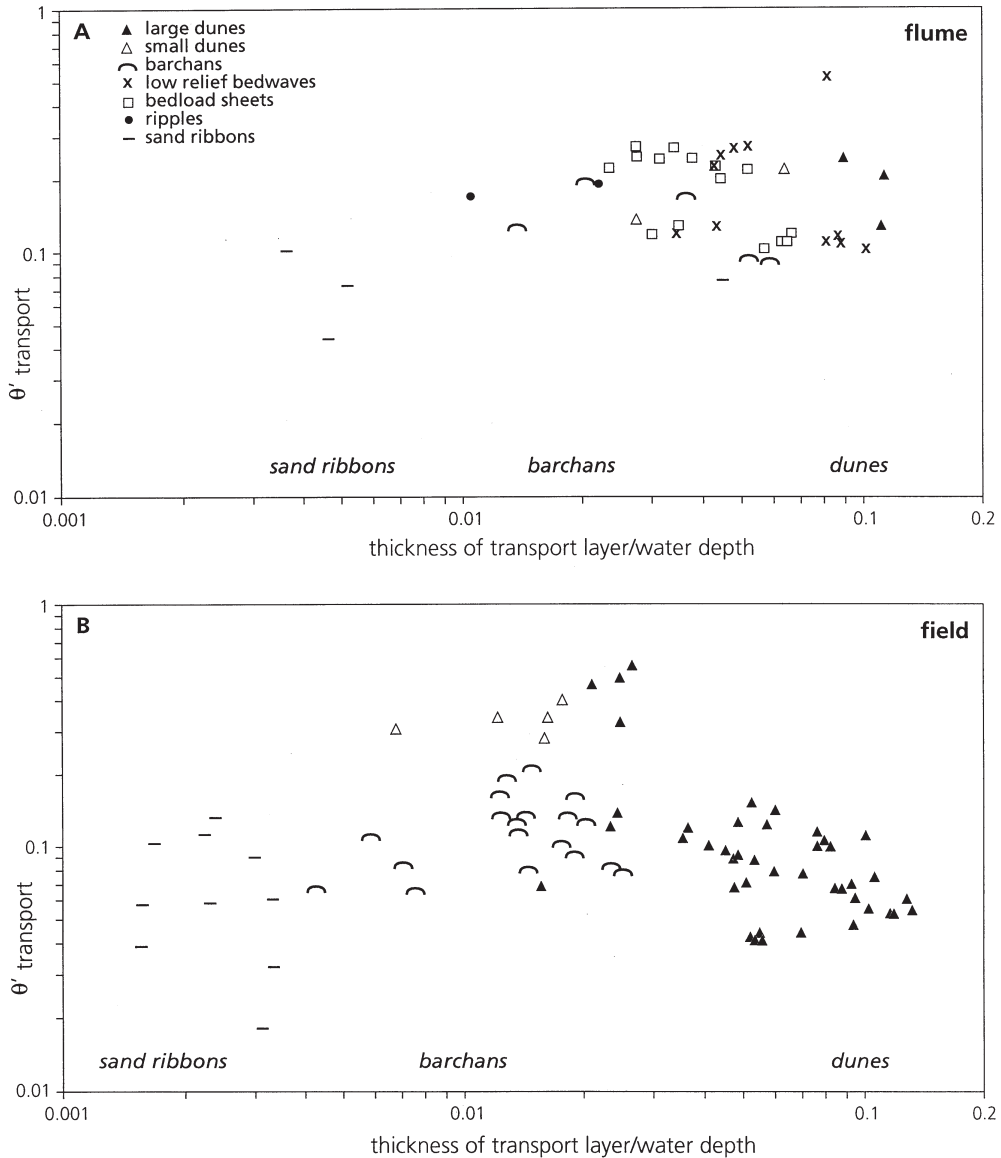


Figure 4.14. The dimensionless transport layer thickness against the modified Shields parameter (based on shear stress on grains of the transported sediment) for flume (A) and field (B) conditions.

A block diagram (Fig. 4.15) based on the dimensionless transport layer thickness (thickness divided by water depth) against the modified Shields parameter is given to illustrate the bedform morphology as derived from visual observations in the flume experiments and the river Allier. This block diagram is taken here as an explanatory model, not a predictive model. The dimensionless transport layer is dependent on bed shear stress, sediment of the bed but also very much on the upstream sediment supply, which cannot be predicted.

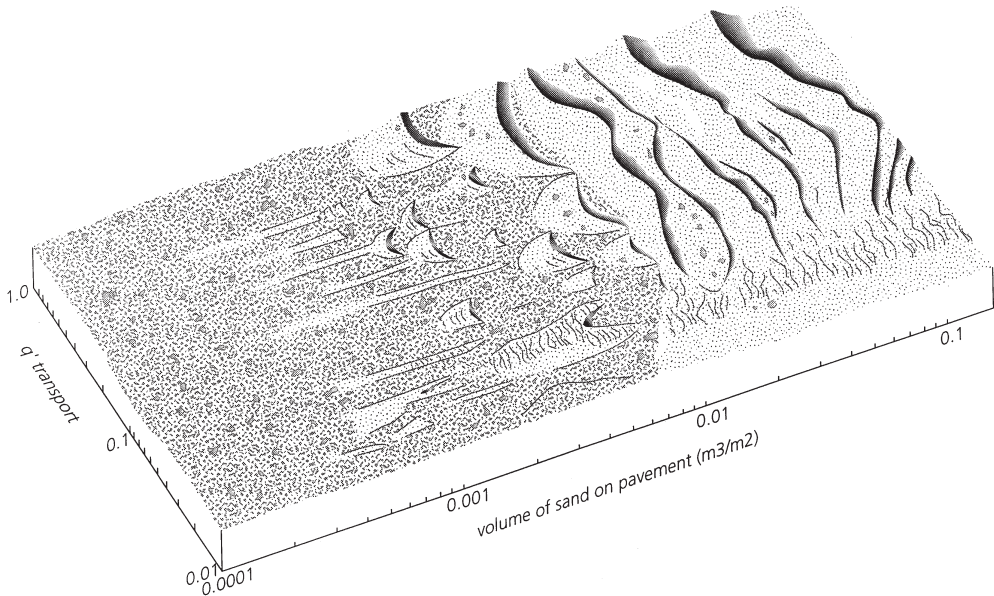


Figure 4.15. Conceptual explanatory (but not predictive) model for the occurrence of bedforms in sediment supply-limited conditions.

The explanatory Figures (Fig. 4.14) and the block diagram (Fig. 4.15) are given for a certain range of conditions. The modified Shields parameter (with grain-related shear stress and D_{50} of bedload sediment) is given for the range of 0.01 to 1. Note that the lower bound is smaller than the Shields criterion for initial motion of the D_{50} of bedload sediment. Because the mobility parameter is given for the bedload sediment, there is no uncertainty related to the fact that the D_{50} of the bed sediment may not be in motion while bedforms consisting of much finer sediment may occur. The main reason here for the low critical value of the mobility parameter is the definition of initial motion. The standard Shields criterion refers to the initiation of general particle motion, while the criterion here is for less mobile conditions. Since the sediment is segregated into sandy bedforms, the grains are not hindered by collisions with coarse immobile particles but can together develop into bedforms over time. Thus the dunes in the block diagram do not occur for a mobility below 0.03, which is about equal to the lower limit for stability of dunes in the stability diagram of Van den Berg & Van Gelder (1993).

The relative transport layer thickness is limited at the lower bound because it cannot become smaller than, say, the D_{90} of the bed surface sediment, because then there is no significant transport anymore. The upper bound is given by the maximum (equilibrium) height that a dune can attain in rivers, which is about 20% of the water depth.

In flume experiments and some rivers the sediment supply may be limited due to some (relatively weak) armouring, while at increasing flow velocities more sediment may be entrained to counteract the sediment supply limitation. In other rivers with stronger armour layers that cannot be broken up, the sediment may only be supplied by upstream inputs like bank failures. Further, sand stored in meander pools (and comparable areas in braided rivers) may be entrained by a small

increase in discharge, leading to the formation of a wave of sand which provides the sediment for the local bedforms. Concluding, the more or less independent processes of armouring, sand storage in pools and bank erosion may play roles to some extent in one and the same river. Only if these processes were fully understood and the boundary conditions well known, a prediction of the sediment supply might be feasible.

4.7 Conclusions

Sand ribbons and barchans are supply-limited bedforms that may occur frequently in rivers with non-uniform sediment, i.e. in flows below the critical threshold of motion of the coarser particles in or on the bed.

Bedform stability diagrams from literature can be extended for coarse sand and gravel, as was also indicated with more data by Carling (1999). In non-uniform sediment the particle parameters must be derived from the transported sediment instead of the bed sediment, as a consequence of the supply limitation of sediment.

The sediment supply limitation determines the morphology of the bedforms. Sand ribbons occur both in the ripple and in the dune regime, indicating that the secondary currents that create these bedforms occur in both high and low flow. In the dune regime, sand ribbons are extremely sediment supply-limited bedforms. If more sediment becomes available, barchans may emerge, which only occur in the dune regime. With even more sediment, the barchans may develop into barchanoid dunes or fully developed dunes.

In the case of supply-limited bedforms that move over a more or less immobile substrate, the sediment supply depends mostly on upstream sources and cannot be predicted from the local flow and bed sediment conditions. An explanatory (but not predictive) diagram, based on a dimensionless transport layer thickness and a modified Shields parameter, accounts for the observed bedform types and morphology.

Acknowledgments

The National Institute for Inland Water Management and waste water Treatment (RIZA) and the Directorate Eastern Netherlands of Rijkswaterstaat in the Netherlands financed and carried out the measurements in the rivers Waal and Bovenrijn. The Sand Flume experiments were financed by 1) the Transport and Mobility of Researchers programme of the European Commission and 2) the consortium of Twente University, the Institute for Inland Water Management and Waste Water Management (RIZA) and WL|Delft Hydraulics. Joanne Horton (of Leeds University) is gratefully acknowledged for providing her data on bedforms in sand-gravel sediment and for discussions. Ward Koster and Gerrit Klaassen are acknowledged for comments and discussion that helped to improve this paper. Jan Alexander, John Southard and an anonymous reviewer are thanked for their useful and stimulating comments.

References

- ALLEN, J. R. L. (1970), Physical processes of sedimentation. London, Allen and Unwin.
- ALLEN, J. R. L. (1984), Sedimentary structures, their character and physical basis, 1. Developments in Sedimentology 30. Amsterdam, Elsevier, 593 pp.
- ALLEN, J. R. L. & COLLINSON, J. D. (1974), The superimposition and classification of dunes formed by

- unidirectional aqueous flows. *Sedimentary Geology*, 12, p. 169-178.
- BAKKER, B. (1984), Straight sand flume description. Delft Hydraulics, report R657-XV, The Netherlands.
- BELDERSON, R. H., JOHNSON, M. A. & KENYON, N.H. (1982), Bedforms. In: STRIDE, A.H. (ed.), (1982), *Offshore tidal sands, processes and deposits*. London, Chapman and Hall, pp. 27-57.
- BENNETT, S. J. & BRIDGE, J. S. (1995), An experimental study of flow, bedload transport and bed topography under conditions of erosion and deposition and comparison with theoretical models. *Sedimentology*, 42 pp. 117-146.
- BLOM, A. & KLEINHANS, M. G. (1999), Non-uniform sediment in morphological equilibrium situations. Data Report Sand Flume Experiments 97/98. University of Twente, Rijkswaterstaat RIZA, WL|Delft Hydraulics. University of Twente, Civil Engineering and Management, The Netherlands.
- BLOM, A., RIBBERINK, J. S. & VAN DER SCHEER, P. (2000), Sediment transport in flume experiments with a trimodal sediment mixture. Proc. Gravel Bed Rivers Conference 2000, 28 August - 3 September, New Zealand, in NOLAN, T. & THORNE, C. (eds), Special publication CD-ROM of the New Zealand Hydrological Society, (<http://www.geog.canterbury.ac.nz/services/carto/toc.htm>).
- CARLING, P. A. & GOELZ, E. (1993), Investigation and numerical modelling of subaqueous dunes in the Rhine near Niederwalluf (Rheingau), Germany. (in German) Bundesanstalt fuer Gewaesserkunde (BfG) and Institute of Freshwater Ecology, Koblenz, Germany.
- CARLING, P. A. (1999), Subaqueous gravel dunes. *Journal of Sedimentary Research*, 69(3), pp. 534-545.
- CARLING, P. A., GOELZ, E., ORR, H. G. & RADECKI-PAWLIK, A. (2000a), The morphodynamics of fluvial sand dunes in the river Rhine, near Mainz, Germany. I. *Sedimentology and morphology*. *Sedimentology*, 47, pp. 227-252.
- Carling, P. A., Williams, J. J., Goelz, E., and Kelsey, A. D. (2000b), The morphodynamics of fluvial sand dunes in the river Rhine, near Mainz, Germany. II. *Hydrodynamics and sediment transport*. *Sedimentology*, 47, pp. 253-278.
- CHIEW, Y. M. (1991), Bed features in nonuniform sediments. *Journal of Hydraulic Engineering*, 117(1), pp. 116-120.
- COLOMBINI, M. (1993), Turbulence driven secondary flows and the formation of sand ridges. *Journal of Fluid Mechanics*, Cambridge, England, 254, 701-719.
- COSTELLO, W. R. & SOUTHARD, J. B. (1981), Flume experiments on lower-flow-regime bed forms in coarse sand. *Journal of Sedimentary Petrology*, 51(3), pp. 849-864.
- DINEHART, R. L. (1989), Dune migration in a steep, coarse-bedded stream. *Water Resources Research*, 25(5), pp. 911-923.
- DINEHART, R. L. (1992), Evolution of coarse gravel bed forms: field measurements at flood stage. *Water Resources Research*, 28(10), pp. 2667-2689.
- HAVINGA, H. (1983), Discussion: bed load discharge coefficient. *Journal of Hydraulic Engineering* 109(1), pp. 157-160.
- HESP, P. A. & HASTINGS, K. (1998), Width, height and slope relationships and aerodynamic maintenance of barchans. *Geomorphology*, 22, pp. 193-204.
- HORTON, J., BENNETT, S., BEST, J. & KUHNLE, R. (2000), Morphological and textural characteristics of bedforms generated in a bimodal sand-gravel mixture. Proc. Gravel Bed Rivers Conference 2000, 28 August - 3 September, New Zealand, in NOLAN, T. & THORNE, C. (eds), Special public. CD-ROM of the New Zealand Hydrological Society (<http://www.geog.canterbury.ac.nz/services/carto/toc.htm>).
- ISEYA, S. & IKEDA, H. (1987), Pulsation in bedload transport rates induced by a longitudinal sediment sorting: a flume study of sand and gravel mixtures. *Geografiska Annaler*, 69A, pp. 15-27.
- JINCHI, H. (1992), Application of sandwave measurements in calculating bedload discharge. Proceedings Symposium Erosion and Sediment Transport Monitoring Programmes in River Basins, Oslo. Publication 210, 63-70. International Association of Hydrological Sciences, Wallingford.
- KLAASSEN, G. J. (1986), Morphology of armoured beds: experiments with discharge waves (in Dutch). Report M2061 Delft Hydraulics, Delft, The Netherlands.
- KLEINHANS, M. G. (1999), Sediment transport in the River Waal: high discharge wave, November, 1998. (in Dutch) Netherlands Centre for Geo-ecological Research / Utrecht University Physical Geography. report ICG 99/6.
- KLEINHANS, M. G. (2000), The relation between bedform type, vertical sorting in bedforms and bedload

- transport during subsequent discharge waves in large sand gravel bed rivers with fixed banks. Proc. Gravel Bed Rivers Conference 2000, 28 August - 3 September, New Zealand, in NOLAN, T. & THORNE, C. (eds), Special public. CD-rom of the New Zealand Hydrological Society, (<http://www.geog.canterbury.ac.nz/services/cartto/toc.htm>).
- KLEINHANS, M. G. & TEN BRINKE, W. B. M. (2001), Accuracy of cross-channel sampled sediment transport in large sand-gravel-bed rivers, *Journal of Hydraulic Engineering* 127(4), pp. 285-269, see chapter 3.
- KLEINHANS, M. G. & VAN RIJN, L. C. (2002), Stochastic prediction of sediment transport in sand-gravel bed rivers, *Journal of Hydraulic Engineering* 128(4), ASCE, pp. 412-425, special issue: Stochastic hydraulics and sediment transport, see chapter 5.
- LISLE, T. E. & HILTON, S. (1999), Fine bed material in pools of natural gravel bed channels. *Water Resources Research*, 35(4), pp. 1291-1304.
- MCCULLOCH, D. S. & JANDA, R. J. (1964), Subaqueous river channel barchan dunes. *Journal of Sedimentary Petrology*
- MCKEE, E. D. (1979), A study of global sand seas, introduction. USGS Prof. paper 1052, Washington, USA, pp. 1-20.
- MCLEAN, S. R. (1981), The role of non-uniform roughness in the formation of sand ribbons. *Marine Geology*, 42, pp. 49-74.
- MCLELLAND, S. J., ASHWORTH, P. J., BEST, J. L. & LIVESEY, J. R. (1999), Turbulence and secondary flow over sediment stripes in weakly bimodal bed material. *Journal of Hydraulic Engineering*, 125(5), pp. 463-473.
- MEYER-PETER, E. & MUELLER, R. (1948), Formulas for bed-load transport. Third Conference of the International Association of Hydraulic Research, Stockholm, Sweden, pp. 39-64, 1948.
- PYE, K. & TSOAR, H. (1990), Aeolian sand and sand dunes, Chapter 6: Aeolian bedforms. Unwin Hyman, London, pp. 152-220.
- ROSZA, P. & JOZSA, J. (1999), Interaction of sandy bed-load and stable gravel bed. 28th International Association of Hydraulic Research, conference proceedings, Graz, Austria.
- RUBIN, D. M. & TOPPING, D. J. (2001), Quantifying the relative importance of flow regulation and grain size regulation of suspended sediment transport α and tracking changes in grain size of bed sediment β . *Water Resources Research*, 37(1), pp. 133-146.
- SHINOHARA, K. & TSUBAKI, T. (1959), On the characteristics of sand waves formed upon the beds of open channels and rivers. Reports of Research Institute for applied mechanics, Kyushu University, pp. 15-45.
- SIMONS, D. B. & RICHARDSON, E. V. (1965), A study of variables affecting flow characteristics and sediment transport in alluvial channels. In: Federal Inter-agency Sediment Conf. 1963 Proc., Misc. Pub. US Agric. 970, Washington, USA, pp. 193-207.
- SOUTHARD, J. B. & BOGUCHWAL, A. (1990), Bed configurations in steady unidirectional water flows. Part 2. Synthesis of flume data. *Journal of Sedimentary Petrology*, 60 no. 5, pp. 658-679.
- VAN DEN BERG, J. H. & VAN GELDER, A. (1993), A new bedform stability diagram, with emphasis on the transition of ripples to plane bed in flows over fine sand and silt. Special Publications of the International Association of Sedimentologists 17, pp. 11-21.
- VAN DEN BERG, J. H. & VAN GELDER, A. (1998), Discussion of: flow and sediment transport over large subaqueous dunes: Fraser River, Canada. *Sedimentology*, 45, pp. 217-221.
- VAN DER ZWAARD, J. J. (1974), Effect of bedload transport on the hydraulic roughness of a bed protection layer (in Dutch). Report M988II, Delft Hydraulics, Delft, The Netherlands.
- VAN RIJN, L. C. (1984), Sediment transport, part I: bed load transport. *Journal of Hydraulic Engineering*, 110 (10) pp. 1431-1456.
- VAN RIJN, L. C. (1993), Principles of sediment transport in rivers, estuaries and coastal seas. Oldemarkt, Aqua Publications, The Netherlands.
- WESSELING, C. & WILBERS, A.W.E. (1999), Manual DT2D version 2.2. Software for dune-tracking in two dimensions (in Dutch). Utrecht University, Dept. of Physical Geography, The Netherlands.
- WHITING, P. J., DIETRICH, W. E., LEOPOLD, L. B., DRAKE, T. G. & SHREVE, R. L. (1988), Bedload sheets in heterogeneous sediment. *Geology*, 16, pp. 105-108.

- WILBERS, A. W. E. (1999), Bedload transport and dune development during discharge waves in the Rhine branches, echo soundings of the flood in November 1998, (in Dutch). Netherlands Centre for Geoeological Research / Utrecht University Physical Geography, report ICG 99/10.
- WILCOCK, P. R. (1998), Two-fraction model of initial sediment motion in gravel-bed rivers. *Science*, 17 April 1998, 280 pp. 410-412.

5

Prediction of bedload sediment transport

“... a success of explanation is a success of adequate and informative description. And while it is true that we seek for explanation, the value of this search for science is that the search for explanation is ipso facto a search for empirically adequate, empirically strong theories.” Bas van Fraassen (1980: p. 157, *The Scientific Image*, Clarendon Paperbacks, Oxford)

Abstract

Classical deterministic bedload transport predictors are applied to sand-gravel bed rivers. The turbulent bed shear stress is modelled according to a probability distribution to obtain realistic bedload transport rates at incipient motion. In extending the predictors to stochastic predictors for non-uniform sediment, many parameters that represent near-bed turbulence and the particle size distribution must be chosen. The parameters that give realistic results are chosen by analyzing the results of a new experimental flume dataset with relatively large water depths. Choosing other combinations of parameters may give equal total bedload transport rates, but at the cost of large errors in fractional transport rates. Attention is given to the hiding-exposure phenomenon and a hindrance effect related to non-uniform sediment. Validation based on two independent field datasets shows that successful predictions of particle sizes near the threshold for motion are feasible using the stochastic approach, while the deterministic approach gives successful predictions well above incipient motion.

This chapter is reproduced from:

Kleinmans, M. G. & Van Rijn, L. C. (2002). Stochastic Prediction of Sediment Transport in Sand-gravel Bed Rivers. *Journal of Hydraulic Engineering* 128(4), ASCE, pp. 412-425, special issue: Stochastic hydraulics and sediment transport, reproduced with permission of the ASCE.

5.1 Introduction

In many rivers with sand-gravel bed material the sand fraction is in motion while the gravel fraction is below the threshold of motion for a significant portion of the year. Using a deterministic bedload predictor (with a critical bed shear stress for incipient motion) the predicted transport of the gravel fraction in the bed might then be zero, while the true transport is non-zero. When the larger sediment particles are below the threshold for motion, the stochastic nature of bedload transport due to flow turbulence should also be represented, because sediment sizes that are on average below the threshold of motion, could well be responsible for some transport due to the turbulence. The effect of turbulence on sediment transport near the threshold of motion was first modelled in detail by Einstein (1937) and Kalinske (1947). There are now several new stochastic predictors available, e.g. Bridge & Bennett (1992) and Van Rijn (1993).

A number of deterministic bedload transport predictors have been tested on field data of the river Waal in the Netherlands (Kleinhans 1996, 1999). The measurements were done with an acoustic doppler instrument for velocity verticals and a Helley-Smith type bedload transport sampler during a high discharge wave. The measurement location was the same location from which the sediment used in the flume tests presented herein, was dredged. Several bedload predictors were tested: Van Rijn (1984), Meyer-Peter & Mueller (1948), Kalinske-Frijlink (1951, in Van den Berg 1987), Parker, Klingeman & McLean (1982), Samaga, Ranga Raju & Garde (1986) and Zanke (1990). The two predictors yielding the best results are Meyer-Peter & Mueller (1948) (MPM) and Van Rijn (1984) (VR). Therefore the present analysis is restricted to these two predictors.

The original VR and MPM are successful in the uniform sediment approach in fully mobile conditions. In this paper the application of the bedload transport predictors of VR and MPM is investigated for sand-gravel sediment in fully mobile conditions and near the threshold of motion. As the original VR and MPM were not developed for these purposes, a basic problem is that several methods can be chosen to represent the turbulent flow and the particle size distribution of the bed material. What choices are physically realistic and which combination of choices gives the best results? The aim is to adapt MPM and VR for non-uniform sediment near incipient motion and fully mobile condition, based on realistic assumptions and understanding of the transport process, including turbulence.

First all possible methods are described and attention is given to the incipient motion of different particle sizes. Next a new dataset from flume experiments is presented on which the methods are tested. Finally the best method is presented and evaluated based on two independent field datasets. The main problem of this paper is the choice between a number of parameters, which in other combinations might give (almost) equal predictions. By dealing with the most sensitive and most clear parameters first, a unique combination is arrived at.

5.2 Types of bedload predictors

Most bedload predictors have been developed for uniform sediment. The bed sediment can then be represented by only one value, e.g. the D_{50} , D_{65} or D_m . Some predictors can be extended for the calculation of transport of several size fractions representing a sediment mixture (non-uniform sediment). In deterministic predictors the flow is characterized by a single value of the grain bed shear stress. To represent turbulence, the grain bed shear stress can be given as a probability density function characterized by an average and a standard deviation (e.g. Bridge & Bennett 1992). These predictors are herein called stochastic. This gives the following classes:

Bedload predictor class	Application		
1. Uniform deterministic	sand bed or gravel bed river	all sediment in motion	$\tau_b \gg \tau_{b,cr}$
2. Uniform stochastic	sand bed or gravel bed river	incipient motion, turbulent flow	$\tau_b \sim \tau_{b,cr}$
3. Non-uniform deterministic	sand-gravel bed river	all sediment in motion	$\tau_b \gg \tau_{b,cr}$
4. Non-uniform stochastic	sand-gravel bed river	incipient motion, turbulent flow	$\tau_b \sim \tau_{b,cr}$

Bedload predictor types 3 and 4 usually are derived from types 1 and 2. Herein the attention is focussed on the general case of sediment transport in a sand-gravel bed river with variable bed shear stresses.

5.3 Prediction methods and parameters

5.3.1 Modification of deterministic predictors for non-uniform sediment

A general method to calculate fractionwise transport is to divide the mixture in a number of size fractions and calculate the sediment transport of each size fraction separately, after which the transport is summed for all fractions (e.g. Einstein 1937, Ribberink 1987, Bridge & Bennett 1992).

The predictor of transport of MPM (Meyer-Peter & Mueller 1948) for a size fraction is as follows:

$$\phi_{b,i} = p_i \alpha \left(\theta'_i - \theta_{cr,i,corrected} \right)^{1.5} \quad (1)$$

in which $\phi_{b,i}$ = dimensionless bedload transport of size class i in the bed material (substrate), α = constant, originally $\alpha = 8$; θ' = Shields grain shear stress; p_i = percentage of occurrence of size class i in the bed material (substrate); and $\theta_{cr,i,corrected}$ = Shields critical shear stress corrected for hiding-exposure effect. Generally it is assumed that $\theta_{cr,i,corrected} = \xi_i \theta_{cr,D_i,Shields}$ or $\xi_i \theta_{cr,D_{50},Shields}$. This choice will be discussed in this paper.

Originally, MPM was based on the total dimensionless shear stress corrected for ripple roughness with a ripple factor. Herein a more direct calculation of the dimensionless grain bed shear stress is preferred, following Van Rijn (1984). The dimensionless (Shields) grain bed shear stress can be calculated from the grain bed shear stress, herein defined as: $\tau' = \rho g (\bar{u} / C')^2$ with ρ = density of water, g = gravitational constant, \bar{u} = depth-averaged flow velocity and C' = Chézy coefficient for grains, given by the White-Colebrook formula $C' = 18 \log(12R_b / k_{s,grains})$ in which R_b is the hydraulic radius (corrected for sidewall-roughness) and $k_{s,grains}$ is the Nikuradse grain roughness. The dimensionless (Shields) grain bed shear stress is given as:

$$\theta'_i = \frac{\tau'}{(\rho_s - \rho) g D_i} \quad (2)$$

The dimensionless transport can be rewritten to transport in kg/sm in two ways:

$$\begin{aligned} q_{b,i} &= \rho_s \phi_{b,i} \cdot \sqrt{(s-1)g} D_{50}^{1.5} & (a) \\ q_{b,i} &= \rho_s \phi_{b,i} \cdot \sqrt{(s-1)g} D_i^{1.5} & (b) \end{aligned} \quad (3)$$

in which ρ_s = sediment density (kg/m³), s = relative density of sediment (ρ_s/ρ), D_{50} = 50% percentile of the particle size distribution (median diameter), D_i = i -th percentile belonging to size fraction i in the bed material.

The predictor of transport of VR (Van Rijn 1984) for a size fraction is as follows:

$$\phi_{b,i} = p_i \beta T_i^{1.5} D_*^{-0.3} \quad (4)$$

in which β = constant, originally 0.1, T_i = transport parameter (relative excess shear stress) and D_* = Bonnefille grain parameter. The dimensionless transport can be rewritten to transport in kg/sm with equation 3a/b.

In the transport parameter T_i two different choices must be combined. The first choice is whether

$$\begin{aligned} T &= \frac{\tau' - \tau_{cr}}{\tau_{cr}} & (a) \\ T &= \frac{\theta' - \theta_{cr}}{\theta_{cr}} & (b) \end{aligned} \quad (5)$$

T_i is written in terms of grain bed shear stress or (dimensionless) Shields grain shear stress.

The second choice is whether the hiding-exposure correction is applied in the denominator of T_i , e.g.:

$$T = \frac{\theta' - \theta_{cr,i,corrected}}{\theta_{cr,i}} \quad (a) \quad T = \frac{\theta' - \theta_{cr,i,corrected}}{\theta_{cr,i,corrected}} \quad (b) \quad (6)$$

Combination of the two different choices gives the following four options:

$$\begin{aligned} T_i &= \frac{\theta'_i - \theta_{cr,i,corrected}}{\theta_{cr,i,corrected}} & (a) & \quad T_i = \frac{\theta'_i - \theta_{cr,i,corrected}}{\theta_{cr,i}} & (b) \\ T_i &= \frac{\tau'_i - \tau_{cr,i,corrected}}{\tau_{cr,i,corrected}} & (c) & \quad T_i = \frac{\tau'_i - \tau_{cr,i,corrected}}{\tau_{cr,i}} & (d) \end{aligned} \quad (7)$$

The D_* is given in two options:

$$D_{*,50} = D_{50} \sqrt[3]{\frac{(s-1)g}{v^2}} \quad (a)$$

$$D_{*,i} = D_i \sqrt[3]{\frac{(s-1)g}{v^2}} \quad (b)$$
(8)

5.3.2 Modification to stochastic predictors (for non-uniform sediment)

The grain shear stress τ' is assumed to have a stochastic nature due to turbulence (Grass 1970). The nature of turbulence as well as the effects on sediment transport have been described by Nelson et al. (1995) and Cao (1997), who found that sweeps and ejections cause the most sediment transport. The probability density function of the grain shear stress can be approximated by a normal distribution, assuming that the combination of turbulent ejections and sweeps cause equally effective grain shear stresses in both upstream and downstream direction. Alternatively, a lognormal distribution could be taken when assuming that the sweeps are more effective sediment entrainers. However, Bridge & Bennett (1992) found that the effect of a lognormal distribution compared to the normal, is small.

The bedload transport is integrated over the whole probability density function. The proportion of time $p_{\tau'_j}$ that τ'_j is active is calculated with the Gaussian probability density function of grain bed shear stress for an interval $\Delta\tau'$ (e.g. Bridge & Bennett 1992, Van Rijn 1993):

$$p_{\tau'_j} = \Delta\tau' \frac{1}{\sqrt{2\pi} \sigma_{\tau'}} \exp\left[-\frac{1}{2}\left(\frac{\tau'_j - \bar{\tau}'}{\sigma_{\tau'}}\right)^2\right] \quad (9)$$

in which $\sigma_{\tau'}$ = standard deviation of the momentaneous τ' . This standard deviation is given as $\sigma_{\tau'} = \gamma\tau'$ in which γ = relative standard deviation of τ' . γ must be chosen appropriately, e.g. De Ruiter (1980) and Bridge & Bennett (1992) give $\gamma=0.4$. Since the transport is zero for $|\tau'_j| < |\tau_{cr,i}|$, the probability density function should only be calculated for $|\tau'_j| > |\tau_{cr,i}|$ in both flow directions:

$$\Phi_i = \int_{-\infty}^{-\tau_{cr,i,corrected}} p_{\tau'_j} \Phi_{i,j} d\tau_j + \int_{\tau_{cr,i,corrected}}^{\infty} p_{\tau'_j} \Phi_{i,j} d\tau_j \quad (10)$$

in which the integration is done numerically using an appropriately small shear stress interval $\Delta\tau'$ and a non-infinite lower and upper boundary of the τ'_j . Bridge & Bennett (1992) assume that six standard deviations include most of the distribution. The interval $\Delta\tau'$ then has a width of $6\sigma_{\tau'}/N$ in which N is the number of intervals (herein $N=16$).

5.4 Critical bed shear stress of particle size fractions in non-uniform sediment

5.4.1 Hiding-exposure correction

When the bed sediment consists of a large range of particle diameters the Shields curve is no longer valid due to the hiding-exposure effect. Coarser particles are more exposed to the flow and therefore have smaller critical shear stresses. Finer particles are hiding in the wake of coarser particles and therefore have larger critical shear stresses. The critical (dimensionless) shear stress of each fraction is often corrected with a hiding-exposure function (he-function):

$$\theta_{cr,i,corrected} = \xi_i \theta_{cr,Shields} \quad (11)$$

A theoretical hiding exposure function (he-function) is given by Egiazaroff (1965):

$$\xi_i = \frac{1.66667}{\left[\log \left(19 \frac{D_i}{D_{50}} \right) \right]^2} \quad (12)$$

In Figure 5.1 the critical bed shear stress is given according to Shields and the he-function of Egiazaroff for $D_{50}=1\text{mm}$. The critical bed shear stress is also given in dimensionless form to simplify comparison with the Shields curve. Alternatively ξ_i is given as an empirical relation of the form (also in Fig. 5.1):

$$\xi_i = \left(\frac{D_i}{D_{50}} \right)^{P_i} \quad (13)$$

in which the power P usually is between 0 (which results in uncorrected Shields values), and -1 (which results in perfect equal mobility according to Parker & Klingeman (1982)).

If the power P is -1 for all size fractions, then all fractions are equally mobile and have equal critical bed shear stresses. Parker et al. (1982) hypothesized that this is the case if the largest fraction is in motion while a mobile armour exists. In a mobile armour the differences in hiding and exposure of the fractions have the effect that the critical Shields value is the same for every particle size (see Fig. 5.1).

Buffington & Montgomery (1997, 1998) gave an exhaustive overview of most existing empirical (power) relations. They conclude that no universal relation can be found, but defendable values should be used for each setting. Both the empirical and theoretical he-functions will be used in this paper.

5.4.2 Critical Shields parameter (θ_{cr}) for D_i or D_{50}

The critical Shields parameter is corrected with a he-function (eqs. 1 and 11). The question is

whether the critical Shields parameter should be described in terms of the median diameter ($\theta_{cr,D50}$) or of the diameter of each fraction ($\theta_{cr,Di}$):

$$\begin{aligned}\theta_{cr,i,corrected} &= \xi_i \theta_{cr,Shields,D50} & (a) \\ \theta_{cr,i,corrected} &= \xi_i \theta_{cr,Shields,Di} & (b)\end{aligned}\tag{14}$$

in which $\theta_{cr,i}$ = corrected critical Shields parameter of size fraction i in the bed material, $\theta_{cr,Shields,D50}$ = critical Shields parameter of the median sediment diameter, and $\theta_{cr,Shields,Di}$ = critical Shields parameter of each size fraction. To show the difference between the two options as clearly as possible, a power function is applied for a D_{50} of 1 mm with a power P of -1 (see Fig. 5.2). If $\theta_{cr,Shields,D50}$ is used then the corrected critical Shields curve is a straight (dashed) line in Figure 5.2. The alternative has the same form as the original curve. The question is whether that form has any meaning in a mixture.

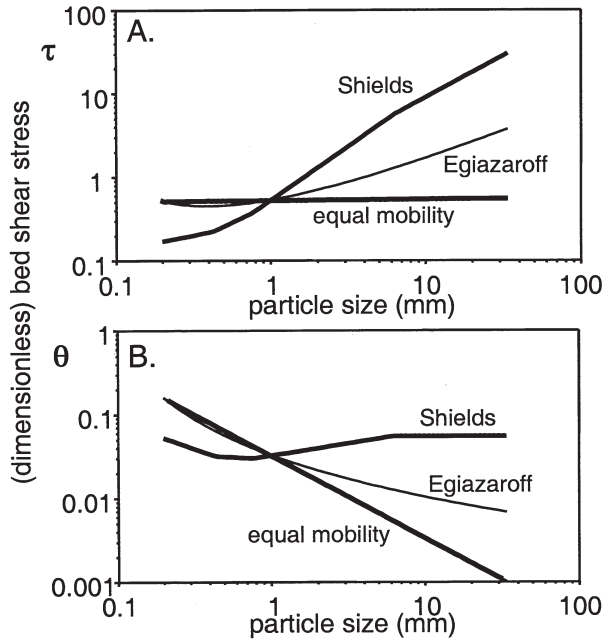


Figure 5.1. Critical bed shear stress according to the Shields curve and with equal mobility and Egiazaroff (1965) hiding-exposure corrections.

A. Dimensional representation.

B. Dimensionless representation comparable to original Shields curve.

The original Shields curve had a Reynolds number ($Re^* = (u_{*cr}D)/\nu$) on the x-axis, describing the flow conditions around grains. If the form of the Shields curve is reflected in the corrected critical Shields curve for a sediment mixture, then the flow conditions around grains as intended in the original Shields curve are also reflected. For Reynolds numbers between 5 and 70 the flow is in a transitional regime from hydraulically smooth to rough, and for Reynolds numbers larger than 70 the flow is hydraulically rough. At a temperature of 15 degrees Centigrade, a Reynolds number of 70 can be rewritten to a diameter of about 2 mm of the sediment, and a Reynolds number of 5 to a diameter of about 0.4 mm.

Let us consider a sand-gravel mixture in a river ranging from 0.4 mm to 40 mm with a median diameter of 2 mm. Equation 14b implies that for the finer half of the bed sediment the hydraulic flow regime around the grains is transitional, and for the coarser half is rough. This presents a problem, because the flow cannot be both transitional and rough at the same time in a completely mixed bed. With reference to $k_{s,grains} = D_{90}$ especially the larger particles have a dominating influence on the near bed flow regime. The flow regime is therefore only rough. Thus it is argued that the second option is not correct. Herein it is therefore proposed to use the $\theta_{cr,Shields,D50}$ in combination with a he-function.

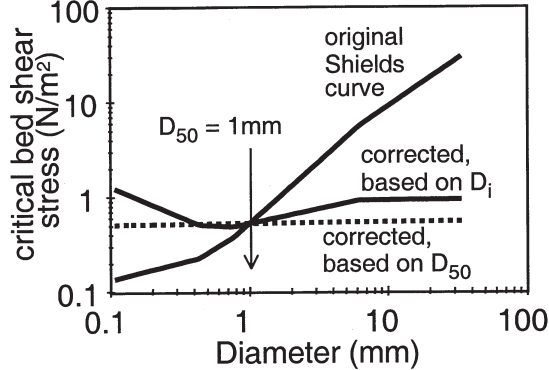


Figure 5.2. Effect on critical bed shear stress ($\tau_{cr,i,corrected}$) based on $\theta_{cr,Shields,D50}$ (straight dashed line) or $\theta_{cr,Shields,D_i}$ (curved line) in combination with a he-function (eq. 14).

5.4.3 Critical bed shear stress of unimodal and bimodal sediment

Recently, several experimenters have determined the critical bed shear stress of the size fractions of non-uniform sediments in laboratory flumes (see Fig. 5.3, Wilcock & Southard (1988), denoted as '1phi', Wilcock & McArdeall (1993, 1997): 'BOMC', Wilcock (1993, 1997): 'LH50', Kuhnle (1993): 'SAND', 'GRAV', 'SG10', 'SG25' and 'SG45', Petit (1994): 'Petit', Misri et al. (1984): 'N1') and in field conditions (Kuhnle (1993): 'Goodwin', Wathen et al. (1995): not given in graph). The experiments of Wilcock and coworkers were done to determine the differences in incipient motion of unimodal, bimodal and extremely bimodal sediments. The experiments of Kuhnle were done to determine the incipient motion of a bimodal sand-gravel mixture with different amounts of sand. The separate mobility of the unimodal sand and gravel modes is given as well. The Petit data is included to extend the present analysis to a large median grain size.

In general these authors found that in unimodal sediments the critical bed shear stress did not vary much with particle size, while in bimodal sediments differences were found in the behaviour of the two modes (e.g. sand and gravel). In Figure 5.3 the data of the critical bed shear stresses are given as a function of the particle diameter. The D_{50} of each mixture is given as well. The critical stresses derived in the flume experiments presented in this paper are also shown but will be discussed later. Four observations can be made.

First, the unimodal sediments are close to equal mobility, while the bimodal sediments show a particle size dependence of the critical bed shear stress.

Second, for bimodal sediment, the mobility differences within the sand mode are small while those in the gravel mode are larger. Thus the gravel mobility increases with particle size.

Third, in bimodal sediment the critical shear stress of the finest particles is slightly larger than that of the D_{50} of the sediment. The same 'inverse mobility' trend is also seen in the widest available

unimodal sediment (Wilcock & Southard 1988) and is predicted with the he-function of Egiazaroff (1965).

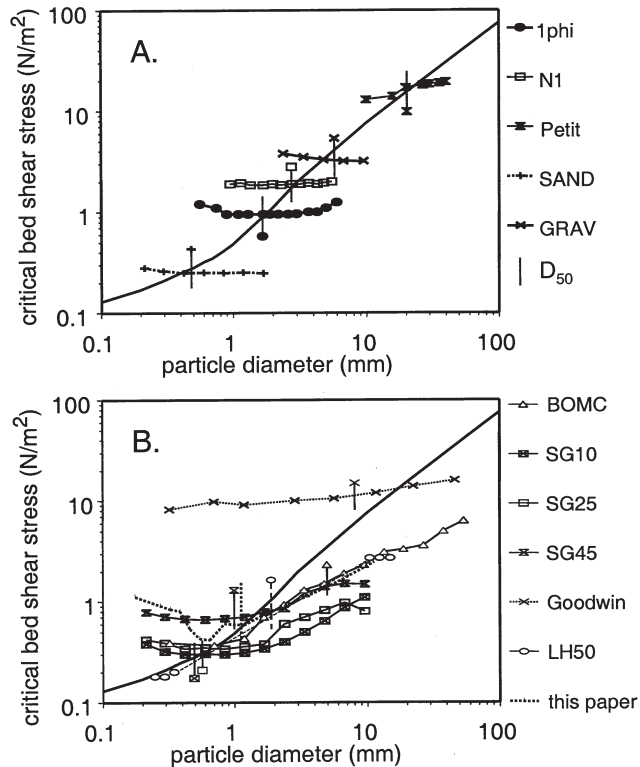


Figure 5.3. Critical bed shear stress of non-uniform sediment. Shields curve is given as the thick line. The D_{50} of each mixture is given as a vertical line with the symbol of that mixture.

A. For unimodal sediments.

B. For bimodal sediments.

Fourth, both in unimodal and bimodal sediment the critical shear stress is equal to that of the D_{50} although in bimodal sediment there is more scatter.

Thus, bimodal sediment shows combined behaviour of uniform and mixed sediment. If the bed sediment is more bimodal, then the sand and gravel fractions show different behaviour. The gravel fraction shows slightly size selective transport, while the sand fraction shows equal mobility. This trend was also found in field conditions (Wathen & al. 1995).

These trends found for bimodal sediment cannot be explained by a simple hiding-exposure concept (with one power P), because then it is assumed that the bed surface is thoroughly mixed. A more likely explanation is local size segregation in the form of longitudinal sand ribbons on gravel beds, which have been observed in all given experiments. If fine sediment is concentrated in more or less homogeneous patches (see Fig. 5.4), then the critical shear stress will approach that of uniform sediment, which in effect is equal mobility within a patch. In the flume experiments presented here local size segregation was also observed. Therefore it is expected that the experiments will exhibit effects related to bimodal sediment: the critical bed shear stress condition will not be equal mobility.

Concluding, for unimodal bed sediment the concept of equal mobility is supported by the data

and is best represented by the $\theta_{cr, Shields, D_{50}}$. Consequently, the transport for fully mobile conditions can be predicted with a deterministic predictor for one size fraction (e.g. Parker et al. 1982, Meyer-Peter & Mueller 1948). For incipient motion a stochastic approach with a uniform predictor might be sufficient but this hypothesis is not tested herein. For bimodal sediment the equal mobility concept is not supported by the data, but the sand fraction shows equal mobility while the gravel fraction shows size-selective entrainment. Consequently, the transport for fully mobile conditions must be predicted with a non-uniform predictor, and for incipient motion also with the stochastic approach. Furthermore, an appropriate hiding-exposure correction must be chosen for each sediment mixture.

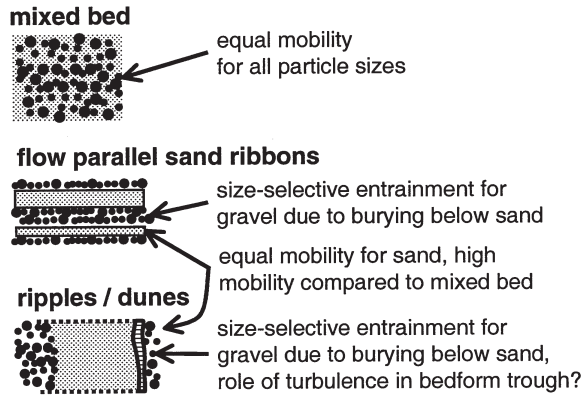


Figure 5.4. The mobility of sand and gravel on different states of the bed surface with increasing bedload transport.

Finally, the results indicate that the hiding-exposure correction is best connected to the D_{50} of the sediment. This agrees with Kuhnle (1993), but disagrees with Meyer-Peter & Mueller (1948) and Egiazaroff (1965) who had the sediment represented by the D_m or D_{65} . Herein, the MPM and Egiazaroff equations are used with the D_{50} .

5.5 Flume experiments

5.5.1 Setup of the flume experiments

The objective of the flume tests was to study the bedload transport process of a sand-gravel mixture in equilibrium conditions (Blom & Kleinhans 1999), both for incipient motion and (almost) fully mobile conditions. As the bedload transport depends on the grain-related bed shear stress (grain bed shear stress), the grain fraction of the bed shear stress therefore needs to be constant in the equilibrium experiments. The grain bed shear stress is herein defined as $\tau = \rho g (\bar{u}/C)^2$ with $C = 18 \log(12R_b/k_{s,grains})$. It was assumed that $k_{s,grains}$ was constant in the experiments, and consequently C is nearly constant. Therefore only the cross-section averaged flow velocity ($= Q/A$, with Q =flow discharge and $A=hW$ is cross-sectional area, h = water depth, W = width of the flume) had to be kept constant while bedforms developed. This cannot be established by using a constant flow discharge, because the growing bedforms will lead to increasing form roughness and hence to decreasing grain bed shear stress. The consequence was

that both the water depth (downstream weir) and discharge had to be adjusted iteratively several times a day. At the same time the flow was kept uniform.

The experiments were done in a flume with a length of 50 m and a width of 1.5 m. The sediment was recirculated with sediment pumps. Bed- and water surface profiles and bedload transport were automatically collected. The water temperature was kept constant at 13° Centigrade. The experiments were started with a mixed bed (see Fig. 5.5) of slightly bimodal sediment, installed at a bed slope that is equal to the expected water surface slope of the experiments. The flow was maintained until the system was in equilibrium, which was simply defined as the condition at which the change of flow roughness, bedform dimensions and sediment transport became smaller than the measurement accuracy and variability. The flume was then drained of water, the bed was photographed, sampled and the sample holes were filled with sediment. The next step was to generate a flow with a different bed shear stress until a new equilibrium was reached, and so on. In Figure 5.6 the sequence of the experiments is presented (Blom & Kleinhans 1999). Only the equilibrium experiments are used in this paper for calculations of the bedload transport (see Table 5.1), which are, in order of increasing shear stress: T0, T10, T5 and T9, and T7. In T0, the gravel is not in motion, while T7 almost all grain sizes are fully mobile.

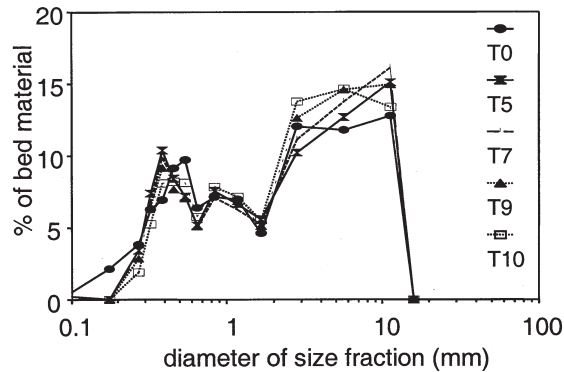


Figure 5.5. Non-cumulative particle size distribution of the bed sediment used in the flume tests.

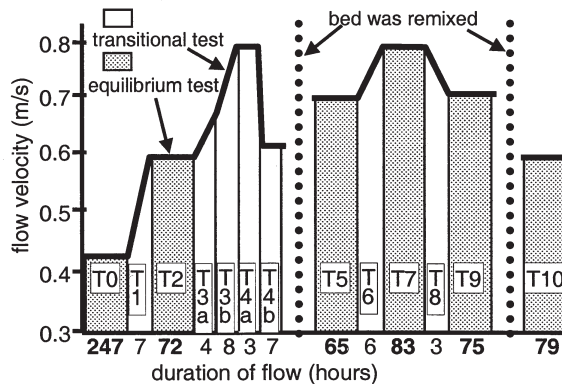


Figure 5.6. Applied flow velocity and duration of the flow.

The sediment transport per size fraction has been determined from the total bedload transport

(kg/s) that was measured automatically in the recirculation system. Samples have been taken from the transported sediment, and have been analyzed by sieving and settling tube to determine the particle size distributions of the transported sediment. The bed and bedload mixtures are represented in 13 particle size fractions with fraction diameters D_i (see Fig. 5.5) that were logarithmically interpolated between the diameters of the sieves. The sediment transport $q_{b,i}$ per size fraction i was obtained by multiplying the total bedload transport q_b with the fractional percentage p_i of the transported sediment ($q_{b,i} = p_i q_b$).

Table 5.1. Experimental conditions.

#	Condition (also see Fig. 5.7)	Hydraulic radius* (m)	Discharge (m ³ /s)	Flow velocity (m/s)	Water surface slope (10 ⁻⁴)	Total bedload transport (g/sm)	Final bed state
<i>bed was mixed and bed slope installed at -4.80 10⁻⁴</i>							
T0	incipient motion	0.17-0.18	0.13-0.13	0.42	-4.48	0.80 ± 0.01	flat bed, sand ribbons
<i>bed was remixed and new bed slope installed at -14.00 10⁻⁴</i>							
T5	incipient motion	0.19-0.23	0.22-0.26	0.69	-14.72	42.0 ± 0.4	small barchans over armour layer
T7	top speed	0.30-0.32	0.41-0.43	0.79	-15.2	66.0 ± 0.8	large dunes over armour layer
T9	incipient motion	0.22-0.25	0.26-0.28	0.7	-16.94	50.8 ± 0.6	large dunes over buried armour layer
<i>bed was remixed and new bed slope installed at -10.60 10⁻⁴</i>							
T10	incipient motion	0.13-0.18	0.14-0.19	0.59	-11.06	14.4 ± 0.1	small barchans over armour layer

*: corrected for side-wall roughness with the Vanoni-Brooks method

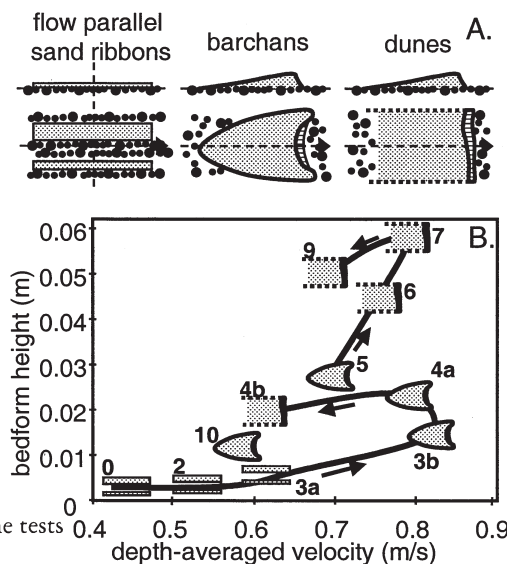


Figure 5.7. Bedform types observed in the flume tests
A. Classification of bedform types.
B. Observed bedform types and heights.

In Figure 5.7 the characteristic bedform types and heights are given as a function of the flow velocity. It can be seen that during the lowest flow velocity mainly flow parallel sand ribbons developed. During higher flow these sand ribbons developed further into barchans, entraining more sediment from the bed, and leaving a lag or armour layer below the bedforms. During the highest flow there was so much sand entrained and winnowed from the bed that the barchans developed into more two-dimensional dunes over the whole width of the flume.

5.5.2 Experimental evaluation of the Nikuradse grain roughness $k_{s,grains}$

The total bed shear stress can be divided in two parts: the bed shear stress related to bedforms (τ'') and the bed shear stress related to the grains on the bed surface (τ'). In most bedload predictors the flow energy is represented by the grain-related bed shear stress. The Chezy parameter related to grains can be calculated from the White-Colebrook formula $C' = 18 \log(12R_b/k_{s,grains})$.

In general $k_{s,grains} = aD_{90}$, in which a is an empirical constant between 1 and 3 (Van Rijn 1993). The present dataset allows an experimental determination of the grain roughness. This is convenient, because the grain bed shear stress is thus more accurately calculated, and consequently the predicted bedload transports are also more reliable. Experiment T0 has a flat bed with only a few flow parallel sand ribbons but no other bedforms. The total bed shear stress in T0 (corrected for sidewall-roughness with Vanoni-Brooks) is assumed to be equal to the grain shear stress for all experiments.

It was found that $k_{s,grains} = D_{75}$ (of the input bed sediment) or in terms of D_{90} , $k_{s,grains} = 0.5D_{90}$. This relatively small grain roughness may be related to the bedform types. The sand ribbons and the sand in the interstices between the gravel particles apparently reduce the grain roughness strongly compared to uniform gravel sediment. Since the bed in the other experiments also was covered partly with sandy bedforms, the grain roughness is probably relatively small in all experiments, though possibly not exactly the same. In further calculations $k_{s,grains} = D_{75}$, and the grain bed shear stress is calculated from this roughness, the measured hydraulic radius and depth-averaged flow velocity.

Major differences between the experiments from literature and the new experiments presented here are the flow depth and the flume dimensions during the experiments. In literature flow depths of 0.08 to 0.12 m are reported for comparable sediment sizes, while the present experiments had much larger flow depths of 0.19 to 0.46 m. Since bedform height in flumes is partly dependent on the water depth, it is not unlikely that the bedforms in the experiments from literature were strongly suppressed, and would have developed better with larger flow depths. It is hoped that the conditions in the present experiments resemble the natural riverbed better.

5.6 Choosing the parameters

The first step is to analyse the prediction of relative transport rate per size fraction ($q_{b,i}/q_b$). The measured values will also be presented as relative transport rates per fraction ($q_{b,i}/q_b$). The second step will be to compare the transport rates q_b (g/sm) integrated over the fractions of measured and predicted values.

The transport predictions will be done with MPM (Meyer-Peter & Mueller) and VR (van Rijn). If all options and he-functions are combined in the final stochastic non-uniform bedload predictors, then the number of possible combinations is inconveniently large. Therefore another

strategy is followed. First the options are tested that occur in the most simple type of bedload predictor, e.g. the non-uniform deterministic predictor of MPM (using standard coefficients). The test result will be accepted for both MPM and VR. Furthermore, the outcome suggests the following order, as the most sensitive are first determined.

5.6.1 Effect of equation 3a/b (conversion from $\phi_{b,i}$ to $q_{b,i}$)

In the conversion from $\phi_{b,i}$ to $q_{b,i}$ (equation 3) the choice is left open between particle size parameters D_{50} and D_i . The effect is studied by comparing the measured transport rates per fraction with the predicted with equation 3a/b. The predictions are made with the deterministic MPM to exclude the effects of choices in the stochastic approach. A deterministic predictor is better suited for experimental conditions well beyond the threshold of motion, therefore T7 is chosen because in this experiment the bed shear stress and transport are the highest. At this stage, it is not yet known which he-function should be chosen, therefore the simple power function with power $P = -0.65$ for all fractions i is applied in equation 13. $P = -0.65$ is more or less the average of values found in literature (Buffington & Montgomery 1997).

When equation 3a is chosen (D_{50}) (see Fig. 5.8) then the predicted bedload transport is extremely sandy, and almost no gravel is predicted to be in transport, contrary to the measurements. On the other hand when equation 3b is chosen (D_i), the predicted particle size distribution is more or less equal to the measured. This result was found to be almost independent of P in the he-function, and was found for all experiments. Therefore it can be concluded that equation 3b is the right one, which is the application of D_i .

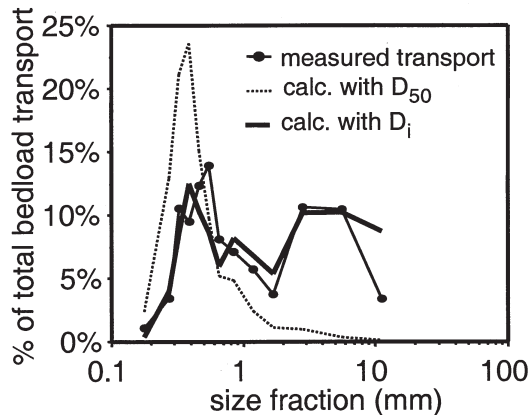


Figure 5.8. Effect of conversion from $\phi_{b,i}$ to $q_{b,i}$ with particle size parameters D_{50} and D_i (eq. 3).

5.6.2 Hiding-exposure function

Egiazaroff (1965) is used here because this he-function is based mostly on theoretical analysis. The power function ($\xi_i = (D_i/D_{50})^{P_h}$) is also used because it can easily be adjusted to measured data, and because most experimental he-functions from literature are power functions. Since most flume experiments in the present dataset have bed shear stresses below the threshold of motion for some

size fractions, the stochastic MPM for non-uniform sediment is used with standard parameters and coefficients and with the Egiazaroff he-function.

To determine the 'true' hiding-exposure coefficient (appropriate for the present dataset), the power of the hiding-exposure function is adjusted to the data as follows. For each fraction the power P_i of the he-function is adjusted to give optimal agreement between measured and computed transport rates. This is done separately for each flume experiment. The result of this procedure is a hiding-exposure power P_i for each fraction, determined per experiment. This gives the experimental he-function for the present dataset according to $\xi_s = (D_i/D_{50})^{P_i}$. In literature, the experimental P_i for very fine sand is sometimes even smaller than -1, which implies an inverse mobility that is confirmed by the data given in Figure 5.3b. The experimental derivation of the powers in the present analysis is therefore done under the condition of $-1.5 < P_i < 0$ for experiments T0, T5, T7, T9 and T10.

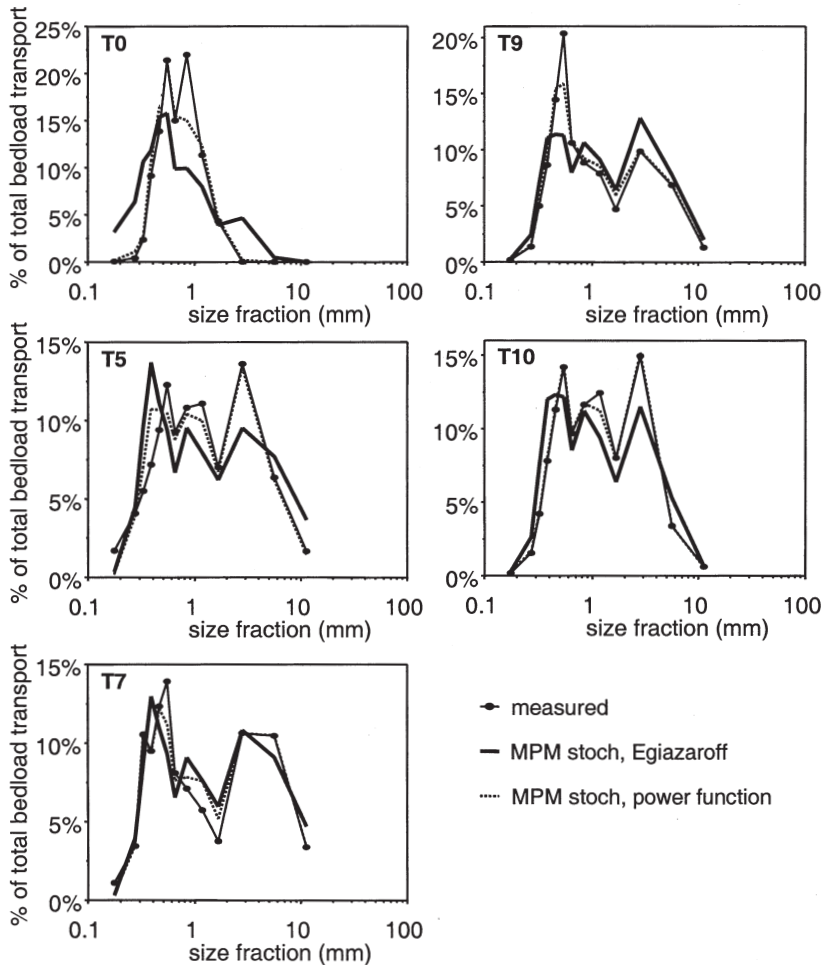


Figure 5.9. Comparison of predicted and measured relative fractional bedload rates for flume experiments T0, T5, T7, T9 and T10 with the Egiazaroff (1965) and the experimental he-function and the stochastic MPM.

The prediction is done for flume experiments T0, T5, T7, T9 and T10 (see Fig. 5.9). For experiments T7 and T10 the predicted relative transport rates per size fraction with the Egiazaroff he-function seem to follow the measured ones well. For T0 and T9 however, too much gravel transport is predicted, and for T5 too little gravel transport is predicted. The experimental he-functions are shown in Figure 5.10. Egiazaroff is shown as well. It can be seen that the Egiazaroff hiding-exposure is smaller than the experimental he-function at the smallest grain sizes and at the largest particle sizes.

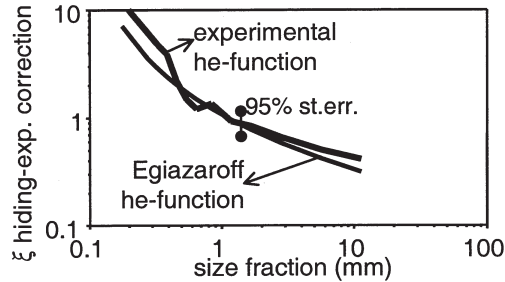


Figure 5.10. Average (of all tests included) experimental he-function compared to the Egiazaroff (1965) he-function. The average two-sided 95% standard error of the experimental he-function is given as an error bar.

The question can now be raised whether the experimental he-function is dependent on the transport condition, because in the experiments with the smallest transports the bedforms were small, but in the experiments with the largest transports the bedforms were large. Averages of the experimental he-functions have been calculated separately for experiment T0 and for experiments T5-T9. No significant difference was found between high and low transport conditions.

Around 0.65 mm there is a dip in the experimental he-function, at which about half of the powers of the experimental he-functions have an extreme value of $P_i = -1.5$ or $P_i = 0$. The he-function barely has any influence on the transport of fractions near the D_{50} if the power is limited within $-1.5 < P_i < 0$. Therefore small differences between the predicted and measured particle size distributions of the bedload transport material around the D_{50} can only be corrected in the experimental adjustment procedure with very small or very large he-functions. The particle sizes around 0.65 mm are very near the D_{50} and may thus be an effect of the small errors in the particle size distributions. Above 8 mm grain size the experimental he-function is less steep than that of Egiazaroff. This means that the critical Shields parameter for the largest grains is larger than is predicted by Egiazaroff. The reason may be that the shape of the grains larger than 8 mm resembles elongated discs which exhibit imbrication.

As a sensitivity experiment the grain bed shear stress was calculated with $k_{s,grains} = D_i$ instead of $k_{s,grains} = D_{75}$. The idea behind this is perfect segregation of all particle sizes, with all sand in the bedforms and all gravel in the patches between the bedforms. The result was that the gravel transport was extremely overpredicted, while the sand transport was underpredicted. The same calculation was also tried without a he-function, but this gave the reverse effect: extreme underprediction of the gravel transport and overprediction of the sand transport. The segregation idea was also tested with two separate roughnesses for sand and gravel: $k_{s,sand} = D_{90,sand} = 0.9$ mm and $k_{s,gravel} = D_{90,gravel} = 10.0$ mm. This gave approximately the same unsatisfactory results as with $k_{s,grains} = D_i$. From this it is concluded that the appropriate grain roughness for the type of predictor used in this paper, is a single grain roughness for the whole mixture in combination with

a he-function for the critical bed shear stress.

The tentative conclusion of the preceding discussion is that the experimental he-function is comparable to the theoretical function of Egiazaroff (1965), although small adjustments of the he-function obviously lead to substantially better predictions (see Fig. 5.9). However, the Egiazaroff function has a theoretical foundation and is therefore preferred.

5.6.3 Effect of the stochastic parameter

There is one additional parameter in the stochastic version of MPM: the relative standard deviation of the applied shear stress which represents the turbulent variation of near bed flow. This is given as $\sigma_{\tau} = \gamma \tau'$, in which γ = relative standard deviation. De Ruiter (1980) found a relative standard deviation of 0.4. Also Bridge & Bennett (1992) found that this value gave reasonable results. In a reanalysis of turbulence flow data over bedforms of De Ruiter & van Mierlo (1988) and of Kornman (1995), also a value was found of approximately 0.4 at the upper stoss sides of the bedforms.

The effect of increasing the relative standard deviation with a factor 2, is more transport of coarse gravel because more large flow fluctuations occur near the bed, which can move more and coarser sediment. Since the predictions are rather well with the selected options, this is an amelioration. To counteract this, ξ_i of the coarsest fractions would have to be adjusted to smaller values (nearer to zero) to give the same predictions as when $\gamma=0.4$ were used in combination with the original experimental he-function. Obviously this degree of freedom introduces the possibility of equal outcomes by different combinations of γ and ξ_i . It may be that the turbulence production is larger for beds with higher protruding elements, and that it is also modified in the presence of dunes, but this remains speculative, pending further research. Considering the values of γ found in literature, $\gamma=0.4$ is used here, and P_i is adjusted without introducing an extra degree of freedom in γ . In conditions of which more is known about the nature of the turbulence, the value can be adapted; here it is assumed that $\gamma=0.4$ represents the present conditions.

5.6.4 Total bedload transport rates with the MPM bedload predictor

The predicted transports using the non-uniform stochastic MPM (eqs. 1, 3b, 9, 10, 12, $\gamma=0.4$ and $k_{s,grains}=D_{75}$) are on average 2 times too large in T5-T10. Fernandez Luque & Van Beek (1976), Jaggi (1994, in Hunziker 1995) and Hunziker (1995) found that the calibration factor of MPM ($\alpha=8$) is too large and should be 5.7, 5.7 and 5.0 respectively. Ribberink (1998) found that the calibration factor had to be adjusted depending on the transport condition. At low transport $\alpha=5.7$, at intermediate transport $\alpha=8$ and at high transport (sand in sheet flow in waves and currents) $\alpha=13$.

The present flume experiments obviously are in the low transport class. It is therefore proposed to use $\alpha = 5.7$ instead of 8, which leads to better predictions (see Fig. 5.11) for the present dataset. Using the adjusted calibration factor, 4 out of 5 predictions fall within a factor 0.5-2 of the measured transports.

5.6.5 Effect of equations 7a/d (T_i in non-uniform VR predictor) and equations 8a/b (D_i in non-uniform VR predictor)

In the transport parameter T_i of VR the first choice in equation 7 is whether T_i is written in terms of grain bed shear stress or (dimensionless) Shields grain shear stress corrected with a he-function. Herein it has been shown that incipient motion for a particle is best represented by $\theta_{cr,D50}$. Based on this, the corrected Shields parameter reads as: $\theta_{cr,i,corrected} = \xi_i \theta_{cr,D50}$, which can be converted to critical bed shear stress as follows:

$$\frac{\tau_{cr,i,corrected}}{(\rho_s - \rho)gD_i} = \xi_i \frac{\tau_{cr,Shields,D50}}{(\rho_s - \rho)gD_{50}} \Leftrightarrow (a)$$

$$\Leftrightarrow \tau_{cr,i,corrected} = \xi_i \frac{D_i}{D_{50}} \tau_{cr,Shields,D50} \quad (b)$$

Thus equations 7b and 7d are equivalent if $\tau_{cr,i,corrected}$ is represented by eq. 15b. Often, the D/D_{50} term in eq. 15b is neglected, resulting in erroneous results.

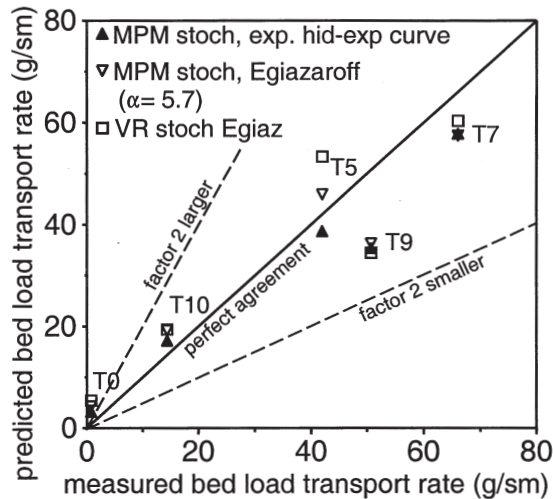


Figure 5.11. Comparison of predicted and measured total bedload transport rates with the stochastic MPM ($\alpha=5.7$) and VR for non-uniform sediment with the Egiazaroff (1965) and the experimental he-function. The line of optimal agreement is also given. The numbers refer to the experiments.

The effect of equations 7a/b is studied by comparing the measured and predicted transport rates per size fraction using equations 7a/b, made with the deterministic VR to exclude the effects of choices in the stochastic approach. Flume experiment T7 is chosen here because in this experiment the bed shear stress and transport are the highest. The he-function of Egiazaroff is used. It is not yet known which of the equations 8a/b (D_* for D_{50} or D_i) must be chosen, therefore equation 8a is chosen. This choice will be evaluated later.

If the he-correction is not applied in the denominator of T_p , then the transport rates per size

fraction of T7 are reasonably well predicted (see Fig. 5.12a). However, if it is applied in the denominator, then the gravel transport is extremely overpredicted. Equation 7b thus gives the best results.

The effect of equations 8a/b, which is the choice between D_{*50} and D_{*p} , is studied in a similar way (see Fig. 5.12b). The sand transport rate is overpredicted if D_{*i} is used, while the relative transport rate per size fraction is reasonably well predicted when D_{*50} is used. Thus D_{*50} gives the best results.

The effect of using the he-function in the denominator of T_i (eq. 7a) was that the gravel transport was overpredicted. This is opposite to the effect of using D_{*i} instead of D_{*50} , and may therefore cancel out. The effect of (not) applying the he-function in the denominator of T_i in combination with D_{*i} , on fractional bedload rates (eqs. 7a/b, 8b) is that the gravel transport is still extremely overpredicted. Thus the results are much more sensitive to equations 7a/b, and the combination of options that gives the best results (regardless of options 8a/b) is equation 7b (not using the he-function in the denominator of T_i) with equation 8a (D_{*50}).

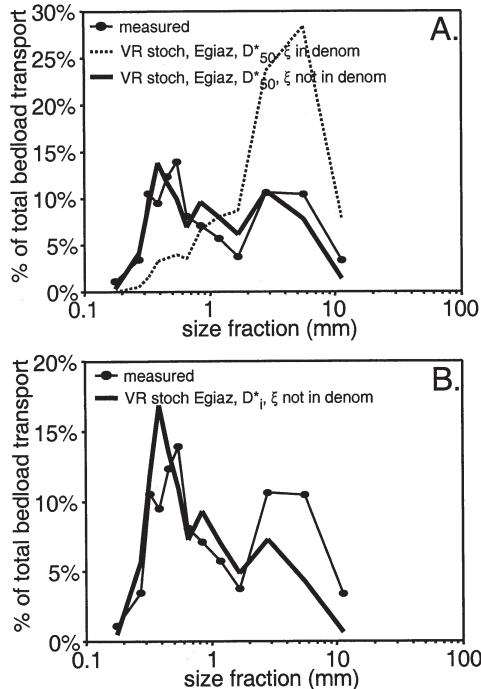


Figure 5.12.

A. The effect of (not) applying the he-function in the denominator of T_i on fractional bedload rates (eq. 7a/b). Calculations were done with D_{*50} for experiment T7.

B. The effect of applying D_{*50} or D_{*i} on fractional bedload rates (eq. 8a/b). Calculations were done without the he-function in the denominator of T_i for experiment T7.

The effect of using some of the other alternative parameters in the VR method (without the hindrance factor) for T7 (Sand Flume) was studied for two cases: with D_{*50} and $\theta_{cr, Shields, D50}$ and with D_{*i} and $\theta_{cr, Shields, Di}$. The difference in predicted total bedload transport was not large, but the transport rates per size fraction differed significantly. The transport of the coarsest particle sizes is extremely underpredicted in the second case.

5.6.6 Fractionwise and total bedload transport rates with the VR bedload predictor

Now the bedload can be predicted with the chosen parameters in the non-uniform stochastic predictor of VR (eqs. 3b, 4, 7b, 8a, 9, 10, 12, $\gamma=0.4$ and $k_{s,grains}=D_{75}$). VR and MPM appear to predict exactly the same relative transport rates per size fraction. In Figure 5.11 the predicted total bedload transport rates based on VR are compared to the measured. It can be seen that the predictions are in general somewhat too large for T0 and T10. Nevertheless, for 4 out of 5 experiments, the transport is predicted within a factor 0.5-2.

5.7 Hindrance at small transport rates

On close inspection of the Sand Flume data there is a trend of overprediction of the total bedload transport using both MPM and VR, especially at lower velocities. The relative transport rates per size fraction are predicted reasonably well and cannot explain the discrepancy. It is suggested here that during low flow the small grains are hindered in their downstream movement by the large immobile particles. First, the small grains of the top surface layer have to pass and collide with the immobile grains. Second, the small grains below the top surface layer are shielded by the larger immobile grains. At higher flow this effect may disappear for two reasons (see Fig. 5.4). First, the number of immobile particles at the bed surface decreases, since more and more are entrained as their critical shear stress is exceeded. Second, the bed surface may be organized in bedforms. The fine sediment is then no longer hindered in its movement while the bedforms bury and move over the coarsest sediment.

Obviously much more research on sediment transport in the case of surface size segregation is needed. Here only a tentative solution is offered in which the transport on a bed near incipient motion without size segregation is corrected. A hindrance factor f_h is proposed for the MPM (and in analogue way for VR) as follows:

$$\phi_{b,i} = f_h p_i \alpha \left(\theta'_i - \theta_{cr,i,corrected} \right)^{1.5} \quad (16)$$

For the low transport condition $\alpha = 5.7$ has been used herein, while originally $\alpha = 8$ is given by Meyer-Peter & Mueller (1948). The $\alpha = 8$ option is combined here with the hindrance factor.

The hindrance factor is assumed to be related to the ratio of the area of the transported coarse grains and the area of the immobile grains: $A_{coarse\ bedload}/A_{immobile\ bed}$ which can be expressed as $(D_{90,bedload}/D_{90,bed})^2$. The areas are used instead of the diameters because drag on the particles is related to the area, and the opportunity for collisions is also related to the area of the largest particles. The ratio $D_{90,bedload}/D_{90,bed}$ also denotes the transport condition and becomes unity at extremely large bed shear stresses, while it is much smaller near incipient motion of the finer sediment, which agrees with the observation of Ribberink (1998) that the calibration factor depends on the flow condition.

The hindrance factor has been calibrated based on Sand Flume experiments T0, T5, T7 and T10, based on:

$$f_h = \frac{\phi_{b,measured}}{\phi_{b,predicted}} \quad (17)$$

T9 is excluded because the armour layer was buried below the bedforms, which makes the transported sediment in T9 independent from the bed sediment. The hindrance factor is given in Figure 5.13 as a function of $D_{90,bedload}/D_{90,bed}$. The following function was calibrated, based on the Sand Flume data (see Fig. 5.13):

$$f_h = 1 - \exp \left[-b \left(\frac{D_{90,bedload,predicted}}{D_{90,bed}} \right)^2 \right] \quad (18)$$

with $b = 7.2$. The measured $D_{90,bedload}$ of the Sand Flume data was used instead of the predicted value, to make the calibration independent of the MPM predictor. In applying equation 18, the predicted $D_{90,bedload}$ can be taken. With $f_h \approx 1$ the hindrance effect disappears and the calibration factor is $f_h \alpha = 8$. The only factor that is calibrated is b .

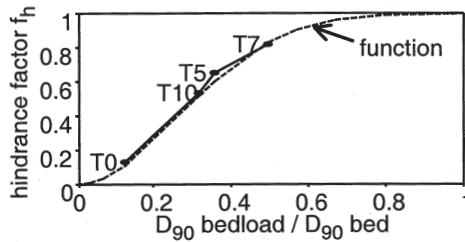


Figure 5.13. The hindrance factor function and observations from the Sand Flume experiments.

5.8 Validation

5.8.1 East Fork, Wyoming data

The stochastic MPM has been tested on the field data of Leopold & Emmett (1976,1977). Hydraulic data and fractional transport rates were collected by the U.S. Geological Survey using flow gages and a conveyor belt bedload trap on the East Fork River, Wyoming. Group averages with comparable flow velocities are used here (see Table 5.2) to obtain more reliable particle size distributions of the transported sediment and the flow data.

The stochastic MPM for transport rates per size fraction with Egiazaroff is used. The grain roughness $k_{s,grains}$ is taken equal to the D_{75} of the bed material: $k_{s,grains} = 7.14$ mm, because the bed sediment is widely graded and probably will exhibit the same roughness-reducing effect of sand in the interstices of gravel as in the Sand Flume. The predicted relative transport rates per size fraction compare well to the measured ones (see Fig. 5.14).

The predicted bedload transport rates are corrected with the f_h based on equation 18 with $b = 7.2$ without any additional calibrating, the predicted $D_{90,bedload}$ and given $D_{90,bed}$ of the East Fork data. The results are given in Figure 5.15 (also see Table 5.2). 3 out of 4 predictions are now within a

factor 2 of the observed transport rates, which is a significant improvement. Neglecting the f_h factor, the transport rate is significantly overpredicted. Using the non-uniform deterministic MPM instead of the stochastic MPM leads to significant underestimation of the transport rates of the coarsest fractions in the lower flow conditions. The results with VR are approximately the same and are not given here.

Table 5.2. Summary of East Fork, Wyoming dataset with velocity group averages.

Dates	Flow velocity (m/s)	Hydraulic radius (m)	Bedload transp. rate (g/sm)
June 14, 16, 20, 1976	0.68	0.453	1.8
June 12b-e*, 1976	0.9	0.743	14.6
June 2-5, 1976	1.11	1.058	73.7
May 28, 30, 1974;	1.29	1.323	136.1
June 15, 16, 1975			

*: several measurements done on this day

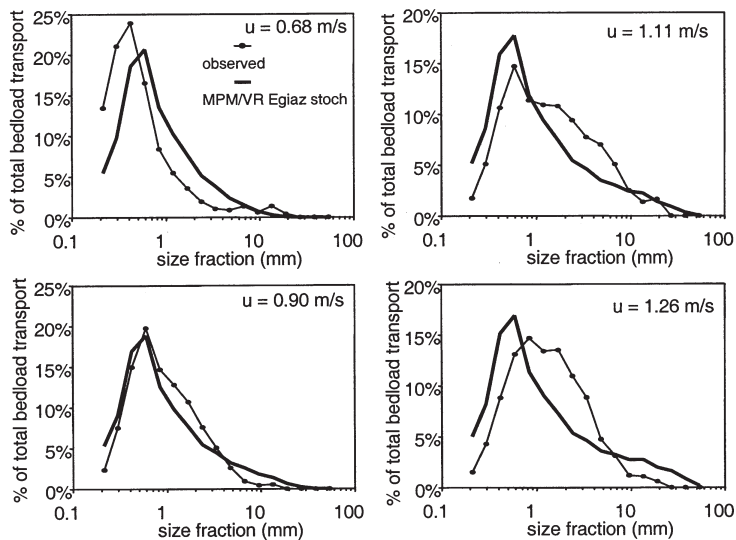


Figure 5.14. Comparison of predicted and measured relative fractional bedload rates for the East Fork dataset for 4 flow velocity classes with the stochastic MPM with the Egiazaroff (1965) he-function.

5.8.2 Sagehen Creek, California data

The bed shear stress in Sagehen Creek in California (Andrews 1994) often is below the threshold of motion for many particle sizes, which provides an ideal test case for the stochastic approach proposed in this paper. Bed shear stresses (but no velocities and water depths) are provided as well as the fractional bedload transport rates, which were measured with a hand-held Helly-Smith sampler. Particles up to 5.6 mm are suspended and were therefore excluded from the bedload data and the present calculations. The data (Andrews 1994) is grouped here in shear stress intervals of

1 Pa (see Table 5.3) to obtain more reliable particle size distributions of the transported sediment and the flow data. Considering the small transport rates, it is not very likely that large bedforms would exist, therefore the grain bed shear stress is assumed to be equal to the bed shear stress given by Andrews (1994).

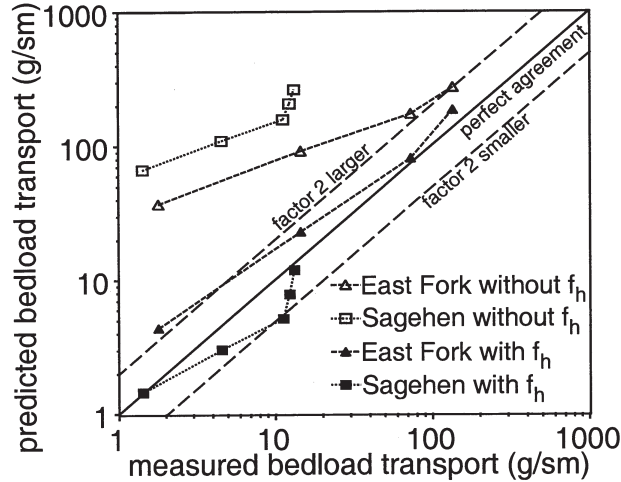


Figure 5.15. Comparison of predicted and measured total bedload transport rates with the stochastic MPM for non-uniform sediment with the Egiazaroff (1965) he-function of East Fork River and Sagehen Creek datasets, with and without the hindrance factor.

The critical Shields value of 0.0384 as given by Andrews (1994) was used instead of the 0.055 given by the Shields curve (see Fig. 5.16). Andrews (1994) suggests that the appropriate he-function is a power function with power $P = -0.887$. This was applied as an alternative to the Egiazaroff function, but did not give good results (see Fig. 5.16).

The Sagehen Creek total bedload transport rates are corrected with f_h (eq. 18) without recalibrating (see Fig. 5.15 and Table 5.3), which significantly improved the predictions. Four out of five predictions are within a factor 2 of the observed transport rates, which is a significant improvement. Using the deterministic instead of the stochastic MPM leads to underestimation of the transport rates of the coarsest fractions in the lower flow conditions.

Table 5.3. Summary of Sagehen Creek, California, dataset with bed shear stress group averages.

Class nr.	Bed shear stress (Pa)	Flow depth (m)	Bedload transport rate (g/sm)
1	15.68	0.360	1.4
2	17.05	0.400	4.6
3	18.24	0.438	11.3
4	19.25	0.556	12.5
5	20.23	0.614	13.3

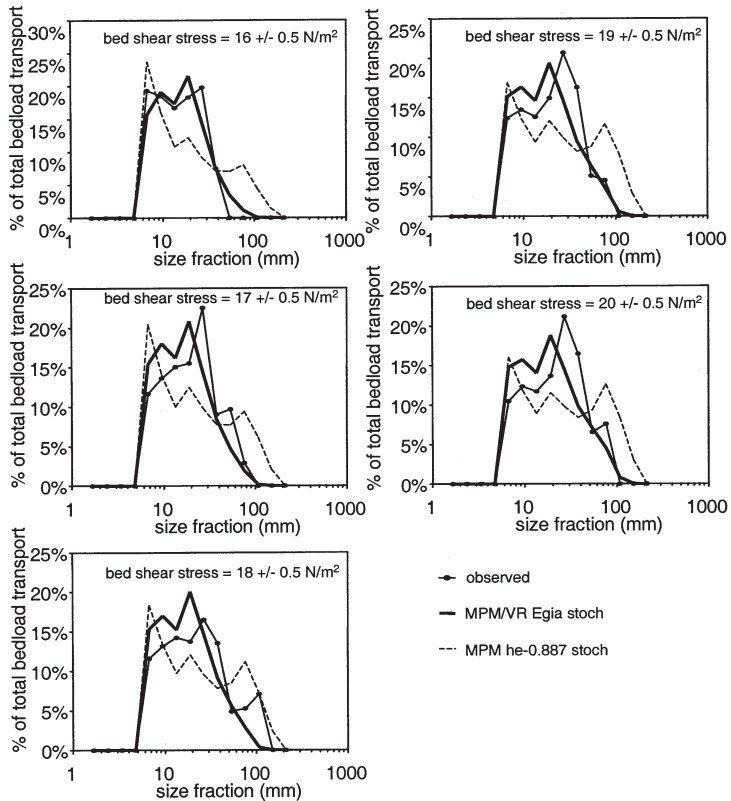


Figure 5.16. Comparison of predicted and measured relative fractional bedload rates for the Sagehen Creek dataset for 5 bed shear stress classes with the stochastic MPM with $\theta_{cr,D50} = 0.0384$ (Andrews 1994) and with the Egiazaroff (1965) and the experimental he-function with $P = -0.887$ (Andrews 1994).

5.9 Discussion

5.9.1 Single- or multi-fraction approach

The effort to predict bedload transport rates per size fraction (multi-fraction approach) is relatively large compared to the classical deterministic method of MPM and VR for uniform sediment (single-fraction approach). In many problems related to non-uniform bed sediment the total bedload transport as well as the fractional transport rates need to be predicted, for example in models that include sorting effects, armour layers, or suspended sediment transport predictors. If one is only interested in the total transport rate, it might be argued whether the single- or multi-fraction method should be applied. Using the single-fraction deterministic MPM the total bedload transport is approximately equal to that of the multi-fraction approach for conditions far above incipient motion. However, for conditions close to the critical bed shear stress (based on D_{50}) it is essential to use the multi-fraction method, because the single fraction method may give

zero transport.

This agrees with Van Rijn (2000), who has presented results for fine graded bed materials (D_{50} in range of 0.2 to 1 mm) using a deterministic bedload (based on eq. 3b, 4, 7b and 8b) and suspended load model including the he-function of Egiazaroff. The multi-fraction method was found to give slightly smaller (10% to 20%) total bedload transport rates than the single-fraction method (based on D_{50}). The total suspended load transport was found to be more significantly affected by the multi-fraction method including hiding-exposure effects. Based on the multi-fraction method, the suspended transport was a factor 3 to 4 larger for small velocities than those of the single-fraction method. Comparison with field data (Enoree River, $D_{50}=0.65$ mm, Andersen 1942) shows that the multi-fraction method yields the best results for the suspended load transport.

5.9.2 Deterministic or stochastic approach

Using the stochastic approach, the transport is not only predicted for each size fraction, but also for all probable bed shear stresses in turbulent flow, modelled with a probability distribution of the bed shear stress. The question is in what conditions the stochastic approach is really necessary, since it involves a considerable extra amount of calculations.

In this paper it is shown that a stochastic approach gives better results if some size fractions are near incipient motion. In Figure 5.17 the prediction of transport rates per size fraction are compared for the stochastic and deterministic MPM for T10 (incipient motion) and T7 (almost fully mobile conditions). The prediction of the coarsest size fractions with the stochastic MPM is much better for T10, while for T7 the difference is smaller. The stochastic method was found to give 20% larger total bedload transport rates than the deterministic fractionwise method, but for the largest 3 grain size fractions (which are near incipient motion) the stochastic method gave 45% to 100% larger transport rates. This conclusion agrees with the findings of Bridge & Bennett (1992), who also found that the turbulence could not be neglected near incipient motion.

5.9.3 Hiding-exposure

Figure 5.9 indicates that the hiding-exposure function is important. The predictions are based on the he-function of Egiazaroff (1965) which gives far from perfect results. The results with the empirical he-function are much better, but deriving an empirical he-function for every sediment mixture is hardly possible. The costs of flume tests are large, and field campaigns in several flow conditions are even more costly while site-specific problems and history effects like armour layers may inhibit a reliable derivation of the empirical he-function.

Egiazaroff gives a better approximation of the experimental he-functions for bimodal sediment than the equal mobility concept, which is more appropriate for unimodal sediment. Note however that at the asymptote $D_i/D_{50} = 1/19$, Egiazaroff predicts an infinite critical shear stress which is not realistic. Egiazaroff should be modified for mixtures with $D_{10}/D_{50} < 1/10$ to $1/12$ approximately, or the very small grain sizes should be excluded from the calculations because these grains would be suspended anyway (e.g. Andrews 1994). Concluding, if it is not possible to obtain an empirical he-function for a specific bimodal sediment, Egiazaroff might be used tentatively as an alternative approximation.

Note, however, that for the coarsest fractions three parameters could be adjusted slightly to obtain

the same results: the turbulent variation of bed shear stress (γ), the dimensionless grain size parameter in VR (D_{*50} or D_*) and the he-function (ξ). This equifinality can be solved by carrying out measurements of the turbulence in each condition.

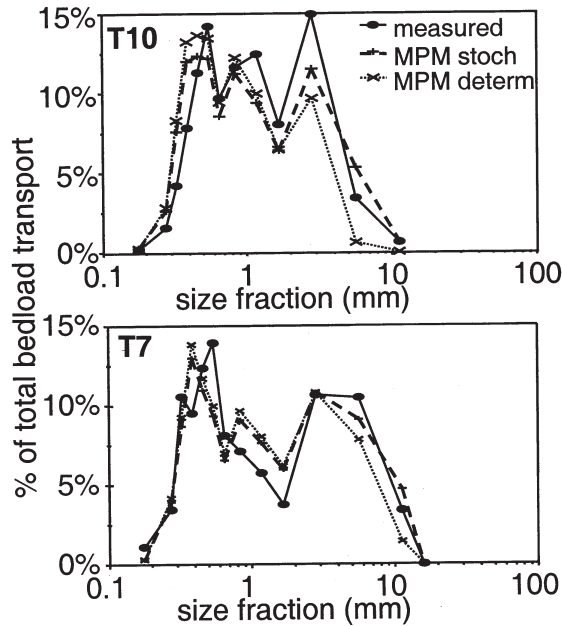


Figure 5.17. Difference between the deterministic and stochastic MPM with the Egiazaroff (1965) he-function for the relative fractional bedload rates in Sand Flume experiments T7 and T10.

5.9.4 Hindrance and armouring

The hindrance of the small mobile grains by large immobile grains is not incorporated in the hiding-exposure correction. The he-correction only accounts for the difference in actual shear stress that acts on different grain sizes. Hindrance only decreases the efficiency of the transport process because the small grains have to pass and collide with the immobile grains and because small grains are shielded by the immobile grains. An extra correction is therefore deemed necessary and was shown to improve the prediction significantly for two independent field datasets. One of the constants in the hindrance function was theoretically based and only one parameter was calibrated based on the Sand Flume data. This gives confidence that the processes in the Sand Flume indeed were comparable to natural rivers.

Armouring has not been included in this study, although it has been observed in the flume experiments. Armouring in itself is a process that occurs below incipient motion of the coarser grains in the bed mixture. The process of armouring does take some time and is therefore time-dependent. In rivers with non-steady flow this may be important. For non-uniform sediment varying spatially the upstream section of the river also influences the armouring process. It is then

no longer possible to predict sediment transport with the predictors presented in this paper because the available bed sediment at the surface (armour layer) depends on former flow conditions in which the armour layer is formed. For this situation, the time-dependent winnowing of fines from the top layer must be modelled while the composition of the top layer itself changes in time, which in turn affects the bedload transport.

The stochastic bedload prediction method for non-uniform sediment as presented in this paper has the advantage that it is a combination of well-known predictors and methods, which have already partly been implemented in many models. A logical next step is the application of the method presented here in a model with an active layer, to enable morphological modelling.

5.10 Conclusions

In this paper it is shown that realistic prediction of bedload transport rates for different size fractions near incipient motion is feasible, and a method is proposed. Classical deterministic predictors of Meyer-Peter & Mueller (1948) and Van Rijn (1984) may give large errors near incipient motion, while a fractionwise and stochastic approach significantly improves the reliability. This approach is an application of a classical bedload predictor for size fractions based on a probability distribution for the bed shear stress to represent the near-bed flow turbulence. The stochastic approach yields 20% higher bedload rates than the deterministic approach, and much better predictions for the largest grain sizes.

The hiding-exposure-function is a main uncertainty in the prediction of transport rates for size fractions. Tentatively it is proposed to use an equal mobility approach for unimodal sediment and the function of Egiazaroff for bimodal sediment.

The predictors were found to overpredict the total bedload transport at small flow velocities. This may be due to hindered movement of the finest sediment by the immobile coarsest sediment. A tentative hindrance factor based on $(D_{90, \text{bedload}}/D_{90, \text{bed}})^2$ is proposed and calibrated based on the flume data. The predictions of two independent field datasets are much improved with the hindrance factor.

Further research is necessary to evaluate whether a local approach of bedload transport prediction is justified or not. If this is not justified the spatial development of the bed composition should be modelled.

Acknowledgments

The investigations were in part supported by the Netherlands Earth and Life sciences Foundation (ALW) with financial aid from the Netherlands Organization for Scientific Research (NWO). The Sand flume tests were financed by 1) the Transport and Mobility of Researchers programme of the European Commission and 2) the consortium of The Institute for Inland Water Management and Waste Water Management (RIZA), Twente University and WL|Delft Hydraulics. The pleasant cooperation with Astrid Blom and Jan Ribberink (Twente University), Klaus Basso (Karlsruhe University), Luigi Fraccarollo (Trento University), Erik Mosselman, Freek de Groot and Joop Ouderling (WL|Delft Hydraulics) is thankfully remembered by the first author, as well as the many informal lessons of Nico Struiksma (WL|Delft Hydraulics) on river modelling, operating flumes and how to 'hinder' causes of stress. Finally we thank Janrik van den Berg and two anonymous referees for their valuable suggestions for improving the manuscript.

Notation

A	=	area of cross-section (m^2)
a	=	factor in $k_{s,grains} = aD_{90}$ (-)
b	=	calibration coefficient (-)
C	=	Chézy coefficient ($m^{0.5}/s$)
C'	=	Chézy coefficient of grains ($m^{0.5}/s$)
c	=	calibration coefficient (-)
D	=	sediment diameter (m)
D_*	=	Bonnefille particle parameter (-)
F_h	=	hindrance factor (-)
g	=	gravitational acceleration ($9.81 m/s^2$)
h	=	water depth (m)
$k_{s,grains}$	=	Nikuradse grain roughness (m)
N	=	number of intervals in discrete approximation of statistical distribution (-)
n	=	number of observations (-)
P	=	power in hiding-exposure function (-)
p	=	proportion of statistical distribution (-)
Q	=	flow discharge (m^3/s)
q	=	sediment transport per unit width (volume m^2/s or weight g/sm)
R	=	hydraulic radius (m)
Re^*	=	Reynolds number of grains: $Re^* = (u_{*cr}D)/\nu$
T	=	transport parameter (relative excess shear stress) in Van Rijn (-)
\bar{u}	=	depth-averaged flow velocity (m/s)
u_{*cr}	=	critical bed-shear velocity (m/s)
W	=	width of river (m)
α	=	calibration factor in MPM (-)
β	=	calibration factor in VR (-)
γ	=	coefficient of variation of bed shear stress (-)
θ	=	Shields parameter (-)
ν	=	kinematic fluid viscosity (m^2/s)
ξ	=	hiding-exposure factor (-)
ρ	=	density (kg/m^3)
σ	=	standard deviation
τ	=	total bed shear stress (N/m^2)
τ'	=	grain bed shear stress (N/m^2)
τ''	=	bed shear stress related to bedform roughness (N/m^2)
ϕ	=	dimensionless sediment transport (-)
Subscripts		
i	=	of grain size fraction
j	=	of grain bed shear stress interval
b	=	bedload
cr	=	critical

References

- ANDERSEN, A. G. (1942), Distribution of suspended sediment in a natural stream. Transactions of the American Geophysical Union, paper Hydrology, 678-683.
- ANDREWS, E. D. (1994), Marginal bed load transport in a gravel bed stream, Sagehen Creek, California. *Water Resources Research* 30 (7) pp. 2241-2250.
- BLOM, A. & KLEINHANS, M. G. (1999), Non-uniform sediment in morphological equilibrium situations. Data Report Sand Flume Experiments 97/98. University of Twente, Rijkswaterstaat RIZA, WL | Delft Hydraulics. University of Twente, Civil Engineering and Management, The Netherlands.
- BRIDGE, J. S. & BENNETT, S. J. (1992), A Model for the Entrainment and Transport of Sediment Grains of Mixed Sizes, Shapes and Densities. *Water Resources Research* 28 (2) pp. 337-363.
- BUFFINGTON, J. M. & MONTGOMERY, D. R. (1997), A systematic analysis of eight decades of incipient motion studies, with special reference to gravel-bedded rivers. *Water Resources Research* 33 (8) pp. 1993-2029.
- BUFFINGTON, J. M. & MONTGOMERY, D. R. (1998), Correction to A systematic analysis of eight decades of incipient motion studies, with special reference to gravel-bedded rivers. *Water Resources Research* 34 (1) pp. 157-157.
- CAO, Z. (1997), Turbulent bursting-based sediment entrainment function. *Journal of Hydraulic Engineering* 123 (3) pp. 233-236.
- DE RUITER, J.C.C. (1980), Stochastic model for incipient motion of sediment grains as a function of local parameters. (in Dutch) Report R657-XI, Delft Hydraulics, Delft, The Netherlands.
- DE RUITER, J.C.C. & VAN MIERLO, M.C.L.M. (1988), Turbulence measurements above artificial dunes. Report Q789-I, Delft Hydraulics, Delft, The Netherlands.
- EGIAZAROFF, I. V. (1965), Calculation of nonuniform sediment concentrations. *Journal of the Hydraulics Division, ASCE* 91 (HY4) pp. 225-248.
- EINSTEIN, H. A. (1937), Bed load transport as a probability problem. *Sedimentation*, ed. H. W. Shen. Zurich:Verlag Rascher & Co. pp. 1-105, 1937.
- FERNANDEZ LUQUE, R. & VAN BEEK, R. (1976), Erosion and transport of bed-load sediment. *J. of Hydraulic Research* 14 (2) pp. 127-144.
- GRASS, A. J. (1970), Initial instability of fine sand bed. *Journal of the Hydraulics Division, ASCE* 96 no. HY3, pp. 619-632.
- HUNZIKER, R. P. (1995), Fractionwise sediment transport. (In German) Versuchsanstalt für Wasserbau, Hydrologie und Glaziologie der Eidgenössischen Technischen Hochschule Zürich, Zürich, Swiss, p. 76-113.
- KALINSKE, A. A. (1947), Movement of sediment as bed load in rivers. Transactions, American Geophysical Union 28 (4) pp. 615-620.
- KLEINHANS, M. G. (1996), Sediment transport in the Dutch Rhine branches: processing of 1988-1995 data and test of sediment transport predictors (in Dutch) Netherlands Centre for Geo-ecological Research / Utrecht University Physical Geography. ICG 96/7.
- KLEINHANS, M. G. (1999), Sediment transport in the River Waal: high discharge wave, November, 1998. (in Dutch) Netherlands Centre for Geo-ecological Research / Utrecht University Physical Geography. ICG 99/6.
- KORNMAN, B.A. (1995), The effect of changes in the lee side shape of dunes on the flow field, turbulence and hydraulic roughness. Report 95-1, Institute for Marine and Atmospheric Research Utrecht, The Netherlands.
- KUHNLE, R. A. (1993), Incipient motion of sand-gravel sediment mixtures. *Journal of Hydraulic Engineering* 119 (12) pp. 1400-1415
- LEOPOLD, L. B. & EMMETT, W. W. (1976), Bedload measurements, East Fork River, Wyoming. *Geology. Proc. Nat. Acad. Sci. USA* 73:4 pp. 1000-1004.
- LEOPOLD, L. B. & EMMETT, W. W. (1977), 1976 bedload measurements, East Fork River, Wyoming.

- Geology. Proc. Nat. Acad. Sci. USA 74:7 pp. 2644-2648.
- MEYER-PETER, E. & MUELLER, R. (1948), Formulas for bed-load transport. 3rd Conf. Int. Assoc. of Hydraul. Res. Stockholm, Sweden. 39-64, 1948.
- MISRI, R. L., GARDE, R. J., & RANGA RAJU, K. G. (1984), Bed load transport of coarse non-uniform sediment. *Journal of Hydraulic Engineering* 110 (3) pp. 312-328.
- NELSON, J. M., SHREVE, R. L., MCLEAN, S. R. & DRAKE, T. G. (1995), Role of near-bed turbulence structure in bed load transport and bed form mechanics. *Water Resources Research* 31 (8) pp. 2071-2086.
- PARKER, G. P. & KLINGEMAN, P. C. (1982), On why gravel bed streams are paved. *Water Resources Research* 18 (5) pp. 1409-1423.
- PARKER, G., KLINGEMAN P.C. & MCLEAN D.G. (1982), Bedload and size distribution in paved gravel-bed streams. *Journal of the Hydraulics Division, ASCE* 108 HY4.
- PETTIT, F. (1994), Dimensionless critical shear stress evaluation from flume experiments using different gravel beds. *Earth Surf.Proc.Land.* 19 pp. 565-576.
- RIBBERINK, J. S. (1987), Mathematical modelling of one-dimensional morphological changes in rivers with non-uniform sediment. Ph.D. thesis, Delft University, The Netherlands.
- RIBBERINK, J. S. (1998), Bed-load transport for steady flows and unsteady oscillatory flows. *Coastal Engineering* 34 pp. 59-82.
- SAMAGA, B.R., RANGA RAJU, K.G. & GARDE, R.J. (1986), Bed load transport of sediment mixtures. *Journal of the Hydraulics Division, ASCE* 112 HY11.
- VAN DEN BERG, J.H. (1987), Bedform migration and bed-load transport in some rivers and tidal environments. *Sedimentology* vol. 34 pp. 681-689.
- VAN RIJN, L. C. (1984), Sediment transport, part I: bed load transport. *Journal of Hydraulic Engineering* 110 (10) pp. 1431-1456.
- VAN RIJN, L. C. (1993), Principles of sediment transport in rivers, estuaries and coastal seas, pp. 7.41-7.43 (stochastic predictor), Oldemarkt:Aqua Publications, The Netherlands
- VAN RIJN, L. C. (2000), Engineering sand model for sand transport. Report Z2099.30, Delft Hydraulics, Delft, The Netherlands.
- WATHEN, S. J., FERGUSON, R. I., HOEY, T. B., & WERRITTY, A. (1995), Unequal mobility of gravel and sand in weakly bimodal river sediments. *Water Resources Research* 31 (8) pp. 2087-2096.
- WILCOCK, P. R. (1993), Critical shear stress of natural sediments. *Journal of Hydraulic Engineering* 119 (4) pp. 491-505
- WILCOCK, P. R. (1997), The components of fractional transport rate. *Water Resources Research* 33 (1) pp. 247-258.
- WILCOCK, P. R. & MCARDELL, B. W. (1993), Surface-based fractional transport rates: mobilization thresholds and partial transport of a sand-gravel sediment. *Water Resources Research* 29 (4) pp. 1297-1312.
- WILCOCK, P. R. & MCARDELL, B. W. (1997), Partial transport of a sand-gravel sediment. *Water Resources Research* 33 (1) pp. 235-245
- WILCOCK, P. R. & SOUTHARD, J.B. (1988), Experimental study of incipient motion in mixed-size sediment. *Water Resources Research* 24 (7) pp. 1137-1151.
- ZANKE, U. (1990), Incipient motion of sediment as a probability problem. (In German) *Wasser + Boden*, 42.Jahrgang Heft 1, Bonn (Germany).

6

Extreme hysteresis of bedload and suspended load transport during a discharge wave in a sand-gravel bed river

“The totality of our so-called knowledge or beliefs, from the most casual matters of geography and history to the profoundest laws of atomic physics or even of pure mathematics and logic, is a man-made fabric which impinges on experience only along the edges. ... A conflict with experience at the periphery occasions readjustments in the interior of the field. ... Having reevaluated one statement we must reevaluate some others, which may be statements logically connected with the first or may be the statements of logical connections themselves. But the total field is so underdetermined by its boundary conditions, experience, that there is much latitude of choice as to what statements to reevaluate in the light of any single contrary experience.” W. V. Quine (1953, *Two dogmas of empiricism*, Harvard University Press, Cambridge, Massachusetts)

Abstract

Plots of bed sediment transport rates in rivers versus a flow parameter often yield hysteresis: a non-unique relation with different outcomes for rising and falling stages. Hysteresis usually is not incorporated in transport predictions, and thus may inhibit realistic sediment transport predictions. A number of hypotheses for explaining hysteresis are tested on a dataset of bed sediment transport in the river Rhine reaches in the eastern Netherlands, which shows an extreme hysteresis in sediment transport. Some of these hypotheses have together the potential to explain the observed hysteresis in the river Rhine and may be relevant for other large rivers as well. The first is hysteresis of hydraulic roughness related to the tardy development of dunes. The second is vertical sorting of bedload sediment by the dunes, combined with the time lag between dune height development and the changing flow. The third is a fine sand wave which migrates through the measurement sections during the discharge wave. However, a full explanation remains a challenge for future field measurements and modelling of hydraulic roughness by dunes, sediment sorting in the river channel bed and sediment transport.

This chapter is based on:

Kleinhans, M. G. (2000). The relation between bedform type, vertical sorting in bedforms and bedload transport during subsequent discharge waves in large sand-gravel bed rivers with fixed banks. Proc. Gravel Bed Rivers Conference 2000, 28 August - 3 September, New Zealand, in Nolan, T. & Thorne, C. (eds), Special public. CD-rom of the New Zealand Hydrological Society

Kleinhans, M. G. (2001). The Key Role of Fluvial Dunes in Transport and Deposition of Sand-Gravel Mixtures, a preliminary note, *Sedimentary Geology* Vol. 143 pp. 7-13.

6.1 Introduction

Magnitude-frequency analyses of bed sediment transport events (cf. Wolman & Miller 1960) and field evaluations of bed sediment transport predictors are usually associated with high uncertainties from a number of sources. One important source is a non-unique relation between transport rates and a flow parameter, which often is a hysteresis loop. The hysteresis can be seen as a time lag or time advance effect and thus shows different transport rates before and after the peak discharge. Hysteresis is defined as clockwise if the sediment transport is larger before the discharge peak and smaller after the discharge peak, and vice versa for counter-clockwise hysteresis. In this paper, field measurements in the river Rhine (The Netherlands) are presented that show an extremely strong hysteresis of suspended and bedload transport.

A number of causes have been cited for hysteresis, among which the development of bedforms (e.g. Allen & Collinson 1974, Ten Brinke et al. 1999) and of armour layers are prominent (e.g. Beschta 1987), which are usually not incorporated in predictions. Dunes usually are associated with sand-bed rivers, while armour layers occur in gravel-bed rivers.

In (bimodal) sand-gravel bed rivers both extensive bedform development (e.g. Klaassen 1991) and armouring (e.g. Klaassen 1987, Reid et al. 1985, Kuhnle 1992) may play significant roles and may both lead to hysteresis. Furthermore the depletion of transportable sediment may play a role, especially in heavily armoured rivers (e.g. Garcia et al. 1999). In addition, the sorting created in antecedent discharge waves may be preserved to some extent and may thus influence the sediment transport in the next discharge wave (e.g. Klaassen 1987). This is sometimes called a history or memory effect of the river. This history effect may cause hysteresis during a discharge wave, and may also cause considerable differences in transport between two discharge waves.

The objective of this paper is to show which mechanisms may be responsible for hysteresis of bedload transport in the eastern reaches of the Dutch river Rhine, a large sand-gravel bed river with fixed banks and low sinuosity. Field data on flow conditions, bed sediment transport, bedform development and sorting in the river bed are presented. The significance of the observed trends is confirmed with an uncertainty analysis. Then a number of hypotheses for hysteresis are discussed in detail. Next, the relative significance of all four hypotheses is determined, using the observations of the Dutch Rhine as constraints. Finally, challenges for future modelling of sediment transport hysteresis are summarized.

6.2 Measurement methods

6.2.1 Field site and general conditions

The measurement area was located both upstream and downstream of the bifurcation point Pannerdense Kop of the river Rhine, the Netherlands (see fig. 6.1), at which the Bovenrijn bifurcates into the Pannerden Canal and the Waal. The Pannerden Canal discharges one-third of the water of the Rhine, and the Waal discharges two-thirds. The rivers are heavily shipped, and their banks are protected with groynes. The average width of the river Waal between the groynes is 240 m and the local water depth varies between 3 and 12 m at low and high discharges respectively. The average discharge of the Waal is 1350 m³/s, with peaks up to 8000 m³/s. The discharge of the Bovenrijn is about 1.5 times that of the Waal, and the width is 360 m. The measurements were done in October and November 1998 (Kleinhans 1999, Wilbers 1999). A maximum discharge of 6400 m³/s in the Waal and 9600 m³/s in the Bovenrijn was reached on 5

November, which has a recurrence interval of 10-20 years.

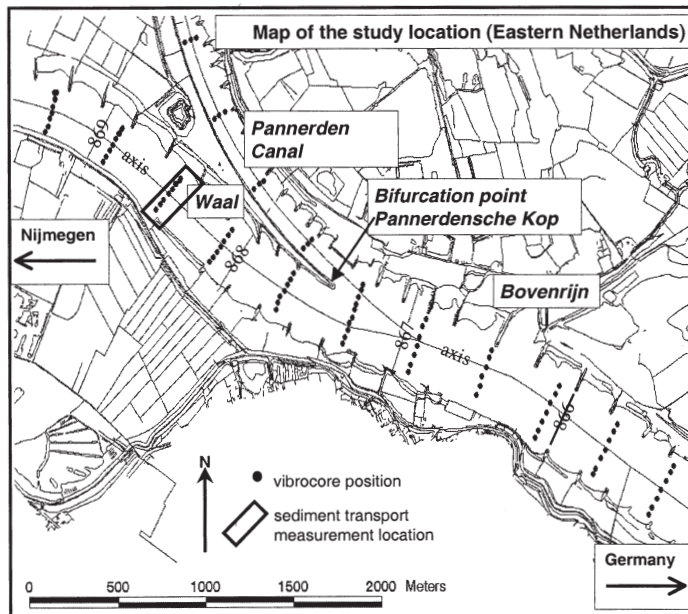


Figure 6.1. Map of the measurement positions of direct sampling of the sediment transport and flow in the river Waal, as well as the vibro-core positions. The whole (submerged) area given by the map was mapped with multibeam echosounders for dunetracking. The numbers at cross-sections are river kilometers.

Vibro-cores were taken in the river bed of the Bovenrijn and Waal (TNO-NITG 2000) in the area where the sediment transport measurements of 1998 were done (see fig. 6.1). In each cross-section, 7 cores were collected at distances of 140, 100, 50 and 0 m off the river axis in the Bovenrijn, and 100, 67, 33 and 0 in the Waal. In the Bovenrijn, this was done in 5 cross-sections and in the Waal in 6 cross-sections, all 400m apart. Particle size analysis was done for samples taken from the cores, usually at 0.0-0.2 m and at 0.6-0.8 m below the bed surface. These cores have been described in Kleinhans (2001a).

At the measurement location the bed consists of a slightly bimodal sand-gravel mixture with a median diameter of about 2.0 mm, with the two modes at 0.7 mm and 11 mm. The sediment averaged over a depth of 0.8 m from the bed surface, is comparable to the surface sediment, though finer (see fig. 6.2). The bed surface sediment of the Bovenrijn is comparable to that of the Waal, only slightly coarser with a median diameter of 2.8 mm (Ten Brinke 1997). The sediment sorting in the bend upstream of the bifurcation has the effect that mainly coarse sediment enters the Pannerden Channel, while a finer mixture enters the Waal. The Pannerden Canal behaves different from the Bovenrijn and Waal, and is therefore not considered in this paper.

6.2.2 Determination of bedload and suspended load transport from direct measurements

Direct transport measurements with bedload and suspended load samplers were done in the river

Waal only (see Figure 6.1). Bedload sediment is herein pragmatically defined as the sediment measured with a bedload sampler. The finer part of the bedload sediment may jump over the dune troughs but still jump into a bedload sampler, thus the dunetracking bedload transport is expected to be slightly lower than the transport measured with the bedload sampler (Van den Berg 1987, Ten Brinke et al. 1999). Suspended load transport is determined from measured vertical transport distributions that were extrapolated to the top of the bedload sampler. Wash load (grain sizes smaller than 0.063mm) is excluded from the analysis.

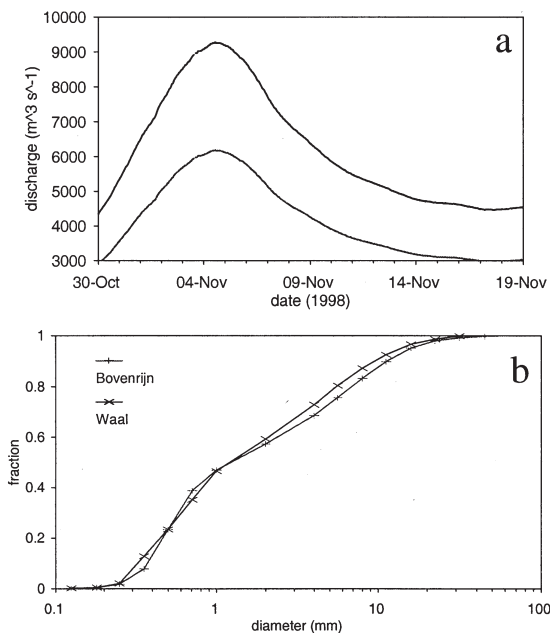


Figure 6.2. a. Discharge of the Waal (lower curve) and Bovenrijn (upper curve) in the measurement period. b. Average grain size distribution of the bed sediment of the Bovenrijn and Waal, averaged over a depth of 0.8 m from the bed surface, determined from the vibro-cores (described in this paper).

The measurement strategy, data processing and accuracy of the resulting data are described in detail by Kleinhans (1999), Wilbers (1999) and Kleinhans & Ten Brinke (2001, see chapter 3). The cross-section of the river was divided in 7 subsections centered at the river axis and 33, 67 and 100 m from the axis at both sides. The width of a subsection, therefore, is about 33 m, except for the outer sections at the banks, which are approximately 40 m wide.

In each subsection, 20 bedload transport samples were taken from each anchoring position, while the dunes migrated downstream approximately one dune length in that period. In every subsection two suspended transport verticals were measured. By doing so it was assumed that samples and verticals were taken at different positions on the dunes and were representative of the conditions along the dunes. The sediment transport was integrated over the width of the channel by summing the average transport of each subsection.

Bedload transport was sampled with an adapted version of the classical Helley-Smith bedload sampler: the Helley Smith for sand-gravel sediment ('HSZ') (Kleinhans & Ten Brinke 2001, see

chapter 3, and Kleinhans 2001b). The dimensions of the sampler orifice are the same as in the original: 7.62 cm wide and high. The mesh bag had a mesh diameter of 250 μm , which is smaller than the 10% diameter percentile of the bed material. The bedload transport sediment was sieved to determine the grain size distributions. The calibration of the bedload sampler is discussed later in this paper.

Both velocity and concentration were measured at several levels above the bed with an Acoustical Sand Transport Meter ('ASTM'): three times subsequently at 0.2, 0.5 and 1 m above the bed, and one time at 2, 3, 4 m etc. above the bed up to the water surface. A pressure sensor in the ASTM was used to determine the water depth (h).

Logarithmic velocity profiles were fitted to the measured velocities to obtain the shear velocity (u^*), which is related to the shear stress as $\tau = \rho u^{*2}$ (with ρ = density of water), and to obtain the height of zero velocity (z_0), which is related to the hydraulic roughness as $k_s = z_0/0.033$ for rough beds.

The suspended sediment transport was calculated as the momentaneous product of velocity and concentration, and was integrated over the water depth. The suspended material was sampled with pump sampling close to the measurement volume of the ASTM. The grain size distribution of the suspended sediment was determined in a settling tube (calibrated in Kleinhans 1998). Kleinhans & Ten Brinke (2001, see chapter 3) discussed the field calibration of the ASTM.

Finally, the water surface slope (i) was measured daily with gauges several hundreds of meters upstream and downstream of the measurement location, and used for the computation of the total bed shear stress as $\tau = \rho g h i$.

6.2.3 Calibration of the applied bedload sampler

The calibration of the bedload sampler is discussed extensively to illustrate that the measured transport trend is not an artefact of the sampling. Furthermore the sampler has not been described before in literature. The calibration coefficient is defined as:

$$\alpha = \frac{\text{true transport}}{\text{transport measured with sampler}} \quad (1)$$

The true transport at the sampler location cannot directly be measured but can be estimated with the transport measured at a nearby location with a trap or conveyor belt in the flume or river. Ideally, $\alpha = 1$.

The long history of bedload samplers illustrates that the problems related to the calibration and design are not trivial. In 1971, E.J. Helley and W. Smith introduced a bedload sampler that was based on the older Bedload Transport Measurement instrument from Arnhem (BTMA), the Netherlands (Bakker 1959). The Helley Smith sampler (HS), named after their designers, is used all over the world today. The original HS had a square, expanding nozzle with 7.62 cm entrance, and a nylon bag with mesh size 200 to 250 μm . The HS was calibrated in the field by Emmett (1980) and in flume experiments by Hubbell (1987) and Thomas & Lewis (1993). The original instrument was meant to be lowered to the bed manually in clear, shallow water. For use in deep water the nozzle is usually attached to a fish-like frame.

The orifice of the new HSZ (Helley Smith 'Zand') sampler for sand-gravel sediment is designed to prevent scooping of bed sediment during landing and lifting. The sampler is suspended from a winch cable connected to the orifice, which hangs in its upward position in the frame of the HS.

When the frame lands on the bed, the orifice takes a few seconds to lower itself slowly to the bed by means of a damped spring construction. When the sampler is lifted again, first the orifice is lifted because it is attached to the winch directly and a few moments later the frame comes up too, making scooping very unlikely.

Table 6.1. Calibration factors of the original (HS) and adapted (HSZ) Helley Smith. The correction of the calibration factor for the HSZ is derived from the difference between the calibration of the HS from literature and as found by Delft Hydraulics (1996, 1997). The values have been calculated with unrounded calibration factors.

instrument	reference	calibration coefficient	remarks
<i>Original calibrations HS</i>			
original HS	Emmett (1980)	1.00	field, 0.5-16 mm
original HS	Hubbell (1980)	0.75	flume, 1.4-32 mm, fig. 4.3
original HS	Thomas and Lewis (1993)	1.02	flume, 2.1-24 mm
	<i>average</i>	0.923	
original HS	Delft Hydraulics (1996)	0.61	flume, 0.46 mm uniform sed.
original HS	Delft Hydraulics (1997)	0.44	flume, 0.4-16 mm, Waal sed.
	<i>average</i>	0.525	
	<i>correction factor:</i>	<i>1.76</i>	<i>(0.923 / 0.525)</i>
<i>Original calibrations HSZ</i>			
HSZ with VC	Delft Hydraulics (1996)	1.35	flume, 0.46 mm uniform sed.
HSZ with VC	Delft Hydraulics (1997)	1.77	flume, 0.4-16 mm, Waal sed.
	<i>average</i>	1.56	
without VC	Delft Hydraulics (1997)	1.15	flume, 0.4-16 mm, Waal sed.
<i>Corrected calibrations HSZ</i>			
HSZ with VC		2.74	1.56*1.76
HSZ without VC		2.02	1.15*1.76
HSZ	<i>average</i>	2.4	error estimate \pm 0.5

The HSZ was calibrated in a recirculating flume at Delft Hydraulics (1996, 1997). The original Helley Smith sampler (HS) was included in the same experiments for comparison between the HSZ and HS to evaluate the calibration results with the known calibration of the HS. In 1996 the calibration was done with sand, and in 1997 the calibration was done with sediment dredged from the measurement location in the Rhine. In Table 6.1 the resulting calibration coefficients are

given. It can be seen that the calibration coefficients of the HSZ (with or without video camera (VC)) are larger than of the original HS. Lower calibration coefficients were found for non-uniform (bimodal) sediment (Delft Hydraulics 1997) than for uniform sand (Delft Hydraulics 1996).

The found calibration coefficients can now be evaluated by comparison of the known calibration of the HS, and the calibration of the HS found here. Comparison between the extensive field and laboratory calibrations of the original HS (Emmett 1980, Hubbell 1987, Thomas & Lewis 1993) with the present laboratory calibration (Delft Hydraulics 1996, 1997) reveals that the latter yielded a calibration coefficient that was 1.76 times lower. This suggests that the true transport in the flume just upstream of the bedload sampler was larger than assumed, leading to underestimation of the calibration coefficients. Reasons could have been the scour at or just downstream the sampling location, or flow deceleration upstream of the sampler due to the locally increased water depth.

If the calibration coefficient of the HS in the experiments is under- or overestimated compared to the calibration in literature, then the calibration coefficient of the HSZ is probably also under- or overestimated. Therefore the calibration coefficients of the HSZ provided by Delft Hydraulics (1996, 1997) of all instrument configurations are corrected by multiplying them with the factor 1.76 (see Table 6.1). For the HSZ with video camera as used in the Waal in 1998, the corrected calibration coefficient then becomes 2.74 instead of 1.56.

An ideal instrument would have a calibration coefficient of 1.00. It is acknowledged that the calibration factor of the HSZ is rather high and rather uncertain and further investigation is needed. Furthermore the effect of the video camera seems to be unacceptably large. Also, recent advances in the calibration techniques (e.g. Thomas & Lewis 1993) could not be applied for lack of data. In this paper, however, the data are used anyway, because it is not the absolute transport rate but the strong hysteresis of the transport that is of interest. In addition, the bedload transport in the Waal determined with the dunetracking method and with the HS showed good agreement in transport rate and trend (see below).

6.2.4 Determination of bedload transport from dunetracking

Echo soundings were done of the bed both in the river Bovenrijn and in the river Waal with a multibeam echo sounder, yielding on average 10-15 points per m², fully covering the river bed (see fig. 6.1). Software, especially designed to characterise dunes and their migration rates, was used to calculate dune dimensions and to compute bedload transport by dunetracking (Ten Brinke et al. 1999). The echosoundings were done twice a day to be used for one transport calculation for that day. The bedload computation by dunetracking was done for the whole width of the river in subsections of 1 m wide. The sediment transport was integrated over the width of the channel by summing the average transport of each subsection.

The bedload transport is calculated using an equation based on the migration of dunes (Engel & Lau 1980, Van den Berg 1987, Ten Brinke et al. 1999). It is assumed that (1) all material that is eroded from the stoss side is deposited on the lee side, (2) the dune shape does not change between two measurements and (3) there is no bedload transport perpendicular to the main migration direction of the dunes. The calculation is done as follows:

$$q_b = \frac{1}{2} H c f (1-a) \approx \beta H c \quad (2)$$

in which q_b is the bedload transport (m³/s/m, including pore space), H is the dune height (m), c is the migration rate (m/s), f is a formfactor to correct the factor $\frac{1}{2}$ as a dune is somewhat bulkier

than a triangle and $(1-a)$ is a factor that corrects for the fact that the position of zero bedload is not the trough but the reattachment point (as was shown by Engel & Lau 1980).

As both the formfactor and especially the factor a are difficult to determine in field measurements, they usually are combined with the factor $\frac{1}{2}$ into the bedload discharge coefficient (β). The value of β is determined by comparing direct bedload measurements (in flumes or using bedload samplers) with the dune track bedload. As was shown by Havinga (1982), Ten Brinke et al. (1999) and Van den Berg (1987), β usually has a value between 0.5 and 0.6. In calculating the bedload transport in the Waal from migrating dunes a value of $\beta=0.55$ was used.

The celerity (c) is determined with a cross-correlation technique. Two subsequent profiles are compared by computing the cross-correlation for a range of migration distances, i.e. translation distances of the second profile from its actual position. When the cross-correlation is the highest, the profiles fit the best on each other and the translation distance of the second profile is the migration distance. This distance is then divided by the time interval between the two echo soundings to yield the celerity.

6.3 Results of the field measurements

6.3.1 Bedform development

The basic parameters of the measurements in the rivers Waal and Bovenrijn during the discharge wave of 1998 are given in Table 6.2. In the following sections, the bedform parameters, bedload transport by dunetracking, and direct sediment transport samplings are presented.

After 31 October the whole bed of the Waal near the measurement position was covered with dunes that became larger as the discharge rose (see fig. 6.3a). The maximum dune height was reached 1 day after the peak discharge. At that moment the duneheight was 0.53 m and the length was 13 m. From 6 november (during falling discharge) secondary dunes appeared superimposed on the primary dunes that were still present since the peak discharge. The dunelength of the primary dunes still increased up to its maximum of 18 m on 7 november (height 0.48 m). After 7 november the primary dunes could no longer be discerned in the measured profiles. The secondary dunes that appeared on 6 November were 8 m long and 0.35 m high. The dimensions of these dunes decreased as the discharge fell. On 19 november, the whole bed of the Waal was still covered with dunes, 5 m long and 0.2 m high.

In the Bovenrijn the dune development showed more or less the same trend as in the Waal (see fig. 6.3b). Contrary to the Waal bed, the bed of the Bovenrijn was already completely covered with dunes before 31 October, 8 m long and 0.3 m high. Apparently these dunes formed at a discharge below 3500-4000 m³/s. The maximal dimensions (28 m long and 1.2 m high) of the dunes were reached 2 days after the peak discharge. The primary dunes were discernable up to 19 november (last day of measurement). At that moment the primary dunes were 45 m long and 0.5 m high, the secondary (superimposed) dunes were 6m long and 0.2 m high.

The celerity of the smaller dunes is uncertain, because the dunes moved more than a dune length in the period between two echo soundings. Consequently, individual dunes cannot be followed in the subsequent profiles, and the cross-correlation diagram (fig. 6.3d) shows equal peaks at two migration distances. This means that the celerity of the dunes and the sediment transport may have two values, and both are given herein.

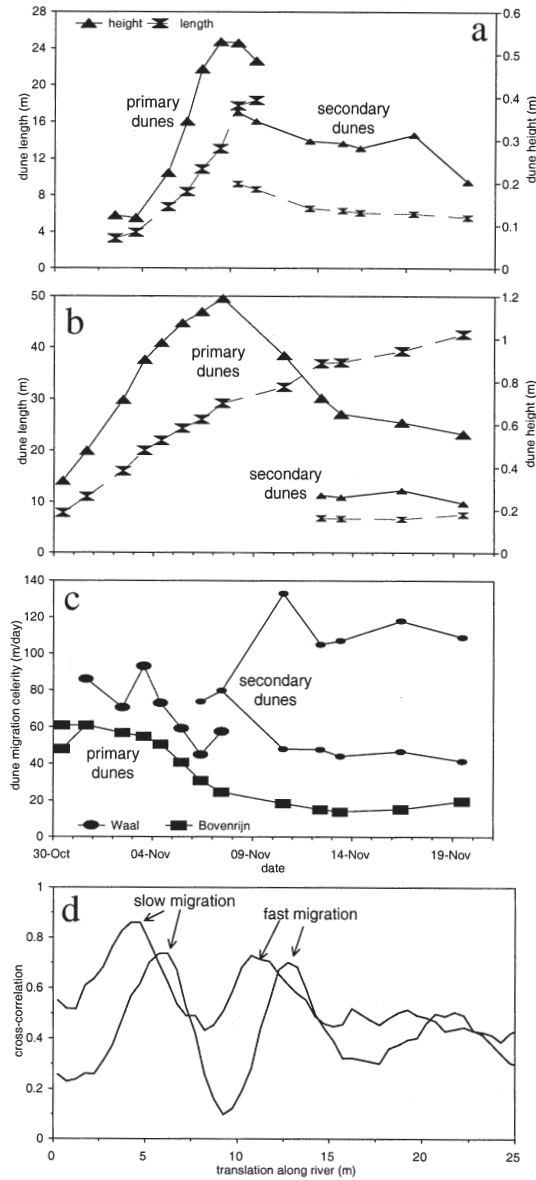


Figure 6.3. Dune height and length in the river Waal (a) resp. Bovenrijn (b), and migration rate in both rivers (c). Large symbols refer to the primary dunes, and small symbols to the secondary dunes. The stochastic error due to noise in the dune height is less than 0.1 m, while the standard deviation of the dune height is about 10-15%. There are two migration celerities possible for the secondary dunes, because there are two high points in the cross-correlation diagram (d).

6.3.2 Bedload transport from dunetracking

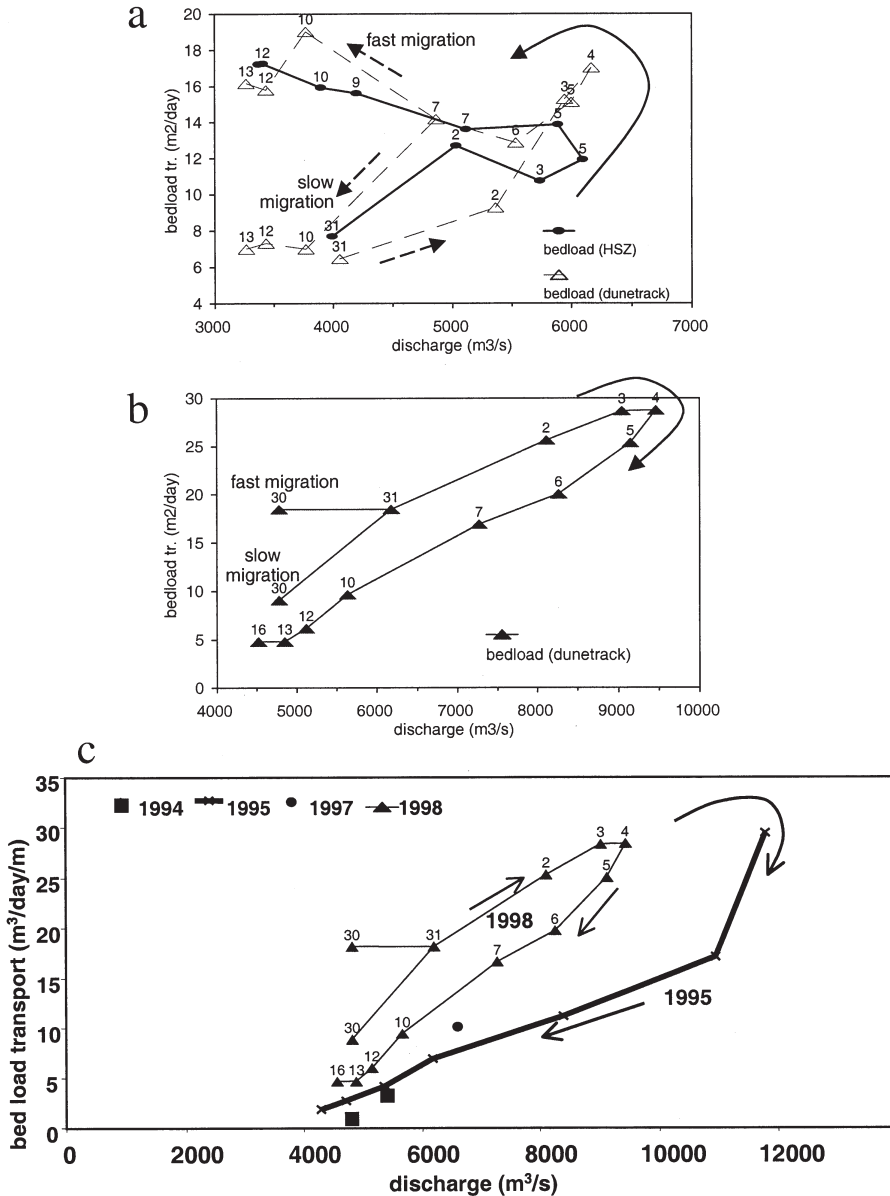


Figure 6.4. Bedload transport computed from dune migration in the river Waal (a) resp. Bovenrijn (b). Numbers refer to dates in the period of 30 October to 19 November in 1998. In figure a, the bedload transport measured with the HSZ is given as well (see text for comparison and discussion). (c) The bedload transport computed from dune migration in the Bovenrijn in several discharge waves. For the dunetracking method, two transports are given for the smallest dunes because it was not clear which migration velocity was correct.

For the total width of the river the bedload transport as determined with dune tracking is shown in Figure 6.4. The bedload transport in the Waal has some counter-clockwise hysteresis, while the hysteresis is clearly clockwise in the Bovenrijn. The hysteresis in the Bovenrijn is also clockwise in the much higher discharge wave of 1995, which in falling stages has even less transport than in 1998 (Wilbers 1998).

The uncertainty in dune celerity, however, leads to a large uncertainty in the hysteresis of bedload transport in the Waal. The bedload transport rate is either very high in falling stages, or near that of the rising stages. It is not clear which one is the realistic transport rate.

6.3.3 Bedload and suspended load sediment transport from sampling

The bedload in the Waal at rising stages consisted of 60% sand and 40% gravel, while it became sandier during the discharge wave, with the sand content rising to 75% near the end of the discharge wave (see fig. 6.5a and b). The bedload sediment is bimodal with mode diameters of 0.5 mm for sand and 8 mm for gravel. Furthermore, the D90 of the bedload sediment sharply decreases after the discharge peak from 10.7 to 7.6 mm.

The bedload transport rates in the river Waal measured with the HSZ are comparable to the bedload calculated with the dunetracking method for rising stages and, in case the highest celerity is correct, also comparable to the falling stages after November 7. This suggests that the calibration coefficient of the HSZ was reasonably well estimated. Both methods show the same trend of low transport at rising stages and higher transport at falling stages, if the highest dune celerity is chosen. Otherwise, the sampled bedload transport rates show a much stronger counter-clockwise hysteresis than the rates determined with the dunetracking method.

The suspended sand transport in the Waal showed a clockwise hysteresis (see fig. 6.5c and d) and was about three times as high as the bedload transport rate during peak flow. The grain size distribution of the suspended sand shows some coarsening during the discharge wave, with the coarsest sediment transported in the falling limb. The suspended sediment had a median diameter of 0.3 mm and a slightly positively skewed lognormal distribution with D95 below 0.8 mm.

6.3.4 Evaluation of the accuracy of the suspended and bedload transport rates

Kleinhans & Ten Brinke (2001, see chapter 3) present a method for estimating and computing the accuracy of cross-channel averaged sediment transport (stochastic error). This method is used for evaluating the uncertainty of the present dataset. The uncertainty of the bedload transport is mainly dependent on the variation coefficient in a subsection: $VC = s_q / (q n^{0.5})$, in which s_q is the standard deviation of the individual bedload transport samples in a subsection, q is the average transport in that subsection, and n is the number of samples. Note that $s_q / n^{0.5}$ is equivalent to the standard error of the average q , thus VC is a relative standard error.

The VC for the 1998 data varies from 15% to 45% for 20 samples, which means that the average of the sampled transport in a subsection has an uncertainty of 15-45%. This agrees with the results of Kleinhans & Ten Brinke (2001, see chapter 3) who used transport data from the Waal sampled in 1997 at the same location. According to their figure 12a, this accuracy leads to an uncertainty of the cross-channel average transport of 20% with 5 subsections. Concluding, the sampled bedload transport as presented herein is in reality at best 20% larger or smaller than the given values. For the suspended sediment transport, a comparable analysis was done (the

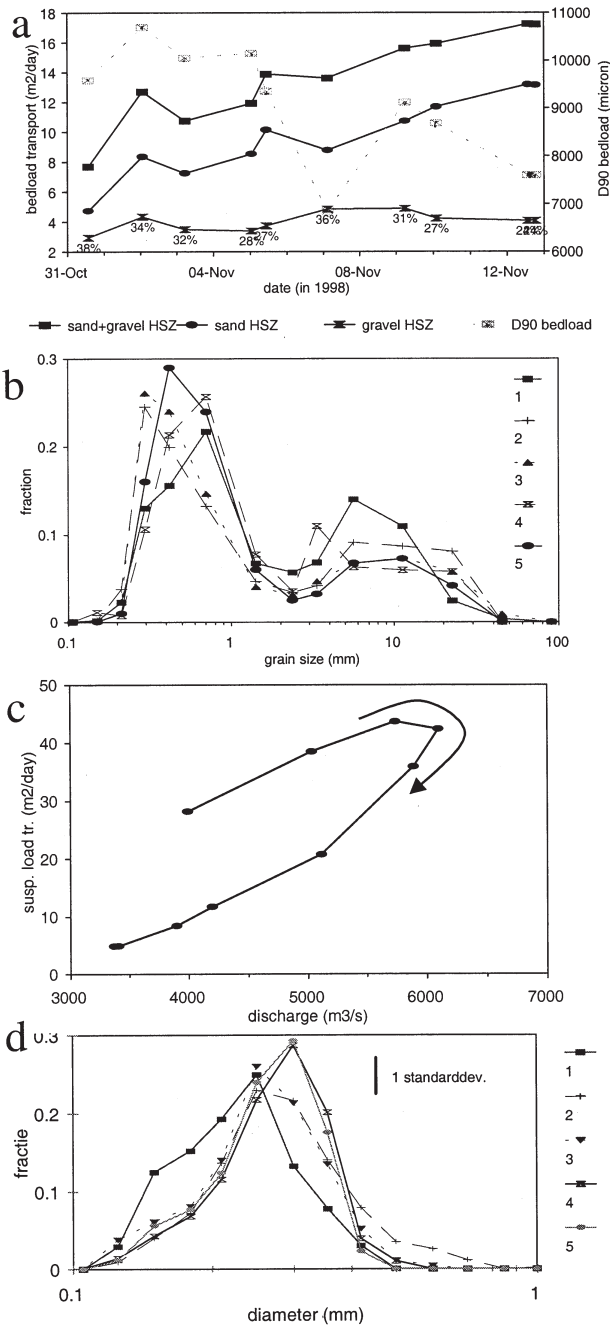


Figure 6.5. a. Bedload transport in the river Waal by the HSZ, and the D90 of the bedload sediment. The percentages refer to the gravel abundance. b. Grain size distributions of the bedload sediment on October 31, November 3, 5, 9 and 12 (numbers 1-5). c. Suspended sand transport in the river Waal by the ASTM. d. Grain size distributions of the suspended load sediment.

calibration is described in Kleinhans & Ten Brinke 2001), leading to an uncertainty of at most 10% uncertainty of the cross-channel averaged suspended sediment transport.

Since the errors of the transports are much smaller than the difference between the transport at rising and falling stages, the hysteresis in suspended and bedload in Waal and in the Rhine is certainly significant. However, the finer details in the measured bedload transport rate trend are not significant.

There is a large uncertainty in dune celerities and transport rates determined by the dunetracking method after November 7. The reason is that the time interval between the echo soundings was too large, so the individual dunes could no longer be recognised to check the cross-correlation method. The cross-correlation peaks at two migration distances, and it is not clear which one is the correct peak. However, the sediment transport sampled with the HSZ is comparable to that determined with dunetracking if the higher celerity and higher transport rates are chosen.

In the analysis below, it is assumed that the strong counter-clockwise hysteresis of bedload transport measured with the HSZ is supported by the dunetracking method. Thus it is assumed that after November 7 the highest celerities and transport rates are correct and not the lower ones. There are three reasons for this assumption:

1. It seems realistic that two independent methods for determining bedload transport give at least the same trend in sediment transport,
2. the hysteresis in the transport rates measured with the HSZ is certainly significant: for several integration methods along the width of the channel, and for several filtering methods to discard the largest samples as scooping, the hysteresis trend does not change, and
3. as shown below, no explanation was found which would explain a strong hysteresis in the transport rates measured with the HSZ and at the same time would explain why the hysteresis in the transport rates determined with the dunetracking method is small (assuming the lowest dune celerity).

6.3.5 Sediment dynamics of the river bed

The deposits as sampled in the Bovenrijn and Waal with the vibro-cores (TNO-NITG 2000) were studied by Kleinhans (2001a) to determine the relation between dunes and vertical sorting in the bed. The key element is the bedform height, which determines at which depth sediment is reworked and redeposited (below the initial plane bed level), and from which depth the bed sediment is entrained. The maximum bedform height determines the depth of lowest level of sediment reworking in the bed, which yields a prediction of the depth of deposits in the bed at 0.5 to 0.6 times the dune height.

There are two processes which promote vertical sorting in the deposits from dunes:

1. by sorting in the grain flows at the lee side of dunes, which yields a fining upward sorting in the dunes, and
2. by selective deposition of coarse sediment in falling stages of discharge waves, which yields a fining upward lag deposit in the troughs of the bedforms.

Both the cross-bedded and lag deposit form a gravelly layer at and just above the depths of the deepest dune troughs in the channel bed. This gravelly layer is overlain by finer sediment, and thus part of the fining upward sorted channel bed sediment. The gravel layers as found in the vibro-cores occurred at depths of 0.5-0.6 times the maximum height of the dunes formed in the discharge waves of 1995 and 1998 in the river Rhine (see fig. 6.6). Kleinhans (2001a) concluded

from this that the deposits formed in the channel bed are indeed related to the dunes.

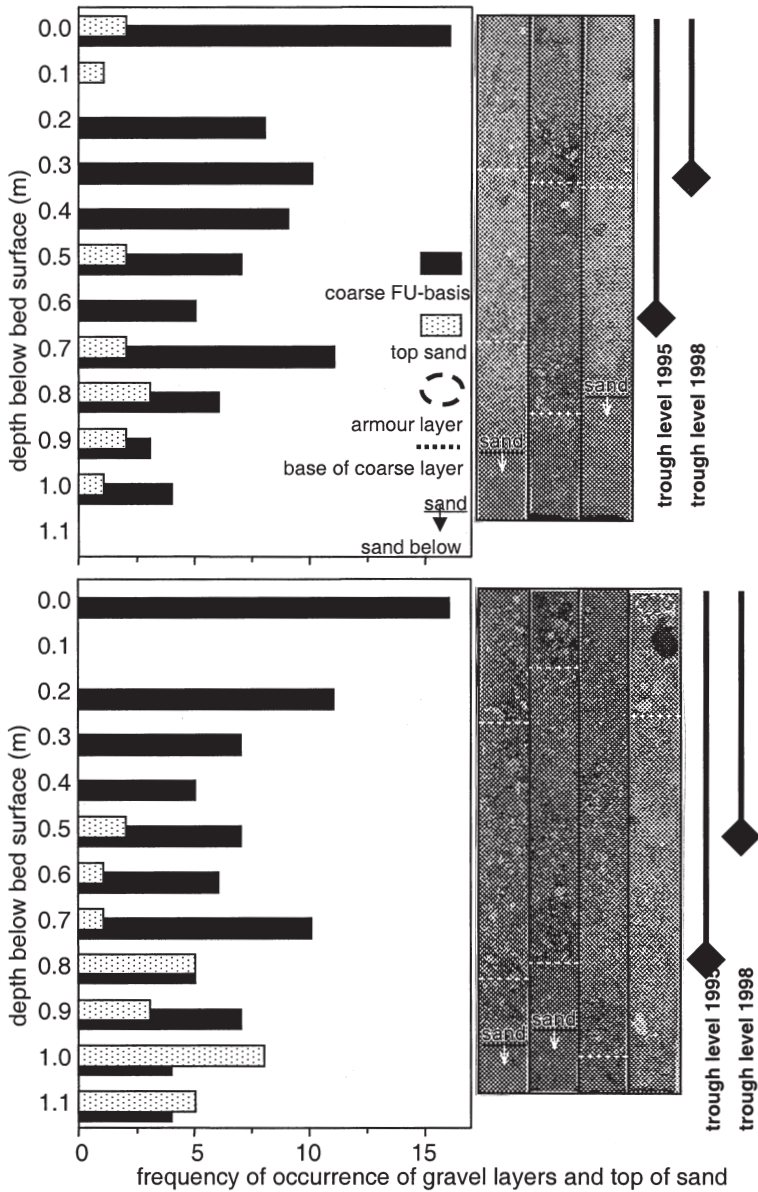


Figure 6.6. Observations of the deposits in the river Waal (a) and Bovenrijn (b). The depths of the top of sand layers and the top of gravelly layers are given as the number of occurrences in all vibrocores. The trough levels are predicted at depths of 0.5 times the observed dune height (after Kleinhans 2001a). In addition, the occurrences of fine sand layers are given in the histogram. Note that this number is higher in the river Bovenrijn than in the Waal. (Also note that the two diagrams have inadvertently been interchanged in Kleinhans 2001a, the one denoted by Waal is for the Bovenrijn and vice versa)

The upward fining trend in the channel bed is difficult to show in the available data, because the cores were sampled for sieving at more or less fixed depths, thus overlapping both the coarse and fine layers. Due to some variation in the depth of the coarse layers, a number of samples (about 6) could be found that represented only the coarse layers of 1995, or only the fine layers of 1995 just above the coarse. The particle size distributions of these selected samples were averaged, yielding a distribution for the fine layers and one for the coarse layers (see fig. 6.7). For the fine layer, the gravel fraction is 43%, and for the coarse it is 59%, which is a significant upward fining. Below some of the dune deposits, a very fine sediment is found that is much finer (see figs 6.6 and 6.7). The relevance of this observation will be discussed later.

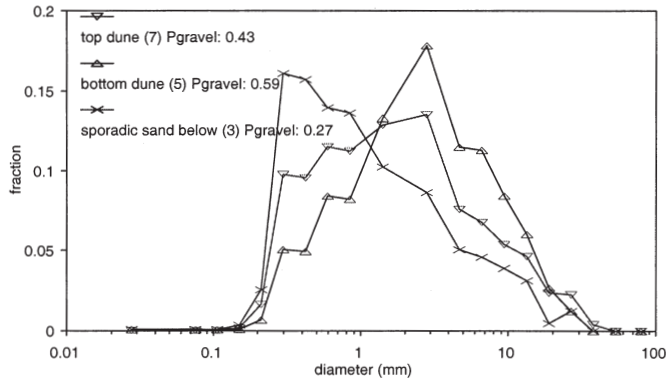


Figure 6.7. Grain size distributions of the sediment in the top and base of dunes in the Waal, and the fine sediment below the dune deposits.

6.4 Bed shear stress determination

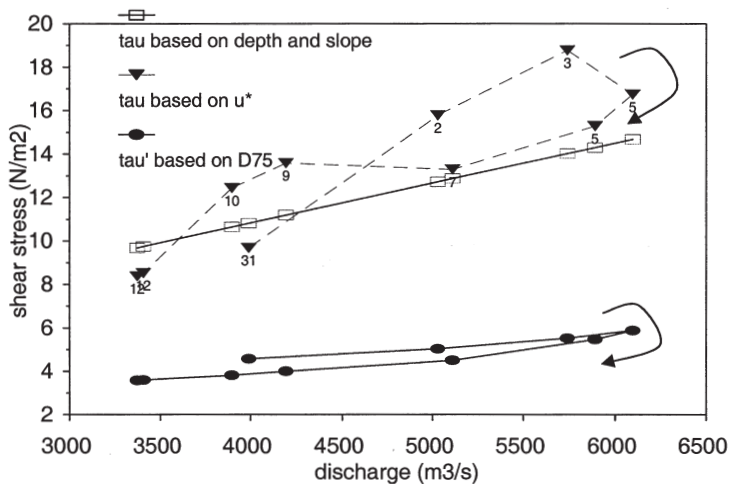


Figure 6.8. Total and grain-related bed shear stress measured in the Waal. The total bed shear stress is based on the depth-slope product and based on u^* from velocity verticals by the ASTM. The grain bed shear stress is based on the flow velocity and the roughness length equal to the D75 of the bed sediment.

The total bed shear stress was computed with two methods (see fig. 6.8):

1. the depth-slope product ($\tau = \rho g h i$) with measured water depth (h) and water surface slope (i), and
2. from the shear velocity ($\tau = \rho (u^*)^2$) determined from the velocity verticals measured with the ASTM and averaged over the width of the river as in the transport measurements (see methods section).

The total bed shear stress is assumed to be the sum of the shear stress related to the bank and groyne roughness, to the bedforms and to the grains. The part of the shear stress that is applied to the grains, is responsible for the bedload sediment transport (Van Rijn 1984a). The aim is therefore to find a method to determine the grain related shear stress (τ'). There are two methods to determine τ' :

1. by subtracting the bedform related shear stress (τ'') from the total shear stress (τ), thus $\tau' = \tau - \tau''$. The bedform related shear stress can be estimated with roughness predictors based on bedform dimensions. However, the bedform related stress is much larger than the grain shear stress. Therefore, small errors in the total shear stress and bedform related shear stress may lead to large errors in the grain shear stress.
2. by estimating the grain roughness (Van Rijn 1984a). The grain shear stress is calculated with the depth-averaged flow velocity and the grain roughness with $\tau' = \rho g (u/C')^2$ with the White-Colebrook equation: $C' = 18 \log(12h/k_s')$, in which C' is the Chezy coefficient related to grains, and k_s' is the Nikuradse grain roughness, usually taken as 1D90 for gravel. In this case, $k_s' = D75$ is taken as empirically determined for the Waal sediment by Kleinhans & Van Rijn (2002, see chapter 5).

For the computation of bedform related shear stress, only crude methods are available, which lead to extreme uncertainties in the residual grain shear stress. Therefore the present analysis is limited to a qualitative consideration of the trends of the total shear stress, from which the contribution of dunes to the total shear stress is derived, and from which the effect of dune behaviour on the grain shear stress is inferred indirectly.

The total bed shear stress in the Waal as determined from the product of water depth and slope, shows no hysteresis. The water surface slope is larger before the discharge peak than after the peak, known as the Jones effect, but this hysteresis is fully offset by the opposite hysteresis in water depth.

However, the determination of total bed shear stress from the depth-slope product may be influenced in addition by the roughness of the banks, groynes and the floodplain, and therefore is not an appropriate measure for flow energy dissipation in the presence of dunes. The locally measured shear velocity, on the other hand, is a local measure for the turbulence and therefore energy dissipation. The total bed shear stress determined from the shear velocity shows a complicated hysteresis (see fig. 6.8).

The grain shear stress is computed only for the river Waal, since no flow velocities were measured in the Bovenrijn. The result is a monotoneous increase of grain shear stress in rising stages, a decrease in falling stages, and a negligible hysteresis (see fig. 6.8).

6.5 Hysteresis of suspended load transport

The suspended load transport was observed to have a significant clockwise hysteresis which was opposite to, and less pronounced than the hysteresis observed in the bedload transport rates in the

Waal. The hysteresis can be explained with the trends in the shear stress during the discharge wave. The measured suspended load transport seems to follow the pattern of the grain shear stress based on D_{75} grain roughness. Also the total shear stress as based on the shear velocity largely follows a clockwise trend for discharges above $4000 \text{ m}^3/\text{s}$ (see fig. 6.8). A suspended load transport predictor like that of Van Rijn (1984b) is based primarily on the shear velocity for the Rouse suspension number, and also on the grain shear stress for sediment entrainment. Such a predictor, if based on the measured flow parameters, predicts the same hysteresis trend as measured, which indicates that the observed trends in shear stress explain the observed trend in suspended load transport.

6.6 Hysteresis of bedload transport

6.6.1 Enumeration of potential explanations

There are a number of possible causes for the strong hysteresis of bedload transport in the Rhine branches, partly borrowed from literature. These are enumerated below. In literature, more hypotheses can be found to explain hysteresis (cf. Beschta 1987, Garcia et al. 1999), but those are not relevant to the present case. One example is hysteresis in suspended silt and clay load may occur due to seasonal depletion of sediment that has been eroded from the mountains and deposited in the river valleys. The present study is focussed on sand-size or coarser sediment. Another example is the depletion of sand from a clast-supported channel bed (clasts connected and air, water or fine sediment in between which does not support the clasts) (Parker et al. 1982). This may be relevant in gravel-bed streams, but not for the matrix-supported (unconnected clasts are supported by finer sediment in between clasts) sediment of a large sand-gravel bed river.

There seem to be two crucial observations in the data which cannot be ignored in evaluating the hypotheses for hysteresis:

1. the bedload transport in the river Waal becomes much sandier in falling stages, and
2. the hysteresis in the Waal and in the Bovenrijn are opposite, and the hysteresis of the Bovenrijn is less pronounced than that in the Waal.

The hypotheses forwarded in this paper can be divided in two groups: those related to the shear stress on the sediment, and those related to the size of the transported sediment. The following phenomena in general may lead to, and may have contributed to the hysteresis of bedload transport in the rivers Waal and Bovenrijn (explained in detail in the next sections):

1. bedload transport and dune migration are enriched and increased respectively by suspended sediment settling in waning flow (Mohrig & Smith 1996),
2. degradation of the channel bed into fine sand,
3. sediment exchange between the active channel of the river and the groyne fields (areas parallel to the river banks that are in between the groynes, which have fine sand in the bed) (after Schans 1998),
4. additional fine sediment entrainment in high stages from meander pools and deposition in low stages (Lisle & Hilton 1999),
5. downstream migration of a fine sand wave (Kleinhans et al. in press, see chapter 4),
6. armouring of the bed surface (Parker et al. 1982, Klaassen 1987, 1991, Reid et al. 1985),
7. lag in bedform height development (and therefore in flow energy dissipation) in a discharge wave (after Allen & Collinson 1974, Kuhnle 1992, Harbor 1998, Ten Brinke et al. 1999),

8. sediment sorting in the channel bed by dunes (Klaassen 1987, 1991, Parker et al. 2000, Kleinhans 2000, 2001a, Blom et al. 2001).

A number of these hypotheses can be rejected easily with the empirical evidence for these hypotheses, but are discussed for the sake of confining the possible explanations and to demonstrate that those hypotheses have been considered. The more promising hypotheses are discussed in more detail.

6.6.2 Suspended sediment settling contributing to bedload transport and dune migration

Suspended and bedload transport are usually defined to be two different modes of transport, but obviously the transition between the two is somewhat gradual (Van Rijn 1984b). It can be argued that the suspended load transport may somehow interfere with the bedload transport as measured in the Waal. If this happened mainly in falling stages and not in the rising stages, then it is conceivable that the sediment transport practically defined as bedload would become sandier and consequently the transport rate would increase. Thus the enrichment of bedload transport with suspended load would result in counter-clockwise hysteresis and fining of the 'bedload' transport. In addition, the suspended load transport would be lower in falling stages than in rising stages. Thus the ratio of suspended and bedload sediment transport is much higher in rising stages than in falling stages.

Three additional hypotheses should be satisfied here to explain the polluting effect of suspended load on bedload transport:

1. This effect is much stronger in falling stages than in rising stages. This is necessary to explain why there is a counter-clockwise hysteresis and fining of the bedload in the first place.
2. A part of the suspended load is inadvertently sampled with the Helley Smith bedload sampler. This is necessary to explain the counter-clockwise hysteresis and fining of the sampled bedload sediment. Since the bedload sampler has a nozzle that is much larger than the layer of sediment rolling and saltating as bedload, it may be expected that some suspended load is indeed sampled with the Helley Smith. Unfortunately, the suspended sediment transport was only measured from 0.2 m upwards above the bed, while the height of the HSZ is 0.076 m. This means that the suspended transport through the upper part of the bedload sampler can only be determined by extrapolating the sediment transport from the points higher above the bed.
3. The suspended sediment contributes to the migration of the dunes, and therefore mainly settles on the lee-sides and in the troughs of the dunes. This is necessary to explain why the counter-clockwise hysteresis in the bedload transport determined with dunetracking shows exactly the same trend as that sampled with the HSZ.

In Figure 6.8, it was observed that the shear velocity, which is a measure for the turbulence, increased when the small secondary dunes appeared on the back of the large primary dunes. It can be hypothesized that the additional turbulence on the back of the primary dunes locally increased the sediment entrainment and incipient suspension. Since this is a local effect, and since the primary dunes are not higher than about 0.3 m, this incipient suspension may have been captured in the bedload sampler, contributing to the hysteresis and fining observed in the sampled 'bedload' rates. This may also explain the increase of bedload transport determined with dunetracking, since the intermittently suspended sediment is expected to settle preferentially in the lee of the primary and secondary dunes.

By extrapolation the transport rates as a function of height above the bed to the near-bed region in the sampler, the amount of suspended load sampled with the HSZ can be estimated. It is assumed that suspended load is caught between the top of the sampler (0.076 m above the bed) and the bedload layer, here assumed to be 0.03 m thick which is twice the D90. The ratio of this amount to the sampled 'bedload' transport is given in Figure 6.9 as a function of discharge. The suspended transport which was sampled with the HSZ appears to be larger before the discharge peak than after, which is the opposite of the hypothesized effect.

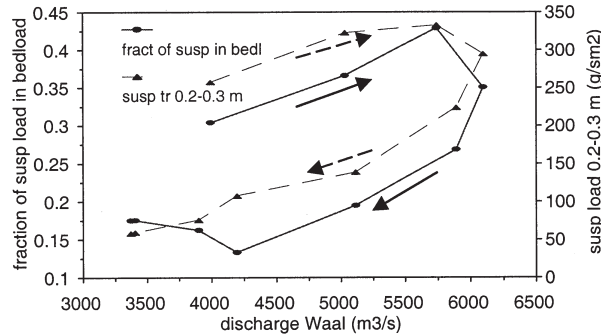


Figure 6.9. Fraction of suspended load sediment that is potentially sampled with the HSZ (between 0 and 1, i.e. between 0% and 100%) (left vertical axis), and the suspended sediment transport between 0.2 and 0.3 m above the bed surface (right vertical axis).

The extrapolated suspended load transport in the near-bed region is, however, very uncertain (Van Rijn 1984b). If the local suspension rate is increased by the secondary dunes of 0.3 m high, then it is reasonable to expect an increase of suspension in the transport measured at the lowest points above the bed. These measured values (not extrapolated), averaged in the cross-section, are given in Figure 6.9 as well, and the hysteresis loop appears to agree very well with the extrapolated suspended load transports. Again, the suspended transport in the near-bed region is larger before than after the peak. It is therefore concluded that suspended sediment enrichment does not explain the observed hysteresis and fining in bedload transport.

6.6.3 Transport hysteresis due to degradation and fine sand scour

In the past hundreds of years, the river has been narrowed with man-made structures like groynes. The effect is that the channel has become deeper, that is, eroded down into its own deposits. In the same period, considerable volumes of sediment were often dredged from the channel bed. From a decennia long record of echo soundings it is known that the river Waal is indeed degrading at a pace of 0.4 m per 50 years (Goelz 1994, Visser et al. 1999).

At the same time, many human-induced changes took place in the catchment of the river Rhine, which have lead to higher discharge peaks. In these higher discharge peaks, the dune height is expected to be higher as well, and so are the related dune scour depth and thickness of the active layer during those peaks.

If the deposits below the active river bed are much finer than that in the active river bed itself, while the bed degrades, then each large discharge wave will scour some of that fine sediment. During the peak discharge, this fine sediment would be mixed into the active layer of the river, which would as a whole become finer after the discharge peak than before. Since finer sediment is easier to transport than coarser sediment, the effect of the sand scour could be higher transport

rates after the discharge peak than before.

The erosion of fine sand at any upstream location within a few kilometers of the measurement location would cause fining of the bedload sediment. The vibro-cores revealed that at some locations, notably in the Bovenrijn at river kilometers 866.9 and 866.5, there are sandy deposits at the surface or just below (see figs 6.6 and 6.7). Furthermore, there is much sand in the bed at kilometers 868.1 and further. Thus, the hypothesis of sand scour may explain part of the fining and counter-clockwise hysteresis of bedload sediment transport at the Waal measurement location (see fig. 6.10).

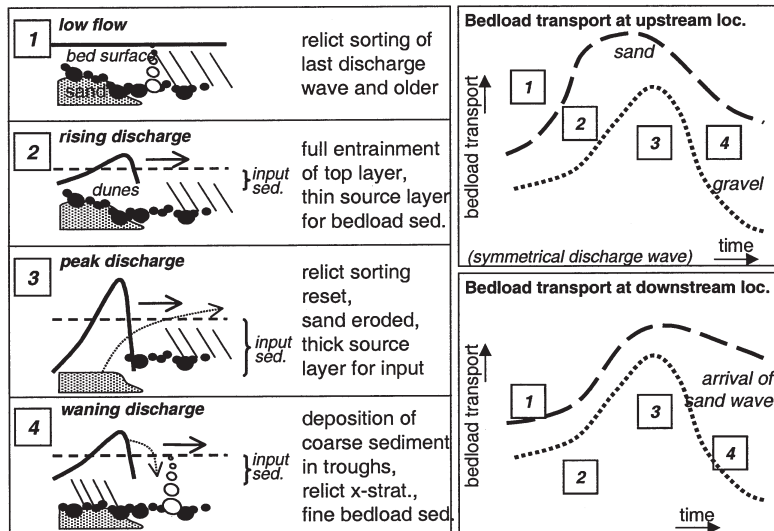


Figure 6.10. Conceptual model of sediment transport at two locations when fine sediment is eroded just upstream of the first location. The gravel transport curves at the two locations are hypothesised to be equal.

However, the scour of fine sediment would take place only during discharge waves that are large enough to create dunes that are high enough to reach the fine sediment. In 1995 this may have been the case, but the dunes of 1998 did not entrain sediment below the trough levels of 1995 (Kleinhans 2001a). This means that the fine sand scour hypothesis cannot explain the observed hysteresis and bedload fining that was observed in 1998.

6.6.4 Transport hysteresis due to fine sand exchange with groyne fields

Fine sand leading to hysteresis could also be entrained from other sources than fine deposits below the active river bed. Along the branches of the river Rhine, groynes have been built to defend the river banks and maintain enough flow depth for shipping. At low flow, the water bodies in between the groynes are subject to large scale turbulence exchange with the main flow and wave action from passing ships. At high flow the groynes are submerged and the water bodies also have a net downstream velocity. The bed in these areas mainly consists of sand. If this sand is preferentially entrained during high discharges, then one could expect a counter-clockwise hysteresis of bedload sediment due to the fining of the transported sediment.

Averaged over the last 10 years, no significant erosion or aggradation of these sandy beaches in

between the groyne fields took place (Schans 1998). This does not mean that the erosion-aggradation cycle could not take place on a smaller time scale. The sand might be entrained from the groyne fields into the river channel during high discharges, and deposited back into the groyne fields during a long period of low discharge. However, measurements of the transport during low flow (Schans 1998) indicate that the transport is directed out of the groyne fields, instead of inward. In addition, the groyne field hypothesis might explain the counter-clockwise hysteresis in the river Waal, but not the clockwise hysteresis in the Bovenrijn. It is not likely that the sediment in the groyne fields in the Waal is entrained during high stages while that in the Bovenrijn is not, because the groyne fields have been designed in such a way that they start to overflow at the same time (flow stage) in all Rhine branches. Groyne fields as a source area for fine sand is therefore not a likely explanation for the hysteresis and fining of bedload sediment.

6.6.5 Transport hysteresis due to sand deposition in meander pools at low stages and entrainment at high stages

The dynamics of the bed in meander bends during discharge waves and in periods with low discharges may cause hysteresis in the following way. (Pool denotes the deep outer bend of a meander, point bar the shallower inner bend, and riffle the shallow area in between two bends.) Sand accumulates in the deep meander pools in low stages, and is eroded again in high stages. When it is eroded, it migrates downstream, possibly as a sandy wave (as reported in Kleinhans et al. in press for the river Allier, France, see chapter 4). The sand enriches the transport layer and leads to higher transport rates. There are two ways in which sand may accumulate in meander pools:

1. The first is related to the shear stress reversal that may take place between pool and riffle. For low discharges, the shear stress on the riffle is high enough to cut into the bed while that in the pools is almost zero (Lisle & Hilton 1999). The sand in the riffle bed is winnowed and deposited in the pools. When the discharge increases, the helicoidal flow in the meander bends becomes stronger and eventually the bed shear stress in the pools is larger than on the riffles (which is the reason why the pools and riffles are formed in the first place). In this process, the sand is eroded from the pools, leading to temporary high sand transport rates in rising stages, and possibly clockwise hysteresis. This shear stress reversal probably occurs only in streams with low discharges that are so small that the water surface is near or on the riffle surfaces.
2. The second is more likely to occur in larger rivers, and is related to helicoidal flow. The bed shear stress between pools and riffles is not reversed, because the water depth during low flow is much larger and the energy slope above pools and riffles much nearer to each other than for shallow flow. The helicoidal flow during high discharges leads to deepening of the meander bend during high discharges. The pool partly fills in during low discharges. In the deepening process, the pool bed surface armours, and in the infilling process, finer sediment (than the armour layer) is deposited in the pool. If this finer sediment is eroded again in the next discharge wave, it may locally lead to the fining of the bedload sediment in rising stages (clockwise hysteresis). Further downstream, this could lead to counter-clockwise hysteresis, depending on the time it takes to be transported downstream.

In Kleinhans & Ten Brinke (2001, see chapter 3), and in Ten Brinke et al. (submitted) the composition of the bed surface is reported to be very coarse in the meander pools and fine in the inner bends and on the riffles. Also in the vibro-cores a coarse surface layer was observed in the

pools. This confirms that an armour layer is formed in the outer bends. However, the sediment layer deposited on top of that armour layer is not very thick; at most 0.1 m in some of the vibro-cores.

If the migration velocity of dunes is considered, then it can be calculated that sediment eroded from the first pool upstream of the measurement location in the Waal takes a few days to reach that measurement location as bedload. This means that fine sediment eroded from the pool in the Bovenrijn in rising stages might reach the Waal in falling stages. This hypotheses might thus explain the clockwise hysteresis in the Bovenrijn and the counter-clockwise hysteresis in the Waal. However, the bedlevel variations as observed with the echosounder were smaller than 0.1 m. This is small compared to the thickness of the active layer, and mixing this fine sediment into the active transport sediment will therefore have a relatively small effect. It must therefore be concluded that this hypothesis cannot play a large role in the explanation of the observations.

6.6.6 Transport hysteresis due to a downstream migrating fine sand wave

Some upstream source of sand may lead to the delivery of sediment to the measurement location in the form of a fine sand wave. Especially if this sediment is sandy, this might help to explain the observed hysteresis and fining of bedload transport during the discharge wave. A fast migrating sand wave would cause high sediment transport before the discharge peak near its source area, but after the discharge peak further downstream. Thus it has the potential to explain the opposite hysteresis in the Bovenrijn and Waal. Waves like these have for example been observed in the river Allier (France, Kleinhans et al. in press, see chapter 4).

Before potential scour areas can be identified, the question is first how far downstream the scoured sediment is able to travel during the discharge wave, since it is useless for this analysis to identify scour areas that are too far upstream to have any effect.

A simplified approach to estimate the sediment celerity is to assume that the bedload sediment was transported in the dunes. The sediment celerity would then be the same as the dune celerity. The dune celerity was determined from the echo soundings, and appeared to be dependent on the dune dimensions. The larger the dune, the smaller was the dune celerity, as was also found by Ten Brinke et al. (1999). The daily values are integrated over the time period. The cumulative distance that the dunes travelled since October 31 to November 12 was about 2000 m. This means that the potential source area for sediment arriving at the HSZ measurement location (868.500 km) could be located up to 1 km upstream of the Pannerdense Kop (bifurcation point). However, the smallest grain sizes may be transported as bedload on the stoss side of dunes but bypass the dune trough instead of depositing at the lee side to participate in the propagation of the dune (Mohrig & Smith 1996). Part of the trajectory of the small grains is then in an intermittent suspension mode, which is much faster than bedload. Furthermore, the gravel may not have been in motion during the whole discharge wave, thus travelled less far than the fine sand. Therefore the sand wave may also have come from areas further upstream.

The sand may have been delivered as a migrating sand wave which arrived in the Bovenrijn section before the discharge peak and in the Waal after the peak. Although this is a realistic possibility that has been reported in other rivers, it is not at all clear where the wave could have come from. Bank erosion as a sediment source is not possible with the defended banks, and no dredging or other human activities were recorded upstream of the measurement locations.

It is inferred from the echosounding data that a number of complicated interactions take place between the different Rhine branches up- and downstream of the bifurcation point. During high discharges, a large bar forms just downstream of the bifurcation point in the rivers Waal and

Pannerdensch Kanaal. In the Waal, this bar migrates downstream with the Bovenrijn dunes entering the Waal during a discharge wave. It is not known yet how this bar affects the transport rate, and how much. It may be that the water levels above the bar are relatively low in falling stages, leading to rapid erosion and possibly more sediment transport (of selectively finer sediment) in the Waal after the discharge peak. This is yet purely hypothetical.

Although it cannot firmly be concluded that scour of fine sediment or a migrating sand wave caused a significant hysteresis of transport, it is potentially an explanation since it explains the opposed hystereses in the Waal and Bovenrijn.

6.6.7 Transport hysteresis due to armouring

The field data of vibro-cores clearly indicate that armouring occurs at low flow in the Rhine branches near Pannerdensche Kop. It is the question how much this armouring influences the sediment transport. Above a certain discharge, dunes emerge. At that point, the armour layer on the low-stage plane bed is destroyed or becomes discontinuous with only armouring in the dune troughs and possibly partly on the stoss side (Kleinhans et al. in press, see chapter 4). Armouring will hinder the entrainment of bed sediment, even if it only occurs in the dune troughs. If the entrainment of bed sediment is hindered by armouring during rising discharge, but not during falling discharge, this leads to a counter-clockwise hysteresis. This is under the assumption of stable armouring.

A dynamic armour layer on the other hand exists both during lower and higher flow stages (Parker et al. 1982). The surface of the bed remains coarser than the underlying bed sediment, while the bedload sediment composition approximates that of the underlying bed sediment (equal mobility condition). At extremely high flow stages, the difference between the bed surface and the underlying and bedload sediment disappears completely.

A dynamic armour layer might cause hysteresis when the time-rate of change of the flow is larger than the time-rate of change of the armour layer. It needs time to develop the armour layer, so at the beginning of a discharge wave it could be less well developed than at the end of a discharge wave. In the latter case the armour layer hinders the entrainment of sediment more than in rising stages, leading to clockwise hysteresis of bedload transport.

Klaassen (1986, 1987) (see also Klaassen et al. 1999) did experiments in a sediment-recirculating flume with sediment with a median grain size of 10 mm and a geometric standard deviation of 5, which was subjected to two discharge waves. The experiments were scaled to the river Meuse (The Netherlands), which is an armoured gravel-bed river. Initially, the bed was allowed to armour in an intermediate discharge, while the transported sediment was not recirculated to simulate the upstream depletion due to armouring of sediment in the real river. Then two discharge waves in order of increasing discharge were simulated, while recirculating the sediment to account for upstream sediment input during high discharge in the natural river. In high discharges, isolated sandy bedforms migrated over the armour layer, locally breaking up or lowering the armour and entraining sediment from the underlying sediment. The armour layer of the second, higher discharge wave was less coarse than that of the first discharge wave, and both were less coarse than the initial armour layer. The reason was that the dynamic armour layer could not reform fast enough in the quickly changing discharge. The sediment transport in both discharge waves showed a clear counter-clockwise hysteresis, with the peak in transport after the peak in discharge. The sediment transport rate in the second wave in rising stages was higher than in the rising stages of the first wave, which is due to the finer armour layer of the second experiment. These experiments prove that hysteresis of transport can occur in (dynamically)

armoured rivers.

There are three arguments why armouring is probably not very important in the Rhine branches:

1. armouring might occur in the Waal and Bovenrijn below discharges of about 4000 m³/s, but above that discharge large dunes develop. It is therefore not likely that armouring affects the bedload transport in any but low flow conditions and during rising discharges. Bedload transports at low and rising stages may be slightly lower than in the absence of an armour, e.g. after the discharge peak, and thus may explain a small part of the hysteresis only.
2. While the sediment in the Bovenrijn is coarser and thus more prone to armouring, the hysteresis is counter-clockwise which suggests no influence of armouring in rising stages at all.
3. The dunes in the river Rhine do not have forms which indicate the existence of an armour layer below the dunes, that is, the dune troughs are rounded and the dunes do not show barchan forms.

It is therefore concluded that armouring plays a minor role only in this part of the river Rhine.

6.6.8 Transport hysteresis due to lag in dune height development

When dunes are large, it takes time to change their dimensions, simply because it takes time to transport the large volumes of sediment involved in the adaptation. The tardy reaction of large dunes to changing flow causes a time lag (c.q. hysteresis) between dune height and flow discharge. Thus the dune height is larger after the discharge peak than before. This is even more so for the dune length, which tends to become larger until the dunes have disappeared. This behaviour has been observed in many rivers (e.g. Allen & Collinson 1974).

Turbulence generated by dunes is in fact a dissipation of the flow energy at the expense of the energy available for bedload transport (McLean et al. 1999). In general, higher dunes are hydraulically rougher and therefore generate more turbulence. However, if the dunes are longer, then there simply are less dunes that generate turbulence, so the roughness is smaller. It is therefore the question whether the turbulence created by dunes is less after the discharge peak than before, or the other way around.

The energy that is available for the bedload transport is the difference between the total energy (total bed shear stress) and the dissipated energy by dunes. Therefore the dune behaviour must have an effect on the bedload transport, which is generated by the remainder of the energy (grain-related shear stress). The direction of the grain shear stress hysteresis is expected to be opposite to the direction of the dune-related shear stress. For example, if the dune-related shear stress is larger in falling stages than in rising stages because the dunes become much higher in waning flow, then it may be hypothesized that the grain shear stress and therefore bedload transport is the largest before the discharge peak and the smallest after (clockwise hysteresis). The observations of total shear stress based on the measured u^* (see fig. 6.8) may be related to the dune development as follows.

From 31 October to 8 November, the shear velocity is largest just before the peak discharge and shows a clockwise hysteresis, concurrent with the formation and growth of the dunes. After 8 November, secondary dunes emerge superimposed on the primary dunes, and are no longer destroyed as they arrive at the top and lee side of the primary dunes. This means that there is probably no flow separation related to the primary dunes and that their hydraulic roughness is negligible. After 8 November, the shear velocity increases temporarily, concurrent with the emergence of the secondary dunes and the diminishing primary dunes, leading to a counter-

clockwise hysteresis of u^* .

The appearance of the secondary dunes and the u^* increase (compare figs 6.3 and 6.8) is concurrent with a temporary decrease followed by an increase in the bedload transport rate. This could be interpreted as follows. The combined roughness of appearing secondary dunes and disappearing primary dunes is relatively large and goes at the expense of the grain shear stress and bedload transport. However, when the primary dunes have disappeared, only the secondary dunes are present, which are smaller and less rough than the primary dunes immediately before the discharge peak. Therefore the energy available for bedload transport increases after the temporary decrease. This remains, however, highly speculative until detailed measurements and turbulence model analyses have been done over dunes with superimposed dunes.

Secondary dunes have been described by Allen & Collinson (1974), who found that these emerge when large dunes adapt too slow to follow the change in flow conditions. Also Harbor (1998) found secondary dunes superimposed on primary dunes in the lower Mississippi river, while both were actively migrating. Harbor suggested that the secondary dunes were the result of the shear stress structure due to the primary dunes, and were not related to the reach-average flow conditions.

For the Bovenrijn no measurements of the shear velocity are available. The measured bedload transport by dunetracking shows the opposite hysteresis as in the Waal. Interestingly, this might be related to the timing of the emergence of secondary dunes. In the Waal, these occur after November 8, while in the Bovenrijn they appear much later. Thus the primary dunes remain active much longer, leading to a relatively larger hydraulic roughness after the discharge peak in the Bovenrijn compared to the Waal. As a result, the energy dissipation by the dunes in the Bovenrijn may have been larger, and therefore the bedload transport lower in falling stages.

Concluding, the (timing of) emergence of secondary dunes superimposed on the primary dunes seems to be essential in an explanation of bedform related flow roughness, and may lead to different directions of hysteresis in the total bed shear stress. Consequently, the bed shear stress related to the grains and used for bedload transport prediction, will also be affected by the emergence of secondary dunes. It seems that essential elements of the sediment transport trends may be explainable with the development lag of dune height, but the correct separation of grain and bedform related shear stress from the total shear stress provides an important challenge before this can conclusively be decided.

6.6.9 Transport hysteresis due to (antecedent) vertical sorting by dunes

It was observed that the bedload sediment became finer in the course of the discharge wave of 1998. Since finer sediment is more easily transported than coarse sediment, this fining may have contributed to the hysteresis. A mechanism that creates this fining in the bed, is the vertical sorting of sediment in dunes, combined with the time-lag of dune growth during the discharge wave as explained in the previous hypothesis.

Two processes sort the sediment vertically in dunes:

1. the grain flowing of bedload sediment at the lee side of dunes (Bagnold 1954, Allen 1963, Kleinhans 2001a). Due to kinematic sorting in the avalanche, the large grains are deposited preferentially in the lower part of the dune and the small grains preferentially in the upper part of the dunes. The result is a fining upward deposit. This sorting process is, however, far from perfect and both in the top and bottom of the dune all grain size fractions are still present. Nevertheless it is found in many cases of grain flowing of sediment mixtures.

2. The size-selective deposition of sediment in waning flow (Ribberink 1987, Kleinhans 2001a). After the peak discharge, the bed shear stress decreases and the largest grain sizes are deposited first. This deposition takes place in the trough zones of the dunes because the sorting of sediment in the avalanches along the lee side of dunes promotes it, and because the turbulent flow strength in the dune troughs is relatively lower due to dune development lag. In short, the gravel lag deposition preferentially takes place in falling stages, depleting the bedload sediment of gravel. This gravel is deposited as an upward fining lag deposit. This leads to sandier sediment transport after the peak discharge which was observed. Since sand is more easily transported, this may lead to larger sediment transport after the peak, that is, counter-clockwise hysteresis.

It is acknowledged that armouring is the same or a related process as the lag deposition described here. The point of view taken here is that armouring is limited to the bed surface only, while the sorting processes due to dunes result in sediment sorting down into the bed as well. Both the processes and effects are much more complicated than in armouring and therefore deserve a separate discussion.

Partial evidence for this hypothesis follows from the observations: in the vibro-cores in the Rhine branches, coarse layers and fining upward sorting were identified (see Kleinhans 2001a), which were the result of upward fining processes in the dunes and selective deposition in waning flow. In addition, a pronounced lag in dune height development was demonstrated.

The hypothesized effect on bedload transport has been estimated with scenario predictions of bedload transport for the Rhine (Kleinhans 2001a, summarised below). The predictions were done for the following three conditions:

1. peak discharge (5 November),
2. waning flow (12 November), including the effect of upward fining due to dunes, and
3. as a reference, the flow conditions of 12 November without fining upwards in the sediment.

The scenario predictions comprise the following steps (Kleinhans 2001a):

1. The sediment available for transport must be estimated by incorporating the vertical sorting effect. This is done with the data on upward fining of the vibro-cores (see fig. 6.7). It is assumed that the preserved deposit (which was the active layer) from dunes has a thickness of 0.55 times the dune height. For peak discharge (condition 1), the sediment over the full depth of 0.55 times the measured dune height is averaged, yielding 48% gravel. For the low discharge (condition 2), only the finer sediment in a shallow layer related to the smaller dune height after the peak is available, yielding 30% gravel. For condition 3 the same gravel abundance as in the peak discharge is assumed because there is no fining upward in condition 3.
2. The bedload transport predictions for all three conditions are done with the adapted Meyer-Peter & Mueller bedload predictor as described in Kleinhans & Van Rijn (2002, see chapter 5), which has the gravel and sand abundances determined in the previous step as one set of input parameters. The calculations are done for two grain-size fractions, sand and gravel. The grain sizes of the sand and gravel fractions are 0.7 and 11 mm respectively. The hiding-exposure phenomenon is incorporated with the Egiazaroff (1965) function as explained in Kleinhans & Van Rijn (2002).

The used parameters and results are given in Table 6.2. The grain shear stresses are based on the grain roughness only, since the aim here is not to predict the transport rate itself, but the change

of trend due to the fining effect compared to a condition without fining.

Table 6.2. Bedload transport hindcast parameters and results for the river Waal with and without the effect of fining of the active layer in falling stages (after Kleinhans 2001a).

case	u (m/s)	h (m)	C' ($\sqrt{m/s}$)	τ' (N/m^2)
Waal peak flow	1.86	10.7	75.9	5.9
Waal waning flow, vertical sorting	1.42	8.7	74.3	3.8
Waal waning flow, no sorting	1.42	8.7	74.3	3.8
	D50 (mm)	bedload transport (m^3/ms)		
Waal peak flow	1.8	17.1×10^{-5}		
Waal waning flow, vertical sorting	0.9	9.45×10^{-5}		
Waal waning flow, no sorting	1.8	7.47×10^{-5}		

The result is that the sediment transport rate in waning flow was predicted larger with the upward fining effect than without (see Table 6.2). These calculations indicate that the hysteresis effect is partly explained with the vertical sorting hypothesis. As expected, the bedload transport in waning discharge for the finer bed sediment is larger than for the coarser bed sediment, which results in hysteresis. The bedload transport for the finer bed sediment contains more gravel than for the coarser sediment, which is explained with the increased mobility of the whole fine mixture due to the lower critical shear stress of the D50.

However, the observed hysteresis in the field is still much larger than predicted with the fining, and the gravel abundance of the predicted bedload transport is still smaller than in reality. The sediment transport in the Waal continued to be large and much more sandy during relatively low discharges, which cannot be explained with this hypothesis alone.

Furthermore, the vertical sorting occurred in the Bovenrijn as well, while the hysteresis in the Bovenrijn is in the opposite direction. If the vertical sorting hypothesis is important, then there must be a mechanism acting only in the Bovenrijn to counteract the hysteresis due to vertical sorting so much that the resulting hysteresis in the Bovenrijn is in the opposite direction.

In favour of this hypothesis is the observation that the bedload transport rate in the Bovenrijn in 1998 is larger than in 1995. If the sediment in 1995 is vertically sorted in fining upward mode, then the sediment entrained in the smaller discharges in 1998 has to be finer and therefore should be larger. It must be concluded that vertical sorting plays a significant role in the hysteresis and fining of bedload transport in the Waal but that it cannot alone explain the observations fully. The sorting process provides a challenge for future models.

Finally, the order and magnitude of discharge waves may be extremely important. The larger the peak discharge, the deeper the sediment is reworked. But depending on the adaption of dune height to the flow, thicker or thinner gravel lag layers may be deposited. The dunes in rising stages of the next discharge wave may have to overcome the resisting effect of such a gravel lag layer, leading to a complex pattern of hysteresis depending on more than one antecedent discharge wave. In the Rhine, a small discharge wave with small dunes occurred in 1997, which might have created a gravel lag that played the resisting role in the next discharge wave of 1998. Thus the transport in 1998 may have depended on the antecedent sorting created in 1995 but also the sorting created in 1997, even though the 1997 wave was smaller than the 1998 wave.

6.7 Integration of the hypotheses

Three mechanisms have the greatest potential to explain the observations:

1. the lagging dune height development effects,
2. the vertical sediment sorting process by dunes, and
3. a migrating body of fine sand from unknown origin (meander pool, a bar created at the bifurcation, a sand wave from an unknown upstream location).

It was seen that none of these three hypotheses can alone explain the observations, while they do not contradict or counteract each other. On the contrary, it is likely that they act together. Below a conceptual model is described that tentatively explains the observations and is not in contradiction with any observation or with processes proposed in literature (see fig. 6.11).

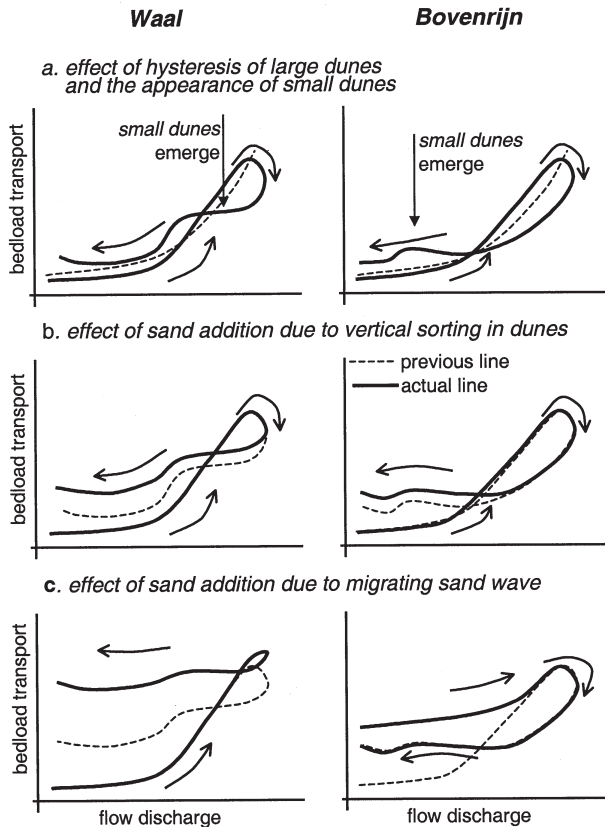


Figure 6.11. Conceptual model explaining the observed hysteresis of sediment transport (see text for explanation). In figures b, c, the previous step is given as well as a dashed line.

Starting from a relation between flow discharge and sediment transport of the bed sediment mixture that shows no hysteresis at all (dashed line in fig. 6.11a), the effects of the three causes of hysteresis is assessed for the Waal and Bovenrijn by adding them one by one (see fig. 6.11):

1. the dune heights show a counter-clockwise hysteresis. Since flow energy is dissipated in the turbulence, there is more bedload transport at the rising limb (see fig. 6.11a). The emergence of the small dunes decreases this hysteresis in the falling limb. Note that the hypothesized bedload transport in Figure 6.11a more or less mirrors the u^* given in fig. 6.8; the falling limb is S-shaped because of the emergence of the small dunes. The contribution of the turbulence due to the emerging small dunes causes the bedload to increase temporarily, leading to a reversed hysteresis after November 8.
2. The dunes sort the sediment vertically, but since the dunes and bedload transport are smaller before the discharge peak than after it, there is more sediment and relatively more sand available for bedload transport after the peak discharge. Sand is easier to transport, even though the dunes also become larger, leading to higher bedload transport in the falling limb (see fig. 6.11b).
3. The arrival of a fine sand wave delivers extra sand to the Bovenrijn before the discharge peak, and to the Waal after the peak (see fig. 6.11c). In the Bovenrijn this effect must be enough to explain the shift from counter-clockwise to clockwise hysteresis in the rising limb, while in the Waal it only has to be large enough to increase the counter-clockwise hysteresis in the falling limb. This is not unreasonable as it can be expected that a sand wave will diffuse and attenuate in migration, and therefore have less pronounced effects in the Waal than in the Bovenrijn.

6.8 General value of the identified mechanisms causing transport hysteresis

These conclusions beg the question whether they occur in other sand-gravel bed rivers as well, that is, what the general validity of the described mechanisms is. The simultaneous occurrence of the phenomena sediment sorting, armouring and dune emergence may be typical for more sand-gravel bed rivers, and thus cause hysteresis of sediment transport in these rivers.

Large sections of the rivers Rhone, Allier (France), Meuse (The Netherlands), Fraser (Canada), Elbe (Germany), Mississippi (United States of America) and the Nile (Egypt) for example, have both sand and gravel in the bed. These are all large systems, in which mobile bars or dunes may occur simultaneously with sorting effects and armour layers. In many smaller rivers, only a few or one of the mentioned mechanisms may cause hysteresis, as large dunes are not relevant there. Thus it seems reasonable that dunes, sorting phenomena and armour layers occur simultaneously in other rivers as well, causing complicated hysteresis patterns in sediment transport. This may not have been reported in literature for two reasons:

- it has never been measured because large measurement campaigns like the one reported here are difficult and expensive to do, and
- it has been observed but was not reported because a report without an explanation is not very satisfactory.

It is a challenge for future field measurements and modelling to explain the hysteresis in sediment transport rates which are caused by tardy reactions of dunes to changing flow, superposition of small bedforms on dune, sorting phenomena like armour layers and fining upward sorting in dunes, and finally the occurrence and behaviour of sediment waves in large rivers.

6.9 Conclusions and recommendations

A strong hysteresis of sediment transport has been observed in the Rhine branches. Three processes that potentially cause this hysteresis were observed to act in the Rhine branches Bovenrijn and Waal. Potentially these occur in other rivers as well. A combination of the three processes is necessary to explain the observed hysteresis in the Rhine branches. The first is hysteresis of hydraulic roughness related to development hysteresis in time of the dunes. The second is vertical sorting of bedload sediment in the dunes combined with the lag between dune height development and the changing flow. The third is the migration of a fine sand wave which arrives in the Waal after the discharge peak.

However, the conclusions remain tentative because the effects of these three on sediment transport cannot yet be quantified, pending modelling and field measurements in the future. In specific:

- Field measurements during a high discharge wave should be repeated at the same measurement position in the Rhine, and should also be done at a comparable bifurcation with the same planform (Merwede bifurcation point further downstream) which does not have a sediment mixture but almost uniform sand in the bed. Preparations for these measurements are currently under way.
- The flow over dunes should be modelled in detail, to compare the hydraulic roughness and its effects on the grain shear stress before and after the discharge peak, and to determine the effect of secondary dunes.
- The vertical sorting by bedforms should be modelled, and coupled to a model for the sediment transport, to determine the potential role of this sorting in the sediment transport hysteresis.

Acknowledgments

The National Institute for Inland Water Management and waste water Treatment ('RIZA') and the Directorate Eastern Netherlands of Rijkswaterstaat in the Netherlands financed and carried out the measurements in the rivers Waal and Bovenrijn, as well as the vibro-cores (in cooperation with the Dutch Institute for Applied Geology ('TNO-NITG')). Furthermore RIZA financed part of the investigations by the author. The comments by Janrik van den Berg, Leo van Rijn, Ward Koster, Wilfried ten Brinke (RIZA) and Gary Parker are much appreciated.

References

- ALLEN, J. R. L. (1963), Sedimentation to the lee of small underwater sand waves: and experimental study. *Journal of Geology* 73 pp. 95-116.
- ALLEN, J. R. L., & COLLINSON, J. D. (1974), The superimposition and classification of dunes formed by unidirectional aqueous flows, *Sedimentary Geology* v. 12, p. 169-178.
- BAGNOLD, R. A. (1954), Experiments on a gravity-free dispersion of large solid spheres in a Newtonian fluid under shear. *Roy. Soc. London, Proc. Ser. A(225)* pp. 49-63.
- BAKKER, M. J. (1959), Calibration of the BTMA, WL|Delft Hydraulics report nr. M601-I, Delft, The Netherlands (in Dutch).
- BESCHTA, R. L. (1987), Conceptual models of sediment transport in streams, in: Thorne, C. R., BATHURST, J. C. & HEY, R. D. (eds.) *Sediment transport in gravel-bed rivers*. Wiley & Sons, UK.
- BLOM, A., PARKER, G. & J.S. RIBBERINK (2001), Vertical exchange of tracers and non-uniform sediment

- in dune situations, Proc. River, Coastal and Estuarine Morphodynamics, IAHR, Obihiro, Japan.
- DELFT HYDRAULICS (1996), Test and calibration measurements with an adapted Helley Smith for bedload transport measurements in sand-bed rivers. (in Dutch) Delft Hydraulics report Q2141, Delft, The Netherlands.
- DELFT HYDRAULICS (1997), Calibration and comparison Helley-Smith Sand. Delft Hydraulics report Q2345, Delft, The Netherlands.
- EGIAZAROFF, I. V. (1965), Calculation of nonuniform sediment concentrations. Journal of the Hydraulics Division, ASCE 91 (HY4) pp. 225-248.
- EMMETT, W. W. (1980), A Field Calibration of the Sediment-Trapping Characteristics of the Helley Smith Bedload Sampler. Geol. Surv. Prof. Pap. 1139, U.S. Dep. of the Interior, U.S. Gov. Print. Office, Washington, USA.
- ENGEL, P. & LAU, Y. L. (1980), Computation of bedload using bathymetric data. Journal of the Hydraulics Division, ASCE 106 pp. 161-162.
- GARCIA, C., LARONNE, J. B. & SALA, M. (1999), Variable source areas of bedload in a gravel-bed stream. Journal of Sedimentary Research 69(1) pp. 27-31.
- GÖLZ, E., 1994. Bed degradation - nature, causes, countermeasures. Water, Science and Technology 29, 325-333.
- HARBOR, D. J. (1998), Dynamics of bedforms in the lower Mississippi river. Journal of Sedimentary Research 68(5) pp. 750-762.
- HAVINGA, H. (1982), Bed load determination by dune tracking. Rijkswaterstaat District Zuid-oost, report 82.3, Arnhem, The Netherlands.
- HUBBELL, D.W. (1987), Bed Load Sampling and Analysis. In: Sediment Transport in Gravel-Bed Rivers. Eds. THORNE, C.R., BATHURST, J.C. & HEY, R.D., John Wiley & Sons, Chichester, UK.
- KLAASSEN, G. J. (1986), Morphology of armoured river beds, experiments with high discharge waves (in Dutch), Delft Hydraulics report M2061.
- KLAASSEN, G. J. (1987), Armoured river beds during floods. Euromech 215, Genova, Italy, September 15-19, also Delft Hydraulics publication 394, Delft, The Netherlands.
- KLAASSEN, G. J. (1991), Experiments on the effect of gradation and vertical sorting on sediment transport phenomena in the dune phase. Grain Sorting Seminar, 21-25 October, 1991, Ascona (Switzerland).
- KLAASSEN, G.J., LAMBEEK, J., MOSSELMAN, E., DUIZENDSTRA, H.D. & NIEUWENHUIJZEN, M.E. (1998), Re-naturalization of the Meuse River in The Netherlands, In: KLINGEMAN, P.C.(1998), Gravel-bed rivers in the environment : workshop held at Gold Bar, Washington, 20-26 August 1995. Highlands Ranch [CO-USA] Water Resources Publications, pp. 655-674.
- KLEINHANS, M. G. (1998), Calibration of the settling tube at the Utrecht University, department of Physical Geography (in Dutch) Netherlands Centre for Geo-ecological Research / Utrecht University Physical Geography. ICG 98/13.
- KLEINHANS, M. G. (1999), Sediment transport in the River Waal: high discharge wave, November, 1998. (in Dutch) Netherlands Centre for Geo-ecological Research / Utrecht University Physical Geography. ICG 99/6.
- KLEINHANS, M. G. (2000), The relation between bedform type, vertical sorting in bedforms and bedload transport during subsequent discharge waves in large sand-gravel bed rivers with fixed banks. Proc. Gravel Bed Rivers Conference 2000, 28 August - 3 September, New Zealand, in NOLAN, T. & THORNE, C. (eds), Special public. CD-rom of the New Zealand Hydrological Society.
- KLEINHANS, M. G. (2001a), The Key Role of Fluvial Dunes in Transport and Deposition of Sand-Gravel Mixtures, a preliminary note, Sedimentary Geology 143 pp. 7-13.
- KLEINHANS, M. G. (2001b), Calibration of bedload transport measurement methods (in Dutch) Netherlands Centre for Geo-ecological Research / Utrecht University Physical Geography. ICG 01/3.
- KLEINHANS, M. G. & TEN BRINKE, W. B. M. (2001), Accuracy of cross-channel sampled sediment transport in large sand-gravel-bed rivers. Journal of Hydraulic Engineering 127 4, pp. 258-269.
- KLEINHANS, M. G. & VAN RIJN, L. C. (2002), Stochastic prediction of sediment transport in sand-gravel bed rivers, Journal of Hydraulic Engineering 128(4), ASCE, pp. 412-425, special issue: Stochastic hydraulics and sediment transport, see chapter 5.
- KUHNLE, R.A. (1992), Bed load transport during rising and falling stages on two small streams. Earth

- Surface Processes and Landforms 17 pp. 191-197.
- LISLE, T. E. & HILTON, S. (1999), Fine bed material in pools of natural gravel bed channels. *Water Resources Research* 35(4) pp. 1291-1304.
- MCLEAN, S. R., WOLFE, S. R. & NELSON, J. M. (1999), Predicting boundary shear stress and sediment transport over bedforms. *Journal of Hydraulic Engineering* 125 7 pp. 725-736.
- MOHRIG, D. & SMITH, J. D. (1996), Predicting the migration rates of subaqueous dunes, *Water Resources Research* 32(10) pp. 3207-3217.
- PARKER, G.P., KLINGEMAN, P.C. & MCLEAN, D.G. (1982), Bedload and size distribution in paved gravel-bed streams. *Journal of Hydraulic Engineering* 108 (HY4) pp. 544-571.
- PARKER, G., PAOLA, C. & LECLAIR, S. (2000), Probabilistic Exner sediment continuity equation for mixtures with no active layer, *Journal of Hydraulic Engineering* 126 (11) pp. 818-826.
- PROFFITT, G. T. & SUTHERLAND, A. J. (1983), Transport of non-uniform sediments. *J. of Hydraulic Research* 21(1) pp. 33-43.
- REID, I., FROSTICK, L. E., & LAYMAN, J. T. (1985), The incidence and nature of bedload transport during flood flows in coarse-grained alluvial channels. *Earth Surface Processes and Landforms* 10 pp. 33-44.
- SCHANS, H. (1998), Representativity of measurements in between groynes in 1996 and 1997 for the whole river Waal. (in Dutch) Netherlands Centre for Geo-ecological Research / Utrecht University Physical Geography ICG 98/15.
- TEN BRINKE, W. B. M. (1997), The composition of bed sediment in the rivers Waal and IJssel in the years 1966, 1976, 1984 and 1995. Report Rijkswaterstaat-RIZA 97.009, Lelystad, The Netherlands.
- TEN BRINKE, W. B. M., WILBERS, A. W. E. & WESSELING, C. (1999), Dune growth, decay and migration rates during a large-magnitude flood at sand and mixed sand-gravel bed in the Dutch Rhine river system. *Spec. Publs int. Ass. Sediment.* 28 pp. 15-32.
- TEN BRINKE, W. B. M., GRUYTERS, S.H.L.L., KOOMANS, R.L., WILBERS, A.W.E. & KLEINHANS, M.G. (submitted), Sediment transport and morphological processes near a river bifurcation in the Dutch Rhine, submitted to the Proc. 7th Int. Conf. Fluv. Sed.
- THOMAS, R.B. & LEWIS, J. (1993), A new model for bed load sampler calibration to replace the probability-matching method. *Water Resources Research* 29(3) 583-597.
- TNO-NITG (2000), Descriptions and photographs of the vibro-cores in the Niederrhein, Bovenrijn, Waal and Pannerdensch Kanaal. Dutch Institute for Applied Geology (TNO-NITG), The Netherlands. Core numbers 40D0155 - 40D0214 and 40G0110 - 40G0150.
- VAN DEN BERG J. H. (1987), Bedform migration and bed-load transport in some rivers and tidal environments, *Sedimentology* 34, pp.681-698.
- VAN RIJN, L. C. (1984a), Sediment transport, part I: bed load transport, *Journal of Hydraulic Engineering* 110 (10) pp. 1431-1456.
- VAN RIJN, L. C. (1984b), Sediment transport, part II: suspended load transport, *Journal of Hydraulic Engineering* 110 (11) pp. 1613-1641.
- VISSER, P.J., H. HAVINGA & W.B.M. TEN BRINKE, (1999), How do we keep the river navigable? (in Dutch). *Land+Water* 9, 24-27.
- WILBERS, A. W. E. (1998), Bedload transport and dune development during discharge waves in the Bovenrijn and the Waal, (in Dutch) Netherlands Centre for Geo-ecological Research / Utrecht University Physical Geography. ICG 98/12.
- WILBERS, A. W. E. (1999), Bedload transport and dune development during discharge waves in the Rhine branches, echo soundings of the flood in November 1998, (in Dutch) Netherlands Centre for Geo-ecological Research / Utrecht University Physical Geography. ICG 99/10.
- WOLMAN, M.G. & MILLER, J.P. (1960), Magnitude and frequency of forces in geomorphic processes. *Journal of Geology* 68, p.54-74.

7

Sorting in grain flows at the lee-side of dunes: review

“The chief importance of knowledge by description is that it enables us to pass beyond the limits of our private experience. In spite of the fact that we can only know truths which are wholly composed of terms which we have experienced in acquaintance, we can yet have knowledge by description of things which we have never experienced. In view of the very narrow range of our immediate experience, this result is vital ...” Bertrand Russell (1912, p. 32, *The problems of philosophy*, Oxford University Press, Oxford)

Abstract

Sediment sorting at the lee-side of ripples, dunes and bars has already been recognized long ago. A predictive model of the sorting is necessary but unavailable for implementation in sediment transport models for sediment mixtures. Relevant processes in sedimentological and physical literature are reviewed and compared to the sparse data of sediment sorting. A synthesis is given of the most important variables governing the sorting processes for the benefit of future experimentation and modelling. These variables are the sorting (standard deviation) of the sediment mixture delivered to the brinkpoint, the height of the dune or bar relative to the average grain size of the mixture, the velocity of the flow above the brinkpoint relative to the settling velocity for all grain size fractions, and the frequency of the grain flows. In addition, the dynamics of the grain flows in different conditions seem to affect the sorting.

7.1 Introduction

A well known feature of fluvial sediments is the cross-stratified deposit, caused by the propagation of the bedforms by discontinuous grain flows of bedload sediment at the lee side of a dune (Allen 1963, 1984) and by settling from suspension on the foreset (Jopling 1965, Hunter 1985b). The angle of the lee-slope of such bedforms is in the order of the angle of repose of the sediment, which is about 25-40 degrees, while the height of these bedforms ranges from 0.01 m to 3 m. Within a cross-stratified set the sediment is often sorted vertically. The gravel usually is mainly deposited on the lower part of the lee slope, while the finer grades are predominantly deposited in the upper part. The result is an upward fining deposit with cross-stratification.

Although this sorting principle related to grain flows is well known, a mathematical description of the process is not available. This notwithstanding, that sorting process is relevant for sediment transport prediction as follows. Part of the resulting fining upward sequence of the largest dunes that occurred during a discharge wave, is preserved in the bed. Furthermore the sediment is entrained and deposited size selectively in the dune troughs, which also results in an upward fining deposit. This combined deposit is the source for sediment entrained during the next discharge wave, which will depend on the relict vertical sorting and on the depth from which it is entrained (Klaassen et al. 1987, Kleinhans 2001). The entrainment and deposition depth of the sediment depends on the dune trough level below the average bed level and therefore on the dune height (Ribberink 1987). Thus subsequent discharge waves of decreasing magnitude will leave the upward fining cross-stratified sets at depths related to the concurrent dune height (Kleinhans 2001). A discharge wave of high magnitude will reset the bed and leave a fresh upward fining deposit. Vertical sorting in a river bed is thus intimately linked with sediment transport, which is the rationale herein for studying the deposition processes at the lee-side of dunes. Herein the emphasis is thus on dunes, although most of the processes are relevant as well for bars, Gilbert-type delta's, growing volcanic scoria cones, etc.

The objective of this paper is to explore sediment sorting and deposition processes at the lee-side of dunes, specifically for poorly sorted sediment mixtures of sand and gravel. This is done in the following steps. First, basic sedimentological definitions and well-known processes and deposits are defined. Second, the sparse datasets of vertical sorting in bedforms from literature are presented and discussed. Third, the main vertical sorting processes are discussed in detail, and secondary effects are summarised. Fourth, it is attempted to distill the most important variables that govern grain flow and sorting behaviour, to serve as a guideline for future systematic experiments and field measurements. The results are combined in a phase diagram that qualitatively predicts the vertical sorting curves in different sediments and conditions.

7.2 Basic sedimentological definitions, units and processes

7.2.1 Bedforms and transport

Based on literature, basic sedimentological units and processes are identified for dunes (see Figs 7.1 and 7.2). They are generalized and their implications for vertical sorting in the river bed are discussed below in more detail. Dunes are here loosely defined as asymmetrical bedforms with a height and length in the order of magnitude of the water depth, as opposed to ripples of which the dimensions are scaled by the grain size. Ripples occur only in sand with grain sizes below 0.7-0.8 mm (Southard & Boguchwal 1990).

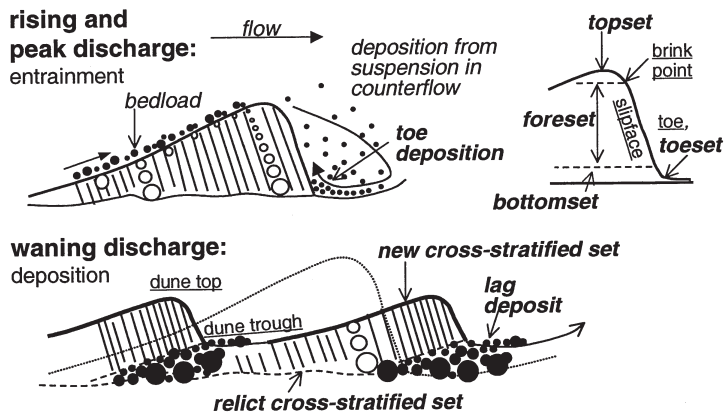


Figure 7.1. Basic definitions of depositional units in river dunes in peak and waning discharge (after Kleinhans 2001). The dunes leave a lag deposit in the river bed below their troughs, which consists of coarse sediment that is no longer mobile.

The dune height is defined as the vertical distance between the trough and top. The brinkpoint is the location at which the flow separates from the bed surface, causing a turbulent counterflow in the lee of the dune (see Fig. 7.2). The zone at which the flow impinges on the bed surface is called the reattachment zone. Downstream of that zone the flow is in the downstream direction and is called coflow, which is herein taken roughly as restricted to the trough zone. ‘Trough’ and ‘top’ are used to denote the zones above the deepest bed height and below the uppermost bed surface height, respectively, in this paper. With ‘bed surface’, the local interface between water or air and sediment is denoted, while ‘average bed level’ denotes the level of the bed averaged over the whole dune length.

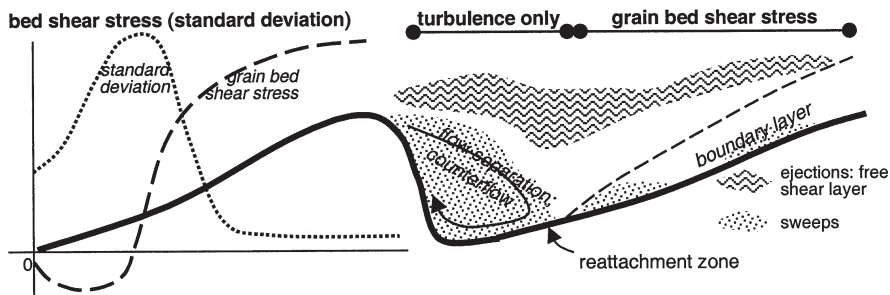


Figure 7.2. Flow conditions over dunes. The average shear stress on the grains (dune surface) is negative (upstream directed) in the trough region, and positive and growing downstream of the reattachment zone. The standard deviation of that grain shear stress is maximal near the reattachment zone, where the turbulent flow variations are the largest. In terms of turbulent flow structures, in the trough zone the counterflow is dominated by sweeps, while the free shear layer flow above the dune tops is dominated by ejections. Downstream of the reattachment zone and upstream of the point where the flow separates from the dune top (called brink point), a boundary layer develops (After Bennett & Best 1995).

The sediment is transported over the dunes in three different basic ways:

1. sliding, rolling and saltating of grains over the bed due to the shear stress exerted by the flow, which is called bedload sediment,

2. suspended sediment transport, which occurs when the saltation height and length of the grains is much larger than the grain size, and
3. gravity-driven movement of sediment downslope, i.e. grain flows, usually at an angle that is larger than the angle of repose.

7.2.2 Deposits and sorting

Within dunes, three basic depositional units can be distinguished, being a bottomset, a foreset c.q. cross-stratified set and a topset (see Fig. 7.1). Bedload sediment is transported on top of the dune, and may be preserved as a topset, which has an erosional boundary with the underlying sediment. In addition, the largest particles are partially mobile and form an armour layer on top of the dune or in the trough. This armour layer protects the underlying dune or bed to some extent against erosion.

Sediment that arrives at the brinkpoint of the dune is partly deposited on the lee slope. A finer part of the sediment is suspended, to be deposited on the lee slope, in the trough zone or on the stoss side of the downstream dune.

It is important to distinguish between two possible directions of sorting (see Fig. 7.3) (Allen 1984):

1. tangential: the direction of the flow of water or grains,
2. perpendicular: upward normal to the plane of flow

The deposition in a cross-stratum of the largest grains near the toe of a dune and the smallest grains near the top gives a net fining upward sorting in the whole dune. Thus vertical sorting in dunes is the result of tangential sorting, which is, for the gravity driven grain flows, parallel to the cross-strata.

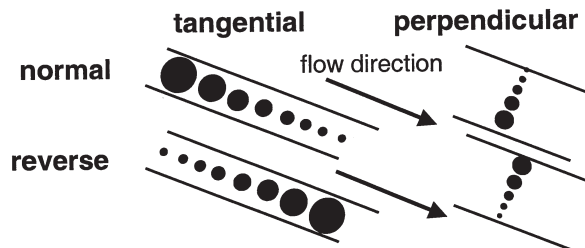


Figure 7.3. Definitions of directions of sorting in four cases, in this case drawn in a cross-stratum, according to Allen (1984). Tangential and perpendicular refers to the direction of sorting relative to the direction of the moving sediment. Normal and reverse refers to the fining or coarsening trend in the deposit.

Furthermore, the fining or coarsening of sediment is defined as follows (see Fig. 7.3) (Allen 1984). Sorting in the tangential direction is called normal when the largest particles are deposited upstream of the smallest grains, as is the case in downstream fining rivers. Sorting in the perpendicular direction is called normal when the smallest particles are on top of the largest, for example in the fining upward deposit of suspended sediment settling in waning flow. Sorting in the tangential direction is called reverse when the largest grains are deposited downstream of the smallest grains. Thus the upward fining in a dune is a case of reverse tangential sorting. Sorting in the perpendicular direction is called reverse when the largest particles are located on top of the smallest, as is the case in river bed armouring.

Three important types of sediment movement and deposition in foresets on the lee side of bedforms are identified between Jopling (1965), Allen (1984), Hunter (1985b), Carling & Glaister (1987) and others: individual grains rolling down on the lee-slope, grain flows, and grain falls. A grain flow refers to a mass of grains that moves downward while the individual moving grains collide and interact. The sediment on the lee slope will accumulate until the angle of repose of the sediment is exceeded. (The angle of repose is sometimes called angle of internal friction, to denote the critical angle of a mass of sediment (internal friction) as opposed to that of the individual grains (repose).) Then the accumulated sediment will roll (individual grains) or flow (grain flow) down the lee slope of the dune. This gravity-driven movement stops at the toe of the lee slope, where the local bed slope decreases. The moving layer of sediment on the lee slope is deposited as a cross-stratum. A number of cross-strata are called the cross-stratified set, and the cross-strata are also called laminae. Cross-stratified sets may range in thickness from a few millimeters in ripples to more than one hundred meters in Gilbert-type deltas. A grain fall on the other hand refers to the settling of single grains from the flow, in which interaction between grains which move is much less important than the interaction between a moving grain and static grains on the lee-slope.

The grain fall mechanism is not only the cause of the formation of the sediment mass prior to grain flow initiation, but also of the toeset and bottomset deposition. Suspended sediment is partly captured in the counterflow and settles on the lee slope and in the trough to form a bottomset. The part of the bottomset at the toe of the lee slope is called the toeset when it is not buried (yet). The sediment in the trough is transported both upstream and downstream, depending on the position relative to the reattachment zone. Both the counterflow and the coflow may form ripples. With very small flow energy, the bottomset may be preserved when the dune migrates over it by deposition of cross-strata at its lee side on top of the bottomset. With higher flow energy, an armour layer may form because the smaller grains are winnowed from the bed and are suspended, while the largest grains of the sediment are partially mobile or immobile.

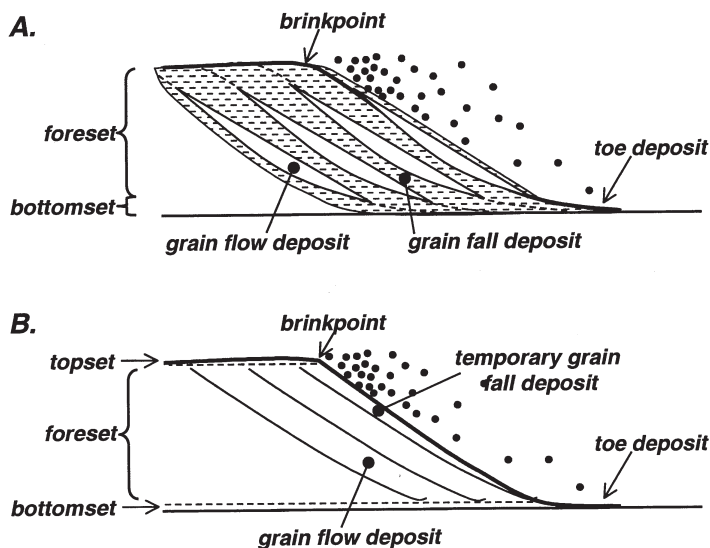


Figure 7.4. a. Sorting and definitions in dune deposits after Hunter (1985b). b. Modified sorting in dune deposits for the case where only grain flow deposits are preserved.

Obviously, the description above is simplified, and the number of processes, interactions and possible combinations between the deposits is large. Different processes are governing the formation of bottomsets, foresets and topsets. The formation of foresets and bottomsets is herein emphasized, since this is the most commonly found deposit in sand-gravel and gravel bed rivers, where vertical sorting is most relevant, and because these are the most important units in an active river bed with dunes while bottomsets are not often preserved.

Table 7.1. Literature on vertical sorting data in grain falls and grain flows.

author(s) and year	sediment	conditions
Datasets used herein		
Allen 1963, 1970	sand	small flume
Blom et al. 2000	trimodal sand-gravel	large flume
Dillingh 1990	sand	field active dunes
Kleinhans 2000	sand-gravel	large flume
Love et al. 1987	sandy gravel	field relict dunes after flood
Ribberink 1987	sand-gravel	large flume
Termes 1986	sand-gravel	small flume, Gilbert-type delta
Hunter & Kocurek 1986	sand	small flume, Gilbert-type delta
Descriptions		
Allen 1984	sand	small flume
Bagnold 1954	sand	laboratory, air
Bak et al. 1988	sand	laboratory, air
Boersma et al. 1986	gravelly sand	field deposits
Carling 1996	gravel	field relict dunes after flood
Carling & Glaister 1987	gravel	flume
Hunter 1985	sand	small flume, Gilbert-type delta
Jopling 1965	sand	small flume, Gilbert-type delta
Klaassen 1987, 1991	gravelly sand	large flume
Nemec	sandy gravel	field Gilbert-type delta
Shaw & Gorrell 1991	sandy gravel	field relict dunes after flood
Modelling and related experimenting with artificial sediments		
author(s) and year	phenomena	model
Boutreux 1998	segregation	microscopic grain interactions
Boutreux et al. 1998	stratification and segregation	microscopic grain interactions
Cizeau et al. 1999	stratification and segregation	continuum flow
Koeppe et al. 1998	stratification and segregation	microscopic grain interactions
Makse 1997	stratification and segregation	stability analysis
Makse et al. 1997a	stratification	-
Makse et al. 1997b	stratification	-
Makse et al. 1998	stratification and segregation	- (detailed measurements)
Makse and Herrmann 1998	stratification and segregation	microscopic grain interactions

The sorting within rolling grain, grain fall and grain flow deposits is obviously different. In the grain fall, roughly the largest grains are deposited near the brinkpoint and the smaller ones further downslope. Grains may roll down individually and the largest grains may be transported further

downslope due to their larger momentum. In the grain flow, the grains drag the neighboring grains and a number of sorting processes occur that are discussed later. It is therefore relevant to assess the importance of both grain fall and flow for the sorting in the end products. It can be hypothesized that fine-grained sediments will have a much stronger grain fall deposition all over the lee-slope (Fig. 7.4a), especially in wind-blown deposits, while coarse-grained sediments have little or no grain fall deposition on most of their lee-slope, resulting in a grain flow dominated deposit (Fig. 7.4b), or, for the coarsest sediments, rolling grain deposits.

Not many papers have specifically addressed the problem of quantifying vertical sorting within a dune. Some present data on the sorting, and a group of physicists attempted to model the vertical sorting for grain flows in air. In Table 7.1, the available data used in this paper are summarized. In the next section, the available data and observations (from Allen (1963), Blom et al. (2000), Dillingh (1990), Kleinhans (2000), Love (1987), Ribberink (1987) and Termes (1986)) are reviewed with special attention to the relative importance of individual grain rolling, grain falls and grain flows and other possible sorting processes. Subsequently, the three types of sediment movement and deposition on lee-slopes (grain fall, individual grain rolling and grain flow) are discussed in detail.

7.3 Sorting data in literature

7.3.1 Vertical sorting in foresets in laboratory experiments

Allen (1963) experimented with sand in a small laboratory flume, in which a single dune or delta-like feature was created. Allen found that sediment was deposited in a wedge on the upper lee-slope of the dune. This wedge of sediment failed above a certain angle and then created a new cross-lamina. Above a certain transport rate, the wedge no longer formed and there were continuously grain flows. Using a sand with a D50 (median grain size) of 590 μm , a D10 of 350 and a D90 of 1200 μm , he found that the D50 in the dune varied with a factor 1.5-2 between dune top and toe (see Fig. 7.5a). The general trend was fining upward, which decreased with increasing flow velocity and sediment transport and grain flow frequency. With the highest flow velocity (1.36 m/s) and continuous grain flows, the trend vanished or even inverted partly.

Termes (1986) created a Gilbert-type delta about 0.1 m high in a small flume, in which he studied the vertical sorting formed at the lee side of the delta (see Fig. 7.5b). The sediment had a D10 of 320 μm , a D50 of 750 and a D90 of 3600 μm . An upward fining trend was found, with a sharp decrease in the lower part of the delta. An armour layer was observed on the top surface of the delta. Termes reported that ripples of coarse sediment (here meant as partly gravel) migrated over the top of the delta, but since ripples only exist in sediment finer than about 700 μm , these bedforms probably have to be classified as bedload sheets. Also, in experiments T1, T4 and T6 (the highest flow velocities, see Fig. 7.5b) the lower lee slope was enriched with sand from suspension, and sand was also deposited on the bed just downstream of the lee slope, and later overrun by the delta foresets. These fine deposits can be interpreted as toesets and bottomsets. It is not clear from the data whether the foreset itself was enriched with the sand, or whether the lowest sampled layer included both an unenriched lowest foreset and the underlying sandy bottomset and thus was finer than the layer of foreset material just above the lowest one.

Ribberink (1987) sampled the vertical sorting in dunes of about 0.04 m high after experiments in a large flume with a bimodal sediment with modes at 0.78 and 1.19 mm (see Fig. 7.5c). He found that the coarse sediment which was immobile or less mobile than the finer sediment, was deposited as a lag near the level of the deepest dune troughs. Furthermore, the sediment at the

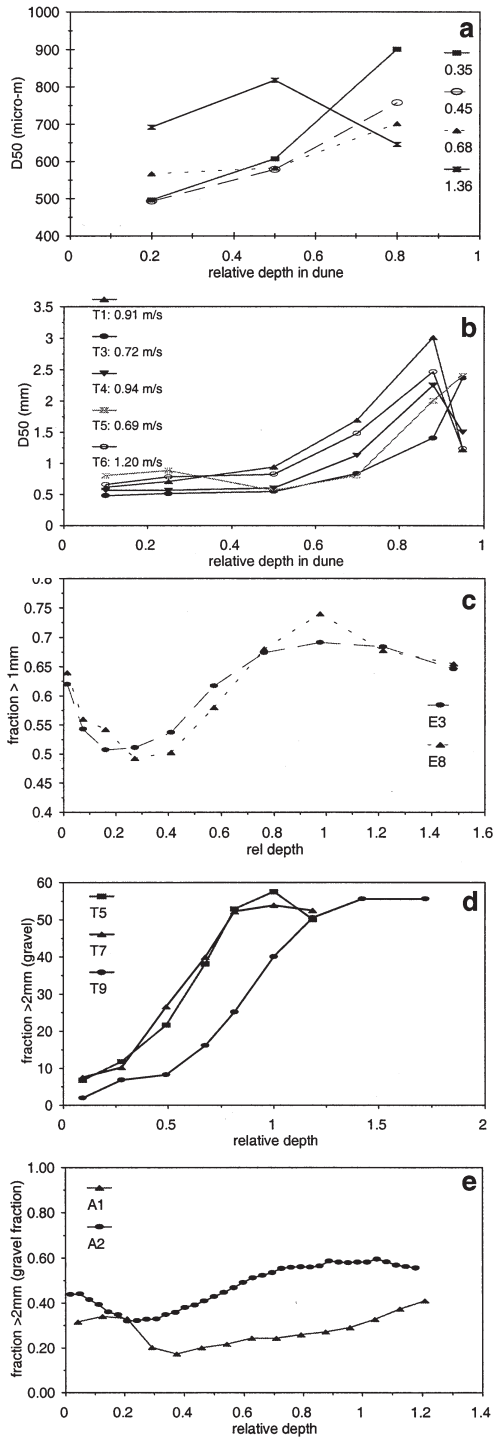


Figure 7.5. Vertical sorting measured in experiments. The dune or bar top is on the left-hand side of the graphs, and the base is on the right-hand side. A horizontal line means no fining or coarsening upward trend at all, and a line with a positive slope means a strong fining upward trend.

- a. Vertical sorting in the dune in Allen (1963). Data is derived from his figure 12. The fining upward trend decreases with increasing flow velocity and grain flow frequency.
- b. Vertical sorting in the Gilbert-type delta in Termes (1986), experiments T1, and T3 to T6. The flow velocity is given as well to indicate the conditions. In experiments T1, T4 and T6 a bottomset can be observed in the lowest part of the delta.
- c. Vertical sorting in the dunes in Ribberink (1987) in his experiments E3 and E8. The sediment is divided into two grain size fractions: coarser and finer than 1.0 mm. The top of the dune shows the presence of coarse bedload sediment, and at the level of the dune troughs there is a lag deposit of gravel.
- d. Vertical sorting in the dunes in Kleinhans (2000), Blom & Kleinhans (1999), experiments T5, T7 and T9. The sediment is here divided into two grain size fractions (sand and gravel), coarser and finer than 2.0 mm. The level of the dune troughs agrees with the level of the armour layer in T5 and T7, while in T9 the armour layer of T7 can still be observed.
- e. Vertical sorting in the dunes in Blom et al. (2000) in experiments A1 and A2. The sediment is here divided into two grain size fractions (sand and gravel), coarser and finer than 2.0 mm. The top of the dune shows the presence of coarse bedload sediment and a gravel lag layer.

top of the dune was rather coarse. This may be interpreted either as the bedload sediment on top of the dune, possibly as a less clear sorting in the upper part of the dune, or as an armour layer on top of the dune.

Klaassen (1991) and Blom & Kleinhans (1999, see also Kleinhans 2000) did comparable experiments as Ribberink (1987). The data of Klaassen are not shown here. The Blom & Kleinhans experiments were done with a coarser and less bimodal sediment than in the Ribberink experiments, with a D₅₀ of 1.8mm and a D_{max} of 16mm. In these experiments (T5 with 0.7 m/s and 28 mm dune height, T7 with 0.8 m/s and 57 mm dune height, T9 with 0.7 m/s and 49 mm dune height) a clear fining upward trend was found without the coarsening at the dune top as observed by Ribberink (see Fig. 7.5d). The main mechanism of foreset formation was grain flows. It was observed that many grain flows were rejuvenated by overrunning subsequent grain flows, and that protruding large grains were captured by the overrunning grain flows to be transported even further down the lee slope. However, halfway the crest of the dune, a coarse surface gravel lag was observed on many dunes, which sank to the trough level as the dune migrated. A clear armour layer was observed at the level of the dune troughs. In the last experiment (T9) the armour layer formed in T7 was still present, and a new upward fining accumulation of lag deposits formed on top of this armour layer as the dune height decreased. Thus the vertical sorting in these experiments clearly are the result of both sorting in the grain flows at the lee of dunes, and selective deposition of gravel in the dune troughs.

Blom et al. (2000) sampled the vertical sorting in and below the dunes in a large flume (see Fig. 7.5e). The sediment was trimodal, with modes at 0.74, 2.0 and 6.1 mm. From base to top, the general trend is fining upward. The sediment just below the dune top, however, shows an increase in grain size. This is interpreted as a combination of bedload transport and a gravel lag layer on top of the dunes. This may be expected to be a thin layer, but was here smeared out in the averaging procedure; the given curves are averages of more than 10 cores at several locations on the dunes. Comparison of tests A1 (lower flow velocity, dune height 24 mm) and A2 (higher flow velocity, dune height 62 mm) indicates that with the higher flow velocity not only more gravel is entrained, but also that the sorting curve in the lower 2/3 of the dune changes from straight to convex.

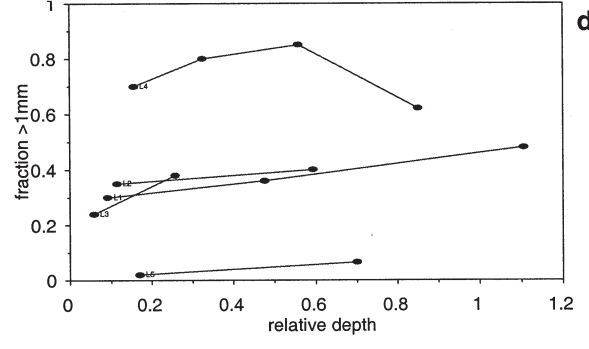
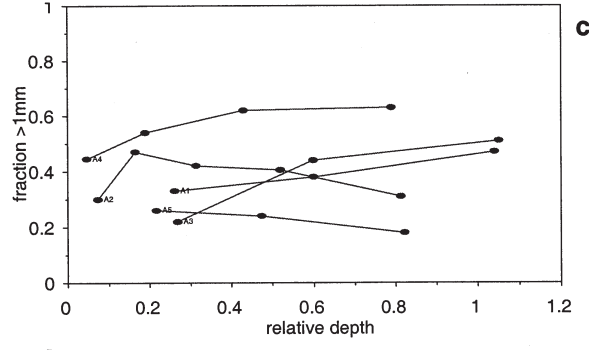
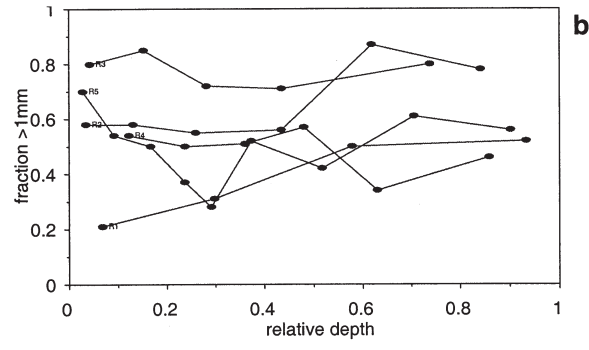
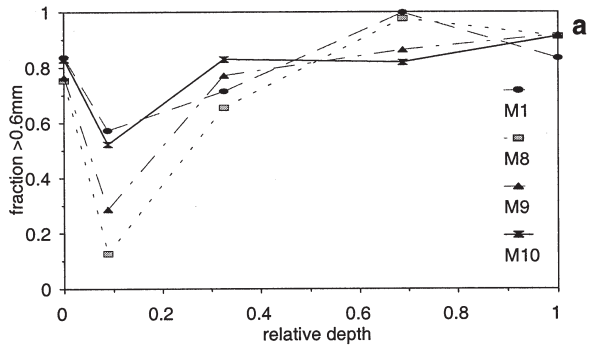


Figure 7.6. Vertical sorting measured in natural river dunes. The dune top is on the left-hand side of the graphs, and the base is on the right-hand side. A horizontal line means no fining or coarsening upward trend at all, and a line with a positive slope means a strong fining upward trend.

- a. Vertical sorting in four gravelly bedforms (M1, M8, M9 and M10) in the in the Conveyance Channel of the Rio Grande (Love et al. 1987). The sediment is divided into two grain size fractions: coarser and finer than 0.6 mm. The armour layer can clearly be seen, and some indication of a slightly finer bottom set is visible in two of the four dunes.
- b-d. Vertical sorting in 15 sand dunes in the left (b), middle (c) and right (d) side of the river IJssel, The Netherlands (Dillingh 1990). Numbers refer to individual dunes. The sediment is divided into two grain size fractions: coarser and finer than 0.5 mm. Curves R1-R5 are located in the right half of the river, L1-L5 in the left half and A1-A5 on the river axis.

Recently a number of highly controlled laboratory experiments with grain falls and flows of granular mixtures in air has been done by Makse and coworkers (Makse 1997, 1998, Boutreux 1998, Boutreux et al. 1998, Makse & Herrmann 1998, Makse et al. 1997a,b, 1998) and by Koeppe et al. (1998). The experiments were done with a vertical Hele-Shaw cell, which is (in Makse's case) a flume of width 0.5cm, length 30cm and depth 20cm, in which the sediment is poured at one upper corner. Bimodal sediments were used with different forms and size ratios. Two mutually almost exclusive types of sorting occurred:

- segregation which results in reverse tangential sorting of small and large round grains. This segregation is almost perfect for $D_{large}/D_{small} > 1.5$, otherwise it is more gradual. Segregation leads to a strong fining upward trend.
- cross-stratification with reverse perpendicular sorting of large cubic grains and small round grains. With a decreasing size difference, the stratification becomes less clear and vanishes at $D_{large}/D_{small} < 1.5$. Stratification yields almost no fining upward trend.

The fact that segregation and cross-stratification are mutually exclusive in these experiments seems to be at variance with the common observation that both can occur in the same set in nature, therefore these experiments must be interpreted with caution.

7.3.2 Vertical sorting in foresets in rivers

Love et al. (1987) measured vertical sorting in relict gravelly megaripples of 0.12 m high that were formed during a flash flood in the Conveyance Channel of the Rio Grande (Central New Mexico) (see Fig. 7.6). An armour layer on top of the bedforms was observed, and ripples migrated over the armour layer. The lower foreset was interpreted by Love et al. to be reworked in the waning flow of the flood: the winnowing of sand from the lower foreset lead to an excellent sorting of the gravel at that height in the bedform.

Dillingh (1990) measured the vertical sorting in sand dunes in the river IJssel near Deventer (The Netherlands) (see Fig. 7.6b). The sediment has a D_{50} of 500-550 μm , a D_{10} of 340 and a D_{90} of 1300 μm . The dunes had a height of 1-1.5 m and their crests continued over the full width of the river channel. The vertical sorting is widely varying and the trend is only slightly fining upward. Allen (1963) on the other hand found a clear sorting in a comparable sediment, except for the high velocity with continuous grain flows. Although his results refer to a small, artificially created dune in laboratory conditions, they imply that the grain flows in the IJssel might have been continuous as well because of their negligible sorting. However, since the dunes at that location have a rather long adaptation time, it is quite possible that a single dune consists of the deposits of several flow stages and amalgated dunes, which would blur any sorting trend within

one active foreset.

Summarizing the laboratory and field observations:

1. the sorting trend in foresets is stronger in wide mixtures than in almost uniform sediment.
2. A higher frequency of individual grain flows decreases the sorting trend. This frequency is related to the celerity of bedforms (bedload transport in $\text{m}^3\text{s}^{-1}\text{m}^{-1}$ divided by dune height) and the thickness of individual grain flows.
3. There seem to be two different modes of sorting: stratification and segregation.
4. Secondary phenomena affecting the sorting trend are deposition of suspended sediment on the foreset and in the trough, armouring on the dunes, and gravel lag deposition below the dunes in changing flow conditions.

In the next section, the three principal modes of sediment motion and deposition on the lee-slopes are discussed, based on literature and compared to the laboratory and field datasets presented here. These are grain fall (deposition from bedload and suspended load on the foreset), individual grain movement on the lee-slope, and grain flows.

7.4 Grain fall process and deposition

A sediment-laden flow arriving at the brinkpoint decelerates rapidly due to the strong water depth increase. The sediment is deposited from this flow on the foreset slope after a short path of suspension. Large grains are deposited immediately downstream of the brinkpoint, while smaller grains may take more time to settle and are deposited lower on the foreset slope. Thus the concentration and settling rate of sediment decreases in downstream direction from the brinkpoint. Allen (1970) and Hunter (1985b) found that the decrease of settling rate for a single grain size follows a power function or exponential function with a faster decay for larger grain sizes. The result of this settling pattern is a sediment wedge with the form of this function (Hunter 1985). This wedge builds up until the angle of static repose is exceeded. Then the mass fails and initiates individual grains rolling or a grain flow (see Fig. 7.7e).

The relation between the flow velocity above the brinkpoint and the settling velocity of the sediment is well known. When the ratio of the bed shear velocity u^* and the fall velocity w_s of the sediment is larger than a certain value, the grains are suspended. Since the boundary between saltating bedload transport and suspended transport is a gradual one, the critical value depends on the definition of suspension. Bagnold (1966, cited in Van Rijn 1993) found that fully developed suspension occurs when $u^*/w_s > 1$, while Engelund (1965, cited in Van Rijn 1993) found $u^*/w_s > 0.25$ for initial suspension. Van Rijn (1993) defined suspension as the shear velocity at which the grains have saltation jump lengths larger than 100 grain diameters, which was experimentally found to be $u^*/w_s > 0.4$.

Experimental evidence is provided by Jopling (1964) and Allen (1968). Jopling measured the deposition of suspended sediment in the lee of a laboratory Gilbert type delta (i.e. a fluvial deposit with its downstream slope at the angle of repose, deposited from a river entering a basin with a much larger depth than the river, e.g. a lake or an ocean). He found that the amount of deposited sediment decreases from brinkpoint to trough, as well as the grain size of that sediment. A combination of the vertical distribution of flow velocity with that of the suspended sediment concentration was used to calculate the flow path of grains of different sizes c.q. different settling velocities. The results of that calculation agreed reasonably with the measurements. Allen (1968) extended this approach and found that the concentration of settling sediment decreases

downstream as a power function with power $\sim u/w_s$. Furthermore, grains with a large settling velocity are deposited mostly very near the brinkpoint.

Obviously the settling pattern also depends on the flow pattern, which is highly turbulent in the lee zone of a negative step, Gilbert type delta or dune. High-frequency flow measurements with laser-doppler instruments above fixed dunes reveal consistent spatial patterns of flow turbulence (e.g. Bennett & Best, McLean etc) (see Fig. 7.2). The water circulates in the lee, resulting in a backward or return flow near the foreset slope. The length of this zone generally is 4 to 5 times the height of the step, delta or dune. In the case of dunes, any deposition of sediment downstream of the reattachment zone is not so likely to be preserved. The stoss side of dunes is erosional and the bottomset is probably more often than not removed (Allen 1968). Therefore the model of Jopling cannot be used for river dunes, but still might be useful for bars and Gilbert-type deltas. The counterflow may even rework the deposits on the lower foreset and in the dune trough, which is discussed in a next section.

When the sediment wedge on the upper foreset exceeds the static angle of repose, the sediment mass in the wedge fails and starts to move downslope (see Fig. 7.7e). The downslope movement refers to individual grains, when only little sediment is involved, and to a grain flow, when so many grains are involved that they start to behave as a flow. The transition between individual grain movement and grain flow is obviously gradual, but for clarity the two are discussed separately.

7.5 Sorting in foreset deposits from individual rolling grains

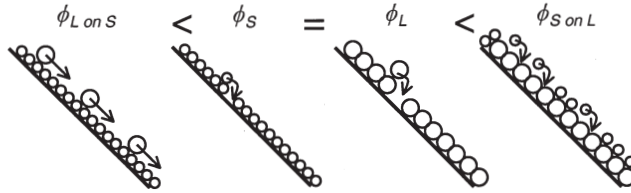
7.5.1 The role of angles of repose

During the descent of individual grains down the lee-slope, the weight and angle of repose as well as the relative size of the rolling and fixed grains determine the probability of deposition on the slope (see Fig. 7.7). Richardson (1903, cited in Allen 1984) already argued that large grains 'experience' a smooth surface when rolling over small grains, but a rough surface when rolling over grains of their own size. Mobile grains that are large with respect to immobile grains in the bed have a very small probability of encountering a niche in which they may deposit. Thus, when a grain flow is in motion, irregularities below it are relatively large to small grains which may lead to their end of motion. The large grains on the other hand continue rolling and thus pass over the surface.

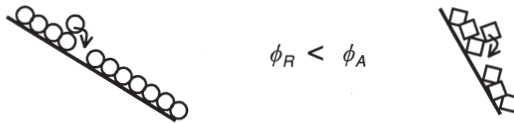
In addition, a large and therefore heavier grain gains more momentum than a small grain in its downwards movement. Consequently the grain has less probability of deposition because it bounces out of possible niches. As a result, the largest grains are deposited near the toe of the lee slope, and the smaller grains near the top (see Fig. 7.7a). This process is known as overpassing (although the term has been used for other, related phenomena as well). Overpassing on the lee slope is not under influence of the flow, but solely attributed to the difference in size between the large and small grains.

It can be expected that these processes are affected by grain shape. Since more angular grains have a higher angle of repose, angularity of grains determine their role in the sorting (see Fig. 7.7b). Makse and coworkers (Makse 1997, 1998, Boutreux 1998, Boutreux et al. 1998, Makse & Herrmann 1998, Makse et al. 1997a,b, 1998) and Koeppe et al. (1998) used these principles in a mathematical model of grain flows and sorting (although they were unaware of Richardson, Allen and Bagnolds work). They were able to reproduce the observations discussed in the section

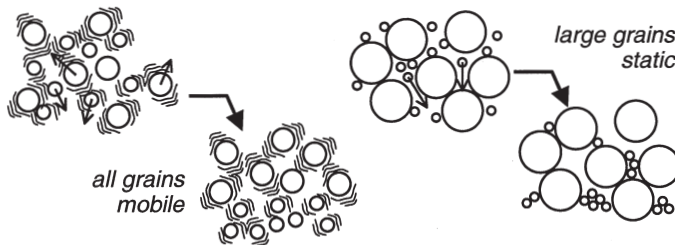
A. Angles of repose (ϕ) of large (L) and small (S) grains



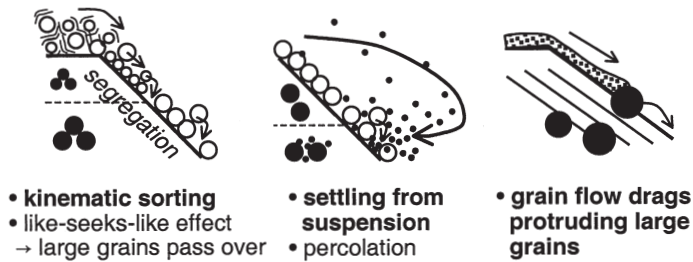
B. Angles of repose of round (R) and angular (A) grains



C. Kinematic sorting and (static) percolation



D. Resulting sorting effects in grain falls and flows



E. Initiation mechanisms of grain flows

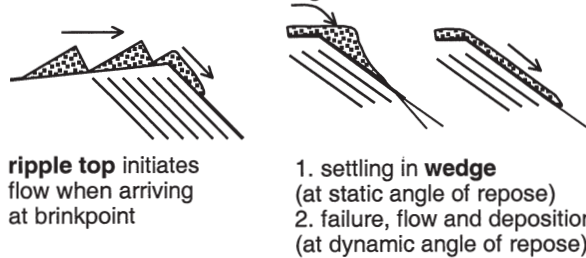


Figure 7.7. Concepts of sorting mechanisms. See text for explanation.

- a. The relations between the angles of repose of uniform sediment, large grains on small grains and small grains on large grains.
- b. The relations between the angles of repose of rounded and angular sediment.
- c. Difference between kinematic sorting and percolation is that all grains are in motion in the former, while the large grains in the latter are static. The opportunity for percolation depends solely on the pore space between the large grains, while the opportunity for kinematic sorting also depends on the kinetic energy of the sediment.
- d. Three sorting mechanisms in sediment motion at the lee side of a bedform.
- e. Initiation mechanisms of grain flows according to Hunter (left) and Allen (right).

devoted to laboratory and field observations herein (see Fig. 7.8). The model by Makse and coworkers did only explicitly include the grain weight of the two grain species and the angles of repose of the pure grain species and of the two species on each other. The latter two were not even included in the model by Koeppel et al., who therefore reproduced the phenomena with even less variables in the model. In the next section, their results are discussed in detail.

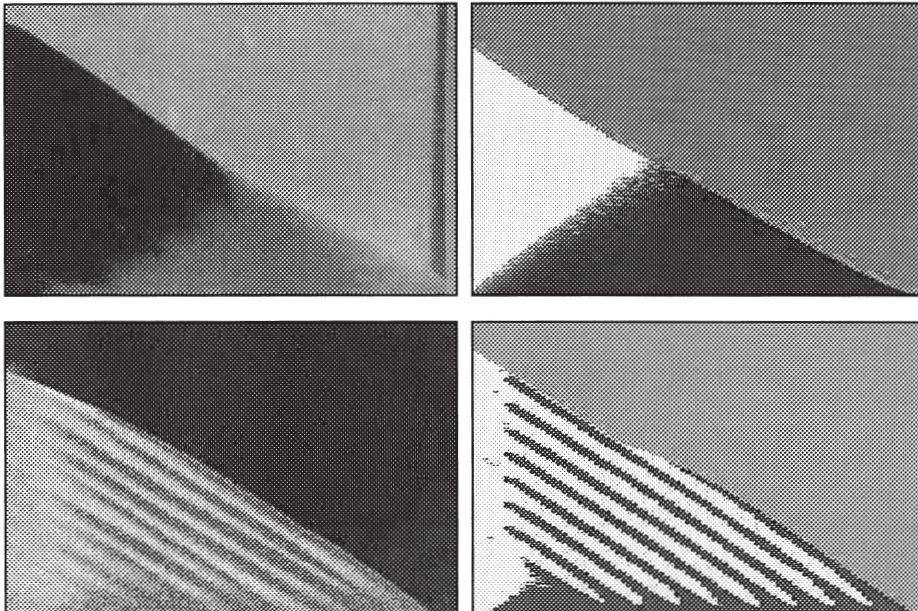


Figure 7.8. Comparison of experimental (left) and modelling (right) results by Makse and coworkers (after Cizeau et al. 1999). Top panels: segregation of the two grain species. Bottom panels: stratification. See text for explanation.

7.5.2 Physical modelling of highly idealised conditions

Makse and coworkers and Koeppel et al. found two mutually almost exclusive types of sorting occur in strictly bimodal sediment. The first is segregation due to the difference in grain size and the like-seeks-like effect (see chapter 2), which results in reverse tangential sorting only. This

segregation is almost perfect for $D_{large}/D_{small} > 1.5$, otherwise it is more gradual. The second type is stratification as a result of competition between size segregation and shape segregation due to difference in grain form and therefore the angle of repose of each grain species and of the one on the other. For two grain species with a different form but equal size, the angle of repose is the largest for the most angular grain species. Thus the most angular grains are deposited on the top part of the lee slope, and the smoother grains on the lower part (see Fig. 7.7b). When the size of the angular grains is larger than the round grains, there is obviously an unstable situation. With large cubic grains and small round grains, a clear cross-stratification emerges. With a decreasing size difference, the stratification becomes less clear and vanishes at $D_{large}/D_{small} < 1.5$.

The explanation by Makse and coworkers is that with these grain species, there is a competition between size segregation and shape segregation. The size segregation would lead to reverse tangential sorting, while the shape segregation would lead to the roughest (cubic) grains in the top part of the lee and the smoothest (round) grains in the lower part. Consequently the whole mixture flows down without significant tangential segregation. When reaching the bottom of the flume (or the trough of the dune), the small grains stop first. The reason is that the small grains on a mixture or on the large grains are more easily captured by the like-seeks-like mechanism. The small grains stop first, large grains are deposited on top of the small, and a static pile c.q. kink develops. The front of this kink moves up the slope as more grains are deposited on it, maintaining the reverse perpendicular sorting. This leads to the development of one cross-stratum. Obviously, stratification is quickly established by the like-seeks-like effect, as the whole slope becomes covered with large grains and the small grains of the next grain flow are easily captured on top of the large grains. The moving front also was observed by Allen (1972) in subaqueous sand dunes in a flume. Both Makse et al. and Allen observed that the kink moved at about the same velocity as the grain flow.

Before these concepts and model for highly idealised sediments can be applied to more natural field and flume conditions, it is worth questioning whether the results of the work by these physicists is representative for any natural condition. Their flume was only 5mm wide, while the coarsest particles were 0.8mm and the thickness of the grain flows up to 7mm, suggesting that wall effects may be large. Makse et al. report that the effect of the wall was only that the angles of repose of the sediment were large compared to the case without walls. This increased angle of repose was fed into the model, but they found that the observed phenomena occurred for much lower angles of repose as well, suggesting that the qualitative results are independent of the magnitude of the angle of repose. Furthermore, the principal experiments were reproduced in a flume of double width with equal results. Therefore they concluded that the wall effect has no effect on their conclusions. However, Koeppe et al. found a strong effect of the width of the flume: it determined the transition from stratification to segregation. In addition, Makse and coworkers found that segregation (tangential sorting) and stratification are almost mutually exclusive, while in natural sediments the combination has often been found. It would be strange if many observations in nature and laboratory should fall exactly in the small range Makse found in which both stratification and segregation occur, therefore it is concluded that these experiments and models cannot without modification be applied to more natural conditions.

Koeppe et al. (1998) found that stratification may occur in bimodal sediment with the same angle of repose (both round grains). They were able to relate each cross-stratum to a single failure of the sediment wedge as described by Allen (1970). It may be that the formation of the wedge in Makse's experiments was inhibited by the large initial velocity of the grains, that were poured from a certain height into the flume. This has the effect that the sediment has an initial vertical velocity. The large grains gain more kinetic energy than the small, which may promote the segregation they found. At the brinkpoint of more natural dunes, on the other hand, the sediment arrives with a horizontal velocity component only. The flow separates from the bed at an angle

of about 10 degrees, while the angle of repose of the sediment is in the order of 30 degrees. Thus the bedload sediment is dropped on the top of the lee slope and a wedge-shaped deposit forms (Allen 1970) which was not observed by Makse. It is more likely that the mechanism as described by Allen occurs on natural dunes, because the wedge has been observed in a number of different settings, and because it explains the simultaneous formation of perpendicular and tangential sorting. The cross-stratification mechanism described by Makse and coworkers may be limited to a laboratory setting and need not play a dominating role in more natural dunes.

Makse and coworkers also studied the effect of grain shape. Angular grains have a larger angle of repose than round grains of the same size. Consequently the angular grains are deposited on the upper lee slope while the round grains are deposited on the low lee slope, as was corroborated by numerical and analog experiments. This agrees with the findings of Carling & Glaister (1987), who found that the most angular grains were deposited on the upper part of the slip face, and the rounder grains on the lower part. Also Nemec & Postma (1993) found the oblate and blade cobbles preferentially on the upper slope of a debris fan.

This shape effect is explained as follows. For two grain species with different sizes but equal forms, the angles of repose of the pure species are equal. However, the angle of repose of the small grains on the large grains is larger, while the angle of repose of the large grains on the small grains is smaller. This is of course explained by the difference in size between the grain species; the large grains when rolling over the small grains, experience a smooth surface, while the small grains rolling over the large ones, experience a rough surface. Thus the large grains tend to end on the lower part of the slope, while the small grains end on the upper part. This trend is quickly amplified by the like-seeks-like effect, as the upper part of the slope becomes smoother for the large grains. The result is a reverse tangential sorting along the slope.

To summarise, in conditions with individual grain movement, the angles of repose of the grains on grains of their own size or different sizes determine their position on the foreset slope. This includes effects of grain shape. In addition, the formation and failure of a sediment wedge on the upper foreset slope is the steering mechanism in grain mobilisation. The demobilisation and deposition occurs from the bottom of the foreset slope to the top (kink moving up) as a compaction 'wave' of the sediment, which is initiated when the grains reach the bottom (dune trough). There may be two modes of deposition that exclude each other, stratification and segregation (see also earlier section about vertical sorting datasets in laboratory conditions), depending on the angles of repose of the grain species on each other.

7.6 Sorting in foreset deposits from grain flows

Two different stages in the grain flow are described. First the initiation is discussed, and the effect of the mode of initiation on the sediment sorting. Second the motion of, and sediment sorting in the grain flow itself are discussed.

7.6.1 Initiation of the grain flow

The initiation of grain flows has been ascribed to two different phenomena. These are ripples and bedload sheets arriving at the brinkpoint of dunes, and the formation of a sediment wedge that fails above a certain angle (see Fig. 7.7e). They are discussed below and compared with empirical evidence.

Hunter (1985a) discussed the possibility of ripples being the initiator. He found that the frequency of grain flows was much larger than that of ripple passage. In addition, it can be argued ripples do probably not occur on the top of dunes, especially not on gravel dunes which occur in flows with a large energy. Concluding, ripples are probably not very important for the sorting in dunes. The sorting is therefore mainly a function of what happens on the lee slope.

Allen (1963, 1984) ascribed the regularity of the grain flow process and cross-stratification to the formation of a wedge of sediment on top of the lee slope (as discussed in the previous section). He found a difference between the static angle of repose and the dynamic angle of repose: the static angle of repose before failure is larger than the dynamic angle of repose at which the grain flow is deposited. The difference between the two angles is called the dilatation angle, because the dynamic angle is that of a dilated sediment mass, being the grain flow. Just after the deposition of a grain flow, a wedge of sediment will build up at the brinkpoint until the static angle of repose is reached. Since the dilatation angle is more or less constant for a certain sediment, the process yields regular cross-strata of comparable thickness (neglecting suspended sediment settling). In very coarse sediment, the wedge has not been observed (Carling & Glaister 1987), and grains dropped by the flow downstream of the brinkpoint moved down the slope individually.

Disregarding the wedge, it has been suggested that grain flows are critically self-organized. Bak et al. (1988) describe how a subaerial pile of drying sand may show grain flows of all possible sizes, consisting of a few grains to the length in the order of the slope length. They argue that the pile of sand is in a self-organized critical state and shows fractal behaviour of grain flow frequency versus size. The upshot is that the grain flows of small sizes occur much more frequently and the bigger it gets, the smaller the frequency. However, in the drying pile of sand the sand supply to grain flows is all over the slope, instead of only at the brinkpoint as in moving dunes. This is confirmed by Allen (1963, 1970), who found that small grain flows occurred now and then on the top of the lee slope, but these accumulated in the wedge (described before) to yield one large grain flow of regular size. Thus, the self-organized critical grain flowing process is repressed by the formation of the wedge, which is only a function of the dilatation angle.

Grain flows are limited in width, and thus are three-dimensional. Allen (1970) and many others observed that grain flows in wide flumes and on subaerial dunes have a lobate form, often with coarse grains at the leading edge. Furthermore, Allen (1970, 1984) and others observed that grain flows do not cover the whole lee side in one sweep, but tend to deposit at some point on the slope, to be activated again when pushed by an adjacent grain flow. This probably has the effect that the vertical sorting in the cross-stratification is less well developed than predicted by the one-dimensional segregation models of Makse and Koepe and coworkers.

There are indications (Hunter & Kocurek 1986) that the frequency of grain flows is to some extent affected by the turbulent vortex shedding of flow at the brinkpoint of dunes, superimposed bedforms on the dune, and lee-eddy impingement on the lower slipface (from the counterflow). Although there is no data at all to assess the importance of these phenomena for grain flow frequency (and therefore grain flow thickness), it is assumed here that these effects are of secondary importance only.

Concluding, the size of the wedge of sediment that is deposited at the top of the lee slope determines the dynamics and size of the grain flows in sands and gravelly sands. Thus the cross-strata thickness is dependent on the volume of the wedge and therefore on the dilatation angle. As a secondary effect, the grain flows are limited in width and do not only push coarse sediment downslope but also to the sides. The sorting processes in a grain flow are discussed in the next section.

7.6.2 Sediment sorting within grain flows

Within the grain flow, the large grains are worked upwards to the surface of the flow. As a result, these large grains have more opportunity to reach the lower foreset slope to yield net vertical fining upward sorting in dunes. The first question is therefore how the sorting within a grain flow takes place. Two hypotheses of sorting mechanisms within grain flows on the lee slope will be discussed: 1. dispersive stress and 2. kinematic sorting or percolation (see Fig. 7.7c). Both mechanisms yield a reverse perpendicular sorting in the grain flow due to which the large grains occur mainly in the top of the flow, allowing the overpassing mechanism to act which results in a tangential inverse sorting. In this way the sorting in the grain flow promotes the sorting along the lee slope of the dune, and thus the vertical sorting in a dune (see Fig. 7.7d first panel).

1. Dispersive stress: Bagnold (1954) experimented with unimodal sediments to determine the dispersive stress in the sediment due to shearing. Viscous and inertial regimes were distinguished in parallel with laminar and turbulent flow. In the viscous regime, he found that the collision-related forces are independent of grain size, and therefore cannot cause any sediment sorting. However, the forces in the inertial regime are dependent on grain size. Bagnold argued that the larger grains of a mixture will migrate to the surface of the grain flow under influence of the dispersive pressure gradient. The result is a reverse perpendicular sorting in the cross-stratum. Furthermore, in a mixture of grains with equal size but different densities, the heaviest grains will migrate to the surface. So dispersive stress sorting is related to sediment size and density. However, Bagnold's analysis refers to well-sorted sediment, and it is not clear whether the size-dependence of forces would apply to individual grains in a poorly sorted sediment and to much thinner grain flows.
2. Kinematic sorting (Dyer 1929, in Sallenger 1979) and percolation are related to the relative size differences between grains. For kinematic sorting the sediment mixture must be in motion (moved, transported or shaken). As a consequence, the sediment is dilated (i.e. the pore space is increased because the colliding grains push neighbouring grains away) and the small grains tend to filter down between the large grains. The effect is that the small grains move downwards and the large grains upwards, irrespective of their weight, resulting in a reverse perpendicular sorting in the cross-stratum. This mechanism can easily be demonstrated by shaking any mixture of small grains and large grains. Percolation is defined here to refer to static sediment in which the small grains are small enough to fall through the interstices of the large grains without dilation, as opposed to kinematic sorting where the sediment is in motion and dilated.

For modelling purposes it would be necessary to determine whether kinematic sorting or dispersive stress or a combination of both is responsible for the sorting. The result of the two is the same for sediments with equal densities, which makes it difficult to distinguish between the two. The evidence concerning the dispersive stress and kinematic sorting hypotheses is conflicting. In experimental subaerial grain flows and in natural beach foreshore deposits, Sallenger (1979) found that the dispersive stress sorting was dominant, based on the behaviour of heavy minerals. Hunter (1985a) on the other hand found contrary evidence in favour of kinematic sorting, also based on heavy minerals in grain flow foresets.

Legros (2002) argued that the dispersive stress gradient necessary for reverse perpendicular sorting immediately causes expansion of the grain flow, until the dispersive stress has become equal to the hydrostatic pressure gradient. Then only lighter grains can be worked up, therefore the larger and heavier grains tend to migrate downwards while the smaller and lighter grains migrate upwards. This means that the dispersive stress cannot be responsible for reverse perpendicular sorting. Legros also provided arguments why the conclusions of Sallenger are not substantiated by his data.

As grain flows on foresets is of interest here, a reasonable working hypothesis is that sorting is dominated by kinematic sorting (not dispersive stress), following Hunter and Legros.

7.6.3 Sorting by grain flows rejuvenating underlying sediment

The overpassing mechanism allows the large grains to roll further downslope than the small grains in the process of individual grain rolling on the foreset slope. In the case of grain flows (with higher transport rates), an additional sorting mechanism may take place. In the experiments of Blom & Kleinhans (1999) an hitherto unrecognised sorting mechanism was visually identified by the author. It was observed that the grain flows were thinner than the largest grain diameter in the flow, which consequently protruded. This may have been amplified by kinematic sorting. The protruding grains were often dragged downslope by a next grain flow that overran the flow deposit of which the grain was a part (see Fig. 7.7d). This may have led to a more pronounced sorting than would have been the case for less protruding grains. Obviously it depends on the size of the largest grains relative to the thickness of the grain flow from which the large grains protrude.

The possibility of this drag mechanism is hinted at by Tischer et al. (2001), who measured velocities of individual grains in grain flows in uniform sand (0.3-0.5 mm grain sizes) at several locations in the flow. (They claimed that they were the first who did this, but apparently they were unaware of the work by Bagnold, Allen, Makse, Kakalios and others.) They found that the upper part of a grain flow consists mostly of sliding, rolling and saltating particles. Lower on the slope, in the more mature grain flow, the movement becomes a shock wave propagating through the deformable bed, which moves faster than the individual particles. In experiments without a deformable bed, the shock wave part of the grain flow did not develop at all. Tischer et al. conclude that a necessary condition for the occurrence of grain flows is the presence of a deformable bed below that grain flow.

If grain flows indeed need a deformable bed to develop, then this has consequences for the sorting. This hypothesis is developed as follows. The deformable-bed condition means that the grain flow exerts drag on the previously immobile bed, which leads to mobilisation of the underlying material. In non-uniform sediment, this underlying material is sorted coarsening upward in the perpendicular direction (within a grain flow) due to the kinematic sorting. Therefore it is preferentially the coarse sediment that is dragged down the slope. In addition, large grains on small grains are much affected by resistance than small grains on large grains (Makse 1997). Thus the large grains in the deformable bed, which are on top due to the kinematic sorting, are preferentially mobilised. The drag is not transferred into the underlying sediment in a gradual way, but in a non-linear decrease with depth, with a strong reduction or maybe even slip condition at the transition from coarse to fine sediment. This non-linearity is obviously stronger for bimodal sediment. The result obviously is that the downslope part of the foreset becomes enriched in coarse sediment, leading to the fining-upward sorting in the whole dune. Most importantly, the deformable-bed condition thus implies that the sorting in grain flows can be a two-stage process; some of the sorting takes place in the initial grain flow, and the sorting is continued in the rejuvenation induced by the next grain flow. It can be expected that the vertical sorting is thus much more effectively attained than without this drag effect.

7.7 Additional factors affecting sorting in dunes

7.7.1 The effect of sediment bimodality

Sediment bimodality may play an important role. With two strictly bimodal grain species, the opportunity for percolation (without dilatation) is large. Percolation occurs best in a very bimodal mixture, for in a unimodal mixture there are also many grains of intermediate size that block the interstices. Note that three measures are necessary to describe the sediment bimodality: the difference between the grain sizes of the two modes, and the sorting of each mode. For a large difference, the opportunity for percolation is large. However, with two poorly sorted, overlapping modes, the grain sizes in between the modes block the interstices and prohibit percolation. Finally, a relatively large fraction of sediment in the large mode causes the mixture to be open-work gravel with large opportunity for percolation, while a large fraction of sediment in the fine mode gives a matrix-supported gravel without percolation opportunity.

Strictly bimodal sediment may lead to a perfect segregation, as was shown by Makse and coworkers. They found a perfect segregation for grains of equal shape and with a size ratio of $D_{\text{large}}/D_{\text{small}} > 1.5$. Although this was in a controlled laboratory setting, it indicates that the bimodality of the sediment may lead to a more abrupt change of sediment size in the depth of the dune than with a more unimodal sediment.

Furthermore the different sizes may have different angularities, leading to different angles of repose and stratification tendencies. This is clearly indicated by experiments of Carling & Glaister (1987), who experimented with a very bimodal gravel and sand mixture deposited in a Gilbert type delta in a flume. They found a clear reverse tangential sorting but no cross-stratification, and the more irregular shaped grains at the top of the slip face. Furthermore the sand percolated into the gravel on the top of the delta, which means that the kinematic sorting already happens without movement of the gravel. Carling & Glaister (1987) argued that the percolation of sand would have been even stronger if the gravel species had been more rounded and uniform.

Shaw & Gorrell (1991) described the sediment sorting of extremely bimodal sediment in subaqueous bedforms formed below a glacier. The large grain size was 64mm while the small grain size was 0.125mm. They found a clear reverse perpendicular sorting in the cross-stratification, but no tangential sorting. The lower part of the cross-strata commonly had more small grains as matrix infilling, while the upper part of the strata had less matrix and sometimes were open worked gravels. Shaw & Gorrell attempted to explain the strong perpendicular sorting with variations in sediment supply due to the migration of bedload sheets, but did not offer any proof. It is likely that percolation alone can explain the perpendicular sorting in their case.

Concluding, both the reverse perpendicular and tangential sorting are more efficient in more bimodal sediment with more or less equal amounts of sediment in both modes. When one of the modes is very dominant, the sorting mechanism tends to the behaviour of unimodal sediment. The vertical change of grain size in the dune is more abrupt than for unimodal sediment.

7.7.2 Counterflow effects on the foreset and bottomset deposits

Termes (1986) suggested that the downward movement of grains is somewhat counteracted by the counterflow in the lee of the dune or delta. Also Carling & Glaister (1987) observed a decreased downslope dip of asymmetric grains on the lee slope, which they attributed to the counterflow. However, the counterflow acts on the grains as a function of their area, say, $\sim D^2$,

while gravity in the settling motion acts on the weight, say, $\sim D^3$. This suggests that the momentum gained by a large falling grain is relatively more important than the counterflow, and modification of the grain flow by the counterflow is at best a secondary effect. The dip angle of the settled grains on the lee slope might be changed but re-entrainment by the counterflow is highly unlikely due to the high slope angle and large weight. The effect of the counterflow on the vertical sorting of large grains is therefore considered to be of secondary importance.

Suspended sediment that is captured in the counterflow, either may be deposited upstream of the reattachment zone or on the toe of the lee slope. Many authors found an enrichment of the lower parts only of gravelly cross-strata by fine sediment, which suggests a counterflow origin, e.g. Termes (1986), Love et al. (1987), and Shaw & Gorrell (1991).

However, in the case of gravel dunes, the flow strength is relatively large, otherwise the gravel would not be transported in the dune phase. Since the gravel dunes are relatively lower than sand dunes due to their larger grain size, the lee zone is smaller and the turbulence in the gravel dune trough is much stronger than in sand dunes with the same height. Consequently, any fine sediment in the trough of a gravel dune is likely to be resuspended, unless it is trapped in the interstices of the gravel in the foreset. The latter probably happened in the cases described by Termes (1986), Love et al. (1987), and Shaw & Gorrell (1991). Nevertheless bottomsets have been found downstream of gravel bedforms, suggesting that it is not impossible. Carling & Glaister (1987) found counterflow ripples at the lee side of their laboratory gravel bar. The effect was matrix infilling by sand of the lower part of the gravel cross-strata.

Depending on the suspended sediment concentration in the counterflow and the strength of the counterflow, the effect of bottomsets on vertical sorting in the river bed is more important in sandier sediments. Hunter (1985a) found that the cross-strata in sandy dunes showed reverse perpendicular sorting halfway down the lee slope, but normal perpendicular sorting at the toe. This can probably be explained with continuous deposition of suspended sediment on the toe. Due to sorting in the grain flow, the largest grains end at the toe, but afterwards are buried below a relatively thick toeset from suspended sediment. The result is a normal perpendicular sorting.

Jopling (1965) and Allen (1963) studied the effect of suspended sediment deposition on the toe of the lee slope on the shape of the cross-strata. Both authors found that the contact between cross-strata and the lower bed is angular when little or no sediment is deposited from suspension, while the contact becomes increasingly tangential when more sediment is deposited from suspension.

Allen (1963, 1970) attributed the lack of sorting in his experiment with the highest flow velocity (see section on experimental data) to the continuous grain flowing. The frequency of grain flowing was so large that grain flows were overrunning each other which prevented effective sorting. It is important to note that some experiments of Hunter & Kocurek (1986) had the condition of continuous grain flowing as described by Allen. In this condition, the slope of the foreset was significantly lower than with a lower frequency of grain flows. This suggests an alternative to Allen's interpretation of overrunning grain flows. The grain fall deposition from suspension may have become so intense that the wedge was buried before it exceeded the critical slope for failure. Or maybe the wedge failed and created a grain flow, but this grain flow only overran but did not rework the thick grain fall deposit. The effect would be that the grain flow deposit is coarsening in the downslope direction, but the grain fall deposit (with the largest grains settling on the upper foreset) is fining in the downslope direction. Thus there is no net sorting within the dune or delta because the two sorting mechanisms oppose each other.

With his model, Hunter (1985b) was able to explain that the grain flows in water are much more frequent than in air, and therefore the ratio of grain flow deposits to grain fall deposits on foresets (see Fig. 7.4) is much larger in water than in air. So in subaqueous dunes, the cross-stratification generally consists of grain flow deposits only, while in air the cross-stratification may consist of

couplets of grain fall and grain flow deposits (Hunter 1985b). Allen (1963) forced a certain combination of dune height and flow velocity in his experiments, and it could be that his conditions were such that both grain fall and flow deposits were preserved in his deposit, leading to the disappearance of the net fining upward sorting. Regardless the truth in that case, it seems to be important to have combinations of flow velocities, sediment transport and dune heights that occur in natural conditions as well.

With very large suspended sediment concentrations in the counterflow, enough sediment may accumulate in the lee zone for the formation of counterflow ripples. Of course the counterflow must be strong enough to form the ripples, although not so strong as to induce much resuspension. Boersma et al. (1967, 1968) found thick sandy bottomsets below cross-stratified deposits of straight crested dunes in gravelly sand. Boersma et al. were able to identify climbing counterflow ripples and wavy lamination from the counterflow, irregular foresets from the reattachment zone, and coflow ripples from downstream of the reattachment zone. A reconstruction of the setting revealed that the sediment was probably deposited on a high part of the point bar, at which the flow velocity rapidly decreased and large concentrations of sediment were deposited. This explains why the coflow ripples and irregular reattachment ripples were also preserved. Lower in the deposits, no sandy bottomsets were found. These findings probably represent a special case which is not very important for foreset deposits in channel beds from dunes.

Concluding, depending on the suspended sediment concentration, the lower part of cross-strata are enriched with fine sediment. Furthermore a bottomset of fine sediment may be preserved, if the turbulence in the dune trough is not so strong that it is immediately resuspended (which is more likely in gravel dunes). The effect on the vertical sorting in dunes is a zone of decreased upward fining or even upward coarsening in the lowest part of the dune. It can be expected that in very wide mixtures, these effects are significant, because when these sediments are in the dune phase, the finer fractions will be in suspension. In addition, in wind-blown deposits and special cases of alluvial deposits, grain fall deposits may be preserved in the foresets and form couplets with the grain flow deposits.

7.7.3 The effect of sediment transport magnitude at the brinkpoint

According to Allen (1963, 1970), the size of the wedge of sediment that is deposited at the top of the lee slope mainly determines the size of the grain flows. Thus the cross-strata thickness is dependent on the volume of the wedge and therefore the dilatation angle. The dilatation angle is more or less constant for a certain sediment mixture in water, and is in the order of 10 degrees. However, the mass of sediment in the wedge depends on the flow at the brinkpoint. The horizontal path length sediment that starts to fall out of the flow at the brinkpoint, depends on the flow velocity as well as the settling velocity of the grains. Thus large grains (which have a large settling velocity) are dropped at the top of the lee slope while smaller grains deposit further downstream. In a larger flow velocity, the sediment is smeared out over a larger distance. The effect is that the wedge of sediment also becomes longer, and contains more sediment and therefore the grain flow will be larger. The larger flow velocity also causes the sediment transport to be larger, which counteracts the smearing out of the sediment over a longer wedge. Consequently, the frequency of grain flowing need not become smaller when the flow velocity is increased. Thus the grain flow thickness and the cross-strata thickness depends on the flow velocity, on which the sediment transport also depends.

The effect of very high sediment transport was studied by Allen (1963, 1970), who distinguished

between discontinuous grain flowing, that occurs at low sediment transport, and continuous grain flowing, that occurs at high sediment transport. The cross-stratification disappeared with increasing (continuous) grain flow frequency.

Also Makse and coworkers found that above a certain limit of input sediment transport, the grain flows are too fast and the kink is not able to develop and there no longer is a competition from shape segregation. The size segregation mechanism on the other hand is still effective, leading to reverse tangential sorting. In intermediate sediment transports the kink and the stratification are only weakly developed, which allows a size segregation in combination with weak stratification.

An unanswered question is how the condition of continuous grain flowing (leading to poorly developed cross-stratification) in high sediment transport is related to dune height. In the experiments for which the fading of cross-stratification was reported (Allen 1970, Makse and coworkers, Koeppel et al. 1998), the dune or delta height was artificially kept constant while the sediment input was increased. In nature, an increase in sediment transport probably is the result of an increase of flow velocity. This increased flow velocity may at the same time lead to higher dunes. The larger sediment transport is then distributed over a longer slip face, and thus the grain flowing need not become continuous if the adaptation of dune height is not very slow. The thickness and frequency of the grain flow thus depends on the flow velocity near the dune top, the sediment transport and the dilatation angle of the mixture. Alternatively, in the very extreme flows and sediment input at which the stratification would disappear according to Allen and Makse, the dunes may have been washed out already.

Hunter & Kocurek (1986) collected data on grain flow dynamics in uniform sand which may provide preliminary answers. They found that the grain flow thickness (or laminae thickness) were independent of the grain flow frequency (see Fig. 7.9a), which can be interpreted as independence from the migration celerity of the slipface, and indirectly of the sediment transport rate. This agrees with the idea that the foreset process is largely independent on the flow and sediment transport condition upstream of the brinkpoint, but depends on the behaviour of the wedge on the upper foreset slope. Interestingly, Hunter & Kocurek found that the thickness of the grain flows is dependent on the height of the bedform (see Fig. 7.9b). In Figure 7.9, symbols denote the bedform type on top of the delta in the flume experiments. It can be seen that there is no obvious trend of bedform type with increasing delta height or laminae thickness, which again suggests that the grain flow magnitude is independent on conditions upstream of the brinkpoint. The conclusion from this set of experiments must be that the sediment volume in the wedge somehow depends on the height of the delta. The larger the delta height, the larger the sediment wedge and therefore the thicker the laminae. A hypothetical explanation is that the flow velocity over higher dunes is larger, leading to higher velocities of the grains downstream of the brinkpoint and therefore a longer and larger sediment wedge on the upper foreset slope, leading to larger grain flows. For the experiments, however, the dune height is not dependent on the flow but is a priori determined by the experimenter. The water depth above the delta is far too small for dunes of that height. Therefore these experiments cannot be used to determine the relation between flow velocity above the delta and wedge size (or laminae thickness).

Concluding, there is a rough relation between dune height, sediment transport and the frequency of grain flows, but there is no suitable data to determine the relations. Since both dune height and sediment transport are related to the (water) flow conditions, it is hypothesized that the effectivity of sorting mechanisms decreases with increasing flow strength.

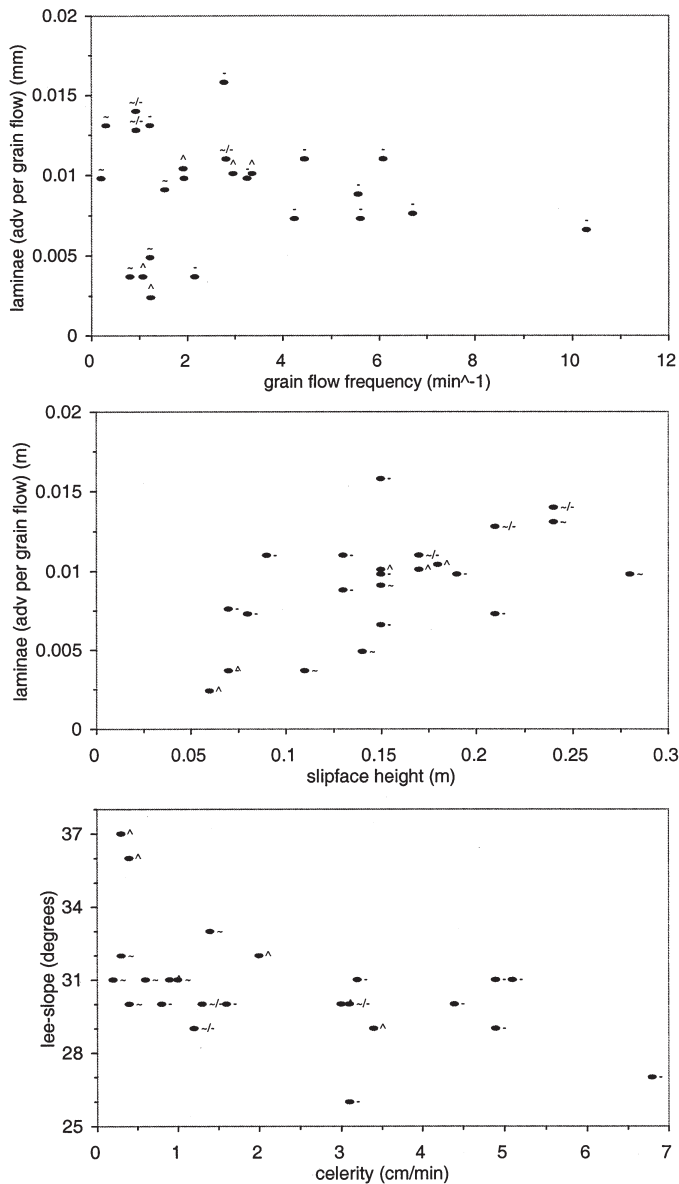


Figure 7.9. Data of Hunter & Kocurek (1986).

- Relation between the thickness of laminae (advance of slip face per grain flow) in cross-bedding and the grain flow. No obvious trend can be found, except that the most frequent avalanching occurs in upper plane bed conditions on the delta. Symbols denote bed condition on the delta: -: upper plane bed, ~: ripples and ^: dunes (classification not defined by Hunter, but Hunter suggests to be following Simons & Richardson 1965).
- Relation between laminae thickness (and related grain flow thickness and wedge volume) and delta height. Hunter & Kocurek (1986) give a rough relation as thickness = 0.060 times the delta height.
- Relation between the slope of the foreset with the celerity of the dune (migration velocity).

7.7.4 Armouring and bottomsets

Sorting of sediment that is in transport in the bedload phase depends on the relative mobility of the different grain sizes. Small grains may already be in transport, while the larger are immobile or less mobile. This may lead to an enrichment of the bed surface of large grains, which is called armouring. An armour layer is essentially an erosional feature, and it is assumed that an armour layer is not formed simultaneously with a bottomset consisting of fine sediment deposited from suspension. An armour layer on dunes was found by Love et al. (1987) and in Blom & Kleinhans (1999) (see figs 5 and 6).

The prediction of incipient motion of sediment has been the topic of extensive research. Obviously, the critical shear stress is larger for larger grains. However, grains in a bed of mixed grain sizes experience a shear stress that is related to their position relative to the other grains. Large grains may protrude above the bed and thus be more exposed to the flow. As a consequence, they become entrained at a lower shear stress than it would have on a bed of uniform grain size. Small grains may hide in the wake of large grains and become entrained at a higher shear stress than in the uniform sediment case. Wilcock (1993) and Kleinhans & Van Rijn (2001, see chapter 5) show that unimodal sediment mixtures tend to show near equal mobility of large and small grains, while in bimodal sediment mixtures, the two modes are increasingly independent, tending to the mobility related to uniform sediment of each mode separately.

Concluding, for unimodal but non-uniform sediments, the size selection is small as well as the range of bed shear stresses in which the larger grains are immobile or partially mobile while the smaller grains are already in transport. For bimodal sediment, the size selection becomes increasingly important for increasing difference in grain size of the two modes in the grain size distribution. Consequently, armouring becomes more likely with increasing differences in grain size, that is, stronger bimodality.

Furthermore, deposition of a bottomset is unlikely when the bed is armouring at the same time. When the armour layer in the dune troughs is being depleted of transportable grains, especially those grain sizes above the threshold for suspension will be entrained and not deposited.

7.8 Synthesis: processes and variables

7.8.1 Primary controls on grain fall, individual grains rolling and grain flows

The characteristics of the sediment mixture (grain size, standard deviation of the mixture, and angularity of the different grain size fractions) are the primary controls on the processes. For almost uniform sediment, there is not much to be sorted, while widely non-uniform mixtures may show strong sorting. The bimodality of the sediment determines the kinematic sorting and percolation effectivity.

The flow and therefore the mobility of the sediment is important in only three aspects:

1. suspension and therefore the grain fall process from the sediment-laden flow downstream of the brinkpoint depends on the ratio of (shear) velocity and settling velocity of each size fraction. Especially in the case of bimodal sediment, this ratio also determines which size fractions may settle at all on the foreset or in the trough, and which remain in full suspension,
2. the flow and sediment mobility determine the height of dunes and thus the length of the foresets along which the sediment is sorted, and

3. the volume of the wedge of sediment forming at the upper foreset slope may depend on the flow velocity above the dune top, roughly leading to larger wedges for higher dunes.

The resulting deposit is a sediment wedge with a downslope decrease in thickness following the exponential or power function of deposition from suspension with distance from the brinkpoint. The counterflow at the lee-side of the foreset slope may induce secondary effects like suspended sediment deposition on the lower foreset slope and skewing the dipping angles of larger grains on the foreset.

The sediment wedge fails when its angle (at some point, usually the upper) becomes larger than the static angle of repose. Both individual grain movement and grain flows on the foreset slope are initiated by this failure. The sediment wedge volume, grain flow thickness, and laminae thickness seem to be dependent on the dune height.

The individual grain movement is governed by the static angles of repose of the individual grain size fractions, and by the static angles of repose of the grain size fractions on fractions of other grain sizes. The individual grain movement may lead to stratification and to segregation of the grain size fractions. The mechanism of kinematic sorting or percolation plays a limited role in bringing the large grains to the top of the moving sediment, leading to stratification or segregation depending on the mutual angles of repose of fine and coarse sediment. Individual grain movement on foreset slopes is relevant for dunes or bars in very coarse sediment, where the ratio of grain flow thickness to grain diameter is small.

In grain flows the condition of a mobile underlying bed is important. A two-stage process leads to net vertical sorting in a dune:

1. in an individual grain flow, kinematic sorting or percolation leads to coarsening upward in the reverse perpendicular direction. The angle of repose of large grains on small grains is relatively small, therefore the large grains are much more unstable than the small underlying grains.
2. the next grain flow drags the underlying sediment of the previous grain flow. The drag is not transferred into the underlying sediment in a gradual way, but mainly applied to the protruding large grains of the previous grain flow. The result obviously is that the downslope part of the foreset becomes enriched in coarse sediment, leading to the fining-upward sorting in the whole dune.

Summarizing, the following variables seem to be the most important for the vertical sorting in dunes:

- sorting (standard deviation) of the sediment mixture delivered to the brinkpoint,
- height of the dune or bar relative to the average grain size of the mixture,
- velocity of the flow above the brinkpoint relative to the settling velocity for all grain size fractions (determining the size of the wedge and therefore the thickness of the grain flow),
- frequency of the grain flows, determined by celerity of the dune (in turn determined by sediment transport divided by dune height) and celerity of the grain flows on the foreset slope.

The frequency of grain flows can either directly be measured, or derived from the celerity of the dunes (m/s) divided by the thickness of the grain flows (m), yielding the frequency (s^{-1} = Hz).

7.8.2 Hypothetical explanation for difference between segregation and stratification

In the experiments of Koepe et al. (1998) it was found that the phenomena stratification and segregation cannot occur simultaneously. Koepe et al. seem to explain the disappearance of the stratification with increasing transport rate like Allen does with the continuous grain flowing. Makse and coworkers explain the transition from stratification to segregation with angles of repose for the two grain species (and did not investigate the effect of transport rate). All these experiments and models refer to small differences in grain sizes of strictly bimodal sediments. In nature, the sediment usually is not strictly bimodal, and continuous grain flowing is not the condition at which segregation (fining upward in the whole dune) occurs. On the contrary, in continuous grain flowing the segregation disappears. It is therefore the question whether the explanations provided by the physicists can be extended to natural conditions.

Clues as to what governs stratification or segregation in nature, can be derived from the literature. There seem to be several types of cross-stratification, distinguishable with diagnostic characteristics, some of which are:

- in ripples and dunes of fine sediment, visible due to the drape of very fine sediment from suspension on the whole foreset,
- in dunes of fine sediment, visible due to the couplets of grain flow and grain fall deposits,
- in ripples and dunes, visible due to the reverse perpendicular sorting caused by kinematic sorting,
- in dunes and bars of mixed coarse sediment, visible due to relicts of kinematic sorting,
- in dunes and bars of mixed coarse sediment, visible due to the direction of dipping (asymmetric) grains, and
- in dunes and bars of mixed coarse sediment, visible due to variations of mixture composition between the different laminae.

The point is that a certain deposit may be recognised as a cross-stratified unit but does not necessarily have the same origin as the stratification *sensu* Makse and Koepe and coworkers, who call the latter three types of 'cross-stratification' segregation.

A hypothesis is forwarded here of the natural conditions in which pure stratification (cross-stratification) without any segregation (fining upward trend in whole dune) *sensu* Makse and Koepe and coworkers occurs. Hypothesised conditions for pure stratification could be:

1. dunes in equilibrium with the flow, combined with much suspension of sediment in a sand bed river, in which grain fall and grain flow deposits are preserved. For such a case to happen in alluvial conditions, the settling from suspension must be extremely high, while the flow strength must not be too high to erode the dunes into upper plane bed. It is the question whether this happens in nature at all.
2. this condition is based on the hypothesis forwarded earlier in this paper: the sorting on foresets is a two-stage process, first with kinematic sorting in a grain flow, and then drag by the second grain flow by which the coarse sediment is preferentially dragged downslope. To create true stratification, the second stage of this process should not take place. This stage would not take place if the grain flow thickness were much larger than the size of the protruding large grains below the grain flow, and if the grain size differences in the sediment is small. It is hypothesised here that these conditions are fulfilled when the sediment volume in the wedge is large (therefore in high dunes), while the sediment is relatively fine (sand) and not too poorly sorted (ratio of dune height over

average grain size). Stratification without any segregation would thus occur in moderately sorted sandy sediment with high dunes. This hypothesis can easily be tested in a flume experiment, and it is important to do so as the occurrence of pure stratification does not lead to fining upward sorting in dunes at all, and therefore has no history effect on sediment transport at all.

7.8.3 Conceptual model

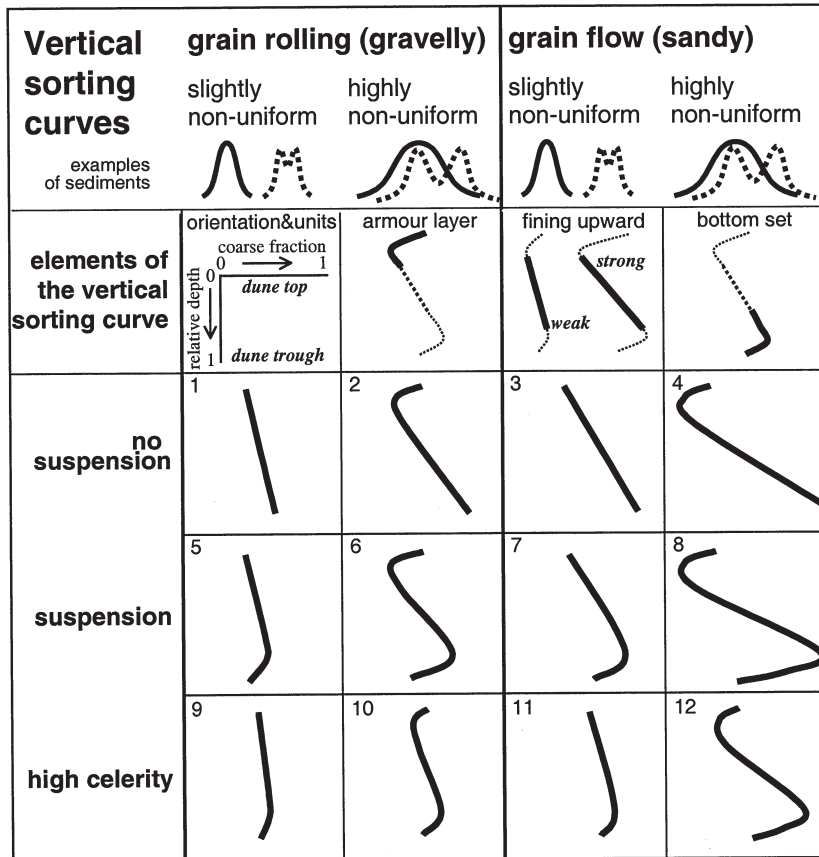


Figure 7.10. Conceptual model of sorting as a function of the most important variables. The curves denote the abundance of the coarse sediment at different heights in the bedforms. A vertical line means no significant upward fining, while a low-sloping line means a strong fining upward trend. See text for explanation.

Based on this review and the sparse sorting data, a conjecture of vertical sorting is given in Figure 7.10. For simplification, each sediment mixture is simply divided into two grain size fractions with about an equal percentage of sediment in each class. The vertical distribution of the larger grain size fraction in the dune is given qualitatively in Figure 7.10, to indicate the form of the vertical sorting curve. On the vertical axis the height above the base of the dune is given, and on the horizontal axis the fraction in the larger grain size fraction is given. For example, the sorting in

a dune consisting of sand and gravel is given as a gravel fraction or percentage as a function of depth below the dune top. The slope of the lines indicates the strength of the upward fining trend. The essential elements of the vertical sorting curves are related to the different types of deposits: foreset and bottomset deposits, as well as armouring in a topset (see Fig. 7.10).

The ideas behind the columns in the conceptual model are primary factors determining the sorting efficiency. These are: for highly non-uniform sediment the sorting is better developed than near-uniform sediment, for grain flows the sorting is better developed than for individual grain rolling due to the drag effect, and grain flows are more often expected in sandier sediment than in coarse gravel. Gravelly armour layers may be expected on dunes in highly non-uniform sediment. The ideas behind the rows in the model are that suspension of finer fractions enriches the lower foreset, and with higher dune celerity the sorting efficiency becomes less large, while the effects of suspension obviously remain important. A number of secondary effects and bimodality of the sediment have not been included. The model does not include the (maybe rare) case of high dune celerity without significant suspension of sediment.

The cells of Figure 7.10 have been numbered for quick reference. The datasets can be compared to this conjectured curves as follows. The Rio Grande channel data (Love et al. 1987) fits in cells 2 or 4, or 6 or 8 if the bottomset deposition is taken into account. The IJssel data (Dillingh 1990) fits in cell 3 or 7, depending on the interpretation of the flow conditions. The laboratory conditions of Ribberink (1987), Kleinhans (2000) and Blom et al. (2000) probably fit in cell 4, while the Termes (1986) data fits in either cells 4 and 8. The case described by Boersma et al. (1968) is an extreme case of cell 8. The relict gravel dunes described by Carling (1996) and by Shaw & Gorrell (1991) should probably be classified in cell 6. All the Makse and Koeppel experiments belong in cell 1. The Allen experiments finally belong in cells 7 and 11.

7.9 Concluding remarks

This review was limited to a qualitative analysis of the sparse available data of vertical sorting in dunes, and a discussion of the possible sorting mechanisms in a large number of settings from models of grain behaviour in air to sand and gravel dunes in laboratory flumes and rivers to relict dunes of extreme floods. The following factors seem to be the most important for the vertical sorting in dunes:

- sorting (standard deviation) of the sediment mixture delivered to the brinkpoint,
- height of the dune or bar relative to the average grain size of the mixture,
- velocity of the flow above the brinkpoint relative to the settling velocity for all grain size fractions,
- frequency of the grain flows, determined by celerity of the dune (in turn determined by sediment transport divided by dune height) and celerity of the grain flows on the foreset slope.

Although the vertical sorting is relevant for sediment transport models, no quantitative model has been developed that is generally applicable to the alluvial setting. Neither are experimental data available with systematic variation in a range of relevant factors and conditions. The obvious next step is to do those experiments and to develop a physical model for the vertical sorting in natural conditions. A logical set-up for such a set of experiments would be to build laboratory Gilbert-type deltas in a narrow flume with different sediments, heights and celerities (determined with input sediment transport), whereby the flow is adapted such that the sediment feed can be

transported at the same energy slope for all experiments. The deltas can be recorded on film for grain flow dynamics analysis and can be sampled in layers to quantify the upward fining trend. Finally, the transition from stratification to segregation, and the different types of stratification, should be studied further in natural deposits and flume experiments.

Acknowledgments

D. Dillingh and D. Beukers of the laboratory of Soil Mechanics, Delft, are thanked for providing the sorting data of the river IJssel dunes. T. Buijse is kindly thanked for providing a highly interesting overview of the gravel dunes and other flood relicts in the Altai Mountains, Siberia, which pointed the way to the identification of different genetic types of cross-bedding. The many stimulating discussions with my advisor Janrik van den Berg are much appreciated. This paper benefitted from comments by Janrik van den Berg, Chris Paola, Gary Parker and Ward Koster.

References

- ALLEN, J. R. L. (1963), Sedimentation to the lee of small underwater sand waves: and experimental study. *Journal of Geology* 73 pp. 95-116.
- ALLEN, J. R. L. (1970), The avalanching of granular solids on dune and similar slopes. *Journal of Geology* 78 pp. 326-351.
- ALLEN, J. R. L. (1984), Sedimentary structures, their character and physical basis. *Developments in Sedimentology* 30, Elsevier, Amsterdam, The Netherlands.
- BAGNOLD, R. A. (1954), Experiments on a gravity-free dispersion of large solid spheres in a Newtonian fluid under shear. *Roy. Soc. London, Proc. Ser. A*(225) pp. 49-63.
- BAK, P., TANG, C. & WIESENFELD, K. (1988), Self-organized criticality. *Physical Review A*, July 1, The American Physical Society, p. 364-374.
- BENNETT, S. J. & BEST, J. L. (1995), Mean flow and turbulence structure over fixed, two-dimensional dunes: implications for sediment transport and bedform stability. *Sedimentology* 42, p. 491-513.
- BENNETT, S. J. & BRIDGE, J. S. (1995), An experimental study of flow, bedload transport and bed topography under conditions of erosion and deposition and comparison with theoretical models. *Sedimentology* 42 pp. 117-146.
- BLOM, A. & KLEINHANS, M. G. (1999), Non-uniform sediment in morphological equilibrium situations. Data Report Sand Flume Experiments 97/98. University of Twente, Rijkswaterstaat RIZA, WL|Delft Hydraulics. University of Twente, Civil Engineering and Management, The Netherlands..
- BLOM, A., RIBBERINK, J. S., & VAN DER SCHEER, P. (2000), Sediment transport in flume experiments with a trimodal sediment mixture. *Proc. Gravel Bed Rivers Conference 2000*, 28 August - 3 September, New Zealand, in NOLAN, T., & THORNE, C. (eds), Special public. CD-rom of the New Zealand Hydrological Society.
- BOERSMA, J. R., VAN DE MEENE, E. A. & TJALSMA, R. C. (1968), Intricated cross-stratification due to interaction of a mega ripple with its lee-side system of backflow ripples (upper-pointbar deposits, Lower Rhine), *Sedimentology* 11 pp. 147-162.
- BOUTREUX, T. (1998), Surface flows of granular mixtures: II. Segregation with grains of different size. *Eur. Phys. J. B* 6, p. 419-424.
- BOUTREUX, T., MAKSE H.A., & DE GENNES, P.G. (1998), Surface flows of granular mixtures: III. Canonical model. *Eur. Phys. J. B* 9, p. 105-115.
- CARLING, P.A. (1996), Morphology, sedimentology and palaeohydraulic significance of large gravel dunes, Altai Mountains, Siberia. *Sedimentology* 43, p. 647-664.
- CARLING, P.A. & GLAISTER, M.S. (1987), Rapid deposition of sand and gravel mixtures downstream of a negative step: the role of matrix-infilling and particle-overpassing in the process of bar-front accretion.

- Journal of the Geol. Soc., London, 144, p. 543-551.
- CIZEAU, P., MAKSE, H.A., & STANLEY, H.E. (1999), Mechanisms of granular spontaneous stratification and segregation in two-dimensional silos. *Physical Review E*, 59 4.
- DILLINGH, D.A. (1990), Transport layer sampling in the river IJssel near Deventer, The Netherlands (in Dutch), Soil Mechanics Laboratory Delft, Delft, report nr. CO318420, The Netherlands.
- EGIAZAROFF, I. V. (1965), Calculation of nonuniform sediment concentrations. *Journal of the Hydraulics Division, ASCE* 91 (HY4) pp. 225-248.
- HUNTER, R.E. (1985a), Subaqueous sand-flow cross-strata. *Journal of Sed. Petrology* 55(6), p. 886-894.
- HUNTER, R.E. (1985b), A kinematic model for the structure of lee-side deposits. *Sedimentology* 32, p. 409-422.
- HUNTER, R.E. & KOCUREK, G. (1986), An experimental study of subaqueous slipface deposition. *Journal of Sed. Petrology* 56 (3) p. 387-394.
- JOPLING, A. V. (1965), Laboratory study of the distribution of grain sizes in cross-bedded deposits, in: Middleton, G. V. (ed.) *Primary sedimentary structures and their hydrodynamic interpretation*, spec. publ. 12, Soc. of Econ. Paleontologists and Mineralogists, Oklahoma, U.S.A.
- JULIEN, P. Y. & KLAASSEN, G. J. (1995), Sand-dune geometry of large rivers during floods, *Journal of Hydraulic Engineering* 121 (9) pp. 657-663.
- KLAASSEN, G. J. (1987), Experiments on the effect of gradation on sediment transport. *Euromech 215 Colloquium, Genova, Italy, September 15-19*, also Delft Hydraulics publication 394, Delft, The Netherlands.
- KLAASSEN, G. J., RIBBERINK, J. S. & DE RUITER, J. C. C. (1987), On the transport of mixtures in the dune phase. *Euromech 215 Colloquium, Genova, Italy, September 15-19*, also Delft Hydraulics publication 394, Delft, The Netherlands.
- KLAASSEN, G. J. (1991), Experiments on the effect of gradation and vertical sorting on sediment transport phenomena in the dune phase. *Grain Sorting Seminar, 21-25 October, 1991, Ascona (Switzerland)*.
- KLEINHANS, M. G. (1999), Sediment transport in the River Waal: high discharge wave, November, 1998. (in Dutch) *Netherlands Centre for Geo-ecological Research / Utrecht University Physical Geography. ICG 99/6*.
- KLEINHANS, M. G. (2000), The relation between bedform type, vertical sorting in bedforms and bedload transport during subsequent discharge waves in large sand-gravel bed rivers with fixed banks. *Proc. Gravel Bed Rivers Conference 2000, 28 August - 3 September, New Zealand*, in NOLAN, T. & THORNE, C. (eds), Special public. CD-rom of the New Zealand Hydrological Society.
- KLEINHANS, M. G. (2001), The Key Role of Fluvial Dunes in Transport and Deposition of Sand-Gravel Mixtures, a preliminary note, *Sedimentary Geology* 143 pp. 7-13.
- KLEINHANS, M. G. & VAN RIJN, L. C. (2002), Stochastic Prediction of Sediment Transport in Sand-gravel Bed Rivers. *Journal of Hydraulic Engineering* 128(4), ASCE, pp. 412-425, special issue: Stochastic hydraulics and sediment transport, see chapter 5.
- KOEPPE, J.P., ENZ, M. & KAKALIOS, J. (1998), Phase diagram for avalanche stratification of granular media. *Physical Review E*. 58 4.
- LEGROS, F. (2002), Can dispersive pressure cause inverse grading in grain flows? *Journal of Sedimentary Research* 72(1), pp. 166-170.
- LOVE, D.W., GUTJAHN, A. & ROBINSON-COOK, S. (1987), Location-dependent sediment sorting in bedforms under waning flow in the Rio Grande, Central New Mexico. *The Society of Economic Paleontologists and Mineralogists, spec. publ. 39*, ETHRIDGE, F.G., FLORES, R.M. & HARVEY, M.D. (eds), *Recent developments in fluvial sedimentology*, p. 37-47.
- LOWE, D.R. (1976), Grain flow and grain flow deposits. *The Society of Economic Paleontologists and Mineralogists*.
- MAKSE, H.A. (1997), Stratification instability in granular flows. *Phys. Rev. E* 56, p. 7008-7016.
- MAKSE, H.A., HAVLIN, S., KING, P.R. & STANLEY, H.E. (1997a), Spontaneous stratification in granular mixtures. *Nature* 386, p. 379-381.
- MAKSE, H.A., CIZEAU, P. & STANLEY, H.E. (1997b), Possible stratification mechanism in granular mixtures. *Physical Review Letters* 78, p. 3298-3301.
- MAKSE, H.A. & HERRMANN, H.J. (1998), Microscopic model for granular stratification and segregation.

- Europhys. Lett. 43, p. 1-6.
- MAKER, H.A., BALL, R.C., STANLEY, H.E. & WARR, S. (1998), Dynamics of granular stratification. *Physical Review E* 58, p. 3357-3368.
- MCLEAN, S. R., WOLFE, S. R. & NELSON, J. M. (1999), Predicting boundary shear stress and sediment transport over bedforms. *Journal of Hydraulic Engineering* 125 7 pp. 725-736.
- MEYER-PETER, E. & MUELLER, R. (1984), Formulas for bed-load transport. 3rd Conf. Int. Assoc. of Hydraul. Res. Stockholm, Sweden. 39-64, 1948.
- MOLINAS, A. & BOASHENG WU (2000), Comparison of fractional bed-material load computation methods in sand-bed channels. *Earth Surf. Proc. Land.* 25 pp. 1045-1068.
- NEMEC, W. (1990), Aspects of sediment movement on steep delta slopes. *Spec. Publ. int. Ass. Sediment.* 10, p. 29-73.
- NEMEC, W. & POSTMA, G. (1993), Quaternary alluvial fans in southwestern Crete: sedimentation processes and geomorphic evolution. *Spec. Publ. Int. Ass. Sediment.* 17, p. 235-276.
- PARKER, G., PAOLA, C. & LECLAIR, S. (2000), Probabilistic Exner sediment continuity equation for mixtures with no active layer, *Journal of Hydraulic Engineering* 126 (11) pp. 818-826.
- RIBBERINK, J. (1987), Mathematical modelling of one-dimensional morphological changes in rivers with non-uniform sediment, PhD thesis, Delft University, 1987.
- SALLENGER, A.H. (1979), Inverse grading and hydraulic equivalence in grain-flow deposits. *Journal of Sed. Petrology* 49 (2) p. 553-562.
- SHAW, J. & GORRELL, G. (1991), Subglacially formed dunes with bimodal and graded gravel in the Trenton drumlin field, Ontario. *Geographie Physique et Quaternaire*, 45(1), p. 21-34.
- SIMONS, D. B., & RICHARDSON, E. V. (1965), A study of variables affecting flow characteristics and sediment transport in alluvial channels; In: *Federal Inter-agency Sediment Conf. 1963 Proc.*, Misc. Pub. US Agric. 970, Washington, USA, pp. 193-207.
- SOHN, Y.K., KIM, S.B., HWANG, I.G., BAHK, J.J., CHOE, M.Y. & CHOUGH, S.K. (1997), Characteristics and depositional processes of large-scale gravelly Gilbert-type foresets in the miocene Domsan fan delta, Pohang basin, Se Korea. *Journal of Sedimentary Research* 67 (1) p. 130-141.
- SOUTHARD, J. B. & BOGUCHWAL, A. (1990), Bed configurations in steady unidirectional water flows. Part 2. Synthesis of flume data; *Journal of Sedimentary Petrology*, 60 5, pp. 658-679..
- TERMES, A.P.P. (1986), Vertical composition of sediment in a dune. Report R657-XXX, WL|Delft Hydraulics, Delft, The Netherlands.
- TISCHER, M., BURSIK, M. I. & PITMAN, E. B. (2001), Kinematics of sand avalanches using particle-image velocimetry. *Journal of Sedimentary Research*, 71 3 p. 355-364.
- TNO-NITG (2000), Descriptions and photographs of the vibrocores in the Niederrhein, Bovenrijn, Waal and Pannerdensch Kanaal. Dutch Institute for Applied Geology (NITG-TNO), The Netherlands. Core numbers 40D0155 - 40D0214 and 40G0110 - 40G0150.
- VAN RIJN, L. C. (1984), Sediment transport, part I: bed load transport. *Journal of Hydraulic Engineering* 110 (10) pp. 1431-1456.
- WATHEN, S. J., FERGUSON, R. I., HOEY, T. B., & WERRITTY, A. (1995), Unequal mobility of gravel and sand in weakly bimodal river sediments. *Water Resources Research* 31 (8) pp. 2087-2096.
- WILBERS, A. W. E. (1998), Bedload transport and dune development during discharge waves in the Bovenrijn and the Waal, (in Dutch) Netherlands Centre for Geo-ecological Research / Utrecht University Physical Geography. ICG 98/12.
- WILBERS, A. W. E. (1999), Bedload transport and dune development during discharge waves in the Rhine branches, echo soundings of the flood in November 1998, (in Dutch) Netherlands Centre for Geo-ecological Research / Utrecht University Physical Geography. ICG 99/10.
- WILCOCK, P. R. (1993), Critical shear stress of natural sediments. *Journal of Hydraulic Engineering* 119 (4) pp. 491-505.
- WILCOCK, P. R. (1998), Two-fraction model of initial sediment motion in gravel-bed rivers. *Science* 17 April 1998, 280 pp. 410-412.

8

Sorting in grain flows at the lee-side of dunes: experiments

"Scientists frequently judge theories for the simplicity properties that they exhibit ... No agreement has so far been reached about the extent to which scientists' simplicity considerations are empirical or aesthetic. ... We have no guarantee that there is a correlation between particular aesthetic properties and high degrees of empirical adequacy in theories. Like all policies of inductive projection, however, the aesthetic induction can be expected - provided that it is pursued for long enough - to discern any such correlation that may exist." James McAllister (1996: p. 4, *Beauty and revolution in science*, Cornell University Press, Ithaca)

Abstract

The sorting of sediment mixtures at the lee slope (at the angle of repose) of dunes, bars and deltas is studied with experiments in a narrow, deep flume with Gilbert-type deltas using various conditions and different sediment mixtures. Sediment deposition and sorting on the lee slope of the delta is the result of three processes. First, the grains fall from suspension that is initiated at the top of the delta. Second, by kinematic sieving the small grains on the lee slope are worked down into the sediment, meanwhile working up the large grains to the surface. Third, the sediment on the lee slope flows downslope as a grain flow, in which preferentially large grains are dragged downslope. The result is a fining upward vertical sorting in the delta. Variations in this trend are dependent on the angularity and grain size distribution of the sediment, the delta height, the migration celerity of the delta front and the flow conditions above the delta top. However, the variations in sorting cannot adequately be described with a set of meaningful dimensionless parameters based on these variables. This suggests that the grain fall and grain flow process are indistinguishably intertwined. The relevance of these results with respect to dunes and bars in rivers and laboratory flumes is discussed.

8.1 Introduction

8.1.1 Scope and objective

The downstream propagation of dunes, bars and (small) Gilbert-type deltas proceeds by deposition of sediment on the lee slope, often at the angle of repose. In the wake of the dune, bar or delta, the transported sediment is deposited on the top of the lee slope (grain fall), until a threshold is exceeded and the sediment mass flows downslope. The repeated grain flows (Allen 1963) as well as the preserved part of the grain fall (Jopling 1965, Hunter 1985) make the dune, bar or delta migrate downstream. When the sediment is a mixture of sand and gravel, sorting takes place both by grain fall and grain flow, usually yielding a fining upward trend within the dune, bar or delta deposit. This process is well-known and has often been observed in experiments and in the field (e.g. Allen 1963, 1984, Brush 1965, Love et al. 1987, Makse 1997, Pye & Tsoar 1990, and Ribberink 1987).

However, no quantitative model has been developed that successfully predicts the vertical sorting in various conditions and for different sediment mixtures. Since the advent of morphodynamic models for rivers with sediment mixtures (e.g. Ribberink 1987, Parker et al. 2000), quantification of vertical sorting is a prerequisite. Although the process of vertical sorting during lee slope deposition is well known, experiments in which this has been measured, are scarce. Hence, the principal variables which govern the sorting have never unequivocally been determined from systematic measurements in nature or in the laboratory to the knowledge of the author. For the benefit of future modelling, the objectives herein are:

1. to quantify vertical sorting,
2. to describe the sorting processes in detail, and
3. to find the principal variables for this sorting.

This is done for a range of flow conditions, sediment transports and slipface lengths, and for various mixtures.

8.1.2 Review and definitions

For an extensive review the reader is referred to chapter 7. A grain flow refers to a mass of grains that moves downward while the individual moving grains collide and interact. A grain fall on the other hand refers to the settling of single grains from the flow, in which grain-grain interaction is much less important. The sediment from grain fall is deposited as toesets, while the sediment from grain flows is deposited as (possibly cross-stratified) foresets (see fig. 8.1). Hunter (1985) suggests that both the grain fall and grain flow deposits can be preserved on the lee slope (see fig. 8.1a). However, Hunter mainly studied fine-grained sediments, which are probably near to suspension and give considerable grain fall deposition all over the lee-slope. For coarse-grained sediments and sand-gravel mixtures on the other hand, little or no grain fall deposition takes place on most of their lee-slope, resulting in a grain flow dominated deposit (fig. 8.1b).

The grain flow and grain fall processes are coupled because the sediment incorporated in grain flows has been delivered by grain fall. Sediment arriving at the brinkpoint is deposited on the foreset slope. Large grains are deposited immediately downstream of the brinkpoint, while smaller grains may saltate higher or even be suspended and therefore take more time to settle and are deposited lower on the foreset slope. Thus the concentration and settling rate of sediment decreases in downstream direction from the top of the dune, bar or delta. The finer sediment will

remain suspended for a longer time than the coarser sediment. As a result of this non-linear settling rate, a wedge of sediment builds up on the top of the foreset, with a much faster build-up rate at the top of the foreset than further downstream of the brinkpoint.

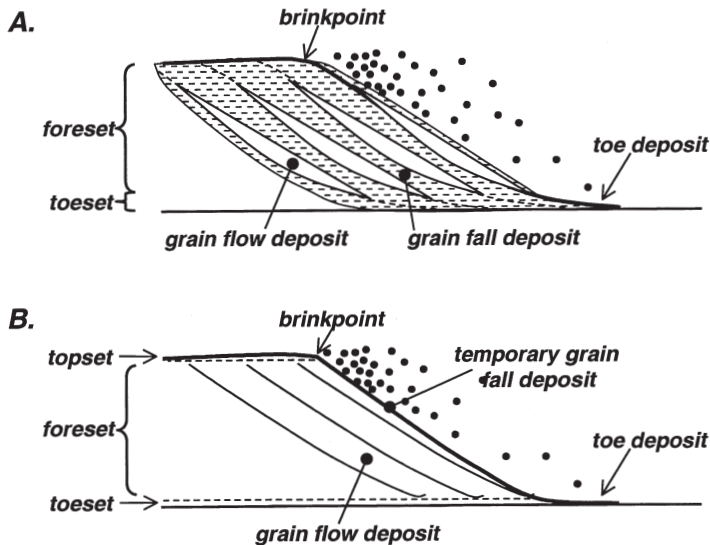


Figure 8.1. A. Sorting and definitions in sand dune deposits (after Hunter 1985). B. Sorting in sand-gravel dune deposits, where only grain flow deposits are preserved on the lee slope.

This sediment wedge fails above a certain threshold, and at that moment a relatively large mass of gravity-driven sediment moves downslope in the form of a grain flow. The threshold is usually specified as a critical slope: the static angle of repose. When the grain flow stops moving, the sediment is deposited at the dynamic angle of repose, which usually is a few degrees smaller than the static angle of repose. During the movement of the sediment mass, kinematic sieving takes place: the small grains work down into the grain flow by occupying the small pores, with the result that the large grains are worked upwards. Kinematic sieving may promote upward fining in dunes, bars and small deltas, because the large grains on top of the lee slope may roll downslope more easily than the small grains below the large ones. This applies especially to grain flow strata and, if preserved, much less to grain fall strata (Pye & Tsaoar 1990).

8.2 Setup of the flume experiments

The experiments were done in a narrowed flume at St. Anthony Falls Laboratory (see fig. 8.2), which had a depth of 0.38 m and a width of 0.075 m. The water depths were between 0.08 and 0.3 m downstream of the delta. Water and sediment were fed at a constant and adjustable rate at the upstream end of the flume.

The water depth in the basin (h_0) was fixed with the downstream weir. The river system on the delta developed to its own equilibrium slope (i) and water depth (h_1). The water depth h_1 was measured through the glass wall and in the middle of the flume, while the bed slope was measured at the end of the experiments from bed level measurement at every 0.1 m along the delta at both

side walls. The flow discharge (Q) was determined twice per run by measuring the time it took to fill a bucket of known volume. The flow velocity (u) over the delta was determined from waterdepth (h_1), flow discharge and flume width (W) from $u=Q/(Wh)$. The slope (i) was determined from the bed elevation along the alluvial topset of the deltas. From the slope and the waterdepth (h_1) the total shear stress (τ) was determined with $\tau=\rho gh_1 i$. The determination of the water depth through the glass wall, however, is very inaccurate: $\pm 1\text{mm}$ which corresponds for most experiments to $\pm 10\%$. The water temperature was $10^\circ \pm 2^\circ$ Centigrade. The dimensionless shear stress θ is computed from the shear stress and the diameter of the sediment in the delta ($D_{g,T}$, explained later): $\theta=\tau/[(\rho_s-\rho_w)gD_{g,T}]$, in which ρ =density of sediment (s) or water (w), and g =gravitational acceleration.

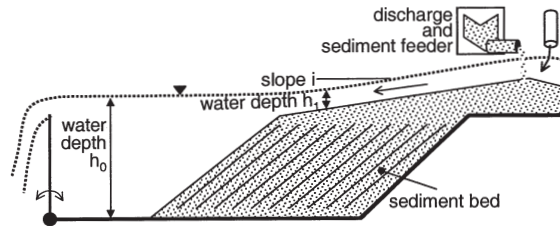


Figure 8.2. Outline of the Delta Flume at St. Anthony Falls Laboratory (vertical scale exaggerated).

During each run, the angle of the prograding deltafront was measured manually just before and after the individual grain flow events, to determine the static and dynamic angles of repose. In addition, the thickness of the individual grain flows was estimated. However, this was very inaccurate: $\pm 2\text{mm}$ which is for most experiments $\pm 25\%$. Also, close-up digital videos were taken for later analysis of the grain flow characteristics like thickness, velocity and frequency (not reported here).

Table 8.1. Description of the sediment mixtures fed into the flume. D_g = geometric mean size (mm), σ_g = geometric standard deviation (in psi-units). All sediments have a density of approximately 2650 kg/m^3 and a porosity varying between 0.30 and 0.36. The symbols of the mixtures are used in the remained of this paper.

mixture name		description	D_g (mm)	σ	gravel fraction (% > 2mm)
Normal	N	unimodal sand-gravel mixture	1.18	2.85	37% gravel
Colored	C	gravel mixture with very fine sand tail	2.71	2.36	88% gravel
Minnesota*	M	slightly bimodal gravel	3.71	1.66	85% gravel
Utrecht*	U	unimodal gravel	2.86	1.34	92% gravel
Sand	S	sand with gravelly tail	0.69	2.26	7% gravel
Angular**	A	sand-gravel mixture with angular gravel	2.11	2.41	64% gravel

*: fractions extracted from the Colored mixture

** : crushed granite

The experiments were repeated for different waterdepths h_0 and therefore different delta heights (Δ). The delta height and the delta celerity (downstream migration of the slip face) were expected to be the most important parameters for the sorting. Therefore these two were systematically varied in combinations of three water depths (0.08, 0.2 and 0.28 m) and three celerities (3, 6 and

9 cm/minute). The celerity (c) is given by $c = q_b / (\Delta)$, in which q_b is the volumetric transport rate including the pore space. The sediment input was between $8.0 \cdot 10^5$ and $3.5 \cdot 10^4 \text{ m}^2/\text{s}$ (including pore space). The delta developed in the basin with a height slightly less than the waterdepth in the basin, and with an alluvial top surface developing at the equilibrium slope for the given conditions. Several sediment mixtures were used to study the effect of sediment size, angularity and bimodality (see Figure 8.3 and Table 8.1).

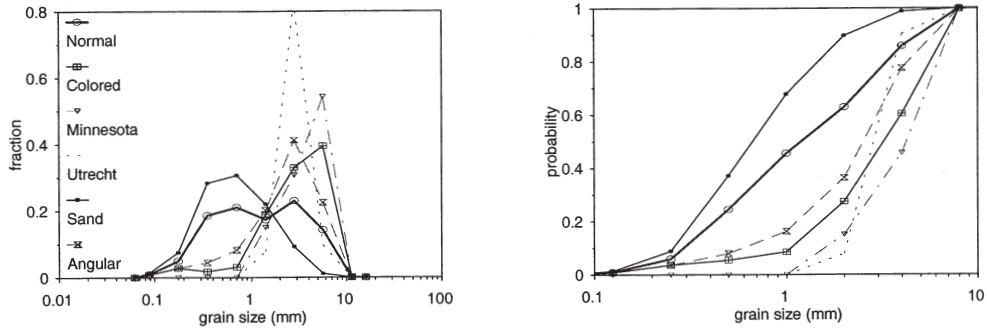


Figure 8.3. Grain size distributions of the sediment mixtures fed into the flume. See Table 8.1 for description.

After the water was drained from the flume, the bed was photographed from both sidewalls and from the top of the flume. The bed surface elevation was measured for the determination of the slope and the total volume of sediment. The celerity was determined from the duration of the experiment and the delta progradation distance. At two positions in the delta (at the delta front and halfway the deposit), the bed was sampled in horizontal layers of 1.5-2 cm thickness over a length of 15-20 cm (comparable to collecting a core and slicing the core in thin layers). The topset (at each forementioned position), the toset (over a length of 0.2 m immediately downstream of the delta slipface) and the foreset (from downstream delta top to toe) were sampled separately. The grain size distributions of the samples were determined by sieving.

The samples are described with the geometric mean sediment size (D_g) and the geometric standard deviation (σ_g) of the mixture, calculated as follows from the grain size distributions:

$$\begin{aligned}
 D_g &= 2^{\psi_m}; & \psi_m &= \sum_{i=1}^N \bar{\Psi}_i p_i \\
 \sigma_g &= 2^\sigma; & \sigma &= \sum_{i=1}^N (\bar{\Psi}_i - \psi_m)^2 p_i
 \end{aligned}
 \tag{1}$$

in which ψ_m = arithmetic mean size (related to the sedimentological grain size scale (Φ) as $\psi = -\Phi$), $\bar{\Psi}_i$ = class middle (in between sieve mesh sizes) of a size fraction, p_i = abundance (probability) in size fraction i , σ_g = geometric standard deviation, and σ = arithmetic standard deviation.

The vertical sorting is described in a nondimensional way as follows. The height (z) at which a sample was taken is made dimensionless as $z^* = z / \Delta$ (Δ = delta height) to be able to compare the sorting in deltas with different heights. The feeder sediment is not the same as the sediment participating in the grain flows because of size-selective sediment transport on the topset. Therefore the composition of the sediment in each 'core', that is, the samples at all heights z at each sampling location in the deltas, was averaged to determine the grain size distribution of the

sediment participating in the grain flows. The arithmetic mean size ($\Psi_{m,z}$), geometric mean size ($D_{g,z}$) and standard deviation ($\sigma_{g,z}$) of the samples at height z are made dimensionless as $\Psi^* = \Psi_{m,z} - \Psi_{m,T}$ and $D^* = D_{g,z}/D_{g,T}$ and $\sigma^* = \sigma_{g,z}/\sigma_{g,T}$, in which the $D_{g,T}$ and $\sigma_{g,T}$ describe the sediment actually going over the top (brinkpoint of the delta) and participating in the grain flowing process at the sampling location. Note that Ψ^* must be made dimensionless by subtraction instead of division for the following reason. Since $D = 2^\Psi$, it follows that:

$$D^* = 2^{\Psi^*} = 2^{\Psi_{m,z} - \Psi_{m,T}} \Rightarrow D^* = \frac{2^{\Psi_{m,z}}}{2^{\Psi_{m,T}}} \Rightarrow D^* = \frac{D_{g,z}}{D_{g,T}} \quad (2)$$

So the dimensionless arithmetic mean size (Ψ^*) is related to the dimensionless geometric mean size (D^*) by $D^* = 2^{\Psi^*}$.

8.3 Results

8.3.1 Basic data

The experimental conditions, transport rates, grain size distributions of the input sediment and delta characteristics are presented in Table 8.2 and Figure 8.4. For N1 to N9 and N11, the delta height and celerity have systematically been varied, and most deltas with other sediment types fall in this range. Two experiments, N10 and S2, have been done with the highest possible celerity.

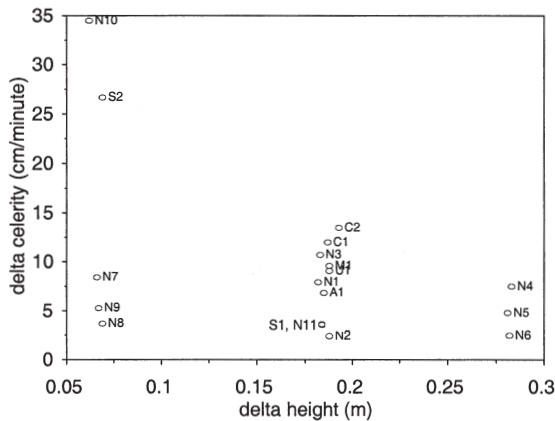


Figure 8.4. The delta height and the delta celerity (downstream migration of the slip face). For N1 to N9, these were systematically varied. N11 is an additional experiment because the celerity of N1 was too large compared to N5 and N9. N10 and S2 were specifically designed for a celerity as high as possible with the given sediment feeder.

Table 8.2. Basic data of the experiments.

#	h ₀ (m)	Q (m ² /s)	h ₁ (m)	i (-)	C (cm/min)	Δ (m)	q _b * (m ² /s)
N1	0.200	3.1E-04	0.008	0.063	7.92	0.18	3.9E-04
N2	0.203	2.9E-04	0.010	0.032	2.40	0.19	1.3E-04
N3	0.200	4.2E-04	0.010	0.066	10.71	0.18	5.4E-04
N4	0.300	4.5E-04	0.010	0.067	7.50	0.28	6.8E-04
N5	0.301	4.2E-04	0.010	0.067	4.79	0.28	4.5E-04
N6	0.299	3.7E-04	0.010	0.037	2.48	0.28	2.3E-04
N7	0.080	3.5E-04	0.011	0.036	8.43	0.07	1.3E-04
N8	0.081	3.3E-04	0.012	0.026	3.69	0.07	5.6E-05
N9	0.082	3.9E-04	0.011	0.014	5.27	0.07	7.7E-05
N10	0.080	5.2E-04	0.013	0.039	34.50	0.06	4.3E-04
N11	0.198	3.9E-04	0.011	0.034	3.53	0.18	1.8E-04
M1	0.200	4.4E-04	0.010	0.069	9.60	0.19	5.7E-04
U1	0.201	4.2E-04	0.010	0.069	9.09	0.19	5.1E-04
S1	0.200	4.2E-04	0.012	0.027	3.62	0.18	1.9E-04
S2	0.080	4.1E-04	0.010	0.036	26.67	0.07	3.6E-04
A1	0.200	3.4E-04	0.010	0.060	6.83	0.19	4.3E-04
C1	0.205	3.9E-04	0.010	0.086	12.00	0.19	7.1E-04
C2	0.208	5.8E-04	0.012	0.072	13.47	0.19	7.8E-04

*: the volumetric bedload transport rate (q_b) includes the pore space.

An example of the sediment sorting and morphology of a delta is given in Figure 8.5. The main body is the fining upward deposit from the grain flows at the lee side of the prograding delta. On top of the delta, there is an alluvial topset at an angle equal to that of the slope of the 'river' which transported the sediment from the inlet to the brinkpoint of the delta. In most experiments a toeset formed by settling of sediment that was suspended at the brinkpoint. When this sediment was overrun by the prograding delta, it became a toeset.

8.3.2 Vertical sorting

Figures 6 and 7 show the vertical sorting in the forementioned non-dimensional way. In all experiments, the sediment was sorted fining upward, and the σ^* at most heights is smaller than unity because the sediment is vertically sorted. The notable exception is the base of most of the deltas, which has a larger σ^* because the fine sediment of the toeset is mixed with the coarse sediment of the lowest part of the foresets. The deltas without fine sediment (M1 and U1) do not have this toeset.

To be able to assess the effect of certain variables on the vertical sorting, the sorting data shown in figures 6 and 7 must be expressed in a convenient parameter. This is done as follows. The fining upward trend along the foreset is expressed as the sorting slope of the relative grain size ψ^* versus the depth (1-z*) in the delta (not the height z*, because the sorting slope is positive for fining upward sorting with 1-z*). The sorting slope $d\psi^*/d(1-z^*)$ is calculated for all samples except the bottom and the top, to exclude the effects of the toeset on the sorting.

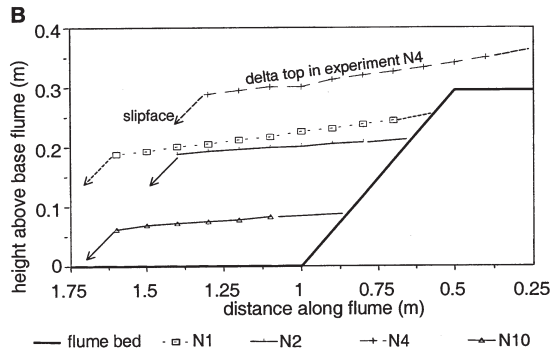
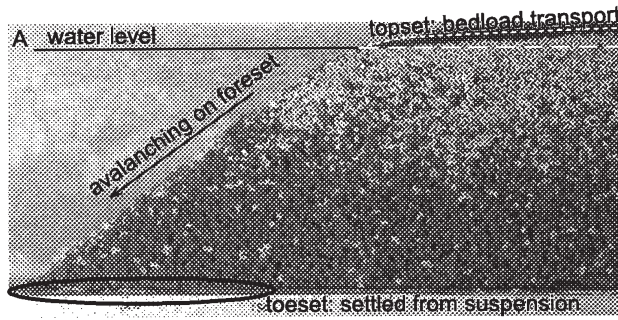


Figure 8.5. a) Photograph showing the sediment sorting in delta M1. The dark grains are large, the light grains are small (note the fining upward). In deltas with finer sediment (not M1), a toe deposit is present, formed of sediment settled out of suspension downstream of the foreset. When this toe deposit is overrun by the delta, it becomes a toeset (location given in the photograph, but not present in experiment M1). b) Examples of surface profiles of some experiments, which were used to determine the alluvial slope and the total volume of the delta (for determination of sediment transport). The base of the flume (already including a delta shape) is given as well.

For the N experiments, three trends (apart from fining upward) in the sorting are manifest. First, the sorting slope becomes smaller with increasing delta celerity, meaning that the sorting becomes less well developed for increasing migration celerity of the delta front. This is also shown in Figure 8.8. This trend is especially obvious for the experiments with the highest celerities: experiment N10 (highest celerity, lowest height) compared to the experiments with the lowest celerities: experiment N8 (lowest celerity, same height) and also experiment S2 (highest celerity) versus S1 (lowest celerity). This dependence on migration celerity seems to be significant as can be seen from the difference in sorting due to migration celerity compared to the difference in sorting due to variation between the samples within one delta. (For most N experiments, two curves are shown as the delta was sampled twice.)

Second, the lines of the σ^* are more curved in the middle of the delta for $\Delta > 0.1$ than for $\Delta < 0.1$. This means that the sediment is actually better sorted (smaller σ^*) in the top and lower parts of the larger deltas than in the middle of the larger deltas and the whole of the small deltas. So, for larger deltas, the sorting process is more efficient at the top and lower parts of the foreset (see also Figure 8.8). This also seems to be the case for the S1 (large delta) and S2 (small delta) experiments.

Third, the toeset is more prominently present in the lowest deltas (top panels, N7 to N10), the measured thickness (not shown here) also indicates this. So, the formation of toesets appears to

be more efficient in smaller deltas.

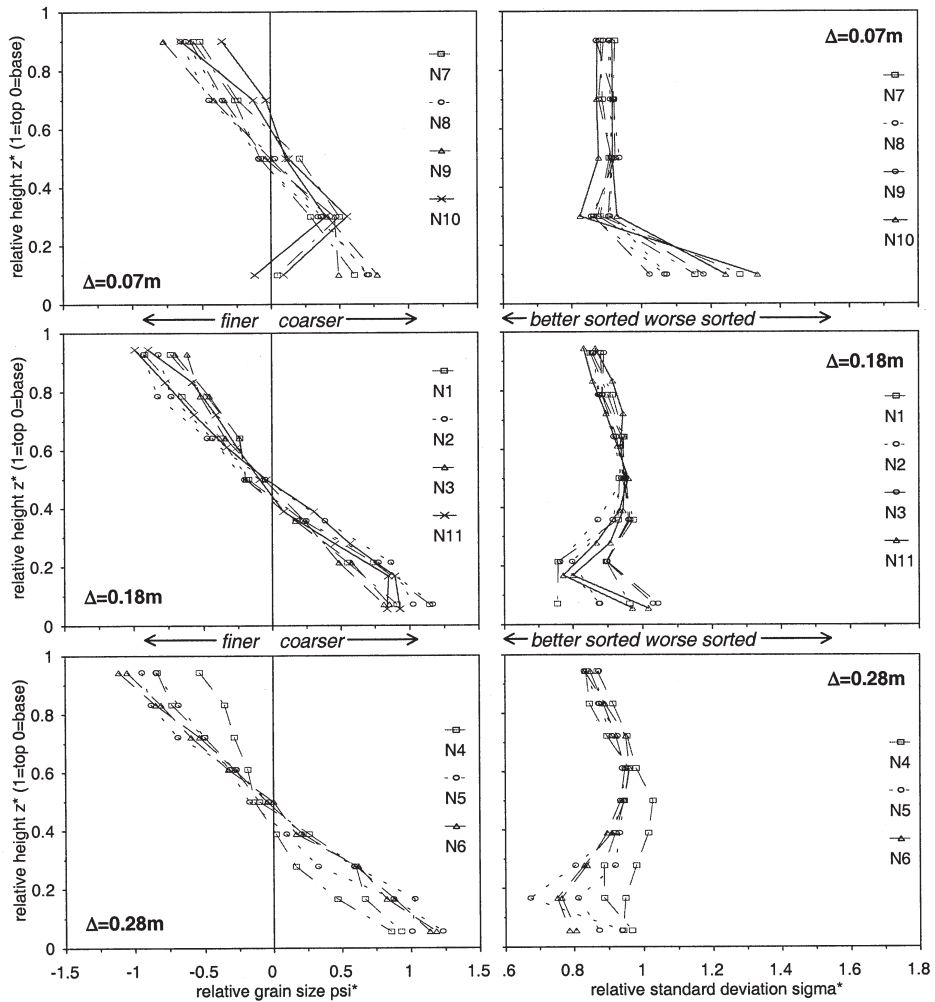


Figure 8.6. The fining upward sorting in the deltas with the N sediment mixture. The horizontal axis of the left-side panels (ψ^*) is the logarithm of the ratio of the sediment diameter at a certain height ($D_{g,z}$) and the diameter of all the sediment in the delta ($D_{g,T}$): $2^{\psi^*} = D_{g,z}/D_{g,T}$. The $\sigma^* = \sigma_{g,z}/\sigma_{g,T}$. The topset and toe deposit have not been included. The toeset, however, is included in the samples taken at the base of the deltas. The sorting curves have been grouped for delta height.

A comparison of the other sediment mixtures (see Figure 8.7) with the N series reveals four additional observations (see also Figure 8.8): Fourth, the mixtures with a smaller geometric standard deviation (M1 and U1) show less vertical sorting; the sorting trend in U1 is very small compared to that of wider mixtures. This was expected, because the uniformer the sediment, the less there is to sort. The differences between all sediment mixtures seem to be much larger than the differences in sorting for one mixture in various conditions.

Fourth, when A1 is compared to the N series, it can be observed that the angularity of the sediment seems to have no significant effect on the sorting. The A and N sediment have comparable grain sizes and standard deviations, while the prominent difference is the angularity. Fifth, when the finest fraction of which the toset consists is much finer than the rest of the sediment (bimodal) as in experiments C1 and C2, then the toset is much stronger developed. So, the flow conditions on the alluvial slope were such that the gravel in the mixture C could be transported, and the fine sand was suspended and deposited in a well-developed toset.

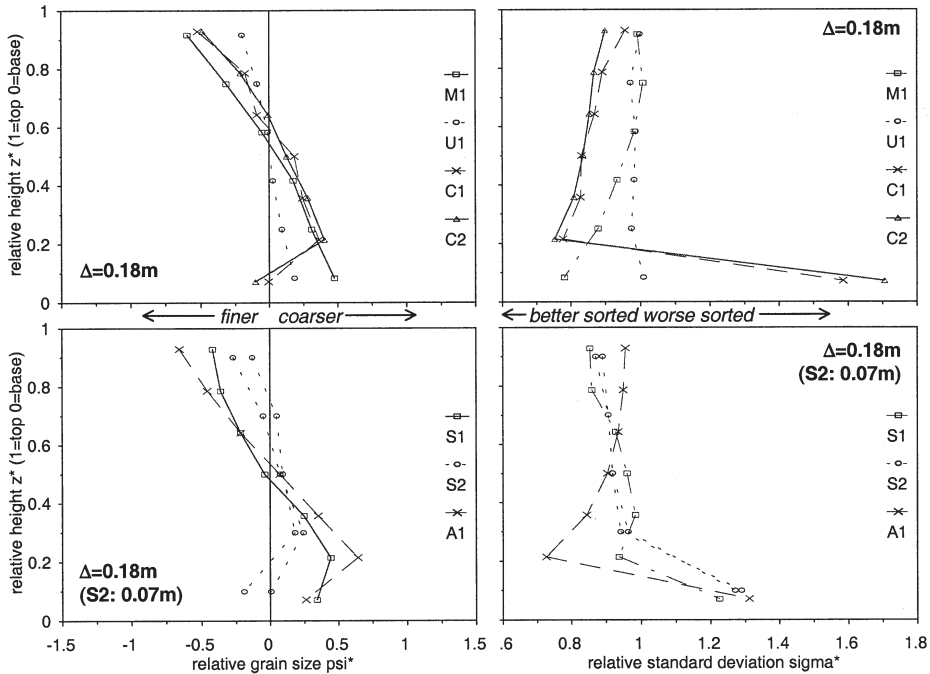


Figure 8.7. Sorting in the deltas with the alternative sediment mixtures. The horizontal axis of the left-side panels (ψ^*) is the logarithm of the ratio of the sediment diameter at a certain height ($D_{g,z}$) and the diameter of all the sediment in the delta ($D_{g,T}$): $2\psi^* = D_{g,z}/D_{g,T}$. The $\sigma^* = \sigma_{g,z}/\sigma_{g,T}$. The topset and toe deposit have not been included. The toset, however, is included in the samples taken at the base of the deltas. The sorting curves have been grouped for delta height.

Sixth, the replica-experiments C1 and C2 were done in the same conditions, except that the flow discharge in C2 was 1.5 times as high as in C1, and the alluvial slope of C2 consequently was smaller while the flow velocity in C2 was 10% higher. The difference in sorting between C1 and C2, however is negligible, so the flow conditions on the alluvial slope seem to have a marginal effect on the sorting at the lee slope of the delta (see Figure 8.8). This is not true, however, for the toe-set formation in the N series: the flow discharge seems to have an effect. For example, for experiment N10 the flow discharge was 1.6 times as high as in N8, and the toset is much more developed in N10 than in N8. So, the flow conditions on the alluvial slope have no obvious effect on the sorting on the foreset, but do have an effect on the toset formation.

8.3.3 Process description of sorting in the grain flow

The following qualitative description is based on visual observations done during the experiments and verified with the videos (see fig. 8.9). The sorting in the grain flows in the N experiments is a three-stage process.

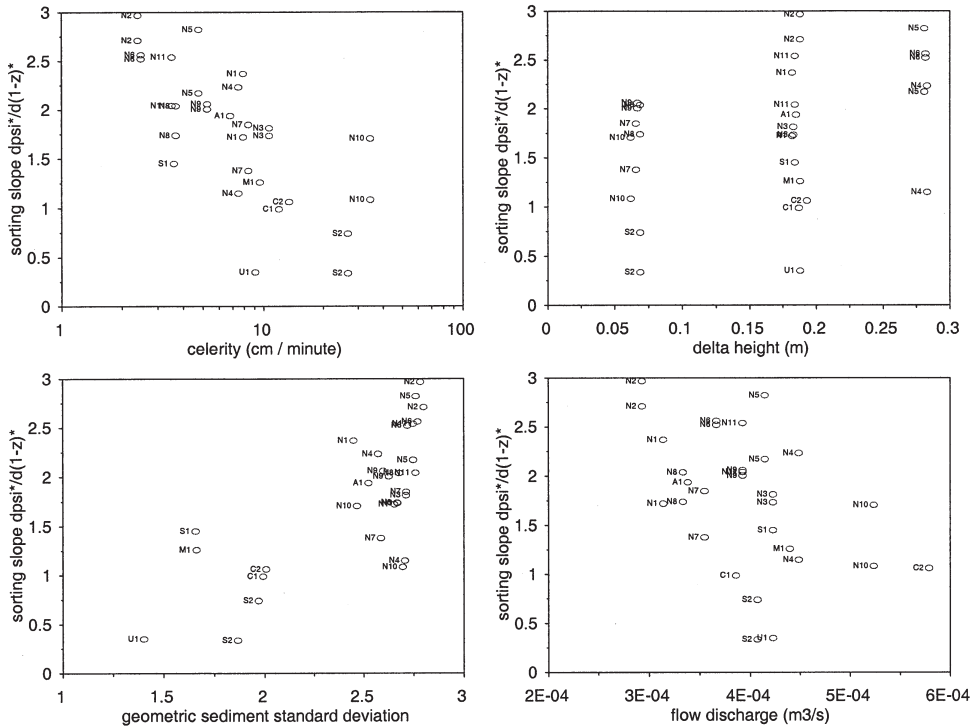


Figure 8.8. Plots of the sorting slope versus the variables celerity, delta height, geometric standard deviation and flow discharge above the delta top. The sorting slope $d\psi^*/d(1-z)^*$ was computed from the data presented in figures 6 and 7 for heights roughly between 0.2 and 0.8 times the delta height.

The first process is the deposition of sediment from grain fall just downstream of the delta top. The flow carries the sediment downstream from the delta top, and meanwhile the grains settle to the slip face. Thus a wedge-shaped mass of mixed sediment is built up at the upper 3 cm of the lee slope. For the smaller grains, this distance is larger, and the smallest are even deposited downstream of the delta as a toeset. The static angle of repose of the wedge-shaped mass is larger (37° for the N experiments) than the dynamic angle of repose of the lower lee slope (32°).

Second, the sediment mass moves down-slope over a small distance (less than half the lee slope length). The accommodation space thus created is filled by the continuous grain fall. During the small down-slope movement of the sediment, the gravel is worked upwards in the moving layer, probably by kinematic sieving. As a consequence, the lee slope is covered with the coarsest sediment from top to toe for most of the time.

Third, at some point roughly the whole upper half of the lee slope sediment fails and moves downslope as a large grain flow, usually about 8 mm thick in the N experiments. The plane at which the sediment fails, seems to be the transition from the gravelly surface of the previous grain

flow deposit with the underlying (in the plane of the lee slope) sediment. This underlying sediment is sandy near the delta top and gravelly near the base, and is finer than the lee slope surface along most of the slope. So mostly the gravelly part of the previous grain flow is dragged down-slope by the next grain flow, which leads to the observed upward fining in the delta. The deposited sediment from grain fall on top of the grain flows seems to have been incorporated into the grain flows by kinematic sieving immediately; no fine sediment drapes were found on the lee slopes and no clear cross-lamination was observed.

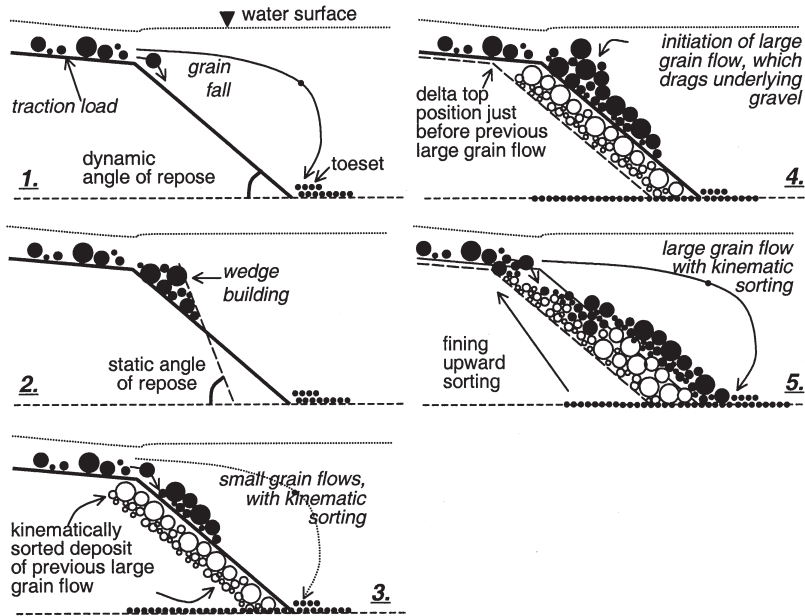


Figure 8.9. Conceptual model of the sediment deposition and sorting on the lee slope of the experimental deltas. The three stages of the process are given: 1,2: grain fall creating the sediment wedge and the toset, 3: small grain flows with kinematic sorting, and 4,5: large grain flows that drag the top of the previous grain flow deposit downslope, leading to the fining upward. For clarity, the dynamic and static angle of repose, the sorted deposit of the previous large grain flow and the previous position of the delta front are introduced in the first four panels, but obviously are present in all time steps in reality.

When the flow reaches the bottom of the flume (top of the toset), the gravelly head of the flowing sediment mass stops moving first and within a second or so all the sediment becomes immobilised. The surface of the stabilised grain flow is again gravelly, while the top of the delta is sandy. Since the slope of the immobilised grain flow (dynamic angle of repose) is smaller than the static angle of repose, there is a new accommodation space for sediment depositing from grain fall, and the process starts anew.

Summarizing, the sediment settles from grain fall as a mixed wedge on the upper lee slope. The gravel in that sediment is worked upwards to the surface by kinematic sorting in small grain flows. When a critical mass has been built up, the sediment along the whole slope fails at the transition between the gravel at the surface of the previous grain flow and the underlying sediment, and the gravel is dragged downslope while the underlying sand remains in place.

8.4 Discussion

8.4.1 Dimensionless numbers affecting vertical sorting: theory

It was found that the variables delta height (Δ), delta celerity (C), geometric mean size ($D_{g,T}$) and the mixture standard deviation ($\sigma_{g,T}$) explained some variation in vertical sorting in foresets. The variation in toeset deposits was found to be related to delta height (Δ), the mixture standard deviation ($\sigma_{g,T}$), the suspended sediment characteristics that is deposited in the toeset and the flow conditions above the delta top. The suspended sediment is characterised by the settling velocity w_s , and the flow conditions above the delta top are conveniently characterised by the depth-averaged flow velocity (u). An additional variable is the submerged specific weight of the sediment: Rg , with $R=(\rho_s-\rho)/\rho$ (with ρ =density of water and ρ_s =density of sediment) and g =gravitational acceleration. By dimensional analysis the variables can be grouped into the following four dimensionless variables.

The transport rate is made dimensionless with the delta height:

$$Tr^* = \frac{q_b(1 - \lambda_p)}{\sqrt{Rg\Delta}} = \frac{C}{\sqrt{Rg\Delta}} \quad (3)$$

in which q_b =volumetric bedload transport rate per unit width, λ_p =porosity or pore space of the deposited sediment, $R=(\rho_s-\rho)/\rho$ (with ρ =density of water and ρ_s =density of sediment) and C =celerity.

The celerity of the delta is made dimensionless with the geometric mean sediment size, roughly to describe the delta progradation in terms of the size of grains deposited on the lee slope, because the individual grain flow laminae thickness scales with this grain size:

$$C^* = \frac{C}{\sqrt{RgD_{g,T}}} \quad (4)$$

The geometric mean grain size, the mixture standard deviation and the length of the lee slope ($\Delta/\sin\beta$, in which β =dynamic angle of repose) can be combined in a dimensionless sorting number. Both the standard deviation and the length of the slope are made dimensionless with the geometric mean size. Assuming that a longer lee slope and a higher standard deviation both lead to more efficient sorting, the sorting number is:

$$S^* = \frac{\sigma_{g,T}}{D_{g,T}} \frac{\Delta}{\sin\beta} \quad (5)$$

The flow conditions at the delta top govern the toe set deposition process. The following reasoning is based on the ideas of Jopling (1965). The settling velocity of the finer sediment (say, of grains with a diameter that is one standard deviation smaller than the mean: $\Psi_{m,T} - \sigma$) acts in the vertical direction (downwards) while the flow velocity at the top gives the grains an initial momentum in the horizontal direction (downstream). It can now be seen that the path of the grains from the

delta top to the toe set deposit is related to u/w_s . Also, the horizontal distance between delta top and toe ($\Delta/\tan\beta$) is then important, as well as the height of the grain in the water column above the delta top (Jopling 1965). Since the water depth h_1 is very small relative to the delta height in the experiments reported here, this grain height is simply assumed to be $0.5h_1$. (For larger water depths, this analysis should include the flow velocity and sediment concentration of all sediment sizes in the vertical direction.) The following dimensionless grain fall number can be constructed:

$$G^* = \frac{u}{w_s} \frac{\tan\beta \left(\frac{1}{2}h_1 + \Delta \right)}{\Delta} \quad (6)$$

The sorting slope (described in a previous section) characterises the fining upward trend in the main body of the deltas. The toset deposits are characterised by the relative geometric standard deviation $\sigma_{g,b}^*$ of the bottom layer in each delta. This standard deviation is so high in these bottom layers, because the bottom layer is a mixture of the extremely fine toset and the extremely coarse lowest part of the foreset deposit.

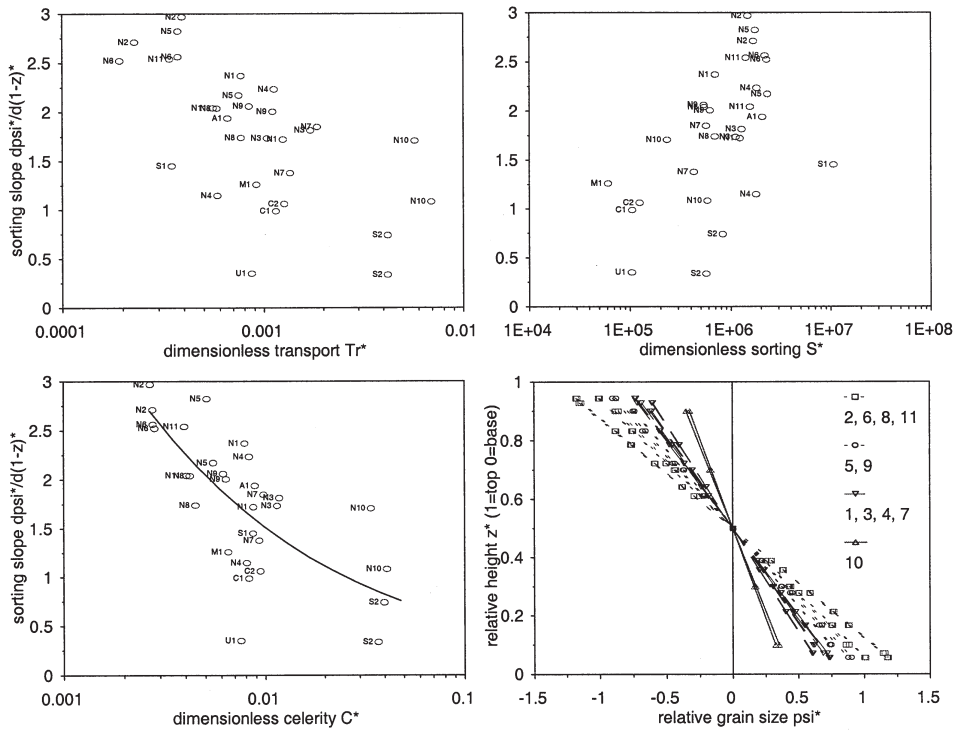


Figure 8.10. Relation between dimensionless numbers and fining upward sorting. Sorting slope $d\psi^*/d(1-z)^*$ as computed from the data presented in figures 6 and 7, versus the dimensionless celerity, transport and sorting numbers. The line in the lower left panel shows the power function of sorting slope versus C^* . The lower right panel shows the predicted vertical sorting based on this power function. The N experiments are grouped for comparable celerities (experiment numbers given in the legend).

In the next section the sorting slope ($d\Psi^*/d(1-z^*)$) and the geometric standard deviation of the bottom sediment ($\sigma_{g,b}^*$) are plotted against the dimensionless numbers Tr^* , C^* , S^* and G^* .

8.4.2 Dimensionless numbers affecting vertical sorting: results

The relation between the dimensionless numbers and the vertical sorting in the foreset deposits is shown in Figure 8.10. The relation between the sorting slope and the celerity (C^*), the transport (Tr^*) and the sorting number (S^*) are comparable. Within the given range of transports and celerities, the sorting slope goes from 3.5 (the maximum) to almost zero (the minimum) with increasing C^* and Tr^* and decreasing S^* . Concluding, the celerity, the related transport rate and the sediment sorting and slope length all have an effect on the sediment sorting, but the scatter is large.

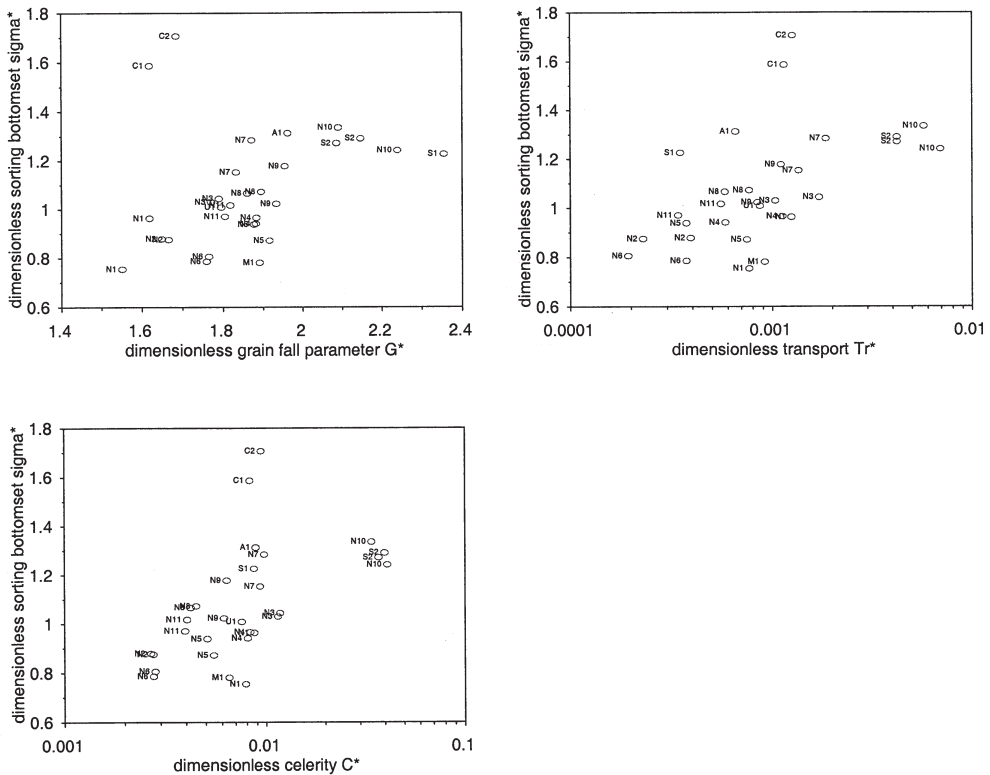


Figure 8.11. Relation between dimensionless numbers and toset deposition. The geometric standard deviation of the bottom sediment ($\sigma_{g,b}^*$) versus the dimensionless celerity, transport and grain fall numbers.

Even though the scatter is large, the predictive capacity of the dimensionless celerity C^* is reasonable. In double logarithmic space, the sorting slope $d\psi^*/d(1-z^*)$ versus C^* is a straight line, so a power function was fitted:

$$\frac{d\psi^*}{d(1-z^*)} = 0.20 C^{*-0.44} \quad (7)$$

So the vertical sorting can now be computed as:

$$\psi_z^* = [(1-z^*) - 0.5] 0.20 C^{*-0.44} \quad (8)$$

The intercept $[(1-z^*) - 0.5]$ of the vertical sorting ψ^* is thus simply taken at $z^*=0.5$ because this is the average intercept for the data presented in figures 6 and 7, which means that the grain size at 0.5 times the delta height is equal to the grain size averaged over the delta. This equation was used to hindcast the vertical sorting of the N experiments. The results (lower right panel in fig. 8.10) agree well with the data (fig. 8.6). Concluding, the dimensionless celerity C^* explains the variation in sorting between the N experiments.

The relation between the dimensionless numbers and the toset deposition is shown in Figure 8.11. The C experiments are outliers in all graphs, which suggests that the fine sand in the bimodal sand-gravel mixture C was much more susceptible to suspension than the coarse sand in the N, A and S experiments. There seems to be a relation between the sorting slope and the dimensionless grain fall parameter (G^*), but the relation is not stronger than that with the dimensionless celerity (C^*) and transport (Tr^*). The problem is that the C^* and Tr^* are both measures for the sediment transport which is related to the flow velocity, while the G^* directly depends on the flow velocity.

It must be concluded that the dimensionless parameters do not fully describe the sorting process. The reason is probably that there are basically two processes that sort the sediment: grain fall and grain flows, which depend on the given variables in a different way, but are indistinguishably intertwined in the observed sorting. The grain fall process mainly depends on the flow conditions and mode of sediment transport (bedload or suspended load) of the grain sizes on top of the delta, while the grain flow process mainly depends on the sediment transport rate, slip face height and the sediment characteristics that determine the grain flow thickness and rate of failure. Another reason could be that the grain size distributions are not well enough described by the average grain size and the standard deviation. The bimodality of the sediment should somehow be included, but it is not clear how.

A dimensionless analysis probably does not suffice, but a model is needed that predicts the sediment deposition on the lee slope and beyond from grain fall for different size fractions, and furthermore predicts the initiation and sorting in grain flows resulting from the wedge-building process.

8.4.3 Comparison between sorting in deltas, bars and dunes

Weak relations were found between the vertical sediment sorting and the height, flow conditions and celerity of the experimental deltas. To test the applicability of the present results to river dunes and bars, it is necessary to compare the experimental range of flow conditions and celerity

with those in natural rivers and in some relevant experiments with measured sediment sorting from literature. Dunes are loosely defined here as features that scale with water depth, while bars scale with river width. Deltas do not occur in a typical river reach, but only in sudden and large flow decelerations, for example in lakes or the ocean.

It is expected that dunes in gravel bed rivers are much smaller than in sand bed rivers, but move much faster, which obviously has consequences for the vertical sorting. The datasets are summarized in Table 8.3, and include relevant flume experiments for studying the sorting in grain flows (see also **chapter 7** for a more complete description), and cover the range from sand-bed rivers to gravel-bed rivers with known dune parameters (dune height and celerity) that are relevant for the sorting.

Table 8.3. Description of the datasets used in the comparison between the experiments presented here, experiments in literature and three field datasets.

author	code*	condition	grain size (D50, mm)	flow depth** (m)
Gabel (1993)	C	Calamus river	0.25 - 0.41	0.34 - 0.61
Dinehart (1992)	NF	North Fork Toutle river	22.2 - 36	1.4 - 2.24
this thesis, chapter 6	R	Rhine river	1.58 - 1.58	8.6 - 10.69
Blom and Kleinhans (1999)	BK	dunes in flume	0.59 - 0.73	0.19 - 0.35
Blom et al. (2000)	B	dunes in flume	1.34 - 1.34	0.16 - 0.32
Termes (1986)	T	bar in flume	0.64 - 0.96	0.17 - 0.21
this thesis, chapter 10	K	dunes in flume	1.12 - 1.56	0.13 - 0.21

author	flow velocity** (m/s)	tau** (-)	bedform height (m)	bedform celerity (cm/minute)
Gabel (1993)	0.47 - 0.77	0.46 - 0.88	0.097 - 0.195	1.2 - 2.4
Dinehart (1992)	2.14 - 2.74	0.1 - 0.24	0.143 - 0.41	67.2 - 255
this thesis, chapter 6	1.42 - 1.86	0.33 - 0.74	0.119 - 0.53	4.2 - 14.4
Blom and Kleinhans (1999)	0.59 - 0.79	0.14 - 0.37	0.011 - 0.057	5.4 - 7.8
Blom et al. (2000)	0.63 - 0.82	0.13 - 0.21	0.024 - 0.062	6 - 18
Termes (1986)	0.69 - 1.2	0.15 - 0.43	0.08 - 0.1	1.2 - 9.6
this thesis, chapter 10	0.78 - 1.08	0.24 - 0.25	0.018 - 0.035	55.8 - 81

*: the code of the dataset as used in figure 12.

** : average flow parameters, for Termes the flow parameters above the bar

The comparison of the (suspended) grain fall conditions is based on the dimensionless shear stress and the median or mean grain size of the sediment in the bedforms. The comparison of the grain flow conditions is based on the dimensionless celerity C^* and the ratio of grain size over delta, bar or dune height (see fig. 8.12). The dimensionless shear stresses and grain sizes of the experiments presented here are roughly in the range of the field and flume data of literature, although none of the experimental values is near those of the gravel bed river dunes in North Fork Toutle river. The celerities of the experiments are somewhat lower than the range of field and flume data. In addition, the conditions of the Calamus sand bed river are just below the criterion for suspension (see fig. 8.12), which means that an increase of shear stress will not lead to an increase of dune celerity but to the suspension of sediment that previously moved with the dunes as bedload.

Therefore, in the sand bed rivers the dimensionless celerity can probably not become much larger than observed in the Calamus river. In general, the conditions found in rivers are rather well represented by the sorting data presented herein for the most important parameters for sorting. It must be emphasised, however, that the dimensional analysis did not give very strong relations, while the dunes, bars and deltas should be compared with parameters that describe the sorting very well to be certain of their comparability.

8.4.4 Applicability of the results to natural river dunes

The general conditions of the experiments are comparable to those in rivers, but it is the question whether the sorting at the lee side of deltas is comparable to the sorting at the lee side of dunes. There are two ways to view this: comparing the nature of the sorting processes that actually take place, and comparing the vertical sorting quantitatively between the deltas presented here and dunes in literature.

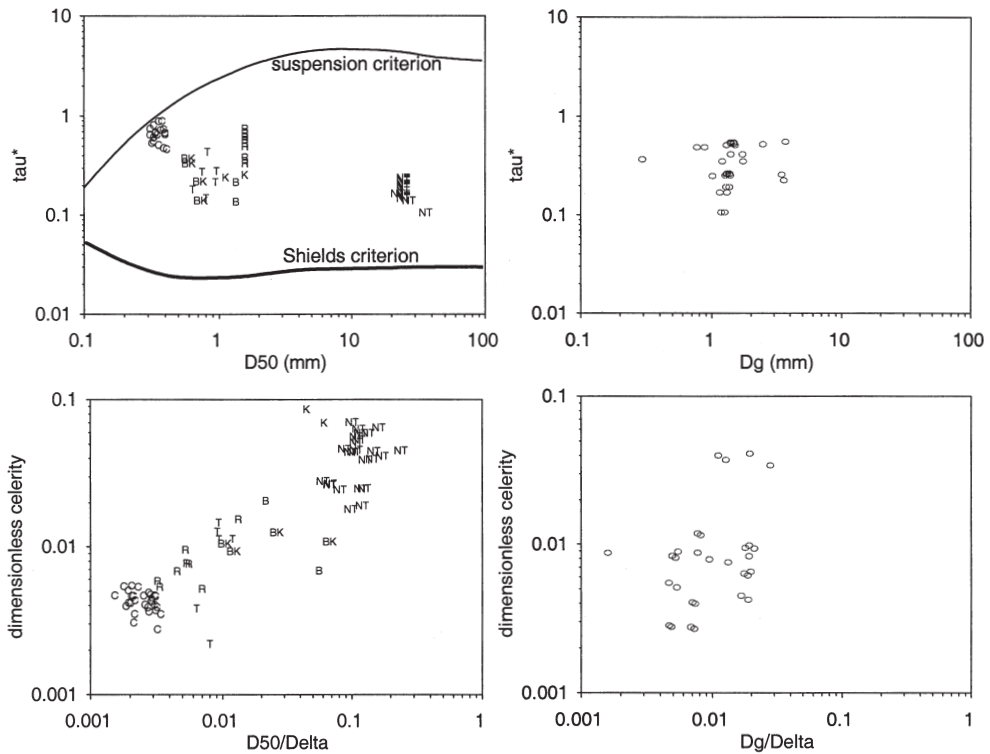


Figure 8.12. Comparison between field and experimental datasets from literature with the experiments presented here. The upper two panels give the sediment mobility, and the lower two panels give the dune parameters. The two left panels show the datasets summarised in Table 8.3, and the two right panels show the experiments presented in this paper. The upper left panel has the Shields criterion for incipient sediment motion and the suspension criterion (Parker in prep.).

There are two obvious differences between deltas and bars and dunes. The first is that the

sediment on deltas is delivered from an alluvial system on top of the delta, while on bars, and even more extremely on dunes, the sediment is mostly delivered from the eroding stoss side of the dune or bar. This may have consequences for the sorting in a bar or dune, but this effect is removed when the sediment sorting is made dimensionless as it is in figures 6 and 7 (with locally delivered sediment), and when the topset and toset are removed.

The second difference between deltas and bars and dunes is the flow structure over them. Over deltas, there is uniform flow over the top of the delta and then a sudden and large increase of the water depth. Over dunes, and less pronounced also over bars, the flow is strongly non-uniform, with accelerations on the stoss sides and decelerations on the lee sides, though less strong than for deltas because the water depth over dunes is much larger than over deltas. As a consequence, the turbulent flow structure at the lee side of the deltas, bars and dunes differ. The counterflow at the lee side of deltas is much weaker and extends further downstream than that at the lee side of dunes, while over dunes the counterflow is much stronger but the extension of the counterflow is suppressed by the coflow impinging on the stoss side of the dunes (McLean and Smith 1986). In addition, the turbulence intensity at the lee side of dunes is much stronger than for deltas and bars. The expected consequence for the sorting is that the grain fall and toset deposition is less well developed in dunes than in bars and deltas. Since part of the sorting along the lee side of the deltas reported herein is related to the grain fall, it may be expected that the sorting in dunes is somewhat different.

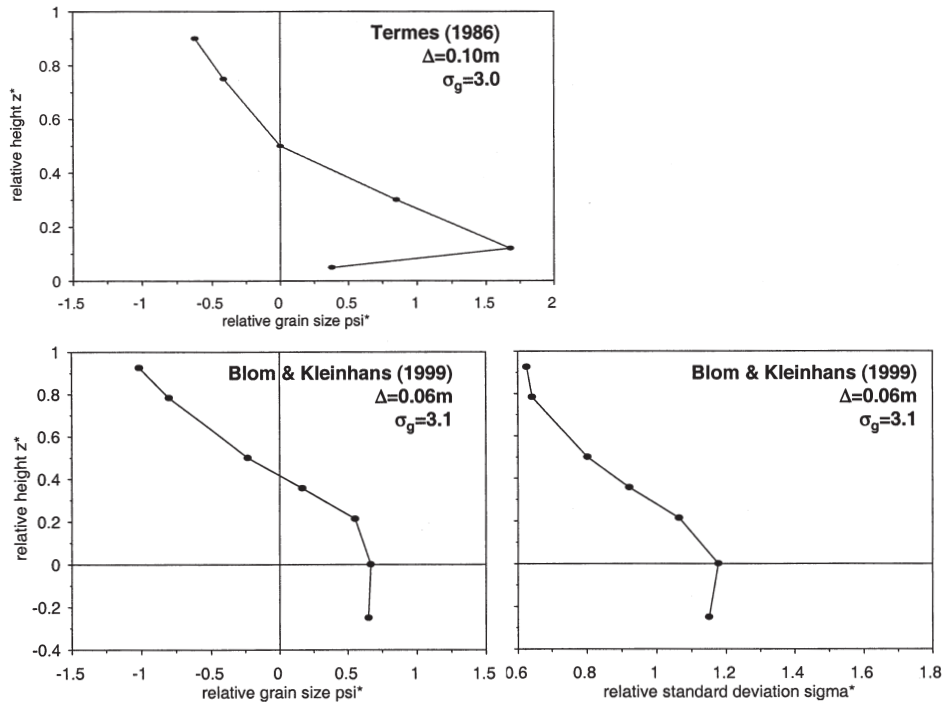


Figure 8.13. Examples of vertical sorting in experiments reported in literature, plotted in the same way as figures 6 and 7 for comparison. The celerity is within a factor two of that of the N1-N9 experiments, and the height is comparable to that of the N7-N9 experiments. The geometric standard deviation of the sediment is slightly larger than in the N experiments. The Terms data is from a bar in a flume, and the Blom & Kleinahns data from dunes in a flume.

The sorting in deltas, bars and dunes can also be quantitatively be compared for more or less comparable conditions (see fig. 8.13, compare to figs 8.6 and 8.7). The following observations can be done: First, the sorting in the dune (Blom & Kleinahns (1999) data) and the bar (Termes (1986) data) is as strongly fining upward as in the N deltas (fig. 8.6 upper left panel).

Second, the bar has a clear toset like N10, which is logical because the shear stress above the bar was even larger than in N10. The dune on the other hand has no clear toset, but shows a lag deposit as described in Kleinahns (2001). This agrees with the expected effect of the turbulent flow structure over dunes compared to that over bars and deltas.

Third, the relative standard deviation σ^* of the dune shows a much stronger increase with depth than in the N experiments. Possibly there was some enrichment of the lower lee slope from grain fall of the finest sediment. Another explanation might be that the sediment sorting in the grain flows at the lee side of the dunes is affected by the strong counterflow. Especially the coarse sediment, which is moving on top of the grain flow, might be susceptible to drag by the counterflow, which is in the upward direction at the lee slope.

Concluding, the sorting process in grain flows at the lee side of dunes, bars and deltas is well comparable, but the grain fall process may be different due to the turbulent flow structure, which results in a stronger counterflow and a higher turbulent intensity in the troughs of dunes, and consequently much less opportunity for the formation of toset deposits.

Further research should be directed to additional dimensional analysis, modelling of the grain fall and grain flow processes and study of the deposits of natural river dunes instead of the small dunes from laboratory conditions. Experiments with dunes with heights of 0.5-1 m would be very useful, but logistically difficult to do. Experiments with smaller dunes, with the deltas presented here, and measurements in nature may be sufficient for testing models.

8.4.5 Comparison of the grain flow sorting process description with literature

The given observations on grain flows agree with most records in literature (e.g. Allen 1963, Bagnold 1954, Jopling 1965, Hunter & Kocurek 1986, Kleinahns 2002, Koeppel et al. 1998, Makse 1997, Pye & Tsoar 1990, and Tischer et al. 2001). However, the observation that the sorting is established by drag of a large grain flow on the gravelly top of the underlying grain flow deposit seems to be new.

In contrast with this observation, the kinematic sorting has been mentioned in literature as the main cause of the sorting. Combined with the kinematic sorting, the difference between the angle of repose of gravel on sand and the angle of repose of sand on gravel leads to easier downslope movement of gravel than of sand (Makse 1997, Koeppel et al. 1998). The resulting sorting is fining upward because the gravel was more likely to move, as it was lying on top already. This way of sorting may be the case for subaerial conditions with very thin grain flows or individual grains rolling (as in Makse 1997), but for the thicker grain flows reported here, the difference between the two mentioned angles of repose did not lead to fining upward sorting. It was the subsequent big grain flow that sorted the sediment. The shearing plane of that big grain flow was indeed at the transition between gravel and sand in the underlying grain flow deposit, which can be explained with the smaller angle of repose of that gravel on the sand being smaller than the angle of repose of the overlying sand on the underlying gravel.

8.5 Conclusions

A strong fining upward trend has been found in the deposits of deltas produced from various sediment mixtures in a narrow laboratory flume. The fining upward trend is caused by the three-stage sediment sorting process at the angle of repose at the lee side of the delta. Sediment arriving at the top of the delta is deposited from grain fall on the upper lee slope. This mass of sediment moves downslope in small and large grain flows. In the (small) grain flows, the gravel is worked to the top of the flow by kinematic sorting. The subsequent large grain flow has its shearing plane at the transition from this gravel to the underlying sand, and drags mainly the gravel downslope which leads to the fining upward trend. The finest sediment deposition from grain fall may take place downstream of the delta, leading to a toeset that is preserved as a toeset below the migrating delta.

The efficiency of the sorting process in the experimental deltas mainly depends on the geometric standard deviation of the sediment: if the mixture is very wide, then the sorting is better developed than when the mixture is very narrow (almost uniform). In addition, an increase in the celerity of the delta front (increase of transport rate) leads to a decreased efficiency of sorting. Other important parameters are the delta height, the flow velocity above the delta top and the grain size and settling velocity of the sediment. An explanation of the sorting trend for different sediments and conditions with meaningful dimensionless parameters was not very successful. This indicates that the sorting is the result of two intertwined processes, being grain fall and grain flow, must be modelled in concert.

The sorting found in the deltas is partly comparable to the sorting found in a laboratory bar and in laboratory dunes. The main difference between deposits of dunes and of deltas is that the turbulence in the troughs of dunes is stronger, so the grain fall deposition is affected and no toeset is able to develop. The conditions in which the experiments were done, are comparable to those in sand-gravel bed rivers and therefore suitable for a further analysis of sorting in river dunes and bars.

Acknowledgments

First of all I would like to thank Gary Parker for his invitation to the St. Anthony Falls laboratory and his help with the design of the experiments. Furthermore I thank Mike, Scott, Randy, Nikki and the students Dan, Andrew and Shandy for all their help with flume modifications and the many necessary sieve samples. Gary Parker, Suzanne Leclair, Chris Paola, James Kakalios and Janrik van den Berg are thanked for discussing the sorting process by grain flows. The investigations were in part supported by the St. Anthony Falls Laboratory, Minneapolis MN, USA.

References

- ALLEN, J. R. L. (1963), Sedimentation to the lee of small underwater sand waves: and experimental study. *Journal of Geology* 73 pp. 95-116
- ALLEN, J. R. L. (1984), Sedimentary structures, their character and physical basis. *Developments in Sedimentology* 30, Elsevier, Amsterdam, The Netherlands
- BAGNOLD, R. A. (1954), Experiments on a gravity-free dispersion of large solid spheres in a Newtonian fluid under shear. *Roy. Soc. London, Proc. Ser. A*(225) pp. 49-63
- BLOM, A. & KLEINHANS, M. G. (1999), Non-uniform sediment in morphological equilibrium situations.

- Data Report Sand Flume Experiments 97/98. University of Twente, Rijkswaterstaat RIZA, WL | Delft Hydraulics. University of Twente, Civil Engineering and Management, The Netherlands.
- BLOM, A., RIBBERINK, J. S., & VAN DER SCHEER, P. (2000), Sediment transport in flume experiments with a trimodal sediment mixture; Proc. Gravel Bed Rivers Conference 2000, 28 August - 3 September, New Zealand, in NOLAN, T., & THORNE, C. (eds), Special public. CD-rom of the New Zealand Hydrological Society, (<http://www.geog.canterbury.ac.nz/services/cartotoc.htm>).
- BRUSH, L. M. (1965), Sediment sorting in alluvial channels. In: MIDDLETON, G. V. (ed.) Primary sedimentary structures and their hydrodynamic interpretation, Society of Economic Paleontologists and Mineralogists, Special Publication 12, Oklahoma, USA, pp. 25-33
- DINEHART, R. L. (1992), Evolution of coarse gravel bed forms: field measurements at flood stage; Water Resources Research, 28(10), pp. 2667-2689.
- GABEL, S. L. (1993), Geometry and kinematics of dunes during steady and unsteady flows in the Calamus River, Nebraska, USA. Sedimentology, 40, pp. 237-269
- HUNTER, R.E. (1985), Subaqueous sand-flow cross-strata. Journal of Sed. Petrology 55(6), pp. 886-894
- HUNTER, R.E. & KOCUREK, G. (1986), An experimental study of subaqueous slipface deposition. Journal of Sed. Petrology 56 (3) pp. 387-394
- JOPLING, A. V. (1965), Laboratory study of the distribution of grain sizes in cross-bedded deposits, in: Middleton, G. V. (ed.) Primary sedimentary structures and their hydrodynamic interpretation, Spec. Publ. 12, Soc. of Econ. Paleontologists and Mineralogists, Oklahoma, U.S.A.
- KOEPPE, J.P., ENZ, M. & KAKALIOS, J. (1998), Phase diagram for avalanche stratification of granular media. Physical Review E. 58 (4)
- LOVE, D.W., GUTJAHR, A. & ROBINSON-COOK, S. (1987), Location-dependent sediment sorting in bedforms under waning flow in the Rio Grande, Central New Mexico. The Society of Economic Paleontologists and Mineralogists, Spec. Publ. 39, ETHRIDGE, F.G., FLORES, R.M. & HARVEY, M.D. (eds), Recent developments in fluvial sedimentology, pp. 37-47
- MAKSE, H.A. (1997), Stratification instability in granular flows. Physical Review E 56, pp. 7008-7016
- MCLEAN, S. R. & SMITH, J. D. (1986), A model for flow over two-dimensional bed forms. Journal of Hydraulic Engineering 112 (4) pp. 300-317
- PARKER, G., PAOLA, C. & LECLAIR, S. (2000), Probabilistic Exner sediment continuity equation for mixtures with no active layer, Journal of Hydraulic Engineering 126 (11) pp. 818-826
- PYE, K., & TSOAR, H. (1990), Aeolian sand and sand dunes. Unwin Hyman Ltd, London, UK, 396 p.
- RIBBERINK, J. (1987), Mathematical modelling of one-dimensional morphological changes in rivers with non-uniform sediment, PhD thesis, Delft University, The Netherlands
- TERMES, A.P.P. (1986), Vertical composition of sediment in a dune. Report R657-XXXX, Delft Hydraulics, Delft, The Netherlands
- TISCHER, M., BURSİK, M. I. & PITMAN, E. B. (2001), Kinematics of sand avalanches using particle-image velocimetry. Journal of Sedimentary Research, 71 (3) pp. 355-364

Linking the bedload transport process and sorted sand gravel deposits in fluvial channels with dunes

Abstract

Subaqueous dunes, sediment transport and deposition in sand-gravel bed rivers are intimately related, as shown in this paper with flume experiments, field data and a behavioural model. The sediment mixture is vertically sorted in the channel bed by two processes. The first is by grain flows at the lee side of the dunes. Part of the resulting fining upward sequence of the largest dunes that occurred during a discharge wave, is preserved in the bed. The second process is grain size-selective entrainment and deposition in the dune troughs, which results in a second type of upward fining deposit (gravel lag deposit). These two types of deposits are the source for sediment entrained during the next discharge wave. The bedload sediment transport depends partly on grain size, and therefore on the relict vertical sorting left in the bed by former discharge waves, and on the depth from which the sediment is entrained. The entrainment and deposition depth of the sediment depends on the dune trough level below the average bed level and therefore on the dune height. Thus subsequent discharge waves of decreasing magnitude will leave the upward fining cross-bedded sets and gravel lag layers at depths related to the concurrent dune height. A discharge wave of high magnitude will reset the bed and leave a fresh upward fining deposit.

The importance and role of the two sorting processes in bedload transport and deposition is demonstrated with flume experiments, vibrocores done in the river Rhine (The Netherlands) and with sediment transport and bedform data in the river Rhine. A behavioural model is developed for the prediction of bed sediment reworking, vertical sorting and deposition by dunes. The model is applied to two subsequent discharge waves of different magnitude, and predicts the same vertical sorting characteristics as observed in the vibro-cores in the Rhine after two subsequent discharge waves. The outlines for further model development to include quantitatively the effect of the sorting on the sediment transport are discussed.

This chapter is based on:

Kleinhans, M. G. (2001). The Key Role of Fluvial Dunes in Transport and Deposition of Sand-Gravel Mixtures, a preliminary note, *Sedimentary Geology* Vol. 143 pp. 7-13

Kleinhans, M. G. (submitted). Subaqueous Dunes, Transport and Deposition of Sand-Gravel Mixtures: linking process and deposit in fluvial channels. Submitted to the conference proceedings of the 7th International Conference on Fluvial Sedimentology 2001, Nebraska, to be published as a Special Publication of the International Association of Sedimentologists, eds. Mike Blum and Sue Marriott.

9.1 Introduction

9.1.1 Relevance of sediment sorting and scope

This paper explores two types of sediment sorting in fluvial channel deposits in relation to dune development. The underlying objective is to determine the relation between antecedent sorting in channel deposits on the sediment transport of sediment mixtures. Flume experiments are used to identify sorting patterns and relations with transport, which are conceptually summarized. This concept is validated with field data from the river Rhine in two subsequent discharge waves. The deposits in the river bed are characterised based on recently collected vibrocores, and the sediment transport and dune characteristics have been measured. Finally, a behavioural model is developed for the sorting in the bed, and the necessary elements are identified which are necessary for a future mathematical model by which both the sorting patterns and the relation between this sorting and the bedload transport can be predicted.

In a number of publications it has been established that sediment transport and deposition in rivers with sand and gravel in the channel bed invokes consideration of the different sediment sizes and their sorting in the river bed (e.g. Klaassen 1987, 1991, Klaassen et al. 1987, Wathen et al. 1995, Wilcock 1993, 2001). In gravel-bed rivers without significant bedforms, the sediment transport can reasonably well be understood and modelled by considering the sorting in, and exchange between substrate sediment, surface sediment (active layer of a few grains thick) and transported sediment (Wilcock 2001). In sand-bed rivers with significant bedforms as the other limiting case, the sorting of the sediment is relatively unimportant. However, in sand-gravel-bed rivers with both large bedforms (dunes) and significant grain size variation, the sorting within the active layer becomes important and the sediment transport and deposition cannot be understood without considering the sorting of sediment within the dunes. Therefore the concept of a surface layer of several grains thick as an active layer is insufficient to capture the essential aspects of sediment transport and sorting in sand-gravel-bed rivers.

There has been some confusion about the definition of the surface layer (Kleinhans & Blom 2001). The definition of the surface layer depends on the time scale of interest. In Wilcock (2001) and elsewhere, the surface layer thickness scales with grain size. If, in the case of large dunes, the sediment transport variations over the dune length were studied, then the active layer again would scale with grain size (the thin layer of moving sediment over the dune). In the case presented in this paper on the other hand, the time scale is longer and envelopes significant changes in dune height, thus the surface layer thickness scales with dune height.

The importance of the dune height variation has been shown, in the sense that the sediment from below the transporting layer of dunes is entrained in the (deepest) troughs (Ribberink 1987). The sorting in the bed was modelled in two layers by Ribberink (1987), one transport layer and an exchange layer between the transport layer and the underlying sediment. The exchange layer represented the sediment entrainment and deposition for the deepest dune troughs, thus incorporating the trough-depth variation of natural dunes. However, the sorting within dunes was not modelled in the transport layer. Recently Parker et al. (2000) developed a mathematical morphological model concept with a continuous description of sediment sorting in the dunes and the bed (no layers like in Ribberink's model), but could not implement it because a general predictor for the sediment sorting in depth was not available.

A generic understanding of the sorting mechanisms is crucial for the further development of morphological models for sand-gravel-bed river channel behaviour. This paper attempts to find the necessary elements for a predictor of stratigraphy and sorting in channel bed deposits, addressing the topics of sorting in the transport layer and within individual dunes, and the role

of dune height variation in this sorting. Furthermore the effect of this vertical sorting in the channel bed on bedload transport is discussed.

9.1.2 Cross-bedded and lag deposits

Two types of deposits are distinguished genetically, based on Ribberink (1987) and Kleinhans (2001): the cross-bedded deposit with an upward fining sorting, and the lag-deposit. These types were found in the flume experiments described in the next section and are explained a priori for reasons of clarity.

1. Cross-bedded deposits (alternatively called foreset deposit) are formed by the propagation of the bedforms by discontinuous grain flows of bedload sediment at the lee side of a dune. The sediment is sorted vertically in the grain flow process (Fig. 9.1): the gravel is mainly deposited on the lower half of the lee slope, while the finer grades are predominantly deposited in the upper half. The result is an upward fining deposit. Allen (1963, 1970), Boersma et al. (1968), Kleinhans (2000) and many others in sedimentological literature found a distinct upward fining within subaqueous dunes in the laboratory and in the field, indicating that sorting in the grain flow plays an important role. Although this sorting principle related to grain flows is well known, a mathematical description of the process is not available. Bagnold (1954) proposed semi-empirical relations describing the velocity of grain flows in air. The stress distribution within the thin layer of each avalanche promotes a coarsening upward of the sediment within each stratum. This would allow the coarse sediment to roll down further. Hunter (1985) extended this work to subaqueous lee-side deposits, but referred only to well-sorted sand. Jopling (1965) developed a model for the composition of foresets (due to grain flows) and toesets (due to settling from suspension) at the lee side of a laboratory delta, but focussed mainly on conditions with significant suspension which is not relevant for gravel.

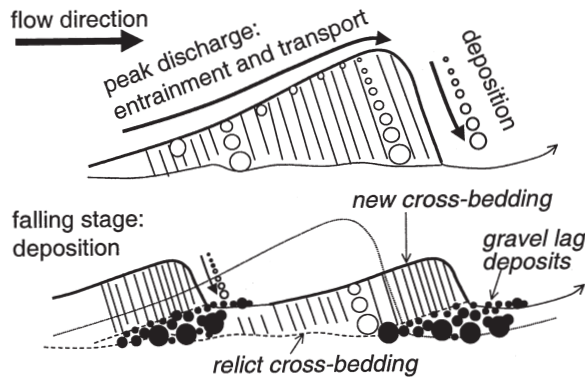


Figure 9.1. Hypothesized channel bed deposits based on literature. During peak discharge the transported sediment is sorted in the grain flow at the lee side of a dune. In waning discharge, the dunes diminish and leave cross-bedding relicts. Due to selective deposition, an upward fining accumulation of lag deposits is created in addition.

2. Lag deposits are formed as a result of size-selective entrainment and deposition during the different stages of a waning discharge wave. The largest grains that are in motion during the peak

discharge, will be deposited in lowering discharge while smaller grains remain in transport. This results in an upward fining accumulation of lag deposits without cross-bedding. Obviously the process of sorting in grain flows at the lee side of dunes may help to transfer the coarser grades down into the active layer (Fig. 9.1), but is distinguished here from the lag deposits by the (im)mobility of the grain sizes and the absence of cross-bedding.

The relevance of these two types of deposits are assessed with flume experiments in the next section.

9.2 Flume experiments

Three flume experiments have recently been done with a natural sand-gravel mixture in a flume of 50m long and 1.5m wide (T5, T7 and T9 in Blom & Kleinhans 1999, Kleinhans 2000, Kleinhans & Van Rijn 2002, see chapter 5). Basic data is given in Table 1. Uniform flow conditions were maintained to avoid large-scale erosion and sedimentation. The transported sediment was recirculated. The tests were continued until a morphological equilibrium was reached, which took a few days. T5 and T9 had approximately the same flow conditions (0.7 m/s), while T7 had a larger flow velocity (0.8 m/s). The bed shear stresses were just above the initial motion threshold of the coarsest sediment sizes for T7, while suspension of sand was negligible. The bed was not remixed after T5 and T7 but was allowed to develop further from the previous condition.

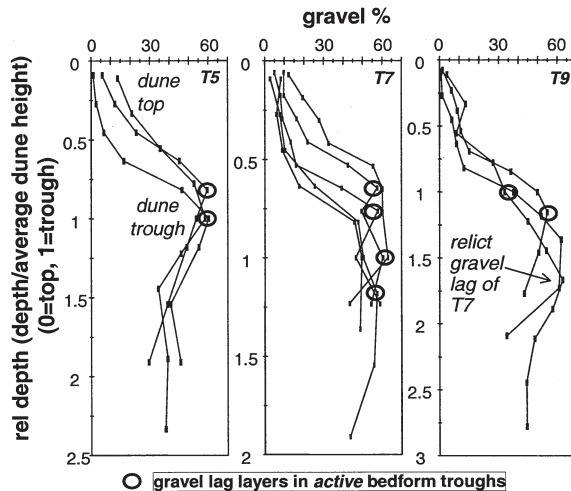


Figure 9.2. Vertical sorting measured in the dunes in the flume experiments (Kleinhans 2000), expressed as the gravel fraction in the sediment ($D_{\text{gravel}} > 2\text{mm}$, rest is sand). The depth of the dune troughs (and armour layers in T5 and T7) are given as circles. The gravel fraction clearly decreases to the dune top (upward fining). For T9 there is also a relict upward fining deposit below the dune trough level, which consists of relict cross-bedding and the accumulation of lag deposits (Fig. 9.1). For some cores, more than one gravel layer can be observed, which probably is the result of dune trough depth variation. Data from Blom & Kleinhans (1999).

In T5, the preferential entrainment of sediment finer than the bulk bed sediment led to the formation of a coarse layer (at the level of dune troughs, which is defined here as the level at which the bedform troughs on average occur, as opposed to the low-stage bed level (LSB) which is flat)

or armour layer below the propagating bedforms (Fig. 9.2) (Kleinhans 2000). Furthermore the sediment was vertically sorted in the dunes due to the grain flows. T7 had higher dunes, while the armour at the level of the troughs was lowered due to the winnowing of the extra sediment used to increase the dune volume. Comparable findings are presented by Klaassen et al. (1987) and Klaassen (1991). In T9 the largest particles from the dunes of T7 were only partially or no longer mobile. This led to a decrease of the dune height and deposition in the bedform troughs. Thus the armour layer of the previous experiment was buried below a fining upward lag deposit of fine gravel, seen in Fig. 9.2 as a fining upward trend below the dune trough level of T9.

The transport rate and composition is affected by the sorting in the bed, as revealed by sediment transport measurements. The sediment transport and the fraction of gravel in transport were the highest in T7, and were considerably different in T5 and T9 despite their equal flow velocities (Kleinhans & Van Rijn 2002, see chapter 5). The sediment transport in T9 was 15% higher than in T5, while the fraction of gravel in T9 was about the same factor lower (table 1). The entrained gravel of T5 and T7 were deposited in the troughs of the dunes in T9, and of course the finer sediment of T9 was more easily transported. This was also found by Klaassen et al. (1987) and Klaassen (1991).

Table 9.1. Basic data of the flume experiments presented by Kleinhans & Van Rijn (2002, see chapter 5) and Blom & Kleinhans (1999).

#	Condition	Hydraulic radius* (m)	Discharge (m ³ /s)	Flow velocity (m/s)	Water surface slope (10 ⁻⁴)	Total bedload transport (g/sm)	Final bed state
<i>bed was mixed and bed slope installed at -14.00 10⁻⁴</i>							
T5	incipient motion	0.19-0.23	0.22-0.26	0.69	-14.72	42.0 ± 0.4	small barchans over armour layer
T7	top speed	0.30-0.32	0.41-0.43	0.79	-15.20	66.0 ± 0.8	large dunes over armour layer
T9	incipient motion	0.22-0.25	0.26-0.28	0.70	-16.94	50.8 ± 0.6	large dunes over buried armour layer

*: corrected for side-wall roughness with the Vanoni-Brooks method

Summarizing, the vertical sorting and the dune development in T9 compared to T5 illustrate the importance of the history of the bed for both the sediment transport and the deposits. Under the high shear stress of T7, much more sand and gravel was entrained from the bed below the armour layer than in T5. This sediment thus still was available for transport in T9, while not in T5, because then it had not yet been entrained above the dune base. The experiments showed that a coarse layer is left in the bed that reflects the level of the troughs of the highest dunes in the recent past. The whole bed above this layer shows upward fining sets.

9.3 Deposition and transport concept

These findings are conceptualized as follows. The sediment sorting processes by dunes will affect sediment transport rates and composition and these two must therefore be linked (Kleinhans 2001). Furthermore, the concept must show how a channel deposit with an age in the order of a

decade can be composed of pluriform sets of different ages. As an outcome, it should explain history effects, i.e. variations in the composition of the bed sediment that is available for sediment transport during subsequent discharge waves. After validation of this concept with the field data (next sections), a quantitative behavioural model is constructed (later section in this paper).

The key element of the concept is the bedform height, which determines at which depth sediment is deposited (below the initial plane bed level), and from which depth the bed sediment is entrained. The maximum bedform height determines the depth of lowest level of gravel deposition in the bed, which yields a prediction of the depth of deposits in the bed. Lag layers are deposited at the trough level of dunes, and are preserved in lowering discharge when the dune height is decreasing. Thus the deposit above the lag layer can consist of more lag layers and cross-bedded deposits which are relicts of dunes (Fig. 9.1).

River bed sorting model with dunes in two discharge waves

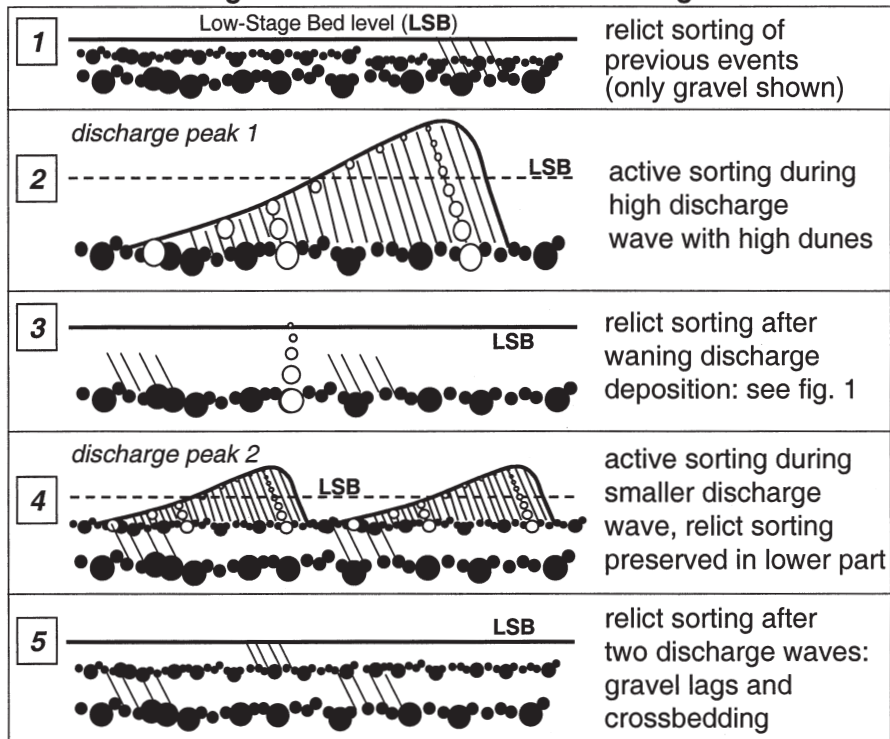


Figure 9.3. Conceptual model of sediment sorting with emphasis on the role of dunes in two subsequent discharge waves in order of decreasing magnitude (here only the gravel lag layers are shown, also see Figure 9.1). The smaller dunes of the second discharge wave erase part of the sorting due to the first wave, and leave a comparable but less deep vertical sorting.

These sorting patterns are erased by the dunes of a next discharge event, down to the depth of the deepest troughs of these dunes. For discharge wave in order of decreasing magnitude, all the deposits can therefore be preserved. Suppose that two subsequent discharge waves rework the river bed (no measurable net aggradation or degradation), and the first discharge wave is a large one (e.g. recurrence interval of ten years or so, panel 2 in Fig. 9.3) and the second is smaller (panel 4 in Fig. 9.3). The resulting deposit (panel 5) may consist of two lag layers, one at the trough depth of dunes which occurred in the first discharge wave (panel 3), and one at the trough depth of the

second. In between and above the lag layers, the channel bed may consist of both cross-bedded and lag deposits. In Fig. 9.3, only the lag layers are shown, which are the hypothesized result of two subsequent discharge waves of which the second one was smaller than the first one.

The bedload transport during one event will be affected by gravelly layers deposited in a previous event as follows:

- In rising discharge, the bedforms attempt to lower their troughs through a relict gravelly layer.
- As a consequence, this gravel is being incorporated in the active layer.
- Thus the sediment available for transport (i.e. transport layer) is relatively coarse, and the bedload transport rate consequently is relatively small.
- In lowering discharge, the gravel is worked down deeper into the active layer by the grain flow process and in the form of lag deposits.
- While the dunes become lower and rework an increasingly shallower active layer, the gravel layers are abandoned and the transport layer becomes finer.
- As a result of the fining of the transport layer, the bedload rate in falling stages is relatively larger than in rising stages, leading to a hysteresis of bedload rate as a function of discharge.

The bedload transport (capacity) in turn affects the sorting of the bed. If the transport capacity of gravel is high enough to transport all available gravel in the dune layer, then a gravel layer in the dune troughs will not be very thick. Thus bedload transport capacity, availability of sediment in the dune layer and vertical sorting in the deposits are intimately linked.

On the time scale of several discharge waves (decade), the characteristics of the bed sediment that is available for entrainment in subsequent discharge events can be predicted, starting from the vertical sorting of the largest previous discharge wave in the relevant time span as a boundary condition (Kleinhans 2001). A significant effect of the sorting is expected on bedload transport rate and composition over several years. If the net sorting in the river bed as a result of many discharge waves is fining upward, then it can be expected that the small discharge waves have relatively higher bedload transport rates and finer bedload sediment than the large discharge waves. This might have a significant effect on the sediment transport averaged over decades, compared to computations based on fully mixed bed sediment of constant composition.

Summarizing, sorting patterns (with most outstanding the gravelly lag layers) of subsequent discharge waves are preserved in the channel bed if the discharge waves occur in order of decreasing magnitude. The bedload transport rate during one discharge wave is expected to show hysteresis due to the difference in vertical sorting before and after the discharge peak. Also between subsequent discharge waves, transport rates change due to antecedent sorting. These are new extensions of the work of Klaassen (1987) and Klaassen et al. (1987), which should be applied in a model like the one described by Parker et al. (2000) for the case of rivers with dunes.

9.4 Test of the concept with data from the river Rhine

9.4.1 Field site description

The concept outlined above is tested with data collected in the river Rhine, using vibro-cores of the channel bed (TNO-NITG 2000), statistics on dune dimensions and propagation in 1995 and 1998, as well as suspended and bedload sediment transport during the discharge wave in 1998

(Kleinhans 1999, Wilbers 1999, Kleinhans 2000, Kleinhans & Ten Brinke 2001, see chapter 3). These datasets were all collected near the bifurcation Pannerdensche Kop, where the Rhine spits into a large branch, the river Waal (two thirds of the discharge) and a small branch, the Pannerden Channel (one third of the discharge, Fig. 9.4). The Rhine upstream of the bifurcation point is called Bovenrijn. The sediment at that point consists of sand and gravel with $D_{50} = 2\text{mm}$ and $D_{90} = 14\text{mm}$. The basic data for 1995 and 1998 are both given in Table 9.2.

Table 2a. Depth- and width-averaged flow parameters and sediment transport in the river Waal.

Date and time	Flow discharge Waal	depth-averaged velocity	Chezy	Shear velocity u^*	Roughn. length ks	flow depth	Susp. load	Bed load transp	bed load sand	bed load gravel
	(m^3/s)	(m/s)	($\text{m} \wedge 0.5/\text{s}$)	(m/s)	(m)	(m)	($\text{g}/\text{s}/\text{m}$)	($\text{g}/\text{s}/\text{m}$)	($\text{g}/\text{s}/\text{m}$)	($\text{g}/\text{s}/\text{m}$)
10 31 98 01:55:43 PM	3993	1.61	50.6	0.098	0.17	9.2	476	130	80	50
11 02 98 01:27:51 AM	5032	1.70	40.5	0.126	0.65	9.7	650	214	141	73
11 03 98 05:21:26 AM	5741	1.80	39.7	0.137	0.76	10.2	737	181	122	59
11 05 98 01:04:17 AM	6097	1.86	38.9	0.129	0.88	10.7	715	201	144	57
11 05 98 10:38:34 AM	5891	1.79	39.3	0.124	0.83	10.5	606	234	171	63
11 07 98 02:45:00 AM	5114	1.62	40.9	0.115	0.65	10.1	351	230	148	82
11 09 98 05:53:34 AM	4198	1.51	39.1	0.117	0.76	9.4	199	264	181	83
11 10 98 02:12:51 AM	3899	1.48	39.4	0.112	0.72	9.2	143	269	197	71
11 12 98 01:40:43 PM	3407	1.42	44.4	0.092	0.35	8.7	83	291	222	69
11 12 98 06:34:17 PM	3372	1.42	44.5	0.092	0.35	8.6	83	291	222	69

Notes

- Flow parameters (except discharge) and suspended sediment transport were measured with the Acoustic Sand Transport instrument ASTM (Kleinhans and Ten Brinke 2001).
- Calibration factor of Helley Smith: 2.74 (so all samples multiplied with this factor to obtain transport given herein).
- Data from Kleinhans (1999)

Table 2b. Dune parameters and bedload transport from dune tracking in Waal and Bovenrijn.

Date	Waal			Bovenrijn			dune celerity (m/day)	dune length (m)	dune height (m)	dune track length (m)	dune track bed load (g/s/m)	dune track bed load transp (m ² / day)	dune track bed load transp (m ² / day)	dune track load (g/s/m)
	Flow discharge (m ³ /s)	dune height (m)	dune length (m)	dune celerity (m/day)	dune track bed load transp (m ² / day)	Flow discharge (m ³ /s)								
30-10-98	3166	0.12	3.29	250	3	59	4783	0.34	7.84	120	19	19	313	
31-10-98	4056	0.12	3.93	210	3	55	6180	0.48	10.97	61	18	18	311	
02-11-98	5363	0.22	6.76	70	5	76	8119	0.72	15.99	57	20	20	341	
03-11-98	5946	0.34	8.39	93	14	233	9045	0.90	19.99	55	22	22	379	
04-11-98	6168	0.47	10.87	73	15	261	9464	0.98	21.92	51	22	22	378	
05-11-98	6002	0.53	13.09	59	14	233	9149	1.07	24.30	41	20	20	337	
06-11-98	5536	0.53	17.75	45	12	197	8267	1.13	26.03	31	16	16	264	
07-11-98	4863	0.49	8.65	80	13	217	7273	1.19	29.16	25	13	13	223	
10-11-98	3770	0.30	6.57	130	17	290	5640	0.92	32.30	18	8	8	128	
12-11-98	3436	0.29	6.31	105	14	240	5122	0.27	6.80	108	12	12	205	
13-11-98	3267	0.28	6.07	105	14	243	4851	0.26	6.68	110	12	12	204	
16-11-98	3045	0.31	5.98	119	17	287	4522	0.29	6.60	111	14	14	239	
19-11-98	3042	0.20	5.58	110	7	126	4527	0.23	7.52	96	11	11	181	

Notes

- Unit of transport g/s/m: grammes per second per meter width. Density of sediment including pores is 1460 kg/m³.
- Small dunes become active (and large inactive) on 7 November in the Waal and on 12 November in the Bovenrijn.
- From this date on, the parameters of the small dunes are given.
- Data from Wilbers (1999)

In 1995 the largest discharge wave of the past decades occurred, in 1997 a small discharge wave occurred, and in 1998 a bigger one occurred, and between 1998 and the moment of vibro-coring, no significant discharge wave occurred. (The discharge was determined daily from water levels and calibrated relations between discharge and water level throughout the years).

It is important to keep in mind that the river Rhine has been affected by engineering works throughout the last centuries. One important aspect is the construction of groynes to increase the flow strength in the low-stage channel, resulting in deeper channels from which ships and barges

benefit. The effect also was that the flow strength during discharge peaks was increased, and therefore the mobility of the sediment, the dune height, the sediment transport, etc. In reaction, the river bed eroded and coarsened. Thus there is much more coarse sediment in the active river bed than is expected on basis of the composition of the channel belts in the Rhine delta.

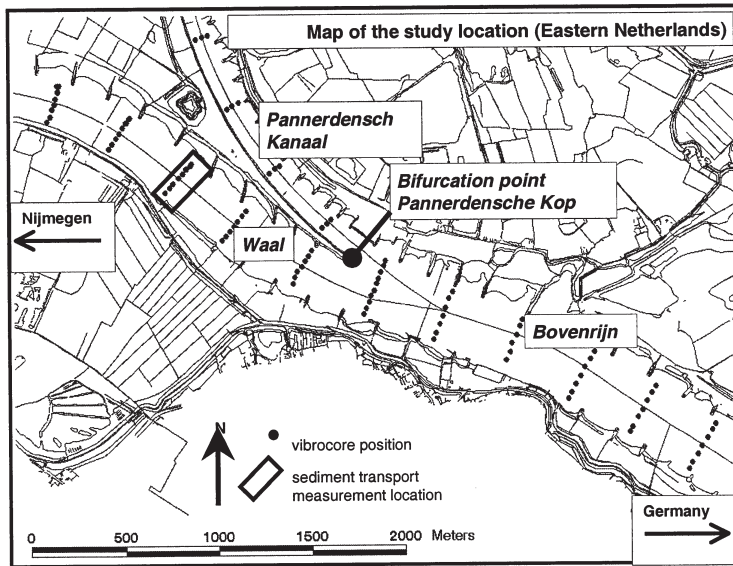


Figure 9.4. Map of the measurement positions of direct sampling of the sediment transport and flow in the river Waal and of dunetracking in the Waal and Bovenrijn, as well as the vibro-core positions. The whole area was mapped with multibeam echosounders. The numbers at cross-sections are river kilometers.

Nevertheless this study may be relevant for other rivers than the Rhine because there are many rivers in the world that have been affected by comparable engineering works with comparable goals and effects. Also, there are many rivers reaches with sand and gravel in the bed along a considerable length in between the upstream gravel river and downstream sand-bed river. Large sections of the rivers Rhine, Meuse (The Netherlands), Rhone, Allier (France), Fraser (Canada), Elbe (Germany), Mississippi (United States of America) and the Nile (Egypt) for example, have both sand and gravel in the bed. These are all large systems, in which dunes may occur simultaneously with sorting effects and armour layers. In the Dutch Rhine, significant amounts of gravel (circa 60-20%) are present in the bed over distances as far downstream of the Dutch-German border as 60 kilometers in the Waal and 25 kilometers in the IJssel.

In addition, the man-induced narrowing of the channel has the coincidental effect that the dunes are very two-dimensional and regular in length and height. This has the advantage that the dunes in the river Rhine can well be represented by the average dune height in many applications.

9.4.2 Dune height and sediment transport measurements

The bedform dimensions were obtained from three-dimensional echo soundings. The echo soundings of 1998 were also used for dunetracking to estimate the bedload transport rate from the propagation and dimensions of the dunes with the method of Ten Brinke et al. (1999). Both the bedload sampling method with the Helley Smith type sampler and the dunetracking method in 1998 show small bedload transport rates (of sand plus gravel) at rising stage and large transport at falling stage (Fig. 9.5), i.e. a considerable hysteresis. At falling stage the transport measured with the Helley Smith and determined with the dunetracking method remained more or less constant and large for days while the flow velocity decreased. The measurements with the Helley Smith have a high accuracy: the uncertainty of cross-channel averaged sediment transport related to natural variability and due to the sediment transport measurement methods is 15-20% (Kleinhans & Ten Brinke 2001, see chapter 3).

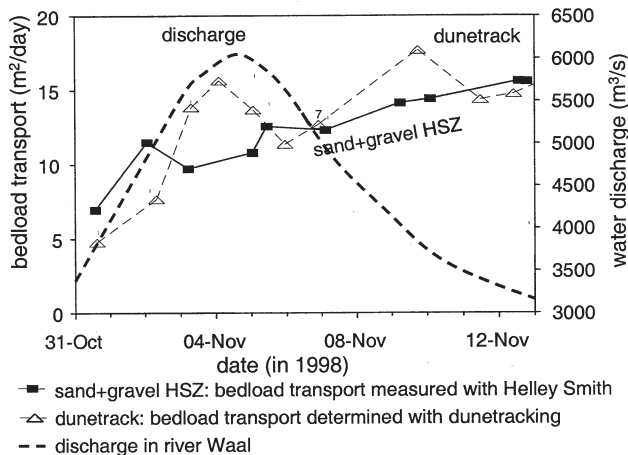


Figure 9.5. Measured sediment transport in the Waal during the discharge wave of 1998, given as total bedload divided by channel width. The measurements with the Helley Smith type bedload sampler (HSZ) have also been split in the gravel and sand bed load transport.

The bedload sediment was slightly bimodal with mode diameters of 0.5 mm for sand and 10 mm for gravel, allowing a convenient division between sand and gravel. The bedload at rising stage consisted of 60% sand and 40% gravel, while it became sandier during falling stages, with the sand content rising to 75% near the end of the discharge wave (Kleinhans 1999, 2000). Thus, the bedload transport was larger after the discharge peak than before. This relative rise was solely due to the absolute rise in rate of sand transport, since the rate of gravel transport decreased after the discharge peak. This observation agrees with the hypothesis derived from the sorting concept that the bedload transport during one discharge wave should show hysteresis.

However, the hysteresis observed in the river Rhine is much larger than that observed in the flume experiments, and than can reasonably be expected from differences in grain sizes (bedload predictors are not overly sensitive to grain size). It is likely that other factors amplify the hysteresis. The possible causes of this hysteresis are discussed in detail in chapter 6 and are summarized here. For lack of more definite data or modelling, the explanations remain hypothetical to some extent. A key point to be kept in mind is that in the Rhine upstream of the bifurcation point, the hysteresis in bedload (measured with the dunetrack method) was opposite

to that in the lower Rhine branch. The causes of hysteresis are as follows:

1. Hydraulic roughness hysteresis due to dune development hysteresis (cf. Allen and Collinson 1974) may contribute to the hysteresis as follows. The tardy reaction of large dunes to changing flow causes a time lag (c.q. hysteresis) between dune height and flow discharge. Thus the dune height is larger after the discharge peak than before. The energy that is available for the bedload transport is the difference between the total energy (total bed shear stress) and the dissipated energy by dunes, while higher dunes generally dissipate more energy. At some point after the discharge peak, secondary dunes emerge superimposed on the primary dunes (chapter 6), and are no longer destroyed as they arrive at the top and lee side of the primary dunes. This means that there is probably no flow separation related to the primary dunes and that their hydraulic roughness is negligible. Thus the hydraulic roughness is lower than it was before the discharge peak, and there is more energy available for the transportation of bedload after the discharge peak, leading to counter-clockwise hysteresis of the bedload transport rate. The suspended load transport on the other hand is larger before the discharge peak (clockwise hysteresis) because the suspension depends on the turbulence generation by dunes.
2. Vertical sorting of bedload sediment in the dunes combined with the dune height development hysteresis causes hysteresis as follows. Because the dune height is lagging behind the discharge, the bed shear stress in falling stages is lower than it was before the discharge peak at the same dune height. Due to the lower bed shear stress, the gravel is worked down to form a lag deposit. As the dunes further diminish in height, this gravel layer is abandoned. As a result, the sediment in the transport layer is finer than it was before the discharge peak. This leads to higher sediment transport rates after the peak than before, i.e. counter-clockwise hysteresis.
3. The erosion of fine sediment from sand deposits below the active river bed at a location upstream of the measurement section may lead to hysteresis as follows. This fine sediment moves downstream as a sand wave, and is more easily transported than the sand-gravel mixture in the active river bed. Depending on the arrival time of the sand wave (and thus the measurement location), clockwise or counter-clockwise hysteresis of bedload results.

Presumably all these hypotheses together are responsible for some part of the hysteresis. The first hypothesis should be tested with a mathematical turbulence model for flow over bedforms, which is outside the scope of this paper. Only the last hypothesis is able to explain why the hysteresis in the Rhine-branch (Bovenrijn) upstream of the bifurcation point is opposite to that in the lower branch (Waal). However, there are no measurements that could indicate the plausibility of a migrating sand wave, therefore this hypothesis remains unfounded for the time being. Since neither of the processes responsible for the hysteresis are incorporated in the model presented in this paper, it is not expected that the hysteresis of bedload transport is correctly hindcast by the model. Yet the model presented later in this paper is a first step towards a model that can also predict the bedload transport correctly.

9.4.3 Gravel lag layers

In each cross-section, 7 vibro-cores were collected at 140, 100, 50 and 0 m on both sides of the river axis in the Bovenrijn, and 100, 67, 33 and 0 in the Waal. This was done in 5 cross-sections

in the Bovenrijn, and in 6 cross-sections in the Waal, which were all 400m apart (Fig. 9.4). The vibrocoreing was done with a modern technique, which gives less disturbances in the cores due to fluidization and vibrations than with previous methods (Dr. A. Bosch, TNO-NITG, pers. comm. 2000). This allows the determination of details like vertical sorting, armour layers and some cross-bedding. Coarse layers could be identified in the cores (Fig. 9.6), although differences between lag layers and cross-bedding were not clear due to the relatively small width of the cores and the disturbance of the sedimentary structures. The depths of the bottom of these layers below the top of the cores were measured, rounded to 0.1 m accuracy, and are given as frequency distributions for the Waal and the Bovenrijn (Kleinhans 2001). The total depth of the vibro-cores often exceeded 3 m below the low stage plane bed.

From the measured dune height, the likely depth of gravel lag deposition can be estimated. This estimate will be compared here to the observed depth of gravel lags in the cores. Dunes can be seen as more or less triangular bed level fluctuations around the low stage bed level (LSB), with the troughs at 0.5 times the dune height below the LSB, and the tops at 0.5 times the dune height above the LSB (Figs 9.1 and 9.3). The observed level of the troughs below the LSB (0.30 m), as compared with the concurrent dune height of 1998 in the Waal, verifies this relation. When the vibro-cores were taken, the relict dunes of previous discharge waves had been eroded and the river bed was plane. Thus, the level of the troughs is 0.5 times the dune height below the low stage plane bed. With the echo-soundings, no measurable net erosion or aggradation was found.

The gravelly layers are expected at that same depth of 0.5 times the dune height below the LSB. Since the dunes are slightly convex and the dune height is rather variable with a standard deviation of 0.1 m, it may be expected that the deeper troughs of the larger dunes cause the coarse layer to sink somewhat lower than 0.5 times the height of the dunes. Furthermore, dunes can be expected to be somewhat assymmetric with deeper troughs and less high tops. However, for the very regular two-dimensional dunes of the river Rhine these variations are small (shown later). The coarse layers from the trough levels of the largest dunes of 1995 and 1998 are thus predicted at 0.5 to 0.6 times the dune height below the top of the vibrocores (table 3).

Table 9.3. Predicted and observed depths (in m \pm 0.1m) below the low-stage bed level of gravel layers in the Rhine branches for two subsequent discharge waves.

year of discharge wave	Bovenrijn duneheight	Bovenrijn predicted	Waal observed	Waal duneheight	predicted	observed
		gravel layer depth			gravel layer depth	
1995	1.5	0.8	0.7	1.4*	0.6*	0.7
1998	1.0	0.5	0.3	0.6	0.3	0.3

* In 1995 no dune height measurements were done in the Waal. The dune height used here is estimated from the measured dune heights in 1993, during a comparable discharge wave. The maximum reach-averaged bedform height in the Waal was 0.6 m in 1998. The maximum reach-averaged bedform height in the Bovenrijn was 1.0 m in 1998 and 1.5 m in 1995. In 1995 no echo soundings were done at the measurement location but from measurements done in 1993 at more or less the same discharge peak both upstream and downstream of the measurement location, a probable maximum dune height of 1.4 m is obtained.

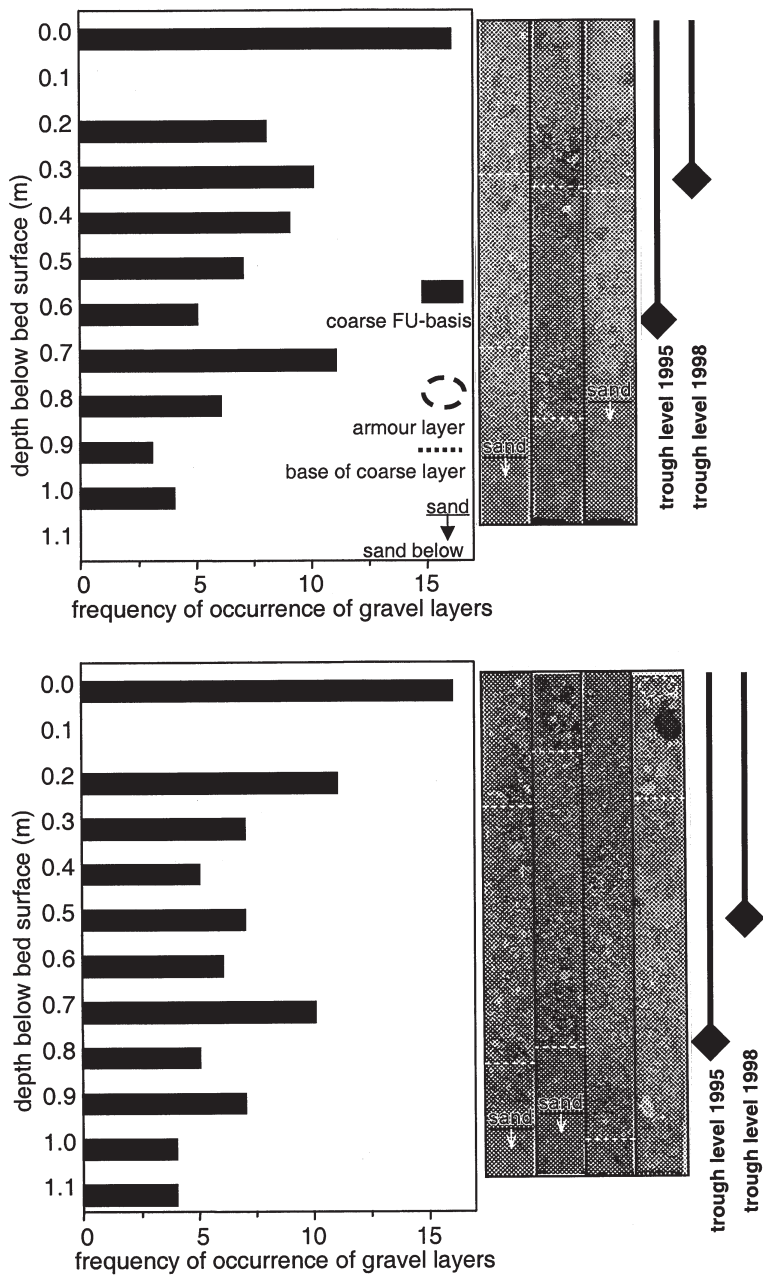


Figure 9.6. Observations of the deposits in the river Waal (a) en Bovenrijn (b). The depths of the gravelly layers were measured and used for the histograms (given as the frequency of gravel layer occurrence in the total number of used borings: 35 in Bovenrijn and 42 in Waal). A few examples of vibro-cores are given, which show the gravel layers. The gravel layers at the bed surface are armour layers, while the lower gravel layers are interpreted as the bases of relict cross-bedding and lag deposits (Fig. 9.1). The lower gravel layers are dominantly found at the depth of dune troughs observed during the discharge waves of 1995 and 1998 (Fig. 9.2).

The depths of the gravel layers were determined in all vibro-cores, including the gravelly bases of upward fining, often cross-bedded sets. A histogram was made of the number of gravel layers in the cores occurring at depths between 0 and 0.1m below the bed surface, 0.1 to 0.2m, etc. m below the bed surface (Fig. 9.6, Kleinmans 2001). Two maxima are found in both the Bovenrijn and the Waal (Fig. 9.6 and table 3). It can be concluded that the observed depth of these layers is about the same as that predicted from the dune heights of 1995 and 1998, which corroborates the conceptual model.

Concluding, the gravel layers in the field can indeed be related to dune trough depth as predicted by the concept. Differences in transport between several discharge waves could not be studied for lack of consistent field datasets in subsequent discharge events. The next step herein is the development of a more quantitative behavioural model.

9.5 Behavioural model of vertical sorting

9.5.1 Model rationale

A behavioural model for the prediction of vertical sorting in the river bed is described below. It predicts the potential for the formation of gravel lag layers and the fining upward pattern in channel deposits as a result of two discharge waves. The objective for modelling is to hindcast the sorting in the river Rhine for the discharge waves of 1995 and 1998, and determine the relative importance of cross-bedding and gravel lag layer deposits.

It is assumed that the dunes for a certain condition have no significant variation in trough depth, i.e. are extremely regular, which seems reasonable for the Rhine but will be discussed later. An active layer is herein defined as half the dune height in depth, where the dune height is predicted from flow parameters and empirical dune height predictors which provisionally include the dune height hysteresis during discharge waves. For simplicity, the sediment is represented in only two grain size fractions: sand and gravel. Two depositional units are modelled: the cross-bedded deposit with a linear upward fining sorting (linear decrease of gravel content in upward direction), and the lag deposit (deposit of gravel only).

The cross-bedding is assumed to be preserved over the full depth of the active layer in the bed (details explained below), except when a certain portion of the active layer is filled with lag deposits (from base upwards). A highly simplified method for the prediction of lag deposits is followed here. From flow parameters, the bedload transport capacity of that flow is predicted (with the method of Kleinmans & Van Rijn 2002, see chapter 5, details explained below). The bedload transport sediment composition is compared to that of the transport layer at the same moment. If there is more gravel present in the transport layer than can be transported by the flow, then the difference is potentially available for the formation of a gravel lag layer.

This model is only intended to predict the sediment sorting in the channel bed and serves to illustrate the potential importance of gravel lag layers in the channel deposits, but cannot be used for accurate quantitative modelling of the sediment transport. The reason is that bedload predictors always predict that bedload sediment is finer than bed sediment (except for extremely high discharges). Given enough time, the process would therefore detrain all gravel, which is not realistic. Furthermore, in this model it is assumed that the gravel lag layer forms instantaneously, and is (for increasing dune height) instantaneously entrained into transport in the next time step. Obviously the deposition and entrainment processes take time in reality. In point of fact, the entrainment of a gravel lag layer by growing dunes may be so difficult that it causes the previously discussed hysteresis of bedload transport. The bedload transport computation in the model will not give

hysteresis, since this effect is not incorporated in this simplified behavioural model. However, the prediction of potential gravel lag layers will indicate how relevant lag layers transport in reality may be for bedload transport (as argued in previous sections). Below, the equations and predictors in the model are given, and finally the model is applied to the river Waal for the discharge waves of 1995 and 1998.

9.5.2 Model description

In short (Fig. 9.7), the model 1) computes flow parameters, 2) predicts the dune height, 3) derives the transport layer from the dune height, 4) sorts the sediment vertically in the transport layer, 5) predicts the bedload transport from the grain-related shear stress and the sediment in the transport layer, and 6) deposits the gravel that cannot be transported in a lag deposit at the base of the transport layer. The input and output parameters are summarized in table 4.

Table 9.4. Input and output parameters of the model for sediment transport and deposition.

Input	Output
flow discharge	dune height
depth-averaged flow velocity	bedload transport of sand and gravel
water depth	depth and thickness of gravel lag layers
grain size distribution of average bed sediment	vertical sorting between and above gravel lag layers

The transport layer thickness is calculated from the (average) dune height (H) as 0.5 H. The choice of the average dune height (rather than the 90th percentile of the dune height distribution as representing the deepest scour depth) is evaluated later. The dune height is usually observed to lag behind the discharge wave: the dune height before the discharge peak is smaller than after the discharge peak, leading to a hysteresis. The dune height is therefore predicted including this hysteresis of dune height as follows. During rising discharge, the dune height lags behind the changing flow, and the dune height is computed with an empirical predictor derived from measurements of 1995, 1997 and 1998 discharge waves:

$$H_{\text{rise}} = h 0.025 (D_{50}/h)^{0.3} T^{1.7}$$

(in m). For falling discharge the dune height predictor of Van Rijn (1993) is used (cf. Wilbers, this issue):

$$H_{\text{fall}} = h 0.11 (D_{50}/h)^{0.3} (1 - e^{-0.5T})(25 - T),$$

(in m) in which the D_{50} is the median grain size of the average bed sediment. The transport parameter T (Van Rijn 1984) is:

$$T = (\tau' - \tau_{cr}) / \tau_{cr}$$

(dimensionless) with τ_{cr} based on the Shields criterion of the D_{50} of the average bed sediment.

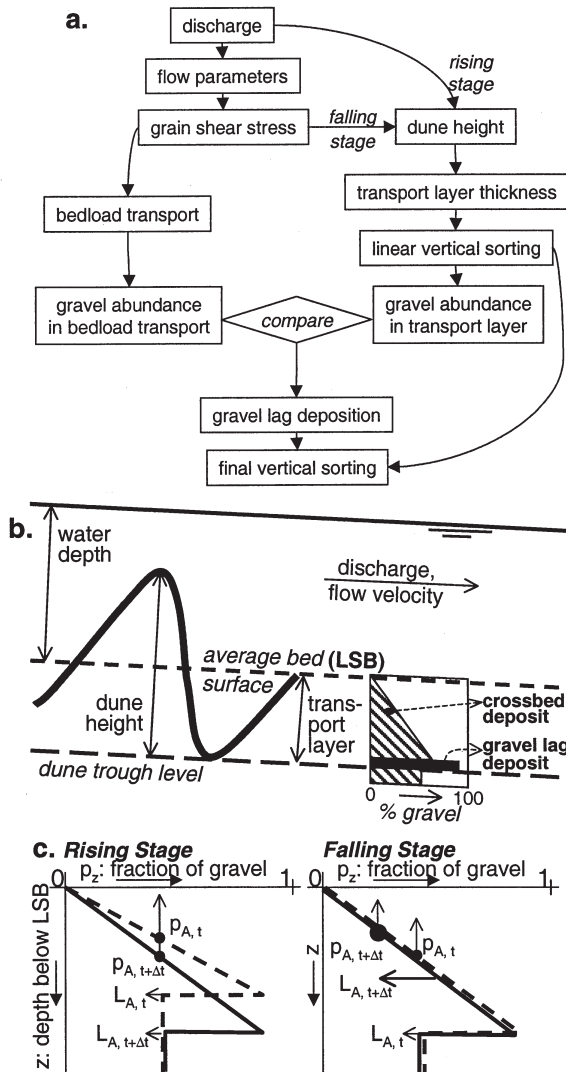


Figure 9.7. The structure of the behavioural model for bedload transport and vertical sorting (a), a sketch of the principal parameters (b), and the different response of cross-bedded sorting in the model in rising and falling stage (c). In rising stage, the sorting is worked down deeper in the bed, while in falling stage, only the active part of the antecedent sorting is reworked, leading to the same sorting curve but a lower gravel abundance in the active layer ($p_{A, t+\Delta t}$).

The grain shear stress τ' is based on the grain roughness as follows (Van Rijn 1984):

$$\tau' = \rho g (u/C')^2,$$

(in $N\ m^{-2}$) in which the Chezy grain roughness coefficient (C') is computed from the White-

Colebrook equation:

$$C' = 18 \log(12h/k'_s),$$

(in $m^{0.5} s^{-1}$) in which the Nikuradse grain roughness length is given as $k'_s = D_{90} = 0.012m$ with the D_{90} of the average bed sediment.

Although the trend of the dune height during lowering discharge is thus predicted well, the dune height itself is systematically overpredicted (Wilbers, this issue) in the Waal. The reason is the time needed for adaptation of the dune dimensions; the actual dune height attained at the discharge peak is lower than the equilibrium dune height at the same discharge. Therefore the second expression for dune height is matched to the first to give the same dune height at peak discharge.

9.5.3 Bedload transport prediction

The grain-related shear stress and the D_{50} and gravel abundance in the transport layer are the input parameters for the prediction of bedload transport for each size fraction with a Meyer-Peter and Mueller (1948) type predictor, adapted for grain size fractions and accounting for near-bed turbulence according to Kleinhans & Van Rijn (2002, see chapter 5) (explained below):

$$q_{b,i} = p_i 5.7 \sqrt{\left(\frac{\rho_s - \rho}{\rho} \right) g D_i D_i (\theta'_i - \xi_i \theta_{cr,D50})^{1.5}}$$

(in $m^3 m^{-1} s^{-1}$), in which the subscript i denotes the gravel or sand fraction, the Shields parameter is:

$$\theta'_i = \tau' / [(\rho_s - \rho) g D_i]$$

(dimensionless) with ρ_s = density of water or sediment (in $kg m^{-3}$) and g = gravitational acceleration $g = 9.81$ (in $m s^{-2}$), and the dimensionless critical Shields criterion for the D_{50} of the bed sediment,

$$\theta_{cr,D50} = \tau_{cr,Shields} / [(\rho_s - \rho) g D_{50}]$$

is derived from the Shields curve. The sand abundance (p_{sand} , p = fraction, 100 p = percentage) is by definition $p_{sand} = 1 - p_{gravel}$. The Shields criterion is corrected for hiding-exposure effects for each size fraction with ξ_i . The gravel grains are more exposed to the flow, compared to a bed with uniform gravel only, while the sand grains hide in the lee of the gravel grains. Thus the gravel grains are more mobile in a mixture and the sand grains less mobile than in uniform sediment. The hiding-exposure correction of Egiazaroff (1965) is used here, following Kleinhans & Van Rijn (2002):

$$\xi_i = \frac{1.66667}{\left[\log \left(19 \frac{D_i}{D_{50}} \right) \right]^2}$$

in which D_i either refers to the sand or the gravel fraction.

9.5.4 Sorting modelling

In the model, the average bed level (equal to the initial plane bed level) is at vertical coordinate $z=0$ (Fig. 9.7), and z is positive in the downward direction. The gravel fraction is actually computed, and, remembering that $p_{sand} = 1 - p_{gravel}$ the composition of the active layer is known. Initially, a completely uniform distribution of gravel in the vertical direction in the bed is assumed:

$$dp_z / dz = 0,$$

in which p is the fraction of gravel. The active layer thickness (L_A) at time t is computed from:

$$L_{A,t} = 0.5 \Delta_t.$$

Now the available gravel is linearly distributed over the depth of the active layer (L_A below $z=0$):

$$dp_z / dz = p_{A,t} / (0.5 L_{A,t}),$$

in which $p_{A,t}$ is the depth-averaged gravel fraction in the active layer at time t . The factor 0.5 determines that the gravel fraction at $z = 0.5 L_{A,t}$ is equal to $0.5 p_{A,t}$, because the depth-averaged gravel fraction in a linear distribution is by definition equal to p_z at $z = 0.5 L_{A,t}$. Obviously, this only works for gravel fractions smaller than 50%, which is the case in the application of this model in this paper. Otherwise, the additional constraint is that $0 < p_z < 1$ for all z .

In time, the dune height and active layer thickness change. In the active layer at $t + \Delta t$, only the sediment in the new active layer is assumed to be entrained from the sorted bed from the previous time step. To calculate the depth-averaged gravel fraction (p_A) of the new active layer, the gravel abundance ($p_{z,t}$) is therefore averaged over the depth of the new active layer at $t + \Delta t$:

$$p_{A,t+\Delta t} = \frac{1}{L_{A,t+\Delta t}} \int_{z=0}^{L_{A,t+\Delta t}} p_{z,t} dz$$

Now the vertical sorting (p_z) in the channel bed at $t + \Delta t$ is computed as:

$$p_{z,t+\Delta t} = \begin{cases} p_{z,t} & \text{for } z > L_{A,t+\Delta t} \\ \frac{dp_{z,t+\Delta t}}{dz} z = \frac{p_{A,t+\Delta t}}{0.5 L_{A,t+\Delta t}} z & \text{for } z \leq L_{A,t+\Delta t} \end{cases}$$

in which the first line accounts for antecedent gravel abundance below the active layer, and the second line for the linearly distributed gravel which is sorted anew for time $t + \Delta t$.

Now the gravel lag layer can be modelled. First, the bedload sediment transport rates of sand, gravel and total (sum of sand and gravel) are predicted, based on the depth-averaged fractions, using $p_{A,t+\Delta t}$ for gravel and $1 - (p_{A,t+\Delta t})$ for sand. The gravel abundance $f_{A,g}$ that can potentially be transported by the flow (and depth-averaged in the transport layer) is computed with:

$$f_{A,g} = q_{b,gravel} / q_{b,total}$$

in which the bedload transport q_b for sand and gravel is computed with the bedload predictor described in the previous section for each time step t . The gravel that is potentially transported by the flow can now be compared to the gravel actually present in the active layer, to find the gravel fraction p_L that will potentially form a gravel lag layer:

$$P_{L,t} = P_{A,t} - f_{g,A,t}$$

This value is used to compute the potential gravel lag layer thickness per unit width and length in the channel bed deposit. Assuming that a gravel lag layer consists of gravel only ($p=1$), the thickness L_G of the potential gravel lag layer can be computed as:

$$L_{G,t} = P_{L,t} L_{A,t}$$

This gravel layer is then deposited in the model at depth $(L_{A,t} - L_{G,t}) < z \leq L_{A,t}$, so the final sorting in the model becomes then:

$$p_{final,z,t+\Delta t} = \left[\begin{array}{l} p_{z,t} \text{ for } z > L_{A,t+\Delta t} \\ \frac{dp_{z,t+\Delta t}}{dz} z = \frac{P_{A,t+\Delta t}}{0.5L_{A,t+\Delta t}} z \text{ for } z < (L_{A,t+\Delta t} - L_{G,t+\Delta t}) \\ 1 \text{ for } (L_{A,t+\Delta t} - L_{G,t+\Delta t}) \leq z \leq L_{A,t+\Delta t} \end{array} \right]$$

in which the first line accounts for antecedent gravel abundance below the active layer, the second line for the linearly distributed gravel which is sorted anew for time $t+\Delta t$, and the third line for the gravel lag deposition ($p_{gravel} = 1$).

Obviously, the resulting distribution of gravel in the model does not conserve the mass of the gravel completely, since it adds gravel to the sediment in the gravel lag layer but does not subtract this amount from the gravel abundance in the active layer. The reason is that no transfer function is known and has been specified for working down the gravel from the foresets to the lag deposits, and therefore it is not known how to subtract the lag gravel from the cross-bedded gravel units. However, this error does not propagate in the model, because the composition of the active layer p_A at $t+\Delta t$ is not computed from $p_{final,z,t}$ but from $p_{z,t}$ in which this gravel has not yet been added. For future purposes of bedload transport and morphological modelling, mass must obviously be conserved.

The model was implemented in a spreadsheet. The vertical grid spacing and time step were chosen such that the change in lag deposit thickness is smaller than the grid spacing for all time steps to prevent unrealistic gaps in the lag deposits. In this case, a vertical grid spacing of 13 mm, which is about equal to the D90 of the sediment mixture. Gravel lag layers thinner than 13 mm have been truncated. The time step was one day.

The 'potential' nature of the gravel lag layer is emphasized here: in reality the potential thickness of gravel lag layers will probably not be attained due to a number of causes, among which the variability of dune height and trough scour, and the time needed to work the gravel down while the discharge and dune height are changing faster. Most importantly, in the prediction of sediment transport composition based on flow parameters and on active layer sediment composition, the predictor always predicts less gravel to be in transport than in the active layer (see details of prediction below). If this process were allowed to continue for a long time, the model concept presented here would eventually work down all the gravel into a lag layer, which is not realistic.

Therefore the model is not allowed to do this, and the potential gravel lag layer is predicted from the composition of the whole active layer (including the mobile and immobile gravel of the previous time step) in every time step.

9.6 Application of the model to the river Rhine

9.6.1 Boundary conditions

The sediment transport and vertical sorting of two recent discharge waves in the Waal branch of the river Rhine are roughly hindcast with the model. The exact form of the discharge wave is of lesser interest and was therefore generalised and smoothed, mainly the maximum discharge and the maximum attained dune height are of importance here (see Fig. 9.8). The first modelled discharge wave must be the largest previous discharge wave of the period of interest. This is because the sorting in the bed is reset at that time and the deposit is predictable as a singular upward fining cross-bedded set. For the Waal, the magnitude of the discharge wave of January 1995 (maximum discharge herein about 10000 m³/s) is chosen as a boundary condition (see model results section for more details). The next discharge wave was in November 1998 (maximum discharge herein about 6000 m³/s). During this event, the extensive field measurements were done as described before. These measurements will be used to evaluate the modelling results. The hindcast of the first, highest discharge wave is intended only to model the relict sediment sorting in the river bed, which is the initial condition for the second wave. The average gravel abundance in the bed sediment in 1995 is 45%, following from the grain size analysis of the vibrocores.

There is no field data available of water depths and flow velocities for the whole range of modelled discharges. Therefore a readily available one-dimensional flow model of the Rhine branches was used to compute width- and depth-averaged water depth (*h*) and flow velocity (*u*) for a large range of discharges (*Q*) in the Waal (A. Wolters, SOBEK-model, Rijkswaterstaat-RIZA, pers. comm.). This flow model has been calibrated on water levels at several stations along the river as well as discharge measurements over a large range of low and high discharges.

The following important assumptions are made in the model. There is no net aggradation or degradation. There is no exchange of sediment with the river bed in the groyne areas parallel to the river. The average dune height is representative for all dunes in the sorting process. These and other assumptions are discussed later.

9.6.2 Modelled flow parameters, dune height and bedload transport

The flow velocity and grain shear stress follow the pattern of the discharge (Fig. 9.8a) as expected. The water depth is attenuated for a discharge above 8000 m³/s due to the flooding of the embanked floodplains, which leads to a sudden increase of the width of the river. In the figure, the measured flow velocities of the second discharge wave are given, and are well reproduced by the model.

The simulated dune height (Fig. 9.8b and 9.9a) shows a strong hysteresis, which agrees with the Waal data for 1998. The simulated maximum dune height in the second wave is about equal to the observed height as expected, although the dune height is somewhat underestimated in rising stage. The predicted sand and gravel transport are in the same order of magnitude as the observed transport (Fig. 9.8c and 9.9b), but the trend is obviously totally wrong. The transport measurements (Fig. 9.5) showed a trend of relatively large and fine bedload transport after the peak, which cannot

be predicted with this model for reasons mentioned earlier.

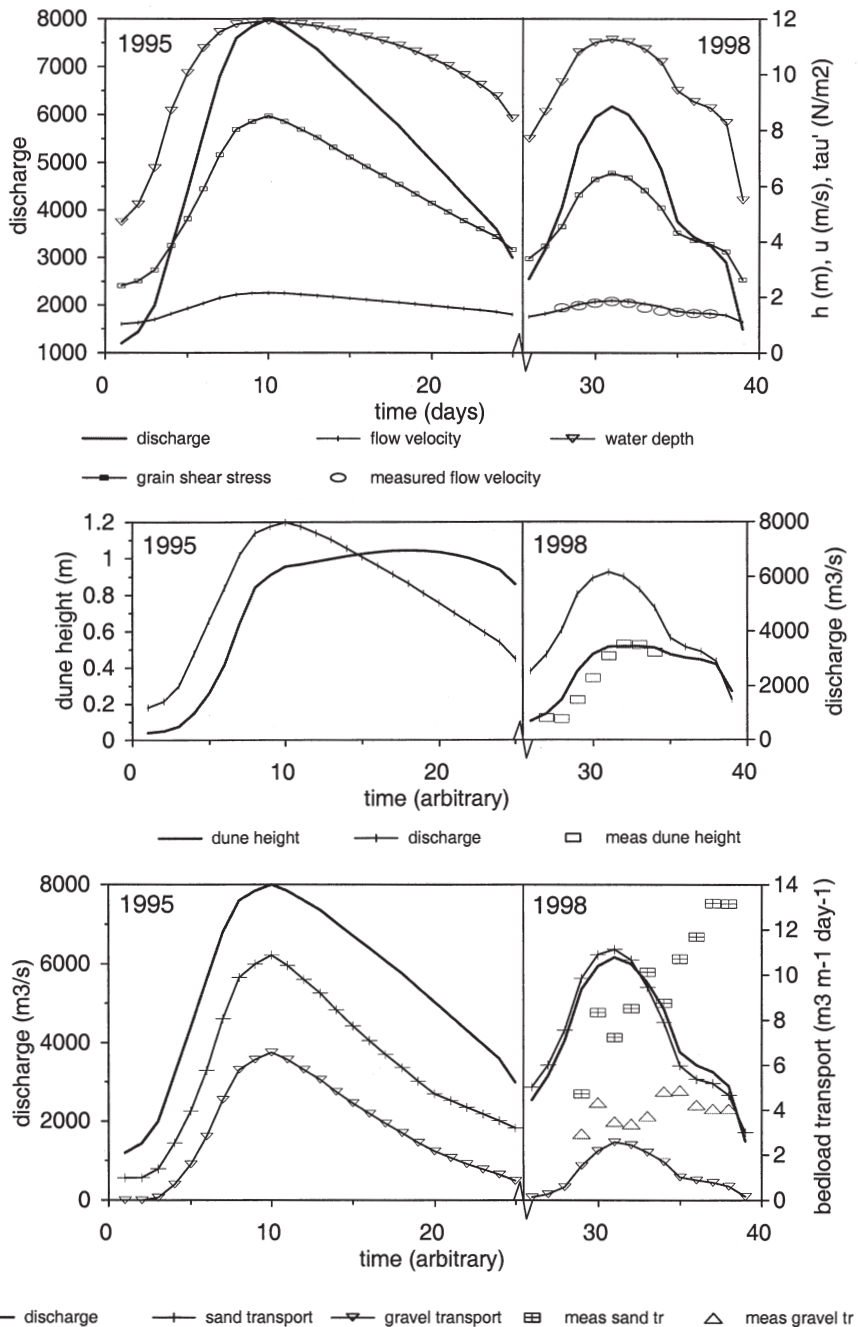


Figure 9.8. a) Discharge, water depth, flow velocity and grain shear stress, as well as the measured velocities, b) Dune height, as well as the measured dune heights, and c) Bedload transport of sand and gravel, as well as the measured transports (with Helley Smith).

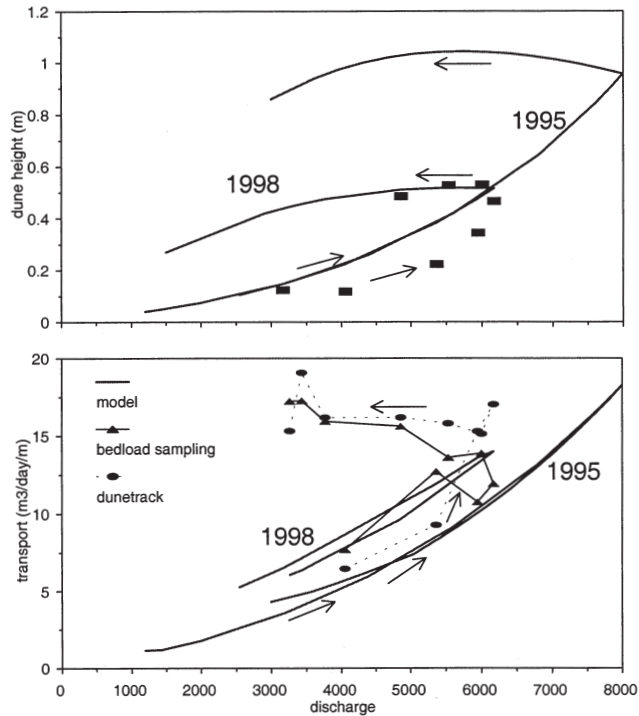


Figure 9.9. Dune height (a) and sediment transport (b) as a function of discharge. The measured bedload transport increases during lowering stages. The predicted bedload transport curve for 1998 lies higher than for 1995, which is caused by the antecedent sorting from 1995 (which itself had not yet antecedent sorting in the model).

9.6.3 Modelled sediment sorting and lag deposits

The modelled sorting in the bed is shown in Figs 10a,b. During rising stages and at peak flow, a thin gravel lag layer formed in the dune troughs and moved downwards in the bed as the dunes grew until peak flow. These thin layers are due to the intrinsic difference between active layer sediment and predicted bedload sediment with the bedload predictor as explained earlier. In falling stages, the modelled gravel lag became thicker at 0.4-0.5 m below the bed surface. During the second discharge wave, the same pattern was found with a gravel lag layer at 0.2-0.25 m below the bed surface, except that it was thinner. An important observation is that the potential for gravel lag formation is the largest during falling stage. The cause is that in falling stage the bed shear stress is decreasing, which leads to increasing demobilization and deposition of the larger grain sizes, while the dune height is still increasing. The resulting sorting agrees with the results from vibro-cores in the Waal, in which also two layers could be found at depths of 0.3 and 0.7 m that were the result of the discharge waves of 1995 and 1998 (see Fig. 9.6).

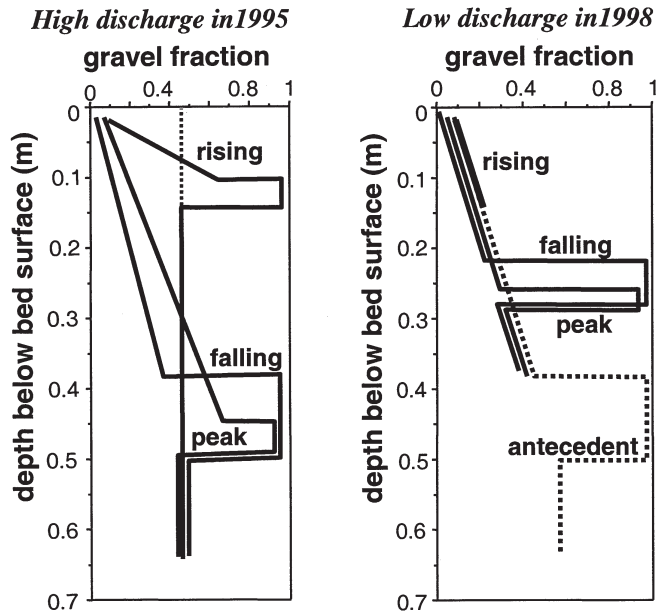


Figure 9.10. Model output: the final sorting of the river bed after the first two discharge waves (a, b). A gravel lag in the dune trough sinks into the bed as the dunes grow. In falling stage, a much thicker gravel lag is formed. In the second discharge wave the same happens, but at a smaller depth. The lines have been given small offsets to be able to distinguish between different steps. Compare to Figure 9.6.

9.6.4 Sensitivity analysis

For two parameters the sensitivity was roughly tested: the maximum dune height and the vertical sorting function:

- The sensitivity to the maximum dune height for the results is marginal. When this maximum dune height is decreased or increased, then the active layer thickness and depth of the gravel layers decreases or increases with the same factor. The sensitivity to the dune height hysteresis was not tested, but a decreased hysteresis will have the effect that the potential gravel layers become less thick.
- The vertical sorting function as given here has the largest slope possible, which means that a perfect sorting efficiency is assumed. When this slope is decreased with 5%, then the gravel layers become thinner. Between 5% and 6% decrease, the gravel layer of the second discharge wave disappears altogether.

Concluding, the model is able to reproduce the sorting in the river bed, and this sorting is genetically tracable to discharge events, but the sensitivity to the vertical sorting function is large.

9.7 Discussion

9.7.1 Effect of variability of dune height and scour depth on gravel lag layer depth

Dune height usually is highly variable (Paola & Borgman 1991, Leclair & Bridge 2001), and so is the concurrent trough scour depth which determines to what depth the sediment is vertically sorted. It is therefore the question whether the dunes are well represented in the model by the average dune height. If the trough scour variation is large in the Waal, then this variation may also be expected in the depth of the gravel layers.

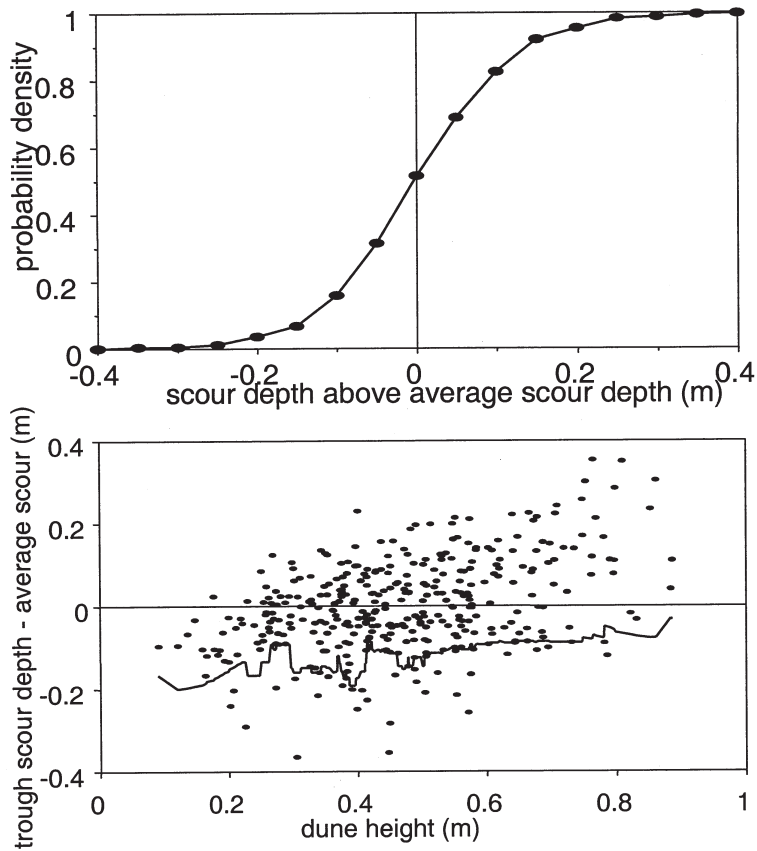


Figure 9.11. Statistics of dune scour depth of 417 dunes at positions varying from -100 m to +100 m from the river axis over a stretch of 0.5 km along the river Waal on 4 November (peak discharge). The average dune height was about 0.5 m. The deviation of scour depth of individual dunes above or below the average scour depth is determined by subtracting the moving average over 10 dunes (to remove the large-scale morphology) from the individual scour depth. a) Probability distribution of the deviation of scour depth. b) Deviation of scour depth as a function of dune height (dots). The line denotes the 90% percentile of deepest trough scours calculated from a moving bin of 20 dunes on the list of all dunes ordered from small to large dune height.

The statistics of the trough level (comparable to the term scour depth in Leclair & Bridge 2001) have been determined from the longitudinal profiles of dunes on 4 November (peak discharge) (Fig. 9.11). Three-dimensional dunes are more irregular than two-dimensional dunes and have therefore deeper troughs every now and then. According to the bedform stability diagrams of Southard & Boguchwal (1990), dunes become more three-dimensional with increasing flow velocity. Using the data from the peak discharge in the Waal ensures that the dunes are as near the condition for three-dimensional dunes as they will get in the river Waal. The coordinates of the dune troughs were determined with the software described earlier. A moving average of 10 trough scour depths was subtracted from each individual (midpoint) scour depth to obtain normalised trough scours. The normalised trough scours were used to compute the trough scour probability distribution (see Fig. 9.11 first panel). In addition, the individual normalised trough scour depths are shown as a function of the concurrent dune height (see Fig. 9.11 second panel).

Only 10% of all dunes scour more than 0.13 m below the average scour depth of the surrounding 10 dunes. This variation encompasses at best two classes in the histogram of gravel layer depth (Fig. 9.6). This means that the dune height and scour depth variation is not very relevant for the modelled depth of gravel deposition in this case, where the depths of the gravel layers from the two events are sufficiently far apart.

In addition, Fig. 9.11b shows that the deepest scour depths are not necessarily related to the largest dunes. The 10% deepest scours are only 0.1 m extra below the average scour depth for the largest dunes, while this is 0.2 m for the average and smaller dunes. Thus the slightly smaller dunes in the dune train may more often have deeper scour holes than the largest dunes. It is concluded here that the average dune height represents the population of dunes best for the present purpose of reach-average scour and deposition modelling.

9.7.2 Effect of variability of trough scour depth on cross-set thickness

The sediment in reality is not sorted in the transport layer, but within each individual cross-set deposited by one migrating dune. Thus, an individual cross-set is enveloped by the scour depth migration paths of individual dunes. The transport layer may therefore be composed of many stacked cross-sets. The variation in scour depth governs the cross-set thickness (Paola & Borgman 1991, Leclair & Bridge 2001). If the preserved cross-set thickness in the river Waal were large (due to large scour depth variation), then several gravel layers and fining-upward sequences would occur on top of each other in the bed.

According to Leclair & Bridge (2001), the average cross-set thickness is approximately one-third (1 over 2.9 [± 0.7] times the dune height. For a dune height of 0.5 m this yields cross-sets of $[1/(2.9-0.7)=0.45$ times 0.5 m is] 0.23 m thickness for scour depths that are one standard deviation (67% percentile) larger than the average scour depth. However, the 10% percentile of scour depth of the dunes in the Waal is less than 0.2 m below the average scour depth. It must therefore be concluded that the scour depth variation, and therefore cross-set thickness, in the Waal is considerably less than predicted with the Leclair & Bridge parameter. Indeed double gravel lag layers with a distance of about 0.1 m or more were only observed in about 10% of the cores in the Waal; in most cases only one gravel lag layer was observed at the level created by a single discharge event.

One reason for the small variation may be that the scour depth variation (and therefore the cross-set thickness) in dunes consisting of sediment mixtures is much less than in dunes consisting of well-sorted sediment (Leclair, pers. comm.). The gravel in the trough of dunes may suppress the natural scour depth variation in dune trains. In addition, the dunes in the Rhine are extremely regular, that is, not three-dimensional. Three dimensional dunes have a much larger variation in scour depth as

their height is also much more variable.

Concluding, the scour depth variation and cross-set thickness are estimated to be relatively small in the river Waal, therefore its effect on stratigraphy and sediment transport is probably also small. Thus the sorting in the active layer is assumed to be equal to the sorting in the individual sets. A future version of the model presented herein might be nested in the cross-set deposition model of Leclair (2000) to test these effects more quantitatively, and extend the applicability of the concept presented herein to rivers with more three-dimensional dunes.

9.7.3 Effect of dune response time on stratigraphy

It takes time for the dune height to adapt to the change in flow conditions, and consequently the dune height shows hysteresis. If the dune response is even slower, then the dunes cease to be active in falling stage and small dunes emerge on top of the relict big dunes (Allen & Collinson 1974). This is also the case in the Rhine (Wilbers 1999). Consequently, the big dune tops are eroded and the dune troughs are filled in with this eroded sediment during falling and low stage. This means that an additional cross-bedded unit may exist in channel beds, which is genetically different from the cross-bedding studied so far, in the sense that it consists of much finer sediment. Thus a longitudinal variation in sorting with a wave length in the order of the large dunes is expected in the river bed. This infilling cross-bedding is herein called secondary cross-bedding in contrast with the primary cross-bedded deposits of the primary (big) dunes.

This indicates the importance of the dune height adaptation time. On the one hand, there are dunes that adapt slowly to changing flow, and become inactive in lowering discharge (Allen & Collinson 1974, Wilbers 1999). In this case, truncated primary cross-bedding of the relict dunes and secondary cross-bedding of the trough-infills are both preserved, as well as lag deposits that vary in thickness in the flow direction (thin below relict dunes and thick below trough-infills). On the other hand, for dunes that adapt very quickly to changing flow (no significant hysteresis), the secondary cross-bedding will not occur, but cross-bedding and fining-upward lag deposits will be preserved.

Results of experiments reported in chapter 10 show that this effect indeed occurs, but that the lag deposits and primary foreset deposits for the experimental conditions occur much more frequently in the bed than the fine secondary cross-bedding. This suggests that the effect of the secondary cross-bedding is not of first-order importance. The vibro-cores of the river Rhine show a considerable variation in grain size and sorting, but the core-spacing is much larger than the dune length and it is not clear whether the variation is the result of the primary and secondary cross-bedding or has other causes like sorting of sediment in the meander bends. The question of importance of the secondary cross-bedding in the Rhine remains therefore unresolved.

9.7.4 Effect of sorting function for cross-bedded (foreset) deposits

The vertical sorting at the lee side of the dunes is now assumed to be linear, while this is not yet supported by data or a model. Therefore the transition from cross-stratified deposit to lag deposit seems rather abrupt in the model outcome, which is only partly supported by the field and flume data. In addition, the preservation of cross-stratification (and thus of the linear sorting) depends partly on the migration celerity of the dunes. If this is relatively low (as in the Rhine), then part of the form set (dune body) is preserved and the stratification with it. If, on the other hand, the migration celerity were high, then no part of the dune body would be preserved, and only an upward fining accumulation of lag deposits would be preserved.

The predicted sorting in the river bed agrees well with the measurements and observations. Yet the assumption of a linear sorting function has not been verified with field or laboratory data. In the present model, the sorting is maximal in the sense that it yields the least possible gravel abundance in the top layer, and the maximum possible gravel abundance in the bottom layer. It could well be that the sorting within grain flows in nature is less effective than assumed here. As shown in the sensitivity analysis, this would lead to a less clear sorting in the cross-bedded deposits. At the same time, if the gravel accommodation in the top part of the transport layer would be higher in falling stage, then the potential gravel lag deposits would be thinner or vanish altogether (see section on sensitivity analysis). Concluding, the sorting in the active layer depends heavily on the vertical sorting function. Yet, the most straightforward parameter choices and assumptions give reasonable results, indicating that the conclusions herein are at least in the direction of what may be found with further research. To be able to predict the sorting for more than two grain size fractions, a quantitative predictor must be found for the vertical sorting in grain flows and due to selective deposition.

The results of the Kleinhans (2000, see also Blom & Kleinhans 1999) experiments as given in Figure 9.2 indicate that the sorting function deviates only slightly from linear and indeed comes close to zero gravel in the top of the dunes. Also preliminary results of experiments to study the vertical sorting (done by the author at Saint Anthony Falls Laboratory in Minneapolis (USA) in the fall of 2001) show that the optimal sorting does not deviate very much from a linear profile. However, the sorting in those datasets is slightly less strong, i.e. less efficient. This means that the model slightly exaggerates the vertical sorting trend, and consequently, that the gravel lag layers are thinner in reality.

9.7.5 Future model development

Essential elements of a model that should predict sediment transport and vertical sorting in rivers with dunes and sand-gravel mixtures are:

1. a vertical sorting function for equilibrium sorting in the foreset (cross-bedded) deposits,
2. a time-dependent approach to this equilibrium to account for the time necessary to deposit or entrain the gravel at the base of dunes, and
3. a dune height predictor including a time-dependent approach to the equilibrium dune height.

As a result, the model should reproduce:

1. sediment transport hysteresis during a single discharge wave,
2. relative sediment transport differences between subsequent discharge events (for the same discharge), and
3. secondary, sandy cross-stratification (infilling of dune troughs with sediment from the tops of these dunes) in the case of strong dune height hysteresis, in addition to primary cross-stratification and lag deposits, and their relative abundance in the channel bed for different dune height adaptation time scales.

9.8 Conclusions

River channel bed deposition of sand-gravel mixtures is strongly coupled to the dune development and the sorting of sediment in the grain flow at the lee side of dunes, as well as grain size-selective deposition in the dune troughs (gravel lags). Data of the river Rhine clearly indicate that the vertical sorting leaves a genetically traceable deposit in the river bed at a depth depending on the maximum dune height.

Consequently, strong feedbacks between bedload sediment transport rate and composition versus deposition in the bed are expected. The bedload sediment transport rate and composition is dependent on the sediment in the active layer (down to the dune troughs), which is determined by the sorting in previous events. The deposits on the other hand are governed by the selective transport and by sorting in dunes, as well as the dune height development during a discharge event. Consequently, the vertical sorting of previous discharge waves may cause hysteresis of the sediment transport, which can only be hindcast by incorporating this sorting.

The behavioural model developed in this paper is able to reproduce the main characteristics of vertical sorting in the bed of the river Rhine due to two recent discharge waves. This approach should be seen as a first exploratory attempt to model vertical sorting. The model shows that both vertical sorting due to grain flows at the lee-side of dunes and due to selective deposition play an important role in the sediment transport and deposition of sand-gravel sediment. The dune height adaptation to changing flow determines the ratios of lag deposits and cross-stratification. The deposition of gravel lag layers in the bed occurs mainly during falling stage, because the grain shear stress is then decreasing while the dune height is still increasing. However, sediment transport is not correctly predicted with this model, because the phenomena that cause strong transport hysteresis were not included in the model. The order and magnitude of discharge waves is important, as the largest wipes out all antecedent sorting, while the processes in smaller ones depend on the depositions of previous waves.

Acknowledgments

The National Institute for Inland Water Management and waste water Treatment (RIZA) and the Directorate Eastern Netherlands of Rijkswaterstaat in the Netherlands financed and carried out the measurements in the rivers Waal and Bovenrijn, as well as the vibrocores (in cooperation with the Dutch Institute for Applied Geology (TNO-NITG)). RIZA is gratefully acknowledged for the permission to use the vibrocores. Antoine Wilbers (Utrecht University) is thanked for providing the bedform statistics from the multibeam echo soundings. Ard Wolters is thanked for providing the SOBEK model output. The comments by Janrik van den Berg, Leo van Rijn, Suzanne Leclair and Gary Parker were much appreciated.

List of symbols

apostroph / refers to 'related to grains'

subscripts $i, 50, 90$, etc. refer to grain size fractions i or grain size distribution percentiles

- C Chezy coefficient ($m^{0.5} s^{-1}$)
- D grain size (m)
- f_i fraction of grain size i in bedload sediment

g	gravitational acceleration (9.81 m s^{-2})
h	water depth (m)
H	dune height (m)
ks	hydraulic roughness (m)
L_A	thickness of active layer
L_D	thickness of gravel lag layer
LSB	low-stage bed level (plane bed)
p	probability / abundance of grain size fraction (100 times p yields p in %) (-)
q_b	bedload transport ($\text{m}^3 \text{ m}^{-1} \text{ s}^{-1}$)
Q	flow discharge ($\text{m}^3 \text{ s}^{-1}$)
T	relative excess shear stress parameter: $(\tau' - \tau_{cr}) / \tau_{cr}$ (-)
t	time coordinate
u	flow velocity (m s^{-1})
z	depth coordinate, $z=0$ at LSB
θ	Shields parameter (subscript cr refers to critical Shields parameter) (-)
ξ	hiding-exposure coefficient (-)
ρ	density (subscript s refers to sediment) (kg m^{-3})
τ	bed shear stress (N m^{-2})

References

- ALLEN, J. R. L. (1963), Sedimentation to the lee of small underwater sand waves: and experimental study
Journal of Geology 73. pp. 95-116.
- ALLEN, J. R. L. (1970), The avalanching of granular solids on dune and similar slopes. Journal of Geology 78
pp. 326-351.
- ALLEN, J. R. L. & COLLINSON, J. D. (1974), The superimposition and classification of dunes formed by
unidirectional aqueous flows, Sedimentary Geology 12, pp. 169-178.
- BAGNOLD, R. A. (1954), Experiments on a gravity-free dispersion of large solid spheres in a Newtonian fluid
under shear. Roy. Soc. London, Proc. Ser. A(225). pp. 49-63.
- BENNETT, S. J. & BRIDGE, J. S. (1995), An experimental study of flow, bedload transport and bed topography
under conditions of erosion and deposition and comparison with theoretical models. Sedimentology 42. pp
117-146.
- BLOM, A. & KLEINHANS, M. G. (1999), Non-uniform sediment in morphological equilibrium situations. Data
Report Sand Flume Experiments 97/98. University of Twente, Rijkswaterstaat RIZA, WL | Delft Hydraulics
University of Twente, Civil Engineering and Management, The Netherlands.
- BOERSMA, J. R., VAN DE MEENE, E. A. & TJALSMA, R. C. (1968), Intricated cross-stratification due to
interaction of a mega ripple with its lee-side system of backflow ripples (upper-pointbar deposits, Lower
Rhine), Sedimentology 11, pp. 147-162.
- EGIAZAROFF, I. V. (1965), Calculation of nonuniform sediment concentrations. Journal of the Hydraulics
Division, ASCE 91 (HY4), pp. 225-248.
- HUNTER, R. E. (1985), A kinematic model for the structure of lee-side deposits. Sedimentology 32, pp. 409-
422.
- JOPLING, A. V. (1965), Laboratory study of the distribution of grain sizes in cross-bedded deposits, in
MIDDLETON, G. V. (ed.), Primary sedimentary structures and their hydrodynamic interpretation, spec
publ. no. 12, Soc. of Econ. Paleontologists and Mineralogists, Oklahoma, U.S.A.
- JULIEN, P. Y. & KLAASSEN, G. J. (1995), Sand-dune geometry of large rivers during floods, Journal of
Hydraulic Engineering 121 (9), pp. 657-663.

- KLAASSEN, G. J. (1987), Experiments on the effect of gradation on sediment transport. Euromech 215 Colloquium, Genova, Italy, September 15-19, also Delft Hydraulics publication 394, Delft, The Netherlands.
- KLAASSEN, G. J., RIBBERINK, J. S. & DE RUITER, J. C. C. (1987), On the transport of mixtures in the dune phase. Euromech 215 Colloquium, Genova, Italy, September 15-19, also Delft Hydraulics publication 394, Delft, The Netherlands.
- KLAASSEN, G. J. (1991), Experiments on the effect of gradation and vertical sorting on sediment transport phenomena in the dune phase. Grain Sorting Seminar, 21-25 October, 1991, Ascona (Switzerland).
- KLEINHANS, M. G. (1999), Sediment transport in the River Waal: high discharge wave, November, 1998. (in Dutch) Netherlands Centre for Geo-ecological Research / Utrecht University Physical Geography. ICG 99/6.
- KLEINHANS, M. G. (2000), The relation between bedform type, vertical sorting in bedforms and bedload transport during subsequent discharge waves in large sand-gravel bed rivers with fixed banks. Proc. Gravel Bed Rivers Conference 2000, 28 August - 3 September, New Zealand, in NOLAN, T. & THORNE, C. (eds), Special public. CD-rom of the New Zealand Hydrological Society.
- KLEINHANS, M. G. (2001), The Key Role of Fluvial Dunes in Transport and Deposition of Sand-Gravel Mixtures, a preliminary note, *Sedimentary Geology* Vol. 143 pp. 7-13.
- KLEINHANS, M. G. & BLOM, A. (2001), Discussion of Wilcock, P. R. (2001), The flow, the bed and the transport: interaction in the flume and field, in: MOSLEY, M. P. (ed.) *Gravel-bed rivers V*, pp. 212-214, New Zealand Hydrological Society Inc, Wellington, New Zealand.
- KLEINHANS, M. G. & TEN BRINKE, W. B. M. (2001), Accuracy of cross-channel sampled sediment transport in large sand-gravel-bed rivers. *Journal of Hydraulic Engineering* 127 (4), pp. 258-269, see chapter 3.
- KLEINHANS, M. G. & VAN RIJN, L. C. (2002), Stochastic prediction of sediment transport in sand-gravel bed rivers, *Journal of Hydraulic Engineering* 128(4), ASCE, pp. 412-425, special issue: Stochastic hydraulics and sediment transport, see chapter 5.
- LECLAIR, S. F. (2000), Preservation of cross-strata due to migration of subaqueous dunes. Unpublished Ph.D. Dissertation, Binghamton University, New York.
- LECLAIR, S. F. & BRIDGE, J. S. (2001), Quantitative interpretation of sedimentary structures formed by river dunes. *Journal of Sedimentary Research* 71 5.
- MCLEAN, S. R., WOLFE, S. R. & NELSON, J. M. (1999), Predicting boundary shear stress and sediment transport over bedforms. *Journal of Hydraulic Engineering* 125 (7), pp. 725-736.
- MEYER-PETER, E. & MUELLER, R. (1948), Formulas for bed-load transport. 2nd Conf. Int. Assoc. of Hydraul. Res. Stockholm, Sweden. pp. 39-64.
- PAOLA, C. & BORGMAN, L. (1991), Reconstructing random topography from preserved stratification, *Sedimentology* 38, pp. 553-565.
- PARKER, G., PAOLA, C. & LECLAIR, S. (2000), Probabilistic Exner sediment continuity equation for mixtures with no active layer, *Journal of Hydraulic Engineering* 126 (11), pp. 818-826.
- RIBBERINK, J. (1987), Mathematical modelling of one-dimensional morphological changes in rivers with non-uniform sediment, PhD thesis, Delft University, 1987.
- SOUTHARD, J. B. & BOGUCHWAL, A. (1990), Bed configurations in steady unidirectional water flows. Part 2. Synthesis of flume data; *Journal of Sedimentary Petrology*, 60 (5), pp. 658-679..
- TEN BRINKE, W. B. M., WILBERS, A. W. E. & WESSELING, C. (1999), Dune growth, decay and migration rates during a large-magnitude flood at sand and mixed sand-gravel bed in the Dutch Rhine river system. *Spec. Publ. int. Ass. Sediment.* 28, pp. 15-32.
- TEN BRINKE, W. B. M., GRUYTERS, S.H.L.L., KOOMANS, R.L., WILBERS, A.W.E. & KLEINHANS, M.G. (submitted), Sediment transport and morphological processes near a river bifurcation in the Dutch Rhine, submitted to the Proc. 7th Int. Conf. Fluv. Sed.
- TNO-NITG (2000), Descriptions and photographs of the vibrocores in the Niederrhein, Bovenrijn, Waal and Pannerdensch Kanaal. Dutch Institute for Applied Geology (TNO-NITG), The Netherlands. Core numbers 40D0155 - 40D0214 and 40G0110 - 40G0150, see also Ten Brinke et al.,
- VAN RIJN, L. C. (1984), Sediment transport, part I: bed load transport. *Journal of Hydraulic Engineering* 110 (10), pp. 1431-1456.
- VAN RIJN, L. C. (1993), Principles of sediment transport in rivers, estuaries and coastal seas, Aqua Publications, Oldemarkt, The Netherlands.
- WATHEN, S. J., FERGUSON, R. I., HOEY, T. B., & WERRITTY, A. (1995), Unequal mobility of gravel and

- sand in weakly bimodal river sediments. *Water Resources Research* 31 (8), pp. 2087-2096.
- WILBERS, A. W. E. (1998), Bedload transport and dune development during discharge waves in the Bovenrijn and the Waal, (in Dutch) Netherlands Centre for Geo-ecological Research / Utrecht University Physical Geography. ICG 98/12.
- WILBERS, A. W. E. (1999), Bedload transport and dune development during discharge waves in the Rhine branches, echo soundings of the flood in November 1998, (in Dutch) Netherlands Centre for Geo-ecological Research / Utrecht University Physical Geography. ICG 99/10.
- WILBERS, A.W.E. & TEN BRINKE, W.B.M. (in prep), Bed form response to floods in sand and gravel bed reaches of the Dutch Rhine river system: hysteresis in dune dimensions and bed load transport
- WILCOCK, P. R. (1993), Critical shear stress of natural sediments. *Journal of Hydraulic Engineering* 119 (4), pp. 491-505.
- WILCOCK, P. R. (2001), The flow, the bed and the transport: interaction in the flume and field, in: MOSLEY, M. P. (ed.) (2002), *Gravel-bed rivers V*, pp. 183-220, New Zealand Hydrological Society Inc, Wellington, New Zealand.

Sand-gravel sorting in channel beds by non-equilibrium, three-dimensional dunes

Abstract

Vertical sediment sorting by migrating dunes in sand-gravel bed rivers is relatively well understood for equilibrium conditions with regular, two-dimensional dunes, but not for non-equilibrium conditions (discharge events) and irregular, three-dimensional dunes. This understanding is prerequisite for morphological modelling of the channel morphology. Experiments are herein reported in which both were simulated in a straight flume, 0.9 m wide and 14 m long. Apart from equilibrium experiments, a series of tests was done with two discharge peaks in order of decreasing magnitude alternated with low flow discharge. The dunes formed in the intermediate discharge were two-dimensional with straight crests and little variation in dune trough scour depth, whereas those formed in the high discharge were three-dimensional with sinuous crests and much trough scour variation. The former left a continuous gravel layer at their bases at a constant depth, while the latter left discontinuous, multiple gravel layers at highly variable depths. The main difference between equilibrium and non-equilibrium conditions was the deposition of fine sand in the dune troughs during low discharge, originating from eroded dune tops.

It is found that three sets of controls determine the characteristics of the deposits and vertical sorting. The first is the three-dimensionality (irregularity) of the dunes, which is determined by the bed shear stress and grain size of the dunes. The second is the mobility of the coarsest sediment fractions, which determines whether the gravel is fully mobile or a gravel lag deposit is formed which hinders entrainment of sediment from deeper layers. This control competes with the first control (although the first control is dominant): dunes cannot develop deep scour holes if there is a strong lag layer, but in time, lag layers may be broken up by three-dimensional dunes, which strive to develop deep scour holes. The third control is the adaptation time scale of the dune height during changing flow conditions. If the dune height adapts slowly and the dunes become inactive in waning flow, then sandier trough-fill deposits will form. The consequences for the net vertical sorting in the channel bed are discussed.

10.1 Introduction

10.1.1 Scope

Morphological modelling of channel beds with sediment mixtures has made strong progress in the past decennium. To model the sediment transport process and the exchange between transported and bed sediment in rivers with dunes correctly, the bed level variations due to migrating dunes must be accounted for (Ribberink 1987, Parker et al. 2000, Leclair & Bridge 2001) as well as the vertical sediment sorting in the dunes (Parker et al. 2000, Kleinhans 2001). These two elements, bed level variation and sediment sorting, must be implemented in model concepts (e.g. Parker et al. 2000), but are not yet predictable for various flow conditions and sediments.

Deposits of former dunes in the bed of the river Rhine (The Netherlands), obtained with vibrocoring were studied by Kleinhans (2001). Two gravelly layers were found in the cores, which seemed to be related to dunes formed in two discharge waves in order of decreasing magnitude, in both of which the dunes were not in equilibrium. Zanke (1976) reports a fining upward sorting in the bed of the Lower Weser River (Germany), and by comparison with equilibrium flume experiments, related this to the sorting by dunes. To the knowledge of the author, no other field data are available that couple the vertical sorting to dunes in past events. The flume experiments reported in literature were all done in equilibrium conditions with regular, two-dimensional dunes, which may not give comparable results to the non-equilibrium conditions in natural rivers. The general aim of this paper is to present and explain experimental sorting data from non-equilibrium conditions and three-dimensional dunes, and to verify experimentally that the deposits formed in two discharge waves (as in Kleinhans 2001) can indeed be related to the dunes and concurrent bed level variations. This has not been reported yet in literature to the knowledge of the author. The bed level variation may be strongly coupled to vertical sediment sorting. Therefore it is also aimed to determine the controls on the dune irregularity and the related trough scour depth variation in the presence of gravel layers.

10.1.2 Sorting in deposits of dunes in equilibrium and non-equilibrium conditions

Flume experiments by Ribberink (1987), Klaassen (1991) and Blom & Kleinhans (1999) showed that migrating dunes produce indeed a clear vertical sediment sorting: in grain flows at the lee-side of dunes, sediment is sorted in a fining-upward manner, and below the dunes a gravel lag may be deposited, composed of the coarsest sediment which is not (fully) mobile. Thus a gravelly layer was found at the depth of dune troughs, consisting of sediment from lower parts of the dunes and/or gravel lags. The grain flow process is well known in sedimentological literature (e.g. Bagnold 1954, Allen 1970, Hunter 1985), but the effect on sediment sorting has not been quantified. The flume experiments were mostly done in equilibrium conditions with regular, two-dimensional dunes, and the bed was remixed after each condition.

Such equilibrium conditions are not often found in the field. Notably, during a discharge wave, dunes need a relatively long time to adapt to the rapidly changing flow conditions. If the adaptation is not fast enough, then the dunes may become inactive while small secondary dunes form on their relicts (e.g. Allen & Collinson 1974, Ten Brinke et al. 1999, chapter 6). Obviously this has consequences for the structure of the deposits and the net sorting in such river beds.

10.1.3 Sorting in deposits of regular and irregular dunes

Regular dunes are herein called two-dimensional (2D) and the irregular three-dimensional (3D), following the definition of Costello & Southard (1981). This can be expressed in two directions: the vertical (trough depths, deep scour pits) and the horizontal (sinuosity of the dune crest line and connectivity between crest lines).

Dunes become more irregular and have more variation in their trough scour depth with increasing flow velocity or shear stress (e.g. Boothroyd & Hubbard 1975, Costello & Southard 1981, Terwindt & Brouwer 1986). When dunes have a highly variable trough scour depth, the deposits of the dunes are highly variable in thickness (e.g. Harms & Fahnestock 1965, Reineck & Singh 1973). Corroborating the Paola & Borgman (1991) theory, Leclair & Bridge (2001) experimentally demonstrated that the thickness and length of preserved cross-stratified sets depends on the variability of this trough scour depth. For highly variable trough scour depth the thickness of the preserved sets is large while the length is short, and vice versa for low trough scour variability. The set thickness variability has consequences for the net vertical sorting in the bed: the sediment obviously is better vertically sorted (averaged over several dune lengths and set lengths) in one single set than in several sets which each show the same sorting but are stacked on each other.

It is, however, not known whether high trough scour variability may occur in sediment mixtures. It could be argued that a gravelly lag layer just below the active dunes hinders dune growth and sediment entrainment from the bed below the active dunes (Klaassen 1991), and inhibits the formation of deep scour holes that are characteristic for irregular dunes with much height and trough scour depth variation (Hooke 1968). Thus, the bed level variation may be strongly coupled to vertical sediment sorting.

The flume experiments reported in this paper were designed to have a mobility of coarse grains as high as possible, while the experiments in literature were designed for as little suspended transport as possible and consequently no or low mobility for the coarse fractions. Below, the setup of the experiments is given, and the results described. Next, the controls on gravel lag formation are discussed, and one important control, the mobility of the coarsest sediment, is related to the hiding-exposure phenomenon. Then the controls on dune irregularity are discussed and compared to literature. Subsequently, the effect of gravel lags on dune irregularity is inferred from the results. Next the deposits in non-equilibrium conditions, and their relevance for natural rivers are discussed. Finally, recommendations for modelling these processes are done.

10.2 Setup of the flume experiments

The experiments were done in the Tilting Bed Flume at St. Anthony Falls Laboratory (see Fig. 10.1), which has a length of 14 m and a width of 0.9 m. The water depths were between 0.05 and 0.22 m, and uniform flow was maintained by adjusting the downstream weir. The discharge was determined by measuring the velocity with a pitot tube and manometer in the discharge pipe entering the flume. The discharge was calibrated for the whole range of flow conditions (0.022 to 0.204 m³/s) with weigh tanks. The water temperature was between 10° and 13° Centigrade. The test section was between 4 and 13 m from the beginning of the flume (the latter taken as just downstream of the sediment feeder). Several water surface profiles per test were collected in the middle of the flume with a point gauge at every 0.5 m in the test section. Time series of the bedlevel at a fixed point (11 m) and bed surface profiles were collected in the middle of the flume (and additional profiles at 0.25 m from both sides in the highest discharges) with an ultrasonic device.

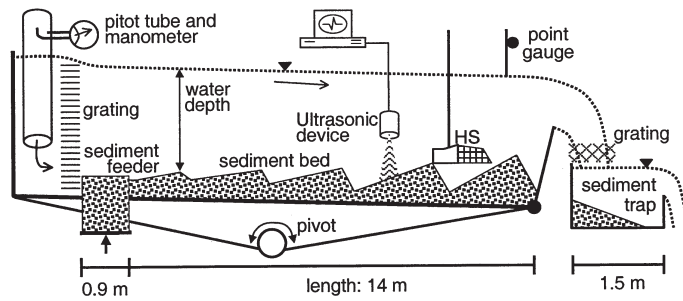


Figure 10.1. Outline of the Tilting Bed Flume at St. Anthony Falls Laboratory (vertical scale exaggerated). The width of the flume is 0.9 m, the length of the flume is 14 m, and the sediment feeder is 0.9 m wide and long. The point gauge and ultrasonic device could be moved along the flume. The Helley Smith (HS) bedload sampler was placed at 13 m. A horizontal grating at the flume entrance reduced the turbulence of the flow coming out of the pipe. A grating on the sediment trap reduced the velocity of the flow over the downstream weir, intended to increase the trapping efficiency.

Equilibrium experiments (Equ) were done to determine the equilibrium flow, dune and transport parameters for low, intermediate and high flow discharge (see Table 10.1). The flow was maintained until the system was in equilibrium, which was simply defined as the condition at which the variations of bedform dimensions and sediment transport became smaller than the measurement accuracy and variability. Non-equilibrium experiments (Non) were done to obtain the transport rates and sorting in the bed from two subsequent discharge peaks in order of decreasing magnitude, with low flow periods in between. The discharge was abruptly changed (see Fig. 10.2) and the flow was kept uniform by adjusting the downstream weir. The durations of the discharge peaks were chosen such that the dunes and transport did not reach equilibrium, while low flow was continued until equilibrium. This duration was taken to be about one-third of the time needed to attain equilibrium, based on the equilibrium experiments. It should be noted that the flume was too short to attain equilibrium of the dune height for the largest flow depth; the dune height increased towards the downstream end of the flume.

The equilibrium experiments and the first non-equilibrium experiment were started with a fully mixed bed of unimodal sediment (see Fig. 10.3), installed at a bed slope equal to that of the flume. The water was slowly fed onto the dry bed at the downstream end, to prevent disturbance of the initial bed and to allow air bubbles to be removed. Sediment of the same composition as the initial bed sediment was fed into the upstream end of the flume by a rising platform of 0.9 m wide and long, which rose at a constant and adjustable speed. The transported sediment accumulated in a trap at the downstream end of the flume, downstream of the weir. Although measures were taken to slow down the flow in the trap and prevent loss of sediment, the fine sand could not be prevented from being transported out of the trap in suspension. Helley Smith measurements (ratio of nozzle exit area to entrance area 1.10, bag of 100 μm mesh size, see Hubbell et al. 1985) were done to determine the transport rate at the downstream end of the flume. In equilibrium, the Helley Smith gave a mean transport rate within a few percent of the feed rate while the sediment trap had a trapping efficiency of only 60%. Herein, only the transport rates and compositions measured with the Helley Smith are reported. When the feeder was emptied in the course of an experiment, the flow was temporarily stopped and the feeder refilled. From the initial bed and the Helley Smith loads, samples were taken for grain size analysis.

The average water depth (h) was determined by subtracting the average bed level from the average water level in the test section. The flow velocity (u) was determined from this water depth,

Table 1. Experimental conditions and results.

exp #	Q m^3/s	u m/s	h m	S -	τ Pa	θ -	Fr	q_b m^2/s	H m	L m	temp. C	durat. hr	bedform types
Equ1	0.022	0.51	0.048	0.0041	1.86	0.096	0.75	1.4E-05	0.002	0	12.2	0.70	sand ribbons, bedload sheets
Equ2	0.092	0.78	0.132	0.0036	4.31	0.222	0.68	7.3E-05	0.018	1.2	12.2	3.00	2D dunes
Equ3	0.204	1.08	0.209	0.0036	6.35	0.327	0.76	2.0E-04	0.035	1.5	11.5	3.10	3D dunes
Non1	0.039	0.54	0.080	0.0036	2.72	0.140	0.61	7.1E-06	0.005	0	10.5	3.38	sand ribbons, bedload sheets
Non2	0.210	1.11	0.210	0.0050	9.08	0.467	0.77	2.8E-04	0.033	1	10.5	0.68	3D dunes
Non3	0.039	0.51	0.085	0.0038	3.00	0.155	0.56	6.9E-06	0.006	0	10.5	1.82	sand ribbons, bedload sheets
Non4	0.090	0.72	0.140	0.0041	5.27	0.271	0.61	5.2E-05	0.016	1.1	10.5	0.68	2D dunes, sand ribbons on top
Non5	0.039	0.54	0.080	0.0047	3.54	0.182	0.61	5.5E-06	0.007	0	10.5	3.08	sand ribbons, bedload sheets

flow discharge (Q) and flume width ($W=0.9$ m). The hydraulic radius (R) was calculated from the average water depth and the flume width, and corrected for side-wall roughness with the method of Vanoni-Brooks. The energy slope (i) was determined with an uncertainty of about 25% as follows: of the Equ experiments by averaging several water surface and bed surface slopes in the test section (4-13 m), and of the Non experiments from several bed slopes, as water surface slopes could not be measured while the time series of bed elevation was measured.

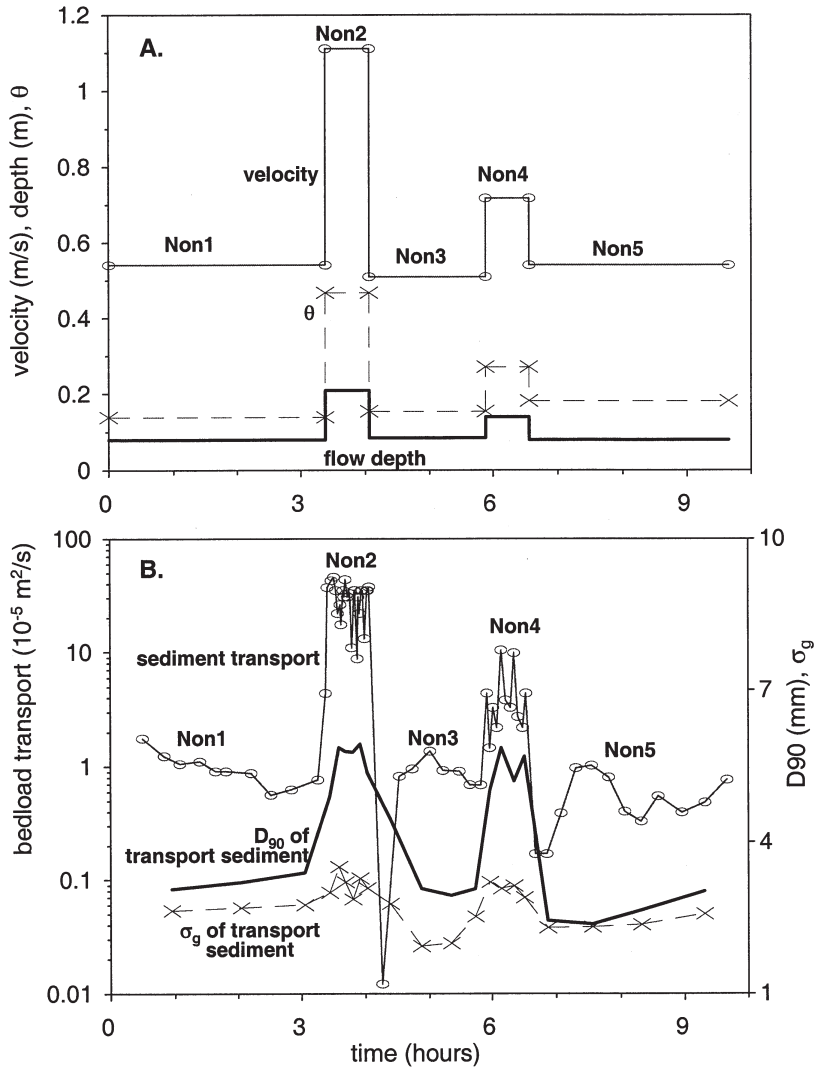


Figure 10.2. Time series of flow parameters (upper panel) and sediment transport (lower panel) of the Non experiments. (The average values of the same parameters of the Equ experiments are given in Table 10.1.) The θ denotes the dimensionless shear stress, the D90 denotes the 90th percentile of the bedload sediment size distribution (measured with the Helley Smith), and the sigma denotes the standard deviation of the bedload sediment size distribution.

From the slope and the corrected hydraulic radius (R_c) the total shear stress (τ) was determined with $\tau = \rho g R_c i$ (ρ = density of water, g = gravitational acceleration). The dimensionless shear stress is computed as $\theta = \tau / [(\rho_s - \rho)gD]$, in which ρ_s = density (of sediment), g = gravitational acceleration and D is sediment diameter (median or mean). The dimensionless shear stress on grains is computed as $\theta'_{s0} = \tau' / [(\rho_s - \rho)gD]$, in which τ' = shear stress on the grains, computed as $\tau' = \rho g [u/C']^2$ (Van Rijn 1984, Van den Berg & Van Gelder 1993) in which u is the depth-averaged flow velocity, C' is the grain-related Chézy coefficient: $C' = 18 \log[12h/k'_s]$, with h the water depth and k'_s the grain roughness, assumed to be equal to the D_{90} of the sediment.

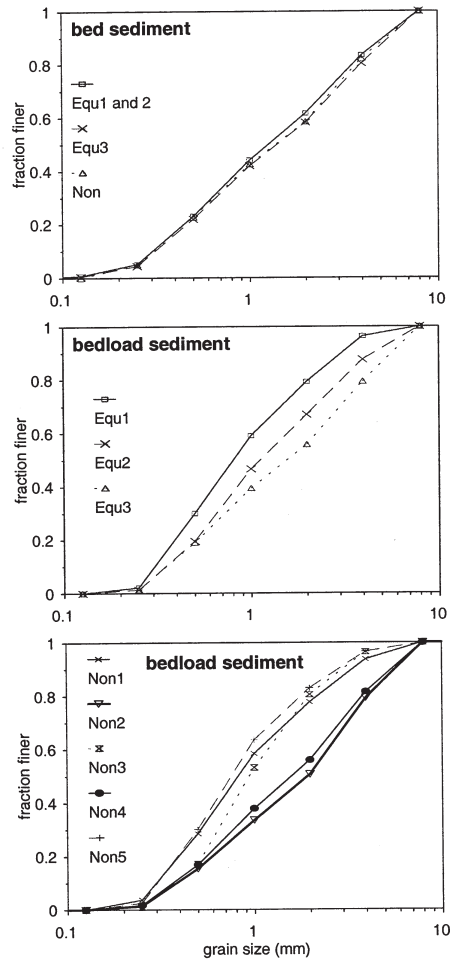


Figure 10.3. Grain size distributions of the bed sediment (equal to the feed sediment) and the bedload sediment at the end of all experiments. The bedload sediment was sampled with the Helly Smith sampler, representing the sediment transport between 0-7.6 cm above the bed surface.

The high Froude numbers ($Fr = u/(gh)^{0.5}$, here $Fr < 0.77$) were inevitable, because the flow velocity needed to exceed the critical flow velocity for motion of the largest grains, while the water depth had to be as large as possible to get high dunes, given the maximum discharge in the flume. With preliminary experiments the appropriate range of the flow conditions was determined.

After the flume was drained of water (in 12 hours), the bed was photographed. The vertical sorting was determined as follows. A trench was dug parallel to the flow, and a vertical section of the sediment bed was exposed in the middle of the flume. This sediment was allowed to air-dry for 18 hours. First the sedimentary structures were recorded with isolation foam profiles along the whole test section, based on the method of C. Bristow (pers. comm.). (The customary cellulose lacquer pouring method of Bouma (1979) did not give good results on the loose and coarse sediment.) To prevent the expanding foam from pushing up the top layers of sediment, the bed was first marked with a colored sediment and then covered with a 5 cm layer of mixed sediment out of the trench (same moisture) to provide enough pressure on the actual bed surface. The foam profiles were made by spraying an expanding poly-urethane isolation foam on cardboard, which was then pressed into the vertical sediment section and kept in place with weights for 3 hours. After removing the profiles, the bed was sampled in layers of 1 cm thickness at a number of locations along the flume, depending on the sedimentary structures (several dune tops and trough zones).

10.3 Results

10.3.1 Flow, sediment transport and dunes

The experimental conditions, transport rates and grain size distributions of the transported sediment are presented in Table 10.1 and Figures 10.2 and 10.3. Near the end of the Equ2 and Equ3 experiments, the composition of the transported sediment is almost equal to that of the original bed sediment (in turn equal to the feeder sediment) (see Fig. 10.3b). This shows that all the grain sizes were in motion in almost the same abundance as they occur in the bed sediment, approximating equal mobility. This is also indicated by the time series of the D_{90} of the transported sediment in the Non experiments, which is about equal for the high and intermediate discharge (see Fig. 10.2b).

In the Non experiments, there is a dip in the sediment transport immediately after a discharge peak, because the bedload sampler was located halfway the stoss-side of a relict dune where the sediment transport rate was small. In low flow, the dunes from discharge peaks were no longer active, but the tops of the dunes were eroded and deposited in the trough. As it took time to fill up the trough, the transport rate just downstream of a trough was very small because the trough temporarily acted as a sediment trap.

The dune characteristics are given in Figures 10.4 to 10.6. The dunes in the high discharge are about twice as high as in the intermediate discharge, while in the low discharge only low relief bedforms (1 times D_{90} high) were observed, interpreted as bedload sheets or incipient dunes, and six well-developed flow-parallel sand ribbons. From the time series taken at a single position, probability distributions of the bedlevel were computed (see Fig. 10.6). These distributions indicate the variations of bedlevel due to passing dunes, averaged over a number of dunes (about 35 for Equ2 and 45 for Equ3, 40 for Non2 and 30 for Non4), and normalized with respect to the average bed level at that position in that time period. The high discharge experiments have skewed distributions with much deeper dune troughs than dune tops, while the distributions for the low and intermediate discharges are about symmetrical. From the photographs (see Fig. 10.4) it can be seen that the dunes in intermediate discharge were much more regular than those in high discharge, in the sense that the latter had more curved crest-lines and deep scour pits every now and then, while the regular ones were more straight-crested and did not have pronounced scour pits.

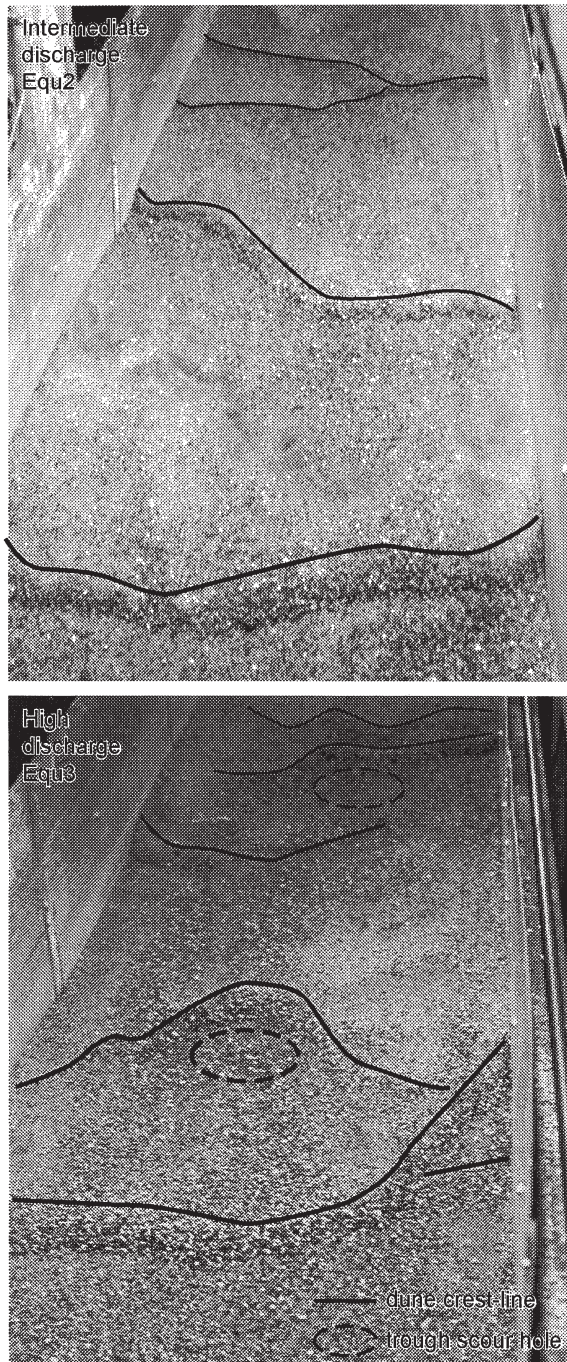


Figure 10.4. Photographs of the dunes in Equ2 and Equ3, which are comparable to those in Non4 and Non2 respectively. Dune crest-lines and pronounced trough scour areas have been marked.

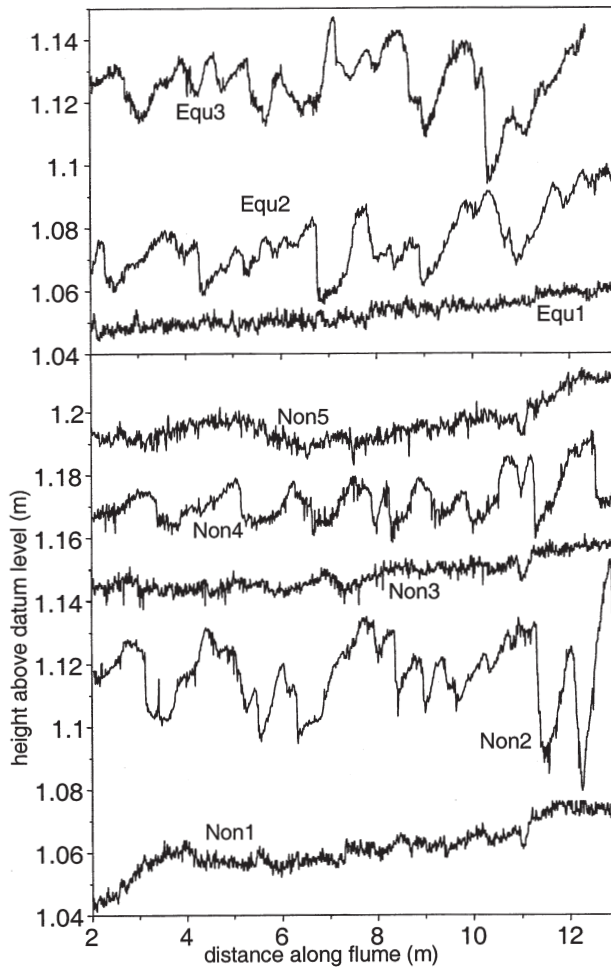


Figure 10.5. Bed profiles at the end of all experiments. The average level is arbitrarily adjusted for each profile for clarity of the graphs; no net aggradation took place. The vertical and horizontal scale is the same for all profiles. The average slope of the profiles as shown is different from their true slope because the flume was tilted.

10.3.2 Sedimentary structures

The sedimentary structures are schematically summarized in Figure 10.7. In the low flow experiments an armour layer formed on the bed surface. In the intermediate and high flow discharges, a thin gravelly layer also formed on the lower stoss sides of the dunes, which may be sediment in transport or a mobile armour. Pronounced gravelly layers were found at the bases of deposits of the intermediate and high discharge experiments, both in equilibrium and non-equilibrium conditions.

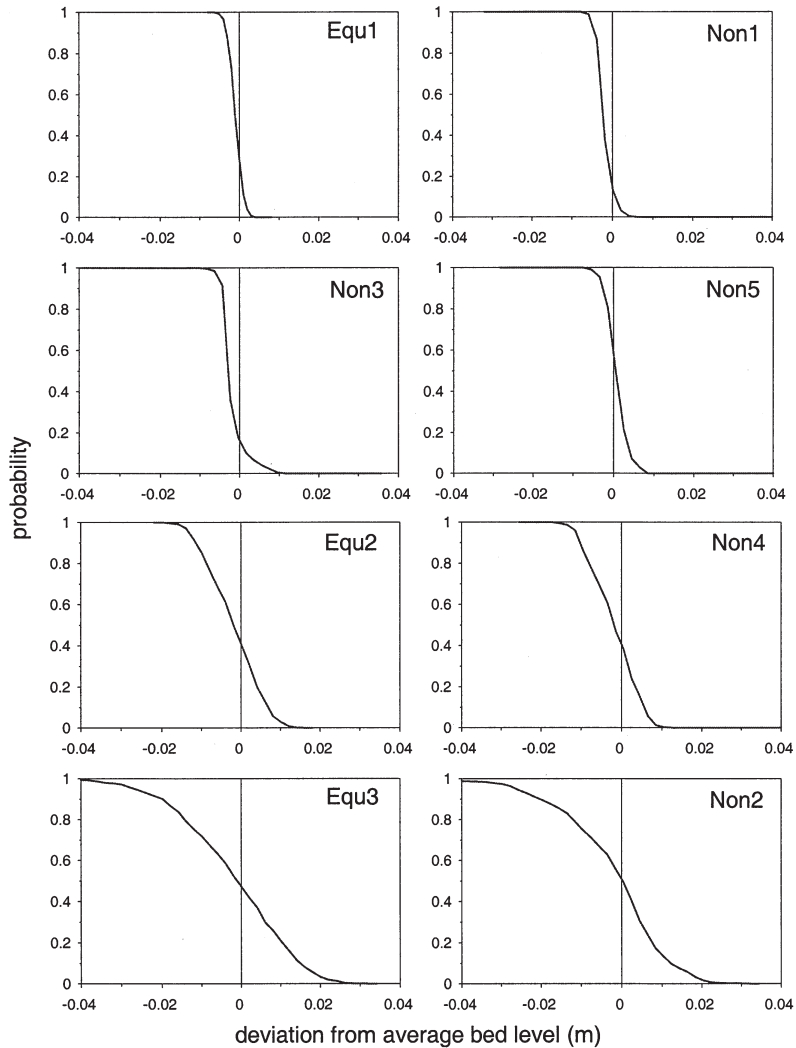
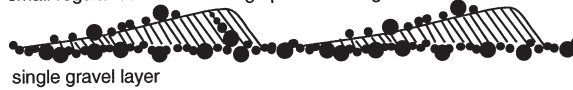


Figure 10.6. Probability distributions of the bed surface, determined from time series of bed level taken at the end of the flume (11 m). The graphs are grouped for comparable flow conditions: Equ1 with Non1, Non3 and Non5, Equ2 with Non4 and Equ3 with Non2. Note the asymmetry due to deep scour pits in Equ3 and Non2.

By correlating the gravel layers on the foam profiles to the dune trough depths recorded in the time series (see Figure 10.8), it is shown that the gravelly layers are deposited at the deepest level of dune troughs. The gravelly layer from the intermediate discharge was found to be very regular and continuous, while the high discharge formed multiple and discontinuous gravelly layers. This characteristic, plus the large difference in dune heights in Non2 and Non4, allowed an unambiguous connection between the gravelly layers and the discharge events. If the dunes in Non4 had been larger, then the irregular gravelly layers of Non2 could not have been distinguished from the gravelly layer of Non4.

Equilibrium

Equ2 small regular dunes with fining upward sorting



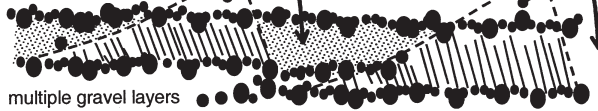
Equ3 large irregular dunes



Non-equilibrium

Non3 relict cross-bedding of Non2 overlain by mobile armour of Non3

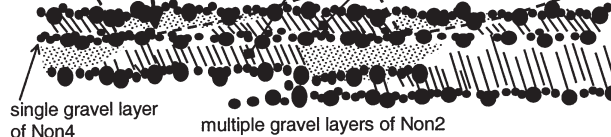
tops of large irregular dunes of Non2 eroded into trough during Non3



Non5 tops of small regular dunes of Non4 eroded into trough during Non5

relict cross-bedding of Non2 and Non4

mobile armour of Non5



Key ●●●●● gravel layer // // // cross-bedding (fining upward) ●●●●● trough-fill deposit from dune top

Figure 10.7. Sedimentary structures found in the experiments. The situation at the end of Non3 and Non5 is more complicated than in Equ2 and Equ3 because the discharge peaks were abruptly followed by low discharge, which caused the erosion of dune tops and the formation of a low-discharge mobile armour.

For the Non-experiments, a longitudinal (and also transversal) heterogeneity in deposits was found. In most locations in the bed, slightly cross-stratified sandy gravel on a gravelly layer was found, interpreted as the fining upward deposits of active dunes. However, at some positions the sediment on the gravelly layer clearly was much more sandy. This sand was interpreted as the sediment transported from the tops of the dunes into the troughs immediately after lowering the flow discharge. Longitudinally this results in a grain-size variation.

The volume of the three types of deposits in the Non experiments are estimated as 35% for gravelly layers, dune deposits: 50% and trough-fill deposits: 15%. The trough-fill deposits have the lowest abundance: only 3% from the large discharge wave, and 12% in the intermediate discharge wave. The abundance is probably lower in the large discharge wave because they have partly been reworked in the intermediate discharge wave.

10.3.3 Vertical sorting

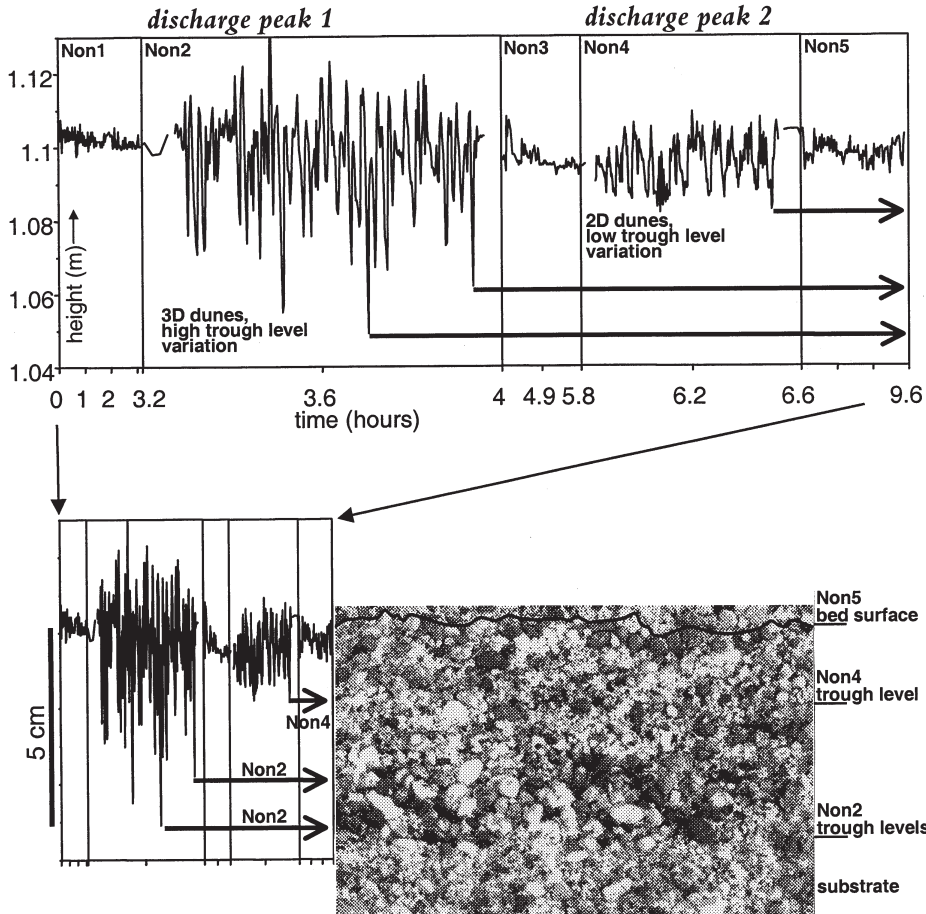


Figure 10.8. Correlation between the bed level variations in time (due to passing bedforms) and the deposition of gravel layers. For clarity, the horizontal scales in the time series have been stretched for the discharge peaks. The gravel layers found on the foam profiles are related to the deepest troughs. The foam profile was taken at the same position as the time series of bed levels.

Examples of the vertical sorting as sampled from the deposits are given in Fig. 10.9. There is a clear fining upward in the dunes of Equ2 and Equ3, though sometimes somewhat obliterated by small dunes overrunning larger dunes (see Fig. 10.9 third panel). The vertically sorted sediment of Non2 and 3 is reworked in Non4, leading to a double peak in the gravel abundance. In some samples, e.g. NonB4, the trough-fill deposit was found. At the same locations bedform troughs were observed in the bed surface profile (see Non4 at 11.3m in Fig. 10.5), and sandy deposits in the foam profiles. The grain size distributions of different parts of the deposits (see Fig. 10.10) also demonstrate the fining upward trend in the dunes.

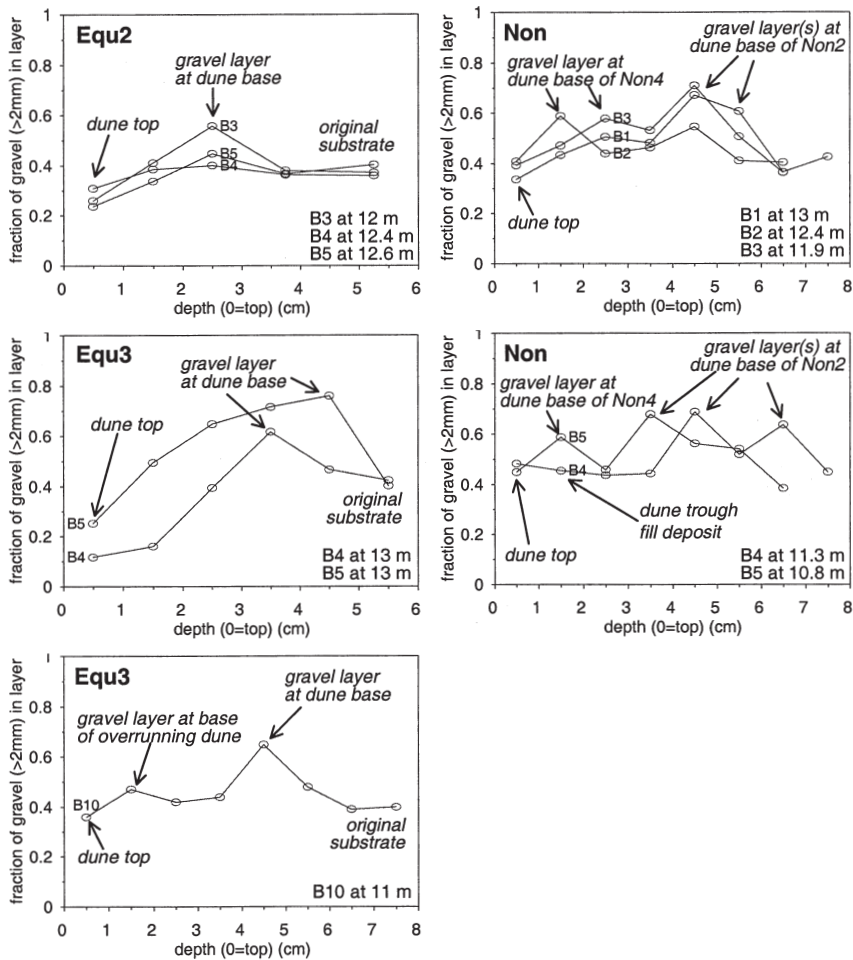


Figure 10.9. Vertical sorting in the bed, given as the gravel abundance ($D > 2\text{mm}$) of the samples against depth below the Non5 bed surface. For Equ2 and Equ3, the given depth is below the dune tops, while for Non it is below the plane low-flow bed surface of Non5. The positions of the samples along the flume are given for comparison with Figure 10.5.

10.4 Discussion

Outstanding characteristics of the experimental channel bed deposits are the occurrence of gravelly layers and the variability of the dune trough scour depth. In addition, a typical deposit for non-equilibrium conditions was found: the sandy trough fill deposit. These phenomena must be understood before morphological modelling in such conditions can be attempted. Four aspects related to vertical sediment sorting are discussed:

1. the formation of gravelly layers,
2. the cause of the variability in the depth of the dune trough scour and the concurrent gravelly layers,

3. the competition between deposition of relatively less mobile gravel in the dune troughs and the dune trough scour, and
4. deposits found in non-equilibrium conditions and their effect on the net vertical sorting.

In addition, there are fundamental differences between experiments conducted in sediment recirculation flumes and sediment feed flumes. These differences, and their effects on the interpretation of the experiments reported here and in literature, are discussed in the appendix.

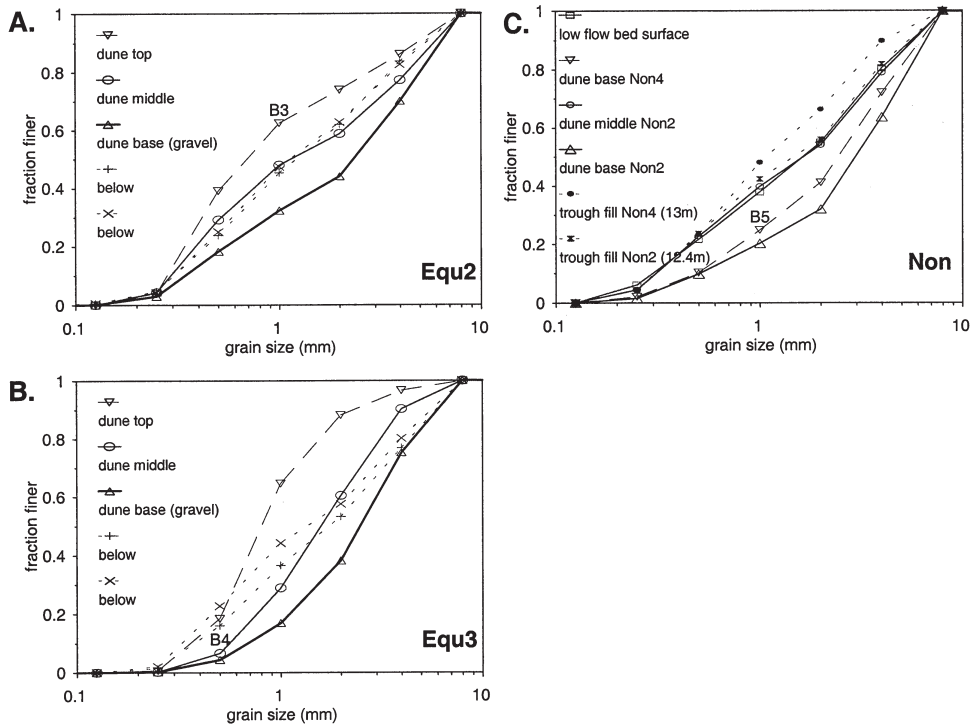


Figure 10.10. Grain size distributions of certain elements of the deposits. The sediment below the dunes is the original substrate. For the Non experiments, also sandy trough-fill deposits from Non4 and Non2 are given. The low-flow armoured bed surface of Non5 was a rather thick sample: some fine underlying sediment was scooped as well, so the armouring is not obvious in the grain size distribution.

10.4.1 Controls on gravel lag formation

For the understanding of the formation process of gravelly layers it is convenient to discuss the two end-members of a continuum of possible cases first:

1. the fully mobile gravelly layer. In Equ3 and Non2, the composition of the transported sediment approximated the feed sediment. Thus the coarse fractions were mobile, and the gravelly layers are therefore not true lag layers. Instead, this gravel is part of the dune body and is worked down in the process of grain flowing at the lee-side of the dunes.

2. the totally immobile gravel lag. The experiments reported by Blom and Kleinhans (1999, see also Kleinhans et al. 2002 in chapter 4) did not have fully mobile gravel fractions, which resulted in an (almost) immobile gravel lag layer below the dunes. The gravel lag layer was formed by working down the gravel below the mobile sediment by grain flowing after it went over the dune top, and when it did not go over the top, by winnowing of the finer sediment from the dune crest.

In extreme cases (very wide mixtures and low shear stresses), the second end-member may be characterized by isolated barchan dunes migrating over a stable armour layer (Carling et al. 2000, Kleinhans et al. 2002, see chapter 4). This phenomenon is not considered herein.

Note that in the absence of dunes, a gravel lag is equivalent to an armour layer. However, in the presence of dunes the formation process is different (grain flowing), therefore the two are distinguished. The difference may be observable when the larger grains are a-spherical: armour layers will have imbrication, while a gravel lag will not have this imbrication.

The control which determines where a certain condition stands between the two end-members, is the mobility of the coarsest fractions. Unfortunately, the mobility of the grains in the trough is not easily predicted, because it depends not only on the abundance of size fractions in the lag layer, but also on the near-bed turbulence characteristics in the wake of the bedforms, which are not understood well enough for predictive purposes (McLean et al. 1994, Bennett & Best 1995). The highest shear stresses of the fluctuating flow in the trough region are expected to entrain the most sediment. Since sediment transport depends non-linearly on the shear stress, the transport must be computed for and integrated over the whole probability distribution of the Reynold shear stress.

The following transport parameter is proposed for prediction of gravel lag occurrence: the net sediment transport q_L of the sediment in the gravel lag layer compared to the transport rate q_b of the bedload sediment. If the ratio q_L/q_b is small, then the gravel lag deposition is promoted. Thus the ratio q_L/q_b determines the opportunity for gravel lag formation.

The sediment transport of the lag layer zone could be based on Bridge & Bennett (1992) and Kleinhans & Van Rijn (2002, see chapter 5):

$$q_L = \int_{\tau = \tau_{cr,L}}^{\tau = 6\sigma_\tau} p_\tau q_\tau d\tau - \int_{\tau = -6\sigma_\tau}^{\tau = -\tau_{cr,L}} p_\tau q_\tau d\tau \quad (1)$$

in which q_L =transport rate of the gravel lag layer sediment, the left integral is the downstream transport rate and the right integral is the upstream transport rate, τ =momentaneous bed shear stress described by an appropriate probability distribution, $\tau_{cr,L}$ =critical shear stress of the gravel in the lag layer in the upstream (negative) and downstream (positive) direction, σ_τ =standard deviation (from the probability distribution) of the momentaneous τ , and p_τ = proportion of the time in which a momentaneous τ is active, described by the same appropriate probability distribution.

The procedure is proposed as follows (Kleinhans & Van Rijn (2002, see chapter 5). The sediment transport rate is computed for each momentaneous shear stress interval in the probability distribution. The portion of the probability distribution in which $-\tau_{cr,L} < \tau < \tau_{cr,L}$ is excluded, because then the transport is zero. The transports are integrated over the whole probability distribution of the momentaneous shear stress in the upstream and downstream direction.

In non-equilibrium conditions, the problem is even more complex. In increasing shear stress the

dunes are growing by sediment entrainment from the substrate, but the growth may be hindered by the gravel lag layer between the dunes and the substrate. The turbulence intensity in the relatively small dunes is high, which promotes the entrainment. For decreasing shear stress, the deposition of a lag layer is promoted by the low turbulence intensity in the troughs of the relatively large dunes. This problem provides a challenge for future modelling.

Although the transport rate of the gravel lag sediment has been approached so far as if it were uniform sediment, in reality it is a sediment mixture. The mobility of grains with different sizes in a mixture varies with mixture characteristics, for instance unimodal or bimodal grain size distributions, and therefore affects gravel lag layers. In the extreme case of equal mobility (Parker & Klingeman 1982), gravel lag layers will not form because the gravel is not less mobile than the rest of the sediment. However, most experimental mixtures and river sediments seem to deviate at least slightly from equal mobility (Wilcock 1993), therefore gravel lag layers may form. Bimodal mixtures show the largest difference in mobility between coarse and fine sediment (Wilcock 1993). Experiments with extremely bimodal sediment are reported by Hooke (1968), where a pea gravel lag in dunes in fine sand seemed to hinder the deep scour erosion, and by Van der Zwaard (1973) with comparable results in a bimodal mixture of coarse sand and coarse gravel. Concluding, gravel lag formation is more likely to occur in bimodal sediment than in unimodal sediment.

10.4.2 Controls on dune irregularity

Dunes become more irregular (3D) when the shear stress is increased (Reineck & Singh 1973, Boothroyd & Hubbard 1975, Costello & Southard 1981, Terwindt & Brouwer 1986). Thus it is the velocity and grain size, or alternatively the dimensionless (grain-related) shear stress of the mean or median grain size (θ_m or θ_{50} or θ'_{50}) that determines the three-dimensionality of the dunes (see Fig. 10.11). The crest lines become sinuous and there is much more variation in dune height, length and scour depth. Reineck & Singh (1973) describe the transition from 2D to 3D features as going from straight-crested, undulatory dunes (with continuous wavy crests), lunate (non-continuous crestlines and spoon-shaped scours) to linguoid dunes (tongue-formed like bars in shallow rivers). The conditions referred to in this paper produced 2D forms (straight-crested), moderately transitional 2D-3D forms (undulatory), and 3D forms (lunate).

The probability distributions of bed levels for 3D dunes (Equ3) have a much longer tail down into the bed than for 2D dunes (Equ2) (see Fig. 10.6). This was exactly the same for Non2 and Non4. Thus, the trough scour depth variation for 3D dunes is much higher than for 2D dunes, and there is no difference between the non-equilibrium and equilibrium case.

This irregularity is relevant here because of the depth of deposition of the sorted sediment (Harms & Fahnestock 1965, Reineck & Singh 1973, Leclair & Bridge 2001) (see Fig. 10.8). For 2D dunes like those in Equ2 and Non4, the deposit is extremely regular, that is, the height of the (cross-stratified) sets is zero and the length is as large as the flume. (With cross-set thickness, Paola & Borgman (1991) do not mean the upper set, but the sets between the upper set and the substrate sediment.) These sets are described as planar cross-bedding. For 3D dunes like those in Equ3 and Non2, the height of the sets (*sensu* Paola & Borgman 1991) is larger while the set length becomes smaller. These sets are described as trough crossbedding. The effect is that the vertical sediment sorting averaged over several dune lengths is less well developed for 3D dunes than for 2D dunes (see Fig. 10.9 third panel). Concluding, increasing the complexity of dune behaviour decreases the net averaged vertical sorting efficiency.

The relation between dune three-dimensionality and the probability distribution of the bed level

is confirmed by data from literature. Leclair & Blom (2001) compared the probability distributions of the bed surface for the experiments A1 and A2 of Blom et al. (2000) and 29SAFL of Leclair & Bridge (2001), of which the former were done with a wide sand-gravel mixture while the latter was done with a narrow sand mixture. The wide mixture had a more or less symmetric probability distribution (see Fig. 10.12), while the narrow mixture had a long tail from the deep irregular scour. Leclair & Blom attributed the difference to the presence of coarse sediment in the trough zone, but in the light of the analysis above, it is more likely that the three-dimensionality of the dunes is the principal parameter (also see next section). From the photographs in Blom et al. (2000) and Leclair & Blom (2001) it is obvious that the dunes in the narrow mixture (29SAFL) were in the three-dimensional regime, while those in the wide mixture (A1, A2) were in the two-dimensional regime as discussed before.

To demonstrate the predictability of three-dimensionality of the dunes, the available experiments reported in this paper and in literature are plotted in the bedform stability diagram of Southard & Boguchwal (1990, see Fig. 10.11). The Equ3 and Non2 experiments plot more in the upper part of the dune regime and therefore are likely to give 3D dunes, while all other experiments plot in the lower half of the dune stability field. From Figures 10.6 and 10.12, it is indeed obvious that the largest asymmetry of bed level probability distributions due to scour holes occur in Equ3 and Non2.

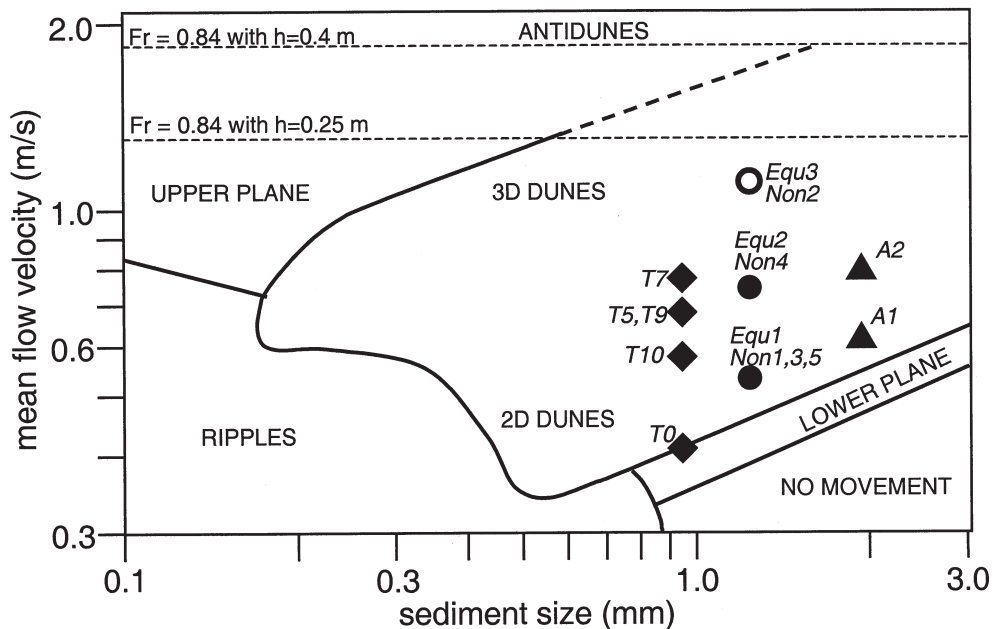


Figure 10.11. Bedform stability diagram of Southard & Boguchwal (1990) from their Figures 10.3 and 10.8 for water depths of 0.1-0.4 m. Antidunes occur above Froude numbers of 0.84, which is given for two water depths in the graph. The experiments plotted are reported in this paper (Equ and Non), the barchan dunes of A1 and 2D dunes of A2 from Blom et al. 2000 (with water depths of 0.16 and 0.32 m respectively), and lower plane bed of T0, barchan dunes of T10 and 2D dunes of T5,7,9 from Blom & Kleinhans (1999) and Kleinhans et al. (2002) (with water depths from 0.2-0.35 m). The transition from dunes to antidunes is for Froude numbers above 0.84.

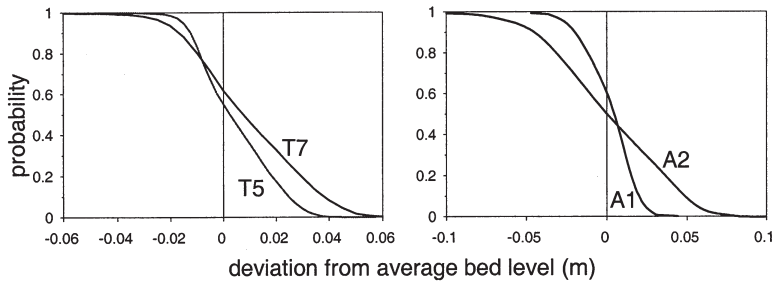


Figure 10.12. Probability distributions of the bed surface, determined from bed level profiles along the axis of the flume, from Blom & Kleinhans (1999) and from Blom et al. (2000).

10.4.3 Competition between deep scour and gravel lag layers

In a previous section, it was argued that the formation of a gravel lag layer hinders the deepening of trough scour areas. There might be cases in which the θ_m or θ'_{50} is high enough for the formation of 3D dunes, but the q_l/q_b is still far below unity, leading to gravel lag formation which may inhibit or hinder the deepening of trough scour areas. Thus the tendency to develop three-dimensional dunes may be frustrated by gravel lags. So there are two controls on the irregularity of dunes and resulting trough scour depth variation (excluding the case of barchan dunes): the θ_m or θ'_{50} and the q_l/q_b . There is a competition between the two, the first inducing irregular deep trough scour and the second inhibiting that trough scour.

It is the question which one is the more important. It could be argued that, when the shear stress is high enough to form 3D dunes, then q_l/q_b approaches unity, that is, the larger grains are far above the threshold of motion anyway. This depends on two things: the deviation from equal mobility and the history (thickness and strength) of the gravel lag layer. In the case of equal mobility, no gravel lag layer is formed at all, in which case the parameter q_l/q_b is unimportant for the explanation of dune trough scour variation. In the case of strong deviations from equal mobility and/or a thick gravel lag layer, the q_l/q_b might become important.

In Figure 10.13, the threshold for motion of grain size fractions is compared to the actual shear stress in the experiments, and the upper limit for dune formation from the bedform stability diagrams of Southard & Boguchwal. The actual shear stress for the Equ2 and Equ3 experiments is never smaller than the critical shear stress for mixtures, which means that all grain sizes are in motion. It can also be seen that the upper limit for dune formation has a much steeper slope than the Egiazaroff (1965) function. Consequently, when an experiment is in the 3D dune regime (e.g. Equ3), then only extremely large grains would be immobile, if they occurred in the mixture at all. This is very rare because there are not many rivers with both dunes and such extremely wide mixtures. It can be concluded that the largest grains in mixtures are in motion for most natural sediments when the dunes are in the 3D regime, therefore the θ_m or θ'_{50} is the dominating parameter for three-dimensionality of dunes.

The analysis above is limited to equilibrium conditions. In rising discharge in rivers, time starts to play a role. The dunes could very well be in the 3D-dune regime as far as the flow is concerned. Yet, the presence of a thick or coarse gravel lag in the bed might inhibit the variation in trough scour depth, temporarily leading to 2D dunes. This is confirmed by Costello & Southard (1981), who observed that dunes in the 3D dune flow regime remained 2D when the non-erodible base of the flume was continuously visible over considerable surface areas in the troughs. The reason is that it takes time to remove the gravel from the lag layer, and during that time the dunes

cannot scour down but must remain two-dimensional.

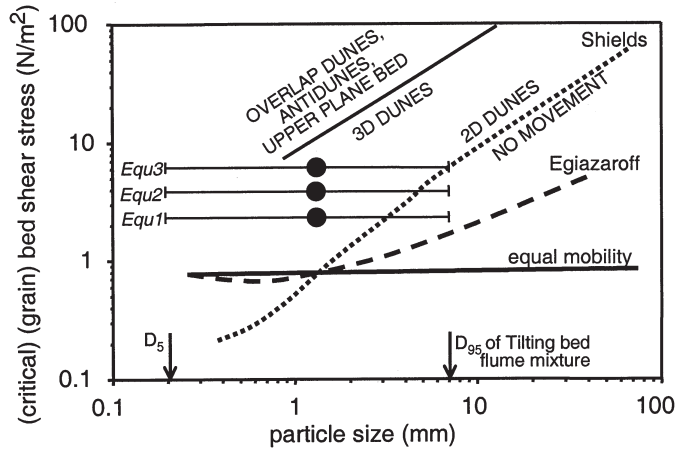


Figure 10.13. Plot of the threshold for motion of uniform mixtures (critical shear stress as a function of grain size according to the Shields curve) and mixtures. For the mixtures, the Egiazaroff (1965) function and the equal mobility function (Parker & Klingeman 1982) are given. In addition, the actual shear stresses of the Equ experiments are given as horizontal lines, ranging from the D_5 to the D_{95} of the Tilting bed flume sediment mixture. If these horizontal lines crossed the lines of critical shear stress for mixtures, then grains with sizes larger than those at the intersection would be immobile, which is not the case. In addition, parts of the bedform stability fields of Southard & Boguchwal (1990, their Figure 10.12) are given.

For future modelling, it is recommended that the trough scour depth (that is, the skewedness) of the bed level probability distributions is coupled to the θ_m , and in addition that the time-dependent process of dunes digging through a resistant gravel lag layer (q_t/q_b in the trough region) is experimentally measured and somehow included in models.

10.4.4 Deposits of dunes in lowering discharge

Until now, the comments on non-equilibrium conditions have been limited to rising discharges. In these conditions, dunes are growing and reworking bed sediment at increasing depth in the channel bed. In doing so, the dunes are affected by antecedent sediment sorting in the bed (e.g. gravel lag layers hinder dune trough scour). It is therefore important to study how the sediment is deposited in lowering discharges as well, since that sorting is the antecedent sorting for the next discharge peak (Kleinhans 2001).

The sandy dune tops from the intermediate and high discharge peaks were eroded and deposited in the dune troughs during low discharge in the Non-experiments. This led to a horizontal variation in grain size (see Fig. 10.7). The reason is that the transition from high or intermediate discharge to low discharge was abrupt, and in low discharge no dunes occurred (*viz.* Equ1) so the relict dunes were eroded. The net fining upward sorting in the bed with the eroded dunes in Non2 and Non4 is less pronounced than in the dunes of Equ2 and Equ3 (Fig. 10.9), because in the latter the dunes were not eroded. The longitudinally averaged vertical sorting of a river bed with patches of fine and coarse sediment is obviously less strong than in dunes with a fining-upward sorting

trend.

Whether such fine trough fill deposits are formed, depends on the adaptation of the dunes to changing flow, as revealed by a comparison with the experiments T7 and T9 of Blom & Kleinhans (1999, see Kleinhans 2001). In T7, the flow velocity was 0.8 m/s, while in T9 it was 0.7 m/s. (in the short transition experiment T8 the flow depth and discharge were gradually decreased.) In both experiments T7 and T9, dunes occurred, but in the latter the coarser gravel was no longer mobile (which it was in T7). The resulting sorting was a fining upward lag deposit below the active dunes of T9, which consisted of the sediment that was mobile in T7 but no longer in T9. There were no relict cross-bedded dune deposits from T7; all the sediment that was active in T7 was reworked in the slow transition, resulting in lag deposits only. In the experiments reported here, on the other hand, mainly cross-stratified dune deposits with gravelly bases were preserved, and in addition the sandy trough fills. The obvious cause for the difference is the time-rate of change of discharge: the transition is sudden and large (dunes to lower stage plane bed), while it is gradual and much smaller in the Blom & Kleinhans experiments (dunes in both cases). In Non3 and Non5 the dunes get no time at all to adapt to the changing flow, while this opportunity is much larger in T8 and T9.

Both cases are relevant in real rivers. Time is needed to adapt dune dimensions to changing discharge during a discharge wave. This time depends on the time-rate of change of the discharge, the sediment transport rate, and the difference between actual dune dimensions and the equilibrium dimensions in the actual flow conditions. Usually this leads to little hysteresis of dune dimensions as a function of shear stress (or discharge), with relatively smaller dimensions in rising discharge and larger in lowering discharge. In such rivers the sorting pattern found in the Blom & Kleinhans experiments is expected: a lag deposit that is fining upward as increasingly finer sediment becomes immobile. This implies a significant deviation from equal mobility, otherwise no lag deposit would be left but only the gravelly lower parts of the dunes.

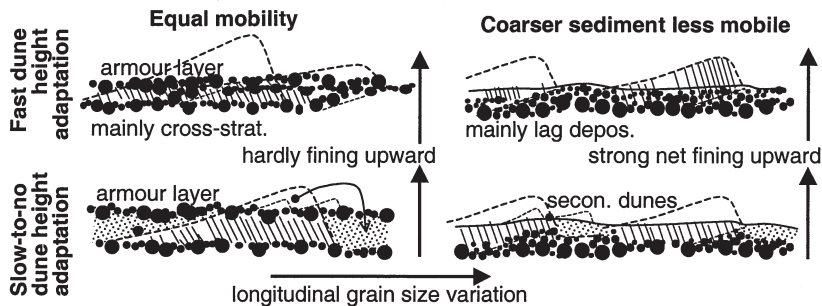


Figure 10.14. Conjecture of sediment sorting in the bed (key is the same as in Figure 10.7) in cases with equal mobility, and with lower mobility of the larger grains, and in cases with fast dune height adaptation to changing flow, and with slow or no adaptation. In the latter case, secondary dunes may emerge. Trough-fill deposits only occur when dunes adapt slowly. True lag deposits only occur in non-equal mobility conditions, and the fining upward trend is stronger than for equal mobility.

In other rivers, however, dunes are reported to become inactive and subject to erosion, analogous to the transitions from Non2 to Non3 and from Non4 to Non5. Field studies by Allen & Collinson (1974), Harbor (1998), Ten Brinke et al. (1999) and reported in chapter 6 show that small secondary dunes emerge on the relicts of the large, inactive primary dunes. These secondary dunes act as the conveyor belt that transports the sediment from the tops of the primary dunes to the troughs, working towards lower stage plane bed while the secondary dunes disappear as well. Now a combination of gravelly (lag) deposits, cross-stratified primary dune deposits and

trough fills is expected as in the Non experiments. Possibly the secondary dunes leave their own fingerprint in the deposits, but this could not be studied here.

Summarizing (see Fig. 10.14), in events where the dunes are able to adapt to some extent to the changing flow conditions, combined with a strong deviation from equal mobility, mainly fining upward lag deposits are expected. When there is equal mobility, a barely fining upward stacking of cross-stratified dune deposits is expected. In rivers where dunes do not adapt to changing flow but become immobile, the fining-upward cross-stratified dune deposits of these primary dunes are preserved, and trough fill deposits are formed consisting of the eroded dune top sediment. For deviations from equal mobility, lag deposits can be expected below the primary dunes and in the troughs. If, however, there was equal mobility in the higher discharge, then only the gravelly layers formed as the lowest parts of cross-stratified dune deposits are expected. A challenge for future modelling is to parameterize the effect of lagging dune height adaptation as a decreased vertical sorting efficiency.

10.4.5 Towards modelling

Recollect that two essential elements for morphological models (cf. Parker et al. 2000) are unknown: the vertical sorting in and by dunes, and the variation of the dune trough scour (see the introductory sections in this paper). Before modelling of the vertical sorting, sediment transport and morphological change can be attempted, the following issues therefore need to be addressed in experimental and field studies:

- The dune trough scour variation, i.e. the three-dimensionality of dunes and the resulting asymmetry of the probability distributions of the bed surface, needs to be quantified as a function of flow parameters and grain size.
- The effect of gravel lag layers on dune development (in specific trough scour) and sediment transport in non-equilibrium conditions need to be quantified.
- The hysteresis of dune height and the favourable conditions for and timing of the emergence of secondary dunes must be understood and predictable.
- The vertical sorting at the lee side of dunes needs to be measured as a function of a large range of flow and dune parameters for different sediment mixtures.

The question is now how these results could be implemented in morphological models for sediment mixtures. One way is to calibrate a rough vertical sorting function and to use measured probability distributions of the bed surface for each modelling case. The disadvantage of such calibrations is that expensive and difficult measurements are needed in each river that is modelled. Calibrating the model on flume experiments is not sufficient, because the vertical sorting and dune behaviour in a flume may be completely different from that in a river for various reasons.

A more physically-based approach without such calibrations would be to model the vertical sorting and the bed level probability distributions based on the measurements proposed above. Three relevant types of models can be distinguished in order of decreasing length scale:

1. Morphological models for sediment mixtures (e.g. Hirano 1971, Ribberink 1987, Parker et al. 2000). These models average the sorting and dune behaviour over a length of several dunes, which means that the variation between individual dunes is not considered.
2. Models for dune development and behaviour and the resulting sedimentary structures (e.g. Raudkivi & Witte 1990, Paola & Borgman 1991, Leclair & Bridge 2001). These

models explicitly include the variation between individual dunes, for example the trough scour variation, to predict the dimensions of relict deposits of individual dunes. However, these models have not been developed for sediment mixtures.

3. Models for the grain flow characteristics at the lee side of dunes (e.g. Bagnold 1954, Allen 1970, Hunter 1985) which predict the characteristics of cross-stratification. These models have not been developed for sediment mixtures.

A nested modelling approach is herein proposed as follows. First, a type-3 model is used to predict the vertical sorting in individual dunes. Obviously the type-3 models first need to be extended for sediment mixtures and sorting at the lee side of bedforms.

The second step is to use a type-2 model to predict the structure of deposits by a train of individual dunes for a sufficient number of dunes. This deposit consists of two parts: 1) the cross-stratified units deposited by individual dunes with vertical sediment sorting modelled by the type-3 model, and 2) the gravel lag deposits, neglecting sandy trough fills. The type-3 model can then be nested in the type-2 model to predict the vertical sorting in the whole deposit.

The third step is to parametrise the results of the previous steps for a large range of flow conditions and different sediment mixtures for use in a type-1 model. Thus, a useful result of the type-2 and type-3 models would be a bed level probability distribution function that depends on the θ , and a vertical sorting function that depends on the θ and the dune height, and which includes both sorting by grain flows and gravel lag deposits.

10.5 Conclusions

The sorting of sediment mixtures in river channel beds with dunes is controlled by dune characteristics and the mobility of the coarser grains in the mixture. In general, the deposits are fining upward with fine sediment deposited in the upper parts of the dune and coarse in the lower part, found as gravelly layers. For two-dimensional dunes in equilibrium, a continuous gravelly layer is deposited with little variation in thickness and depth below the bed surface. For three-dimensional dunes, the variation in trough scour depth causes a more complex stacking of deposits with multiple, discontinuous gravelly layers. As a result, the net vertical sorting is less pronounced than with two-dimensional dunes. For two discharge waves in order of decreasing magnitude and with enough difference in dune height, the gravelly layers from the lower parts of the dunes can be related to individual events.

There is a tendency for dunes to become more three-dimensional at higher shear stresses, with more trough scour depth variation and crest sinuosity. At the same time, the formation of lag layers below the dunes depends on the mobility of the coarsest sediment. Such a lag layer hinders trough scour, especially in rising discharge. Usually, however, all grain sizes are probably mobile when the dunes are in the 3D regime and gravel lag formation does not inhibit trough scour.

A third control is the dune height adaptation in lowering discharge. When dunes simply become smaller while migrating, then mostly fining upward lag deposits are expected in the channel bed. When, on the other hand, dunes become inactive, then the fining upward deposits of these dunes are preserved, and the fine sediment of the dune tops is deposited in the troughs. The latter pattern leads to a horizontal (downstream) patchiness of the deposit, and as a consequence a less pronounced vertical sorting averaged over the length of several dunes.

Acknowledgments

First of all I would like to thank Gary Parker for inviting me to St. Anthony Falls laboratory and for his help with the experiments. Jeff Marr is thanked for all his help with starting up the experiments, finding all the materials in the lab and deciphering the slang of Minnesotan suppliers of sediment and hardware. Without Jeff, the number of experiments feasible in the three-month stay would have been halved. Furthermore I acknowledge Mike, Scott, Randy and the students Dan, Andrew and Shandy for all their help with flume modifications, sediment mixing, the many sieve samples and sediment feeders that broke down, and Miguel, Horatio, Jake and Ben for fast bedload sampling during the high discharge experiments. Suzanne Leclair, Charlie Bristow, Arnold Bouma and Janrik van den Berg are thanked for their discussion and support in the making of lacquer profiles and foam profiles, which was a tricky job in the rather coarse and loose sediment, and needed much experimenting before good results were obtained. Chris Paola and Suzanne Leclair are thanked for discussing the complex interaction between dunes and sorting, and John Bridge is thanked for mentioning 'three-dimensionality of dunes' to me, which put me on the trail towards the competition between gravel lag formation and dune scour variation. The investigations were in part supported by the Netherlands Earth and Life sciences Foundation ('ALW') with financial aid from the Netherlands Organization for Scientific Research ('NWO'), and by the St. Anthony Falls Laboratory, Minneapolis MN, USA.

Appendix: Effect of the difference between sediment feed and recirculation flumes

A final point remains to be discussed, namely how the type of flume may have affected the observed sorting patterns. The experiments by Blom and Kleinhans (1999) were done in a sediment recirculating flume, while the present experiments were done in a sediment feed flume. Parker and Wilcock (1993) point out that there is an important difference between these two types of flumes. In both flumes, the discharge, water depth and the initial slope are specified (and uniform flow is maintained). In the sediment feed flume, the rate and composition of the sediment entering the flume is specified, while in the recirculating flume, it is determined by the selective transport process; thus the transport rate and composition is a dependent parameter. Thus the recirculating flume has an additional degree of freedom.

The effect of this difference is best illustrated for a case with an initial combination of slope, discharge and water depth and sediment mixture properties, for which the coarsest sediment is immobile in both flumes. Starting with a fully mixed bed, in a recirculating flume the finer sediment is entrained and migrates over the immobile coarse sediment. The sediment entering the flume is this same fine sediment. The result is therefore fine mobile sediment (possibly in dunes) migrating over immobile coarse gravel (lag deposit), which is a strong deviation from equal mobility. In the feed flume on the other hand, the coarse fractions in the feed sediment cannot be transported and therefore are deposited in the upstream part of the flume. This leads to an increase in bed slope (and, maintaining uniform flow, also water surface slope), and consequently to an increase of the bed shear stress, until the coarser sediment is transported as well. The feed system is eventually (in equilibrium) forced to transport all the sediment that is fed in. In moderate discharge, this equal mobility condition is only attained when a mobile armour layer is formed (Parker and Klingeman 1982) which was indeed observed during low and intermediate discharge.

A wrong conclusion would be that a true gravel lag layer cannot be formed in a sediment feed flume. This is only true for equilibrium conditions. For example, immediately after Non2 and Non4, the only sediment in transport in the downstream half of the flume, was that on the dune tops, while the underlying sediment was a gravel lag. In the upstream half, also coarse sediment was in motion, as the dunes were not yet well developed while the shear stress was for the larger portion applied to the grains (and not dissipated in the turbulence in the wake of bedforms).

It can be stated that the tendency for gravel lag formation is larger in sediment recirculating flumes

than in feed flumes. The flume experiments reported in this paper were designed to have a mobility of coarse grains as high as possible, in which case the gravel lag formation is not very important anyway. The experiments reported by Blom and Kleinhans, on the other hand, were designed for as little suspended transport as possible and no or low mobility for the coarse fractions, in which case a true lag layer is expected to occur anyhow. No true gravel lag layers would have formed in the recirculating flume if the shear stress were far above the threshold of motion for the coarsest grains. Thus, almost the same result could have been obtained with a recirculating flume as was obtained with a feed flume. However, immobile coarse sediment with a true lag layer could not be obtained in a feed flume in equilibrium where the feed sediment is the same as the original bed sediment. Therefore the results of Blom and Kleinhans could not have been obtained in a feed flume. Thus the two flume types were used for the conditions for which they are the best applicable. At best, the difference between the flume types may have made the differences between the deposits more pronounced, but this effect on the general conclusions herein is expected to be negligible.

Literature

- ALLEN, J. R. L. (1970), The avalanching of granular solids on dune and similar slopes. *Journal of Geology* 78, pp. 326-351.
- ALLEN, J. R. L., & COLLINSON, J. D. (1974), The superimposition and classification of dunes formed by unidirectional aqueous flows, *Sedimentary Geology* v. 12, pp. 169-178.
- BAGNOLD, R. A. (1954), Experiments on a gravity-free dispersion of large solid spheres in a Newtonian fluid under shear. *Roy. Soc. London, Proc. Ser. A(225)* pp. 49-63.
- BENNETT, S. J. & BEST, J. L. (1995), Mean flow and turbulence structure over fixed, two-dimensional dunes: implications for sediment transport and bedform stability, *Sedimentology* 42, p. 491-513.
- BLOM, A. & KLEINHANS, M. G. (1999), Non-uniform sediment in morphological equilibrium situations. Data Report Sand Flume Experiments 97/98. University of Twente, Rijkswaterstaat RIZA, WL | Delft Hydraulics. University of Twente, Civil Engineering and Management, The Netherlands.
- BLOM, A., RIBBERINK, J. S., & VAN DER SCHEER, P. (2000), Sediment transport in flume experiments with a trimodal sediment mixture. Proc. Gravel Bed Rivers Conference 2000, 28 August - 3 September, New Zealand, in NOLAN, T., & THORNE, C. (eds), Special public. CD-rom of the New Zealand Hydrological Society, New Zealand.
- BOOTHROYD, J. C. & HUBBARD, D. K. (1975), Genesis of bedforms in mesotidal estuaries. In: CRONIN, L. E. (ed.), *Estuarine Research, Volume II: Geology and Engineering*, pp. 217-234, Academic Press, New York, USA.
- BOUMA, A. H. (1979), *Methods for the study of sedimentary structures*, Robert E. Krieger Publishing Company, Huntington, New York.
- CARLING, P. A., GOELZ, E., ORR, H. G., & RADECKI-PAWLIK, A. (2000), The morphodynamics of fluvial sand dunes in the river Rhine, near Mainz, Germany. I. *Sedimentology and morphology; Sedimentology*, 47, pp. 227-252.
- COSTELLO, W. R. & SOUTHARD, J. B. (1981), Flume experiments on lower-flow-regime bed forms in coarse sand. *Journal of Sedimentary Petrology*, 51, 3, pp. 849-864.
- EGIAZAROFF, I. V. (1965), Calculation of nonuniform sediment concentrations. *Journal of the Hydraulics Division, ASCE* 91 (HY4) pp. 225-248.
- HARBOR, D. J. (1998), Dynamics of bedforms in the lower Mississippi River. *Journal of Sedimentary Research*, 68, 5, pp. 750-762.
- HARMS, J. C. & FAHNESTOCK, R. K. (1965), Stratification, bed forms, and flow phenomena (with an example from the Rio Grande), In: MIDDLETON, G. V. (ed.) *Primary sedimentary structures and their hydrodynamic interpretation*, Society of Economic Paleontologists and Mineralogists, Special Publication 12, Oklahoma, USA, pp. 84-115.
- HIRANO, M. (1971), River bed degradation with armouring, *Transactions of the JSCE*, 3, part 2.
- HOOKE, R. LEB. (1968), Laboratory study of the influence of granules on flow over a sand bed. *Geological*

- Society of America Bulletin 79 p. 495-500.
- HUBBELL, D.W., STEVENS, H.H. JR., SKINNER, J.V. & BEVERAGE, J.P. (1985), New approach to calibrating bed load samplers. *Journal of Hydraulic Engineering* 111, 4, pp. 677-694.
- HUNTER, R. E. (1985), A kinematic model for the structure of lee-side deposits. *Sedimentology* 32, pp. 409-422.
- KLAASSEN, G. J. (1991), Experiments on the effect of gradation and vertical sorting on sediment transport phenomena in the dune phase, Grain Sorting Seminar 21-25 October 1991, Ascona, Switzerland, Mitteilungen 117, Versuchsanstalt fuer Wasserbau, Hydrologie und Glaziologie der Eidgenoessischen Technischen Hochschule Zuerich (ETH).
- KLEINHANS, M. G. (2001), The Key Role of Fluvial Dunes in Transport and Deposition of Sand-Gravel Mixtures, a preliminary note, *Sedimentary Geology* 143 pp. 7-13.
- KLEINHANS, M. G., WILBERS, A. W. E., DE SWAAF, A. & VAN DEN BERG, J. H. (2002), Sediment supply-limited bedforms in sand-gravel bed rivers. *Journal of Sedimentary Research* in press, see chapter 4.
- LECLAIR, S. F. & BLOM, A. (2001), Relation between the probability distribution of bed elevation and the vertical sorting in subaqueous dunes. In: *Fluvial Sedimentology 2001*, Eds. MASON, J. A., DIFFENDAL, R. F. JR. & JOECKEL, R. M., Open-File report 60, Conservation and survey division, Institute of agriculture and natural resources, University of Nebraska-Lincoln, USA.
- LECLAIR, S. F. & BRIDGE, J. S. (2001), Quantitative interpretation of sedimentary structures formed by river dunes. *Journal of Sedimentary Research* 71 5.
- MCLEAN, S. R., NELSON, J. M. & WOLFE, S. R. (1994), Turbulence structure over two-dimensional bed forms: Implications for sediment transport. *Journal of Geophysical Research*, 99, C6, pp. 12729-12747.
- PAOLA, C. & BORGMAN, L. (1991), Reconstructing random topography from preserved stratification, *Sedimentology* 38, pp. 553-565.
- PARKER, G. P. & KLINGEMAN, P. C. (1982), On why gravel bed streams are paved. *Water Resources Research* 18 (5) pp. 1409-1423.
- PARKER, G. P. & WILCOCK, P. R. (1993), Sediment feed and recirculating flumes: fundamental difference. *Journal of Hydraulic Engineering*, 119 11 p. 1192-1204.
- PARKER, G., PAOLA, C. & LECLAIR, S. (2000), Probabilistic Exner sediment continuity equation for mixtures with no active layer, *Journal of Hydraulic Engineering* 126 (11) pp. 818-826.
- RAUDKIVI, A. J. & WITTE, H. H. (1990), Development of bed features. *Journal of Hydraulic Engineering* 116, 9, pp. 1063-1079.
- REINECK, H.-E. & SINGH, I. B. (1973), *Depositional sedimentary environments*, Springer-Verlag, Heidelberg, Germany, p. 439.
- RIBBERINK, J. S. (1987), Mathematical modelling of one-dimensional morphological changes in rivers with non-uniform sediment. Ph.D. thesis, Delft University, The Netherlands.
- SOUTHARD, J. B. & BOGUCHWAL, A. (1990), Bed configurations in steady unidirectional water flows. Part 2. Synthesis of flume data; *Journal of Sedimentary Petrology*, 60 5, pp. 658-679.
- TEN BRINKE, W. B. M., WILBERS, A. W. E. & WESSELING, C. (1999), Dune growth, decay and migration rates during a large-magnitude flood at sand and mixed sand-gravel bed in the Dutch Rhine river system. *Spec. Publs int. Ass. Sediment.* 28, pp. 15-32.
- TERWINDT, J. H. J. & BROUWER, M. J. N. (1986), The behaviour of intertidal sandwaves during neap-spring tide cycles and the relevance for palaeoflow reconstructions. *Sedimentology*, 33, pp. 1-31.
- VAN DEN BERG, J. H., & VAN GELDER, A. (1993), A new bedform stability diagram, with emphasis on the transition of ripples to plane bed in flows over fine sand and silt; *Spec. Publs. Int. Ass. Sediment.* 17, pp. 11-21.
- VAN RIJN, L. C., (1984), Sediment transport, part I: bed load transport; *Journal of Hydraulic Engineering*, 110 (10) pp. 1431-1456.
- VAN DER ZWAARD, J. J. (1973), Roughness aspects of sand transport over a fixed bed, XVth IAHR-congress, Istanbul, also Delft Hydraulics publication 118, Delft, The Netherlands.
- WILCOCK, P. R. (1993), Critical shear stress of natural sediments. *Journal of Hydraulic Engineering* 119 (4) pp. 491-505.

Synthesis, conclusions and scientific recommendations

"All our ideas are nothing but copies of our impressions." David Hume

"As far as the laws of mathematics refer to reality, they are not certain; and as far as they are certain, they do not refer to reality." Albert Einstein about David Hume

"When I saw the earth flow moving into that river, I immediately thought of Leibnitz's rule." Gary Parker

11.1 Introduction

The general objective of this PhD-thesis is to gain a better understanding of the sediment transport and depositional processes of sand-gravel mixtures in the presence of dunes. There are two complementary approaches to the objective: first, working from basic principles (sediment continuity, other physical laws) with models and testing these models on experimental results, and second, the empirical study of processes in nature and under more controlled laboratory conditions. The latter approach is followed in this thesis.

First, the conclusions are summarised, and their relevance discussed for rivers in the continuum from sand-bed rivers to gravel-bed rivers. Next, the role of sediment sorting phenomena in the sediment transport processes is considered at the length scales of grains, dunes and river reaches (see **chapter 2**). How to implement the findings in morphological models is explicitly indicated for some existing and new model concepts. Finally, a number of crucial processes and their importance for sediment transport and sorting are outlined which are not well understood, but of which understanding is a prerequisite for further progress.

11.2 Conclusions

The general conclusions of this study, referring to the four hypotheses given in **chapter 2**, are:

- I.
 1. The bedload sediment transport rate and the bedload grain size distribution can be predicted for conditions near incipient motion of the largest grains in the bed sediment by using an appropriate hiding-exposure function and a stochastic approach to the bed shear stress on the grains (see **chapter 5**).
 2. The appropriate hiding-exposure function depends on sediment mixture characteristics: it represents near equal mobility of all grain sizes for unimodal sediment, and in bimodal sediment a lower mobility of the coarser mode than of the finer mode of the grain size distribution(see **chapters 2 and 5**).
- II. In flow conditions with heavy armouring, bedload sediment in the bedforms is not exchanged with the sediment in the armour layer and the sediment below. The bedload

transport rate and composition, and the bedform characteristics depend in this case on upstream sediment delivery, which cannot be predicted from local conditions (see **chapter 4**).

III. Vertical sediment sorting in the river bed is the result of two processes: 1) sorting at the lee-side of bedforms, preserved in the individual cross-stratified sets, and 2) gravel lag deposition in the trough-zone of bedforms (see **chapters 9 and 10**).

1. The sorting at the lee side of bedforms depends on sediment characteristics, the bedform height and celerity, and the local flow conditions above the top of the bedform (see **chapters 7 and 8**).

2. Whether a gravel lag is deposited, depends primarily on the mobility of the coarsest sediment, and in addition on the vertical sorting at the lee side of bedforms and on the dune adaptation time to changing flow.

a. The mobility of the coarsest sediment is determined by the turbulent flow conditions in the trough zone of bedforms. The depth in the bed at which the gravel lag is deposited and the variation of this depth, depend on the trough-level variation of the dunes. This variation, in turn, depends on the dune irregularity (three-dimensionality of dunes), which is a function of sediment grain size and flow conditions (see **chapter 10**) and may be affected by antecedent gravel lag layers in the river bed (history effect).

b. The opportunity for gravel lag formation is affected by the vertical sorting at the lee side of bedforms (see **chapter 9**). Gravel lag formation is specifically promoted if the coarse sediment is mainly accommodated on the very lowest part of the lee side, while a more uniform distribution of gravel over the lee side reduces the opportunity.

c. The opportunity for continuous lag layer formation depends on the dune adaptation time in changing flow (see **chapter 10**). The faster the reaction of the dunes, the more likely is the formation of a continuous lag layer.

IV. 1. Due to the vertical sorting processes mentioned in the previous conclusion, a sedimentary record is left in the river bed of one or more discharge events (see **chapters 6, 9 and 10**). As the grain size of the bed sediment affects the sediment transport rate and composition, this sorted deposit is the antecedent sorting which affects sediment transport in subsequent discharge events. As a result, the sediment transport rate is not uniquely dependent on the flow discharge, but may show a hysteresis during a discharge wave. In addition, this 'history effect' may lead to differences in transport rates between two subsequent discharge waves (see **chapter 9**).

2. The prediction of sediment transport during a discharge wave in large sand-gravel bed rivers is hampered by lack of knowledge of:

a. the bedform development during a discharge wave (see **chapter 6**),

b. the partitioning of bed shear stress into grain-related shear stress (causing the transport) and bedform-related shear stress (see **chapter 6** and the discussion in a later section), and

c. the interaction between (antecedent) sediment sorting (e.g. thick gravel lag layers) in the bed on the dune development and transport rate (see **chapter 9**).

11.3 A continuum from sand-bed rivers to gravel-bed rivers

The findings in this thesis refer to rivers with both sand and gravel in the bed. The importance of vertical sediment sorting in the river bed for the sediment transport process is due to three phenomena: mobility of the sediment, the presence of a sediment mixture that can be sorted (i.e. not uniform sand), and the presence of dunes in which and by which the sorting takes place.

Concerning the role of the sediment mobility, in **chapter 4** it is shown what happens when the coarser part of the sediment is rather immobile: the bedforms cannot develop well, and the actual sediment transport rate is determined by the sediment delivered from upstream sections of the river. In this condition, the vertical sorting in the river bed will not develop as described in **chapters 8 and 9**, but is dominated by armouring. The armouring condition is more likely to take place in very wide mixtures and/or bimodal sediment.

If the sediment in the river bed is rather uniform, then the vertical sorting is negligible (see for example the sorting of sediment in dunes in the river IJssel, **chapter 7**). It is the question when exactly the sorting becomes unimportant. Sandy sediment usually has a rather small geometric standard deviation while gravel usually has a large geometric standard deviation (gravel-bed rivers with well sorted sediment are exceptional) (see **chapter 2**). So one generalisation may be that the coarser the sediment is (D_{50} or D_g), the more important sediment sorting becomes.

In addition, in sand-bed rivers the sediment is much more mobile than in gravel bed rivers, so the role of suspension is more important and obscures the vertical sorting caused by grain flows at the lee side of dunes (see **chapter 7**). So, a second generalisation may be that in sand-bed rivers the role of sorting is negligible.

A prerequisite for the vertical sorting mechanisms as described in this thesis is the presence of dunes. To develop dunes, the shear stress must at least be approximately twice as large as the critical shear stress. However, many gravel-bed rivers have shear stresses at bankful discharge that are only just above the critical shear stress (see **chapter 2**, figure 2.1). It is therefore unlikely that dunes of significant height will generally develop in gravel-bed rivers. Consequently, vertical sorting by dunes will be negligible.

This notwithstanding, many gravel-bed rivers are braided, and their sedimentary structures are related to the bars. In **chapters 7 and 8** it was argued that the sediment sorting at the lee-side of bars is comparable to that at the lee-side of dunes. So the vertical sediment sorting in bars might still be significant in gravel bed rivers. This is, however not well known, and the effect of this vertical sorting on sediment transport is not known at all.

Summarising, in typical sand-bed rivers the vertical sediment sorting is negligible because the sediment is too uniform, while in typical gravel-bed rivers the vertical sediment sorting by dunes (disregarding armouring) is negligible because dunes do not occur. The (effect of) sorting in bars is not well known. In all rivers with sand and gravel in the bed and in which dunes occur and in which the coarsest sediment is so mobile that armouring is not too strong for dune development, the vertical sediment sorting patterns as described in **part 2** of this thesis may develop. It has sufficiently been made clear in **chapter 6 and 9** that, once present, vertical sorting will certainly affect the sediment transport.

11.4 Roles of sediment sorting on different scales

Eventually, the object of this research is the modelling of sediment transport and morphological change in rivers during discharge waves. Only when the behaviour at the time scale of several

discharge waves is understood, it can be attempted to model the long-term behaviour of a river. If a river were modelled without the effects of vertical sediment sorting as described in this thesis, one may expect that both the rate and composition of the predicted sediment transport in subsequent discharge waves deviates from the true rate and composition. The magnitude of this deviation depends on the discharge history, and might lead to a long-term under- or overestimation of the sediment transport rate and morphological change.

The conceptual framework for modelling has been given in **chapter 2** (figure 2.12). In working towards the mathematical modelling of sediment sorting and transport (described in a next section), an overview is given below of the different sediment sorting processes in the order of increasing length scales as described in **chapter 2**:

- sorting at the grain scale: incipient sediment motion,
- sorting at the bedform scale: at the lee-side of bedforms,
- sorting at the reach scale: by several dunes.

The sorting on even larger length scales like that of the meander bends and of the downstream fining will be discussed in a later section. The sediment sorting phenomena at the grain scale are the *hiding-exposure phenomenon* described in **chapters 2 and 5**, the bed-surface armouring (see **chapters 2 and 4**) and the *like-seeks-like effect* (and related overpassing phenomena, see **chapter 2**). These have a considerable effect on the mobility of the sediment. This mobility is incorporated into sediment transport predictors (see **chapter 5**), while the like-seeks-like effect is either unimportant in sand-gravel bed rivers or incorporated in the overall mobility of the sediment and the hiding-exposure function. The sediment sorting at the bedform scale is the *sorting at the lee-side of bedforms by grain fall and grain flows* (see **chapters 7 and 11**). Part of the vertically sorted dune sediments are preserved in the river bed, and it is this part that affects the sediment transport rate. It is not yet clear how this sorting can be predicted, but it is understood in terms of the most important variables.

These sorting processes, together with the sorting at the river reach scale by several bedforms, make-up the whole complex of sediment sorting in the river bed. Sediment sorting by several dunes includes the deposition of gravel lag layers (see **chapter 9**), includes the variation in depth of *sorting due to dune trough scour*, and includes the *sorting from eroded dunes in waning flow* (see **chapter 10**). This whole complex of sediment sorting phenomena affects the sediment transport rate and composition.

Therefore this complex of sorted sediment (dune scale and reach scale) must be predicted and incorporated *en block* in a mathematical model (see figure 2.12). At least, the dune height and the variation in dune height must be predicted, as well as the sorting within a single representative dune and the vertical sorting in the bed due to the passage of several (irregular) dunes. The resulting sorting must be recorded in the model, because it will affect the sediment transport in subsequent discharge waves. So in the model there must be feedbacks between the sediment transport module and the sorting module, as well as between the dune height prediction module and the sorting module.

11.5 How to implement the results into (morphological) models?

“It does not help matters when reductionists mulishly insist that the only way decent physical models can be constructed is to start from the most primitive equations possible, or when synthesists cavalierly suggest that fundamental mechanics somehow becomes irrelevant just because a system happens to be complicated.” Chris Paola (2001: p. 35 in Mosley, M. P. (Ed.), *Gravel-bed rivers V*, New Zealand Hydrol. Soc.)

11.5.1 Modelling sediment sorting at the lee side of dunes

In **chapter 8** it was found that the sorting at the lee side of dunes, bars and deltas is probably not a simple function of a number of dimensionless parameters, but instead the result of two intertwined processes: grain fall deposition and grain flow reworking and deposition. It must be concluded that, for a correct prediction of the vertical sorting, these two processes must be dynamically modelled. In this section the outlines for a physically-based model of vertical sorting are given, based on three existing model concepts. This model does not include the deposition of gravel lag layers, as this is a different process. In literature, three unrelated model concepts have been reported that together form the essential elements of a model that should be able to predict the vertical sorting:

1. The grain fall deposition model concept by Jopling (1965), which predicts the paths of grains with different diameters from the top of a delta where they are suspended, to the lee slope or toe of the delta. This grain fall deposition causes the building of a wedge of sediment at the top of the lee slope, which may at some point fail and become a grain flow. The suspended grains start off with a certain horizontal velocity at a certain level above the top of the delta, and after the rapid flow deceleration just downstream of the delta the grain becomes subject to the settling velocity only. Based on these parameters Jopling was able to predict the position on the lee slope or toe where the grain was deposited, and the grain size and thickness of toe deposits in laboratory deltas. This concept must be extended to the situation with dunes and sediment mixtures with a suspended sediment transport predictor for sediment mixtures, as well as some information on the turbulent structure of the flow in the lee of dunes (as far as it affects grain fall deposits). This extension could be done based on the model of Mohrig (1994) and Mohrig & Smith (1996), who predicted the ratio of sediment that passes over to the downstream dunes and the sediment that is deposited on the lee slope.
2. Hunter (1985) provided a model concept for grain flows in uniform sediment, based on earlier work by Allen (1970). Based on the angle of repose of the sediment and on the deposition of grain fall as described under the previous point, Hunter was able to explain the initiation and thickness of the grain flows, as well as the preservation of grain flow or grain fall deposits on the lee slope. However, some of Hunter's conclusions are at variance with those in **chapter 8**, and his results may not be applicable to coarser and less well sorted sediment. This model therefore needs to be adapted. The video recordings of the experiments reported in **chapter 8** may provide the necessary clues how to adapt Hunters model, and provide the data for calibration of such a model.
3. For the sorting of grains of different sizes rolling down a slope, Koeppel et al. (1998) have been able to reproduce the vertical sorting and stratification of their experiments with bimodal sediment in air. The model is based on particle interactions; the energy exchange in collisions is modelled with the angle of repose and initial velocities of the grains as input parameters. A next step could be to incorporate more of the grain flow character in the model, that is, increase the sediment flux and model the interactions between the moving grains as well.

The sorting in grain flows provides a major challenge for both modellers and experimentators. A physically-based model for sorting at the lee-side of dunes and deltas could be used for the

parametrisation of a simple vertical sorting function. This simple function, in turn, could then be implemented in morphological models. This is computationally more attractive than nesting the whole grain flow model into a morphological model (see **chapter 10**).

In addition, more experiments and additional modelling may provide insight in sediment characteristics and flow conditions for which the vertical sorting vanishes. As explained in **chapter 7**, Koeppel et al. (1998) indicate that there is a sudden transition between vertical segregation of small and large grains with a strong fining upward trend but no stratification on the one hand, and pure cross-stratification without a fining upward trend on the other hand. This seems to contrast with the combined cross-stratification and fining upward found in the experiments in **chapters 8-10**, but was confirmed by one experiment with a bimodal sand mixture reported in **chapter 8**. In that experiment no vertical sorting was found but only pure cross-stratification. More experiments are needed to clarify whether and when this transition takes place in natural conditions. Eventually this may provide a fundamental explanation for the occurrence of cross-stratification in natural deposits, and whether vertical sorting occurs in that cross-stratification.

11.5.2 Point model of sediment sorting and transport

Recall that the model in **chapter 9** predicts a linear vertical sorting for two grain size fractions (sand and gravel), and predicts gravel lag layer formation by comparing the bedload sediment (determined by the bedload predictor of **chapter 5**) with the sediment in the transport layer (determined by dune height and antecedent sorting). An extension of this model is necessary to be able to predict the link between deposits and sediment transport, and potentially explain reach-averaged sorting and sediment transport hysteresis like that described in **chapters 6 and 9**.

To couple the vertical sorting to the transport process, the model described in **chapter 9** needs improvement for the following reason. Sediment transport predictors almost always predict that the bedload sediment is finer than the sediment in the bed (or in this case, in the transport or surface layer). Given enough time, this approach would therefore disentrain all the gravel from the transport layer, which is not realistic. If, on the other hand, a bedload predictor were used that assumes equal mobility, then the model would never predict gravel lag layers. Another reason is that the model assumes a linear vertical sediment sorting by dunes, and instantaneous formation of the gravel lag layer, which is also unrealistic.

An improved model concept for sediment sorting and transport might comprise the following:

1. the less mobile the gravel is, the lower it rides in the transport layers,
2. it takes time to move the gravel up or down,
3. it takes time to change the dune height (and related transport layer thickness), and
4. the gravel never becomes totally immobile (no threshold for motion).

The first idea is essential to create the model equivalent of a gravel lag layer. The second idea is necessary because the hindrance of sediment entrainment by the lag layer is essential for the prediction of hysteresis in the sediment transport rate. The dune time scale of the third idea together with the sorting time scale of the second idea determines how strong the hysteresis can be. If the sorting adaptation is very fast compared to that of the dune height, then almost no hysteresis is the result as shown in **chapter 9**. The fourth idea, finally, is necessary to prevent that all the gravel is worked down in time.

These processes might be modelled as follows. The transport layer thickness depends on the dune height. The dune height itself needs time to adapt to changing flow, for which the time scale can be derived from field measurements.

An equilibrium vertical sorting function would describe the distribution of sand and gravel in the vertical direction. The sorting function would have to be a function of the dimensionless shear stress to obey the first idea. The sorting adaptation in time could be modelled with diffusion. The sediment transport, finally, could be computed with a surface-based predictor, in which the sediment at the surface is here taken to be the sediment in the whole transport layer.

11.5.3 Continuous sorting in the Exner sediment continuity concept

Modelling sediment transport and morphological changes for river beds with dunes composed of sediment mixtures has first been done by Hirano (1971). In this model, it was assumed that an active mixing or transport layer could be defined, based on the grain size or dune height. In reality dunes are irregular and the deepest dune troughs allow sediment from deeper layers in the river bed to be exchanged with the mixing layer. Therefore Ribberink (1987) introduced an additional layer which accounts for sediment exchange between substrate and transport layer by the deepest dune troughs. Models developed since then mostly have one (following Hirano), two or more discrete layers (following Ribberink) (see Blom and Ribberink 1999 for a review).

The combination of choices of a) the thickness of the active layer, and b) the bedload transport predictor may have large effects on the modelling results, especially when the river bed is armoured. To investigate this, the author modelled the graded sediment transport in East Fork River (US) with an existing model based on the Hirano concept and the transport predictor of chapter 5. The modelling results are not described in detail herein, because it was beyond the scope of this study. The author attempted to reproduce the modelling results of Vogel et al. (1992), who modelled graded sediment transport in the East Fork River. They were able to hindcast the bedload transport rates and the bedload material composition during two discharge waves very well. Although the water discharge in the second peak is higher than in the first, the measured transport rate in the second is a factor 3 lower because the active layer is depleted of transportable fine sediment (Vogel et al. 1992). However, the model study by the present author, using the same boundary conditions as in Vogel et al., had a much different outcome. Notably, the modelled transport rate lagged two days behind the measured rate. Moreover, the time lag and difference in transport between the two discharge waves depended strongly on the thickness of the active layer and the bedload transport rate and composition. In other words, the coarsening of the active layer (armouring) depended strongly on the thickness of the active layer and on the bedload transport predictor. This illustrates that the bedload transport and active layer dynamics play a crucial role in the modelling. These, therefore, need more attention.

The model concept of Parker et al. (2000) obeys sediment continuity in such a way that the exchange of sediment with underlying layers can be modelled stochastically in a continuous way. This gives an advantage over the modelling in discrete layers, namely that the vertical sorting in dunes can be incorporated, and that the variability of dune trough scour depth can be incorporated more realistically. To develop this model concept further for rivers with dunes but without significant armouring, the following processes need to be included:

- incipient sediment motion including the effects of hiding-exposure in different sediment mixtures, and including the effect of near-bed turbulence,
- gravel lag layer formation,
- dune trough scour depth variation, which varies with the dimensionless shear stress, and
- vertical sorting at the lee-side of dunes.

For modelling purposes (reducing the number of parameters) the separate modelling of sorting due to gravel lag deposition and sorting at the lee side of dunes may not be feasible nor desirable

because of the large number of parameters involved. Instead, a continuous sorting function may be constructed which includes the sorting due to both phenomena, which should contain the most important parameters for both gravel lag deposition and sorting at the lee side of dunes.

The latter approach is followed by Blom et al. (2001; pers. comm.), who developed submodels in the Parker et al. (2000) model for the dune-averaged deposition rate and for the vertical sorting. The dune trough scour variation is specified for each condition in an empirical probability distribution function. Furthermore, from the analysis of dune-averaged deposition rate it followed that deposition at the stoss (upstream) side of the dunes cannot be ignored. This is confirmed by observations of the armouring and traction carpet on the dunes in the Sand flume experiments (chapter 7), the effect of which needs further study.

The vertical sorting submodel predicts the same straight lines of vertical sorting as observed in chapter 8 (see figure 8.6). The sorting slope can be calibrated in Blom's model, which gives the possibility to specify the sorting slope for various sediment mixtures and conditions. So the model by Blom et al. (2001) is able to combine the dune trough scour variation with a linear vertical sorting in dunes.

As pointed out in the previous section, the vertical sorting is a combination of sorting in grain flows at the lee side and gravel lag deposition. The gravel lag deposition itself may be a combination of deposition of coarse grades on the stoss side and in the troughs of the dunes. It is promising that vertical sorting curves in laboratory deltas (chapter 8) can mostly be represented with straight lines, but sorting data from laboratory dunes and from the Waal (this thesis, Blom and Ribberink 1999) indicates that this approach is too simple to account for the observed gravelly layers and the possible history effects on sediment transport rates, bedload sediment composition and dune growth. The logical next step in modelling therefore seems to be the implementation of a non-linear vertical sorting function.

11.6 Opening Pandora's Box: scientific challenges

11.6.1 Shear stress acting on grains

From chapters 5 and 6 it follows that the existing methods for the computation of grain shear stress may be fallible, and depend on assumptions that have only been verified for plane bed and uniform sediment. In addition, from chapter 10 it follows that prediction of the variation of shear stress acting on the large grains in the trough zones of dunes is crucial for the understanding of gravel lag formation. Finally, in chapter 6 it is concluded that partitioning the shear stress on grains and on bedforms is far from routine in rivers with dunes in non-equilibrium conditions. Below, these shortcomings of the present methods for grain shear stress computation are discussed in more detail.

In general, there are two methods for the computation of grain shear stress in the presence of bedforms:

- a. Van Rijn (1984a) computes the grain shear stress from depth-averaged flow velocity and the Chezy coefficient related to grain roughness: $\tau' = \rho g (u/C')^2$, in which $C' = 18 \log(12h/k_s')$ (for notation see chapter 5). The crucial assumption is the grain roughness k_s' . Van Rijn suggests $k_s' = 1D_{90}$ for gravelly sediment, and $3D_{90}$ for sand. Values that have experimentally been determined for a limited number of sediment mixtures (see Van Rijn 1984a for discussion), however, are widely at variance with these rules of thumb. For instance, the fines may fill in the pores of the coarse sediment, which leads to a reduction

in skin friction and therefore grain shear stress. This, however, depends on the shear stress, as this effect vanishes when the fine sediment becomes more mobile.

- b. The frequently used alternative is a relation between the total shear stress and the grain shear stress, e.g. Engelund & Hansen proposed in 1967: $\theta' = 0.06 + 0.4\theta^2$. Since then, many comparable functions have been given which essentially all have the same crucial assumption: that the hydraulic roughness of the bedforms (i.e., the bedform-related θ'') is a simple and unique function of the total shear stress (e.g. Smith & McLean 1977, White et al. 1979, Van Rijn 1984b). This is, given the variety of dune shapes in various conditions, of dune roughness predictors, differences in graded sediment, etc. not the case.

The first method is more often used in deep sand-bed rivers and has been extended for waves, currents and sandy near-shore zones. The second, on the other hand, is more often used in gravel-bed rivers with relatively low-relief bedforms. It must be concluded that the determination of grain shear stress is not straightforward, on the contrary, it contains a subjective element. The order of magnitude of the grain shear stress may be right in many cases, but that is no guarantee that it is correct for the three more complicated cases described below.

- It has not been studied well whether the grain shear stress can be represented with a single value for a river bed with dunes and mixed sediment. The local bed shear stress over a dune varies from negative to positive values when going downstream from the dune toe to the top. The turbulent variations are extremely large in the dune troughs and small on the tops. For dunes with uniform sediment, a sort of average grain bed shear stress could be conceived. The situation is even more complex with sediment mixtures due to fining upward sorting in the dunes. Then the sediment mixture varies from gravel to sand when going downstream from the dune toe to the top. The shear stress regime on the gravel is thus very different from that on the sand. It is not known whether the sediment transport conditions are then accurately represented by averages over the length of the dune of grain shear stress, the surface sediment composition and a hiding-exposure correction.
- Likewise, it is not known how the shear stress acting on grains in the dune troughs can be determined, taking account of the turbulent flow at the lee side of bedforms. This is very important when the coarser fractions of a sediment mixture are incipiently mobile, because gravel lag layers are formed in those conditions.
- Recollect that the dunes in the Rhine in falling stages become inactive while new, secondary dunes form on the relicts of the primary dunes. This phenomenon has been observed in other rivers as well. It is unknown how the shear stress on grains should be computed in these cases, while it is relevant as it potentially explains hysteresis in sediment transport rates (see **chapter 6**).

Concluding, the computation of grain shear stress is a topic that deserves further attention.

11.6.2 Hiding-exposure relations

The doubts about the grain shear stresses affect related areas as well; empirical sediment transport relations that are based on a certain method of grain shear stress computation may not work well with another method, because the behaviour of transport relations changes with different methods. This is probably the reason why most workers use sediment transport predictors only with the grain shear stress and roughness relations recommended by the authors of the transport predictors. It is argued here that, although comparisons of transport predictors with several datasets remain very useful, it is very necessary to compare the shear stress computations also as argued in the previous section.

For example, many recent bedload predictors for sediment mixtures are based on a similarity collapse of the transport rate of each size fraction as a function of some parameter containing the grain shear stress. A similarity collapse involves the empirical determination of relations between transport rate and shear stress for each grain size fraction, and an empirical determination of the hiding-exposure relation for that dataset. Often these transport relations collapse onto one single relation. Here it is hypothesised that these predictors would have been significantly different, had another method for grain shear stress computation been used.

This has considerable consequences for the hiding-exposure functions derived with those predictors. A number of empirical hiding-exposure functions have been described in literature, and some differences in form could be related to sediment characteristics (see **chapter 5**). However, not all differences could be explained, which may be due to the different approaches to the grain shear stress with which the functions have been derived.

Especially for the wider sediment mixtures, bedforms consisting of fine sediment exist while the coarsest sediment is not yet in motion. Therefore the partitioning of grain shear stress and bedform related shear stress is relevant, and different methods may result in different hiding-exposure functions. Summarising, a study on the effect of using different grain shear stress computations is in order. This can easily be done by performing the similarity collapse on a number of datasets with systematically varied independent parameters with different grain shear stress computation methods.

11.6.3 Interactions up- and downstream of river bifurcations

Partly related to the section on meandering effects is the behaviour of river reaches upstream and downstream from a bifurcation. In general, the dynamics of sediment transport and morphology at a river bifurcation are not well understood. At the Pannerdensche Kop bifurcation in the Rhine, the Rhine splits into the Waal and the Pannerden Canal. In **chapter 6** it was found that these reaches behave different during a discharge wave, and in fact show extreme and opposite hysteresis of sediment transport and dune parameters as a function of discharge, and it is the question why. The Pannerden Canal splits off from a point where the Rhine has an outer bend. Consequently the better part of the coarse sediment of the Rhine enters the Pannerden Canal, while a finer sediment mixture enters the river Waal. At the same time, the discharge in the Waal is twice as high as that in the Pannerden Canal. The mobility of the sediment in the Waal is therefore higher, and dunes are expected to form more quickly in the Waal than in the Pannerden Canal.

A testable hypothesis is that the different behaviour of the dunes (and consequent hydraulic roughness) in the three reaches is related to the difference in sediment mobility. For this, measurements should be done at the bifurcation of the Merwede river, which has the same planform as the bifurcation at Pannerdensche Kop, but has only fine sand in the river bed. Such a study will allow a comparison between the bifurcation with and without a sediment mixture in the bed, and possibly lead to the isolation of (one of) the cause(s) of the strong hysteresis of dune parameters and sediment transport.

11.6.4 Interactions with sediment sorting in meander bends

Sediment is sorted in meander bends (see **chapter 2**), with coarse sediment in the outer bend, fine sediment in the inner bend and a mixture in the cross-over (riffle) from one bend to a downstream

opposite bend. Virtually nothing is known about the interaction between this sediment sorting pattern and the sorting on the bedform scale as studied in this thesis. However, the following observations from the river Rhine at Pannerdensche Kop during bankful discharge make clear that it is important:

- although the bed shear stress in the (shallower) inner bend is smaller than in the (deeper) outer bend, the dune height on both sides of the river is approximately equal, suggesting that the effect on dune height of the grain size decrease towards the inner bend counteracts the decrease of shear stress (dune height depends on grain size as well as shear stress);
- the outer bends erode temporarily while the inner bends aggrade temporarily, which obviously must have an effect on the preservation of sorted dune deposits on both sides of the river;
- in the coarsest parts of the outer bends no dunes occur at all.

These observations give the impression that the riffles, inner and outer bend regions react differently during a discharge wave, and that the flow and sorting pattern at the meander bend scale affects the dune development and therefore the sorting in the bed. If this is true, then the cross-channel averaged sediment transport in a meandering river may be different from that in a straight channel. This is a hypothesis that may be tested with two-dimensional and one-dimensional models which incorporate the effect of vertical sediment sorting, e.g. the model developed by Mosselman et al. (1999).

11.6.5 Interactions with downstream fining

In this section, it is hypothesised how vertical sorting in the river bed can lead to large-scale downstream fining. Among the most basic properties of river systems is a tendency of their bed sediments to become finer downstream. Strongly related to this is the downstream concavity of the bed and water surface profile. These trends are strong forcings on the river behaviour at smaller scales (e.g. Sambrook Smith & Ferguson 1996). The bed sediment composition at a certain location determines the amount of sediment that can be transported on a small time-scale, and also the occurrence and size of subaqueous river dunes. Also the channel pattern is partly determined by these factors; a braided pattern is often found in the upstream, gravel-bed reaches whereas meandering patterns dominate the gently sloping lower course (Van den Berg 1995). The downstream fining is thus intimately part of the natural morphological expression of an alluvial river. The understanding of downstream fining in large rivers is essential for assessments of the river behaviour on a decadal time scale.

The following main causes for downstream fining in rivers have been identified:

- selective transport and deposition of grains with different sizes (e.g. Paola & Seal 1995, Lisle et al. 1997, Toro-Escobar et al. 2000),
- abrasion, through which the clasts become smaller by breaking, which eventually may lead to bimodal bed sediment (e.g. Cui & Parker 1998, Lewin & Brewer 2002), and
- input of different sediment from tributaries (e.g. Rice 1999), and from older deposits in the case of degradation (see [chapter 6](#)).

The downstream fining of rivers has already been described by Sternberg (1875), who suggested an exponential law for downstream grain size decrease due to the abrasion or fracturing of clasts into finer sediment. However, this approach remains essentially empirical. A number of recent studies have attempted to apply process-based models for short river reaches (10^0 - 10^1 km) to

longer reaches (10^2 - 10^3 km) with the aim to capture the observed downstream fining of the river bed (Cui & Parker 1998, Paola & Seal 1995, Lisle et al. 1997). However, these models have all been applied to flume experiments, small mountain streams and moderate gravel bed rivers, in which dunes play no significant role.

Two mechanisms of selective transport and deposition of sediment mixtures that may promote downstream fining in the lower Rhine are identified: the rapid suspended transport of sand versus the slow transport of gravel at the bed, and vertical sorting of sediment (explained below). The role of abrasion is not yet fully clear. Based on a petrological study, it was concluded that abrasion is unimportant to downstream fining in the Dutch Rhine branches (Terwindt 1963). Goelz et al. (1995) on the other hand studied the downstream development of crushed granit supplied to counteract severe bed degradation in the German Rhine, and found that abrasion played a significant role for the broken material. Lewin and Brewer (2002) argued that laboratory simulations of abrasion may have significantly underestimated the abrasion rates in rivers.

It can be argued that the vertical sediment sorting as described in this thesis may contribute significantly to downstream fining. Two factors are prerequisite: a fining upward sorting, and a higher frequency of low discharge waves compared to high discharge waves. The sediment transport integrated over a whole discharge wave can be thought of as a layer of sediment that has been moved downstream. The thickness of the layer is related to the dune height (approximately half the dune height, see **chapter 9**). In high discharge waves, this dune height is large, and a thick layer of sediment will be displaced, while the layer is thin in small discharge waves. Since small discharge waves occur more often than large discharge waves, more often a thin layer is displaced downstream than a thick layer. If the sediment in the bed is fining upward, then it can be seen that the fine sediment near the bed surface is more often displaced than the coarse sediment deeper in the bed. This might lead to downstream fining.

A test of this hypothesis would involve the implementation of a one-dimensional model like that of Parker et al. (2000) with a flood-frequency hydrograph over a long reach (for the Rhine: say, from Iffezheim in Germany to the Pannerdensche Kop in the Netherlands), and field measurements of dune height and sediment transport at least at the upstream and downstream boundary of the modelling reach.

References

- ALLEN, J. R. L. (1970). The avalanching of granular solids on dune and similar slopes. *Journal of Geology* 78, pp. 326-351.
- BLOM, A. & RIBBERINK, J. S. (1999). Non-uniform sediment in rivers: vertical sediment exchange between bed layers, Proceedings of River, Coastal and Estuarine Morphodynamics, IAHR, Genova, Italy, pp. 45-54.
- BLOM, A., PARKER, G. & RIBBERINK, J. S. (2001). Vertical exchange of tracers and non-uniform sediment in dune situation, Proceedings of River, Coastal and Estuarine Morphodynamics, IAHR, Japan.
- CUI, Y. & PARKER, G. (1998). The arrested gravel front: stable gravel-sand transitions in rivers Part 2: general numerical solution, *Journal of Hydraulic Res.* 36(2) pp. 159-182.
- ENGELUND, F. & HANSEN, E. (1967). A monograph on Sediment transport. Technisk Forlag, Copenhagen, Denmark.
- GOELZ, E. SCHROETER, M. & MIKOS, M. (1995). Fluvial abrasion of broken quartzite used as a substitute for natural bed load, 6th int. symp. on River sedimentation, New Delhi, 1995, pp. 387-395.
- HIRANO, M. (1971). River bed degradation with armouring, *Transactions of the JSCE*, 3, part 2.
- HUNTER, R.E. (1985). A kinematic model for the structure of lee-side deposits. *Sedimentology* 32, pp. 409-422.
- JOPLING, A. V. (1965). Laboratory study of the distribution of grain sizes in cross-bedded deposits, in:

- MIDDLETON, G. V. (ed.) Primary sedimentary structures and their hydrodynamic interpretation, Spec. Publ. no. 12, Soc. of Econ. Paleontologists and Mineralogists, Oklahoma, U.S.A.
- KOEPPE, J.P., ENZ, M. & KAKALIOS, J. (1998). Phase diagram for avalanche stratification of granular media. *Physical Review E* 58 4.
- LEWIN, J. & BREWER, P. A. (2002). Laboratory simulation of clast abrasion. *Earth Surface Processes and Landforms* 27, pp. 145-164.
- LISLE, T. E., PIZZUTO, J. E., IKEDA, H., ISEYA F. & KODAMA, Y. (1997). Evolution of a sediment wave in an experimental channel, *Water Resources Research* 33(8) pp. 1971-1981.
- MOHRIG, D. (1994). Spatial evolution of dunes in a sandy river. PhD dissertation, 119 pp., University of Washington, Seattle, USA.
- MOHRIG, D. & SMITH, J. D. (1996). Predicting the migration rates of subaqueous dunes. *Water Resources Research* 32 10, pp. 3207-3217.
- MOSELMAN, E, SIEBEN, J., SLOFF, C.J. & WOLTERS, A. (1999). Effect of spatial grain size variations on two-dimensional river bed morphology. In: Proc. IAHR-Symp. on River, Coastal and Estuarine Morphodynamics, University of Genoa, p. 499-507.
- PAOLA, C. & SEAL, R. (1995). Grain size patchiness as a cause of selective deposition and downstream fining, *Water Resources Research* 31(5) pp. 1395-1407.
- PARKER, G., PAOLA, C. & LECLAIR, S. (2000). Probabilistic Exner sediment continuity equation for mixtures with no active layer, *Journal of Hydraulic Engineering* 126 (11), pp. 818-826.
- RIBBERINK, J. S. (1987). Mathematical modelling of one-dimensional morphological changes in rivers with non-uniform sediment. Ph.D. thesis, Delft University, The Netherlands.
- RICE, S. (1999). The nature and controls on downstream fining within sedimentary links, *J. of Sedimentary Research*, 69, 1, pp. 32-39.
- SAMBROOK SMITH, G. H. & FERGUSON, R. I. (1996). The gravel-sand transition: flume study of channel response to reduced slope, *Geomorphology* 16, pp. 147-159.
- SMITH, J. D. & MCLEAN, S. R. (1977). Spatially-averaged flow over a wavy surface. *J. of Geophysical Research* 82 pp.1735-1746.
- STERNBERG (1875). Untersuchungen uber Langen- und Querprofil geschiebefuhrender Flusse, *Zeitschrift fur Bauwesen* 25, pp. 483-506, cited in RICE (1999).
- TERWINDT, J. H. J., DE JONG, J. D. & VAN DER WILK, E. (1963). Sediment movement and sediment properties in the tidal area of the lower Rhine (Rotterdam waterway). *Verhandelingen van het Koninklijk Nederlands geologisch mijnbouwkundig genootschap, Geologische serie deel 21-2*, Transactions of the Jubilee convention, part two, pp. 243-258, Mouton & Co. Den Haag, The Netherlands.
- TORO-ESCOBAR, C., PAOLA, C., PARKER, G., WILCOCK, P., & SOUTHARD, J. (2000). Experiments on downstream fining of gravel. II: wide and sandy runs, *Journal of Hydraulic Engineering* 126(3) pp. 198-208.
- VAN DEN BERG, J. H. (1995). Prediction of alluvial channel pattern of perennial rivers, *Geomorphology* 12, pp. 259-279.
- VAN RIJN, L. C. (1984a). Sediment transport, part I: bed load transport. *Journal of Hydraulic Engineering* 110 (10), pp. 1431-1456.
- VAN RIJN, L. C. (1984b). Sediment transport, part III: alluvial roughness. *Journal of Hydraulic Engineering* 110 (12), pp. 1733-1754.
- VOGEL, K. R., VAN NIEKERK, A., SLINGERLAND, R. L. & BRIDGE, J. S. (1992). Routing of heterogeneous sediments over movable bed: model verification. *Journal of Hydraulic Engineering* 118 (2), pp. 263-279.
- WHITE, W., PARIS, E. & BETTESS, R. (1979). A new general method for predicting the frictional characteristics of alluvial streams. H.R.S. Wallingford report No. IT187, UK.

Sorting out sand and gravel; sediment transport and deposition in sand-gravel bed rivers

Summary

1 Objectives

The general aim of this PhD-project was to gain better understanding of the sediment transport and depositional processes of sand-gravel mixtures in rivers with subaqueous dunes. The understanding of the fundamental processes of sediment transport and deposition in channel beds is crucial for morphological models. Processes outside the channel, for instance in the flood plains, are beyond the scope of this work.

Rivers with mixtures of sand and gravel in their channel bed combine characteristics from sand-bed rivers and gravel-bed rivers. Sand-bed rivers are characterised by rather uniform, very mobile sand and subaqueous dunes. Gravel-bed rivers, on the other hand, seldom have dunes and are characterised by gravelly sediment which is usually near incipient motion. Sand-gravel bed rivers have a mixture of sand and gravel in their beds, and have dunes while the coarsest sediment is near incipient motion. The sediment mixtures is vertically sorted by migrating dunes. The resulting vertical sorting considerably influences sediment transport and dune development, and vice versa. This interaction is probably typical for sand-gravel bed rivers but is not well understood.

Specific objectives in this thesis were to:

1. develop a predictor for selective sediment transport of mixtures, including the probability of movement for different size-fractions near incipient motion and fully mobile conditions,
2. identify the bedform types that occur in sediment mixtures, and their significance for the sediment transport, and develop a predictor for the bedform types,
3. identify vertical sediment sorting processes and determine their role in sediment transport,
4. identify and quantify how dune development in non-equilibrium conditions (discharge waves) affects vertical sorting processes and the sediment transport, and
5. develop a model for dune-related sorting processes and selective sediment transport of mixtures.

How these objectives were met, is summarised in the following five sections.

2 Prediction of bedload transport of sediment mixtures

The sediment transport rate in rivers is usually computed with predictors that are based on the flow shear stress on the bed and the grain size of the sediment in the bed. Below a critical shear stress, no sediment transport is predicted. For coarse sediment, lower transport rates are predicted than for fine sediments. These predictors are valid for uniform sediment, but not for sediment mixtures. In mixtures, the small grains may be mobile while the large grains are immobile, therefore large errors in the transport rates could be made. In addition the effects of typical phenomena like armour layers are not incorporated.

A basic problem is that several methods can be chosen to represent the turbulent flow, the grain size distribution of the bed material and the interaction between grains of different sizes. In

chapter 5 a predictor for bedload transport of sediment mixtures is developed by extending existing deterministic bedload transport predictors for uniform sediment to non-uniform sediment, based on flume experiments reported herein. The sediment is represented by grain-size fractions which are derived from the grain size distribution of the underlying bed sediment (substrate). The near-bed turbulence is modelled stochastically to obtain realistic bedload transport rates at incipient motion. The difference in mobility of small and large grains is represented by hiding-exposure functions.

However, such an approach gives wrong results for the river Rhine, the Netherlands, during a discharge wave in 1998. The measured bedload transport (see **chapter 6**) showed a strong hysteresis. Hysteresis of bed sediment transport rates in rivers as a function of a flow parameter yields different outcomes for rising and falling stages. The hysteresis was not predicted because the causes of the hysteresis are not incorporated in the predictors. The cross-channel averaged sediment transport rates have an uncertainty of less than 20% (see **chapter 3**), which shows that the hysteresis is significant, while the hysteresis was also observed with an independent bedload measurement method. A potential explanation of part of the observed hysteresis is vertical sorting of bedload sediment by the dunes, combined with the time lag between dune height development and the changing flow. Part 2 of this thesis focusses on the role of sediment sorting (summarised below).

3 Bedforms and sediment transport over armour layers

In conditions of stable armouring, the predicted sediment transport is zero. Yet, often a little bedload transport is observed in the form of bedforms of various shapes moving over the armour layer. In **chapter 4**, observations of bedforms in sediment mixtures are systematised, and the conditions for which bedload predictors are not valid, are discussed. These observations were done in flume experiments and field measurements in the river Rhine, the Netherlands, in the river Allier, France, and taken from literature. Existing bedform stability diagrams are shown to be extendable to sediment supply-limited bedforms in sand-gravel sediment.

Three bedform types are characteristic for sediment mixtures: bedload sheets (low relief dune-like features of a few grains thick and downstream coarsening), flow parallel sand ribbons and flow transverse barchans (crescent shaped dunes with horns pointing downstream and the immobile substrate exposed between individual barchans). Barchans and sand ribbons occur when not enough transportable sediment is available for the formation of fully developed ripples or dunes, because a part of the bed sediment is immobile. When the bed surface is armoured, barchans and sand ribbons are dependent on the sediment supply from upstream. This supply is often not predictable from the local hydraulics and sediment characteristics.

4 Vertical sorting processes and their role in sediment transport

Bedload transport rates measured in the river Rhine and in flume experiments indicate that vertical sediment sorting in dunes affects both the transport rate and the composition of the bedload transport (see **chapters 6 and 9**). During a discharge wave, the development of the dunes and the vertical sorting in those dunes may interact in such a way that the bedload transport is larger and more sandy in falling stages than in rising stages. In addition, a record of sorted sediment is left in the channel bed after a discharge wave, which is the antecedent sorting for the next discharge wave, often called 'history effect'. This vertical sorting is in general fining upward.

In the Rhine, gravelly layers were found at two depths in the channel bed (see **chapter 6**). The deepest layer was related to the dunes formed in the very high discharge wave of 1995, and the second layer was related to the dunes formed in the smaller discharge wave of 1998. This is confirmed by a behavioural model (**chapter 9**) and by flume experiments (**chapter 10**) with a sediment mixture that was subjected to two discharge events in order of decreasing magnitude. The sediment mixture is vertically sorted by two processes (**chapters 6 and 9**). The first is by grain flows at the lee side of the dunes, leading to fining upward sorting. The second process is grain size-selective entrainment and deposition in the dune troughs, which results in a second type of upward fining deposit (gravel lag deposit). The base of the grain flow deposits and the gravel lag deposit are both observed as gravelly layers. Thus, these two types of deposits are the source for sediment entrained during the next discharge wave. Since bedload sediment transport rates depend partly on grain size, it also depends on the relict vertical sorting left in the bed by former discharge waves, and on the depth from which the sediment is entrained. The entrainment and deposition depth of the sediment depends on the dune trough level below the average bed level and therefore on the dune height. Thus subsequent discharge waves of decreasing magnitude will leave the upward fining cross-bedded sets and gravel lag layers at depths related to the concurrent dune height. A discharge wave of high magnitude will reset the bed and leave a fresh upward fining deposit.

Sediment sorting in grain flows at the lee-side of ripples, dunes, bars and small Gilbert-type deltas has already been recognized long ago, yet a predictive model is unavailable for implementation in sediment transport models for sediment mixtures. Relevant processes in sedimentological and physical literature are reviewed in **chapter 7**. A synthesis is given of the most important variables governing the sorting processes for the benefit of experimentation. From such experiments (reported in **chapter 8**), it follows that the sediment deposition and sorting on the lee slope of a delta is the result of three processes. First, the grains fall from suspension that was initiated at the top of the delta. Second, by kinematic sieving the small grains on the lee slope are worked down, meanwhile working up the large grains to the surface. Third, the sediment on the lee slope flows downslope as a grain flow, in which the large grains are dragged downslope. The result is a fining upward vertical sorting in the delta. This sorting trend depends on the sediment mixture characteristics, the delta height, the migration celerity of the delta front and the flow conditions above the delta top.

Gravel lag deposits have been generated in flume experiments with low, intermediate and high discharges (see **chapter 10**). The dunes formed in the intermediate discharge were two-dimensional with straight crests and little variation in dune trough scour depth, whereas those formed in the high discharge were three-dimensional with sinuous crests and much trough scour variation. The former left a continuous gravel layer at their bases at a constant depth, while the latter left discontinuous, multiple gravel layers at highly variable depths. Consequently, in the latter case the net vertical sediment sorting (averaged over a number of dune lengths) is less well developed than in the former. Thus, the first factor governing gravel lag formation is the three-dimensionality (irregularity) of the dunes, which is determined by the bed shear stress and grain size of the dunes. The second factor is the mobility of the coarsest sediment fractions, which determines whether the gravel is fully mobile or a gravel lag deposit is formed which hinders entrainment of sediment from deeper layers. This control competes with the first control (although the first control is dominant): dunes cannot develop deep scour holes if there is a strong lag layer, but in time, lag layers may be broken up by three-dimensional dunes, which strive to develop deep scour holes.

5 Bedforms, vertical sorting and sediment transport in non-equilibrium conditions

Vertical sediment sorting by migrating dunes in sand-gravel bed rivers is relatively well understood for artificial equilibrium conditions, but not for natural non-equilibrium conditions (discharge events). This understanding is a prerequisite for morphological modelling of rivers with natural flow discharge regimes. Two subsequent discharge waves were experimentally simulated in order of decreasing magnitude, alternated with low flow discharge (**chapter 10**). The main difference between equilibrium and non-equilibrium conditions was the deposition of fine sand in the dune troughs during low discharge, originating from eroded dune tops. Whether this type of deposit occurs, is controlled by the adaptation time scale of the dune height during changing flow conditions. If the dune height adapts slowly and the dunes become inactive in waning flow, then sandy trough-fill deposits will form, while this is not the case for quickly adapting dunes. In the river Rhine, the sandy trough-fill deposits are formed by transporting the sand from the inactive dune tops to the troughs. This transport takes place by superimposed secondary dunes which are formed when the primary dunes become inactive. However, the conditions favourable to secondary dune formation are not understood. The consequence of sandy trough-fill deposition is a patchy sediment sorting pattern in the downstream direction. As a result, the net vertical sorting in the channel bed (averaged over a number of dune lengths) is less well developed than without sandy trough-fill deposits.

6 Modelling vertical sorting processes and sediment transport

Morphological modelling of channel beds with sediment mixtures has made strong progress in the past decennium, but many of the observed phenomena are not yet incorporated or predictable with those models. The question is therefore how these results could be implemented in those models (**chapter 11**).

To model the sediment transport process and the exchange between transported and bed sediment in rivers with dunes correctly, the bed level variations due to migrating dunes must be accounted for as well as the vertical sediment sorting in the dunes. These two elements, bed level variation and sediment sorting, must be implemented in model concepts, but are not yet predictable for various flow conditions and sediments.

In specific, the following processes should be included in the models:

- gravel lag layer formation,
- incipient sediment motion of different grain sizes in sediment mixtures, including the effect of near-bed turbulence,
- dune trough scour depth variation, and
- vertical sorting at the lee-side of dunes.

For non-equilibrium conditions (discharge waves), the following processes should be added:

- the effect of historic gravel lag layers on dune development (in specific trough scour) and sediment transport,
- the hysteresis of dune height and the favourable conditions for and timing of the emergence of secondary dunes superimposed on the primary dunes.

For modelling purposes (reducing the number of parameters) it could well be that the separate modelling of sorting due to gravel lag deposition and sorting at the lee side of dunes is not feasible and desirable because of the large number of parameters involved. Instead, a continuous sorting function may be constructed which includes the sorting due to both phenomena, which should contain the most important parameters for both gravel lag deposition and sorting at the lee side of dunes. The trough scour variation by dunes could possibly be parameterised with bed level probability distributions in which the deepest scour depends on the three-dimensionality of the dunes, which is governed by the dimensionless shear stress.

Sedimenttransport en -afzetting in zand-grindrivieren

Behorende bij het proefschrift van Maarten G. Kleinhans, verdedigd op 29 mei 2002

Samenvatting voor de leek

1 Inleiding

“Te veel, te weinig, te vuil”. Zo wordt de wereldwijde waterproblematiek vaak samengevat. In Nederland hebben we al deze problemen ook. In de takken van de Rijn bijvoorbeeld, waar tijdens de perioden met hoogwater in 1993 en 1995 de dijken op springen stonden, terwijl ‘s zomers de schepen tijdens laagwatercondities aan de grond dreigen te lopen. De hoog- en laagwaterproblematiek is gerelateerd aan het gedrag van de bedding van de rivier. Met modellen van de stroming van water kunnen met name de extreme hoogwaterstanden nog niet goed worden voorspeld, mede omdat het gedrag van de rivierbedding in die condities niet voldoende bekend is. De stroming verplaatst sediment, bestaande uit zand en grind, en door die verplaatsing verandert de ligging van de rivierbedding. Dit heeft gevolgen voor de vaargeul, die vaak smaller wordt, hetgeen onveilige situaties oplevert.

Het gedrag van de bedding en het transport van sediment door de rivier wordt redelijk goed begrepen voor zand en voor grind apart, maar niet voor mengsels van zand en grind. Het sediment in de bedding wordt fijner richting de zee. Bij de grens tussen Nederland en Duitsland ligt veel grind in de rivierbedding. Over een traject van vele tientallen kilometers komt daar zowel grof zand als grind in de rivierbedding voor. Tijdens hoge afvoeren wordt daarnaast fijn zand uit het Duitse achterland aangevoerd; dit wordt in de vorm van oeverwallen direct langs de rivier afgezet of verder benedenstrooms gevoerd. Nog verder van de rivierbedding af bezinken klei en slib.

Dit proefschrift richt zich op het gedrag van mengsels van zand en grind in de rivierbedding tijdens hoogwaters, namelijk hoe het sediment getransporteerd wordt, om hoeveel sediment het gaat, en hoe het wordt afgezet. Om dit gedrag te bestuderen, zijn door Rijkswaterstaat metingen gedaan in de Rijn rond het splitsingspunt Pannerdensche Kop (zie **hoofdstuk 3 en 6**, en Kleinhans & Ten Brinke 1998), waar de rivierbedding voor 45% uit grind en 55% uit zand bestaat. Bij dit splitsingspunt verdelen het water en sediment zich over de Waal en het Pannerdensch Kanaal. Dit onderzoek is dus van belang voor alle verder benedenstrooms gelegen Rijntakken. Ter vergelijking met de condities in de Rijn zijn waarnemingen en metingen gedaan in de rivier Allier in Frankrijk. Daarnaast zijn drie series laboratoriumexperimenten gedaan in stroomgoten (zie **hoofdstuk 4, 8 en 10**, en Kleinhans et al. 2000), waarbij sedimentmengsels aan stroming werden blootgesteld. Stroomgoten zijn langwerpige zandbakken van circa 5 tot 50 meter lang en 0.1 tot 1.5 meter breed, vaak met glazen wanden, waarin de waterstroming geheel kan worden ingesteld. In deze experimenten kon het gedrag van sediment en de resulterende afzettingen in de bedding onder gecontroleerde omstandigheden en van dichtbij worden bestudeerd, zonder de extra moeilijkheden die worden ondervonden tijdens een veldmeting. In onderstaande paragrafen worden de waargenomen fenomenen en de gevolgen voor het sedimenttransport en de afzetting samengevat.

2 Sedimenttransport

Herodotos schreef vijftienduizend jaar geleden in zijn Historiën: “Indien ooit de Nijl zijn bedding zou verleggen naar de Arabische Golf, wat zou dan kunnen verhinderen, dat deze binnen 20.000 jaar door de stroom met sediment gevuld zou worden? Ja, ik geloof, dat dat zelfs wel binnen 10.000 jaar zou gebeuren. Zou immers in die lange periode, die vóór mijn geboorte is verstreken, niet een zeeboezem kunnen zijn dichtgeslibd, die nog veel groter is dan deze, door de werking van een zo grote en krachtige rivier?” Deze schatting was zo slecht nog niet. Nu, een industriële en vele maatschappelijke revoluties verder, kunnen we het gemiddeld sedimenttransport van de Waal in Nederland niet veel nauwkeuriger inschatten dan tussen de 400.000 en 900.000 m³ per jaar. Dit komt door het gebrek aan kennis over het gedrag van de rivier tijdens hoogwater en de technische moeilijkheden van transportmetingen in de natuur (zie hoofdstuk 3 en 6).

Sedimenttransport van zand of van grind kan worden berekend met empirische functies, zogenaamde transportvoorspellers, waarbij het sedimenttransport evenredig is met de schuifspanning tot de macht 1.5 (macht 3 tot 5 voor stroomsnelheid in plaats van schuifspanning) en in mindere mate van de korreldiameter. Schuifspanning is gedefinieerd als de sleepkracht van het water op de rivierbedding per eenheid van oppervlak, en is gerelateerd aan de waterdiepte en de hellingshoek van de rivier of de stroomsnelheid. Door die macht van circa 1.5 is het sedimenttransport tijdens een hoogwater relatief veel groter dan tijdens laagwater.

De vage ondergrens van schuifspanning waarbij het sediment in beweging komt, wordt hier de kritieke schuifspanning genoemd. Deze hangt af van de korrelgrootte: grindkorrels zijn groter en dus zwaarder dan zandkorrels en dus lastiger om in beweging te krijgen dan zand (zie ook Kleinhans & Ten Brinke 1998). De kritieke schuifspanning wordt belangrijker naarmate het sediment grover wordt, omdat het dan vaker voorkomt dat het sediment niet mobiel is. In werkelijkheid is de kritieke grens vaag om twee redenen. De eerste is dat de stroming over de bedding sterk variabel is door turbulentie. De tweede reden is dat sommige korrels op de bedding instabieler liggen dan andere en daardoor gemakkelijker in beweging komen. Het gevolg is dus dat in werkelijkheid een klein beetje transport plaatsvindt waar dit door de transportformules die uitgaan van een kritieke ondergrens van korrelbeweging, niet wordt voorspeld. In hoofdstuk 4 wordt een kansverdeling voor de schuifspanning gebruikt om met name het effect van turbulentie in de berekening mee te nemen, wat aantoonbaar betere voorspellingen oplevert voor condities nabij het begin van sedimentbeweging.

3 Transport van sedimentmengsels

Zand-grindmengsels vertonen bijzonder gedrag dat niet of nauwelijks in zand of grind apart voorkomt. Zandkorrels die zich in de luwte van grindkorrels bevinden, zijn meer afgeschermd van de stroming, terwijl de uitstekende grindkorrels juist meer zijn blootgesteld. Hierdoor wordt het zand relatief minder mobiel en het grind mobieler, ofschoon zand nog steeds wat makkelijker in beweging komt dan grind. Dit wordt het afschermings-/blootstellingsfenomeen (Engels: ‘hiding-exposure’) genoemd, wat kan worden beschreven in empirische functies (zie ook Kleinhans et al. 2000). Zo’n functie beschrijft het verminderde verschil in mobiliteit tussen zand en grind. In hoofdstuk 4 wordt de kritieke schuifspanning in transportvoorspellers ermee gecorrigeerd, om het sedimenttransport van de afzonderlijke zand- en grindfracties te berekenen. Hiermee is dus een transportvoorspeller geconstrueerd voor zand-grindmengsels.

Wanneer de transportvoorspeller met ‘hiding-exposure’-correctie en turbulentie-correctie wordt

toegepast op de rivier de Rijn tijdens het hoogwater van 1998, blijken de voorspellingen echter niet goed overeen te komen met de gemeten transporten (zie **hoofdstuk 6**). Het sedimenttransport bij stijgende waterstanden verschilt sterk van dat bij dalende waterstanden. In de Bovenrijn het transport voor de hoogwaterpiek hoger dan erna en in de Waal is dit andersom. Dit fenomeen wordt hysteresis genoemd. De voorspelde transporten vertoonden deze hysteresis niet, ofschoon de voorspellingen gebaseerd waren op gemeten stromingsparameters en samenstelling van het beddingsediment.

Verskillende hypothesen om de hysteresis te verklaren werden getoetst, waaruit bleek dat met name het gedrag van rivierduinen op de rivierbedding en de sortering van zand en grind in de bedding een belangrijke rol spelen. Deze fenomenen zijn daarom nader onderzocht.

4 Rivierduinen onder water en hun effect op sedimenttransport

Als de schuifspanning groter wordt en meer sediment wordt verplaatst, krijgt de bedding van de rivier langzamerhand een golvende vorm; er ontstaan beddingvormen die stroomafwaarts bewegen. Bij lagere snelheden zijn dat nog ribbels van enkele meters lengte en een paar decimeters hoog, maar als het hoogwater hoog genoeg wordt en lang genoeg duurt, kunnen ze uitgroeien tot duinen van honderd meter lengte en enkele meters hoog. Bij de Pannerdensch Kop verdwijnen de duinen bij laagwater weer. De hoogste punten worden duintoppen genoemd en de laagste duintroggen.

De flauwe loefzijde (bovenstrooms) van het duin wordt voortdurend geërodeerd. Dit geërodeerde materiaal wordt vervolgens benedenstrooms op de steile lijkzijde van het duin afgezet. Op deze wijze beweegt het hele duin zich stroomafwaarts. Anders gezegd, bodemgebonden sedimenttransport vindt plaats in de vorm van bewegende duinen en is ongeveer gelijk aan het verplaatste volume van de duinen per tijdseenheid. Overigens vindt daarnaast ook zwevend transport plaats van fijn sediment dat in suspensie wordt gehouden door de turbulentie in de stroming, maar dit valt buiten het bestek van dit proefschrift.

De stroomafwaartse kant van een beddingvorm is steil, zodat de waterstroming daar het bodemoppervlak niet meer kan volgen. Er ontstaan turbulente wervelingen aan de steile lijkzijde van de duinen, die een extra weerstand vormen voor het stromende water. Het verlies aan energie ten gevolge van die wervelingen gaat ten koste van de energie die beschikbaar is voor het sedimenttransport. Hogere duinen met een kleine lengte veroorzaken meer turbulentie, meer energieverlies en meer stromingsweerstand.

Daarnaast is het zo dat het tijd kost voordat de duinen in grootte aan de stroming zijn aangepast. Als gevolg daarvan loopt de duinhoogte in ontwikkeling vaak achter bij het verloop van de schuifspanning gedurende een hoogwater, wat dus ook hysteresis geeft, maar dan van de duinhoogte. Na de hoogwaterpiek zijn de duinen daarom meestal hoger dan ervoor, bekeken bij dezelfde waterafvoer. Het grootste energieverlies treedt dus ook op na een hoogwater. Dit kan hysteresis in het sedimenttransport opleveren, met relatief meer transport bij stijgende waterstanden dan bij dalende. Dit speelt een belangrijke rol in de Rijntakken (**hoofdstuk 6**). De duinvorming is in de Rijn nog complexer, daar bij dalende waterstanden de grote duinen op een gegeven moment inactief worden en er secundaire duinen op de rug van de grote ontstaan. De effecten van deze secundaire duinen op de stroming en het sedimenttransport zijn echter nog niet doorgond (**hoofdstuk 6**).

Een belangrijk neveneffect is overigens dat de extra weerstand een waterstandverhoging veroorzaakt. Het ontstaan van duinen, turbulentie in de stroming en het effect op de waterstand is echter nog onvoldoende begrepen, zodat vooral de voorspelde waterstanden voor extreem grote

hoogwaters met grote onzekerheid zijn omgeven.

5 Verticale sortering van sediment

Bij schudden of transport van een mengsel van korrels met verschillende grootten ontstaat al snel een verticale sortering. Dit kan ook worden waargenomen als gemengde noten of muesli worden geschud. De kleine korrels vallen omlaag in de door de beweging ontstane poriën. De grote korrels passen daar echter niet in. Het gevolg is dat het lichte zand onderop komt te liggen, terwijl het zwaardere grind juist omhoog wordt gewerkt. Dit fenomeen wordt 'kinematische sortering' genoemd en speelt een belangrijke rol in zand-grindrivieren (**hoofdstuk 7**).

Een gerelateerd fenomeen is een afpleisteringslaag aan het beddingoppervlak, kortweg pleisterlaag. Een pleisterlaag is in beginsel een erosief verschijnsel; het makkelijk transporteerbare zand is door de stroming afgevoerd terwijl de grotere korrels zijn blijven liggen. Hierdoor ontstaat een grove laag die het onderliggende sediment beschermt tegen verdere erosie. Het eerder genoemde 'hiding-exposure'-fenomeen speelt dus een belangrijke rol bij de pleisterlaagvorming. Ook kinematische sortering kan een rol spelen. De dikte van de pleisterlaag blijkt in de praktijk niet groter te zijn dan de diameter van de grootste korrels die in het sediment aanwezig zijn. Een tijdens laagwater ontstane pleisterlaag kan het sedimenttransport gedurende enige tijd (tot het falen van de pleisterlaag) tegenhouden. Hierdoor kan hysteresis in het sedimenttransport ontstaan, waarbij het transport bij stijgende waterstanden lager is dan bij dalende waterstanden (**hoofdstuk 6**). Dit effect op sedimenttransport is dus omgekeerd aan dat van duinen. Pleisterlaagvorming is in de Nederlandse Rijntakken waarschijnlijk van ondergeschikt belang, maar speelt in de Allier en de Grensmaas (tussen Maastricht en Venlo) een prominente rol omdat daar meer grind in de rivier voorkomt.

Zoals gezegd bewegen duinen zich over de bedding voort doordat sediment wordt afgezet op de steile lizijde van de duinen, dus in de luwte van de stroming. Tijdens deze afzetting vindt sortering van zand en grind plaats, welke deels bewaard blijft in de rivierbedding. Boven in de duinen komt vooral zand voor, terwijl naar onderen toe steeds meer grind voorkomt. De sortering ontstaat op twee manieren.

De eerste manier van sortering vindt plaats in de lawines van sediment die plaatsvinden op de steile lizijde van de duinen. Het sediment dat getransporteerd wordt over de loefzijde van de duin, zakt uit in de luwte van de duintop en valt vooral op het bovenste deel van de lizijde. Zodra dit sediment een kritieke hoek overschrijdt, ontstaat een lawine en stroomt het sediment naar beneden over de lizijde totdat het beneden de kritieke hoek weer tot rust komt (**hoofdstuk 7**). Zo'n lawine is een aantal korrels dik. Uit experimenten met verschillende sedimenten en stromingscondities (**hoofdstuk 8**) blijkt hoe het sediment in de lawine wordt gesorteerd. In de lawine vindt kinematische sortering plaats, zodat vooral grind aan het oppervlak van de lizijde komt te liggen. Tegelijk schuift en rolt grind veel gemakkelijker over zand dan andersom, net zoals een fiets makkelijker over kinderkopjes rolt dan een rolschaats. In de daaropvolgende lawine wordt vooral dat onderliggende grind naar beneden meegesleept, terwijl het zand op de plaats blijft. Het is dus de kinematische sortering in combinatie met de sleepkracht van opeenvolgende lawines die de vergroving naar onderen toe veroorzaakt. Deze vergroving kan worden waargenomen als een grindige laag onder een meer zandige laag. De sortering wordt zwakker naarmate de duinen sneller bewegen (**hoofdstuk 8**).

De tweede manier van sortering vindt plaats in de troggen van de duinen. Bij dalende waterstanden zijn de duinen relatief hoog en is er dus minder energie voor bodemtransport. Tegelijk worden de duinen kleiner als reactie op de afnemende stromingsenergie, en vindt dus

afzetting van sediment plaats in de troggen. Het minst mobiele sediment, namelijk het grind, wordt als eerste afgezet. Hierbij spelen het eerder genoemde 'hiding-exposure'-fenomeen maar ook de complexe turbulente stroming in de duintroggen een belangrijke rol. Het gevolg is dat op de diepte van de duintroggen een grindlaag ontstaat. Deze laag is gevonden in de experimenten (hoofdstuk 4 en 10). Ook in de rivier de Rijn zijn twee grindlagen gevonden, welke zijn ontstaan als gevolg van sedimentsoortering in de hoge duinen in het extreme hoogwater van 1995 en in de minder hoge duinen in het hoogwater van 1998 (hoofdstukken 6 en 9).

6 Effect van verticale sortering op sedimenttransport

Pleisterlagen hebben vooral een remmende werking op het transport. Dit blijkt ook uit het type beddingvorm dat voorkomt. Als het beddingsediment is afgedekt met een pleisterlaag, kan een beddingvorm geïsoleerd raken en een sikkelvorm krijgen. Zo'n beddingvorm heet een barchaan, en komt ook als windduin in woestijnen op Aarde en Mars voor. Barchanen ontstaan als sediment zich voortbeweegt over een vlakte waaruit bij de gegeven omstandigheden geen extra sediment (zand) kan worden opgenomen, omdat de wind- of stroomsnelheid niet voldoende sterk is om dat zwaardere sediment (grind) in transport te krijgen, of bijvoorbeeld omdat de ondergrond bevroren of vochtig is. Het eerste was in de experimenten van hoofdstuk 4 inderdaad het geval: de zandige barchaan bewoog zich voort over een pleisterlaag, waarin geen zand meer aan de oppervlakte voorkwam. Als er nog minder zand beschikbaar is voor de vorming van beddingvormen, ontstaan dunne slierten van zand op de pleisterlaag die parallel aan de stroming liggen. De waargenomen beddingvormtypen variëren systematisch met de hoeveelheid sediment die beschikbaar is voor transport, maar onder deze condities kan het lokale sedimenttransport niet goed worden voorspeld, zodat ook de beddingvormtypen niet goed voorspeld kunnen worden (hoofdstuk 4). Deze condities worden daarom verder buiten beschouwing gelaten, en de nadruk ligt verder op rivieren met een hogere sedimentmobiliteit of hoogwaters.

De verticale sortering in duinen uit zich vooral in grove lagen of vergroving naar onderen toe. Het effect hiervan op het sedimenttransport kan aanzienlijk zijn, zowel tijdens een hoogwater als op het daaropvolgende hoogwater (zie hoofdstuk 6 en 9). Tijdens een hoogwater ontstaat vooral na de hoogwaterpiek een afzetting van grind in de troggen van de duinen. Dat betekent dus dat bij dalende waterstanden minder grind beschikbaar is voor het sedimenttransport dan bij stijgende waterstanden. Aangezien grind moeilijker te transporteren is dan zand, is het transport voor de hoogwaterpiek wat lager dan erna, beschouwd bij dezelfde waterafvoer. De verticale sortering kan dus een hysteresis veroorzaken. De grindlagen beïnvloeden ook het transport tijdens het daaropvolgende hoogwater. Bij stijgende waterstanden kunnen deze grindlagen, wanneer ze aangesneden worden door groeiende duinen, het transport gedurende enige tijd remmen (hoofdstuk 10). Dit wordt ook wel een geschiedenis-effect genoemd omdat de grindlaag een overblijfsel is van een vorig hoogwater. Het is echter niet zo eenvoudig om dit effect te voorspellen, omdat de stroming in de duintroggen dusdanig complex is dat een eenvoudig verband tussen sedimenttransport en schuifspanning niet voldoet (hoofdstuk 9-11). De verticale sortering kan in elk geval leiden tot aanzienlijke hysteresis in het sedimenttransport. Hoe deze hysteresis zich verhoudt tot de hysteresis die wordt veroorzaakt door andere fenomenen en in hoeverre deze elkaar versterken of verzwakken, lijkt te verschillen per riviertak van de Rijn (hoofdstuk 6).

De vorming van grindlagen onder de duinen is niet alleen afhankelijk van de mobiliteit van het grind in de duintroggen, maar ook van de regelmaat van de duinvormen. Uit experimenten (hoofdstuk 10) blijkt dat de duinen in zand-grindmengsels onregelmatiger van vorm worden naarmate de schuifspanning toeneemt. Dit werd in de literatuur al eerder geconstateerd voor zandige duinen, maar niet voor duinen met meer grind, omdat de schuifspanningen in de

experimenten met mengsels uit de literatuur daarvoor te laag waren. De onregelmatigheid van de duinen komt tot uiting in meer golvende duinkammen en vooral een grotere variatie in diepte van de troggen. Het effect op de verticale sortering is dus dat er ook een grotere variatie in de diepte van de grindlagen ontstaat. Dit leidt tot een minder sterke gemiddelde sorteringstrend van vergroving in de diepte. Daarmee zou de hysteresis van sedimenttransport ook weer minder kunnen worden, maar dit effect kon niet worden geïsoleerd in de experimenten of veldmetingen.

7 Toekomstig onderzoek

Uit dit proefschrift volgt dat een aantal bijzondere fenomenen moeten worden meegenomen in berekeningen om de waterstand, de stroomsnelheid, het sedimenttransport en de veranderingen in de hoogteligging van de bedding goed te kunnen voorspellen. Deze fenomenen zijn:

- de vorming van grindlagen,
- het begin van beweging van zand en grind en het effect van turbulentie daarop,
- de variatie in diepte van de duintroggen, en
- de verticale sortering als gevolg van de lawines aan de lizijde van de duinen.

Voor condities met snel veranderende stroming, zoals tijdens hoogwaters, zouden bovendien de volgende processen beter moeten worden bestudeerd en worden meeberekend in modellen:

- het effect van begraven grindlagen uit vorige hoogwaters op het sedimenttransport en de duingroei bij stijgende waterstanden, en
- de achterblijvende ontwikkeling van duinen, en het ontstaan en de effecten van secundaire duinen bij dalende waterstanden.

Literatuur

- KLEINHANS, M. G. & TEN BRINKE, W. B. M. (1998), Vervoer onder de rivier. *Natuur & Techniek*, 66e jaargang, 1, pp. 32-40.
- KLEINHANS, M. G., VAN DEN BERG, J. H., WILBERS, A. & DE KRAMER, J. (2000), De Allier als morfologisch voorbeeld voor de Grensmaas. III: sedimenttransport en afpleistering. *Natuurhistorisch Maandblad*, september 2000, pp. 202-207.

Curriculum Vitae



Maarten Kleinhans was born on April 28, 1972 in Velp (The Netherlands). He went through primary and secondary education in Zwolle and married in 1999. He studied Physical Geography at Utrecht University between 1991 and 1995 and specialised in Coastal and Riverine Morphodynamics. During an internship at WL|Delft Hydraulics he participated in a scale model study of the gravel-bed river Meuse (The Netherlands), and graduated (Msc equivalent level) on a field study of infragravity waves off the coast of Terschelling (The Netherlands).

From December 1995 to March 1997 Maarten was employed at Utrecht University under contract of Rijkswaterstaat-RIZA to analyse sediment transport data and determine the annual sediment budget of the river Rhine in The Netherlands.

Meanwhile, he wrote the proposal for this PhD study. It was funded for four years by the Netherlands Science Foundation (NWO), commenced in April 1997, and was extended with additional contracts of Rijkswaterstaat-RIZA to March 2002. Laboratory flume experiments were conducted in cooperation with other workers at WL|Delft Hydraulics (The Netherlands) in 1997-1998, and at the Dept. of Earth Sciences, Utrecht University, in 1999 and at St. Anthony Falls Hydraulics Laboratory (Minneapolis, USA) in 2001. In the river Rhine, field studies were done in cooperation with Rijkswaterstaat in 1997, 1998 and 2001. In the sand-gravel bed river Allier (France), a field study was done in 1999 together with four MSc-students.

Maarten attended the international conferences and workshops of Gravel Bed Rivers in New Zealand in 2000, Graded Sediment in Wallingford (UK) in 2001 and Fluvial Sedimentology in Lincoln, Nebraska (USA) in 2001. Presently Maarten is employed by Utrecht University for a three-year postdoctoral study of offshore sediment transport in the European research project 'SANDPIT'.

Spare time was spent partly in the Dutch Youth Association for Astronomy. In 1989 Maarten designed a low-cost telescope that can easily be built by children, and has been built about a hundred times. Between 1998 and 2001, Maarten was the chairman of the Dutch Youth Association for Astronomy. Since 1990, he has been giving astronomy and planetary geology courses for children, and helped organise meetings and holiday camps.

Since 1995, Maarten has studied how philosophy of science in literature relates to philosophy of earth science, presented some results at a national conference for philosophers of science, and is now a guest-member of the Philosophy of Science research group at the Free University in Amsterdam.

Publications by Maarten Kleinhans

Peer-reviewed publications

- KLEINHANS, M. G.** (submitted), Subaqueous Dunes, Transport and Deposition of Sand-Gravel Mixtures: linking process and deposit in fluvial channels. Submitted to the conference proceedings of the 7th International Conference on Fluvial Sedimentology 2001, Nebraska, to be published as a Special Publication of the International Association of Sedimentologists, eds. MIKE BLUM & SUE MARRIOTT.
- KLEINHANS, M. G., WILBERS, A. W. E., DE SWAAF, A. & VAN DEN BERG, J. H.** (2002), Sediment supply-limited bedforms in sand gravel bed rivers, in press by Journal of Sedimentary Research.
- KLEINHANS, M. G. & VAN RIJN, L. C.** (2002), Stochastic prediction of sediment transport in sand-gravel bed rivers, Journal of Hydraulic Engineering 128(4), ASCE, pp. 412-425, special issue: Stochastic hydraulics and sediment transport.
- KLEINHANS, M. G.** (2001). The Key Role of Fluvial Dunes in Transport and Deposition of Sand-Gravel Mixtures, a preliminary note, Sedimentary Geology 143 (1-2) (ExpresSed), pp. 7-13.
- KLEINHANS, M. G. & TEN BRINKE, W. B. M.** (2001), Accuracy of cross-channel sampled sediment transport in large sand-gravel-bed rivers. Journal of Hydraulic Engineering 127 (4), pp. 258-269.
- HESSELINK, A.W., KLEINHANS, M. G. & BOREEL, G.L.** (submitted), Discharge of Rhine distributaries calculated from historic flow measurements. Submitted to J. of Hydr. Engineering.
- RUSSINK, B. G., KLEINHANS, M. G., & VAN DEN BEUKEL, P. G. L.** (1998), Observations of swash under highly dissipative conditions. Journal of Geophysical Research 103 (C2), pp. 3111-3118.

Conference publications

- KLEINHANS, M. G. & BLOM, A.** (2001), Discussion of WILCOCK, P. R. (2001) The flow, the bed and the transport: interaction in the flume and field, in: MOSLEY, M. P. (ed.) Gravel-bed rivers V, pp. 212-214, New Zealand Hydrological Society Inc, Wellington, New Zealand.
- KLEINHANS, M. G. & BUSKES, C. J. J.** (2001), Philosophy of Earth Science: just sloppy physics? 2nd Flemish/Dutch Congress for General and Special Philosophy of Science, Leusden, 18-20 May.
- KLEINHANS, M. G.** (2001), Prediction of sand-gravel bedload transport. Graded sediment workshop, Wallingford (UK), May 2001.
- KLEINHANS, M. G.** (2001), Sorting and Deposition of Sediment Mixtures in Subaqueous River Dunes (review). 7th International Conference on Fluvial Sedimentology, 2001, Lincoln (Nebraska), in: J.A. MASON, R.F. DIFFENDAL JR. AND R.M. JOECKEL (eds), Open-File report 60, Conservation and Survey Division, Institute of Agriculture and Natural Resources, USA.
- KLEINHANS, M. G.** (2000), The Relation between Bedform Type, Vertical Sorting in Bedforms and Bedload Transport During Subsequent Discharge Waves in Large Sand Gravel Bed Rivers with Fixed Banks, Gravel Bed Rivers 2000 conference, New Zealand, in NOLAN, T. & THORNE, C. (eds), Special public. CD-rom of the New Zealand Hydrological Society.
- KLEINHANS, M. G.** (2000), Relevant Phenomena for Predicting Bed Load Transport in Sand Gravel Bed Rivers, Netherlands Centre for River research symposium, Soesterberg, October 2000.
- KLEINHANS, M. G.** (2000), Sorting of Sand and Gravel in Bedforms as a Possible Explanation for Hysteresis in Bed Load Transport during High Discharges in the Waal, Netherlands Earth Science Congress (NAC5), Veldhoven, April 2000.

Professional publications

- KLEINHANS, M. G., VAN DEN BERG, J. H., WILBERS, A. W. E. & DE KRAMER, J.** (2000), De Allier als morfologisch voorbeeld voor de Grensmaas. III: sedimenttransport en afpleistering. *Natuurhistorisch Maandblad*, september 2000, pp. 202-207.
- DE KRAMER, J., WILBERS, A. W. E., VAN DEN BERG, J. H. & KLEINHANS, M. G.** (2000), De Allier als morfologisch voorbeeld voor de Grensmaas. II: oevererosie en meandermigratie. *Natuurhistorisch Maandblad*, augustus 2000, pp. 189-198.
- VAN DEN BERG, J. H., DE KRAMER, J., KLEINHANS, M. G. & WILBERS, A. W. E.** (2000), De Allier als morfologisch voorbeeld voor de Grensmaas. I: vergelijkbaarheid en rivierpatroon. *Natuurhistorisch Maandblad*, juli 2000, pp. 118-122.
- KLEINHANS, M. G. & TEN BRINKE, W. B. M.** (1998), Rivieren in beweging. *Natuur & Techniek* 1, januari 1998, pp. 32-40.

Reports

- KLEINHANS, M. G., WILBERS, A. W. E., & VAN DEN BERG, J. H.** (2001), Effect van getij op sedimenttransport in de Merwede, Proefmeting splitsingspunt Werkendam 2001. Netherlands Centre for Geo-ecological Research / Utrecht University Physical Geography. ICG 01/6, 2001.
- KLEINHANS, M. G.** (2001), Calibratie van bodemtransportmeetmethoden, literatuurstudie. Netherlands Centre for Geo-ecological Research / Utrecht University Physical Geography. ICG 01/3, 2001.
- WILBERS, A. W. E. & KLEINHANS, M. G.** (1999), Gevoeligheidsanalyse dunetracking in 2 dimensies. Netherlands Centre for Geo-ecological Research / Utrecht University Physical Geography. ICG 99/8, 1999.
- BLOM, A. & KLEINHANS, M. G.** (1999), Non-uniform sediment in morphological equilibrium situations, Data Report Sand Flume Experiments 97/98. University of Twente, Rijkswaterstaat RIZA, WL | Delft Hydraulics. 1999. University of Twente, Civil Engineering and Management.
- KLEINHANS, M. G.** (1999), Sedimenttransport in de Waal: Hoogwater november 1998. Netherlands Centre for Geo-ecological Research / Utrecht University Physical Geography. ICG 99/6, 1999.
- KLEINHANS, M. G.** (1998), Kalibratie van de Valbuis Fysische Geografie Utrecht. Netherlands Centre for Geo-ecological Research / Utrecht University Physical Geography. ICG 98/13, 1998.
- KLEINHANS, M. G.** (1997), Sedimenttransport in de Waal: Betrouwbaarheidsanalyse en meetstrategie. Netherlands Centre for Geo-ecological Research / Utrecht University Physical Geography. ICG 97/3, 1997.
- KLEINHANS, M. G.** (1997), Sedimenttransport in de Waal: Hoogwater maart 1997. Netherlands Centre for Geo-ecological Research / Utrecht University Physical Geography. ICG 97/7, 1997.
- KLEINHANS, M. G.** (1996), Sedimenttransport in de Nederlandse Rijntakken, verwerking metingen 1988-1995 en toetsing transportvergelijkingen. Interuniversitair Centrum voor Geo-ecologisch Onderzoek / Universiteit Utrecht Fysische Geografie. ICG 96/7, 1996.
- KLEINHANS, M. G.** (1996), Sediment transport in the Dutch Rhine branches, annual transport and interim sediment budget. Netherlands Centre for Geo-ecological Research / Utrecht University Physical Geography. ICG 96/9, 1996.